



agronomy

Special Issue Reprint

New Insights into Pathogen, Insect Pest, and Weed Control in Field and Greenhouse Cropping Systems

Edited by
Hideyoshi Toyoda

mdpi.com/journal/agronomy



New Insights into Pathogen, Insect Pest, and Weed Control in Field and Greenhouse Cropping Systems

New Insights into Pathogen, Insect Pest, and Weed Control in Field and Greenhouse Cropping Systems

Editor

Hideyoshi Toyoda



Basel • Beijing • Wuhan • Barcelona • Belgrade • Novi Sad • Cluj • Manchester

Editor

Hideyoshi Toyoda
Kindai University
Nara
Japan

Editorial Office

MDPI
St. Alban-Anlage 66
4052 Basel, Switzerland

This is a reprint of articles from the Special Issue published online in the open access journal *Agronomy* (ISSN 2073-4395) (available at: https://www.mdpi.com/journal/agronomy/special_issues/TS29410019).

For citation purposes, cite each article independently as indicated on the article page online and as indicated below:

| |
|--|
| Lastname, A.A.; Lastname, B.B. Article Title. <i>Journal Name</i> Year , <i>Volume Number</i> , Page Range. |
|--|

ISBN 978-3-7258-0895-3 (Hbk)

ISBN 978-3-7258-0896-0 (PDF)

doi.org/10.3390/books978-3-7258-0896-0

© 2024 by the authors. Articles in this book are Open Access and distributed under the Creative Commons Attribution (CC BY) license. The book as a whole is distributed by MDPI under the terms and conditions of the Creative Commons Attribution-NonCommercial-NoDerivs (CC BY-NC-ND) license.

Contents

| | |
|--|------------|
| About the Editor | vii |
| Preface | ix |
| Hideyoshi Toyoda Electrostatic Techniques for Physically Managing Pathogens, Insect Pests, and Weeds in Field and Greenhouse Cropping Systems Reprinted from: <i>Agronomy</i> 2023 , <i>13</i> , 2855, doi:10.3390/agronomy13122855 | 1 |
| Teruo Nonomura and Hideyoshi Toyoda Electrostatic Spore-Trapping Techniques for Managing Airborne Conidia Dispersed by the Powdery Mildew Pathogen Reprinted from: <i>Agronomy</i> 2022 , <i>12</i> , 2443, doi:10.3390/agronomy12102443 | 8 |
| Shin-ichi Kusakari, Yoshinori Matsuda and Hideyoshi Toyoda Electrostatic Insect Repulsion, Capture, and Arc-Discharge Techniques for Physical Pest Management in Greenhouses Reprinted from: <i>Agronomy</i> 2023 , <i>13</i> , 23, doi:10.3390/agronomy13010023 | 22 |
| Li Jia, Shicai Xu, Huanzhang Shang, Jiao Guo, Xia Yan, Changhai Liu, et al. High-Voltage Electrostatic Fields Adversely Affect the Performance of Diamondback Moths over Five Consecutive Generations Reprinted from: <i>Agronomy</i> 2023 , <i>13</i> , 1008, doi:10.3390/agronomy13041008 | 38 |
| Yoshinori Matsuda, Yoshihiro Takikawa, Kunihiro Shimizu, Shin-ichi Kusakari and Hideyoshi Toyoda Use of a Pair of Pulse-Charged Grounded Metal Nets as an Electrostatic Soil Cover for Eradicating Weed Seedlings Reprinted from: <i>Agronomy</i> 2023 , <i>13</i> , 1115, doi:10.3390/agronomy13041115 | 54 |
| Yoshinori Matsuda, Koji Kakutani and Hideyoshi Toyoda Unattended Electric Weeder (UEW): A Novel Approach to Control Floor Weeds in Orchard Nurseries Reprinted from: <i>Agronomy</i> 2023 , <i>13</i> , 1954, doi:10.3390/agronomy13071954 | 65 |
| Koji Kakutani, Yoshinori Matsuda and Hideyoshi Toyoda A Simple and Safe Electrostatic Method for Managing Houseflies Emerging from Underground Pupae Reprinted from: <i>Agronomy</i> 2023 , <i>13</i> , 310, doi:10.3390/agronomy13020310 | 78 |
| Yoshinori Matsuda and Hideyoshi Toyoda Target-Size-Dependent Application of Electrostatic Techniques for Pest Management in Greenhouses Reprinted from: <i>Agronomy</i> 2023 , <i>13</i> , 125, doi:10.3390/agronomy13010125 | 94 |
| Mireille van Damme, Romanos Zois, Martin Verbeek, Yuling Bai and Anne-Marie A. Wolters Directions from Nature: How to Halt the Tomato Brown Rugose Fruit Virus Reprinted from: <i>Agronomy</i> 2023 , <i>13</i> , 1300, doi:10.3390/agronomy13051300 | 111 |
| Lei Cui, Michiel C. van den Munckhof, Yuling Bai and Roeland E. Voorrips Resistance to Anthracnose Rot Disease in <i>Capsicum</i> Reprinted from: <i>Agronomy</i> 2023 , <i>13</i> , 1434, doi:10.3390/agronomy13051434 | 134 |

**Eleni Koseoglou, Matthijs Brouwer, Derek Mudadirwa, Jan M. Van der Wolf,
Richard G. F. Visser and Yuling Bai**
Identification of Two Novel Loci Underlying Tolerance to *Clavibacter michiganensis* Originating
from *Solanum arcanum* LA2157
Reprinted from: *Agronomy* **2023**, *13*, 953, doi:10.3390/agronomy13040953 **154**

Márk Z. Németh, Diána Seress and Teruo Nonomura
Fungi Parasitizing Powdery Mildew Fungi: *Ampelomyces* Strains as Biocontrol Agents against
Powdery Mildews
Reprinted from: *Agronomy* **2023**, *13*, 1991, doi:10.3390/agronomy13081991 **167**

**Yutaka Kimura, Márk Z. Németh, Kana Numano, Asami Mitao, Tomomi Shirakawa,
Diána Seress, et al.**
Hyperparasitic Fungi against Melon Powdery Mildew Pathogens: Quantitative Analysis of
Conidia Released from Single Colonies of *Podosphaera xanthii* Parasitised by *Ampelomyces*
Reprinted from: *Agronomy* **2023**, *13*, 1204, doi:10.3390/agronomy13051204 **183**

About the Editor

Hideyoshi Toyoda

Professor Hideyoshi Toyoda was born in December 1949 in Osaka City, Osaka Prefecture, Japan. He obtained a Bachelor of Education degree from Osaka Kyoiku University in 1972 and a Doctor of Agriculture degree from Kyoto University in 1980. Following two years as a research fellow with the Japan Society for the Promotion of Science, he began his career as an assistant professor at the Faculty of Agriculture, Kindai University in 1981. In 1998, he was promoted to professor at the Faculty and Graduate School of Agricultural Science. Throughout his tenure, he held various administrative roles, including Dean of the Department of Agriculture, Director of the Library and Vice Dean of Students until his retirement. In recognition of his contributions, he was awarded the title of Professor Emeritus in 2016. He also had the privilege of delivering invited lectures at the National University of Singapore (Department of Botany) and serving as a specially invited professor at East China Normal University (Department of Life Science). Within academic societies, he served as a councilor for the Japan Society of Plant Pathology and the Japan Society of Plant Cell and Molecular Biology, as well as the Japan Society for Biological Environmental Regulation. In government-related capacities, he participated as a member of the candidate selection committee (Biotechnology section) for the Japan Prize Foundation. Currently, he serve as the President of the Research Association of Electric Field Screen Supporters (AEFSS).

Preface

This Special Issue compiles cutting-edge research on pesticide-independent strategies for tackling agricultural pests, including pathogens, insect pests and weeds. It emphasizes innovative physical control methods based on electrostatic principles and sheds light on novel approaches to pest management.

The cornerstone of this Special Issue lies in the utilization of electrostatic techniques to develop simple yet effective devices. These devices leverage the generation of electric fields through charged conductors, both insulated and non-insulated. Insulated charged conductors create static electric fields capable of trapping airborne fungal spores, plant pollen and flying insect pests. Moreover, the repellent effect of the static electric field on insects adds another dimension to pest management. On the other hand, non-insulated charged conductors generate dynamic electric fields, facilitating the electrocution of conductive pests such as insects nesting in stored dried crop products.

The editorial and review articles provide insights into the structural design of electrostatic devices and their application in quantitative sporulation analysis for fungal phytopathogen and pest trapping. Original articles delve into the impact of electrostatic fields on diamondback moth population dynamics and introduce innovative techniques for electrocuting weed seedlings and emerging flies. Clear criteria for target size in the trapping and electrocuting processes are also elucidated.

Complementing electrostatic methods, this Special Issue explores biotechnological approaches to pest resistance. Screening for genetic traits conducive to pest resistance in major crop plants and strategies for breeding resistant cultivars are discussed. Articles focus on resistance to Tomato brown rugose fruit virus and anthracnose in a capsicum species, highlighting the role of viral RNA silencing, host resistance proteins and hormone-based resistance.

The efficacy of combining physical and resistance breeding technologies with biological control measures is underscored. Various bacterial and fungal agents are explored as biocontrol agents against plant pathogens and insect pests. The use of hyperparasitic fungi such as *Ampelomyces* spp. is highlighted for controlling powdery mildew colonies on leaves. Morphological and molecular characterization, along with quantitative analyses, elucidate their biocontrol functionality.

This Special Issue showcases a comprehensive approach to pest management, integrating innovative electrostatic techniques with biotechnological advancements and biological control measures. By harnessing these diverse strategies, agricultural systems can achieve more sustainable and effective pest control.

Hideyoshi Toyoda

Editor



Editorial

Electrostatic Techniques for Physically Managing Pathogens, Insect Pests, and Weeds in Field and Greenhouse Cropping Systems

Hideyoshi Toyoda

Research Association of Electric Field Screen Supporters, Nara 631-8505, Japan; toyoda@nara.kindai.ac.jp

1. Introduction

The primary focus in pest management across all pest classes, including pathogens, insect pests, and weeds, is on shifting towards methods that do not rely on pesticides. This shift is driven by the emergence of pesticide-resistant pests due to the extensive use of chemicals [1–4] and increasing public demand for reduced or pesticide-free agriculture. In alignment with this research direction, this editorial introduces a new wave of electrostatics-based physical pest control methods.

A thorough understanding of electrostatics has laid the foundation for the development of innovative tools to combat plant pathogens, insect pests, and weeds in both field and greenhouse settings. These tools encompass devices that create an electric field [5], defined as the region surrounding an electric charge where it can exert a noticeable force on another electric charge [6]. The core component of these devices is an insulated conductor charged negatively using a voltage generator [5]. The insulation of the charged conductor is crucial to establish a non-discharging electric field around it. These electric field-based devices are known as electric field screens and are of three types: single-charged monopolar, single-charged dipolar, and double-charged dipolar [5]. The force generated by these electric field screens has been harnessed to capture airborne spores [7], plant pollen [8], and flying insect pests [9,10]. In contrast, a different type of device, constructed with a non-insulated charged conductor, generates an arc (spark) discharge aimed at targets [11]. This device is referred to as an arc-exposing electric field screen and is employed to manage insects and weed seedlings emerging from the ground [9]. Hence, these devices can be customized to suit the specific electrostatic characteristics based on the nature of the targets.

The most notable feature of these electric field-based devices is their straightforward design, which allows ordinary workers to construct them inexpensively using readily available materials or modifying them as required. Electrostatic traps have demonstrated practicality in preventing wind-borne pathogen spores and flying insect pests from infiltrating greenhouses [12] and in monitoring their spatial and temporal patterns to design safe crop production areas [13]. Safe arcing devices can also serve as practical tools for simultaneously eliminating weeds and insect pests emerging from crop fields [14].

In this editorial, the author provides basic information and explanations about electric field screens for ordinary crop growers who may not be familiar with the technical aspects. The aim is to encourage their active participation in new research endeavors related to pest control. Ongoing research in this area offers fresh insights for developing reliable plant protection methods and ensuring sustainable crop production that can effectively adapt to various changes in different cropping systems.

2. Charging of an Insulated Conductor

A conductor can be charged either negatively or positively by connecting it to a grounded voltage generator. This voltage generator increases the initial voltage to the

Citation: Toyoda, H. Electrostatic Techniques for Physically Managing Pathogens, Insect Pests, and Weeds in Field and Greenhouse Cropping Systems. *Agronomy* **2023**, *13*, 2855. <https://doi.org/10.3390/agronomy13122855>

Received: 28 October 2023

Accepted: 15 November 2023

Published: 21 November 2023



Copyright: © 2023 by the author. Licensee MDPI, Basel, Switzerland. This article is an open access article distributed under the terms and conditions of the Creative Commons Attribution (CC BY) license (<https://creativecommons.org/licenses/by/4.0/>).

desired level [15]. When using a negative voltage, the generator takes free electrons (negative charge) from the ground and transfers them to the conductor, resulting in negatively charging the conductor. Conversely, when using a positive voltage, the generator pushes free electrons out of the conductor into the ground, causing it to acquire a positive charge. To prevent the discharge of the conductor, it is coated with an insulating material like soft polyvinyl chloride, which has a recommended volume resistivity of $10^9 \Omega\text{cm}$ [5].

3. Construction of Electric Field Screens

Figure S1 illustrates the components (Figure S1A–E) and units (Figure S1F–H) needed to build electric field screens. These components consist of a negative or positive voltage generator (Figure S1A), a grounded line (Figure S1B), a layer of insulated metal wires (Figure S1C) arranged horizontally at specific intervals and interconnected, a metal net (Figure S1D), and a polypropylene frame (insulator) (Figure S1E) [5]. A voltage generator is connected to both a grounded line and a layer of insulated metal wires or a metal net. A layer of insulated metal wires is secured within a frame and serves as a metal-wire unit for screen construction (Figure S1F). The framed metal net is connected to a negative voltage generator to function as a charged metal-net unit (Figure S1G) or connected to a grounded line to serve as a grounded metal-net unit (Figure S1H).

4. Single-Charged Monopolar Electric Field Screen for Trapping Airborne Spores

Figure S2A depicts a single-charged monopolar electric field screen (SM-screen), which consists of a layer of insulated metal wires (metal-wire unit) connected to either a negative [16] or positive voltage generator [17]. The SM-screen was originally designed to capture airborne conidia of the powdery mildew pathogen [16]. Each insulated charged metal wire (conductor) creates an electrostatic field (a monopolar electric field that does not produce electric discharge) concentrically in the surrounding space, and an electric field barrier is created when multiple insulated charged conductors are arranged in parallel at specific intervals. Within this electric field barrier, small particles such as fungal spores are attracted to the charged conductor due to their dielectrophoretic movement [18]. Specifically, airborne spores become polarized positively on the side facing the charged conductor and negatively on the opposite side. An attractive force is generated between the positive charge on the spore and the negative charge on the conductor, causing the spore to be drawn towards the charged conductor [16]. In the case of a positively charged insulated conductor, the spore is oriented in the opposite direction due to dielectrophoresis. When the applied voltage is the same in both conductors, an attractive force of equal strength is generated between the spore and the charged conductor [17].

In practical spore trapping scenarios, the target is typically wind-borne spores. The movement of these spores within an electrostatic field is influenced by the wind velocity vector and dielectrophoretic attractive force. To capture the spores effectively, an attractive force greater than the force associated with the wind velocity is required. Increasing the voltage applied to the conductor results in a stronger attractive force. However, it is important to note that the SM-screen was not very effective at trapping small flying insect pests, even when the highest achievable force was applied.

5. Single- and Double-Charged Dipolar Electric Field Screens for Trapping Flying Insect Pests

A single-charged dipolar electric field screen (SD-screen) (Figure S2B) was designed to capture small flying insect pests that could pass through a typical insect-proof net with a mesh size of around 1.5 mm on a greenhouse window [19]. In the SD-screen, an electric field was created in the space between oppositely charged poles. This involved a layer of negatively charged insulated metal wires (the metal-wire unit, serving as the negative pole) and a grounded non-insulated metal net (the metal-net unit, functioning as the positive pole) positioned within the electrostatic field formed by the metal-wire unit [20]. In this setup, a negative voltage generator collected negative charge from the

ground and transferred it to the insulated metal wires. An insulating cover (made of a soft polyvinyl chloride tube) prevented the dissipation of surface charge from the charged metal wires. Simultaneously, it became dielectrically polarized due to the negative charge on the metal wire. This polarization resulted in a negative charge on the outer surface and a positive charge on the conductor-facing surface of the insulator cover due to dielectric polarization [21]. The negative charge on the insulator surface induced a positive charge on the grounded metal net via electrostatic induction [22]. Essentially, the opposite charges on the insulated metal wires and the grounded metal net established an electric field between them [20].

A crucial factor for the dipolar electric field was the volume resistivity (Ωcm) of the insulator used to cover the charged conductor. While the insulating cover could prevent discharge from the charged conductor, if the voltage applied to the conductor exceeded a certain threshold, a negative charge could pass through the insulator cover and move to the ground through the electric field and the metal net (continuous corona discharge) [23]. In the SD-screen, a metal wire was coated with a soft polyvinyl chloride tube ($10^9 \Omega\text{cm}$) with a voltage limit of 8 kV, causing no discharge below this voltage. In other words, at voltages below 8 kV, the SD-screen formed a static electric field (a dipolar electric field with no discharge) between the charged metal wires and the grounded metal net [20].

A significant characteristic of the static electric field was that the negative charge on the insulated charged conductor exerted a repulsive force on another negative charge within the electric field. Consequently, when an insect entered this field, its free electrons were pushed out of its body, making it positively charged (discharge-mediated positive electrification of an insect). Eventually, these positively charged insects were attracted to the negatively charged insulated conductor. This force was strong enough to prevent insects from escaping, and based on this electrostatic principle, an electrostatic insect sweeper was developed to eliminate insect pests that infest host plants [24].

A double-charged dipolar electric field screen (DD-screen) was also created to trap flying insect pests in a greenhouse [25,26]. The DD-screen was constructed by pairing metal-wire units connected to negative and positive voltage generators (Figure S2C). A static electric field was established in the space between these two units. When an insect enters this electric field, it can be captured in two ways [27]. The first scenario involves the insect entering the vicinity of the negatively charged insulated metal wire. The insect loses its free electrons, becoming positively charged, and is attracted to the negative pole [27]. This is essentially the same phenomenon observed in a single-charged dipolar electric field. In the second scenario, the insect enters the region near the positively charged pole. In this case, the insect acquires electrons from the surrounding space, becoming negatively charged and being attracted to the positive pole [27].

The explanations above apply to a static electric field. When the applied voltage surpasses the insulating limit and results in a silent discharge between the opposite poles, the static electric field is converted into a dynamic electric field. However, the generation of electric current does not affect the capture of insects. In fact, the insects are securely trapped, even when an electric current is generated in the dynamic electric field.

6. SD-Screen for Repelling Insect Pests

The SD-screen is composed of negatively charged insulated metal wires placed at specific intervals and a grounded metal net (Figure S2B). Insects that entered the electric field were strongly drawn towards the charged conductor wire due to the discharge-mediated positive electrification of their bodies [28,29]. Conversely, insects that landed on the outer surface of the net exhibited a completely different behavior. These insects, upon reaching the net, stopped and extended their antennae into the static electric field, displaying a ‘searching’ behavior inside the field [30]. This behavior deterred them from fully entering the static electric field, and they ultimately flew away without going inside. This avoidance behavior was observed in a wide range of insects, including 17 orders, 42 families, 45 genera, and 82 species [31]. These findings strongly suggest that all insects

are deterred by a static electric field, making the devices utilizing this electric field a promising tool for repelling insect pests.

Some studies [32,33] reported that cockroaches are capable of detecting electric fields with their antennae. Cockroaches, when subjected to an electric field, deflect their antennae in response to the attraction forces, moving their antennae towards the electrode [32]. The force arose from the uneven charge distribution on the cockroach, with negative charges being attracted to the oppositely charged electrode [32]. Recently, Matsuda et al. [34] used cockroaches to analyze how insects avoid this electric field and concluded that cockroaches perceive an attractive force acting on their antennae when introduced into a static electric field due to the removal of electrons from the antennae. In other words, when an antenna is inserted into a static electric field, it becomes positively charged due to discharge-mediated positive electrification and is attracted to the oppositely charged insulated metal wire. The insect then instinctively retracts its antennae and moves backward. Positively polarized antennae attract free electrons from the air, neutralizing the charge when pulled back out of the electric field [35]. Gordon et al. [36] reported that mosquitoes are capable of recognizing and avoiding entry into a static electric field generated by non-insulated charged and grounded metal plates.

7. Arc Discharge-Generating Electric Field Screen for Eliminating Insect Pests and Weed Seedlings

A discharge-generating electric field screen (DG-screen) was created by connecting two metal-net units: one linked to a negative voltage generator and the other to a grounded line (Figure S2D). This setup generated a dynamic electric field in the space between the two units. Two types of DG-screens were established by adjusting the applied voltage: corona discharge and arc discharge.

The arc discharge-generating type was initially developed to exterminate rice weevils infesting dried rice grains after harvesting [37] and was later applied to pigsty windows to eliminate mosquitoes [38]. The occurrence of an arc discharge (spark) depended on the applied voltage and the distance between the two units, with higher voltages and shorter distances generating stronger arc discharges in the electric field [37]. In the arc discharge-generating DG-screen, the two units were set at a distance where no arc discharge occurred. When insects entered the space between the units, regardless of their location, they effectively became intermediate poles. Consequently, these insects experienced an arc discharge from the negatively charged metal net due to their conductive cuticle outer layer. As a result, the negative charge was transferred to the insect and then to the grounded metal net via a two-step arc discharge process [11]. This electrocution method effectively eliminated the insects. Despite its simple structure, this screen demonstrated excellent functionality.

An electric weeding method based on an arc discharge exposure was originally proposed by Wilson and Anderson [39] and subsequently adopted by others [40–45]. The arc discharge-generating devices were operated using a continuous-charging type of voltage generator. This type had a high output power for charging but carried the risk of electric shock from the charged metal net. In contrast, a pulse-charging type of voltage generator was safer and commonly used with electric fences to deter wild animals [46]. In cases of unintentional human contact with electric fences, it resulted in only temporary discomfort [46]. For safe usage, the pulse-charging type of voltage generator was employed to operate screens for eliminating invasive kudzu vines climbing on a fence [47], weed seedlings emerging in crop fields [48], and adult houseflies emerging from underground pupae [49]. Recently, Matsuda et al. [50] integrated a continuous-charging type of voltage generator into an unattended electric weeder and effectively controlled ground weeds in a greenhouse orchard while ensuring safety.

8. Conclusions

Electric field-based devices for pest control have been categorized based on whether the conductor is insulated for charging purposes. Insulating the charged conductor is crucial for creating insect-capturing and repelling devices. In laboratory-scale experiments, an insulated conductor wire is created by passing a metal wire through a soft polyvinyl chloride tube. The volume resistivity of polyvinyl chloride is typically 10^{15} Ωcm , but it can be reduced to the range of 10^{14} to 10^8 Ωcm by adding plasticizers or ultraviolet absorbents to enhance weather resistance. Various polyvinyl chloride materials mixed with different substances are available in the market as soft polyvinyl chloride, each with distinct properties and varying volume resistivities. Previous devices were effectively operated using a conductor covered with a soft polyvinyl chloride tube with a resistivity of 10^9 Ωcm . In future studies, it is crucial to investigate the relationship between the volume resistivities of insulating materials and their functionalities.

The DG-screen could be constructed more easily because it did not require conductor insulation; in fact, it was simply created by pairing two non-insulated metal nets. A metal net was suitable for this purpose because numerous convex portions on the net surface served as sites for discharge generation. Depending on the applied voltage, the type of discharge at these convex sites could be adjusted from corona to arc discharges. Specifically, two types of DG-screens could be constructed by varying the applied voltage. While this editorial mainly focused on the arc discharge-generating types to present the current state of arc-based pest control methods, the use of corona discharge-generating types may provide opportunities to develop new devices for managing a wide range of targets.

In a corona discharge-generating electric field, numerous negative ions were generated at the convex sites of the negatively charged metal net and transferred to the positively charged grounded metal net. Previous studies have shown that these negative ions were attached to small particles, such as tobacco smoke [51] or small droplets containing viral pathogens [52], which were present within the electric field. This ionization process negatively charged these particles, ultimately leading to their capture by the oppositely charged grounded metal net. Therefore, these successful applications may provide insights into the development of discharge-based electric field screen technologies for pest control in the next stage.

Supplementary Materials: The following supporting information can be downloaded at: <https://www.mdpi.com/article/10.3390/agronomy13122855/s1>, Figure S1: Components (A–E) and units (F–H) for constructing electric field screens; Figure S2: Different types of electric field screens constructed using combinations of metal wire units and/or metal-net units.

Funding: This research received no external funding.

Conflicts of Interest: The author declares no conflict of interest.

References

1. Yin, Y.; Miao, J.; Shao, W. Fungicide resistance: Progress in understanding mechanism, monitoring, and management. *Phytopathology* **2023**, *113*, 707–718. [CrossRef] [PubMed]
2. Naqqash, M.N.; Gökçe, A.; Bakhsh, A. Insecticide resistance and its molecular basis in urban insect pests. *Parasitol. Res.* **2023**, *115*, 1363–1373. [CrossRef] [PubMed]
3. Green, J.M. Current state of herbicides in herbicide-resistant crops. *Pest Manag. Sci.* **2014**, *70*, 1351–1357. [CrossRef] [PubMed]
4. Heap, I. Global perspective of herbicide-resistant weeds. *Pest Manag. Sci.* **2014**, *70*, 1306–1315. [CrossRef] [PubMed]
5. Toyoda, H.; Kusakari, S.; Matsuda, Y.; Kakutani, K.; Xu, L.; Nonomura, T.; Takikawa, Y. Electric field screen structures. In *An Illustrated Manual of Electric Field Screens: Their Structures and Functions*; Toyoda, H., Ed.; RAEFSS Publishing Department: Nara, Japan, 2019; pp. 9–15.
6. Jones, E.; Childers, R. Electric charge and electric field. In *Physics*, 3rd ed.; McGraw-Hill: Boston, MA, USA, 2002; pp. 495–525.
7. Nonomura, T.; Toyoda, H. Electrostatic spore-trapping techniques for managing airborne conidia dispersed by the powdery mildew pathogen. *Agronomy* **2022**, *12*, 2443. [CrossRef]
8. Toyoda, H.; Kusakari, S.; Matsuda, Y.; Kakutani, K.; Xu, L.; Nonomura, T.; Takikawa, Y. Practical application of earth-net free electric field screens. In *An Illustrated Manual of Electric Field Screens: Their Structures and Functions*; Toyoda, H., Ed.; RAEFSS Publishing Department: Nara, Japan, 2019; pp. 69–73.

9. Kakutani, K.; Matsuda, Y.; Nonomura, T.; Toyoda, H. An electrostatic pest exclusion strategy for greenhouse tomato cultivation. *Horticulturae* **2022**, *8*, 543. [CrossRef]
10. Kusakari, S.; Matsuda, Y.; Toyoda, H. Electrostatic insect repulsion, capture, and arc-discharge techniques for physical pest management in greenhouses. *Agronomy* **2023**, *13*, 23. [CrossRef]
11. Toyoda, H.; Kusakari, S.; Matsuda, Y.; Kakutani, K.; Xu, L.; Nonomura, T.; Takikawa, Y. Structure and functions of discharge-generating screens. In *An Illustrated Manual of Electric Field Screens: Their Structures and Functions*; Toyoda, H., Ed.; RAEFSS Publishing Department: Nara, Japan, 2019; pp. 75–85.
12. Takikawa, Y.; Kakutani, K.; Matsuda, Y.; Nonomura, T.; Kusakari, K.; Toyoda, H. A promising physical pest-control system demonstrated in a greenhouse equipped with simple electrostatic devices that excluded all insect pests. *J. Agric. Sci.* **2019**, *11*, 1–20. [CrossRef]
13. Kakutani, K.; Matsuda, Y.; Nonomura, T.; Takikawa, Y.; Osamura, K.; Toyoda, H. Remote-controlled monitoring of flying pests with an electrostatic insect capturing apparatus carried by an unmanned aerial vehicle. *Agriculture* **2021**, *11*, 176. [CrossRef]
14. Matsuda, Y.; Shimizu, K.; Sonoda, T.; Takikawa, Y. Use of electric discharge for simultaneous control of weeds and houseflies emerging from soil. *Insects* **2020**, *11*, 861. [CrossRef]
15. Wegner, H.E. Electrical charging generators. In *McGraw-Hill Encyclopedia of Science and Technology*, 9th ed.; Geller, E., Moore, K., Well, J., Blumet, D., Felsenfeld, S., Martin, T., Rappaport, A., Wagner, C., Lai, B., Taylor, R., Eds.; The Lakeside Press: New York, NY, USA, 2002; pp. 42–43.
16. Matsuda, Y.; Ikeda, H.; Moriura, N.; Tanaka, N.; Shimizu, K.; Oichi, W.; Nonomura, T.; Kakutani, K.; Kusakari, S.; Higashi, K.; et al. A new spore precipitator with polarized dielectric insulators for physical control of tomato powdery mildew. *Phytopathology* **2006**, *96*, 967–974. [CrossRef] [PubMed]
17. Shimizu, K.; Matsuda, Y.; Nonomura, T.; Ikeda, H.; Tamura, N.; Kusakari, S.; Kimbara, J.; Toyoda, H. Dual protection of hydroponic tomatoes from rhizosphere pathogens *Ralstonia solanacearum* and *Fusarium oxysporum* f. sp. *radicis-lycopersici* and airborne conidia of *Oidium neolycopersici* with an ozone-generative electrostatic spore precipitator. *Plant Pathol.* **2007**, *56*, 987–997. [CrossRef]
18. Cross, J.A. Dielectrophoresis. In *Electrostatics: Principles, Problems and Applications*; De Barr, A.E., Ed.; Adam Hilger: Bristol, VA, USA, 1987; pp. 269–276.
19. Kakutani, K.; Matsuda, Y.; Nonomura, T.; Kimbara, J.; Kusakari, S.; Toyoda, H. Practical application of an electric field screen to an exclusion of flying insect pests and airborne conidia from greenhouses with a good air penetration. *J. Agric. Sci.* **2012**, *4*, 51–60. [CrossRef]
20. Matsuda, Y.; Nonomura, T.; Kakutani, K.; Takikawa, Y.; Kimbara, J.; Kasaishi, Y.; Kusakari, S.; Toyoda, H. A newly devised electric field screen for avoidance and capture of cigarette beetles and vinegar flies. *Crop Prot.* **2011**, *30*, 155–162. [CrossRef]
21. Halliday, D.; Resnick, R.; Walker, J. Electric discharge and electric fields. In *Fundamentals of Physics*; Johnson, S., Ford, E., Eds.; John Wiley & Sons: New York, NY, USA, 2005; pp. 561–604.
22. Griffith, W.T. Electrostatic phenomena. In *The Physics of Everyday Phenomena, a Conceptual Introduction to Physics*; Bruflo, D., Loehr, B.S., Eds.; McGraw-Hill: New York, NY, USA, 2004; pp. 232–252.
23. Kaiser, K.L. Air breakdown. In *Electrostatic Discharge*; Kaiser, K.L., Ed.; Taylor & Francis: New York, NY, USA, 2006; pp. 1–93.
24. Takikawa, Y.; Matsuda, Y.; Kakutani, K.; Nonomura, T.; Kusakari, S.; Okada, K.; Kimbara, J.; Osamura, K.; Toyoda, H. Electrostatic insect sweeper for eliminating whiteflies colonizing host plants; a complementary pest control device in an electric field screen-guarded greenhouse. *Insects* **2015**, *6*, 442–454. [CrossRef] [PubMed]
25. Tanaka, N.; Matsuda, Y.; Kato, E.; Kokabe, K.; Furukawa, T.; Nonomura, T.; Honda, K.; Kusakari, S.; Imura, T.; Kimbara, J.; et al. An electric dipolar screen with oppositely polarized insulators for excluding whiteflies from greenhouses. *Crop Prot.* **2008**, *27*, 215–221. [CrossRef]
26. Kakutani, K.; Matsuda, Y.; Nonomura, T.; Takikawa, Y.; Okada, K.; Shibao, M.; Kusakari, S.; Toyoda, H. Successful single-truss cropping cultivation of healthy tomato seedlings raised in an electrostatically guarded nursery cabinet with non-chemical control of whiteflies. *GJPDCP* **2017**, *5*, 269–275.
27. Matsuda, Y.; Kakutani, K.; Nonomura, T.; Kimbara, J.; Kusakari, S.; Osamura, K.; Toyoda, H. An oppositely charged insect exclusion screen with gap-free multiple electric fields. *J. Appl. Phys.* **2012**, *112*, 116103. [CrossRef]
28. Kakutani, K.; Matsuda, Y.; Haneda, K.; Sekoguchi, D.; Nonomura, T.; Kimbara, J.; Osamura, K.; Kusakari, S.; Toyoda, H. An electric field screen prevents captured insects from escaping by depriving bioelectricity generated through insect movements. *J. Electrostat.* **2012**, *70*, 207–211. [CrossRef]
29. Kakutani, K.; Matsuda, Y.; Haneda, K.; Nonomura, T.; Kimbara, J.; Kusakari, S.; Osamura, K.; Toyoda, H. Insects are electrified in an electric field by deprivation of their negative charge. *Ann. Appl. Biol.* **2012**, *160*, 250–259. [CrossRef]
30. Nonomura, T.; Matsuda, Y.; Kakutani, K.; Kimbara, J.; Osamura, K.; Kusakari, S.; Toyoda, H. An electric field strongly deters whiteflies from entering window-open greenhouses in an electrostatic insect exclusion strategy. *Eur. J. Plant Pathol.* **2012**, *134*, 661–670. [CrossRef]
31. Matsuda, Y.; Nonomura, T.; Kakutani, K.; Kimbara, J.; Osamura, K.; Kusakari, S.; Toyoda, H. Avoidance of an electric field by insects: Fundamental biological phenomenon for an electrostatic pest-exclusion strategy. *J. Phys. Conf. Ser.* **2015**, *646*, 012003. [CrossRef]

32. Newland, P.L.; Hunt, E.; Sharkh, S.M. Static electric field detection and behavioral avoidance in cockroaches. *J. Exp. Biol.* **2008**, *211*, 3682–3690. [CrossRef]
33. Jackson, C.W.; Hunt, E.; Sharkh, S.; Newland, P.L. Static electric fields modify the locomotory behaviour of cockroaches. *J. Exp. Biol.* **2011**, *214*, 2020–2026. [CrossRef]
34. Matsuda, Y.; Nonomura, T.; Toyoda, H. Turkestan cockroaches avoid entering a static electric field upon perceiving an attractive force applied to antennae inserted into the field. *Insects* **2021**, *12*, 621. [CrossRef]
35. Jonassen, N. Electrostatic effects and abatement of static electricity. In *Electrostatics*, 2nd ed.; Jonassen, N., Ed.; Kluwer Academic Publishers: Norwell, MA, USA, 2007; pp. 75–120.
36. Gordon, U.; Tanveer, F.; Rose, A.; Paaijmans, K. Repelling Mosquitoes with Electric Fields. In *Advances Arthropod Repellents*; Corona, C., Debboun, M., Coats, J., Eds.; Elsevier BV: Amsterdam, The Netherlands, 2022; pp. 95–112.
37. Matsuda, Y.; Takikawa, Y.; Nonomura, T.; Kakutani, K.; Okada, K.; Shibao, M.; Kusakari, S.; Miyama, K.; Toyoda, H. Selective electrostatic eradication of *Sitophilus oryzae* nesting in stored rice. *J. Food Technol. Preserv.* **2018**, *2*, 15–20.
38. Kakutani, K.; Matsuda, Y.; Takikawa, Y.; Nonomura, T.; Okada, K.; Shibao, M.; Kusakari, S.; Miyama, K.; Toyoda, H. Electrocutation of mosquitoes by a novel electrostatic window screen to minimize mosquito transmission of Japanese encephalitis viruses. *Int. J. Sci. Res.* **2018**, *7*, 47–50.
39. Wilson, R.G.; Anderson, F.N. Control of three weed species in sugar beets (*Betavulgaris*) with an electrical discharge system. *Weed Sci.* **1981**, *29*, 93–97. [CrossRef]
40. Diprose, M.F.; Benson, F.A. Electrical methods of killing plants. *J. Agric. Eng. Res.* **1984**, *30*, 197–209. [CrossRef]
41. Nagura, A.; Tenma, T.; Sakaguchi, Y.; Yamano, N.; Mizuno, A. Destruction of weeds by pulsed high voltage discharges. *J. Inst. Electrostat. Jpn.* **1992**, *16*, 59–66.
42. Mizuno, A. Destruction of weeds by high voltage discharge. *J. Plasma Fusion. Res.* **1999**, *75*, 666–671. [CrossRef]
43. Minoda, A. A basic study on weeding method by using high voltage. *Jpn. J. Ind. Appl. Eng.* **2021**, *9*, 21–24.
44. Lati, R.N.; Rosenfeld, L.; David, I.B.; Bechar, A. Power on! Low-energy electrophysical treatment is an effective new weed control approach. *Pest Manag. Sci.* **2021**, *77*, 4138–4147. [CrossRef] [PubMed]
45. Lehnhoff, E.A.; Neher, P.; Indacochea, A.; Beck, L. Electricity as an effective weed control tool in non-crop areas. *Weed Res.* **2022**, *62*, 149–159. [CrossRef]
46. Burke, M.; Odell, M.; Bouwer, H.; Murdoch, A. Electric fences and accidental death. *Forensic Sci. Med. Pathol.* **2017**, *13*, 196–208. [CrossRef]
47. Matsuda, Y.; Takikawa, Y.; Kakutani, K.; Nonomura, T.; Okada, K.; Kusakari, S.; Toyoda, H. Use of pulsed arc discharge exposure to impede expansion of the invasive vine *Pueraria montana*. *Agriculture* **2020**, *10*, 600. [CrossRef]
48. Matsuda, Y.; Takikawa, Y.; Shimizu, K.; Kusakari, S.; Toyoda, H. Use of a pair of pulse-charged grounded metal nets as an electrostatic soil cover for eradicating weed seedlings. *Agronomy* **2023**, *13*, 1115. [CrossRef]
49. Kakutani, K.; Matsuda, Y.; Toyoda, H. A simple and safe electrostatic method for managing houseflies emerging from underground pupae. *Agronomy* **2023**, *13*, 310. [CrossRef]
50. Matsuda, Y.; Kakutani, K.; Toyoda, H. Unattended electric weeder (UEW): A novel approach to control floor weeds in orchard nurseries. *Agronomy* **2023**, *13*, 1954. [CrossRef]
51. Matsuda, Y.; Takikawa, Y.; Nonomura, T.; Kakutani, K.; Okada, K.; Shibao, M.; Kusakari, S.; Miyama, K.; Toyoda, H. A simple electrostatic device for eliminating tobacco sidestream to prevent passive smoking. *Instruments* **2018**, *2*, 13. [CrossRef]
52. Kakutani, K.; Matsuda, Y.; Nonomura, T.; Takikawa, Y.; Takami, T.; Toyoda, H. A simple electrostatic precipitator for trapping virus particles spread via droplet transmission. *Int. J. Environ. Res. Public Health* **2021**, *18*, 4934. [CrossRef] [PubMed]

Disclaimer/Publisher’s Note: The statements, opinions and data contained in all publications are solely those of the individual author(s) and contributor(s) and not of MDPI and/or the editor(s). MDPI and/or the editor(s) disclaim responsibility for any injury to people or property resulting from any ideas, methods, instructions or products referred to in the content.

Review

Electrostatic Spore-Trapping Techniques for Managing Airborne Conidia Dispersed by the Powdery Mildew Pathogen

Teruo Nonomura ^{1,2,*} and Hideyoshi Toyoda ³

¹ Laboratory of Phytoprotection Science and Technology, Faculty of Agriculture, Kindai University, Nara 631-8505, Japan

² Agricultural Technology and Innovation Research Institute, Kindai University, Nara 631-8505, Japan

³ Research Association of Electric Field Screen Supporters, Nara 631-8505, Japan

* Correspondence: nonomura@nara.kindai.ac.jp

Abstract: This review examines the progress of electrostatic spore-trapping research and the potential for the practical application of electrostatic apparatuses in powdery mildew control. These apparatuses produce an electric field by charging an insulated conductor wire (ICW). Airborne pathogen spores are subjected to an attractive force in the electric field and are drawn to the charged ICW as a result of dielectrophoretic movement. The strength of the attractive force is commensurate with the field strength (determined by the magnitude of the voltage applied to the ICW). Single-charged monopolar electric field screens (SM screens) are constructed by arraying negatively charged cylindrical ICWs in parallel at a specific interval. The connected electric fields of these ICWs form a gap-free air-shielding barrier. Wind-dispersed spores are precipitated by this barrier to create spore-free air. Oppositely charged SM screens have been combined to develop double-charged dipolar electric field screens, which generate a stronger spore attraction force under lower voltage application. Thus, electric field screens represent a promising physical method for creating spore-free spaces in cropping facilities, where plants can be cultivated without risk of infection by airborne fungal pathogens.

Keywords: attractive force; electrostatic field; *Pseudoidium neolycopersici* L. Kiss; *Penicillium digitatum*; physical pathogen control; spore collection probe; spore-free space; static electric field

Citation: Nonomura, T.; Toyoda, H. Electrostatic Spore-Trapping Techniques for Managing Airborne Conidia Dispersed by the Powdery Mildew Pathogen. *Agronomy* **2022**, *12*, 2443. <https://doi.org/10.3390/agronomy12102443>

Academic Editor: Caterina Morcia

Received: 2 September 2022

Accepted: 6 October 2022

Published: 9 October 2022

Publisher's Note: MDPI stays neutral with regard to jurisdictional claims in published maps and institutional affiliations.



Copyright: © 2022 by the authors. Licensee MDPI, Basel, Switzerland. This article is an open access article distributed under the terms and conditions of the Creative Commons Attribution (CC BY) license (<https://creativecommons.org/licenses/by/4.0/>).

1. Introduction

Powdery mildew was first detected in our greenhouse tomatoes in 2001 [1]. The isolated strain (KTP-01) was identified as *Oidium neolycopersici* L. Kiss (syn. *Pseudoidium neolycopersici* L. Kiss) [2], which was identical to isolates collected in various regions worldwide [3]. KTP-01 was found to be highly infectious to all tested commercial tomato cultivars [1,2], as well as a breed line resistant to a European tomato powdery mildew isolate [4]. Although conventional fungicides for powdery mildew pathogens are effective for its control, non-chemical control measures were adopted to reduce the risk of inducing fungicide-resistant strains of the pathogen [5,6]. The initial approach was to screen wild-type tomato plants resistant to new isolates [7–9] and identify resistance genes in these plants [10–12]. A new tomato line bred through interspecific hybridization was found to be highly resistant to the target pathogen isolate until a new pathogenic strain appeared [4,8]. Another biological approach was to use plant resistance-inducing bacteria or pathogen-antagonistic microbes to control powdery mildew. Yamamoto et al. [13] reported that the application of *Bacillus amyloliquefaciens* to soil induced systemic resistance in tomato plants against powdery mildew and bacterial wilt caused by *Ralstonia solanacearum*. Németh et al. [14] inoculated *Ampelomyces* strains into powdery mildew colonies on leaves and reported their mycoparasitic activity against colonial mycelia. Despite much interesting work, there has been little practical progress in this field because these protective effects are easily attenuated, and due to problems with agent preparation, limited application targets, high susceptibility to environmental conditions, and high cost.

By contrast, physical pathogen control methods are largely unaffected by biological and environmental conditions. With electrostatic methods, which are promising for physical pathogen control, an electric field is generated by an electric charge on a conductor as follows: a voltage generator picks up a negative charge from the ground and supplies it to a linked conductor; negative charge accumulates on the surface of the conductor; and an electric field is formed in the space surrounding the charged conductor. If another grounded conductor is placed within the electric field and the applied voltage exceeds a certain limit, the negative charge on the conductor moves to the ground via the grounded conductor (i.e., discharge between two conductors) [15]. By exploiting this discharge phenomenon, Nonomura et al. [16] devised a portable pen-shaped corona discharge generator, in which a powdery mildew colony on a leaf touched by a ground line is directly exposed to a plasma jet stream from the pointed tip of the generator. This exposure treatment destroyed all conidia and conidiophores in the colony instantaneously. However, due to its labor-intensive nature, this treatment is effective for only limited numbers of colonies at the initial stage of disease expansion.

Negative charge on an insulated conductor causes different phenomena within an electric field. If the applied voltage does not exceed the limit, the insulating coating of the conductor prevents discharge (i.e., charge movement) from the charged conductor. Charge remaining on the conductor negatively electrifies the outer surface and positively electrifies the inner surface of the coating through dielectric polarization [17]. An electric field forms around the insulated conductor due to surface charge on the insulator. Importantly, this surface charge imparts a perceivable force to any other charge entering the electric field. Matsuda et al. [18] utilized this force to design a spore trap based on an electric field screen, in which cylindrical insulated conductors were arrayed in parallel at a specific interval, thereby creating an electric field between the charged insulated conductors. Eventually, this spore trap device was further developed as an electrostatic air-shielding barrier to create spore-free spaces for plant cultivation [19].

In this review, we discuss the progress of electrostatic spore trapping research, from its initial experiments to the development of electric field screens targeting fungal spores subject to long-distance dispersal by wind. Most fungal spores are plant pathogens, which have varying spore production rates; powdery mildew is relatively prolific in the pre-harvest stage [20], whereas green molds are common post-harvest [21]. These fungi are often used as model biological materials for capture experiments. Based on results obtained using these species, we offer new insights into fungicide-independent control methods for airborne fungal pathogen spores, based on major contributions made by our joint researchers.

2. Construction of Electrostatic Spore Collection Probes

The powdery mildew pathogen infects tomato plants and typically produces white colonies (pustules) on leaves (Figure 1A). As shown in Figure 1B, numerous conidiophores (rod-shaped structures emerging from superficial hyphae) are produced in the pustules, and spores (conidia) develop at the tips of conidiophores [22]. Using a glass needle held by the micromanipulator of a high-fidelity digital microscope (Figure 1C), Matsuda et al. [23] collected mature conidia from the tips of conidiophores under the microscope. Conidia jumped toward the glass needle before coming into contact with it (Figure 1D). This phenomenon suggested electrostatic attraction between the conidia and needle. A glass needle was fabricated by heating, expanding, and cutting a glass tube (Figure S1). Frictional electrification occurred between the glass surface and surrounding air as the glass tube expanded [24]. Frictional electricity accumulated on the tip of the glass needle, producing an electrostatic field in the surrounding space (Figure S1). The spores were attracted to the needle as a result of an attractive force created by the electrostatic field.

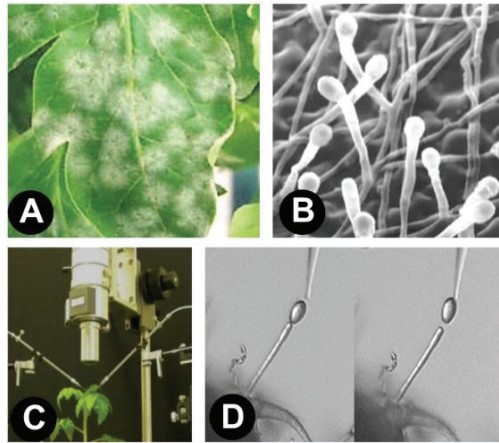


Figure 1. (A) Fungal colonies on tomato leaves; (B) electron micrograph of conidiophores within a colony; (C) a high-fidelity digital microscope equipped with two micromanipulators; and (D) tomato powdery mildew spore collected with a glass needle held under a high-fidelity digital microscope.

To demonstrate the involvement of an electrostatic force in spore attraction, an electrostatic field was created using another electrostatic technique. In this experiment, Nonomura et al. [22] used an electrostatic spore collection probe (i.e., a pointed ebonite rod) (Figure 2A). Mature conidia on the conidiophore were collected using the attractive force created by the electrostatic field produced at the pointed tip of the electrostatic spore collection probe (Figure 2B). Mature conidia that had detached from the conidiophore were attracted to the probe tip, without requiring physical contact, demonstrating that our the hypothesis of electrostatic involvement was correct. The electrostatic spore collection probe was created by touching the flat end of the pointed ebonite rod to a negatively charged metal cap. The ebonite became electrified via dielectric polarization [17], thus producing an electrostatic field around the pointed tip. In the area occupied by an electrostatic field, a charged body will experience an electrostatic force directly proportional to the applied voltage.

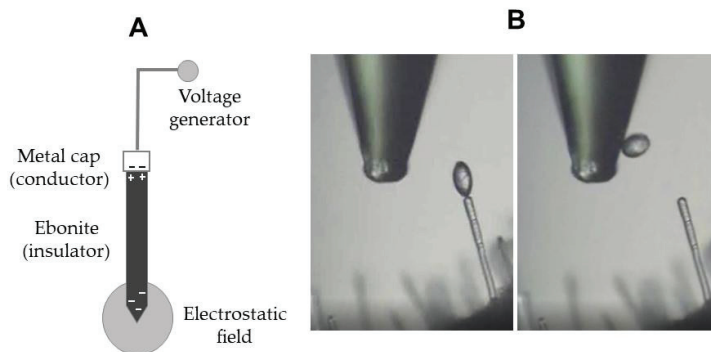


Figure 2. (A) Structure of an electrostatic spore collection probe; and (B) attraction of a mature spore (conidium) on a tomato powdery mildew conidiophore by an electrostatic spore collection probe.

Under a digital microscope, the electrostatic spore collection probe was brought close to a mature conidium on a conidiophore. Mature conidia were easily distinguished due to the clear constriction between a conidium and the conidiophore tip end. A conidium was attracted to the probe tip without direct contact (Video S1A), providing clear evidence of the involvement of electrostatic force in spore attraction. These results laid the groundwork for our further electrostatic engineering research and electric field screen development.

The electrostatic spore collection probe was used for microscopic analysis of conidogenesis by barley powdery mildew (*Blumeria graminis* f. sp. *hordei*) [25] and Cucurbitaceae powdery mildew (*Podosphaera xanthii*) [26]. The probe was modified to fabricate a time-controlled electrostatic spore attraction plate (Video S1B), to collect all conidia produced by these powdery mildew pathogens throughout their lifetime [27,28].

3. Dielectrophoretic Movement of Spores in an Electrostatic Field

3.1. Construction of an Electrostatic Field

The application of negative or positive voltage to an insulated conductor allows negative or positive charge to accumulate on the conductor surface, in turn producing an electric field in the surrounding space. This field induces surface charges in the insulating coating of the conductor. For example, when the insulator is an acrylic cylinder, opposite charges are created on the inner and outer surfaces of the cylinder through dielectric polarization (Figure S2) [17]. The outer surface charge of the monopolar cylinder produces an electrostatic field in the surrounding space (Figure S2), such that there is no current flow in the space, only charge.

With either negative or positive voltage application, a voltage applied at the same magnitude will produce the same field intensity, as the potential difference with respect to the ground remains the same. The same field intensity in turn creates the same magnitude of electrostatic force. Field intensity is strongest in the region closest to the charged/electrified body (in this case, the insulator). The electric field intensity gradient is used to capture objects that enter the field.

3.2. Airborne Spore Capture by an Electrified Insulated Conductor

Dielectrophoresis is a phenomenon by which a force is exerted on a dielectric (oppositely polarized) particle in an electric field [29]. This force does not require the particle to be charged, because all particles exhibit dielectrophoretic activity in the presence of the electric field. According to dielectrophoresis theory, the relative polarizability of the particles changes along the electric field strength gradient. Field strength, i.e., the force intensity at a given point in the electric field, becomes stronger as a point moves closer to the charged pole. Thus, particles in an electric field are attracted to a charged pole that produces an electric field.

In a negatively charged acrylic cylinder, airborne spores reaching the electrostatic field are positively polarized on the cylinder side and negatively polarized on the opposite side of the spore (Figure 3A). An attractive force is generated between the positive charge of the spore and the negative charge of the cylinder, and the spore is drawn to the cylinder according to its dielectrophoretic movement [18].

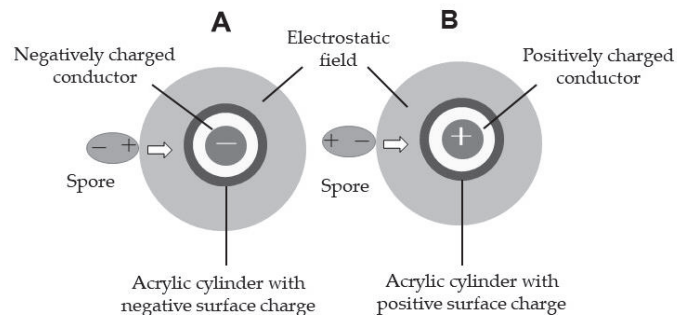


Figure 3. Schematic representation of attraction of spores entering the electrostatic field of an insulator: (A) negatively or (B) positively electrified by dielectrophoresis.

In a positively charged acrylic cylinder (Figure 3B), spore polarization is oriented in the opposite direction. The spore is polarized negatively on the cylinder side and positively

on the opposite side of the spore through dielectrophoresis [30]. If the applied voltage is the same in both insulated conductor wires (ICWs), an attractive force of the same strength (magnitude) is generated between the spore and cylinder. This spore attraction phenomenon prompted additional investigations into the use of electric field screens for capture applications.

In real-life spore capture applications, the targets are wind-dispersed spores. The movement of these spores in an electrostatic field is determined by the wind velocity vector and dielectrophoretic attractive force [18]. Naturally, an attractive force surpassing the force associated with the wind velocity is necessary to capture the spores.

3.3. Fabrication of a Single-Charged Monopolar Electric Field Screen

3.3.1. Air-Shielding Barrier Formed by Connected Electrostatic Fields

An insulator covering a charged conductor generates an electrostatic field in the surrounding space via electrification through dielectric polarization. A cylindrical insulator produces the electrostatic field concentrically (Figure 3). Thus, an air shield can be created by placing several electrostatically charged cylinders in close proximity to other cylinders in a screen-like configuration, allowing interaction between the associated electrostatic fields of individual cylinders (Figure 4A). Wind-dispersed spores that reach the field are uniformly attracted to the nearest cylinder (Figure 4B), and do not pass through the electrostatic barrier [18,30].

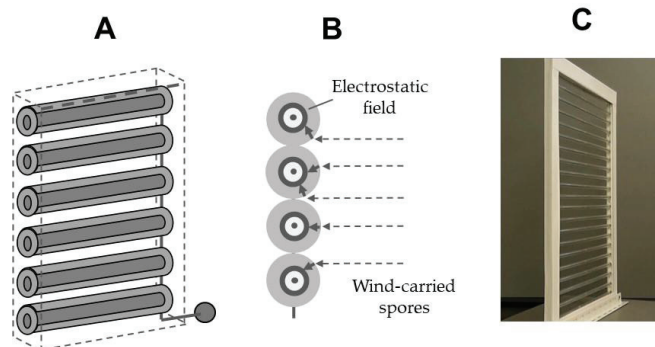


Figure 4. (A) Vertically arrayed insulated conductor wires (ICWs); (B) air-shielding barrier of connected electrostatic fields comprising vertically arrayed ICWs (cross-sectional view); and (C) single-charged monopolar electric field screen.

One apparatus that utilizes this phenomenon is the electric field screen (Figure 4C), which is an air shielding device constructed using electrostatic engineering techniques. The electrostatic field created by the parallel array of insulated conducting wires allows air to permeate freely through the barrier while capturing wind-dispersed spores by establishing a strong attractive force. The electric field screen is air-permeable, allowing use in conjunction with other ventilation equipment. For example, in a greenhouse containing windows furnished with electric field screens, wind-dispersed spores precipitate from the ventilated air to the screen, while air passes freely through the screen. As a result, spore-free air is supplied to plants cultivated in the greenhouse [19]; this allows the plants to avoid infection by airborne pathogens, for non-agrochemical control of pathogens during crop cultivation.

There is a positive relationship between applied voltage and radial expansion of an electrostatic field (Figure S3A). A higher voltage produces a wider electrostatic field. In an electric field screen, the interval between the ICWs necessary for capture applications increases at twice the rate of the applied voltage (Figure S3B). As the necessary separation interval between the ICWs of the screen increases with the application of higher voltages, the screen becomes more permeable to air. However, higher voltages increase the likelihood of discharge at the electric connection points. In practical applications, 5-kV charging

(separation interval, 10 mm) is often selected to minimize discharge events while promoting satisfactory air permeability.

3.3.2. Powdery Mildew Pathogen Control by a Single-Charged Monopolar Electric Field Screen

A single-charged monopolar electric field screen (SM screen) was designed to protect greenhouse tomatoes from infection by airborne conidia of the tomato powdery mildew pathogen. Insulated cylindrical conductor wires were installed on the roof and four lateral faces of a box-shaped frame to create an electric field screen box (Figure 5A). This box was used to cover a hydroponic trough used for growing tomato seedlings.

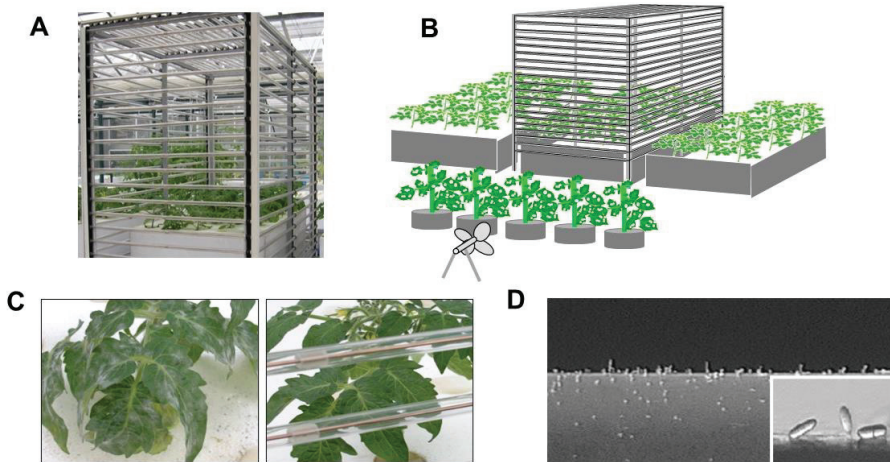


Figure 5. (A) Rectangular box furnished with single-charged monopolar electric field screens to cover a hydroponic trough for culturing plant seedlings; (B) schematic representation of a method for inoculating powdery mildew pathogen conidia into tomato seedlings in screen-guarded and unguarded hydroponic troughs; (C) heavily infected tomato seedlings in the unguarded hydroponic trough (left) and healthy non-infected tomato seedlings in the screen-guarded hydroponic trough (right) at 1 month after inoculation; and (D) digital micrographs of conidia captured by the insulated conductor wire of the electric field screen box used to cover the hydroponic trough.

Powdery mildew pathogen conidia are dispersed by wind to reach host plant leaves, where they germinate and initiate infection. After infection has been established, the pathogen produces pustules (colonies) on the leaf surface, in which numerous conidia are produced and dispersed by wind to neighboring host plants, thereby spreading the infection.

The occurrence of powdery mildew disease in greenhouse tomatoes indicates that an outside source is responsible for the infection. The origin of the conidia remains unclear; however, several studies have suggested that these pathogens can travel several kilometers [31–33]. Once the pathogen invades a greenhouse, the disease spreads quickly after the first infection is established. Therefore, preventing the initial entry of conidia into the greenhouse is vital.

In an inoculation assay, conidia were mechanically blown onto tomato plants under the assumption that the conidia are wind-dispersed. Three hydroponic troughs culturing tomato seedlings were used for the experiment; the center trough was covered with an electric field screen box (Figure 5B). Inoculated tomato plants producing abundant conidia were used as spore (inoculum) sources. Air was blown continuously, at a rate of 3 m/s, toward the hydroponic tomato seedlings by an electric fan for one month. As conidia were produced daily on the inoculum plants [22], the test plants were continuously infected by the pathogen; thus, particularly severe infection conditions were established as an exacting

test of the electric field screen system. This degree of infection is rarely encountered under natural conditions.

The spacing between the ICWs in the electric field screen box was 60 mm (30 kV charge; Figure 5C) to facilitate observation of the tomato seedlings. Photographs showed the external appearance of leaves of guarded and unguarded tomato seedlings after one month. Powdery mildew colonies expanded over the leaf surfaces of unguarded seedlings (Figure 5C, left), indicating severe infection. By contrast, tomato seedlings within the screen box remained uninfected throughout the experimental period (Figure 5C, right), confirming that healthy and successful growth could be attained under severe inoculation conditions.

At the end of the experiment, all ICWs were detached from the box to observe their surfaces using a high-fidelity digital microscope. Many conidia were detected on the conductor surfaces (Figure 5D). These results demonstrate that the electric field screen was able to capture all conidia blown at a rate of 3 m/s toward the screen box, thereby fully protecting tomato seedlings from the powdery mildew pathogen.

4. Spore Trapping by Two- and Three-Layer Double-Charged Dipolar Electric Field Screens

4.1. Negative and Positive Voltage Generators for Double Charging

The ICW is electrified by connecting a grounded negative or positive voltage generator. A negative voltage generator draws free electrons from the ground, which is an infinite source or sink of electrons, to the conductor wire (Figure S4A). Negative electricity accumulates on the surface of the wire conductor. In turn, negative charges are induced on the outer surface of the insulating wire coating, thereby negatively electrifying the insulator through dielectric polarization. A positive voltage generator pushes free electrons to the ground to positively charge the conductor wire (Figure S4B). The surface of the conducting wire becomes positively charged due to electrostatic induction [34]. A positive charge is induced on the outer surface of the insulating coating surrounding the conducting wire, and the coating becomes positively charged through dielectric polarization.

The amount of electricity required for electrification is proportional to the voltage applied by the voltage generator. The applied voltage corresponds to the potential difference with respect to the ground; a larger potential difference enhances electrostatic phenomena, as a larger attractive or repulsive force is generated. This allows the capture of spores.

Both voltage generators can be operated by a 12-V storage battery. A voltage generator is used to boost the initial voltage (12 V) to the designated voltage (up to 30 kV) using a transformer (coil) and Cockcroft circuit integrated into an electric circuit in the voltage generator [35]. The difference between the negative and positive voltage generators is that the Cockcroft circuit is set in reverse, such that negative electricity moves in the opposite direction (Figure S4). The greatest advantage of this voltage generator is that it can be operated using a 12-V direct current (DC) source. The electric power consumption (5 W) approaches that of a small lightbulb, such that the screen can operate for long periods of time using a regular storage battery. This is useful for practical implementation of the electric field screen.

4.2. Soft Polyvinyl Chloride Tube for Insulating Conductors

Acrylic resin has strong insulative properties, such that high voltages can be applied to a conductor insulated with this resin. However, acrylic resin is very difficult to process, which complicates the development of new types of electric field screens and limits real-world applications. To solve this problem, we employed polyvinyl chloride resin, which is commonly used to insulate metal materials. As we had no equipment in our laboratory capable of producing or coating materials with this resin, we used a commercially available soft vinyl chloride (Toalon) tube. The most serious drawback of this material is that it has extremely low volume resistivity, which limited our ability to charge it. Unexpectedly, this limitation motivated us to develop a new method for achieving the necessary capture capabilities at lower voltages.

The major factors that should be considered when designing an electric field screen are the quality of the insulation material, pole distance, range of applied voltage, and presence or absence of discharge, particularly arc discharge. All these factors are closely related. For example, for the same applied voltage, if the pole distance is shortened, discharge occurs more readily between the opposite poles. Therefore, we modified several screen parameters such as the applied voltage, while fixing other factors. The fixed parameters included the use of soft vinyl chloride tube to insulate the conductors and a 5-mm separation distance between the adjacent insulated conductors used to create the screen. The ICW was prepared by passing a copper or iron wire through the soft polyvinyl chloride tube and arranging these wires in parallel at a constant 5-mm interval as a skeletal structure for subsequent electric field screens.

4.3. Fabrication of the Double-Charged Dipolar Electric Field Screen

Conductor wires insulated with soft polyvinyl chloride tubes were arrayed in parallel at a specific interval (5 mm), linked to each other (and to a negative or positive voltage generator), and fixed with a polypropylene frame to construct the SM screen (Figure 6A). A double-charged dipolar electric field screen (DD screen) was constructed by pairing two SM screens linked to negative and positive voltage generators, respectively, to realize a two-layer DD screen (Figure 6B). A three-layer DD screen was constructed by placing the negatively charged SM screen beside a positively charged two-layer SM screen (Figure 6C). Two- and three-layer DD screens have oppositely charged ICWs in an offset configuration, where the electric field is created in the space between the oppositely charged ICWs (dipole) (Figure 6D,E). The insulating coating of the charged conductor prevents charges on the conductor surface from moving to the electric field (discharge of the charge conductor). The electric field formed between the oppositely charged poles can result in an electric discharge if the applied voltage exceeds a certain limit. Thus, this type of electric field is distinguished by the presence or absence of discharge, where the non-discharging electric field can be described as a static electric field [36]. Within the voltage range of the DD screen, a static electric field between the oppositely charged ICWs forms a zigzag pattern in two-layer screens (Figure 6D) and an x-shaped pattern in three-layer screens (Figure 6E).

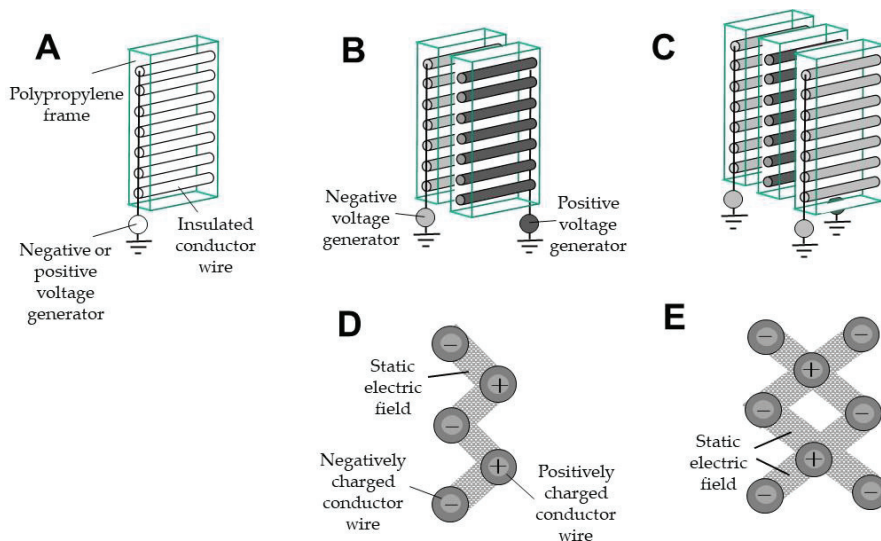


Figure 6. (A) Single-charged monopolar electric field screen; (B, C) double-charged dipolar electric field screens (DD screens) constructed with (B) two and (C) three layers; (D,E) static electric fields formed between oppositely charged conductor wires of (D) two-layer and (E) three-layer screens (cross-sectional view).

4.4. Spore-Capturing Ability of Two- and Three-Layer DD Screens

In this experiment, lemon fruit was inoculated with green mold (*P. digitatum*) and the abundant spores that formed were used for inoculation (Figure S5A,B) [37]. Spores from the inoculated fruit were dusted onto a parchment paper-covered tray by gently tapping the fruit. The spore density was fixed at 10^4 – 10^5 spores/cm²/tray by counting the spores in several randomly selected areas of the tray using a high-fidelity digital microscope. The collected spores were placed in a pressure bottle and blown by compressed air from the outlet nozzle toward the DD screen (Figure S5C). The spore capture rate was determined by counting the spores trapped by the ICWs of the DD screen and the electrostatic spore attraction plate [27] placed over the screen (Figure S5D). Two- and three-layer DD screens were used for the assay to determine their ability to capture wind-dispersed spores, as these screen types had shown good results in preliminary experiments.

To determine the total number of microscopic spores used in this experiment, the surfaces of the ICWs were scanned with a high-fidelity digital microscope to ensure that all trapped spores were counted. Because spores that escaped the trap by passing through the screen remained uncounted in preliminary experiments, an electrostatic spore attraction plate was installed as an additional trapping apparatus on the opposite side of the screen [27]. Despite this precaution, we were unable to guarantee that all escaped spores had been trapped for counting. Nevertheless, the number of spores trapped by the electrostatic spore attraction plate at lower applied voltages declined gradually as the voltage increased, indicating enhancement of the spore capturing rate. The spore capturing rate was determined by calculating the numbers of spores trapped by the ICWs of the DD screen and electrostatic spore attraction plate.

The three-layer screen prevented all spores from passing through the apparatus at a charge of -0.9 kV (Table 1). Two- and three-layer screens use the same mechanism to trap spores; therefore, the two-layer screen was expected to prevent passage of the spores. However, the two-layer screen failed to capture even a small number of spores, as they appeared to escape via a ‘jumping’ phenomenon.

Table 1. Numbers of *Penicillium digitatum* spores passing through electric field screens with double or triple layers of oppositely charged insulated conductor wires [37].

| Electric Field Screens | Experiments | Voltages (-kV) Oppositely Applied to ICWs | | | | |
|------------------------|-------------|---|-------------------------|------------------------|------------------------|------------------------|
| | | 0 | 0.3 | 0.6 | 0.9 | 1.2 |
| Double layers | 1 | 24,959.5 (100) | 10,892.1 (43.6) | 1790.0 (7.2) | 227.2 (0.9) | 221.6 (0.9) |
| | 2 | 17,705.4 (100) | 7444.9 (42.0) | 1574.1 (8.9) | 291.9 (1.6) | 250.8 (1.4) |
| | 3 | 25,908.6 (100) | 10,411.8 (40.2) | 2019.3 (7.8) | 330.8 (1.3) | 291.4 (1.1) |
| | 4 | 19,141.7 (100) | 8663.7 (45.3) | 1458.9 (7.6) | 188.5 (1.0) | 150.8 (0.8) |
| | 5 | 21,498.2 (100) | 8512.9 (39.6) | 1601.8 (7.5) | 201.4 (0.9) | 176.5 (0.8) |
| | Average % | 100 ^a | 42.1 ± 2.4 ^b | 7.8 ± 0.7 ^c | 1.2 ± 0.3 ^d | 1.0 ± 0.3 ^d |
| Triple layers | 1 | 28,411.3 (100) | 6967.0 (24.5) | 109.8 (0.4) | 0 (0) | 0 (0) |
| | 2 | 18,849.4 (100) | 4671.1 (24.8) | 96.5 (0.5) | 0 (0) | 0 (0) |
| | 3 | 24,449.9 (100) | 2654.5 (10.9) | 76.2 (0.3) | 0 (0) | 0 (0) |
| | 4 | 28,212.2 (100) | 5254.2 (18.6) | 108.1 (0.4) | 0 (0) | 0 (0) |
| | 5 | 13,548.6 (100) | 2662.8 (19.7) | 73.6 (0.5) | 0 (0) | 0 (0) |
| | Average % | 100 ^a | 19.7 ± 5.1 ^b | 0.4 ± 0.1 ^c | 0 ^d | 0 ^d |

Numbers in parentheses represent percentages of trapped spores relative to the uncharged control. Different letters in each horizontal row indicate significant differences ($p < 0.05$; Tukey’s test).

4.5. Spore Jumping Caused by Creeping Discharges

Within the electric field, minute particles such as spores are attracted to the nearest charged pole due to dielectrophoresis. However, when the spores reached the surface of the negatively charged pole, they were rarely electrified by negative discharge. When multiple spores were within the closed area, spores contiguous to other spores jumped away as a

result of the charge between them. Thus, when a second spore was attracted to a negatively charged insulator close to a precedent, positively electrified spore, the first spore jumped away, instead of the second spore. This phenomenon can be explained in terms of creeping discharge between proximate spores.

When a second spore is captured at a site adjacent to a previously captured spore, both spores attain opposite charges (Figure 7A); this promotes the transfer of electricity (free electrons) between them. This flow of electricity occurs on the surface of the insulator as creeping discharge [38]. Eventually, the second spore becomes positively charged, and the first spore attains a negative charge. The first spore is subjected to a repulsive force from the same-charged insulator, which induces the jumping effect. For the green mold spores (diameter, 5 μm) used in this experiment, spore jumping was observed when two spores coexisted within a circle with a 20- μm radius [37]. If the separation of the two spores exceeded this distance, no creeping discharge (i.e., no spore jumping) occurred.

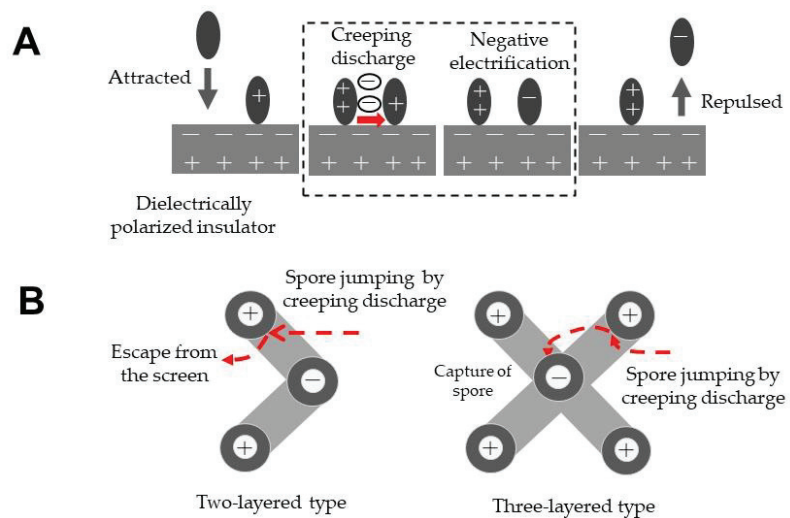


Figure 7. (A) Schematic representation of creeping discharge between two spores and spore jumping on the electrified insulator covering a charged conductor; and (B) schematic representation of the escape (left) and recapture (right) of a jumping spore in two- and three-layer electric field screens, respectively.

Spore jumping occurs more frequently as spore density increases, as creeping discharge between the spores is generated more easily. From an electrostatic perspective, creeping discharge occurs more frequently when an insulator with lower surface resistivity is used or when the applied voltage is higher. The three-layer screen was effective in capturing spores (Table 1); therefore, to determine whether there is a difference in spore-capturing functionality between two- and three-layer screens, Takikawa et al. [37] re-examined the settings of the experiment. Large numbers of spores were blown onto the electric field screen, which readily induced creeping discharge (and therefore spore jumping). Microscopic observation indicated that spore jumping occurred when subsequent spores entered the area at an inter-spore distance of 20 μm . As shown in Figure 7B, spores that jumped were more easily trapped by the additional electric field in the three-layer screen.

The density of spores in air is very low; thus, the likelihood of creeping discharge between captured spores is also very low. From this perspective, the jumping of captured spores seldom occurs under ordinary circumstances. Therefore, two-layer screens can be applied for spore capture in most situations, as they exhibit the same capture ability as three-layer screens and are more cost-effective.

5. Practical Control of Powdery Mildew Conidia by Electric Field Screens

A three-layer DD screen with an ungrounded circuit (Figure 8A) was used to construct an electrostatic shelter (Figure 8B) to raise healthy plant seedlings in a pathogen-free space [39]. In the ungrounded circuit, free electrons in the conductor wires were supplied directly to other conductor wires according to the voltage produced by generators (Figure S6). An electric field screen with such a circuit requires no ground line. Based on this reasoning, the electric field screen may be placed arbitrarily and effectively acts as a portable device. This equipment is designed to be used in a greenhouse without an installed electric field screen. Three-layer screens are appropriate for such usage because they prevent entry by both pests and pathogen spores [39]. Because their structure is very simple, their size may be freely altered according to the scale of seedling cultivation. To enhance air permeation, the screens were installed on opposite faces of the shelter, along with a small axis fan.

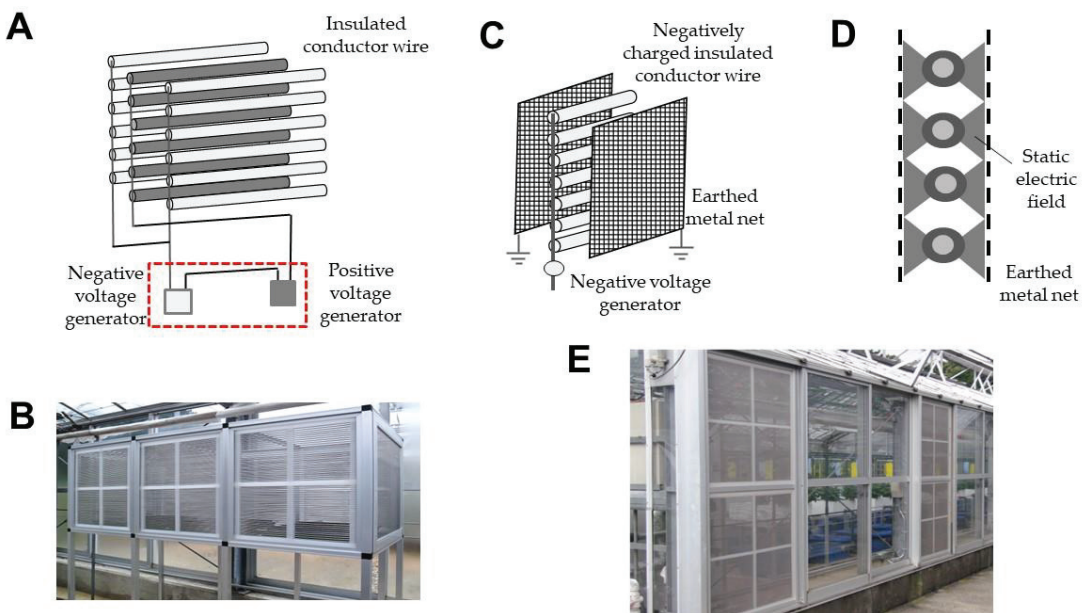


Figure 8. (A,B) Schematic representation of (A) a three-layer DD screen with a non-grounded circuit and (B) an electrostatic seedling shelter furnished with three-layer DD screens; (C,D) schematic representation of (C) a single-charged dipolar electric field screen, consisting of grounded metal nets on either side of a layer of negatively charged insulated conductor wires (ICWs); and (D) static electric fields formed between the negatively charged ICWs and grounded metal nets; and (E) installation of single-charged dipolar electric field screens in the lateral windows of a greenhouse.

Matsuda et al. [40] devised a single-charged dipolar electric field screen (SD screen) to trap insect pests. This screen was constructed by placing two grounded metal nets on either side of the SM screen (Figure 8C); static electric fields were created in the space between the negatively charged conductor wires and grounded net (Figure 8D). Insects blown into the electric field were captured by the negatively charged conductor wire [40]. Nonomura et al. [41] reported that the single-charged dipolar screen repelled insects that reached the grounded metal net of the screen, as they instinctively avoided entering the static electric field. More importantly, Kakutani et al. [42] found that the negatively charged ICW of the SD screen trapped airborne powdery mildew conidia; these screens were applied to greenhouse windows to create a conidium- and pest-free greenhouse environment (Figure 8E).

The ICW is the heart of the electric field screen. These wires are easily constructed in a laboratory by passing a metal wire through a soft polyvinyl chloride tube. However, in outdoor, longer-term experiments, the tubes are susceptible to severe deterioration such as cracking, deformation, and discoloration due to changes in temperature, humidity, and ultraviolet irradiation levels. These issues limit practical implementation of the electric field screen.

Coating of a metal wire with weatherproof polyvinyl chloride resin is advisable to prolong screen operation in outdoor environments with minimal deterioration. In the preliminary experiments, a soft polyvinyl chloride tube showed optimal volume resistivity (10^8 – 10^9 Ωcm) for electric field screen functionality. The volume resistivity of polyvinyl chloride (10^{15} Ωcm) can be adjusted to 10^{14} – 10^8 Ωcm through the addition of plasticizers or ultraviolet absorbers, thereby enhancing weather resistance [43]. Polyvinyl chloride materials mixed with various substances are sold commercially as soft polyvinyl chloride; these materials have distinct qualities with different volume resistivity values. A remaining problem in electric field screen research is the selection of coating materials that meet the requirements for practical implementation and weather resistance of ICWs.

6. Conclusions

Electrostatic spore trapping techniques are based on the dielectrical polarization of an insulative coating by a charged conductor, and the creation of an electric field in the space surrounding the insulated charged conductor. Spores are captured within the electric field created by the insulated charged conductor. Unique arrangements of cylindrical charged ICWs were used to generate various types of electric field screen, which act as air-shielding barriers comprising combined electric fields to precipitate wind-dispersed pathogen spores from the air. This review provides an experimental basis for the development of physical strategies for the control of plant fungal pathogens.

Supplementary Materials: The following supporting information can be downloaded at: <https://www.mdpi.com/article/10.3390/agronomy12102443/s1>, Figure S1: Formation of an electrostatic field by frictional electricity accumulated on the tip of a glass needle, Figure S2: Schematic representation of an electrostatic field produced by a (left) negatively or (right) positively electrified insulator covering the negatively or positively charged conductor, Figure S3: (A) Expansion of an electrostatic field produced by insulated conductor wires (ICWs) applied with different voltages. (B) Different intervals between ICWs charged with different voltages, Figure S4: Schematic representation of the structure and function of (A) negative and (B) positive voltage generators, Figure S5: (A) Superficial colony formed over a lemon inoculated with green mold and (B) electron micrograph of conidia on conidiophores. (C) Instrument set used for a spore blowing assay. Conidia were collected and placed in a pressure bottle, and then blown toward a double-charged dipolar electric field screen (DD) screen by compressed air. (D) Diagram of a test box furnished with a DD screen and an axial-flow fan on the opposite side, Figure S6: Schematic representations of (A) grounded and (B) ungrounded circuits integrated into a DD screen, Video S1: (A) Trapping of a mature conidium by an electrostatic spore collection probe observed under a high-fidelity digital microscope. (B) Trapping of barley powdery mildew conidia with an electrostatic spore attraction plate.

Author Contributions: Conceptualization, H.T. and T.N.; methodology, T.N.; software, T.N.; validation, H.T. and T.N.; formal analysis, H.T.; investigation, T.N.; resources, T.N.; data curation, H.T.; writing—original draft preparation, H.T.; writing—review and editing, T.N.; visualization, T.N.; supervision, H.T.; project administration, T.N. All authors have read and agreed to the published version of the manuscript.

Funding: This research received no external funding.

Data Availability Statement: Not applicable.

Conflicts of Interest: The authors declare no conflict of interest.

References

- Matsuda, Y.; Kashimoto, K.; Takikawa, Y.; Aikami, R.; Nonomura, T.; Toyoda, H. Occurrence of new powdery mildew on greenhouse tomato cultivars. *J. Gen. Plant Pathol.* **2001**, *67*, 294–298. [CrossRef]
- Kashimoto, K.; Matsuda, Y.; Matsutani, K.; Sameshima, T.; Kakutani, K.; Nonomura, T.; Okada, K.; Kusakari, S.; Nakata, K.; Takamatsu, S.; et al. Morphological and molecular characterization for a Japanese isolate of tomato powdery mildew *Oidium neolycopersici* and its host range. *J. Gen. Plant Pathol.* **2003**, *69*, 176–185.
- Kiss, L.; Cook, R.T.A.; Saenz, G.S.; Cunningham, J.H.; Takamatsu, S.; Pascoe, I.; Bardin, M.; Nicot, P.C.; Sato, Y.; Rossmann, A.Y. Identification of two powdery mildew fungi, *Oidium neolycopersici* sp. nov. and *O. lycopersici*, infecting tomato in different parts of the world. *Mycol. Res.* **2001**, *105*, 684–697. [CrossRef]
- Kashimoto, K.; Sameshima, T.; Matsuda, Y.; Nonomura, T.; Oichi, W.; Kakutani, K.; Nakata, K.; Kusakari, S.; Toyoda, H. Infectivity of a Japanese isolate of *Oidium neolycopersici* KTP-01 to a European tomato cultivar resistant to *O. lycopersici*. *J. Gen. Plant Pathol.* **2003**, *69*, 406–408. [CrossRef]
- Van den Bosch, F.; Gilligan, C.A. Models of fungicide resistance dynamics. *Annu. Rev. Phytopathol.* **2008**, *46*, 123–147. [CrossRef] [PubMed]
- Lucas, J.A.; Hawkins, N.J.; Fraaije, B.A. The evolution of fungicide resistance. *Adv. Appl. Microbiol.* **2015**, *90*, 29–92.
- Lindhout, P.; Pet, G.; van der Beek, H. Screening wild *Lycopersicon* species for resistance to powdery mildew (*Oidium lycopersicum*). *Euphytica* **1994**, *72*, 43–49. [CrossRef]
- Matsuda, Y.; Mori, Y.; Nishida, M.; Sakano, S.; Tarumoto, K.; Nonomura, T.; Nishimura, H.; Kusakari, S.; Toyoda, H. Screening of wild *Lycopersicon* species for resistance to Japanese isolate of tomato powdery mildew *Oidium neolycopersici*. *Breed. Sci.* **2005**, *55*, 355–360. [CrossRef]
- Mieslerová, B.; Lebeda, A.; Chetelat, R.T. Variation in response of wild *Lycopersicon* and *Solanum* spp. against tomato powdery mildew (*Oidium lycopersici*). *J. Phytopathol.* **2000**, *148*, 303–311. [CrossRef]
- Li, C.; Bonnema, G.; Che, D.; Dong, L.; Lindhout, P.; Visser, R.; Bai, Y. Biochemical and molecular mechanisms involved in monogenic resistance responses to tomato powdery mildew. *Mol. Plant Microbe Interact.* **2007**, *9*, 1161–1172. [CrossRef] [PubMed]
- Seifi, A.; Nonomura, T.; Matsuda, Y.; Toyoda, H.; Bai, Y. An avirulent tomato powdery mildew isolate induces localized acquired resistance to a virulent isolate in a spatiotemporal manner. *Mol. Plant Microbe Interact.* **2012**, *25*, 372–378. [CrossRef]
- Li, C.; Faino, L.; Dong, L.; Fan, J.; Giovanni, C.; Lebeda, A.; Scott, J.; Matsuda, Y.; Toyoda, H.; et al. Characterization of polygenic resistance to powdery mildew in tomato at cytological, biochemical and gene expression level. *Mol. Plant Pathol.* **2012**, *13*, 148–159. [CrossRef]
- Yamamoto, S.; Shiraishi, S.; Kawagoe, Y.; Mochizuki, M.; Suzuki, S. Impact of *Bacillus amyloliquefaciens* S13-3 on control of bacterial wilt and powdery mildew in tomato. *Pest Manag. Sci.* **2015**, *71*, 722–727. [CrossRef]
- Németh, M.N.; Mizuno, Y.; Kobayashi, H.; Seress, D.; Shishido, N.; Kimura, Y.; Takamatsu, S.; Suzuki, T.; Takikawa, Y.; Kakutani, K.; et al. *Ampelomyces* strains isolated from diverse powdery mildew hosts in Japan: Their phylogeny and mycoparasitic activity, including timing and quantifying mycoparasitism of *Pseudoidium neolycopersici* on tomato. *PLoS ONE* **2021**, *16*, e0251444.
- Kaiser, K.L. Air breakdown. In *Electrostatic Discharge*; Kaiser, K.L., Ed.; Taylor & Francis: New York, NY, USA, 2006; pp. 1–93.
- Nonomura, T.; Matsuda, Y.; Kakutani, K.; Takikawa, Y.; Toyoda, H. Physical control of powdery mildew (*Oidium neolycopersici*) on tomato leaves by exposure to corona discharge. *Can. J. Plant Pathol.* **2008**, *30*, 517–524. [CrossRef]
- Halliday, D.; Resnick, R.; Walker, J. Electric discharge and electric fields. In *Fundamentals of Physics*; Johnson, S., Ford, E., Eds.; John Wiley & Sons: New York, NY, USA, 2005; pp. 561–604.
- Matsuda, Y.; Ikeda, H.; Moriura, N.; Tanaka, N.; Shimizu, K.; Oichi, W.; Nonomura, T.; Kakutani, K.; Kusakari, S.; Higashi, K.; et al. A new spore precipitator with polarized dielectric insulators for physical control of tomato powdery mildew. *Phytopathology* **2006**, *96*, 967–974. [CrossRef]
- Toyoda, H.; Matsuda, Y. Basic concept for constructing an electric field screen. In *Electric Field Screen; Principles and applications*; Toyoda, H., Ed.; Nobunkyo Production: Tokyo, Japan, 2015; pp. 3–17.
- Whipps, J.M.; Budge, S.P.; Fenlon, J.S. Characteristics and host range of tomato powdery mildew. *Plant Pathol.* **1998**, *47*, 36–48. [CrossRef]
- Kanetis, L.; Forster, H.; Adaskaveg, J.E. Determination of natural resistance frequencies in *Penicillium digitatum* using a new air-sampling method and characterization of fluodioxonil- and pyrimethanil-resistant isolates. *Phytopathology* **2010**, *100*, 738–746. [CrossRef]
- Nonomura, T.; Matsuda, Y.; Xu, L.; Kakutani, K.; Takikawa, Y.; Toyoda, H. Collection of highly germinative pseudochain conidia of *Oidium neolycopersici* from conidiophores by electrostatic attraction. *Mycol. Res.* **2009**, *113*, 364–372. [CrossRef]
- Matsuda, Y.; Sameshima, T.; Moriura, N.; Inoue, K.; Nonomura, T.; Kakutani, K.; Nishimura, H.; Kusakari, S.; Takamatsu, S.; Toyoda, H. Identification of individual powdery mildew fungi infecting leaves and direct detection of gene expression by single conidium PCR. *Phytopathology* **2005**, *95*, 1137–1143. [CrossRef]
- Moore, A.D. Frictional electricity. In *Electrostatics, Exploring, Controlling, and Using Static Electricity*, 2nd ed.; Laplacian Press: San Diego, CA, USA, 1997; pp. 22–27.
- Moriura, N.; Matsuda, Y.; Oichi, W.; Nakashima, S.; Hirai, T.; Sameshima, T.; Nonomura, T.; Kakutani, K.; Kusakari, S.; Higashi, K.; et al. Consecutive monitoring of lifelong production of conidia by individual conidiophores of *Blumeria graminis* f. sp. *hordei* on barley leaves by digital microscopic techniques with electrostatic micro-manipulation. *Mycol. Res.* **2006**, *110*, 18–27.

26. Takikawa, Y.; Nonomura, T.; Miyamoto, S.; Okamoto, N.; Murakami, T.; Matsuda, Y.; Kakutani, K.; Kusakari, S.; Toyoda, H. Digital microscopic analysis of conidiogenesis of powdery mildew pathogens isolated from melon leaves. *Phytoparasitica* **2015**, *43*, 517–530. [CrossRef]
27. Moriura, N.; Matsuda, Y.; Oichi, W.; Nakashima, S.; Hirai, T.; Nonomura, T.; Kakutani, K.; Kusakari, S.; Higashi, K.; Toyoda, H. An apparatus for collecting total conidia of *Blumeria graminis* f. sp. *hordei* from leaf colonies using electrostatic attraction. *Plant Pathol.* **2006**, *55*, 367–374. [CrossRef]
28. Suzuki, T.; Nakamura, N.; Takagi, N.; Takikawa, Y.; Kakutani, K.; Matsuda, Y.; Matsui, K.; Nonomura, T. Quantitative analysis of the lifelong production of conidia released from single colonies of *Podosphaera xanthii* on melon leaves using electrostatic techniques. *Aust. Plant Pathol.* **2019**, *48*, 297–307. [CrossRef]
29. Cross, J.A. Dielectrophoresis. In *Electrostatics: Principles, Problems and Applications*; De Barr, A.E., Ed.; Adam Hilger: Bristol, UK, 1987; pp. 269–276.
30. Shimizu, K.; Matsuda, Y.; Nonomura, T.; Ikeda, H.; Tamura, N.; Kusakari, S.; Kimbara, J.; Toyoda, H. Dual protection of hydroponic tomatoes from rhizosphere pathogens *Ralstonia solanacearum* and *Fusarium oxysporum* f. sp. *radicis-lycopersici* and airborne conidia of *Oidium neolycopersici* with an ozone-generative electrostatic spore precipitator. *Plant Pathol.* **2007**, *56*, 987–997. [CrossRef]
31. Aylor, D.E. The role of intermittent wind in the dispersal of fungal pathogens. *Annu. Rev. Phytopathol.* **1990**, *28*, 73–92. [CrossRef]
32. Brown, J.K.M.; Hovmöller, M.S. Aerial dispersal of pathogens on the global and continental scales and its impact on plant disease. *Science* **2002**, *297*, 537–541. [CrossRef] [PubMed]
33. Nonomura, T.; Matsuda, Y.; Yamashita, S.; Akahoshi, H.; Takikawa, Y.; Kakutani, K.; Toyoda, H. Natural woody plant, *Mallotus japonicus*, as an ecological partner to transfer different pathotypic conidia of *Oidium neolycopersici* to greenhouse tomatoes. *Plant Protect. Sci.* **2013**, *49*, S33–S40. [CrossRef]
34. Griffith, W.T. Electrostatic phenomena. In *The Physics of Everyday Phenomena, a Conceptual Introduction to Physics*; Bruflo, D., Loehr, B.S., Eds.; McGraw-Hill: New York, NY, USA, 2004; pp. 232–252.
35. Wegner, H.E. Electrical charging generators. In *McGraw-Hill Encyclopedia of Science and Technology*, 9th ed.; Geller, E., Moore, K., Well, J., Blumet, D., Felsenfeld, S., Martin, T., Rappaport, A., Wagner, C., Lai, B., Taylor, R., Eds.; The Lakeside Press: New York, NY, USA, 2002; pp. 42–43.
36. Toyoda, H.; Kusakari, S.; Matsuda, Y.; Kakutani, K.; Xu, L.; Nonomura, T.; Takikawa, Y. Electric field screen structures. In *An Illustrated Manual of Electric Field Screens: Their Structures and Functions*; Toyoda, H., Ed.; RAEFSS Publishing Department: Nara, Japan, 2019; pp. 9–16.
37. Takikawa, Y.; Matsuda, Y.; Nonomura, T.; Kakutani, K.; Kimbara, J.; Osamura, K.; Kusakari, S.; Toyoda, H. Electrostatic guarding of bookshelves from mould-free preservation of valuable library books. *Aerobiologia* **2014**, *30*, 435–444. [CrossRef]
38. Kebbabi, L.; Beroual, A. Fractal analysis of creeping discharging patterns propagating at solid/liquid interfaces: Influence of the nature and geometry of solid insulators. *J. Physics. D Appl. Phys.* **2006**, *39*, 177–183. [CrossRef]
39. Takikawa, Y.; Matsuda, Y.; Nonomura, T.; Kakutani, K.; Kusakari, S.; Okada, K.; Toyoda, H. An electrostatic nursery shelter for raising pest and pathogen free tomato seedlings in an open-window greenhouse environment. *J. Agric. Sci.* **2016**, *8*, 13–25. [CrossRef]
40. Matsuda, Y.; Nonomura, T.; Kakutani, K.; Takikawa, Y.; Kimbara, J.; Kasaishi, Y.; Kusakari, S.; Toyoda, H. A newly devised electric field screen for avoidance and capture of cigarette beetles and vinegar flies. *Crop. Prot.* **2011**, *30*, 155–162. [CrossRef]
41. Nonomura, T.; Matsuda, Y.; Kakutani, K.; Kimbara, J.; Osamura, K.; Kusakari, S.; Toyoda, H. An electric field strongly deters whiteflies from entering window-open greenhouses in an electrostatic insect exclusion strategy. *Eur. J. Plant Pathol.* **2012**, *134*, 661–670. [CrossRef]
42. Kakutani, K.; Matsuda, Y.; Nonomura, T.; Kimbara, J.; Kusakari, S.; Toyoda, H. Practical application of an electric field screen to an exclusion of flying insect pests and airborne conidia from greenhouses with a good air penetration. *J. Agric. Sci.* **2012**, *4*, 51–60. [CrossRef]
43. Toyoda, H.; Kusakari, S.; Matsuda, Y.; Kakutani, K.; Xu, L.; Nonomura, T.; Takikawa, Y. Basic knowledge in electrostatics. In *An Illustrated Manual of Electric Field Screens: Their Structures and Functions*; Toyoda, H., Ed.; RAEFSS Publishing Department: Nara, Japan, 2019; pp. 1–7.

Review

Electrostatic Insect Repulsion, Capture, and Arc-Discharge Techniques for Physical Pest Management in Greenhouses

Shin-ichi Kusakari ¹, Yoshinori Matsuda ^{2,*} and Hideyoshi Toyoda ¹¹ Research Association of Electric Field Screen Supporters, Nara 631-8505, Japan² Laboratory of Phytoprotection Science and Technology, Faculty of Agriculture, Kindai University, Nara 631-8505, Japan

* Correspondence: ymatsuda@nara.kindai.ac.jp

Abstract: This article reviews the development of electrostatic apparatuses for controlling insect pests in greenhouses. The apparatuses control insects by repelling them, capturing them, and killing them by producing an arc discharge. The single-charged dipolar electric field screen (SD screen) repels insects due to insects' inherent avoidance behavior toward entering the electric field produced. As this behavior is common to many insect pests, the SD screen effectively prevents many pests from entering a greenhouse. The double-charged dipolar electric field screen (DD screen) has a strong attractive force that captures insects entering its electric field. The DD screen is useful for capturing small insects that pass through a conventional insect net, and unique derivatives of this screen have been invented to trap various insect pests on-site in a greenhouse. An arc-discharge exposer was used as a soil cover to kill adult houseflies that emerged from underground pupae transferred along with cattle manure used for soil fertilization. The houseflies were subjected to arc discharge when they appeared at the soil surface. These apparatuses have the common characteristic of a simple structure, so ordinary workers can be encouraged to fabricate or modify them based on their own needs. This review provides an experimental basis for designing efficient physical measures for controlling insect pests in greenhouses.

Keywords: aphid; attractive force; electrostatic field; electrostatic soil cover; housefly; shore fly; static electric field; thrips; tomato leaf miner; whitefly

Citation: Kusakari, S.-i.; Matsuda, Y.; Toyoda, H. Electrostatic Insect Repulsion, Capture, and Arc-Discharge Techniques for Physical Pest Management in Greenhouses. *Agronomy* **2023**, *13*, 23. <https://doi.org/10.3390/agronomy13010023>

Academic Editor: Angelo Canale

Received: 2 December 2022

Revised: 17 December 2022

Accepted: 19 December 2022

Published: 21 December 2022



Copyright: © 2022 by the authors. Licensee MDPI, Basel, Switzerland. This article is an open access article distributed under the terms and conditions of the Creative Commons Attribution (CC BY) license (<https://creativecommons.org/licenses/by/4.0/>).

1. Introduction

The primary strategy for physical pest control in greenhouses is the prevention of their entry [1]. Netting greenhouse windows has been a basic approach for this purpose [2,3]. However, mesh sizes of conventional woven insect-proof nets are ordinarily between 1 and 1.5 mm, so some small pests can pass through. In our tomato greenhouses, whiteflies, *Bemisia tabaci* (Gennadius) (Hemiptera: Aleyrodidae); tomato leaf miners (syn. vegetable leaf miner), *Liriomyza sativae* Blanchard (Diptera: Agromyzidae); western flower thrips, *Frankliniella occidentalis* (Pergande) (Thysanoptera: Thripidae); winged green peach aphids, *Myzus persicae* (Sulzer) (Hemiptera: Aphididae); and shore flies, *Scatella stagnalis* (Fallén) (Diptera: Ephydriidae) frequently enter by passing through such nets. The biggest problem has been that whiteflies, thrips, and aphids transmit viral pathogens: tomato yellow leaf curl virus [4,5], tomato spotted wilt tospovirus [6,7], and cucumber mosaic virus [8], respectively, and shore flies transfer rhizosphere fungal pathogens (*Verticillium dahliae* and *Fusarium oxysporum* f. sp. *radicis-lycopersici*) [9,10]. Tomato plants are vulnerable to direct attacks by these pests, as well as the serious infections caused by viral, bacterial, and fungal pathogens carried by them. Most seriously, a viral disease caused by the tomato yellow leaf curl virus has been a major cause of loss of tomato crops grown in greenhouses nationwide [11].

Insect-excluding woven nets with a fine mesh size have been extensively employed to minimize whitefly entry into greenhouses, but the netting has the disadvantage of reducing

ventilation, which causes overheating and an increase in relative humidity [2]. Electrostatic techniques have been used to solve this problem. Matsuda et al. [12] created an electrified insect net (electric field screen), consisting of a layer of multiple insulated conductor (iron or copper) wires arrayed in parallel at a definite interval and two identical insect nets woven with stainless strands of the same thickness as a conventional net and linked to a grounded line. The nets were placed on each side of the insulated conductor wire layer, and negative charging of the insulated conductor wires formed an electric field between the charged insulated conductor wire and the grounded metal net. In tests, insects that reached the grounded metal net of the electric field screen appeared to sense the electric field inside the screen and were deterred from entering [12,13]. This peculiar reaction, which was considered a result of inherent hesitant behavior, was ultimately detected in 13 orders, 45 families, and 62 genera of arthropods [14]. Based on the results of such studies, the insect-repelling function of the electric field screen was widely acknowledged [15] and it came to be known as the single-charged dipolar electric field screen (SD screen) and was put into practical use [16].

Initially, the concept of the screen was presented as an air-shielding barrier to precipitate wind-carried spores of powdery mildew pathogens [17,18]. The electrostatic principles implemented for this purpose were that the negative charge supplied to a conductor wire accumulates on its surface and polarizes the insulating coating of the conductor dielectrically, negatively on the outer surface and positively on the inner surface of the coating [19]; the surface charge on the insulating coating produces an electrostatic field in the air [20]. In the proposed devices, cylindrical insulated conductor wires negatively charged to produce an electrostatic field concentrically surrounding the wires were arrayed in parallel to combine the electrostatic fields [17]. Spores that reached the air-shielding barrier (combined electrostatic fields) were drawn to the charged insulated conductor wires by their dielectrophoretic movement in the electrostatic field [18,21]. This device was named the single-charged monopolar electric field screen (SM screen) and positioned as a prototype for subsequent types of electric field screens [22].

Another tactic is the use of colored sticky traps for phototactic insect pests that may enter a greenhouse. Due to the strong photosensitive behavior of these insects, colored sticky traps have been widely used to explore the population fluctuations of such flying insects. Yellow and blue sticky traps effectively attract many insect species. In particular, the yellow sticky trap has been used to monitor populations of western cherry fruit fly (*Rhagoletis indifferens*) [23], sweet pepper whitefly (*Trialeurodes vaporariorum*) [24], sweet potato whitefly (*B. tabaci*) [25], western flower thrips (*F. occidentalis*) [26], and chrysanthemum leaf miner (*Liriomyza trifolii*) [27]. Similarly, the blue sticky trap has been used to monitor populations of melon thrips (*Thrips palmi*) [28] and bean flower thrips (*Megalurothrips usitatus*) [29]. Therefore, because the yellow sticky trap has a strong insect-attracting ability, many growers who cultivate plants organically in large greenhouses have used the traps as an insecticide-independent method to reduce populations of phototactic insects. The traps are often hung from crossbeams and lateral pillars near greenhouse windows. However, the stickiness of the trap surface gradually deteriorates with the increasing number of trapped insects, so traps must be exchanged for fresh ones frequently during the peak pest season. Another weak point is the sticky surface of the trap, which limits trap placement in the vicinity of cultivated plants. Thus, greenhouse operators have requested a less expensive and reusable trap with a non-sticky surface that could attract and capture targeted insect pests. This demand has encouraged the development of a new type of electric field screen.

The double-charged dipolar electric field screen (DD screen) was constructed by pairing two oppositely charged SM screens [30]. The insulated conductor wires of the SM screen are negatively and positively charged by linking them to a grounded negative and positive voltage generator, respectively. The opposite charges on the insulated conductor wires of the paired SM screens form a dipolar electric field in the space between the oppositely charged conductor wires. Insects that enter this electric field are subjected to a strong force drawing them toward the nearest charged insulated conductor. This makes it

unnecessary to make the surface of the trap sticky. The insulated conductor wire is prepared by passing a metal wire through an acrylic cylinder or soft polyvinyl chloride tube for insulation, and it is washable for reuse. Importantly, a change in conductor material from metal wire to water enabled the construction of a yellow-colored DD screen [31,32]. Because water conducts electricity, a transparent polyvinyl chloride tube filled with charged water (with watercolors) could be electrified to form an electric field for capturing insects. The colored DD screen can be placed at any location within a greenhouse, and it attracts and captures insects distant from the apparatus. This screen has led to the development of other insect-trapping apparatuses [33–36].

A third application of electrostatic principles is the production of an arc discharge-generating device for electrocuting insects that enter the electric field [37–40]. This technique was originally devised to kill rice weevils *Sitophilus oryzae* (Linnaeus) (Coleoptera: Curculionidae) nesting in dried rice [37,40]. The arc-discharge exposer is simple, fabricated by pairing two identical metal nets in parallel at a definite interval; one net is linked to a negative voltage generator and the other is connected to a grounded line. Negative charge accumulates on the charged metal net and polarizes the grounded metal net positively by electrostatic induction [41]. Eventually, an electric field forms in the space between the oppositely electrified nets. Negative charge on the metal net surface is released as an arc discharge toward an insect that enters the electric field [37], and the insect is killed instantly. This apparatus has been most effective for killing *Musca domestica* (Linnaeus) (Diptera: Muscidae) houseflies emerging from underground pupae at the soil surface, which are possible vectors of pathogenic *Escherichia coli* O-157 and can be introduced with manure used as soil fertilizer [42].

For the remainder of this article, we describe the development of electric field screen research, focusing on the desirable functions that should be conferred to each type of screen. From the perspective of effective pest management, we categorize the major electrostatic techniques based on three functions (repelling, capturing, and electrocuting insect pests), as mentioned above. These works are unique challenges to developing new physical methods for pest control, and the newly devised apparatuses possess a simple structure, allowing ordinary greenhouse workers to fabricate or improve them for their own requirements and exert prominent control functions to target insect pests. While providing a detailed explanation of the electrostatic principles used for constructing electric field screens and the structural characteristics of the screens, we discuss the current state and future potential of electric field screen research.

2. Construction of the SM-Screen

A conductor (metal wire and net) can be charged by linking it to a negative or positive voltage generator. A voltage generator is an amplifier used to increase the initial voltage (12 V) to the desired voltage (1–30 kV) using a transformer and Cockcroft circuit integrated into the voltage generator [43]. A negative voltage generator using an enhanced voltage draws negative charge (free electrons) from the ground and supplies it to a conductor linked to the voltage generator. The negative charge accumulates on the surface of a conductor and produces an electric field in the surrounding space. In the case of an insulated conductor, negative charge on the conductor surface dielectrically polarizes an insulating coating, negatively on its outer surface and positively on its inner surface (dielectric polarization of an insulator) [19]. Eventually, the negative charge on the insulator coating surface generates an electric field in the surrounding space.

Electric fields can be classified into three types: electrostatic, static, and dynamic electric fields. An electrostatic field is the electric field produced by a single-charged conductor (monopole), where the discharge of the charged conductor does not occur (i.e., no electric current). The SM screen was constructed based on this electrostatic field. In the first example of the SM screen, a negatively charged conductor (iron wire) was passed through an acrylic cylinder (volume resistivity of $10^{12} \Omega\text{cm}$) for insulation [17]. The negative charge on the conductor wire polarized the acrylic cylinder dielectrically.

Eventually, an electrostatic field formed concentrically in the air surrounding the cylinder (Figure 1A). The screen was constructed by arraying negatively electrified cylinders in parallel at a definite interval to combine the electrostatic fields (Figure 1B).

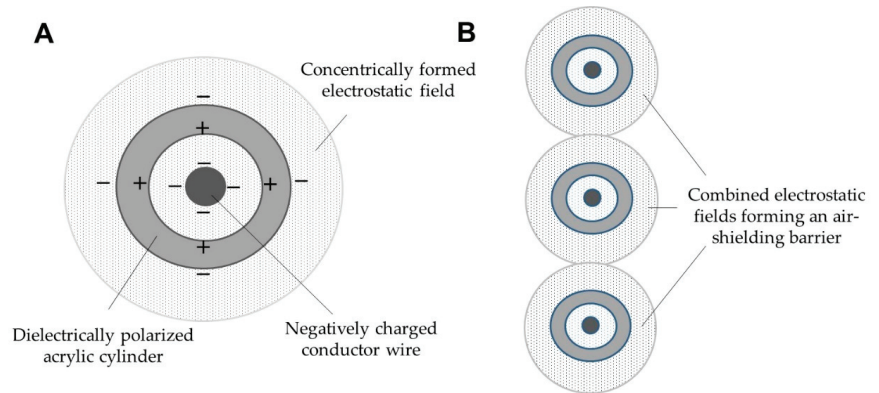


Figure 1. Schematic representation of the electrostatic field produced by a negatively electrified insulator (acrylic cylinder) covering a negatively charged conductor (iron wire) (A) and insulated conductor wires in a vertical array forming an air-shielding barrier of combined electrostatic fields (cross-sectional view) (B).

Acrylic resin is an outstanding insulator, so a high voltage can be applied to a conductor insulated with this resin. However, it is difficult to process. This problem was an obstacle, particularly in the development of new types of electric field screens. To solve this problem, developers turned to polyvinyl chloride resin, which had frequently been used to insulate metal materials. However, because of a lack of equipment to coat metal materials with this resin, commercially available soft polyvinyl chloride tubes had to be substituted. The most substantial disadvantage of using soft polyvinyl chloride tubes is their lower volume resistivity, which was a limiting factor in charging the material. However, this limitation served as a motivating force to develop a new method to create the necessary capabilities with lower voltage applications. The invention of the SD screen was the first such instance.

In subsequent experiments, an insulated conductor was fabricated by passing a metal wire (copper or iron) through a soft polyvinyl chloride tube (volume resistivity of $10^9 \Omega\text{cm}$). The insulated wires were arranged in a parallel configuration, with a constant separation interval of 5 mm, as a common skeletal structure for subsequent electric field screen designs.

3. Dual Functions of the SD Screen: Insect Capture and Repulsion

3.1. Construction of the SD-Screen

Theoretically, the dipolar electric field formed between oppositely charged poles causes an electric discharge if the applied voltage exceeds a certain limit, regardless of whether or not the conductor is insulated. The type of electric field is determined by the existence or nonexistence of discharge. Hereafter, the non-discharging and discharge-generating electric fields are referred to as static and dynamic electric fields, respectively. During electric field screen research, a new method by which a dipolar static electric field could be generated via single charging was devised. The electric field screen integrating this field exhibited revolutionary power for capturing insects.

As described earlier, a negatively charged insulated conductor wire causes dielectric polarization within the insulating coating, thus creating a negatively charged insulator surface. The charged surface of the insulator produces an electrostatic field in the surrounding space. The difference in the design of the SD screen is that a grounded metal net is placed inside the electrostatic field produced by the insulated conducting wire (Figure 2).

Eventually, the grounded metal net was positively electrified as a result of electrostatic induction [41]. The opposite charges of the insulated conductor wire (negatively charged) and the grounded metal net (positively charged) create a dipole, forming an electric field in the space between them. Thus, we can create a positive pole (grounded metal net) without using a positive voltage generator. This is our single-charged dipolar electrification system.

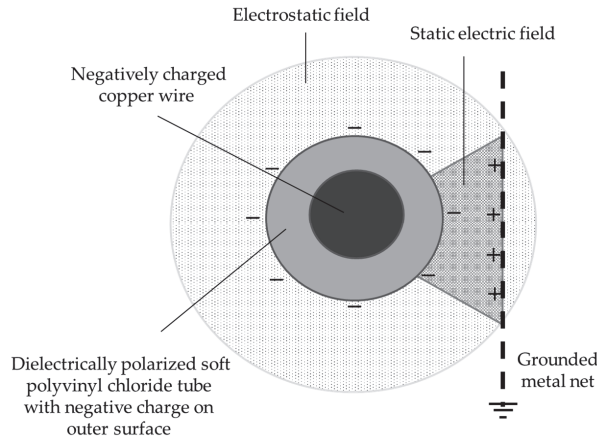


Figure 2. Formation of a static electric field inside the electrostatic field formed by a single-charged monopolar electric field screen (SM screen) (cross-sectional view).

As shown in Figure 2, a static electric field is formed inside the electrostatic field. The static electric field is formed in a bilaterally symmetrical manner by placing another grounded net on the opposite side of the insulated conductor wires (Figure 3A). Accordingly, a new electrostatic barrier of static electric fields is constructed by arranging the insulated conductor wires such that the upper and lower ends of the two static electric fields contact each other (Figure 3A) [12].

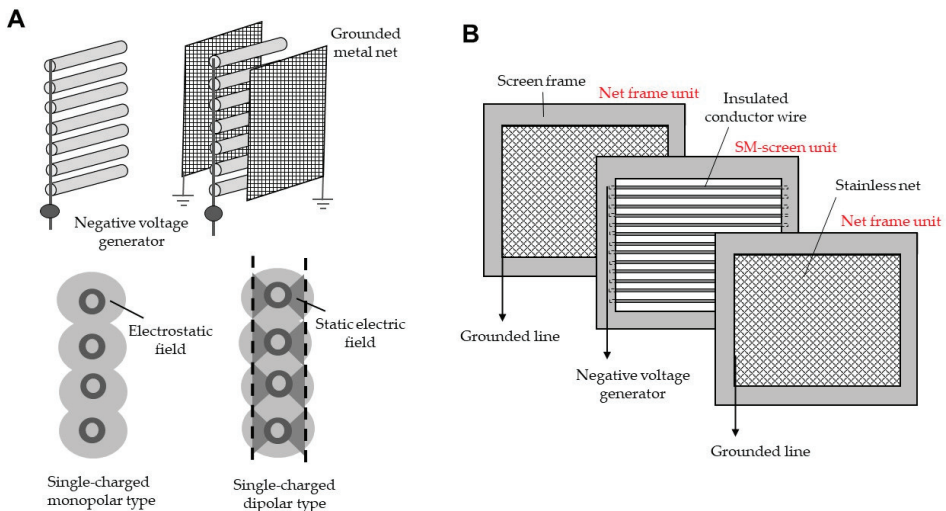


Figure 3. (A) Comparative representation of single-charged monopolar and dipolar electric field screens forming an electrostatic field and static electric field, respectively. (B) Schematic representation of a single-charged dipolar electric field screen (SD screen) consisting of three units. Two net frame units are placed on each side of the SM screen unit.

We produced the unit-type SD screen (Figure 3B), which consists of three units: the insulated conductor wires held with a polypropylene screen frame (SM screen unit), which is linked to a negative voltage generator, and two framed stainless net units (mesh size of 1.5 mm, which is equivalent to a conventional insect-proof net), which are linked to a grounded line. For completion, three frame units are combined simply by placing the two net units on either side of the SM screen unit (Figure 3B).

3.2. Comparison of Insect-Capturing Ability of Single-Charged Monopolar and Dipolar Types

The SD screen is formed by placing two grounded metal nets inside the electrostatic fields produced by the SM screen (Figure 3A). However, there is a remarkable difference in insect-capturing capability between the SM and SD screens. In the SM screen, the insect is attracted to the charged insulated conductor wire by dielectrophoresis. However, the force generated is not sufficiently strong for insect capture. Indeed, the captured insect struggles strenuously to free itself from the attractive force of the insulated conductor wire and ultimately escapes. By contrast, the SD screen exerts a strong attractive force so that the insect cannot escape, despite its struggle.

The static electric field is specialized by the negative charge on the surface of the insulated conductor wire. The negative charge has a strong repulsive force on other negative charges (electrons) in the electric field; eventually, the free electrons are pushed toward the ground via the metal net (Figure S1(A1)). According to this mechanism, any conductor in the static electric field is deprived of its free electrons and becomes positively charged. This phenomenon is called discharge-mediated positive electrification of a conductor [44,45]. In this section, we focus on an insect that enters the static electric field. Most insects possess a solid protective layer (cuticle layer) that covers the body. This layer is highly conductive [46–50]; thus, an insect that enters the static electric field is deprived of its free electrons in the cuticle layer and becomes positively electrified. This implies that discharge-mediated positive electrification can be induced in the insect [44,45]. The positively electrified insects are attracted to the insulated conductor wire (Figure S1(A2)), and this force is strong enough that the captured insect cannot escape the trap. This capturing mechanism is applicable to almost all insects that have a cuticle [44].

3.3. Insect Avoidance of the Static Electric Field: The SD Screen as an Insect-Repellent Type of Screen

Matsuda et al. [12] devised the SD screen and reported that vinegar fly *Drosophila melanogaster* Meigen (Diptera: Drosophilidae) and cigarette beetle *Lasioderma serricorne*; (Fabricius) (Coleoptera: Anobiidae) avoided entering the electric field of the screen. Video S1 shows the remarkable avoidance behavior of the cigarette beetle. In addition, we have frequently observed insects reaching the grounded metal net of the SD screen installed to a greenhouse window and flying away without entering the screen [13]. Video S2A shows that the insects were deterred from entering the static electric field. Video S2B shows that the insects were captured by the strong force of the electric field when they were forcibly pushed inside the electric field. This observation suggests that the screen actually repels the pests.

Matsuda et al. [14] further examined the insect avoidance behavior to the static electric field of the SD screen by placing transparent acrylic cylinders on and beneath the screen and putting test insects at the bottom of the lower cylinder. All of the insects tested, covering 17 orders, 42 families, 45 genera, and 82 species, exhibited avoidance behavior with respect to the static electric field [14]. These results strongly suggest that all insects are deterred by the static electric field of the SD screen.

To capture most of the insects that were forcibly pushed inside, 4.2 kV charging was required [51,52]. Thus, the SD screen is practical as an insect-repelling type of screen because the screen is fully functional with 1.2 kV of charging; in fact, it is capable of repelling all insects with this voltage [15].

4. DD Screens for Insect Capture

4.1. Construction of DD Screens and Their Insect-Capturing Ability

Based on the arrangement of insulated conductor wires, DD screens are classified into three types: the single-layered type, possessing oppositely charged insulated conductor wires arranged alternately (Figure 4A); two-layered type; and three-layered type, possessing oppositely charged insulated conductor wires arranged in an offset configuration (Figure 4B,C). The two- and three-layered types have a shorter distance between insulated conductor wires than the single-layered type (Figure 4) and therefore create a stronger force when the same voltage is applied due to the higher potential difference.

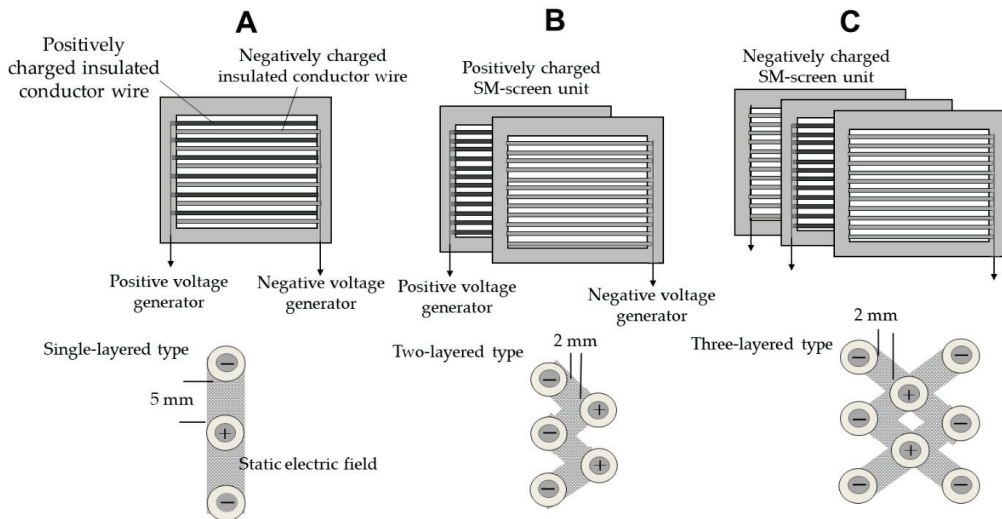


Figure 4. Three types of DD screens for capturing insect pests and the static electric fields formed by the DD screens. (A) A unit of the single-layered DD screen, where oppositely charged insulated conductor wires are arrayed alternately. (B,C) Two- and three-layered DD screens. Two or three oppositely charged SM screen units were combined in an offset arrangement with the oppositely charged insulated conductor wires.

Toyoda et al. [52] discussed the insect-capturing ability of DD screens, in which they determined the appropriate voltage setting for capturing all insect pests tested. The assay was conducted by blowing the insects toward the screen. Table S1 shows that the voltage should be enhanced in response to the wind velocity and size of the test insects. A 2.0 kV charging was sufficient to capture all of the test insects at the highest wind speed and by all screens [52]. Incidentally, the screen was charged with the same magnitude of negative and positive voltage. Therefore, the actual potential difference was twice the difference between the voltages listed in the table. Video S3 shows the successful capture of whiteflies by the single-layered DD screen. At insufficient voltage (-0.6 kV), some whiteflies escaped from the trap (Video S3A) but at 1.2 kV they were not able to escape (Video S3B).

Figure S1B shows the insect-capturing mechanism in the static electric field of the DD screen [53]. In this field, free electrons in the air are drawn to the positively charged insulated conductor wire (positive pole) (Figure S1(B1)). When an insect enters this field, there are two ways that it can be captured. The first is that the insect invades the space near the negatively charged insulated conductor wire (negative pole) (Figure S1(B2)). Here, the insect is deprived of free electrons, electrified, and thus attracted to the negative pole. This is the same phenomenon that occurs in the static electric field (discharge-mediated positive electrification) of the SD screen. The second is the case in which the insect enters

the space of the positive pole (Figure S1(B3)). In this case, the insect receives electrons and is electrified negatively for attraction to the pole (charge-mediated negative electrification).

4.2. Practical Application of DD Screens

4.2.1. Grounded and Ungrounded Circuits for Charging

In the usual electric circuit (grounded circuit) configuration for voltage charging of the DD screen, a negative voltage generator pumps negative charge from the ground and supplies it to the insulated conductor wires while a positive voltage generator pushes free electrons from the linked insulated conductor wires to the ground to generate positively charged insulated conductor wires (Figure S2A). From the viewpoint of electricity movement, the same amount of electricity can be returned to the ground from the conductors.

In the ungrounded circuit, the free electrons of the insulated conductor wires are supplied directly to the other insulated conductor wires by the voltage produced by the two generators (Figure S2B). Therefore, an electric field screen with this circuit has no need for a grounded line. For this reason, the placement of the electric field screen is freely selectable, allowing portability of the electric field screen.

4.2.2. Diversification of DD Screens

The bamboo blind-type electric field screen (Figure S3A) is a single-layered type of screen that was devised to reduce construction costs, particularly for practical applications involving a plastic hoop greenhouse [36]. This screen can be hung easily anywhere and can be positioned at the openings of lateral-side plastic film roll-ups. Although it is not possible to prevent the entry of pests completely, this approach is useful for greatly diminishing the interior pest population.

An electrostatic flying insect catcher (electrostatic racket) is a two-layered apparatus used to capture flying pests directly (Figure S3B) [30]. This apparatus is carried by the greenhouse attendant during ordinary plant care checks and is used to capture flying insects quickly (as they appear). It is possible to reduce the pest population significantly with the continued diligent use of this device. The apparatus can be used in various facilities, such as food-processing factories, warehouses, and facilities that provide meals, in which the use of insecticides is strictly regulated or prohibited.

An electrostatic cabinet (two-layered type) (Figure S3C) system was designed for use inside facilities, including greenhouses [35]. The entire structure has a simple design. The frame is furnished with two electric field screens, which are installed on opposite faces of the frame for better ventilation. The door of the cabinet and the remaining faces are covered with reinforced plastic film. The electrostatic cabinet can be set up affordably compared to more involved greenhouse screen installations. The cabinet can also be used as a cultivation facility for specific plants that should be protected from pests or as a pest-free laboratory and workroom.

An electrostatic nursery shelter (three-layered type) (Figure S3D) is an apparatus used to raise healthy plant seedlings [34]. The shelter is designed so that it can be installed in a greenhouse that is not furnished with electric field screens. The reason for using the three-layered type screen is to prevent the entry of pests as well as pathogen spores [54]. Because the structure is simple, its size can be easily modified to the scale needed for seedling cultivation. To obtain better ventilation, the screens can be installed on opposite faces of the shelter, along with a small axis fan.

4.2.3. Yellow-Coloring of DD Screen for Attracting Phototactic Insect Pests

Many insects are attracted to a particular type of light (or color). We utilized this characteristic in our capture method. The following experiments were conducted to examine whether this behavior could be applied to enhance the capture capability of the DD screen. Although the DD screen was able to capture insects entering the static electric field of the screen, it did not attract distant insects.

Nonomura et al. [33] used a single-layered DD screen backed with a yellow board, gray board, or gray net to examine the effects of better light reflection for bringing out insect photoselectivity (Figure S4A). As insects attracted by the color plate were captured by the insulated conductor wires of the screen, the feasibility of this method was evaluated by counting the number of insects trapped. As a control, DD screens with a gray-colored board and gray net were also used. These three screens were placed in a greenhouse where numerous whiteflies were present. The results showed, as expected, that whiteflies were preferentially trapped by the screen with the yellow-colored board [33].

Takikawa et al. [31,32] used a yellow-colored insulated conductor to fabricate a colored DD screen. For this purpose, the conductor metal wire in the insulator coating was changed to water. Because water conducts electricity, the transparent polyvinyl chloride tube filled with charged water was similarly electrified and produced an electric field in the space surrounding the tube. Two-layered, yellow-colored DD screens were constructed by pairing two identical yellow-colored SM screen units (Figure S4B). In this screen, the yellow-colored tubes of the two units were arranged in an off configuration (Figure S4C). The yellow-colored DD screen was highly effective at attracting and trapping whiteflies, thrips, and leaf miners distant from the apparatus in the greenhouse [31]. The wide selection of commercially available watercolors is useful for constructing devices with the coloration most suitable for attracting phototactic insect pests.

5. Soil-Surface Control of Insect Pests Emerging from Underground Pupae

In our greenhouses, houseflies and tomato leaf miner flies (Figure 5A,B) are problematic insect pests to control using various electrostatic methods because both flies emerge from underground pupae in the soil bed of a greenhouse. Houseflies introduced in cattle manure used for soil fertilization present a risk for transmitting pathogenic bacteria (*Escherichia coli* O-157) [55–57]. Contamination of cultivated and postharvest crops with this pathogen is a serious problem that can endanger the food supply chain [58,59]. On the other hand, adult leaf miners deposit eggs in leaves. The larvae hatched from the eggs form extensive mines within the leaves and then crawl out and fall to the ground. The larvae then enter the ground and pupate, and adult flies emerge from the underground pupae and oviposit eggs on host plants [60]. Thus, tomato leaf miner flies can cause a persistent infestation of greenhouse tomato plants throughout their life cycle [61]. Because of the great body size differences between these two flies (Figure 5), it was impossible to control them simultaneously using a single method. The following sections describe two effective control-measure methods for each fly.

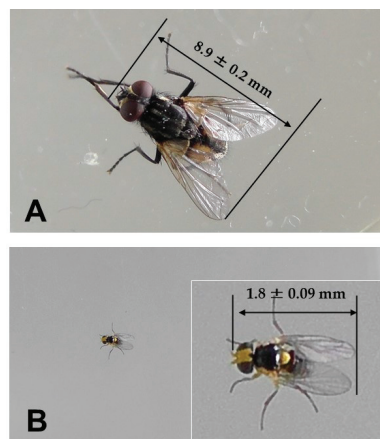


Figure 5. Comparative demonstration with test flies of different body sizes: housefly (A) and tomato leaf miner (B). The inserted photograph in (B) is an enlarged image of the fly.

Figure 6A shows the structure of an arcing-type soil cover method, an arc discharge exposer designed to kill insect pests that emerge from a soil bed instantaneously [42]. The apparatus consisted of two identical expanded metal nets, a square polypropylene frame (height of 6 mm), and a plastic grating (height of 54 mm). One metal net was linked to a negative voltage generator, and the other was connected to a grounded line. The frame was placed between the two nets to create a separation interval of 6 mm. The grating was placed beneath the grounded metal net and on the soil bed. The arc-discharge exposure method was originally devised to eradicate warehouse pests, such as the rice weevil, nesting in dried post-harvest products [37,40]. In addition, Kakutani et al. [38] applied it to a pigsty window to kill mosquitoes that transmit Japanese encephalitis viruses between pigs and humans. In this study, the system was used to kill adult houseflies that emerged from underground pupae.

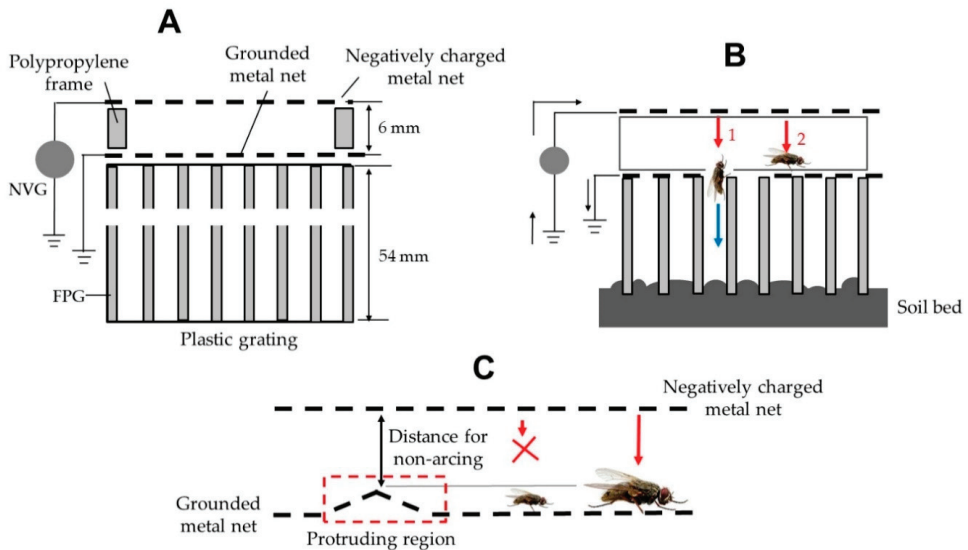


Figure 6. (A) Schematic representation of an arc-type soil cover system developed to kill insect pests that emerge from a soil bed. (B) Two-step arcing from the charged metal net to a fly that climbed along the wall of the grating and reached the electric field (red arrow 1) and a fly that clambered over the grounded metal net (red arrow 2) (cross-sectional view). The black arrow represents the direction of current flow, and the red arrow shows the electricity movement caused by arc discharge. The blue arrow represents the fall of an insect to the bottom of the grating after arc discharge exposure. (C) Successful and unsuccessful arcing to target flies based on their body size difference.

The essential goals were to examine the relationship between the pole distance (the separation distance between the negatively charged and grounded metal nets) and the occurrence of arcing and establish the optimal operating condition, where arcing occurs only when the insect enters the electric field between the two nets and is directed toward the insect. As mentioned earlier, insects are conductive and so become an intermediate pole between the two nets. In this situation, two-step arcing occurs. A first arcing occurs between the charged metal net and the insect, and a second occurs between the insect and the grounded metal net. In the present soil cover system, the insect was subjected to arc discharge from the charged metal net when the adult housefly extended a portion of its body over the grounded net (Figure 6B, red arrow 1) (Video S4). The arcing occurs specifically at any location of the target in the electric field. The insect is then pushed to the bottom by the strong impact caused by arc discharge [42]. In addition, the device produces a second arc discharge toward any housefly that evades the first arc and clammers over the

grounded metal net (Figure 6B, red arrow 2). This two-step arc system was highly effective at controlling houseflies emerging from underground pupae at the soil bed surface.

Nevertheless, it is unsuitable for smaller flies, such as tomato leaf miner flies (Figure 5B). The problem is the low uniformity of the metal nets used for the construction of the apparatus. The separation interval of the two nets is formed by the 6 mm high square frame placed between the two nets. However, any protruding region on the net surface can be a site ejecting or receiving discharge because arcing occurs at the short distance between the nets; moreover, other non-protruding (lower) regions on the net become safety zones for small insects (Figure 6C). In the case of adult tomato leaf miner flies, a small protrusion with a height of less than 1 mm can invalidate the arc discharge exposure treatment. On the other hand, adult houseflies are large enough that a small protrusion from the net surface can be ignored (Figure 6C).

Figure 7A shows the structure of a capturing-type soil cover system [61]. Adult tomato leaf miner flies were effectively trapped by the system when they emerged from pupae and flew upward (Figure 7B) (Video S5). This device consists of two sets of iron rods welded to an iron frame. The iron rods and frame of one set were coated with a soft polyvinyl chloride resin ($10^9 \Omega\text{cm}$) and linked to a negative voltage generator. The iron rods of the other set were not insulated and linked to a grounded line. The iron rods of both sets were arranged in an offset configuration to produce static electric fields between the oppositely charged iron rods (a modified SD screen) (Figure 7B). Adult houseflies emerged from pupae, climbed to the soil surface, and then flew into the static electric field of the soil cover (Figure 7B). The charged insulated conductor wire had a strong force and captured the flies.

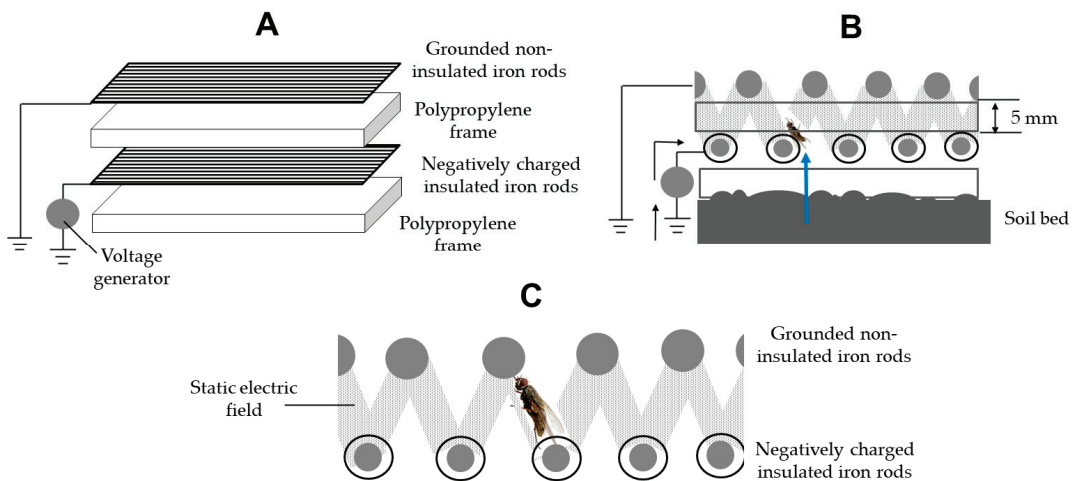


Figure 7. (A) Schematic representation of a capturing-type soil cover system developed to trap adult tomato leaf miner flies emerging from underground pupae. (B) Capture of a fly entering the static electric field of the negatively charged insulated conductor wire (cross-sectional view). The blue line represents the path of adult houseflies emerging from underground pupae. (C) Bridge formation by a fly caught between the opposite poles (negatively charged insulated and grounded non-insulated conductor wires). Larger flies reach both poles and form a direct route for electric current flow between the opposite poles.

This capture-type system, negatively charged at 4 kV, generated a force strong enough to capture the leaf miner flies that flew up toward the charged insulated conductor wire. However, this voltage was insufficient to capture larger insects such as adult houseflies. In fact, -7.5 kV charging is necessary for the successful capture of this fly due to its larger body size [62]. However, if that charge is applied, the charged conductor causes a continuous corona discharge (silent discharge) or spark (arc) discharge between the

poles [63]. Furthermore, a bridge between the opposite poles may be established by an insect's body because the adult housefly is large enough to touch both poles (Figure 7C). In this case, electric current flow occurs easily and eventually causes the insulating coating to break down. Thus, this system was used only for small flies.

6. Current Condition and Future Perspectives of Electrostatic Pest Management Research

This review article provides a summary of the electrostatic approach for greenhouse pest management. The approach consists of techniques for constructing unique apparatuses for generating electric fields. The basic components are conductor materials, insulating coatings for conductors, and negative and/or positive voltage generator(s). A common characteristic of the systems is a simple structure that enables ordinary greenhouse workers to fabricate and implement their own versions cheaply using common materials. In this article, we describe various examples of electric field-generating apparatuses to provide useful guidelines for this purpose. Conversely, the arc discharge-generating devices are even simpler, eliminating the need for any guidance toward designing them.

A voltage generator is an electrical appliance involved in all of the pest management instruments. The difference between a negative and a positive voltage generator is that the Cockcroft circuit is set oppositely. Two configurations are commercially available for both generators: a fixed voltage and an adjustable voltage. In our approaches, the adjustable voltage model was used to examine the relationship between applied voltage and the occurrence of electrostatic phenomena. However, after an optimal voltage is determined, the fixed voltage model is more suitable for practical use because of its lower cost.

In our electrostatic research, two problems remain unresolved. One is theoretical, and the other is practical. The first problem is the volume resistivity of the insulating coatings. This problem is critical, particularly when producing the static electric field of the SD and DD screens. The data obtained indicate that the resistivity range of 10^8 – 10^9 Ωcm is ideal for producing a static electric field that can exhibit the desired functions of repelling or capturing insects entering the field. The resistivity of the insulating coating limits the range of the applicable voltage. We used the voltage range causing no arc discharge between opposite dipoles. Nevertheless, in this voltage range, we detected the occurrence of silent discharge (continuous corona discharge) between the poles, which is accompanied by a very small amount of electric current (approximately equal to or less than 0.01 μA , beyond the detection limit of our current detector). This trace current has no effect on the repelling or capturing function of the electric field screens. In our preliminary analysis, these functions were not detected in either the case of an acrylic resin with higher resistivity (10^{12} Ωcm), which produces a stronger electric field intensity by the higher voltage applied without causing any silent discharge, or a soft polyvinyl chloride tube possessing lower resistivity (10^4 Ωcm), which produces a larger electric current by silent discharge with weaker field intensity. In future work, it is essential to clarify the complicated relationships among volume resistivity, applied voltage, and field intensity in terms of the insect repelling and capturing functions.

The second remaining problem is the improvement of the weatherability of the insulating coating. The insulation of the conducting material is a vital point in electric field screen construction. Conductor wire is typically insulated by passing it through a soft polyvinyl chloride tube. This is easy to prepare, and there is no problem with functionality. However, the insulated conductor wire is susceptible to serious deterioration, such as deformation, discoloration, hardening, and cracking, due to changes in ultraviolet (UV) irradiation, temperature, and humidity in the outdoor environment. Fundamentally, adding a conductive substance to an insulator reduces the insulator's resistivity. For example, adding a plasticizer or UV absorbent material (to improve weatherability) lowers the volume resistivity (10^{15} Ωcm) of polyvinyl chloride resin to the level of 10^{14} to 10^8 Ωcm . In fact, polyvinyl chloride materials mixed with various substances are commercially available as various soft polyvinyl chloride tubes, and these materials have distinct qualities with different volume resistivities and weather resistance levels. From a practical point of view,

an exploration of suitable insulating materials is a vital step in the quality testing of the electric field screen.

7. Conclusions

Various instruments for pest management were introduced based on related electrostatic principles. The wide variety of devices and their structural simplicity enable ordinary greenhouse workers to fabricate a particular tool that is most suited to their demands cheaply and using common materials. Three alternative pest-control functions, repulsion, capture, and arc exposure, were discussed to assess the feasibility of each choice. The repelling function of the SD screen is applicable to a variety of insect pests, irrespective of pest size. The DD screen is applied most effectively to capture small insect pests that pass through a conventional insect-proof net. At present, the use of the arc discharge method is restricted to larger flies that emerge from underground pupae. Thus, this review article provides an experimental basis for developing efficient physical methods to control insect pests in greenhouses.

Supplementary Materials: The following supporting information can be downloaded at: <https://www.mdpi.com/article/10.3390/agronomy13010023/s1>. Figure S1: (A) Schematic representation of insect capture by discharge-mediated positive electrification of the insect in the static electric field of a single-charged dipolar electric field screen (SD screen). (B) Schematic representation of the insect capture mechanism in the static electric field of the double-charged dipolar electric field screen (DD screen); Figure S2: Schematic representations of (A) grounded and (B) ungrounded circuits integrated into a DD screen; Figure S3: Photograph and schematic representation of a bamboo blind-type electric field screen (A), an electrostatic flying insect catcher (B), an electrostatic cabinet (C), and an electrostatic nursery shelter (D); Figure S4: (A) Three types of single-layered DD screen examined during a greenhouse assay. (B) Schematic representation of a DD screen consisting of two identical SM screen units with an insulating coating (transparent soft polyvinyl chloride tube) filled with yellow-colored water. (C) Transparent tubes with yellow-colored water arranged in an offset configuration; Table S1: Capture of insect pests blown toward insulated conductor wires of different types of double-charged dipolar electric field screens (DD screens); Video S1: Demonstration of avoidance of the static electric field of the SD screen by cigarette beetles; Video S2: (A) Avoidance of static electric field of the SD screen (negatively charged with 1.5 kV) by adult whiteflies under the no-blow condition. (B) Capture of whiteflies that were forcibly pushed into the electric field under the blowing condition of 5 m/s; Video S3: Capture of whiteflies by insulated conductor wire of the single-layered DD screen negatively charged with 0.6 kV (A) and 1.2 kV (B); Video S4: Arc-discharge exposure of an adult housefly by the negatively charged metal net of the arc-type soil cover system; Video S5: Emergence of an adult tomato leaf miner from a pupa and capture of the fly with an insulated iron rod of the horizontally placed electrostatic cover (−4 kV charge).

Author Contributions: Conceptualization, H.T., S.-i.K. and Y.M.; methodology, Y.M.; software, Y.M.; validation, S.-i.K., H.T. and Y.M.; formal analysis, S.-i.K. and H.T.; investigation, Y.M.; resources, Y.M.; data curation, S.-i.K. and H.T.; writing—original draft preparation, H.T.; writing—review and editing, S.-i.K. and Y.M.; visualization, Y.M.; supervision, H.T.; project administration, Y.M. All authors have read and agreed to the published version of the manuscript.

Funding: This research received no external funding.

Data Availability Statement: Not applicable.

Conflicts of Interest: The authors declare no conflict of interest.

References

- Weintraub, P.G.; Berlinger, M.J. Physical Control in Greenhouses and Field Crops. In *Insect Pest Management*; Horowitz, A.R., Ishaaya, I., Eds.; Springer: Amsterdam, The Netherlands, 2004; pp. 301–318. [CrossRef]
- Teitel, M.; Barak, M.; Berlinger, M.J.; Lebiush-Mordechai, S. Insect-proof screens in greenhouses: Their effect on roof ventilation and insect penetration. *Acta Hort.* **1999**, *507*, 25–34. [CrossRef]
- Taylor, R.; Shalhevet, S.; Spharim, I.; Berlinger, M.J.; Lebiush-Mordechi, S. Economic evaluation of insect-proof screens for preventing tomato yellow leaf curl virus of tomatoes in Israel. *Crops Prot.* **2001**, *20*, 561–569. [CrossRef]

4. Fukuta, S.; Kato, S.; Yoshida, K.; Mizukami, Y.; Ishida, A.; Ueda, J.; Kanbe, M.; Ishimoto, Y. Detection of tomato yellow leaf curl virus by loop-mediated isothermal amplification reaction. *J. Virol. Methods* **2003**, *112*, 35–40. [CrossRef]
5. Riley, D.G.; Srinivasan, R. Integrated Management of Tomato Yellow Leaf Curl Virus and its Whitefly Vector in Tomato. *J. Econ. Entomol.* **2019**, *112*, 1526–1540. [CrossRef] [PubMed]
6. Houle, J.L.; Kennedy, G.G. Tomato spotted wilt virus Can Infect Resistant Tomato when Western Flower Thrips Inoculate Blossoms. *Plant Dis.* **2017**, *101*, 1666–1670. [CrossRef] [PubMed]
7. He, Z.; Guo, J.-F.; Reitz, S.R.; Lei, Z.-R.; Wu, S.-Y. A global invasion by the thrip, *Frankliniella occidentalis*: Current virus vector status and its management. *Insect Sci.* **2020**, *27*, 626–645. [CrossRef]
8. Rendina, N.; Nuzzaci, M.; Scopa, A.; Cuypers, A.; Sofo, A. Chitosan-elicited defense responses in Cucumber mosaic virus (CMV)-infected tomato plants. *J. Plant Physiol.* **2019**, *234–235*, 9–17. [CrossRef]
9. Gillespie, D.R.; Menzies, J.G. Fungus gnats vector *Fusarium oxysporum* f.sp. *radicislycopersici*. *Ann. Appl. Biol.* **1993**, *123*, 539–544. [CrossRef]
10. El-Hamalawi, Z. Attraction, acquisition, retention and spatiotemporal distribution of soilborne plant pathogenic fungi by shore flies. *Ann. Appl. Biol.* **2008**, *152*, 169–177. [CrossRef]
11. Ueda, S.; Brown, J.K. First report of the Q biotype of *Bemisia tabaci* in Japan by mitochondrial cytochrome oxidase I sequence analysis. *Phytoparasitica* **2006**, *34*, 405–411. [CrossRef]
12. Matsuda, Y.; Nonomura, T.; Kakutani, K.; Takikawa, Y.; Kimbara, J.; Kasaishi, Y.; Osamura, K.; Kusakari, S.-I.; Toyoda, H. A newly devised electric field screen for avoidance and capture of cigarette beetles and vinegar flies. *Crop Prot.* **2011**, *30*, 155–162. [CrossRef]
13. Nonomura, T.; Matsuda, Y.; Kakutani, K.; Kimbara, J.; Osamura, K.; Kusakari, S.-I.; Toyoda, H. An electric field strongly deters whiteflies from entering window-open greenhouses in an electrostatic insect exclusion strategy. *Eur. J. Plant Pathol.* **2012**, *134*, 661–670. [CrossRef]
14. Matsuda, Y.; Nonomura, T.; Kakutani, K.; Kimbara, J.; Osamura, K.; Kusakari, S.; Toyoda, H. Avoidance of an electric field by insects: Fundamental biological phenomenon for an electrostatic pest-exclusion strategy. *J. Phys. Conf. Ser.* **2015**, *646*, 012003. [CrossRef]
15. Toyoda, H.; Kusakari, S.; Matsuda, Y.; Kakutani, K.; Xu, L.; Nonomura, T.; Takikawa, Y. Pest repelling function of an electric field screen. In *An Illustrated Manual of Electric Field Screens: Their Structures and Functions*; Toyoda, H., Ed.; RAEFSS Publishing Department: Nara, Japan, 2019; pp. 51–57.
16. Toyoda, H.; Kusakari, S.; Matsuda, Y.; Kakutani, K.; Xu, L.; Nonomura, T.; Takikawa, Y. Practical implementation of single-charged dipolar electric field screen. In *An Illustrated Manual of Electric Field Screens: Their Structures and Functions*; Toyoda, H., Ed.; RAEFSS Publishing Department: Nara, Japan, 2019; pp. 41–49.
17. Matsuda, Y.; Ikeda, H.; Moriura, N.; Tanaka, N.; Shimizu, K.; Oichi, W.; Nonomura, T.; Kakutani, K.; Kusakari, S.-I.; Higashi, K.; et al. A New Spore Precipitator with Polarized Dielectric Insulators for Physical Control of Tomato Powdery Mildew. *Phytopathology* **2006**, *96*, 967–974. [CrossRef]
18. Shimizu, K.; Matsuda, Y.; Nonomura, T.; Ikeda, H.; Tamura, N.; Kusakari, S.; Kimbara, J.; Toyoda, H. Dual protection of hydroponic tomatoes from rhizosphere pathogens *Ralstonia solanacearum* and *Fusarium oxysporum* f.sp. *radicis-lycopersici* and airborne conidia of *Oidium neolycopersici* with an ozone-generative electrostatic spore precipitator. *Plant Pathol.* **2007**, *56*, 987–997. [CrossRef]
19. Halliday, D.; Resnick, R.; Walker, J. Electric discharge and electric fields. In *Fundamentals of Physics*; Johnson, S., Ford, E., Eds.; John Wiley & Sons: New York, NY, USA, 2005; pp. 561–604.
20. Jones, E.; Childers, R. Electric charge and electric field. In *Physics*, 3rd ed.; McGraw-Hill: Boston, MD, USA, 2002; pp. 495–525.
21. Cross, J.A. Dielectrophoresis. In *Electrostatics: Principles, Problems and Applications*; De Barr, A.E., Ed.; Adam Hilger: Bristol, RI, USA, 1987; pp. 269–276.
22. Toyoda, H.; Matsuda, Y. Basic concept for constructing an electric field screen. In *Electric Field Screen*; Toyoda, H., Ed.; Principles and Applications; Nobunkyo Production: Tokyo, Japan, 2015; pp. 3–17.
23. Yee, W.L. Three-Dimensional Versus Rectangular Sticky Yellow Traps for Western Cherry Fruit Fly (Diptera: Tephritidae). *J. Econ. Entomol.* **2019**, *112*, 1780–1788. [CrossRef] [PubMed]
24. Moreau, T.L.; Isman, M.B. Trapping whiteflies? A comparison of greenhouse whitefly (*Trialeurodes vaporariorum*) responses to trap crops and yellow sticky traps. *Pest Manag. Sci.* **2011**, *67*, 408–413. [CrossRef] [PubMed]
25. Lu, Y.; Bei, Y.; Zhang, J. Are yellow sticky traps an effective method for control of sweet potato whitefly, *Bemisia tabaci*, in the greenhouse or field? *J. Insect Sci.* **2012**, *12*, 113. [CrossRef] [PubMed]
26. Stukenberg, N.; Pietruska, M.; Waldherr, A.; Meyhöfer, R. Wavelength-Specific Behavior of the Western Flower Thrips (*Frankliniella occidentalis*): Evidence for a Blue-Green Chromatic Mechanism. *Insects* **2020**, *11*, 423. [CrossRef]
27. Parrella, M.P.; Jones, V.P. Yellow Traps as Monitoring Tools for *Liriomyza trifolii* (Diptera: Agromyzidae) in Chrysanthemum Greenhouses. *J. Econ. Entomol.* **1985**, *78*, 53–56. [CrossRef]
28. Murata, M.; Yamahama, Y.; Hariyama, T. Synergistic Effects of the Red Light and Blue Traps on Control of Thrips palmi (Thysanoptera: Thripidae). *J. Econ. Entomol.* **2021**, *114*, 627–631. [CrossRef] [PubMed]
29. Tang, L.D.; Zhao, H.Y.; Fu, B.L.; Han, Y.; Liu, K.; Wu, J.H. Colored sticky traps to selectively survey thrips in cowpea eco-system. *Neotrop Entomol.* **2016**, *45*, 96–101. [CrossRef] [PubMed]

30. Takikawa, Y.; Matsuda, Y.; Nonomura, T.; Kakutani, K.; Okada, K.; Shibao, M.; Kusakari, S.; Toyoda, H. Elimination of whiteflies colonizing greenhouse tomato plants using an electrostatic flying insect catcher. *Int. J. Curr. Adv. Res.* **2017**, *6*, 5517–5521.
31. Takikawa, Y.; Nonomura, T.; Sonoda, T.; Matsuda, Y. Developing a Phototactic Electrostatic Insect Trap Targeting Whiteflies, Leafminers, and Thrips in Greenhouses. *Insects* **2021**, *12*, 960. [CrossRef]
32. Takikawa, Y.; Matsuda, Y.; Kakutani, K.; Nonomura, T.; Toyoda, H. Unattended Trapping of Whiteflies Driven out of Tomato Plants onto a Yellow-Colored Double-Charged Dipolar Electric Field Screen. *Horticulturae* **2022**, *8*, 764. [CrossRef]
33. Nonomura, T.; Matsuda, Y.; Kakutani, K.; Takikawa, Y.; Kimbara, J.; Osamura, K.; Kusakari, S.-I.; Toyoda, H. Prevention of Whitefly Entry from a Greenhouse Entrance by Furnishing an Airflow-Oriented Pre-Entrance Room Guarded with Electric Field Screens. *J. Agric. Sci.* **2014**, *6*, 172–184. [CrossRef]
34. Takikawa, Y.; Matsuda, Y.; Nonomura, T.; Kakutani, K.; Okada, K.; Morikawa, S.; Shibao, M.; Kusakari, S.-I.; Toyoda, H. An Electrostatic Nursery Shelter for Raising Pest and Pathogen Free Tomato Seedlings in an Open-Window Greenhouse Environment. *J. Agric. Sci.* **2016**, *8*, 13–25. [CrossRef]
35. Kakutani, K.; Matsuda, Y.; Nonomura, T.; Takikawa, Y.; Okada, K.; Shibao, M.; Kusakari, S.; Toyoda, H. Successful single-truss cropping cultivation of healthy tomato seedlings raised in an electrostatically guarded nursery cabinet with non-chemical control of whiteflies. *GJPDCP* **2017**, *5*, 269–275.
36. Takikawa, Y.; Matsuda, Y.; Nonomura, T.; Kakutani, K.; Okada, K.; Shibao, M.; Kusakari, S.; Miyama, K.; Toyoda, H. Exclusion of whiteflies from a plastic hoop greenhouse by a bamboo blind-type electric field screen. *J. Agric. Sci.* **2020**, *12*, 50–60.
37. Matsuda, Y.; Takikawa, Y.; Nonomura, T.; Kakutani, K.; Okada, K.; Shibao, M.; Kusakari, S.; Miyama, K.; Toyoda, H. Selective electrostatic eradication of *Sitophilus oryzae* nesting in stored rice. *J. Food Technol. Preserv.* **2018**, *2*, 15–20.
38. Kakutani, K.; Matsuda, Y.; Takikawa, Y.; Nonomura, T.; Okada, K.; Shibao, M.; Kusakari, S.; Miyama, K.; Toyoda, H. Electrocutation of mosquitoes by a novel electrostatic window screen to minimize mosquito transmission of Japanese encephalitis viruses. *Int. J. Sci. Res.* **2018**, *7*, 47–50.
39. Matsuda, Y.; Shimizu, K.; Sonoda, T.; Takikawa, Y. Use of Electric Discharge for Simultaneous Control of Weeds and Houseflies Emerging from Soil. *Insects* **2020**, *11*, 861. [CrossRef] [PubMed]
40. Kakutani, K.; Takikawa, Y.; Matsuda, Y. Selective Arcing Electrostatically Eradicates Rice Weevils in Rice Grains. *Insects* **2021**, *12*, 522. [CrossRef] [PubMed]
41. Griffith, W.T. Electrostatic phenomena. In *The Physics of Everyday Phenomena, a Conceptual Introduction to Physics*; Brufloft, D., Loehr, B.S., Eds.; McGraw-Hill: New York, NY, USA, 2004; pp. 232–252.
42. Kakutani, K.; Matsuda, Y.; Toyoda, H. A simple and safe electrostatic method for managing houseflies emerging from underground pupae. *Agronomy* **2022**, submitted.
43. Wegner, H.E. Electrical charging generators. In *McGraw-Hill Encyclopedia of Science and Technology*, 9th ed.; Geller, E., Moore, K., Well, J., Blumet, D., Felsenfeld, S., Martin, T., Rappaport, A., Wagner, C., Lai, B., Taylor, R., Eds.; The Lakeside Press: New York, NY, USA, 2002; pp. 42–43.
44. Kakutani, K.; Matsuda, Y.; Haneda, K.; Nonomura, T.; Kimbara, J.; Kusakari, S.; Osamura, K.; Toyoda, H. Insects are elec-trified in an electric field by deprivation of their negative charge. *Ann. Appl. Biol.* **2012**, *160*, 250–259. [CrossRef]
45. Kakutani, K.; Matsuda, Y.; Haneda, K.; Sekoguchi, D.; Nonomura, T.; Kimbara, J.; Osamura, K.; Kusakari, S.-I.; Toyoda, H. An electric field screen prevents captured insects from escaping by depriving bioelectricity generated through insect movements. *J. Electrostat.* **2012**, *70*, 207–211. [CrossRef]
46. Ishay, J.; Benshalom-Shimony, T.; Ben-Shalom, A.; Kristianpoller, N. Photovoltaic effects in the *Oriental hornet, Vespa orientalis*. *J. Insect Physiol.* **1992**, *38*, 37–48. [CrossRef]
47. McGonigle, D.F.; Jackson, C.W. Effect of surface material on electrostatic charging of houseflies (*Musca domestica* L.). *Pest Manag. Sci.* **2002**, *58*, 374–380. [CrossRef]
48. McGonigle, D.F.; Jackson, C.W.; Davidson, J.L. Triboelectrification of houseflies (*Musca domestica* L.) walking on synthetic dielectric surfaces. *J. Electrostat.* **2002**, *54*, 167–177. [CrossRef]
49. Honna, T.; Akiyama, Y.; Morishima, K. Demonstration of insect-based power generation using a piezoelectric fiber. *Comp. Biochem. Physiol. Part B Biochem. Mol. Biol.* **2008**, *151*, 460. [CrossRef]
50. Moussian, B. Recent advances in understanding mechanisms of insect cuticle differentiation. *Insect Biochem. Mol. Biol.* **2010**, *40*, 363–375. [CrossRef] [PubMed]
51. Kakutani, K.; Matsuda, Y.; Nonomura, T.; Toyoda, H.; Kimbara, J.; Osamura, K.; Kusakari, S. Practical Application of an Electric Field Screen to an Exclusion of Flying Insect Pests and Airborne Fungal Conidia from Greenhouses with a Good Air Penetration. *J. Agric. Sci.* **2012**, *4*, 51–60. [CrossRef]
52. Toyoda, H.; Kusakari, S.; Matsuda, Y.; Kakutani, K.; Xu, L.; Nonomura, T.; Takikawa, Y. Earth net-free electric field screens. In *An Illustrated Manual of Electric Field Screens: Their Structures and Functions*; Toyoda, H., Ed.; RAEFSS Publishing Department: Nara, Japan, 2019; pp. 59–67.
53. Matsuda, Y.; Kakutani, K.; Nonomura, T.; Kimbara, J.; Kusakari, S.-I.; Osamura, K.; Toyoda, H. An oppositely charged insect exclusion screen with gap-free multiple electric fields. *J. Appl. Phys.* **2012**, *112*, 116103. [CrossRef]
54. Takikawa, Y.; Matsuda, Y.; Nonomura, T.; Kakutani, K.; Kimbara, J.; Osamura, K.; Kusakari, S.-I.; Toyoda, H. Electrostatic guarding of bookshelves for mould-free preservation of valuable library books. *Aerobiologia* **2014**, *30*, 435–444. [CrossRef]

55. Nonomura, T.; Toyoda, H. Soil Surface-Trapping of Tomato Leaf-Miner Flies Emerging from Underground Pupae with a Simple Electrostatic Cover of Seedbeds in a Greenhouse. *Insects* **2020**, *11*, 878. [CrossRef]
56. Alam, M.J.; Zurek, L. Association of *Escherichia coli* O157:H7 with Houseflies on a Cattle Farm. *Appl. Environ. Microbiol.* **2004**, *70*, 7578–7580. [CrossRef]
57. Ahmad, A.; Nagaraja, T.; Zurek, L. Transmission of *Escherichia coli* O157:H7 to cattle by house flies. *Prev. Vet. Med.* **2007**, *80*, 74–81. [CrossRef]
58. Mukherjee, A.; Cho, S.; Scheftel, J.; Jawahir, S.; Smith, K.; Diez-Gonzalez, F. Soil survival of *Escherichia coli* O157:H7 acquired by a child from garden soil recently fertilized with cattle manure. *J. Appl. Microbiol.* **2006**, *101*, 429–436. [CrossRef]
59. Brandl, M.T. Plant Lesions Promote the Rapid Multiplication of *Escherichia coli* O157:H7 on Postharvest Lettuce. *Appl. Environ. Microbiol.* **2008**, *74*, 5285–5289. [CrossRef]
60. Ibekwe, A.M.; Grieve, C.; Papiernik, S.; Yang, C.-H. Persistence of *Escherichia coli* O157:H7 on the rhizosphere and phyllosphere of lettuce. *Lett. Appl. Microbiol.* **2009**, *49*, 784–790. [CrossRef]
61. Helyer, N.; Brown, K.; Cattlin, N.D. Pest profiles. In *A Colour Handbook of Biological Control in Plant Protection*; Northcott, J., Ed.; Manson Publishing: London, UK, 2004; pp. 21–41.
62. Takikawa, Y.; Takami, T.; Kakutani, K. Body Water-Mediated Conductivity Actualizes the Insect-Control Functions of Electric Fields in Houseflies. *Insects* **2020**, *11*, 561. [CrossRef] [PubMed]
63. Kaiser, K.L. Air breakdown. In *Electrostatic Discharge*; Kaiser, K.L., Ed.; Taylor & Francis: New York, NY, USA, 2006; pp. 1–93.

Disclaimer/Publisher’s Note: The statements, opinions and data contained in all publications are solely those of the individual author(s) and contributor(s) and not of MDPI and/or the editor(s). MDPI and/or the editor(s) disclaim responsibility for any injury to people or property resulting from any ideas, methods, instructions or products referred to in the content.

Article

High-Voltage Electrostatic Fields Adversely Affect the Performance of Diamondback Moths over Five Consecutive Generations

Li Jia, Shicai Xu, Huanzhang Shang, Jiao Guo, Xia Yan, Changhai Liu, Guangwei Li and Kun Luo *

Shaanxi Engineering and Technological Research Center for Conversation and Utilization of Regional Biological Resources, College of Life Science, Yan'an University, Yan'an 716000, China

* Correspondence: luok1985@gmail.com

Abstract: Changing electrical environments can influence the performance of herbivorous insects and adversely affect their control strategies. The diamondback moth, *Plutella xylostella* (L.), is a pest that devastates cruciferous vegetables. An age-stage, two-sex life table of *P. xylostella* over multiple generations was established to describe the effect of varying high-voltage electrostatic field (HVEF) exposure on their performance after the age-cohort eggs were exposed to HVEF at an intensity of 5.0 kV/cm for different durations. The results show that direct HVEF exposure adversely affected the population dynamics parameters of *P. xylostella* over multiple generations. In particular, the net reproduction rate, intrinsic natural increase rate, and finite increase rate of the *P. xylostella* population significantly decreased in the third and fifth generations under HVEF exposure for 10 min, while the mean generation time and doubling time significantly increased. Similarly, HVEF exposure for 10 min rapidly reduced the survival rate of adult *P. xylostella* in the first generation, and subsequently, it declined evenly and slowly. Meanwhile, the fecundity parameters of *P. xylostella* revealed that HVEF exposure for 10 min had the strongest inhibition effect on reproduction over five consecutive generations. In addition, HVEF exposure significantly increased the superoxide dismutase activity to produce extra hydrogen peroxide; however, increased catalase and peroxidase activity or reduced peroxidase activity triggered the accumulation of malondialdehyde in instar *P. xylostella*, especially after 10 min of treatment. The present findings provide experimental evidence and a theoretical basis for developing control strategies for *P. xylostella* under new HVEF environments.

Keywords: high-voltage electrostatic field (HVEF); *Plutella xylostella*; Cruciferae vegetables; two-sex life table; population dynamics

Citation: Jia, L.; Xu, S.; Shang, H.; Guo, J.; Yan, X.; Liu, C.; Li, G.; Luo, K. High-Voltage Electrostatic Fields Adversely Affect the Performance of Diamondback Moths over Five Consecutive Generations. *Agronomy* **2023**, *13*, 1008. <https://doi.org/10.3390/agronomy13041008>

Academic Editor: Hideyoshi Toyoda

Received: 18 February 2023

Revised: 26 March 2023

Accepted: 28 March 2023

Published: 29 March 2023



Copyright: © 2023 by the authors. Licensee MDPI, Basel, Switzerland. This article is an open access article distributed under the terms and conditions of the Creative Commons Attribution (CC BY) license (<https://creativecommons.org/licenses/by/4.0/>).

1. Introduction

The diamondback moth, *Plutella xylostella* Linnaeus (Lepidoptera: Plutellidae), is a pest that devastates cruciferous vegetables such as pakchoi *Brassica chinensis* Linnaeus [1–3]. During the larval stage, especially the third and fourth instars, larvae gnaw on fresh leaves, severely damaging the leaves and causing significant yield losses in cruciferous vegetable production [4]. To effectively suppress the damage and keep it below the economic threshold, chemical spraying is still a crucial measure for managing the population dynamics of *P. xylostella* in agricultural production [5]. However, in recent decades, the economically irrational frequent spraying of several kinds of pesticides has significantly accelerated the development of pests' resistance to diverse chemicals [6,7]. It has been demonstrated that *P. xylostella* has already developed resistance to approximately 50 kinds of insecticides [8–11]. This is likely because its genetic plasticity stimulates an accumulating increase in resistance to such chemicals, which would serve as a genetic basis for it to adapt to the altered environment, and this poses a serious challenge to cruciferous vegetable production worldwide.

In addition, the artificial electric fields derived from modern industrial civilization have greatly increased the intensity of the natural electric fields to which organisms are directly exposed [12–14]. Previous studies have demonstrated that dramatic alterations in the electric environment affect the performance of plants and animals [15,16]. Similarly, insects are extremely sensitive to environmental changes, and can develop certain adaptive strategies owing to their high evolutionary rate, short growth cycle, small body size, and poor migration of larvae [17]. For instance, direct exposure of the cereal aphid *Sitobion avenae* Fabricius (Hemiptera: Aphididae), a prevalent and economically important wheat pest worldwide, to a high-voltage electrostatic field (HVEF) for 20 min at an intensity of 4 kV/cm had strong adverse effects on the population dynamics parameters of the aphids. However, using the same treatment on *S. avenae* over multiple generations, it was revealed that the aphids gradually recovered from the adverse effects of direct HVEF exposure over the generations, suggesting that the aphids' bodies changed in response to stress [18–20]. Moreover, when *S. avenae* were directly exposed to and fed on plant seeds exposed to the same intensity of HVEF, their antioxidative enzyme activity was affected, which supports the results of previous studies [21]. Similar findings were reported in many other insects, such as *Bombyx mori* (Lepidoptera: Bombycidae) [22], *Drosophila melanogaster* (Diptera: Drosophilidae) [23], and *Myzus persicae* (Hemiptera: Aphididae) [18,24]. Therefore, the rapid adaptation of insects, especially species with high genetic plasticity, to novel electrical environment alternations could make it more difficult to develop environmentally friendly pest control strategies.

To develop an alternative method that uses a more effective and sustainable pest management strategy to control *P. xylostella* larvae, we determined the effects of direct exposure to HVEF on *P. xylostella* larvae. In the field, *P. xylostella* typically passes through multiple generations during the plant growth period. To simulate high-voltage HVEF stress, we directly exposed newborn *P. xylostella* eggs (within 24 h after birth) to an HVEF field for five consecutive generations. An age-stage, two-sex life table of *P. xylostella* was established to determine the effects of direct HVEF exposure on the growth, development, and reproduction of *P. xylostella* over multiple generations. Meanwhile, the antioxidative enzyme activity and malondialdehyde (MDA) levels of fourth-instar *P. xylostella* were evaluated to characterize the physiological alterations after HVEF treatment. The results of the current study have increased our understanding of the performance of *P. xylostella* under HVEF stress, and have provided experimental data and a theoretical basis for the development of *P. xylostella* control strategies in novel HVEF environments.

2. Materials and Methods

2.1. Insect Specimens and Rearing Conditions

Larvae of *P. xylostella* were collected from a vegetable greenhouse in Yan'an (109°35' E, 36°63' N), Shaanxi Province, China. The larvae were taken to the Insect Physiology and Ecology Laboratory of Yan'an University. After five generations of stable reproduction with an artificial diet, they were used as test specimens. In order to avoid biotic and abiotic effects on the *P. xylostella* population, they were maintained on an artificial diet and placed in an artificial climate chamber with a constant temperature of 25 ± 1 °C, relative humidity of $55 \pm 10\%$, and a photoperiod of 12:12 (L:D) until pupation. The preparation of the artificial diet and its main components and proportions was carried out according to the China Invention Patent (Publication No. CN103478486A, 1 January 2014). To attract the moth larvae, the linseed oil in the formulation was exchanged for canola oil [25]. A newly prepared artificial diet was exchanged with the old one every two days. To produce eggs, the pupae of *P. xylostella* were transferred to oviposition cages for adult emergence, and the adults were fed with 10% honey solution until egg laying and death. The cage was covered with a black cloth and maintained in the growth chamber. Newborn larvae of *P. xylostella* were reared in the same manner until a sufficient number was obtained for experiments. To obtain the age-cohort eggs of *P. xylostella* for HVEF treatment, a multitude of male and female diamondback moths were transferred to the oviposition cage, and a

piece of spawning paper was suspended in the middle of the cage. After 24 h, the spawning paper with the age-cohort eggs of *P. xylostella* was removed from the oviposition cage. These newly laid eggs were used in the following experiments within 24 h.

2.2. HVEF Treatment

The HVEF generator used in this study (WJ-II, 0–100 kV output voltage) was purchased from Wuxi Boya Electronic Technology Co., Jiangsu Province, China. Two parallel rectangular aluminum plates (area, $50 \times 50 \text{ cm}^2$; distance between two plates, 8.0 cm) were installed in a wooden frame to form an electrical field. The output wires from the HVEF generator were connected to the aluminum plates, while a ground wire was connected to the field to avoid electrostatic damage. For each treatment, 100 newly laid eggs of *P. xylostella* (within 24 h after birth) were collected and placed in uncovered Petri dishes, which were directly exposed to HVEF with an intensity of 5.0 kV/cm (as determined prior to the experiment, this treatment intensity was appropriate) for 5, 10, 15, and 20 min. Another 100 newborn eggs without HVEF exposure were used as controls (Figure 1). There were three biological replicates for each treatment.

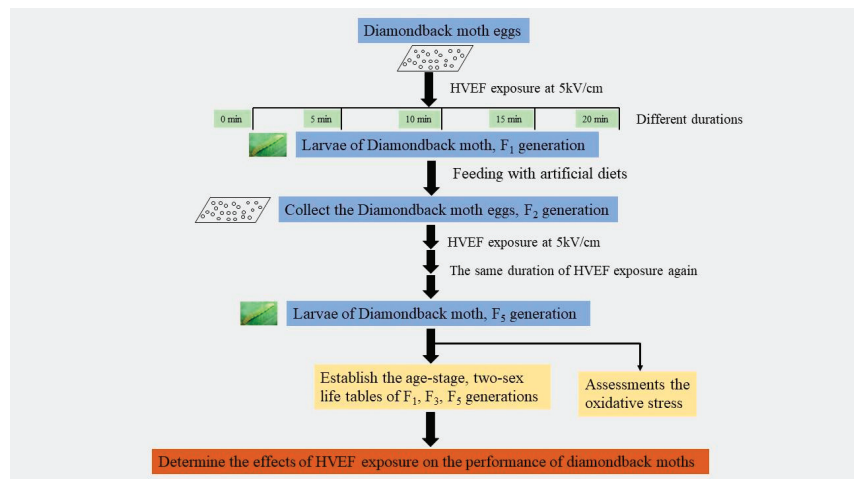


Figure 1. Experimental design for investigating suppression of *P. xylostella* performance over five generations, in response to direct exposure of eggs to HVEF at 5 kV/cm for different durations. The blue rectangles represent the different stages and generations of *P. xylostella* concerned in this study. F₁ to F₅ generation represent the first to the fifth generation of *P. xylostella*. The golden yellow rectangles represent the methods that employed into this study. The orange rectangles represent the main purpose of this study.

2.3. Life Table Analysis

The following experiments were conducted in controlled greenhouse conditions, as described previously. After HVEF treatment, the eggs were individually placed in feeder boxes and transferred to feeder cups (50 mL) containing feed for single rearing after they hatched. A freshly prepared artificial diet was exchanged with the old one every 1 to 2 days during the experimental period. Daily individual observations of larval mortality, larval molt, pupation time, and adult emergence were recorded. The survival rate and development time were obtained for all stages. When the larvae pupated, the artificial diet was removed to keep the inside of the bearing cups dry. When the pupae became adults, males and females that emerged on the same day in each treatment group were paired, and each pair was placed in a plastic oviposition container (14 mL). Each oviposition container also included a small cotton ball soaked in a 10% honey solution on which the adults were able to feed, and a $3 \times 4 \text{ cm}^2$ rectangular piece of spawning paper

was hung inside the cup to collect the eggs. The number of newborn eggs was recorded, and the eggs were removed daily until all female diamondback moths died.

To determine the effects of HVEF on multiple generations of *P. xylostella*, the newly laid eggs produced by the adults in each test group were collected within 24 h for five consecutive generations. They were directly exposed to HVEF for the same treatment time using the physical method described previously. From the onset of reproduction for each female, the number of newborn eggs was recorded daily, and the life data and parameters of the first (F_1), third (F_3), and fifth (F_5) generations of *P. xylostella* were analyzed in the present study. The life table parameters of the population growth of *P. xylostella*, including net reproductive rate (R_0), intrinsic natural increase rate (r), mean generation time (T), finite increase rate (λ), and doubling time (dt), were evaluated to determine the effects of direct HVEF exposure on performance. The life table parameters for each moth cohort were calculated using the equations below [26]. The stage-specific survival rate (l_x) describes the probability of survival of the individuals in a given population under treatment, and the stage-specific fecundity of the total population (m_x) reflects the average number of offspring born to each individual. The parameters l_x and m_x were calculated as follows:

$$l_x = \sum_{j=1}^m s_{xj} \quad (1)$$

$$m_x = \left(\sum_{j=1}^m s_{xj} f_{xj} \right) / \sum_{j=1}^m s_{xj} \quad (2)$$

where S_{xj} is the age- and stage-specific survival, including both the survival situation and the stage differentiation, and f_{xj} is the age- and stage-specific fecundity.

The net reproductive rate was defined as the age-specific survival rate and fecundity for each individual during its lifetime, including females, males, and individuals that died in immature stages, using the following equation:

$$R_0 = \sum_{x=0}^{\infty} \sum_{j=1}^m s_{xj} f_{xj} = \sum_{x=0}^{\infty} l_x m_x \quad (3)$$

In addition, the parameter r was considered to describe the maximum instantaneous growth rate of the population under stable conditions, and was calculated as shown in Equation (4):

$$\sum_{x=0}^{\infty} e^{-r(x+1)} l_x m_x = 1 \quad (4)$$

Meanwhile, other parameters of the population dynamics, T , λ , and dt , were calculated based on the above two parameters; T describes the time required for the population to develop for a whole generation, and was calculated using Equation (5). Parameters λ and dt represent the population growth relative to the population size, and were calculated using Equations (6) and (7):

$$T = (\ln R_0) / r \quad (5)$$

$$\lambda = e^r \quad (6)$$

$$dt = \ln 2 / r \quad (7)$$

Furthermore, to estimate the effects of direct HVEF exposure on *P. xylostella* reproduction, the relevant data from the life tables were employed to calculate the fecundity parameters, including the adult preoviposition period (APOP), oviposition period (OP), oviposition day (OD), and eggs per day during the oviposition period.

2.4. Oxidative Stress Assessment

To determine whether direct HVEF exposure affected physiological alterations in herbivores, the antioxidative enzyme activity and malondialdehyde (MDA) levels of fourth-instar *P. xylostella* were evaluated for each treatment. In parallel with the life table data collection, when eggs reached the fourth instar within 24 h after HVEF stress, the samples from the first and third generations were collected individually in 1.5 mL centrifuge tubes (6 fourth-instar larvae per tube). Then, the collected samples were snap-frozen using liquid nitrogen and stored in an ultra-low-temperature refrigerator at -80°C for enzyme activity assessment. The superoxide dismutase (SOD), catalase (CAT), and peroxidase (POD) activity, as well as the MDA level of fourth-instar *P. xylostella*, were determined according to commercial assay kits purchased from Nanjing Jiancheng Bioengineering Institute (SOD: item no. A001-3-2; CAT: A007-2-1, POD: A084-3-1, MDA: A003-1-2). The reaction mixture of fourth-instar *P. xylostella* tissue was prepared according to the reference manuals, and the absorbance of the mixture of all samples was determined within 10 min. The antioxidative enzyme activity in *P. xylostella* was expressed as U/mgprot, and the MDA level was expressed as nmol/mgprot. Three biological replicates were performed per treatment.

2.5. Statistical Analysis

The population parameters for all *P. xylostella* individuals in the study were analyzed according to an age–stage, two-sex life table using TWOSEX-MSChart software [27]. Based on the TWOSEX-MSChart software, the bootstrap technique with 100,000 resamplings was employed to simulate the effects of the sex ratio on the population parameters of *P. xylostella* and to estimate the standard error (SE). In addition, output files of bootstrap studies on the population parameters of *P. xylostella* relative to reproduction and population growth were used to compare the differences between treatments through one-way analysis of variance (ANOVA), and multiple comparisons among treatments were performed using the Student–Newman–Keuls (SNK) test. Meanwhile, the antioxidative enzyme activity and MDA levels in *P. xylostella* were calculated using Excel software (version 2010; Microsoft, Redmond, WA, USA). Similarly, one-way ANOVA was employed to compare the differences between HVEF exposure durations, and multiple comparisons of enzyme activity were made using the SNK test. All analyses were performed using SPSS 26.0 software (SPSS Inc., Chicago, IL, USA). The level of significance was set to p -value < 0.05 . All graphs were prepared using GraphPad Prism 8.0 software (GraphPad Software, San Diego, CA, USA).

3. Results

3.1. HVEF Treatment Adversely Affected Net Reproduction Rate (R_0) of *P. xylostella*

Direct exposure of *P. xylostella* eggs to HVEF at 5.0 kV/cm adversely affected R_0 , and the adverse effects exhibited different profiles at different time points. In particular, for the first generation of *P. xylostella*, although no significant difference in R_0 was detected when compared to the control group under HVEF stress ($p > 0.05$), HVEF treatment resulted in a reduced R_0 value, with the lowest value observed for the 5 min treatment (Figure 2A). When the stress continued to the third generation, R_0 decreased significantly with treatment times other than 5 min compared to the control, with the most significant decrease observed when the treatment time was 20 min ($p < 0.05$). In the fifth generation, 5 and 10 min treatments resulted in reduced R_0 , and 10 min treatment resulted in significantly decreased R_0 , whereas the R_0 values for 15 and 20 min treatments were close to the controls. In addition, under controlled greenhouse conditions, the presence of HVEF stress resulted in a significantly reduced R_0 in the third generation, especially with 10, 15, and 20 min treatments, while the R_0 values for fifth-generation *P. xylostella* showed an increasing trend with 15 and 20 min treatments (Figure 2B).

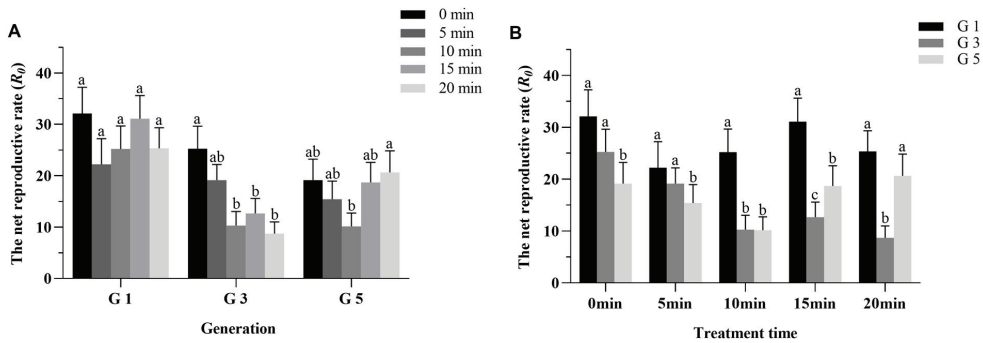


Figure 2. Net reproductive rate (R_0) of the first, third, and fifth generations of *P. xylostella* under HVEF stress. Note: Values are expressed as mean \pm standard error (SE). (A) The different lowercase letters indicates a significant difference at $p < 0.05$ between generations for groups exposed to electrostatic fields (0, 5, 10, 15, and 20 min). (B) The different lowercase letters indicates significant differences at $p < 0.05$ between treatments for 3 generations (G1, G3, and G5). Differences were compared using the paired bootstrap test.

3.2. HVEF Stress Significantly Affected the r of *P. xylostella* in All Generations

To better evaluate the effect of direct exposure of *P. xylostella* to HVEF on population growth, we determined the value of r . The results showed that in the first generation, although r did not exhibit a significant decrease under HVEF treatment compared to the controls ($p > 0.05$), it showed significant differences between treatment durations ($p < 0.05$); the lowest and highest values were found for the 5 and 15 min treatment times, respectively (Figure 3A). In the third generation, except for the 5 min treatment group, r decreased significantly in the experimental groups compared to the control, and the most significant decrease was found with the 20 min treatment ($p < 0.05$). For the fifth generation, r showed a similar decreasing tendency to the first generation; there was a significant decrease between the 5 and 10 min treatments and the control, and the other treatments did not show a significant decrease. Regarding the multigenerational effects, r was significantly decreased at different treatment times, especially at 10, 15, and 20 min (Figure 3B). These results suggest that the reproductive capacity of the *P. xylostella* populations was affected by the reduced r and its derived parameters in the novel HVEF environment.

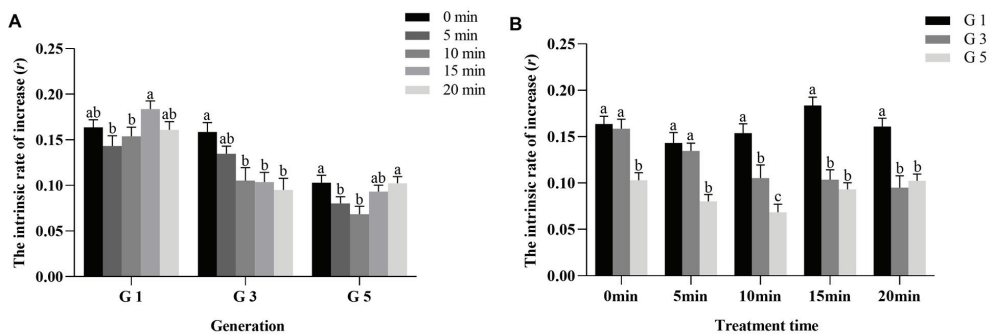


Figure 3. Intrinsic natural increase rate (r) of the first, third, and fifth generations of *P. xylostella* under HVEF stress. Note: Values are expressed as mean \pm standard error (SE). (A) The different lowercase letters indicates a significant difference at $p < 0.05$ between generations for groups exposed to electrostatic fields (0, 5, 10, 15, and 20 min). (B) The different lowercase letters indicates significant differences at $p < 0.05$ between treatments for 3 generations (G1, G3, and G5). Differences were compared using the paired bootstrap test.

3.3. HVEF Treatment Gradually Prolonged the T of *P. xylostella*

In the first generation, the T of *P. xylostella* was decreased after HVEF exposure, with significant decreases at 15 and 20 min (Figure 4A). However, in the third and fifth generations, T was significantly increased by HVEF stress compared to the control ($p < 0.05$). In particular, the T values of *P. xylostella* in the third generation showed an increasing trend at all treatment times, with the most significant increase at 15 min ($p < 0.05$), and a significant increasing trend was also observed at 5 and 10 min in the fifth generation (Figure 4A). Regarding the effects of HVEF on multiple generations of *P. xylostella*, HVEF stress significantly prolonged T as the number of generations increased; the longest T was found for the 5 min treatment in the fifth generation (Figure 4B).

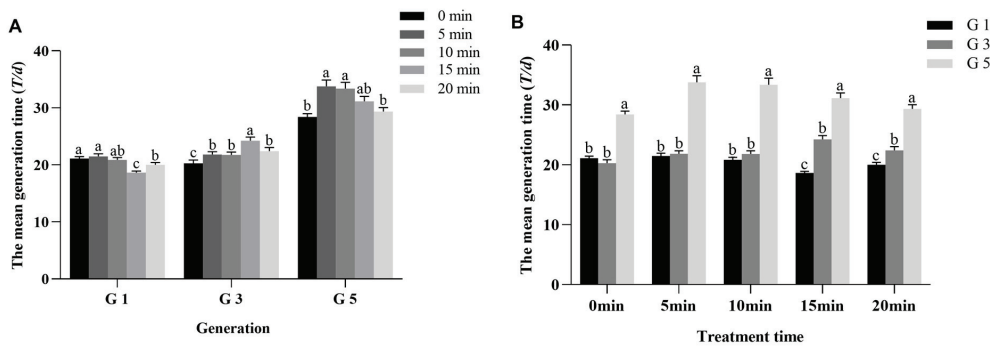


Figure 4. Mean generation time (T) of the first, third, and fifth generations of *P. xylostella* eggs in 5 successive generations after HVEF treatment. Values are expressed as mean \pm standard error (SE). (A) The different lowercase letters indicates a significant difference at $p < 0.05$ between generations for groups exposed to electrostatic fields (0, 5, 10, 15, and 20 min). (B) The different lowercase letters indicates significant differences at $p < 0.05$ between treatments for 3 generations (G1, G3, and G5). Differences were compared using the paired bootstrap test.

3.4. HVEF Stress Exerted a Suppressive Effect on Population Growth of *P. xylostella*

As shown in Table 1, similarly to the tendency of r described above, the value of λ for *P. xylostella* was significantly reduced under HVEF treatment. In the first generation, there was no significant difference between HVEF exposure and the control group ($p > 0.05$). Compared with the control group, the value of λ in third-generation *P. xylostella* was significantly decreased after HVEF exposure, with the lowest value observed at 20 min. In the fifth generation, the value of λ showed a significant decrease with shorter 5 and 10 min treatment times ($p < 0.05$), and no significant decrease was observed with longer times. In addition, the value of λ in each treatment was the greatest for the first generation of *P. xylostella*, and the lowest for the fifth generation.

In comparison with the control, in the first generation, the population doubling time decreased significantly in the 15 min treatment group ($p < 0.05$), while the other treatment groups were not significantly affected by HVEF stress ($p > 0.05$). In the third generation, the population doubling time increased significantly with each treatment duration ($p < 0.05$), and the largest value of dt was observed for the 20 min treatment group. For the fifth generation, the largest value was found with the 10 min treatment time, and was significantly increased compared to the control ($p < 0.05$). When considering the multigenerational effects, the population doubling time of *P. xylostella* significantly increased as the number of generations increased, and direct exposure of eggs to HVEF at 5.0 kV/cm for 10 min resulted in the greatest increase in dt in the fifth generation. These results suggest that 10 min of HVEF exposure exerted a more suppressive effect on population growth.

Table 1. λ and dt parameters of *P. xylostella* for each generation under HVEF at an intensity of 5.0 kV/cm for different durations.

| Statistic | Generation | 0 min | 5 min | 10 min | 15 min | 20 min |
|-----------|------------|--------------------|-------------------|-------------------|-------------------|-------------------|
| λ | G1 | 1.180 ± 0.006 bXY | 1.164 ± 0.009 bX | 1.192 ± 0.011 aX | 1.223 ± 0.004 abX | 1.190 ± 0.013 abX |
| | G3 | 1.208 ± 0.011 aX | 1.178 ± 0.001 bX | 1.160 ± 0.009 bY | 1.155 ± 0.007 bY | 1.121 ± 0.009 cY |
| | G5 | 1.156 ± 0.010 aY | 1.104 ± 0.003 bY | 1.092 ± 0.005 bZ | 1.137 ± 0.008 aY | 1.139 ± 0.008 aY |
| dt | G1 | 4.191 ± 0.116 abXY | 4.600 ± 0.237 aY | 3.974 ± 0.212 abY | 3.450 ± 0.053 bY | 4.025 ± 0.280 abY |
| | G3 | 3.686 ± 0.167 cY | 4.230 ± 0.024 bcY | 4.706 ± 0.236 bY | 4.832 ± 0.201 bX | 6.101 ± 0.388 aX |
| | G5 | 4.819 ± 0.284 bX | 7.014 ± 0.196 aX | 7.944 ± 0.417 aX | 5.415 ± 0.286 bX | 5.341 ± 0.277 bX |

Note: λ and dt represent the finite rate of increase and population doubling time, respectively. Values are expressed as mean ± standard error (SE). SE was estimated by using the bootstrap technique with 100,000 resamplings. Means followed by letters a–c in the same row are significantly different between treatment times in the same generation, according to paired bootstrap tests based on confidence intervals of differences at the 5% significance level, while letters X–Z indicate significant differences between generations (G1, G3, and G5) for the same HVEF duration.

3.5. Effect of HVEF Exposure on Survival and Oviposition Parameters of *P. xylostella*

To more accurately describe the survival probability among individuals, the age–stage survival rate of *P. xylostella* from egg to adult was investigated. The l_x curve showed that the survival duration of *P. xylostella* adults increased as the number of generations increased, and the longest life span was detected in the fifth generation (Figure 5). Under HVEF stress, although the survival rate of each treatment group was higher than that of the control group, the survival rate rapidly declined compared with the control group in the first generation, with the fastest decrease observed for the 20 min treatment time. In addition, the life spans of females were significantly shorter than those of males, and females who received 15 min of treatment had the shortest life spans. With continued HVEF exposure, the survival rates of third-generation *P. xylostella* in the larval and pupal stages were still higher than that those of the control group, and declined rapidly at the pupal and adult stages with 10 min of treatment. In the fifth generation, the survival rate in the pupal stage after HVEF exposure was lower than that of the control group, and it declined evenly and slowly. Meanwhile, the survival times were longer than those of the first and third generations. Notably, the difference in survival rates between females and males in the first and third generations was not significant; however, in the fifth generation, the survival rates of the females were significantly higher than those of the males (Figure 5).

In addition, direct exposure to HVEF had an adverse effect on the adult preoviposition period (APOP) in *P. xylostella*, and the APOP gradually extended in the same generation with increased exposure time. As shown in Table 2, the APOP under 15 min of treatment was significantly longer than the control and the other treatment groups in all generations, except for the fifth. In the fifth generation, the APOP with 15 min of HVEF exposure decreased suddenly compared to other treatments, and was close to that of the control group, while the APOP at 10 min was significantly higher than in the other groups ($p < 0.05$). Although the oviposition period (OP) and oviposition days (OD) of female *P. xylostella* were not significantly affected by direct HVEF exposure, they showed an increasing trend in the generations, with the longest OP and OD detected in the fifth generation after all treatments. The shortest OD and OP were observed with 10 min of treatment. Moreover, although this was not observed in the first generation, HVEF exposure resulted in a decreased number of eggs per day during oviposition in the third and fifth generations compared to the controls, with the lowest number found after 10 min of treatment in all test generations. The fecundity of the females showed a similar trend to the number of eggs per day during oviposition in each treatment group over multiple generations. These results suggest that direct HVEF exposure has an adverse effect on the survival and oviposition of *P. xylostella*.

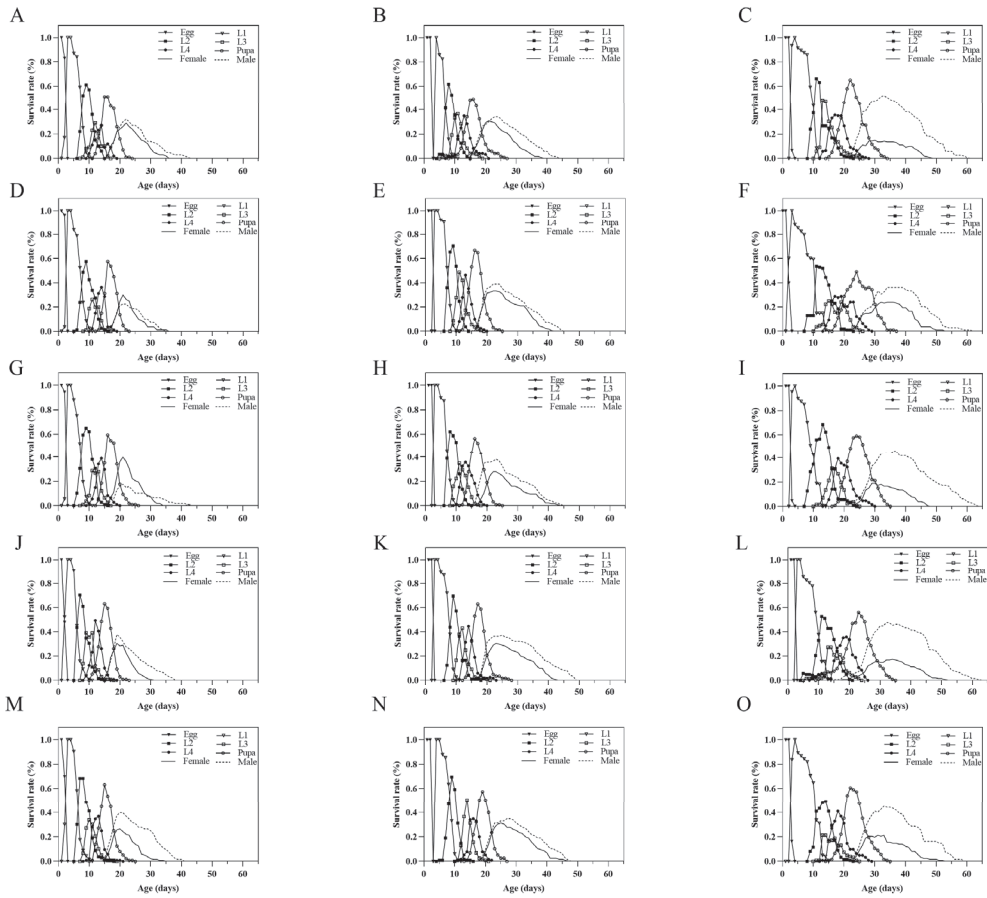


Figure 5. Age-specific survival rates (I_x) at each life stage of the first, third, and fifth generations of *P. xylostella*, with 5 consecutive generations treated with HVEF at 5.0 kV/cm for 0, 5, 10, 15, and 20 min. For each generation, the control group received 0 min of treatment. (A,D,G,J,M) The first column represents the survival rate of each stage at 0, 5, 10, 15, and 20 min for the first generation. (B,E,H,K,N) The second column represents the survival rate with each treatment time for the third generation. (C,F,I,L,O) The last column represents the survival rate of the fifth generation after HVEF stress at each stage.

Table 2. Fecundity parameters of each generation under different treatment times.

| Generation | Treatment Time (min) | Adult Preoviposition Period (APOP) (d) | Oviposition Period (OP) (d) | Oviposition Days (OD) (d) | Eggs per Day during Oviposition Period | Fecundity per Female |
|------------|----------------------|--|-----------------------------|---------------------------|--|----------------------|
| G1 | 0 | 0.77 ± 0.184 aX | 5.66 ± 0.502 aY | 5.23 ± 0.440 aX | 18.866 ± 1.680 abX | 91.714 ± 7.650 aX |
| | 5 | 1.19 ± 0.184 aX | 4.83 ± 0.557 aZ | 4.25 ± 0.501 aY | 16.550 ± 2.272 abX | 74.125 ± 10.856 abX |
| | 10 | 1.13 ± 0.229 aY | 4.30 ± 0.379 aY | 3.83 ± 0.335 aY | 13.339 ± 1.715 bX | 57.957 ± 8.162 bX |
| | 15 | 1.24 ± 0.297 aY | 4.51 ± 0.330 aZ | 4.09 ± 0.291 aY | 22.432 ± 2.099 aX | 95.378 ± 7.606 aX |
| | 20 | 1.04 ± 0.217 aX | 5.12 ± 0.435 aY | 5.23 ± 0.440 aX | 18.145 ± 1.613 abX | 84.049 ± 7.580 abX |
| G3 | 0 | 1.42 ± 0.433 aX | 6.36 ± 0.526 aY | 5.28 ± 0.457 aX | 13.504 ± 1.281 aY | 84.167 ± 8.912 aX |
| | 5 | 2.09 ± 0.401 aX | 7.84 ± 0.709 aY | 5.98 ± 0.504 aXY | 10.156 ± 1.141 abY | 68.911 ± 6.734 abX |
| | 10 | 2.22 ± 0.462 aXY | 5.70 ± 0.658 aY | 4.91 ± 0.579 aXY | 9.140 ± 1.329 abX | 56.348 ± 10.946 abX |
| | 15 | 2.52 ± 0.862 aX | 7.52 ± 0.996 aY | 5.87 ± 0.695 aX | 11.087 ± 2.087 abY | 66.565 ± 9.159 abX |
| | 20 | 1.82 ± 0.440 aX | 5.73 ± 0.715 aXY | 4.64 ± 0.605 aX | 7.608 ± 0.885 bZ | 45.591 ± 8.294 bY |

Table 2. Cont.

| Generation | Treatment Time (min) | Adult Preoviposition Period (APOP) (d) | Oviposition Period (OP) (d) | Oviposition Days (OD) (d) | Eggs per Day during Oviposition Period | Fecundity per Female |
|------------|----------------------|--|-----------------------------|---------------------------|--|----------------------|
| G5 | 0 | 0.25 ± 0.083 bX | 8.36 ± 0.853 aX | 6.57 ± 0.791 aX | 13.253 ± 1.609 aY | 105.143 ± 13.774 aX |
| | 5 | 1.33 ± 0.211 bX | 10.52 ± 1.133 aX | 7.24 ± 0.828 aX | 8.446 ± 0.857 aY | 79.476 ± 9.600 aX |
| | 10 | 2.95 ± 0.671 aX | 7.50 ± 0.947 aX | 5.70 ± 0.758 aX | 8.688 ± 1.256 aX | 64.500 ± 9.876 aX |
| | 15 | 0.60 ± 0.212 bY | 9.77 ± 0.956 aX | 7.27 ± 0.733 aX | 9.467 ± 1.369 aY | 89.000 ± 12.100 aX |
| | 20 | 1.55 ± 0.652 bX | 7.4 ± 0.868 aX | 6.21 ± 0.609 aX | 12.240 ± 1.280 aY | 87.000 ± 10.787 aX |

Note: Values are expressed as mean ± standard error (SE). SE was estimated using the bootstrap technique with 100,000 resamplings. Means followed by letters a–c in the same row were significantly different between treatment times in the same generation according to the paired bootstrap test, which is based on a confidence interval of differences at the 5% significance level, while letters X–Z indicate significant differences between generations (G1, G3, and G5) for the same HVEF duration.

3.6. HVEF Exposure Led to Significant Oxidative Damage to Fourth-Instar *P. xylostella*

Based on one-way ANOVA, HVEF stress significantly affected the antioxidative enzyme activity, subsequently increasing the MDA level of instar *P. xylostella*. In particular, total SOD activity exhibited an increasing trend after HVEF treatment (G1: $F = 16.171$, $d.f. = 4$, $p < 0.05$; G3: $F = 38.938$, $d.f. = 4$, $p < 0.05$), except for the 20 min treatment in the third generation, when compared with the controls (Figure 6A). The first and third generations exhibited the greatest increase in total SOD activity at 10 min. Similarly, when compared with the controls, the CAT (G1: $F = 29.482$, $d.f. = 4$, $p < 0.05$; G3: $F = 35.861$, $d.f. = 4$, $p < 0.05$) and POD (G1: $F = 85.530$, $d.f. = 4$, $p < 0.05$; G3: $F = 27.839$, $d.f. = 4$, $p < 0.05$) activity under most treatment durations showed an increasing trend, while a suppressive effect on POD activity was found with other treatment durations, including 15 min in the first generation and 10 min in the third generation, and the lowest POD activity in each generation was found with these durations (Figure 6B,C). Moreover, alterations in the activity of these antioxidative enzymes induced a significantly increased MDA level in fourth-instar *P. xylostella* (G1: $F = 3.988$, $d.f. = 4$, $p < 0.05$; G3: $F = 5.521$, $d.f. = 4$, $p < 0.05$). The highest MDA level was found after 20 min in the first generation and after 10 min in the third generation, while the controls exhibited the lowest MDA levels (Figure 6D).

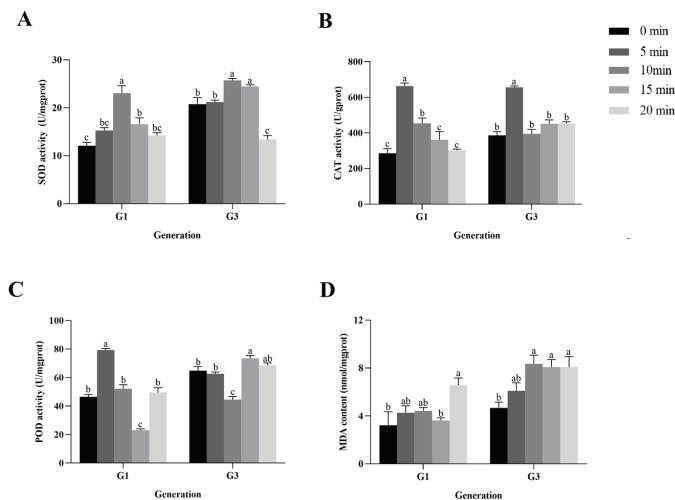


Figure 6. Effects of different durations of HVEF exposure on antioxidative enzyme activity and malondialdehyde levels of fourth-instar *P. xylostella*. Values are expressed as mean ± standard error (SE). (A) Superoxide dismutase (SOD), (B) catalase (CAT), (C) peroxidase (POD), (D) malondialdehyde (MDA). Different lowercase letters indicate significant differences ($p < 0.05$).

4. Discussion

In the present study, direct exposure of *P. xylostella* eggs to HVEF resulted in oxidative damage and adversely affected parameters associated with growth, and development, and reproduction in multiple consecutive generations. Interestingly, the 10 min treatment time had the most significant effect on all studied parameters when compared with the controls. These results were consistent with our previous study on direct and indirect exposure of first-instar cereal aphid nymphs to HVEF [19,28,29]. For instance, the results showed that exposure of either cereal aphids or wheat seeds to HVEF at 4 kV/cm for 20 min significantly affected the growth and reproductive parameters of aphid populations, and that the antioxidant enzyme activity was altered under stress [21,28,29]. In addition, in studies of other types of abiotic stress, we found that treating *P. xylostella* at different temperatures had a reproductive impact, with further evidence of reproductive compensation [30,31]. Furthermore, direct exposure of *P. xylostella* to $^{60}\text{Co-}\gamma$ radiation resulted in significantly reduced nymphal fecundity and postfecundity, as well as reduced adult longevity and fecundity, suggesting that either HVEF or other abiotic stresses adversely affect the performance of *P. xylostella* [32,33].

Previous studies have demonstrated that exposing cereal aphids to HVEF immediately affected their performance, and that they gradually exhibited adaptability to electric field stress when the treatment was continued for 10 more generations [19,29,34]. Interestingly, the growth and development, fecundity, and population growth of *P. xylostella* were not immediately inhibited in the first generation; when the treatment was continued up to the fifth generation, more serious adverse effects on their performance under electric field stress were observed. This is probably because the external eggshells of *P. xylostella* eggs can partially suppress the adverse effects of HVEF exposure, and as a result, some of the population dynamics parameters did not rapidly exhibit significant effects. Meanwhile, some of the parameters, such as r , could be determined by R_0 and T ; a higher value of R_0 and a lower T can lead to a higher value of r in the first generation than subsequent generations. The curve of the age–stage survival rate of *P. xylostella* supports this. For instance, direct HVEF exposure rapidly reduced the survival rate of *P. xylostella* in the first and third generations; when the treatment was continued up to the fifth generation, they adapted to HVEF, which eventually allowed them to survive and persist under electric field stress. Accordingly, the growth cycle of *P. xylostella* is longer than that of cereal aphids, and they recover rapidly from the adverse effects of HVEF exposure. Moreover, it is well known that when the environment is suitable, aphids generally undergo parthenogenesis, while *P. xylostella* is oviparous, producing eggs [35]. Thus, more work is required to unravel the exact nature of the damage to *P. xylostella* that is caused by HVEF exposure.

In addition, the current study suggests that the dose-dependent effects of different intensities of HVEF exposure on *P. xylostella* eggs produce different stress effects. Previous studies have shown that electric or magnetic fields of moderate intensity have the greatest inhibitory effect on the biological performance of different species of organisms [36–38]. For instance, static magnetic field (SMF) exposure at a moderate intensity of 0.2–0.4 T was found to maximally affect leukemia cell proliferation and the cell cycle [39]. Meanwhile, by treating rats with static magnetic fields of different intensities, it was demonstrated that static magnetic fields of moderate intensity inhibited osteocalcin secretion and human osteoblast-like cell proliferation [40]. The same results were reported in a study which attempted to enhance sorghum seed viability by using HVEF [41].

In this study, the life table parameters R_0 and r of the first generation of *P. xylostella* subjected to HVEF stress decreased significantly under moderate treatment durations, but other parameters were not significantly altered compared to the control group. It is possible that electrostatic damage is repaired within the organism by its own defense system, or that the population is maintained by reducing reproductive capacity. Nevertheless, as the number of generations exposed to HVEF treatment increased, the damage caused by HVEF gradually accumulated and reached a threshold where it could be repaired by the moths themselves. Therefore, in the third and fifth generations, there were significant changes in

vital phenotypes compared with the first generation; for example, the population doubling time increased significantly with increased treatment generations, but between generations, it showed a dose effect, i.e., longer population doubling times with shorter treatment durations. In contrast, both reproduction-related parameters, R_0 and r , were significantly lower in the 10 min treatment group than in the control. This proves that different radiation durations can have different toxic effects on insects, but not that a longer duration will produce a more pronounced effect.

In agreement with previous studies, the current study suggests that direct exposure of organisms to different environmental stressors, such as heavy metals, UV radiation, or HVEF, could cause the production of large amounts of reactive oxygen species (ROS). ROS cause an imbalance in the normal oxygen-consuming metabolic processes in the body, and have toxic effects; for example, they cause changes in cell structure and protein function, even causing structural changes in DNA, and, thus, its function [42–45]. For instance, direct exposure of *P. xylostella* eggs to HVEF for 10 min resulted in the greatest oxidative stress and the most significant adverse effects on performance. A similar result was found in *Thitarodes xiaojinensis* (Lepidoptera: Hepialidae) after using heat stress, which indicates that a large number of oxygen radicals were produced. This caused structural and functional damage to mitochondria, resulting in a series of cellular dysfunctions which led to cell and tissue death, and, ultimately, to irreversible damage to the insects, causing them to live longer [46].

In response to various adverse environmental changes, insects have evolved complex antioxidant enzyme protection mechanisms to mitigate the harmful effects of oxidative damage [46–49]. SOD, CAT, and POD play important roles in eliminating extra ROS compounds [50,51], and changes in their gene expression levels or enzyme activity can reflect the state of environmental stress and the degree of oxidative damage to the organism. For example, treating *P. xylostella* eggs with $^{60}\text{Co-}\gamma$ radiation caused significant changes in SOD, CAT, and POD gene expression and enzyme activity [51,52]. Apart from that, the results showed that *P. xylostella* midgut microbes encode for large amounts of SOD, CAT, and POD, which helps the host to reduce ROS to nontoxic compounds [53]. Although symbiotic bacteria are also present in aphids, they have completely different roles; for example, the obligate species *Buchnera aphidicola* can transform nonessential amino acids into amino acids that aphids cannot synthesize, and some species of secondary endosymbionts provide energy materials and some detoxification functions. This might be an important reason why HVEF exposure was shown to have a stronger adverse effect on aphids than *P. xylostella* [29,54,55].

In addition, direct exposure of *P. xylostella* eggs to $^{60}\text{Co-}\gamma$ radiation at 200 Gy resulted in significantly upregulated expression of the heat-stimulated protein (HSP) 70 genes [51]. It was demonstrated that some species of HSP have antioxidant capacity, which means that they can inhibit or scavenge the excess free radicals produced by organisms. Exposure to different external adverse environmental stressors (such as high temperature, low temperature, and UV radiation) impairs regular protein function and disrupts cellular homeostasis. Thereafter, large numbers of HSPs are expressed to help organisms to withstand external stresses and to enhance their resilience [53,56,57]. UV-A irradiation of *Ostrinia furnacalis* resulted in a slow decrease, then a rapid increase, and then a sudden decrease in the expression of vitellogenin receptor (*VgR*), a gene related to reproduction, and a corresponding change in fertility occurred in response to the effects of the external environment [58]. Furthermore, in the present study, a significant increase in malondialdehyde (MDA) content was detected after HVEF exposure, which may be a crucial marker of oxidative damage. This may be because MDA can easily bind to proteins and DNA and damage the structure and function of biomolecules [48,59]. Therefore, in subsequent experiments, we can further explore the biological roles of important proteins, such as HSP and reproduction-related proteins, in the adaptation of organisms to new HVEF environments.

In summary, direct exposure of *P. xylostella* eggs to HVEF at an intensity of 5.0 kV/cm for 10 min had the strongest inhibition effects on their performance, possibly resulting in longer growth cycles and increased population doubling time, as well as reduced

reproductive capacity. The results of this study will help us to understand the effects of HVEF stress on the performance of *P. xylostella* and its adaptation mechanisms, and will provide experimental data and a theoretical basis for control strategies in the new HVEF environment (Figure 7).

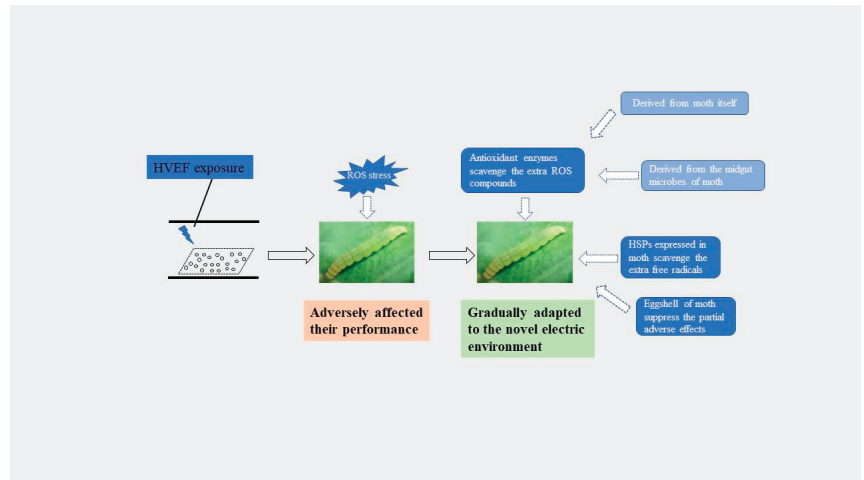


Figure 7. Proposed alterations in *P. xylostella* after exposure to HVEF stress based on findings obtained in or deduced from this study. Solid arrows represent pathways supported by experimental evidence from the present study; dotted arrows represent potential physiological alterations predicted from the literature.

Author Contributions: L.J.: investigation, writing—original draft, data curation. S.X.: conceptualization, data curation, writing—review and editing. H.S.: writing—original draft, data curation, investigation. J.G.: writing—original draft, investigation. X.Y.: investigation, data curation. C.L.: writing—review and editing, data curation. G.L.: writing—review and editing, data curation. K.L.: conceptualization, writing—review and editing, supervision, data curation, funding acquisition. All authors have read and agreed to the published version of the manuscript.

Funding: This work was supported by the Research Fund for the Doctoral Starting up Foundation of Yan’an University, China (No. YDBK2019-65), the Educational Innovation Program of Graduate Students of Yan’an University (YCX2021075), and the Innovation and Entrepreneurship Training Program for College Student of Yan’an University (D2020095).

Institutional Review Board Statement: Not applicable.

Informed Consent Statement: Not applicable.

Data Availability Statement: The data presented in this study are available on request from the corresponding authors.

Conflicts of Interest: The authors have no conflict of interest to declare.

References

1. Furlong, M.J.; Wright, D.J.; Dossall, L.M. Diamondback moth ecology and management: Problems, progress, and prospects. *Annu. Rev. Entomol.* **2013**, *58*, 517–541. [CrossRef]
2. Gautam, M.P.; Singh, H.; Kumar, S.; Kumar, V.; Singh, S.N. Diamondback moth, *Plutella xylostella* (Linnaeus) (Insecta: Lepidoptera: Plutellidae) a major insect of cabbage in India: A review. *J. Entomol. Zool. Stud.* **2018**, *6*, 1394–1399.
3. Jaleel, W.; Saeed, S.; Naqqash, M.N.; Sial, M.U.; Ali, M.; Zaka, S.M.; Sarwar, Z.M.; Ishtiaq, M.; Qayyum, M.A.; Aine, Q.U.; et al. Effects of temperature on baseline susceptibility and stability of insecticide resistance against *Plutella xylostella* (Lepidoptera: Plutellidae) in the absence of selection pressure. *Saudi J. Biol. Sci.* **2020**, *27*, 1–5. [CrossRef]

4. Zalucki, M.P.; Shabbir, A.; Silva, R.; Adamson, D.; Shu-Sheng, L.; Furlong, M.J. Estimating the economic cost of one of the world's major insect pests, *Plutella xylostella* (Lepidoptera: Plutellidae): Just how long is a piece of string? *J. Econ. Entomol.* **2012**, *105*, 1115–1129. [CrossRef]
5. Wang, J.; Zheng, X.B.; Yuan, J.J.; Wang, S.Y.; Xu, B.Y.; Wang, S.L.; Zhang, Y.J.; Wu, Q.J. Insecticide resistance monitoring of the diamondback moth (Lepidoptera: Plutellidae) populations in China. *J. Econ. Entomol.* **2021**, *114*, 1282–1290. [CrossRef] [PubMed]
6. You, S.; Liu, Z.; Xiong, L.; Liao, J.; He, W.Y.; You, M.S. Advances in research on the resistance of *Plutella xylostella* to *Bacillus thuringiensis* (Bt). *Chin. J. Appl. Entomol.* **2018**, *55*, 951–962.
7. Li, Z.Y.; Xiao, Y.; Wu, Q.J.; Shen, A.D.; Wang, X.L.; Zhang, J.M.; Feng, X. Progress in research on diamondback moth (*Plutella xylostella*) outbreaks and the management of resistance in this pest. *Chin. J. Appl. Entomol.* **2020**, *57*, 549–567.
8. Talekar, N.S.; Shelton, A.M. Biology, ecology, and management of the diamondback moth. *Annu. Rev. Entomol.* **2003**, *38*, 275–301. [CrossRef]
9. Luo, Y.J.; Wu, W.W.; Yang, Z.B.; Pu, E.T.; Guo, Z.X.; Yin, K.S.; He, C.X. Advances in insecticide resistance of diamondback moth (*Plutella xylostella* L.) in Yunnan. *J. Yunnan Univ.* **2008**, *30*, 178–182.
10. Santos, V.C.; Haa, D.S.; Da, S.J.; Mjdc, D.F. Insecticide resistance in populations of the diamondback moth, *Plutella xylostella* (L.) (Lepidoptera: Plutellidae), from the state of Pernambuco, Brazil. *Neotrop. Entomol.* **2011**, *40*, 264–270. [CrossRef]
11. Gao, D.L.; Liu, Y.; Wang, L.L.; Xu, N.N.; Zhuang, Z.G.; Xu, Y.; Hu, Z.J.; Zhuang, Z.X. Insecticides against resistance population of *Plutella xylostella*: Toxicity analysis and field control efficacy. *Chin. Agric. Sci. Bull.* **2018**, *34*, 145–149.
12. Bai, Y.; Hu, Y. Original mechanism of biological effects of electrostatic field on crop seeds. *Trans. Chin. Soc. Agric. Eng.* **2003**, *19*, 49–51. [CrossRef]
13. Wu, C.Y.; Zhang, L.; Zhen, S. Biological effect mechanism and application of high voltage electrostatic field on animal body. *Prog. Vet. Med.* **2004**, *25*, 7–9. [CrossRef]
14. Lee, J.Y.; Kang, S.W.; Yoon, C.S.; Kim, J.J.; Choi, D.R.; Kim, S.W. *Verticillium lecanii* spore formulation using UV protectant and wetting agent and the biocontrol of cotton aphids. *Biotechnol. Lett.* **2006**, *28*, 1041–1045. [CrossRef] [PubMed]
15. Yang, X.S.; Sun, H.; Liang, C.Y.; Yi, T.G.; Sun, F. Effect of high voltage electrostatic field on physiological and biochemistry indexes in developmental mice. *J. Jilin Univ.* **2005**, *31*, 839–842. [CrossRef]
16. Wang, G.; Huang, J.; Gao, W.; Lu, J.; Li, J.; Liao, R.; Jaleel, C.A. The effect of high-voltage electrostatic field (HVEF) on aged rice (*Oryza sativa* L.) seeds vigor and lipid peroxidation of seedlings. *J. Electrostat.* **2009**, *67*, 759–764. [CrossRef]
17. Lu, K.; Song, Y.; Zeng, R. The role of cytochrome P450-mediated detoxification in insect adaptation to xenobiotics. *Curr. Opin. Insect Sci.* **2021**, *43*, 103–107. [CrossRef]
18. Cakmak, T.; Cakmak, Z.E.; Dumlupinar, R.; Tekinay, T. Analysis of apoplasmic and symplasmic antioxidant system in shallot leaves: Impacts of weak static electric and magnetic field. *J. Plant Physiol.* **2012**, *169*, 1066–1073. [CrossRef] [PubMed]
19. He, J.; Cao, Z.; Yang, J.; Zhao, H.; Pan, W. Effects of static electric fields on growth and development of wheat aphid *Sitobion avenae* (Hemiptera: Aphididae) through multiple generations. *Electromagn. Biol. Med.* **2016**, *35*, 1–7. [CrossRef]
20. Cao, Z.; Li, G.Y.; He, J.; Zhao, H.Y.; Piyaratne, M.; Hu, Z.Q.; Hu, X.S. Effects of high voltage electrostatic fields on protective enzyme activity in wheat plants and on the population dynamics of *Sitobion avenae* Fabricius (Hemiptera: Aphididae). *Acta Ecol. Sin.* **2016**, *36*, 1001–1009.
21. Luo, K.; Luo, C.; Li, G.Y.; Xin, J.Y.; Gao, R.; Hu, Z.Q.; Zhang, G.S.; Zhao, H.Y. High-voltage electrostatic field-induced oxidative stress: Characterization of the physiological effects in *Sitobion avenae* (Hemiptera: Aphididae) across multiple generations. *Bioelectromagnetics* **2019**, *40*, 52–61. [CrossRef] [PubMed]
22. Zhang, H.L.; Zhao, B.G.; Xia, L.Q.; Xu, J.T. Effects of *Bombyx mori* eggs under the treatment of high voltage electrostatic field on dietary efficiency and larva growth and development. *J. Shandong Agric. Univ.* **2006**, *37*, 505–508.
23. Diebolt, J.R. The influence of electrostatic and magnetic fields on mutation in *Drosophila melanogaster* spermatozoa. *Mutat. Res.* **1978**, *57*, 169–174. [CrossRef] [PubMed]
24. Harutyunyan, H.; Artsruni, G. Biological effects of static electric field: Plasma/serum proteome analysis of rats. *J. Bioelectr.* **2013**, *32*, 79–94. [CrossRef] [PubMed]
25. Chen, Z.Q.; Miao, S.; Luo, K.J. Mass rearing techniques of diamondback moth. *Entomol. Knowl.* **2001**, *38*, 68–70. [CrossRef]
26. Chi, H.; Liu, H. Two new methods for the study of insect population ecology. *Bull. Inst. Zool. Acad. Sin.* **1985**, *24*, 225–240.
27. Chi, H.; Fu, J.W.; You, M.S. Age-stage, two-sex life table and its application in population ecology and integrated pest management. *Acta Entomol. Sin.* **2019**, *62*, 255–262. [CrossRef]
28. Li, G.Y.; Gao, R.; He, J.; Cao, Z.; Hu, Z.Q.; Hu, X.S.; Zhao, H.Y. Effect of high-voltage electrostatic field (HVEF) on the growth and fecundity of *Sitobion avenae* Fabricius (Hemiptera: Aphididae). *Acta Ecol. Sin.* **2016**, *36*, 3987–3994.
29. Luo, K.; Cao, Z.; Gao, R.; He, J.; Li, G.Y.; Gao, H.H.; Zhang, G.S.; Zhao, H.Y. Direct exposure of wheat seeds to high-voltage electrostatic fields adversely affects the performance of *Sitobion avenae* (Hemiptera: Aphididae). *J. Econ. Entomol.* **2016**, *109*, 2418–2423. [CrossRef]
30. Marchioro, C.A.; Foerster, L.A. Development and survival of the diamondback moth, *Plutella xylostella* (L.) (Lepidoptera: Yponomeutidae) as a function of temperature: Effect on the number of generations in tropical and subtropical regions. *Neotrop. Entomol.* **2011**, *40*, 533–541.

31. Zheng, Z.S.; Xing, K.; Zhao, F.; Wang, J.M.; Wen, X.D.; Yang, F. Effects of short hot stress and its duration on longevity and fecundity of diamondback moth adults. *China Plant Prot.* **2015**, *35*, 15–20.
32. Luo, L.Y.; Zhang, X.F.; Wei, X.Q.; Zhang, K.; Weng, Q.F. Effect of $^{60}\text{Co-}\gamma$ radiation on inherited sterility of *Plutella xylostella* (Lepidoptera: Plutellidae). *J. Northwest AF Univ.* **2018**, *46*, 149–154. [CrossRef]
33. Li, X.; Zhang, K.; Deng, Y.K.; He, R.K.; Zhang, X.F.; Zhong, G.H.; Hu, Q.B.; Weng, Q.F. Effects of $^{60}\text{Co-}\gamma$ radiation on testis physiological aspects of *Plutella xylostella* (Linnaeus). *Ecotoxicol. Environ. Saf.* **2019**, *169*, 937–943. [CrossRef] [PubMed]
34. Kim, H.; Seunghwan, L.; Yikweon, J. Macroevolutionary patterns in the *Aphidini Aphids* (Hemiptera: Aphididae): Diversification, host association, and biogeographic origins. *PLoS ONE* **2011**, *6*, e24749. [CrossRef]
35. Hori, T.; Inoue, N.; Suzuki, H.; Harakawa, S. Exposure to 50 Hz electric fields reduces stress-induced glucocorticoid levels in BALB/c mice in a kV/m- and duration-dependent manner. *Bioelectromagnetics* **2015**, *36*, 302–308. [CrossRef] [PubMed]
36. Kim, E.; Park, J.; Noh, G.; Park, S.; Noh, K.; Kwon, I.; Ahn, S. Effects of moderate intensity static magnetic fields on osteoclastic differentiation in mouse bone marrow cells. *Bioelectromagnetics* **2018**, *39*, 394–404. [CrossRef] [PubMed]
37. Wang, D.; Wang, Z.; Zhang, L.; Li, Z.; Tian, X.; Fang, J.; Lu, Q.; Zhang, X. Cellular ATP levels are affected by moderate and strong static magnetic fields. *Bioelectromagnetics* **2018**, *39*, 352–360. [CrossRef]
38. Hu, L.F.; Qian, A.R.; Yang, P.F.; Zhang, W.; Xie, L.; Shang, P. Effects of moderate static magnetic field on cell proliferation and cell cycle of leukemia cells. *J. Fourth Mil. Med. Univ.* **2009**, *30*, 397–400. [CrossRef]
39. Cunha, C.; Panseri, S.; Marcacci, M.; Tampieri, A. Evaluation of the effects of a moderate intensity static magnetic field application on human Osteoblast-Like cells. *Am. J. Biomed. Eng.* **2012**, *2*, 263–268. [CrossRef]
40. Hu, J.F.; Chen, J.; Wang, Y.G.; Du, H.L. Optimization of condition for improving sorghum seed vigor by high voltage electric field. *Trans. CSAE* **2015**, *31*, 253–259. [CrossRef]
41. Grujij, F.; Longstreth, A.J.; Norval, B.M.; Cullen, C.; Slaper, D.H. Health effects from stratospheric ozone depletion and interactions with climate change. *Photochem. Photobiol. Sci.* **2003**, *2*, 16–28. [CrossRef]
42. Zhaorigetu, S.; Yanaka, N.; Sasaki, M.; Watanabe, H.; Kato, N. Inhibitory effects of silk protein, sericin on UVB-induced acute damage and tumor promotion by reducing oxidative stress in the skin of hairless mouse. *J. Photochem. Photobiol. B Biol.* **2003**, *71*, 11–17. [CrossRef] [PubMed]
43. Meng, J.Y.; Zhang, C.Y.; Lei, C.L. A proteomic analysis of *Helicoverpa armigera* adults after exposure to UV light irradiation. *J. Insect Physiol.* **2010**, *56*, 405–411. [CrossRef] [PubMed]
44. Ute, W.; Esser, P.R.; Birgit, S.H.; Martin, S.F.; Jürgen, L.; Schempp, C.M. UVB-induced DNA damage, generation of reactive oxygen species, and inflammation are effectively attenuated by the flavonoid luteolin in vitro and in vivo. *Free. Radic. Biol. Med.* **2015**, *50*, 1081–1093. [CrossRef]
45. Packer, L.; Wirtz, K.W.A. *Signalling Mechanisms—from Transcription Factors to Oxidative Stress*; Springer: Berlin/Heidelberg, Germany, 1995.
46. Wang, M.L.; Zhu, W.; Zhang, J.H.; Xu, A.; Wang, H.T.; Li, X.; Zhou, G.L.; Zhang, H.; Qin, Q.L. Oxidative damage is one of the most important causes of death of *Thitarodes xiaojinensis* (Lepidoptera: Hepialidae) larvae under heat stress. *Acta Entomol. Sin.* **2014**, *57*, 769–776. [CrossRef]
47. Nguyen, T.; Michaud, D.; Cloutier, C. A proteomic analysis of the aphid *Macrosiphum euphorbiae* under heat and radiation stress. *Insect Biochem. Mol. Biol.* **2009**, *39*, 20–30. [CrossRef]
48. Dharshini, L.C.P.; Vishnupriya, S.; Sakthivel, K.M.; Rasmi, R.R. Oxidative stress responsive transcription factors in cellular signalling transduction mechanisms. *Cell. Signal.* **2020**, *72*, 109670. [CrossRef]
49. Blagojevi, D.P.; Grubor-Laji, G. Multifunctionality of antioxidant system in insects. *Arch. Biol. Sci.* **2000**, *52*, 185–194.
50. Ray, G.; Batra, S.; Shukla, N.K.; Suryanarayana, D.; Raina, V.; Ashok, S.; Husain, S.A. Lipid peroxidation, free radical production and antioxidant status in breast cancer. *Breast Cancer Res. Treat.* **2000**, *59*, 163–170. [CrossRef]
51. Li, X.; Luo, L.; Karthi, S.; Zhang, K.; Luo, J.J.; Hu, Q.B.; Weng, Q.F. Effects of 200 Gy $^{60}\text{Co-}\gamma$ radiation on the regulation of antioxidant enzymes, Hsp70 genes, and serum molecules of *Plutella xylostella* (Linnaeus). *Molecules* **2018**, *23*, 1011. [CrossRef]
52. Xia, X.F.; Lin, H.L.; Zheng, D.D.; Guang, Y.; Sheng, Y.M. Identification and expression patterns of heat shock protein genes in the diamondback moth, *Plutella xylostella* (Lepidoptera: Yponomeutidae). *Acta Entomol. Sin.* **2013**, *56*, 457–464. [CrossRef]
53. Alkhedir, H.; Karlovsky, P.; Mashaly, M.A.A.; Vidal, S. Phylogenetic relationships of the symbiotic bacteria in the aphid *Sitobion avenae* (Hemiptera: Aphididae). *Environ. Entomol.* **2015**, *44*, 1358–1366. [CrossRef] [PubMed]
54. Luo, C.; Luo, K.; Meng, L.Q.; Wan, B.; Zhao, H.Y.; Hu, Z.Q. Ecological impact of a secondary bacterial symbiont on the clones of *Sitobion avenae* (Fabricius) (Hemiptera: Aphididae). *Sci. Rep.* **2017**, *7*, 40754. [CrossRef]
55. Yang, C.; Meng, J.Y.; Su, L.; Zhang, C.Y. Cloning of heat shock protein gene *MpHsp70* and its expression analysis under UV-B stress in *Myzus persicae* (Hemiptera: Aphididae). *Acta Entomol. Sin.* **2019**, *62*, 133–140. [CrossRef]
56. Ding, C.Y.; Zhao, L.; Liu, S.; Li, M.Y. Molecular characterization of heat shock protein 70 (HSP70) genes from *Pieris rapae* (Lepidoptera: Pieridae) and their responses to insecticide stress. *Acta Entomol. Sin.* **2021**, *64*, 1407–1416. [CrossRef]
57. Liu, F.; Meng, J.Y.; Su, L.; Zhang, C.Y. Cloning of the vitellogenin receptor gene and its expression under UV-A stress in *Ostrinia furnacalis*. *Chin. J. Appl. Entomol.* **2021**, *58*, 96–107.

58. Seal, J.R.; Havrilla, C.M.; Porter, N.A.; Hachey, D.L. Analysis of unsaturated compounds by Ag⁺ coordination ionspray mass spectrometry: Studies of the formation of the Ag⁺/lipid complex. *J. Am. Soc. Mass Spectrom.* **2003**, *14*, 872–880. [CrossRef]
59. Wang, Z.J.; Niu, C.Y. Influence of ultraviolet light irradiation on HMG-CoA reductase, vitellogenin mRNA expression and oviposition of *Helicoverpa armigera*. *J. Huazhong Agric. Univ.* **2014**, *33*, 46–50. [CrossRef]

Disclaimer/Publisher’s Note: The statements, opinions and data contained in all publications are solely those of the individual author(s) and contributor(s) and not of MDPI and/or the editor(s). MDPI and/or the editor(s) disclaim responsibility for any injury to people or property resulting from any ideas, methods, instructions or products referred to in the content.

Article

Use of a Pair of Pulse-Charged Grounded Metal Nets as an Electrostatic Soil Cover for Eradicating Weed Seedlings

Yoshinori Matsuda ¹, Yoshihiro Takikawa ^{2,*}, Kunihiro Shimizu ³, Shin-ichi Kusakari ⁴ and Hideyoshi Toyoda ⁴

¹ Laboratory of Phytoprotection Science and Technology, Faculty of Agriculture, Kindai University, Nara 631-8505, Japan; ymatsuda@nara.kindai.ac.jp

² Plant Center, Institute of Advanced Technology, Kindai University, Wakayama 642-0017, Japan

³ Mikado Kyowa Seed, Co., Ltd., Chiba 267-0056, Japan; kunihikoshimizunozomi@yahoo.co.jp

⁴ Research Association of Electric Field Screen Supporters, Nara 631-8505, Japan;

kusakari@knsk-osaka.jp (S.-i.K.); toyoda@nara.kindai.ac.jp (H.T.)

* Correspondence: takikawa@waka.kindai.ac.jp

Abstract: An electrostatic technique was developed to generate a simple physical method to eradicate weeds in crop fields. The proposed apparatus consisted of double-expanded metal nets connected to a pulse-charging type negative voltage generator and a grounded line. The two metal nets were arranged in parallel at an interval (6 mm) that caused no arc (spark) discharge between the negatively charged metal net (NC-MN) and the grounded metal net (G-MN). The paired nets were used as a soil cover to zap weed seedlings emerging from the ground. As plant seedlings are biological conductors, the seedling was subjected to an arc discharge from the upper metal net (NC-MN) when it emerged from the soil and passed through the lower net (G-MN). The discharge was strong enough to destroy the seedling with a single exposure. The arc treatment was highly effective for eradicating successively emerging mono- and dicotyledonous weed seedlings, regardless of the number of coexisting weeds or the area of the netted field. Thus, the present study provides a simple and reliable weed eradication method that could be integrated into a sustainable crop production system.

Keywords: electric field; expanded metal net; herbicide-independent method; physical weed control; pulse-charging type voltage generator; weed control

Citation: Matsuda, Y.; Takikawa, Y.; Shimizu, K.; Kusakari, S.-i.; Toyoda, H. Use of a Pair of Pulse-Charged Grounded Metal Nets as an Electrostatic Soil Cover for Eradicating Weed Seedlings. *Agronomy* **2023**, *13*, 1115. <https://doi.org/10.3390/agronomy13041115>

Academic Editor: Ilias Travlos

Received: 10 March 2023

Revised: 6 April 2023

Accepted: 12 April 2023

Published: 14 April 2023



Copyright: © 2023 by the authors. Licensee MDPI, Basel, Switzerland. This article is an open access article distributed under the terms and conditions of the Creative Commons Attribution (CC BY) license (<https://creativecommons.org/licenses/by/4.0/>).

1. Introduction

Weed control is necessary for sustainable crop production. Herbicide-based weed control has been the most commonly used method for half a century [1]. However, due to the intensive use of herbicides, many weeds resistant to major classes of herbicides have evolved [2–4]. In addition to the problem of herbicide resistance in a wide range of weed species, greater public concern about the use of chemicals for managing all classes of pests (i.e., pathogens, insect pests, and weeds) has led to the development of a non-chemical method of weed control. Biological and physical methods can be integrated into total pest management systems as an alternative to chemicals.

The use of bioherbicides is an emerging technique for weed control and sustainable agriculture [5,6]. Bioherbicides include plant-producing phytotoxins [7], allelochemicals [8], and fungal phytotoxins [9,10]. The direct application of living herbivorous insects [11,12] or fungal phytopathogens [13] is another option for biological weed control. However, little practical progress has been made because effective control is difficult to maintain, agent preparation is problematic, there are few application targets, and costs are high. The main barrier to their practical implementation is integrating individual methods into large-scale weed control systems under various environmental conditions.

The most basic conventional methods used to physically control weeds include covering the soil surface with a weeding mulch film [14,15] and mowing, flaming, and tilling practices [16]. Some studies have proposed the use of electrical [17,18] and

robotic weeders [19] to reduce the labor requirements of these operations. However, the high cost of these machine weeders limits their wide use, particularly in developing countries [20]. Electrostatic techniques provide additional ways to kill weeds at the soil-emerging stage by directly exposing young seedlings to a high voltage arc (spark) discharge [17,21] generated in the space between conductors. The soil-emerging weed seedlings act as a biological conductor that receives a discharge from a charged conductor [21]. Matsuda et al. [22] successfully applied this technique to control kudzu creeping along an animal-repelling electric fence by attaching a grounded metal wire to an electrified fence wire at predefined intervals. This approach suggests that a simple electrostatic weed eradicator could be fabricated easily and inexpensively.

The objective of the present study was to provide an electric discharge-generating soil cover for practical weed management, in which a pair of charged grounded metal nets (G-MNs) were placed on a field to kill weed seedlings emerging from the soil. The framework of the apparatus is simple and easy to fabricate using commonly available materials. The main goal was to safely charge a metal net with a voltage generator, which is the only electric part of the present apparatus. A pulse-charging type negative voltage generator used for an electric fence was applied to the present system. Electric fences are used to repel wild animals and are ubiquitous and essential devices in modern agriculture. Accidents associated with agricultural electric fences are very rare [23]. Although unintentional human contact with electric fences occurs regularly, it only causes temporary discomfort [23]. Accordingly, this type of voltage generator is considered safe.

The arc discharge-exposure method was originally developed to prevent rice weevils nesting in dried rice grains [24,25]. Arcing is an electrical phenomenon generated by the movement of a high voltage-mediated negative charge in the air between opposite electric poles [26]. The intensity of the arc is determined by the voltage applied to the conductor and the distance between the opposite poles. The arc generated by the pulse-charging type voltage generator is sufficient to kill weeds effectively and quickly [22]. Thus, we developed an “electric discharge-armed weed zapper” (EDWZ) and determined the frequency of pulsed arc discharge exposure required to kill the seedlings of mono- and dicotyledonous plants. Based on these results, we evaluated the feasibility of the EDWZ for weed control and provided an experimental basis for developing an electrostatic weeding method.

2. Materials and Methods

2.1. Plant Species

Barley (*Hordeum vulgare* cv. Kobinkatagi), oats (*Avena sativa* cv. Negusaredaigi), soybeans (*Glycine max* cv. Natsunokoe), tomatoes (*Solanum lycopersicum* cv. Momotaro fight), watermelons (*Citrullus lanatus* cv. Tahiti), and sunflowers (*Helianthus annuus* cv. Konatsu) were used as model graminaceous, leguminous, solanaceous, cucurbitaceous, and asteraceous weeds, respectively. Germinated seeds of these plants were sown in a tray in soil and newly emerged seedlings were used in the experiments.

2.2. Instrument to Generate Arc Discharge between Two Metal Nets

Two identical expanded stainless nets (Okutani Wire Netting Mfg., Co., Ltd., Kobe, Japan) (Figure 1A) were used to construct the arc discharge instrument. One of the metal nets was held horizontally with a plastic clamp and linked to a solar cell-driven pulse-type negative voltage generator (pulse interval, 1 s; usable voltage, 10 kV) (Suematsu Denshi, Kumamoto, Japan) (Figure 1B), which is commonly used in electric fences to repel wild animals from crop fields. The other metal net was connected to a grounded line and placed on the horizontal platform of a laboratory scissor jack stand to vary the gap between the two nets (Figure 1C). The negative voltage generator amplified the initial voltage (12 V) to achieve the desired voltage (10 kV). The generator draws a negative charge from the ground using this voltage and supplies it to the conductor connected to the voltage generator [27]. A negative charge accumulates on the surface of the charged conductor and forms an electric

field (monopolar electric field) in the surrounding space (Figure 1D). If the grounded conductor is placed inside the electric field, the negative charge on the charged conductor pushes negative electricity (free electrons) out of the grounded conductor by electrostatic induction [28]. The grounded conductor becomes positively electrified, and opposite charges on the nets form a dipolar electric field (Figure 1E). The positively electrified grounded conductor acts as a recipient pole for the negative charge released from the negatively charged conductor via the arc discharge (Figure 1E). Thus, arcing occurs when a dipolar electric field forms between the oppositely charged conductors. In this experiment, the G-MN was brought closer to the negatively charged metal net (NC-MN) by gradually raising the jack platform to determine the longest distance (from the NC-MN) that would cause an arc discharge (arcing distance).

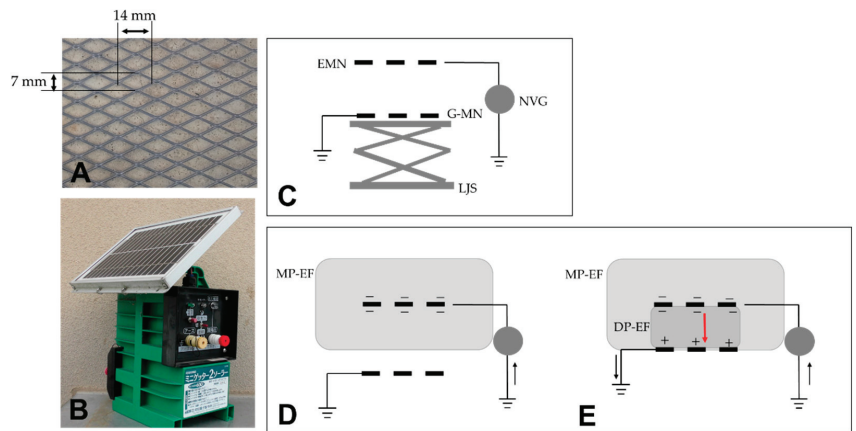


Figure 1. Experimental apparatus generating arc discharge. (A) Expanded stainless net with diamond-shaped 2 mm mesh connected to a voltage generator and grounded line. (B) Pulse-type voltage generator equipped with a solar panel and storage battery. (C) Configuration of the instrument (cross-sectional view), which consisted of two identical expanded metal nets (EMNs): one was maintained in a horizontal position and connected to a negative voltage generator (NVG), while the other was connected to a grounded line and placed on the horizontal platform of a laboratory jack stand (LJS) such that its height could be adjusted relative to the grounded metal net (G-MN). (D,E) Schematic representation of the monopolar electric field (MP-EF) surrounding the negatively charged metal net (D) and the dipolar electric field (DP-EF) formed between the two metal nets (E). The G-MN was moved closer to the charged upper metal net by gradually raising the jack platform. Arc discharge (red arrow) occurred when the G-MN entered the MP-EF and formed the DP-EF between the two metal nets. This distance was denoted as the arcing distance. The black arrow represents the movement direction of the negative charge.

2.3. Construction of the EDWZ

We fabricated the EDWZ using two expanded metal nets ($30 \times 30 \text{ cm}^2$). As the NC-MN caused arcing toward the G-MN when the distance between them was 5 mm (Figure 2A), the G-MN was set at a distance of 6 mm (non-arcing distance) by placing a square 6 mm high polypropylene frame (insulator) between the nets (Figure 2B). The EDWZ was placed on soil in a tray in which seeds had been sown. Arcing occurred preferentially toward a plant seedling when it reached the NC-MN electric field (Figure 2B).

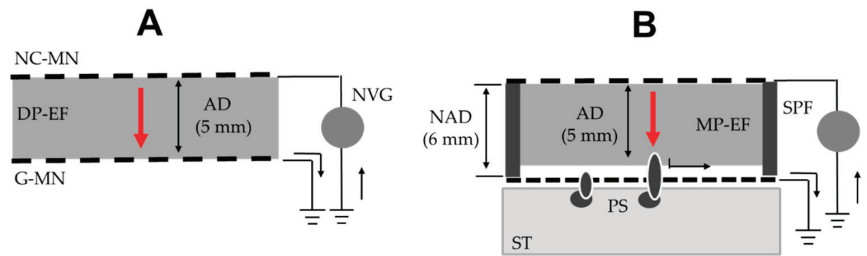


Figure 2. Schematic representation of the experimental instrument used to eradicate weed seedlings emerging from the ground (cross-sectional view). The expanded upper metal net was connected to a pulse-type negative voltage generator (NVG) and the lower net was connected to a grounded line. (A) Arc discharge occurred between the two metal nets, which were parallel to each other and separated by 5 mm (arcing distance, AD). A dipolar electric field (DP-EF) formed between the two nets. (B) The instrument was fabricated by placing a square polypropylene frame (SPF) (6 mm in height) between the NC-MN and G-MN to maintain a non-arc distance (NAD) and set on soil in a tray (ST) containing sown plant seeds. Arcing occurred toward a plant seedling (PS) when it reached the MP-EF of the NC-MN. The black arrow represents the ground-to-ground movement of negative electricity. The red arrow represents the movement of electricity (arcing) through the air.

2.4. Assay of Damages on Plant Seedlings Caused by Arc-discharge Exposure

Arc discharge exposure seriously damages the targets exposed to the arcing [22,29]. In the present study, the plant seeds were sown in a soil tray to determine the arc discharge exposure frequency required to kill the seedlings. The sound associated with arc discharge exposure [21,22] was recorded using a sound-level meter (Sato Tech, Kanagawa, Japan) throughout the entire experiment. A sound profile was generated on a chart to count the number of arc discharge sounds using a spectrum analyzer integrated into a sound-level meter. Twenty seedlings of each plant species were used, and the experiment was repeated five times. In addition, we recorded a video of monocotyledonous (barley) and dicotyledonous (tomato) seedlings subjected to arc discharge to demonstrate the effect on the seedling.

2.5. Practical Application of the EDWZ to Control Weed Seedlings Emerging in a Crop Field

A 1 m² EDWZ was constructed for practical use. Multiple EDWZs were connected with electrical wire (Figure 3A) and used to cover different areas (1 × 6–20 m²) in the field. All EDWZs were operated by a single voltage generator and a ground line. Before starting the apparatuses, the soil covering the top surface of the G-MN was leveled off to avoid exposure of the soil to an arc discharge (leveling-off-soil operation) (Figure 3B). Experiments were conducted at 18 locations in the crop field for 3 months between April and October in 2021 and 2022.

In the study area (Nara Prefecture, Japan), the seedlings of many weeds appear in April and grow vigorously. The present experimental period included the rainy (June–July) and high-temperature (July–September) seasons. At the end of each month, we assessed the weed community that appeared in the region adjacent to the area covered by the apparatuses. The Pl@ntNet application [30] was used to identify weed species.

2.6. Statistical Analysis

Each experiment was replicated five times, and all data are presented as mean and standard deviation. Tukey's test was performed using EZR software (ver. 1.54; Jichi Medical University, Saitama, Japan) to detect differences among the various conditions. A *p*-value < 0.05 was considered significant.

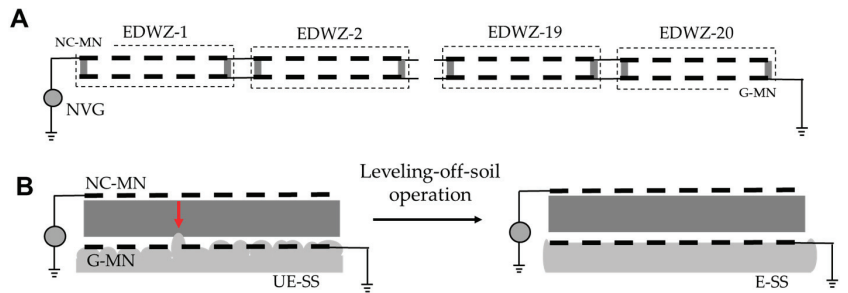


Figure 3. Application of multiple electric discharge-armed weed zappers (EDWZs) to a crop field. (A) Connection between the negatively charged metal nets (NC-MNs) of 20 EDWZs (EDWZ 1–20) and one pulse-charging type negative voltage generator (NVG), and between 20 grounded metal nets (G-MNs) and a grounded line, using an electric wire. (B) Soil covering the top surface of the G-MN was leveled off to transform the uneven soil surface (UE-SS) into an even soil surface (E-SS); undesirable arcing (red arrow) of this soil portion was thus evaded.

3. Results and Discussion

3.1. Determination of Arcing Distance

A negatively charged conductor creates an electric field in the surrounding space, which widens as the voltage applied is increased [26]. In the present study, the -10 kV metal net generated a 5 mm wide electric field and ejected an arc (spark) to the G-MN (Figures 1E and 2A). Based on this result, we designed an electrostatic soil cover consisting of two metal nets arranged in parallel at an interval of 6 mm (Figure 2B). This arrangement made it possible to achieve a distance between the NC-MN and G-MN at which arcing did not occur between them; instead, arc discharge was directed toward a seedling that emerged from the soil and extended 1 mm over the G-MN (Figure 2B). Thus, the EDWZ preferentially killed juvenile plant seedlings emerging from the soil.

3.2. Ability of the EDWZ to Eradicate Mono- and Dicotyledonous Plant Seedlings

The negative voltage generator produced arc discharges at an interval of 1 s. A sound was created at the time of the pulsed arc discharge, i.e., a sonic boom caused by the shock wave from the high-speed electrons moving within the electric field. The intensity of this sound reflected the impact of the shock wave produced by the arc discharge. Previous studies have reported that a pulsed arc discharge produces a force that can destroy the apical tissue of kudzu vines [22] and prompts flight by adult houseflies [29]. In this study, we examined how much arcing was required to kill plant seedlings that entered the NC-MN arcing area. Figure 4 shows the typical profiles of the sound(s) generated by arc discharges targeting the same monocotyledonous (barley) (A) and dicotyledonous (tomato) (B) seedlings during the experimental period (7 days).

The results indicated that the monocotyledonous plants were subjected to several arc discharge exposures (Figure 4A). The monocotyledonous plants first developed coleoptile tissue, which was destroyed by the first exposure (Video S1A). The lower part of the epicotyl remained alive and elongated continuously despite damage to the apical region. However, subsequent discharges destroyed the newly developed epicotyl. Repeated discharges overcame regrowth and killed the seedling. In contrast, the growth of dicotyledonous seedlings was halted after the first arc discharge exposure (Figure 4B). The arc discharge struck the dicotyledonous seedling's hypocotyl hook, which separated the hypocotyl hook from the epicotyl and halted further growth (Video S1B). Figure 5 shows the number of arc discharges required to kill the seedlings of mono- and dicotyledonous plants. There was no significant difference in the number of arcings required to kill the monocotyledonous and dicotyledonous plant seedlings, although there was a significant difference between the

mono- and dicotyledonous plants. Thus, the results suggest that the EDWZ is a practical way to eradicate weed seedlings emerging in a crop field.

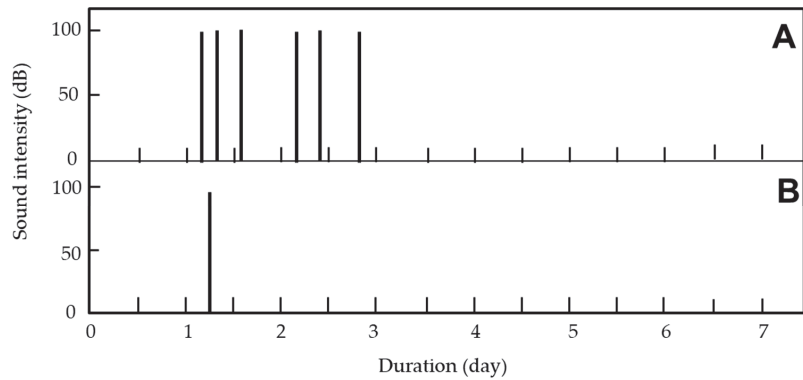


Figure 4. Profile of sound(s) generated by arc discharge(s) produced by the electric discharge-armed weed zapper (EDWZ) targeting barley (monocotyledon) (A) and tomato (dicotyledon) (B) seedlings.

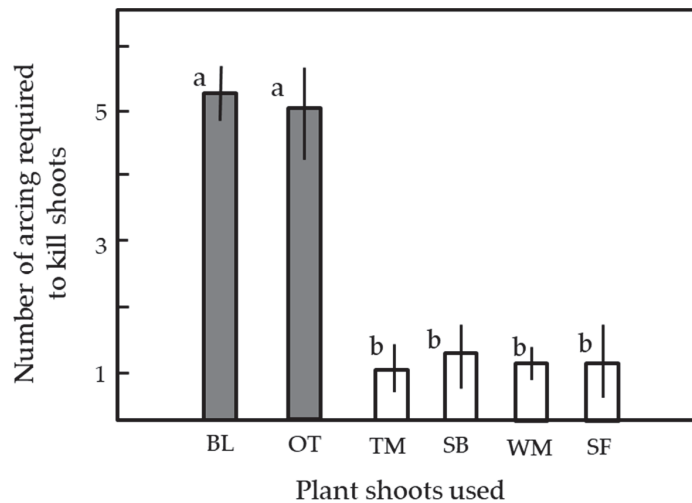


Figure 5. Eradication of elongating mono- and dicotyledonous plant seedlings via exposure to arcing generated by the negatively charged metal net of the electric discharge-armed weed zapper. Barley (BL) and oat (OT) were used as model monocotyledonous weeds, and tomato (TM), soybean (SB), watermelon (WM), and sunflower (SF) served as dicotyledonous weeds. Twenty seedlings were used for each plant species. Mean and standard deviation values were calculated from five experimental replicates. Different letters (a, b) in each vertical column indicate significant differences ($p < 0.05$) according to Tukey's test.

3.3. Practical Application of the EDWZ

3.3.1. Successful Grounding of the EDWZ

A prerequisite for the normal functioning of the EDWZ is successful grounding, which allows the collection of a negative charge from the ground by the voltage generator. The charge is then sent back to the ground. In a laboratory experiment, we inserted the grounded line plug of the voltage generator into the ground-contact outlet of a wall socket, which was equipped with a conductive pipe. The pipe was driven into the earth to a minimum depth of 8 feet (about 2.5 m) to protect against fire caused by electricity

leakage [31]. It was necessary to ground the voltage generator and the grounded line during the field experiments because the dried surface layer of the field increased ground resistance (earth resistance), which impeded current flow to the ground [32]. The manufacturer of the pulse-charging type voltage generator used here recommends driving a 50 cm long iron stake into the ground. The apparatus produced pulsed arc discharges at all 200 points tested in the crop field.

Plant seedlings with roots growing in wet ground are electrically grounded such that they are exposed to an arc discharge when they enter the NC-MN electric field, even if the G-MN is not equipped [21]. The surface layer of the ground soil is easily dried by a change in weather conditions. The dried soil layer was less conducive to intercepting the current flow from the arc discharge-exposed seedling. This is an important factor with respect to suppressing arcing from the NC-MN to a weed seedling. The G-MN was set to ensure a stable ground for the target seedling, regardless of any change in the weather. Seedlings that passed through the G-MN acted as intermediate poles and were subjected to an arc discharge from the NC-MN because of their conductivity. The electricity was eventually transferred to the seedling, and then to the ground, via the G-MN by a two-step arc discharge (Figure 2B) [22].

3.3.2. Leveling-Off of Soil for Preferential Arcing of Plant Seedlings

Wet soil is conductive and acts as an opposite pole receiving a negative charge from the NC-MN if the soil reaches the electric field (Figure 2A) [21]. To avoid undesirable arcing between the NC-MN and the ground, soil that projected over the top surface of the G-MN was leveled off to ensure that arcing to the weed seedlings passed through the G-MN and reached the NC-MN electric field (Figure 2B). The leveling-off of soil was easily achieved by sliding a flat-edge plate over the surface of the G-MN; successful leveling-off was confirmed by the lack of arcing and weed seedlings within the netted area.

3.3.3. Effects of a Change in Weather on EDWZ Functioning

Changes in the weather during the outdoor experiment were of concern. The voltage generator used in the present study was an all-weather generator; therefore, the effect of climate conditions on the generation of arc discharges by the NC-MN was an important consideration. The change in vapor concentration (relative humidity) in the air was the most important factor affecting the generation of arc discharges. Air conductivity changes in response to changes in the water vapor concentration (relative humidity) in the air: air conductivity is higher (i.e., more electricity is transferred) under conditions of higher relative humidity [33]. This implies that, under high humidity conditions, seedlings were exposed to arc discharges with larger amounts of electric current. Accordingly, highly humid conditions promoted effective arc discharge exposure treatment [21,22]. Seedlings that became wet because of rain or morning dew were more susceptible to arc discharge due to the increased conductivity of the wet plant body [21,22]. Temperature changes did not affect the generation of arc discharges by the apparatus. In fact, the EDWZ was not affected by changes in diurnal temperature even when the temperature change increased from 12 °C to 46 °C (at the ground level of 1 cm) over a period of several days in August.

3.3.4. Practical Application of the EDWZ for Weed Control in Crop Fields

The most important characteristic of the apparatus used in this study was that arc discharges were generated toward the seedling nearest to the NC-MN, suggesting that arcing occurs at a point on the charged metal net regardless of the net size or the number of seedlings reaching the electric field. It was possible to increase the size of the charged metal net for practical use. Multiple EDWZs were easily connected by linking their NC-MNs to a voltage generator and connecting the G-MNs to a grounded line (Figure 3A). However, we were concerned that expanding the apparatus would delay exposure to the arc discharge because of the tremendous increase in the number of targeted weed seedlings. The voltage generator generated 60 arcs/min, i.e., 86,400 arcs per

day. Theoretically, this means that the EDWZ can treat approximately 85,000 seedlings per day if all of the targets are dicotyledons, and approximately 14,000 seedlings if they are all monocotyledons. In our preliminary survey, the average density was 328.9 ± 85.4 weeds/m², suggesting that the voltage generator could treat weeds emerging in a 50–280 m² area. These provisional calculations encouraged us to apply the EDWZ for weed control. Ultimately, we fabricated 20 EDWZs because of budget limitations.

We conducted field experiments to demonstrate the practicality of the apparatus. The results indicated that the EDWZs functioned continuously during the experiments. In fact, the emergence of weed seedlings was completely suppressed in all 18 locations, where 6–20 apparatuses were combined to cover different areas. Figure 6 shows two examples of successful applications. Figure 6A–C show where the 20 EDWZs were placed initially (A) and where they were placed after 3 months (B). The results indicate that the apparatuses completely suppressed the emergence of seedlings, and the post-experiment survey indicated that no weed seedlings remained beneath the nets (Figure 6C). Figure 6D,E show the application of six EDWZs, which achieved the complete suppression of weed emergence. We concluded that the EDWZ is a promising tool to eradicate weed seedlings and achieve weed control in crop fields.

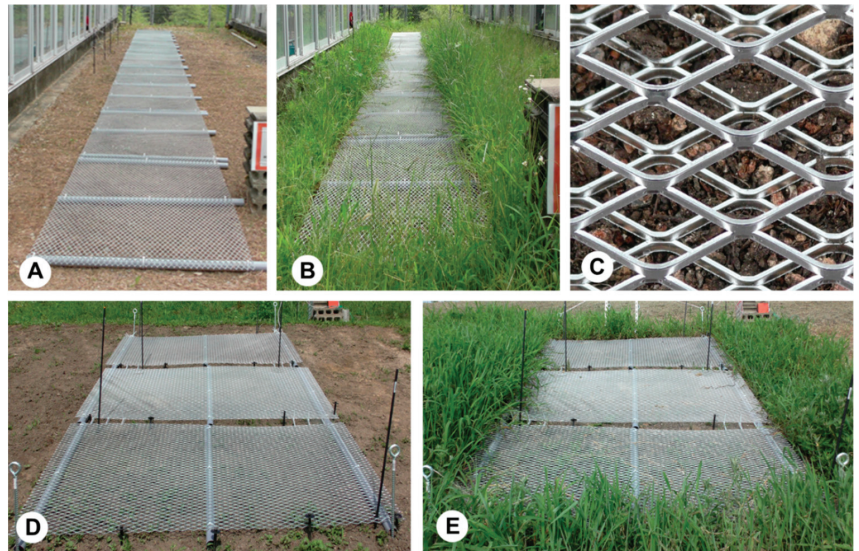


Figure 6. Photograph showing the sustainable functionality of the electric discharge-armed weed zapper (EDWZ). (A–C) Suppression of weed emergence using a soil cover consisting of 20 connected EDWZs at the start of experiment (A) and after 3 months (B,C). The image in C is an enlargement of the image in B. (D,E) Suppression of weed emergence by six connected EDWZs at the start of the experiment (D) and after 3 months (E). No weeds appeared in netted areas, while numerous weeds emerged and grew in areas adjacent to those covered by the apparatus.

To identify the weeds that were controlled, we designated an adjacent control plot where we analyzed the weed population of the soil seedbank. Our survey indicated that several weed species appeared seasonally during the experimental period, including four kinds of dicotyledonous weeds and six monocotyledonous species (Table 1).

Table 1. List of Identified Weeds ^a.

| Types of Cotyledon | Common Name | Scientific Name |
|--------------------|-----------------------|---|
| Dicotyledons | Chickweed | <i>Stellaria media</i> (L.) Vill. |
| | Narrow-leaved Vetch | <i>Vicia sativa</i> L. subsp. <i>nigra</i> (L.) Ehrh. |
| | Philadelphia Fleabane | <i>Erigeron philadelphicus</i> L. |
| | White Clover | <i>Trifolium repens</i> L. |
| Monocotyledons | Green Bristlegrass | <i>Setaria viridis</i> (L.) P. Beauv |
| | Southern Crabgrass | <i>Digitaria ciliaris</i> (Retz.) Koel |
| | Indian Goosegrass | <i>Eleusine indica</i> (L.) Gaertn |
| | Annual Bluegrass | <i>Poa annua</i> L. |
| | Shortawn Foxtail | <i>Alopecurus aequalis</i> Sobol. |
| | Wild Oat | <i>Avena sativa</i> L. |

^a Weeds growing in the area adjacent to the test locations covered by the electric discharge-armed weed zappers.

We have proposed a unique electrostatic weed eradicator. Due to its simple structure, it can be fabricated inexpensively using common materials without requiring any special construction skills. The use of a pulse-charging voltage generator, which has been typically used for electric fences to repel wild animals, reduced the total production cost. The voltage generator was operated by a solar panel-powered storage battery; therefore, it was not necessary to equip the apparatus with electric wiring. This low-cost equipment should be acceptable to many farmers for use as a weed management tool. Moreover, the apparatus is weatherproof such that it can be operated outdoors for extended periods. Importantly, a successful arc discharge depends on the conductivity of the weeds, and all weeds entering the electric field are targeted for eradication, regardless of their biological characteristics. In summary, we have developed a promising new tool for physical weed management.

Despite the prominent weed seedling-eradicating ability of the present apparatus, we have some problems regarding its practicality. The important problems may be identifying how to adequately treat weeds in a crop field that are adjacent to crop plants without harming the crop and how to apply the apparatus to a curved place, such as raised beds, where crops are cultivated. Because weed seeds germinate throughout the year, another problem is how long the apparatus would need to stay in place. Once the system is installed, it may be more difficult to do some farming by tractor. In addition, existing weed populations or perennial weed species are problematic to the present system. Despite these questions, this system could be very useful in specific cropping situations. Some future research to deal with these issues could continue to improve this method.

4. Conclusions

The electrostatic weed eradicator presented here is a newly developed device to kill weed seedlings emerging from crop fields via arc discharge. The convex part of an expanded metal net ejects discharge sparks toward seedlings in any location. The arc discharge treatment can target the tallest emerging weed seedlings with a high accuracy. The present study describes a simple physical herbicide-independent weed management approach for sustainable crop production systems.

Supplementary Materials: The following supporting information can be downloaded at <https://www.mdpi.com/article/10.3390/agronomy13041115/s1>. Video S1: Arc discharge from the negatively charged metal net (NC-MN) and the electric discharge-armed weed zapper (EDWZ) affecting barley (monocotyledon) (A) and tomato (dicotyledon) seedlings (B), respectively.

Author Contributions: Conceptualization, H.T. and Y.M.; methodology, Y.M. and Y.T.; software, Y.M.; validation, H.T., Y.M., K.S., S.-i.K. and Y.T.; formal analysis, Y.M. and Y.T.; investigation, Y.M. and Y.T.; resources, Y.M.; data curation, Y.T.; writing—original draft preparation, H.T.; writing—review and editing, Y.M. and Y.T.; visualization, Y.M.; supervision, H.T.; project administration, Y.M. All authors have read and agreed to the published version of the manuscript.

Funding: This research received no external funding.

Data Availability Statement: Not applicable.

Conflicts of Interest: The authors declare no conflict of interest.

References

- Davis, A.S.; Frisvold, G.B. Are herbicides a once in a century method of weed control? *Pest Manag. Sci.* **2017**, *73*, 2209–2220. [PubMed]
- Green, J.M. Current state of herbicides in herbicide-resistant crops. *Pest Manag. Sci.* **2014**, *70*, 1351–1357. [CrossRef] [PubMed]
- Heap, I. Global perspective of herbicide-resistant weeds. *Pest Manag. Sci.* **2014**, *70*, 1306–1315. [PubMed]
- Duke, S.O. The history and current status of glyphosate. *Pest Manag. Sci.* **2018**, *74*, 1027–1034. [CrossRef] [PubMed]
- Radhakrishnan, R.; Alqarawi, A.A.; Allah, E.F.A.A. Bioherbicides: Current knowledge on weed control mechanism. *Ecotoxic. Environ. Saf.* **2018**, *158*, 131–138. [CrossRef]
- Hasan, M.; Ahmad-Hamdani, M.S.; Rosli, A.M.; Hamdan, H. Bioherbicides: An Eco-Friendly Tool for Sustainable Weed Management. *Plants* **2021**, *10*, 1212.
- Anese, S.; Rial, C.; Varela, R.M.; Torres, A.; Molinillo, J.M.G.; Macías, F.A. Search of new tools for weed control using *Partocrat rotundifolia*, a dominant species in the Cerrado. *J. Agric. Food Chem.* **2021**, *69*, 8684–8694.
- Macías, F.A.; Mejías, F.J.; Molinillo, J.M. Recent advances in allelopathy for weed control: From knowledge to applications. *Pest Manag. Sci.* **2019**, *75*, 2413–2436. [CrossRef]
- Sharma, S.; Pandey, L.M. Prospective of fungal pathogen-based bioherbicides for the control of water hyacinth: A review. *J. Basic Microbiol.* **2022**, *62*, 415–427. [CrossRef]
- Cimmino, A.; Masi, M.; Evidente, M.; Superchi, S.; Evidente, A. Fungal phytotoxins with potential herbicidal activity: Chemical and biological characterization. *Nat. Prod. Rep.* **2015**, *32*, 1629–1653. [CrossRef]
- Catton, H.A.; Lalonde, R.G.; De Clerck-Floate, R.A. Differential host-finding abilities by a weed biocontrol insect create within-patch spatial refuges for nontarget plants. *Environ. Entomol.* **2014**, *43*, 1333–1344. [CrossRef]
- Catton, H.A.; Lalonde, R.G.; De Clerck-Floate, R.A. Nontarget herbivory by a weed biocontrol insect is limited to spillover, reducing the chance of population-level impacts. *Ecol. Appl.* **2015**, *25*, 517–530. [CrossRef]
- Morin, L. Progress in Biological Control of Weeds with Plant Pathogens. *Annu. Rev. Phytopathol.* **2020**, *58*, 201–223. [CrossRef]
- Petrikovszki, R.; Zalai, M.; Bogdányi, F.T.; Ferenc Tóth, F. The effect of organic mulching and irrigation on the weed species composition and the soil. *Plants* **2020**, *9*, 66. [CrossRef]
- Wang, K.; Sun, X.; Long, B.; Li, F.; Yang, C.; Chen, J.; Ma, C.; Xie, D.; Wei, Y. Green production of biodegradable mulch films for effective weed control. *ACS Omega* **2021**, *6*, 32327–32333. [CrossRef]
- Mainardis, M.; Boscutti, F.; Cebolla, M.D.M.R.; Pergher, G. Comparison between flaming, mowing and tillage weed control in the vineyard: Effects on plant community, diversity and abundance. *PLoS ONE* **2020**, *5*, 0238396. [CrossRef]
- Nagura, A.; Tenma, T.; Sakaguchi, Y.; Yamano, N.; Mizuno, A. Destruction of weeds by pulsed high voltage discharges. *J. Inst. Electrostat. Jpn.* **1992**, *16*, 59–66.
- Lati, R.N.; Rosenfeld, L.; David, I.B.; Bechar, A. Power on! Low-energy electrophysical treatment is an effective new weed control approach. *Pest Manag. Sci.* **2021**, *77*, 4138–4147. [CrossRef]
- Fennimore, S.A.; Cutulle, M. Robotic weeders can improve weed control options for specialty crops. *Pest Manag. Sci.* **2019**, *75*, 1767–1774. [CrossRef]
- Ekeleme, F.; Dixon, A.; Atser, G.; Hauser, S.; Chikoye, D.; Korie, S.; Olojede, A.; Agada, M.; Olorunmaiye, P.M. Increasing cassava root yield on farmers' fields in Nigeria through appropriate weed management. *Crop. Prot.* **2021**, *150*, 105810. [CrossRef]
- Matsuda, Y.; Shimizu, K.; Sonoda, T.; Takikawa, Y. Use of electric discharge for simultaneous control of weeds and houseflies emerging from soil. *Insects* **2020**, *11*, 861. [CrossRef] [PubMed]
- Matsuda, Y.; Takikawa, Y.; Kakutani, K.; Nonomura, T.; Okada, K.; Kusakari, S.; Toyoda, H. Use of pulsed arc discharge exposure to impede expansion of the invasive vine *Pueraria montana*. *Agriculture* **2020**, *10*, 600. [CrossRef]
- Burke, M.; Odell, M.; Bouwer, H.; Murdoch, A. Electric fences and accidental death. *Forensic Sci. Med. Pathol.* **2017**, *13*, 196–208. [CrossRef] [PubMed]
- Matsuda, Y.; Takikawa, Y.; Nonomura, T.; Kakutani, K.; Okada, K.; Shibao, M.; Kusakari, S.; Miyama, K.; Toyoda, H. Selective electrostatic eradication of *Sitophilus oryzae* nesting in stored rice. *J. Food Technol. Pres.* **2018**, *2*, 15–20.
- Kakutani, K.; Takikawa, Y.; Matsuda, Y. Selective arcing electrostatically eradicates rice weevils in rice grains. *Insects* **2021**, *12*, 522. [CrossRef]
- Kaiser, K.L. (Ed.) Air breakdown. In *Electrostatic Discharge*; Taylor & Francis: New York, NY, USA, 2006; pp. 1–93.
- Wegner, H.E. Electrical charging generators. In *McGraw-Hill Encyclopedia of Science and Technology*, 9th ed.; Geller, E., Moore, K., Well, J., Blumet, D., Felsenfeld, S., Martin, T., Rappaport, A., Wagner, C., Lai, B., Taylor, R., Eds.; The Lakeside Press: New York, NY, USA, 2002; pp. 42–43.
- Griffith, W.T. Electrostatic phenomena. In *The Physics of Everyday Phenomena, a Conceptual Introduction to Physics*; Brufflodt, D., Loehr, B.S., Eds.; McGraw-Hill: New York, NY, USA, 2004; pp. 232–252.
- Kakutani, K.; Matsuda, Y.; Toyoda, H. A simple and safe electrostatic method for managing houseflies emerging from underground pupae. *Agronomy* **2023**, *13*, 310. [CrossRef]
- Pl@ntNet. 10000 Most Identified Plant Species. Available online: <https://plantnet.org/en/> (accessed on 2 March 2022).

31. National Fire Protection Association. About the NEC®/Grounding & Bonding. Available online: <https://www.nfpa.org/NEC/About-the-NEC/Grounding-and-bonding> (accessed on 21 April 2022).
32. Nor, N.M.; Rajab, R.; Ramar, K. Validation of the calculation and measurement techniques of earth resistance values. *Am. J. Appl. Sci.* **2008**, *5*, 1313–1317. [CrossRef]
33. Jonassen, N. (Ed.) Abatement of static electricity. In *Electrostatics*, 2nd ed.; Kluwer Academic Publishers: Boston, MA, USA, 2002; pp. 101–120.

Disclaimer/Publisher’s Note: The statements, opinions and data contained in all publications are solely those of the individual author(s) and contributor(s) and not of MDPI and/or the editor(s). MDPI and/or the editor(s) disclaim responsibility for any injury to people or property resulting from any ideas, methods, instructions or products referred to in the content.

Article

Unattended Electric Weeder (UEW): A Novel Approach to Control Floor Weeds in Orchard Nurseries

Yoshinori Matsuda ^{1,2}, Koji Kakutani ^{2,3,4,*} and Hideyoshi Toyoda ²

¹ Laboratory of Phytoprotection Science and Technology, Faculty of Agriculture, Kindai University, Nara 631-8505, Japan; ymatsuda@nara.kindai.ac.jp

² Research Association of Electric Field Screen Supporters, Nara 631-8505, Japan; toyoda@nara.kindai.ac.jp

³ Pharmaceutical Research and Technology Institute, Kindai University, Osaka 577-8502, Japan

⁴ Anti-Aging Centers, Kindai University, Osaka 577-8502, Japan

* Correspondence: kakutani@kindai.ac.jp

Abstract: This study developed an unattended electric weeder (UEW) to control floor weeds in an orchard greenhouse. The UEW was a motor-driven dolly equipped with a spark exposer. The spark exposer was constructed by applying an alternating voltage (10 kV) to a conductor net (expanded metal net). The charged conductor net (C-CN) discharged into the surrounding space. Wild oat and white clover were used as test weed species. Weed seedlings growing on the floor were grounded by the biological conductor and were subjected to a spark from the C-CN when they reached the discharge space. The spark-exposed seedlings were singed and shrunk instantaneously. In the present experiment, the UEW was remotely controlled to move on the soil-cover metal nets, which were laid on the floor to make a flat surface, in a stop-and-go manner, and to eject a spark to the weed seedlings that emerged from the floor. All of the mono- and dicotyledonous weed seedlings, which had been artificially sown on the floor, were completely eradicated using this method. Thus, this study provides an experimental basis for developing an unattended technique for controlling floor weeds in an orchard greenhouse.

Keywords: alternating voltage; arc discharge-mediated spark; *Avena fatua* L.; expanded metal net; physical weed control; *Trifolium repens* L.; unattended electric weeder; voltage amplifier

Citation: Matsuda, Y.; Kakutani, K.; Toyoda, H. Unattended Electric Weeder (UEW): A Novel Approach to Control Floor Weeds in Orchard Nurseries. *Agronomy* **2023**, *13*, 1954. <https://doi.org/10.3390/agronomy13071954>

Academic Editor: Baohua Zhang

Received: 19 June 2023

Revised: 16 July 2023

Accepted: 23 July 2023

Published: 24 July 2023



Copyright: © 2023 by the authors. Licensee MDPI, Basel, Switzerland. This article is an open access article distributed under the terms and conditions of the Creative Commons Attribution (CC BY) license (<https://creativecommons.org/licenses/by/4.0/>).

1. Introduction

Many weed control strategies have been used by tree fruit growers, depending on the type of weed, area to be controlled, and availability and feasibility of laborers [1]. Weed control is necessary for sustainable crop production. Herbicide-based weed control is the most commonly used method in greenhouse and field crop production systems [2]. However, the intensive use of herbicides causes the emergence of many weeds resistant to major classes of herbicides [3,4]. In addition, greater public concern about the use of chemicals for managing all classes of pests (i.e., pathogens, insect pests, and weeds) has led to the development of non-chemical weed control methods [5]. Biological and physical methods have been integrated into total pest management systems as an alternative to chemicals [6].

Direct applications of living herbivorous insects [7,8] or fungal phytopathogens [9] are emerging techniques to control weeds biologically. Additionally, the use of bioherbicides provides another option for biochemical weed control. Bioherbicides include fungal phytotoxins [10,11] and plant-producing phytotoxins [12] or allelochemicals [13]. However, effective control is difficult to maintain because of the limited number of application targets, problematic preparation of the agent, and high cost; thus, little practical progress has been made using these methods. The main barrier to practical implementation is that it is difficult to integrate individual methods into large-scale weed control systems under different environmental conditions. In contrast, living and dead mulch methods [14,15]

have been practically implemented because of their easy and eco-friendly use. The most basic conventional physical methods include covering the soil surface with a weeding mulch film [16,17] and mowing [18], flaming [18], heating by steam [19], hot water, or hot foam [20], and tilling practices [18].

The fruit tree growers in our districts use tilling because of the disadvantages of other methods, including mulching, which entailed frequent renewal of the mulch film due to poor durability; flaming, with the potential risk of fire; mowing, with promoted regrowth by roots left in the soil; and other methods (living or dead mulch and thermal means), because the farmers were inexperienced. However, tilling operations require year-round intensive labor. Moreover, tilling has the potential to negatively impact the surface feeder roots of fruit trees [21]. To reduce labor requirements, some studies have proposed the use of robotic [22] or electrical [23–28] weeders. However, the high cost of these machine weeders limits their use, particularly on small farms [29]. Thus, the growers requested our cooperation (Research Association of Electric Field Screen Supporter, RAEFSS) to develop a new electric system, to control weeds automatically. The RAEFSS is a private research association that educates small farmers on electrostatic-based agricultural techniques [30]. Some types of electrostatic apparatus have been launched for insect pest control in response to farmers' requests [31–33]. The present study was conducted to meet the demands of farmers.

The arc discharge-exposure method for weed control was originally developed by Wilson and Anderson [23]. The principles of electricity used for weed control are provided in previous studies [34,35], where weeds at the soil-emerging stage were killed by directly exposing young shoots to a high-voltage arc (spark) discharge. Arcing is an electrical phenomenon generated by the movement of a high-voltage-mediated negative charge in the air between opposite electric conductors [36]. The soil-emerging weed shoots act as biological conductors that receive the discharge from a charged conductor [34]. This technique has been successfully applied to control kudzu (*Pueraria montana* var. *lobata* [Willd.] Ohwi) creeping along an animal-repelling electric fence [37] and for weed populations growing in crop fields [35]. These approaches suggest that a simple electric weed eradicator could be fabricated easily and inexpensively.

The present study aimed to develop an unattended method to control floor weeds in an orchard greenhouse. Thus, we fabricated a motor-driven dolly equipped with a spark-exposing apparatus (charged metal net), clarified the optimal conditions for killing mono- and dicotyledonous weed seedlings using the spark exposure treatment, and applied the system to control weed seedlings growing on the greenhouse floor by automatically moving the electric weeder. Based on these results, we evaluated the feasibility of the present method for controlling floor weeds in an orchard greenhouse and provide an experimental basis for developing an unattended electric weeding system.

2. Materials and Methods

2.1. Plant Species

Wild oat (*Avena fatua* L.) and white clover (*Trifolium repens* L.) were used as the model mono- and dicotyledonous weed species. The seeds (Takii & Co., Ltd., Kyoto, Japan) of these plants were sown in plastic trays containing soil, and elongated seedlings were used for the spark-exposure experiment in the laboratory. The seeds were sown directly on the greenhouse floor for the unattended weed control approach.

2.2. Experimental Instruments Used to Expose the Plant Seedlings to an Electric Spark

2.2.1. The Charged Conductor Net and Determining the Spark Distance

An expanded stainless net (60 × 50 cm²; strand thickness, 0.8 mm) (Okutani Wire Netting Mfg., Co., Ltd., Kobe, Japan) (Figure S1A) was used as the charged conductor net (CN). Alternating voltage was applied to the CN using a voltage amplifier (VA) (useable voltage, 10 kV; maximum current, 120 mA; 10 kHz) (Logy Electric Co., Ltd., Tokyo, Japan). The VA was linked to a grounded line, which was connected to a ground-contact wall

socket, and its charging probe was linked to the CN (Figure S2A). The charged conductor (C-CN) formed a discharge space in the surrounding air (Figure S2A). The expansion of the discharge space was determined by the voltage applied to the conductor [38].

The charged conductor discharges when the grounded conductor reaches the discharge space and causes an arc discharge in the air between the charged and grounded conductors. The arc discharge of the charged conductor is an electric phenomenon in which the high-voltage negative charge moves in the air with an instantaneous spark (spark discharge) [36]. In this experiment, we determined the distance between the C-CN and the grounded conductor required to cause a successful spark by the C-CN. An iron nail (5 cm length; 1 mm thickness) was connected to a grounded line and used as a grounded conductor. The C-CN was held horizontally with a plastic (polypropylene) clamp (insulator), and the grounded nail was vertically held under the C-CN (Figure S2B). The grounded nail was gradually brought closer to the C-CN to determine the point at which the spark discharge occurred (Figure S2C). Thus, we determined the longest distance (4 mm) from the C-CN (the edge of the discharge space) required to cause the spark discharge toward the grounded conductor.

2.2.2. Double-Net System for Exposing Plant Seedlings to an Electric Spark

In this experiment, we used wet soil in a plastic tray ($61 \times 51 \text{ cm}^2$; depth, 2 cm). The soil was grounded by contacting a grounded line that was introduced from the side wall of the tray (Figure 1A). Germinating wild oat and white clover seeds were sown in the soil, and a second expanded metal net ($60 \times 50 \text{ cm}^2$; strand thickness, 2.0 mm) (Figure S1B) was placed on the soil as a soil-cover net to create a flat and horizontal surface (Figure 1A). Seedlings that grew to 3–6 mm high from the upper surface of the soil-cover net were used for the spark exposure treatment. Namely, the C-CN (not charged) was held horizontally and set above the seedling-growing tray at an interval of 6 mm (discharge space of 4 mm and non-contact space of 2 mm) between the C-CN and the soil-cover net (Figure 1A). Then, the VA was switched on to charge the C-CN.

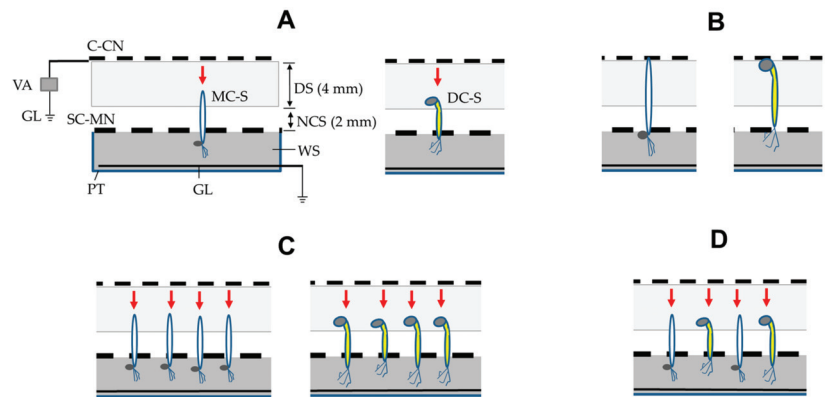


Figure 1. Exposure of wild oat (MC-S) and white clover (DC-S) seedlings to an electric spark generated by a charged conductor net (C-CN). (A) Spark exposure of single MC-S (left) and DC-S (right) that did not reach the C-CN. The C-CN was linked to a voltage amplifier (VA) and formed a 4-mm wide discharge space (DS). The soil-cover metal net (SC-MN) was placed on the wet soil (WS) in a plastic tray (PT) to make a flat surface. Seeds of the test plants were sown in the soil, which was in contact with a grounded line (GL) that was introduced from the tray wall. The distance between the C-CN and the SC-MN was fixed at 6 mm. (B) Exposing a single seedling to the spark that reached the C-CN. (C) Exposing multiple seedlings (2–20 seedlings) to the spark. (D) MC- and DC-Ss were exposed to sparks and growing on the same tray. The red arrow represents the spark from the C-CN to the seedling.

In the first experiment, we exposed single wild oat and white clover seedlings that had reached the discharge space, but not the C-CN (Figure 1A). The coleoptile and hypocotyl were the spark-exposed sites of these weeds, respectively. As the spark exposure stopped automatically, we measured the duration of the spark exposure to compare the tolerance between the two weed species. In the second experiment, the seedlings that had reached the C-CN were similarly treated to compare the time of spark exposure between them and between the C-CN-touched and untouched cases (Figure 1B). In both experiments, 20 seedlings were used for each weed species, and the experiments were repeated five times. In the third experiment, multiple seedlings growing on the same tray were exposed to the spark (Figure 1C). Namely, we prepared 10 groups, which contained 2, 4, 6, 8, 10, 12, 14, 16, 18, and 20 seedlings on the tray, and placed each group beneath the C-CN for spark exposure. As the sparks were launched one by one or stepwise toward all seedlings and then stopped automatically, the duration of the spark exposure was examined to determine the relationship between the time of spark exposure and the number of seedlings of each weed species used. Additionally, we conducted a similar experiment for the wild oat and white clover seedlings that were grown half-and-half on the same tray. All experiments were repeated five times.

2.3. Construction of a Motor-Driven Dolly Carrying the C-CN and Its Application to Greenhouse Floor Weeding

2.3.1. Construction of the Unattended Electric Weeder

We installed the C-CN on a motor-driven dolly (floor area, $70 \times 90 \text{ cm}^2$) (Figure 2A). The C-CN ($60 \times 50 \text{ cm}^2$) was horizontally attached to the outer surface of the bottom of the dolly; the discharge space was formed between the C-CN and the soil-cover metal net that was laid on the ground (Figure 2B). The movement of the dolly was remotely controlled by a motor-operating controller linked to the dolly with a coiled extension electric cable. The C-CN-equipped dolly was used as an unattended electric weeder (UEW) to control floor weeds in an orchard greenhouse.

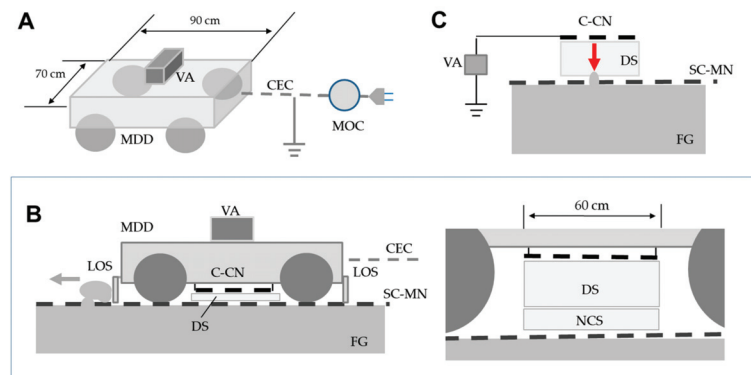


Figure 2. (A) A motor-driven dolly (MDD) carrying a charged conductor net (C-CN). (B) Cross-sectional view of the MDD. The C-CN was linked to a voltage amplifier (VA) and equipped on the outer surface of the bottom of the dolly. The discharge space (DS) (4 mm wide) was formed in the space between the C-CN and the soil-cover metal net (SC-MN) laid on the floor (FG). The interval between the C-CN and the SC-MN was fixed at 6 mm, including 4 mm of DS and 2 mm of non-contact space (NCS). The level-off-soil sliders (LOSs) were equipped in the front and back of the dolly. The dolly was remotely operated by a motor-operation controller (MOC) that was linked with a coiled extension electric cable (CEC). (C) Exposing the soil to a spark that protruded from the SC-MN. The soil over the SC-MN reached the DS to receive the arc-discharge-mediated spark (red arrow) from the C-CN. Extra soil over the SC-MN was removed by the LOS when moving (gray arrow) the dolly (B).

2.3.2. Level-Off-Soil Operation to Avoid Undesired Sparking of the Ground Soil

Five soil-cover metal nets (each, $1 \times 1 \text{ m}^2$) were laid on the greenhouse floor to make the floor flat for the UEW. However, the problem was that the ground soil protruded from the upper surface of the CN, as these soils reached the discharge space to receive the spark from the C-CN (Figure 2C). To avoid this undesired sparking, we attached flat plates to the front and back of the dolly to level off the soil (Figure 2B). The extra soil on the soil-cover metal net was pushed away as the dolly moved (Figure 2B). This leveling-of-soil operation readied the discharge space beneath the C-CN to expose only plant seedlings to the spark. As the arc discharge was always accompanied by a specific sound (arc-discharge sound) [28,29,31], effective elimination of the extra soil was confirmed by checking for the presence or absence of the arc-discharge sound by moving the UEW over the soil-cover metal net at the stage before the weed seedlings appeared.

2.3.3. Application of the UEW to Control Floor Weeds in a Greenhouse

The UEW (Figure 3A) was used for unattended control of floor weeds in a greenhouse. Seeds (300, 600, and 900 seeds) of the test weeds were mixed half and half and sown directly in the seeding area (SA1–3) (each $60 \times 100 \text{ cm}^2$) on the greenhouse floor. The seeded areas were covered with soil-cover metal nets ($1 \times 1 \text{ m}^2$) in a row (Figure 3B). Two additional nets were placed on both sides of the net row to prepare the departure and arrival places for the UEW. The movement of the UEW was controlled remotely using a motor-operated controller. The UEW was moved over the connected soil-cover nets from one end to the other in a stop-and-go manner: 5 cm/s for 10 s and stopping for 3 min. The UEW traveled forward (Figure 3B) and returned (Figure 3C) using the same route. This go-and-return movement of the UEW was repeated twice daily (morning and evening) for 1 week. The exposure treatment started when the first seedling appeared on the soil-cover nets and continued for 1 week. The numbers of seedlings (1) exceeding the C-CN (ECCN-seedlings), (2) reaching the discharge space (RDS-seedlings), and (3) not reaching the discharge space (URDS-seedlings) were counted using a leveling-wire stand (Figure 3C) each day after the evening treatment was completed. As a control, three seeding areas covered with nets were similarly prepared in the neighborhood, but the spark-exposure treatment was not applied. The numbers of whole weeds and ECCN seedlings were counted each day during the experimental periods. Separate experiments were replicated five times. The experiments were carried out from July to August 2022. The diurnal change in the greenhouse temperature and relative humidity during the experimental periods was 16 to 36 °C and 48 to 98%, respectively.

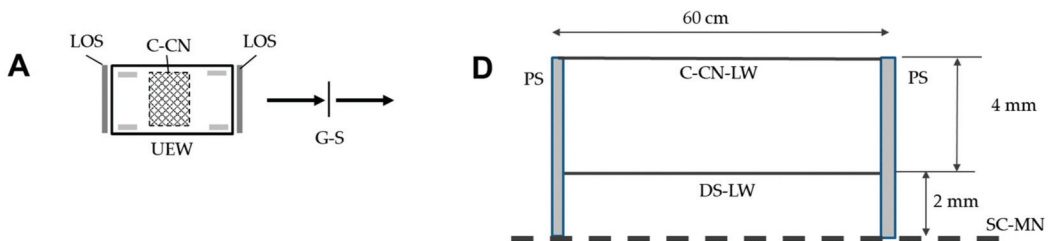


Figure 3. Cont.

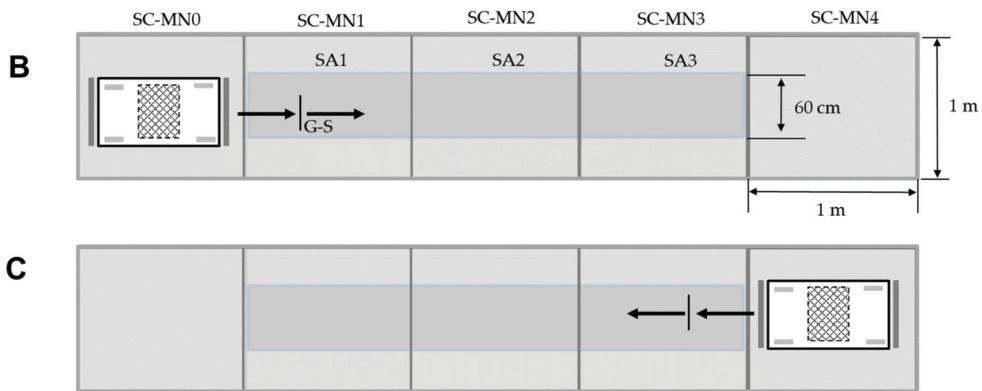


Figure 3. Design of the spark-exposure treatment of greenhouse floor weeds with an unattended electric weeder (UEW). (A) A bird's-eye view of the UEW equipped with a charged conductor net (C-CN) and two level-off-soil sliders (LOSs). (B,C) Weed seeding, placement of metal nets (SC-MNs), and movement of the UEW. Seeds were sown in the seeding areas (SA1–3) of the greenhouse floor, and three SC-MNs nets (SC-MN-1–3) were laid over SA1–3 in a row, respectively. An additional two nets (SC-MN-0 and 4) were placed on both sides of the net row to make departure and arrival places for the UEW. The UEW was moved over the connected SC-MNs from one end to the other in a stop-and-go manner (G-S). The UEW was remotely controlled to go forward (B) and return (C) on the same route. (D) A leveling-wire stand to examine the height of the seedlings (cross-sectional view). Two iron wires (C-CN- and DS-LW) were bridges between two identical plastic stands (PSs) 2 and 6 mm above the SC-MN, respectively. The leveling-wire stand slid on the SC-MNs and allowed the height of each seedling to be checked.

2.4. Statistical Analysis

All experiments were repeated five times, and the data are presented as mean \pm standard deviation. Tukey's test and linear regression analysis were performed using EZR software v1.54 (Jichi Medical University, Saitama, Japan) [39] to detect significant differences between conditions and the correlations among the factors.

3. Results

3.1. Sparking Distance of the C-CN

The primary objective of the present study was to determine the sparking distance of the C-CN. The sparking distance was determined by the voltage applied to the conductor. A conductor charged with a higher voltage produces a wider discharge space in the surrounding area [38]. The spark discharge of the C-CN occurred the moment the pointed tip of the grounded iron nail reached the outer edge of the discharge field (4 mm from the C-CN). This distance was considered the C-CN sparking distance. The importance of the sparking-distance specification was to make it possible to construct an apparatus that ejects a discharge-mediated spark to every grounded conductor that comes into an area within 4 mm from the C-CN. As plant seedlings growing on the ground are grounded biological conductors [34], they can be targeted for the spark by the C-CN.

3.2. Exposure of Plant Seedlings to an Arc Discharge-Mediated Spark

Previous studies [34,35] have suggested that the spark-exposure treatment effectively kills weed seedlings. Thus, we evaluated the effectiveness of an electric spark produced by the present apparatus. In the first experiment, we ejected the spark to single wild oat and white clover seedlings to determine the destructive power of the electric spark. Video S1A,B demonstrates that the energy of the electric spark was highly destructive; the white clover seedlings were singed instantaneously, while the wild oat seedlings were

singed and shrunk after a short exposure. These results strongly suggest the involvement of current-flow-mediated heating (Joule heating) [40] during this type of seedling destruction. These results also indicate that there was a significant difference in the time of spark exposure between the two weed species (Figure 4). The spark exposure of the white clover seedlings stopped in less than 1 s, whereas the exposure of the wild oat seedlings continued for 5–7 s. This result suggests that the different tolerances of the two weed plants were due to different electrical characteristics of the coleoptiles (wild oat) and hypocotyls (white clover) of the seedlings that received the spark. The hypocotyls were more susceptible to spark exposure than the coleoptiles (Video S1B). We considered that the hypocotyls of the white clover seedlings were more conductive than the coleoptile tissue of the wild oat seedlings and, therefore, larger amounts of electric current caused rapid destruction of the white clover seedlings. In addition, we spark-exposed single wild oat and white clover seedlings that reached the C-CN. Video S1A,B shows that similar destructive effects were detected on these two seedlings when they touched the C-CN. Figure 4 indicates no significant difference in the duration of the spark exposure between the seedlings that touched and did not touch the C-CN in either weed species. We concluded that the present apparatus could handle the seedlings that exceeded the C-CN as well as the seedlings beneath the C-CN.

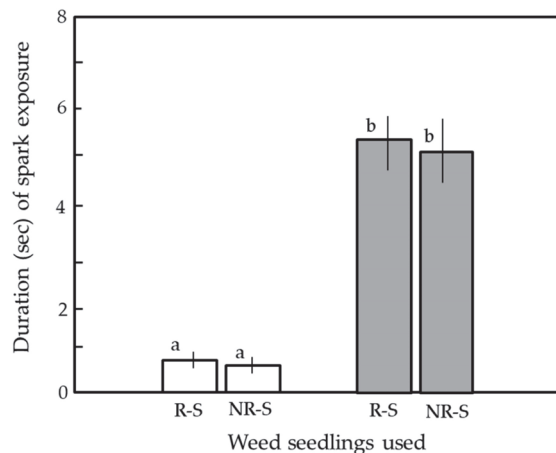


Figure 4. Comparison of the duration of spark exposure of a single white clover (open) and wild oat (gray column) seedlings. R-S and NR-S denote the seedlings that reached and did not reach the charged conductor net, respectively. Twenty seedlings were used for each weed species. Mean and standard deviation values were calculated from five experimental replicates. Different letters (a, b) in each vertical column indicate significant differences ($p < 0.05$) according to Tukey's test.

The main objective of the present experiment was to determine the size of the target population, i.e., the maximum number of weed seedlings that the present apparatus could treat at one time. Thus, we exposed multiple wild oat and white clover seedlings to sparks. The results indicated that there were two spark exposure methods for these plants. Video S2 shows the cases of three wild oat and white clover seedlings. The white clover seedlings were subjected to the spark in a one-by-one manner from the tallest seedling. The seedlings were knocked down by a single spark discharge (Figure S3A). In contrast, the exposure was first directed to the tallest wild oat seedling. However, the exposure was turned to the second tallest and then the third tallest seedling when the height of the first seedling became smaller than these seedlings, and finally returned to the first seedling (Figure S3B). Spark exposure continued until all seedlings were short of the C-CN discharge space. These two types of spark exposures included all cases of both weed species, regardless of the number of seedlings applied.

For the linear regression analysis between the number of the seedlings applied and the time length of the spark exposure, until the exposure stopped automatically, we exposed multiple seedlings (2–20 seedlings) of the test weeds to the spark and measured the duration of spark exposure. Figure 5 shows the results of the wild oat (A), white clover seedlings (B), and a half-and-half mixture of the two weed species (C). In each case, the R-squared value represented a relatively good fit of the line to the data; as the number of the seedlings treated increased, a longer spark exposure treatment was required to eradicate all of the seedlings. Thus, this trend was useful to illustrate the predicted treatment time length in response to an increase in the weeds growing on the floor area.

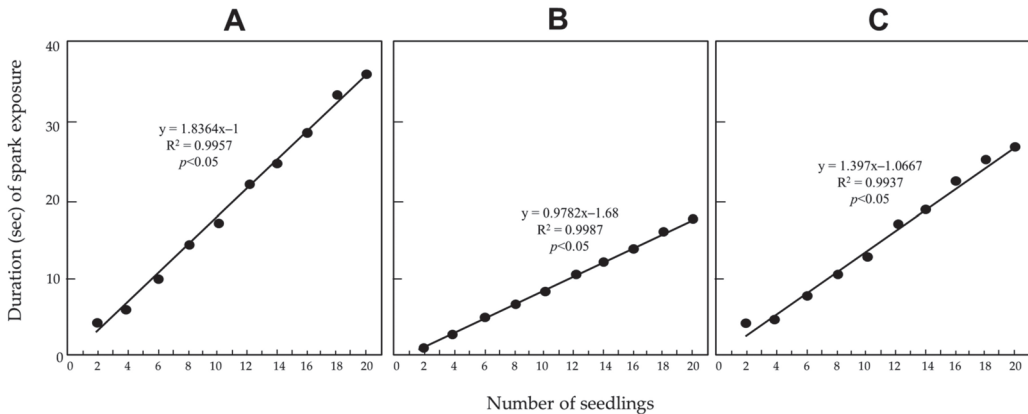


Figure 5. Relationship between the number of weed seedlings and the duration of spark exposure. (A,B) represent a group of wild oat and white clover seedlings, respectively. (C) represents a group that contained half wild oat and half white clover seedlings. Note that each of the R-squared values (0.9957, 0.9987, and 0.9937) obtained was a relatively good fit with the line to the data.

The present study revealed that current-flow-mediated heating was the key mechanism for destroying weed seedlings. Based on this interpretation, the weed destruction efficiency was dependent on the output voltage and current of the apparatus. This was a problem of the VA used in the present study. The maximum output of the present VA was 10 kV/120 mA, which was the limit of the working capacity of the apparatus. We searched for the optimal weeding conditions.

3.3. Application of the UEW to Control Floor Weeds in a Greenhouse

3.3.1. Prerequisite Operations before the Spark-Exposure Treatment

The greenhouse floor can be used as a grounded conductor if the soil is sufficiently wet. Matsuda et al. [34] reported that free water in the ground soil easily evaporates through a low-temperature (30 °C) dehydration procedure and that the soil loses conductance when 60% of the free water is lost by evaporation. Water in the superficial soil layer easily evaporates, particularly during the high-temperature season. Many weeds live in this soil layer, so keeping the soil wet was essential to ensure successful current flow from the spark-exposed plant seedlings to the ground via the floor soil [34]. Thus, watering the floor is an effective way to ground the floor soil; that is, to ensure satisfactory spark-exposure efficiency.

The second prerequisite was the trial run of the UEW to level off the extra soil that protruded from the soil-cover metal net on the floor. The level-off-soil slider attached to the UEW was an effective way to push the soil away (Figure 2B), by which the C-CN was allowed to preferentially eject the spark to target plant seedlings during the spark-exposure treatment.

3.3.2. Greenhouse Assay for Controlling Floor Weeds by the UEW

We developed an unattended method to control weed seedlings growing on a greenhouse floor by automatically moving the UEW in a stop-and-go manner. We had two basic problems applying the present system. The first problem was the number of seedlings that the UEW could treat at one time. The most important parameter was the stopping time, as the spark-exposure treatment was performed while the UEW was stopped. In this experiment, we determined the required exposure time by predicting the number of seedlings involved in the C-CN ($60 \times 50 \text{ cm}^2$) sparking area (Figure 5). Our preliminary observations showed that the emergence rate of the seeds was approximately 90% for both weed species and that these seedlings appeared successively on the ground over 5 days. Based on this observation, we calculated the exposure times (UEW-length of stop time) from the case that 900 seeds (the highest number) of the wild oat required longer exposure times than the white clover were sown. As a result, the UEW C-CN was expected to encounter a maximum of approximately 80 seedlings per stop. Judging from the wild oat trend (Figure 6A), a 3 min exposure would be long enough for the UEW to treat all 80 wild oat seedlings during one stop. The second problem was that the URDS seedlings (seedlings that had not reached the discharge space yet) comprised the majority. The UEW passed over these seedlings without ejecting a spark. Nevertheless, the rapid growth of weed seedlings helped solve this problem. In our preliminary observations, the weed seedlings elongated 2–4 mm per half day and, therefore, the URDS seedlings were expected to grow to be RDS seedlings in half a day. It was possible to treat these seedlings by weeding in the morning and evening. We applied the go-and-return movement of the UEW (Figure 3B,C) twice per day in the morning and evening for 1 week.

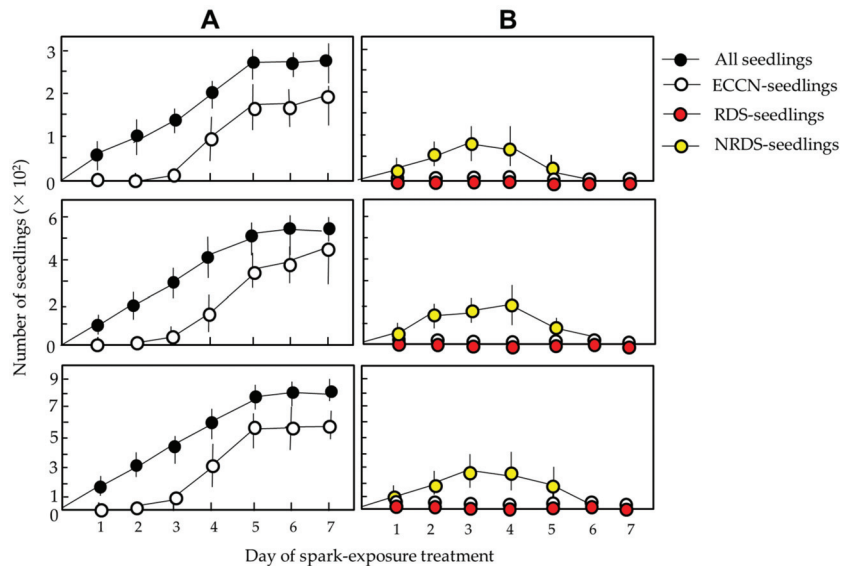


Figure 6. Treatment of the weed seedlings with a spark generated by the charged conductor net (C-CN) on the unattended electric weeder (UEW). The upper, middle, and lower panels represent the seeding area (SA1–3), where 300, 600, and 900 seeds of wild oat or white clover were sown half and half, respectively. (A) Untreated weed seedlings that were grown on the greenhouse floor were covered with an expanded metal net (control). (B) Weed seedlings that were exposed to a spark from the UEW that was automatically moved over the metal nets laid on the seeding area. ECCN, RDS, and URDS seedlings represent the seedlings exceeding the C-CN, reaching the discharge space of the C-CN, and not reaching the discharge space, respectively. Means and standard deviations were calculated from five experimental replicates.

Figure 6 shows the results of the spark-exposure treatment for the weed seedlings on the greenhouse floor. In this experiment, different numbers of wild oat and white clover seedlings (300, 600, and 900 seedlings in seeding areas SA1, 2, and 3) were used. The weed seedlings in the untreated control (Figure 6A) appeared successively between D1 and D5 and rapidly elongated 4–8 mm per day; the seedlings (ECCN seedlings) that exceeded the height of the C-CN first appeared at D4 and increased rapidly thereafter. Neither the RDS nor the URDS seedlings were counted in the untreated seeding area because it was difficult to distinguish them among the numerous vigorously growing seedlings. As a result, the rates of the seedlings that developed from seed were $90.8 \pm 2.5\%$ for the wild oat and $89.3 \pm 4.3\%$ for the white clover in the three seeding areas from five separate experiments.

Figure 6B shows the number of seedlings that were still living after two spark-exposure treatments per day. The most important point was that the taller seedlings (ECCN and RDS seedlings) were not detected in the three seeding areas throughout the entire experimental period, suggesting that the apparatus controlled all of the ECCN and RDS seedlings that appeared on these days. Thus, two (morning and evening) treatments were highly effective to catch up with the URDS seedlings that escaped from the earlier exposure treatment. Figure 6A shows that the newly elongated seedlings appeared successively between days 1 and 5. All of these seedlings grew into the discharge space on days 6 and 7 and were subjected to the spark. All of the seedlings were eventually eradicated by the UEW, twice per day, for 7 days. The spark exposure treatment was effective, regardless of the number of seedlings and different weed species. Figure 7 is an illustrative example of a successful application of the present method to the floor weeds in a greenhouse. The photograph shows the situation on day 7; two rows of the soil-cover metal nets were arranged in parallel on the floor for an easy comparison of the effect (Figure 7A). One row was the untreated control, where the weed seedlings had elongated vigorously depending on the number of seeds sown (300, 600, or 900 seeds in the SA1 to 3, respectively), and the other was the row for the spark-exposure treated division, in which all of the seedlings were effectively eradicated by the treatment (Figure 7A,B). Thus, these results indicate that the unattended method using the UEW was practical for controlling floor weeds in a greenhouse.

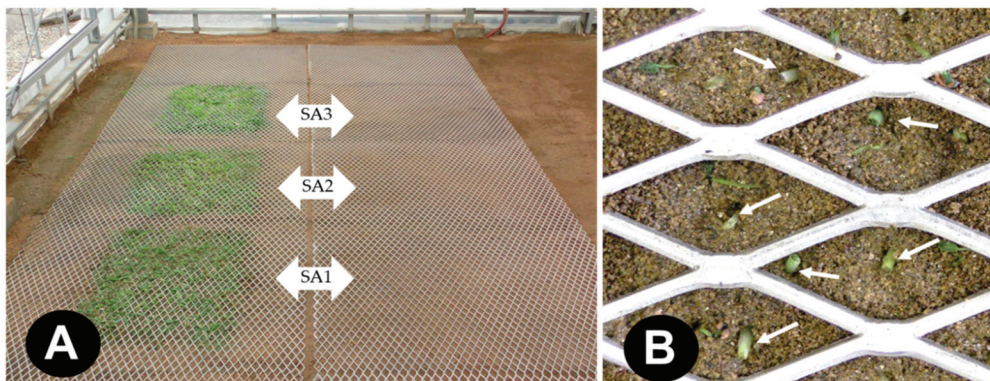


Figure 7. Eradication of weed seedlings growing on the floor of a greenhouse with an unattended electric weeder. (A) Two rows of connected soil-cover metal nets were arranged in parallel on the floor of the greenhouse. The left row was for the untreated weed seedlings (control), and the right row was for the seedlings that were treated with sparks twice a day for 1 week. No seedling appeared in the seeding area (SA1–3) on the right-side net row, in contrast to the vigorous growth of the seedlings in the neighboring control. (B) A close-up of the ground surface beneath the soil-cover metal net shows weed seedlings (arrows) damaged severely by the spark-exposure treatment.

4. Discussion

In the present study, we successfully fabricated a remotely controlled motor-driven dolly that was equipped with a spark-exposure apparatus, demonstrated the ability of the apparatus to kill weed seedlings, and provided an experimental basis for applying the present method to floor weed control in an orchard greenhouse. In addition to this technical progress, many growers have an overriding concern about the costs of manufacturing the UEW and purchasing the soil-cover metal nets. To fabricate the UEW, we purchased a motor-driven dolly and a voltage amplifier. The C-CN, which is the heart of the UEW, was easily installed by linking a flat metal net to a voltage amplifier with an electric wire and attaching it horizontally to the outer surface of the bottom of the dolly. In fact, the expense necessary for preparing the UEW was only the cost of materials, which was approximately \$1500 in U.S. dollars. The costs for the metal nets vary with the size of the floor covered. In our ordinary orchard greenhouse (floor area, $20 \times 20 \text{ m}^2$), approximately 250 metal nets were needed to cover the floor for weeding, and the cost was estimated at approximately \$2000 (approximately \$8 per square meter). Eventually, the growers may be costed this amount of expenses to perform the present system in a greenhouse.

Although the present study revealed that this method can be used to manage mono- and dicotyledonous weed species effectively, some questions need to be clarified in our subsequent study. Our concern now involves how to use this method to control creeping perennial weeds with subterranean stems or rhizomes in the floor [21]. To solve this problem, it may be useful to clarify the conductivity of weed seedlings, which is an issue pertaining to how long the electric current flows in the weed body. The present results suggest that the portions of the weed bodies in which electric current flowed were passively destroyed. Another concern is the possibility of inter-root transfer of a negative charge, particularly between the roots of weeds and young fruit trees. As their root systems may be intertwined in a superficial layer of the soil [21], clarifying this problem would avoid the undesired effects of a negative charge that flows through weed roots reaching the roots of a fruit tree.

The present method required a flat floor surface. Thus, we laid several expanded metal nets on the floor area to be weeded. The metal nets used in this study (2 mm strands) were sturdy enough for workers to conduct operations on the nets. This allowed us to leave the metal nets there throughout the year. Nevertheless, we have no information about how the present metal nets bear the load of heavier farm equipment used in a greenhouse cropping system. Further investigations are required to answer this question. Our orchard greenhouse was an ideal place to lay the metal nets on the floor because there are no ridges for crop cultivation. However, this advantage may be an obstacle to broad applications of the present method to other field and greenhouse crop production systems. In particular, a new device for curved portions, such as a cropping ridge, is essential for this purpose.

Applying the UEW for floor weed control in an orchard greenhouse was expected to reduce labor. From this viewpoint, we designed the next study. The purpose of the study was to completely automate weeding operations and optimize the system. Thus, we used a storage battery-operated VA to save energy and a wireless apparatus for sending and receiving signals to remotely control the movement of the UEW. Then, we examined the relationships between weeding efficiency and (1) the voltage applied, (2) the size of the spark-exposed area (the area of the C-CN), (3) the length of spark exposure (length of stop time), (4) the number and timing of the weeding operations during a day, and (5) the age and types of and population size of the weeds to be targeted. The final purpose was to program a computer with these data for automatic weed operation in the future.

5. Conclusions

We have presented a remote-controllable electric weeder armed with a spark-exposing apparatus. The spark-exposure treatment was highly effective for killing weed seedlings instantaneously, regardless of the cotyledon type. Operation of the weeder was programmed based on the diurnal elongation of the weed seedlings and effectively killed the seedlings

that emerged on the greenhouse floor ground at different times. The use of this weeder is expected to lighten weeding labor by growers. The structure of the weeder is simple, and the parts of the apparatus are affordable, such that the growers could fabricate the weeder without any special skills. Thus, the present study provides beneficial information for realizing the unattended control of floor weeds.

Supplementary Materials: The following supporting information can be downloaded at: <https://www.mdpi.com/article/10.3390/agronomy13071954/s1>, Figure S1: The two expanded stainless nets were used for the present study, Figure S2: Charging of the conductor metal net with an alternating voltage amplifier (VA) and a spark generated by a charged conductor net (C-CN), Figure S3: Exposing three white clover (A) and wild oat (B) seedlings to a spark generated by a charged conductor net (C-CN), Video S1: Wild oat (A) and white clover (B) seedlings exposed to the spark from a charged conductor net (C-CN), Video S2: Three white clover (A) and wild oat clover (B) seedlings were exposed to a spark from the charged conductor net (C-CN).

Author Contributions: Conceptualization, H.T., Y.M. and K.K.; methodology, Y.M. and H.T.; software, Y.M. and K.K.; validation, K.K., Y.M. and H.T.; formal analysis, Y.M.; investigation, Y.M.; resources, Y.M.; data curation, K.K.; writing—original draft preparation, H.T.; writing—review and editing, Y.M. and K.K.; visualization, Y.M.; supervision, H.T.; project administration, Y.M. and K.K. All authors have read and agreed to the published version of the manuscript.

Funding: This research received no external funding.

Data Availability Statement: Not applicable.

Conflicts of Interest: The authors declare no conflict of interest.

References

1. WSU Tree Fruit: Comprehensive Tree Fruit Site. Weed Control. Available online: <https://treefruit.wsu.edu/crop-protection/weed-control/> (accessed on 12 May 2023).
2. Davis, A.S.; Frisvold, G.B. Are herbicides a once in a century method of weed control? *Pest Manag. Sci.* **2017**, *73*, 2209–2220. [CrossRef] [PubMed]
3. Green, J.M. Current state of herbicides in herbicide-resistant crops. *Pest Manag. Sci.* **2014**, *70*, 1351–1357. [CrossRef] [PubMed]
4. Heap, I. Global perspective of herbicide-resistant weeds. *Pest Manag. Sci.* **2014**, *70*, 1306–1315. [CrossRef] [PubMed]
5. Carvalho, F.P. Pesticides, environment, and food safety. *Food Energy Secur.* **2017**, *6*, 48–60. [CrossRef]
6. Lewis, W.J.; van Lenteren, J.C.; Phatak, S.C.; Tumlinson, J.H., III. A total system approach to sustainable pest management. *Proc. Natl. Acad. Sci. USA* **1997**, *94*, 12243–12248. [CrossRef]
7. Catton, H.A.; Lalonde, R.G.; De Clerck-Floate, R.A. Differential host-finding abilities by a weed biocontrol insect create within-patch spatial refuges for nontarget plants. *Environ. Entomol.* **2014**, *43*, 1333–1344. [CrossRef]
8. Catton, H.A.; Lalonde, R.G.; De Clerck-Floate, R.A. Nontarget herbivory by a weed biocontrol insect is limited to spillover, reducing the chance of population-level impacts. *Ecol. Appl.* **2015**, *25*, 517–530. [CrossRef]
9. Morin, L. Progress in Biological Control of Weeds with Plant Pathogens. *Annu. Rev. Phytopathol.* **2020**, *58*, 201–223. [CrossRef]
10. Sharma, S.; Pandey, L.M. Prospective of fungal pathogen-based bioherbicides for the control of water hyacinth: A review. *J. Basic Microbiol.* **2022**, *62*, 415–427. [CrossRef]
11. Cimmino, A.; Masi, M.; Evidente, M.; Superchi, S.; Evidente, A. Fungal phytotoxins with potential herbicidal activity: Chemical and biological characterization. *Nat. Prod. Rep.* **2015**, *32*, 1629–1653. [CrossRef]
12. Anese, S.; Rial, C.; Varela, R.M.; Torres, A.; Molinillo, J.M.G.; Macías, F.A. Search of new tools for weed control using *Partocrat rotundifolia*, a dominant species in the Cerrado. *J. Agric. Food Chem.* **2021**, *69*, 8684–8694. [CrossRef] [PubMed]
13. Macías, F.A.; Mejías, F.J.; Molinillo, J.M. Recent advances in allelopathy for weed control: From knowledge to applications. *Pest Manag. Sci.* **2019**, *75*, 2413–2436. [CrossRef]
14. Sportelli, M.; Frascioni, C.; Fontanelli, M.; Pirchio, M.; Gagliardi, L.; Raffaelli, M.; Peruzzi, A.; Antichi, D. Innovative living mulch management strategies for organic conservation field vegetables: Evaluation of continuous mowing, flaming, and tillage performances. *Agronomy* **2022**, *12*, 622. [CrossRef]
15. Kornecki, T.S.; Price, A.J.; Raper, R.L.; Arriaga, F.J. New roller crimper concepts for mechanical termination of cover crops in conservation agriculture. *Renew. Agric. Food Syst.* **2009**, *24*, 165–173. [CrossRef]
16. Petrikovszki, R.; Zalai, M.; Bogdányi, F.T.; Ferenc Tóth, F. The effect of organic mulching and irrigation on the weed species composition and the soil. *Plants* **2020**, *9*, 66. [CrossRef]
17. Wang, K.; Sun, X.; Long, B.; Li, F.; Yang, C.; Chen, J.; Ma, C.; Xie, D.; Wei, Y. Green production of biodegradable mulch films for effective weed control. *ACS Omega* **2021**, *6*, 32327–32333. [CrossRef] [PubMed]

18. Mainardis, M.; Boscutti, F.; Cebolla, M.D.M.R.; Pergher, G. Comparison between flaming, mowing and tillage weed control in the vineyard: Effects on plant community, diversity and abundance. *PLoS ONE* **2020**, *5*, 0238396. [CrossRef]
19. Bond, W.; Grundy, A.C. Non-chemical weed management in organic farming systems. *Weed Res.* **2001**, *41*, 383–405. [CrossRef]
20. Martelloni, L.; Frascioni, C.; Sportelli, M.; Fontanelli, M.; Raffaelli, M.; Peruzzi, A. Hot foam and hot water for weed control: A comparison. *J. Agric. Eng.* **2021**, *52*, 1167. [CrossRef]
21. Country Folks Grower: Orchard Insights: Weed Control Options in Tree Fruit. Available online: <https://cfgrower.com/orchard-insights-weed-control-options-in-tree-fruit/> (accessed on 12 May 2023).
22. Fennimore, S.A.; Cutulle, M. Robotic weeders can improve weed control options for specialty crops. *Pest Manag. Sci.* **2019**, *75*, 1767–1774. [CrossRef]
23. Wilson, R.G.; Anderson, F.N. Control of three weed species in sugar beets (*Betavulgaris*) with an electrical discharge system. *Weed Sci.* **1981**, *29*, 93–97. [CrossRef]
24. Diprose, M.F.; Benson, F.A. Electrical methods of killing plants. *J. Agric. Eng. Res.* **1984**, *30*, 197–209. [CrossRef]
25. Nagura, A.; Tenma, T.; Sakaguchi, Y.; Yamano, N.; Mizuno, A. Destruction of weeds by pulsed high voltage discharges. *J. Inst. Electrostat. Jpn.* **1992**, *16*, 59–66.
26. Mizuno, A. Destruction of weeds by high voltage discharge. *J. Plasma Fusion Res.* **1999**, *75*, 666–671. [CrossRef]
27. Minoda, A. A basic study on weeding method by using high voltage. *Jpn. J. Ind. Appl. Eng.* **2021**, *9*, 21–24.
28. Lati, R.N.; Rosenfeld, L.; David, I.B.; Bechar, A. Power on! Low-energy electrophysical treatment is an effective new weed control approach. *Pest Manag. Sci.* **2021**, *77*, 4138–4147. [CrossRef] [PubMed]
29. Ekeleme, F.; Dixon, A.; Atser, G.; Hauser, S.; Chikoye, D.; Korie, S.; Olojede, A.; Agada, M.; Olorunmaiye, P.M. Increasing cassava root yield on farmers' fields in Nigeria through appropriate weed management. *Crop Prot.* **2021**, *150*, 105810. [CrossRef]
30. Research Association of Electric Field Screen Supporters. Major Projects. Available online: <http://www.electric-field-screen.org> (accessed on 12 May 2023).
31. Takikawa, Y.; Matsuda, Y.; Nonomura, T.; Kakutani, K.; Okada, K.; Shibao, M.; Kusakari, S.; Miyama, K.; Toyoda, H. Exclusion of whiteflies from a plastic hoop greenhouse by a bamboo blind-type electric field screen. *J. Agric. Sci.* **2020**, *12*, 50–60.
32. Takikawa, Y.; Nonomura, T.; Sonoda, T.; Matsuda, Y. Developing a phototactic electrostatic insect trap targeting whiteflies, leafminers, and thrips in greenhouses. *Insects* **2021**, *12*, 960. [CrossRef]
33. Kakutani, K.; Matsuda, Y.; Nonomura, T.; Takikawa, Y.; Osamura, K.; Toyoda, H. Remote-controlled monitoring of flying pests with an electrostatic insect capturing apparatus carried by an unmanned aerial vehicle. *Agriculture* **2021**, *11*, 176. [CrossRef]
34. Matsuda, Y.; Shimizu, K.; Sonoda, T.; Takikawa, Y. Use of electric discharge for simultaneous control of weeds and houseflies emerging from soil. *Insects* **2020**, *11*, 861. [CrossRef] [PubMed]
35. Matsuda, M.; Takikawa, Y.; Shimizu, K.; Kusakari, S.; Toyoda, H. Use of a pair of pulse-charged grounded metal nets as an electrostatic soil-cover for eradicating weed seedlings. *Agronomy* **2023**, *13*, 1115. [CrossRef]
36. Kaiser, K.L. Air breakdown. In *Electrostatic Discharge*; Kaiser, K.L., Ed.; Taylor & Francis: New York, NY, USA, 2006; pp. 1–93.
37. Matsuda, Y.; Takikawa, Y.; Kakutani, K.; Nonomura, T.; Okada, K.; Kusakari, S.; Toyoda, H. Use of pulsed arc discharge exposure to impede expansion of the invasive vine *Pueraria montana*. *Agriculture* **2020**, *10*, 600. [CrossRef]
38. Jones, E.; Childers, R. Electric charge and electric field. In *Physics*, 3rd ed.; McGraw-Hill: Boston, MA, USA, 2002; pp. 495–525.
39. Free Statistical Software EZR Version 1.61. Available online: <https://www.jichi.ac.jp/saitama-sct/SaitamaHP.files/statmedEN.html> (accessed on 12 May 2023).
40. Jones, E.; Childers, R. Electric current and resistance. In *Physics*, 3rd ed.; McGraw-Hill: Boston, MA, USA, 2002; pp. 557–593.

Disclaimer/Publisher's Note: The statements, opinions and data contained in all publications are solely those of the individual author(s) and contributor(s) and not of MDPI and/or the editor(s). MDPI and/or the editor(s) disclaim responsibility for any injury to people or property resulting from any ideas, methods, instructions or products referred to in the content.

Article

A Simple and Safe Electrostatic Method for Managing Houseflies Emerging from Underground Pupae

Koji Kakutani ¹, Yoshinori Matsuda ^{2,*} and Hideyoshi Toyoda ³

¹ Pharmaceutical Research and Technology Institute, and Anti-Aging Centers, Kindai University, Osaka 577-8502, Japan

² Laboratory of Phytoprotection Science and Technology, Faculty of Agriculture, Kindai University, Nara 631-8505, Japan

³ Research Association of Electric Field Screen Supporters, Nara 631-8505, Japan

* Correspondence: ymatsuda@nara.kindai.ac.jp

Abstract: A simple electrostatic apparatus that generates an arc discharge was devised to control adult houseflies emerging from a soil bed in a greenhouse. Adult houseflies emerging from a soil bed in a greenhouse are a potential vector of pathogenic *Escherichia coli* O157, carried by animal manure used for soil fertilization. A simple electrostatic apparatus that generates an arc discharge was devised to control these houseflies. The apparatus consisted of two identical metal nets; one was linked to a negative-voltage generator to create a negatively charged metal net (NC-MN), and the other was linked to a grounded line to create a grounded metal net (G-MN). A square insulator frame was placed between the two nets, separating them by 6 mm, and a plastic grating with multiple cells was placed beneath the G-MN to provide a climbing path (54 mm in height) to the arcing sites of the apparatus for adult houseflies emerging on the soil surface. Houseflies that climbed up the wall of the grating and reached the arcing zone were subjected to arc-discharge exposure from the NC-MN and thrown down onto the soil by the impact of the arcing. The impact was destructive enough to kill the houseflies. The structure of this apparatus is very safe and simple, enabling ordinary greenhouse workers to fabricate or improve it according to their own requirements. This study developed a simple and safe tool that provides a physical method to manage houseflies.

Keywords: arc-discharge exposer; electric field; expanded metal net; housefly; organic farming; pesticide-independent method; physical control; plastic grating

Citation: Kakutani, K.; Matsuda, Y.; Toyoda, H. A Simple and Safe Electrostatic Method for Managing Houseflies Emerging from Underground Pupae. *Agronomy* **2023**, *13*, 310. <https://doi.org/10.3390/agronomy13020310>

Academic Editor: Stefano Bedini

Received: 2 December 2022

Revised: 12 January 2023

Accepted: 18 January 2023

Published: 19 January 2023



Copyright: © 2023 by the authors. Licensee MDPI, Basel, Switzerland. This article is an open access article distributed under the terms and conditions of the Creative Commons Attribution (CC BY) license (<https://creativecommons.org/licenses/by/4.0/>).

1. Introduction

There is an increasing public concern regarding the use of chemicals for the management of all classes of pests (pathogens, insects, and weeds). Additionally, there is a serious risk of pesticide resistance developing in a wide range of weed species [1,2], pathogens [3,4], and insect pests [5,6]. This has led to the development of the organic farming of tomatoes in greenhouses. In organic farming, the introduction of food-waste compost, or green and animal manure, into soil beds in a greenhouse is a routine approach to for soil fertilization. Cattle manure is the major organic fertilizer in our greenhouse cultivation, and is typically applied once or twice each year. Unfortunately, the cattle manure often contains the larvae and pupae of the housefly *Musca domestica* (Linnaeus) (Diptera: Muscidae), resulting in the frequent emergence of adult houseflies from underground pupae during plant cultivation, because no synthetic insecticides are used in organic greenhouses.

The housefly problem presents a risk of transmitting pathogenic *Escherichia coli* O157 [7,8] posing a potential risk to public health. Food poisoning caused by *E. coli* O157 frequently occurs in people who have eaten fresh food contaminated by this pathogen. *E. coli* O157 in the intestines of cattle and sheep, where they do not cause disease, can spread to the human food chain through feces from these animals [8,9]. Housefly larvae develop in animal feces and very large populations accumulate, both on cattle farms and in other agricultural

facilities [7]. *E. coli* O157 ingested by houseflies remain viable in fly excreta; consequently, houseflies are able to carry and disseminate *E. coli* for several days [7]. Importantly, this bacterial pathogen is transferred from cattle manure used for soil fertilization [10]. Contamination of cultivated and postharvest crops with this pathogen is a serious problem that can endanger the food supply chain [11–13]. Insecticide substitution is therefore essential to control houseflies emerging from soil beds before they come into contact with crops in a greenhouse. The most basic and conventional method is to cover the soil surface with a weeding mulch film [14,15]. Unfortunately, mulch application is unsuitable for plant cultivation in the summer because of the undesirable increase in soil temperature. We therefore focused on electrostatic methods to manage houseflies at the soil bed surface.

Nononura et al. [16] devised an electrostatic soil cover to capture adult tomato leaf miner flies (syn. vegetable leaf miner), *Liriomyza sativae* Blanchard (Diptera: Agromyzidae), which emerged from underground pupae. This apparatus consisted of two sets of iron rods welded onto an iron frame. The iron rods and frame of one set of rods were coated with a soft polyvinyl chloride resin and linked to a negative-voltage generator, while the iron rods of the other set were not insulated and linked to a grounded line. Both sets of iron rods were arranged in an offset configuration to produce static electric fields between the oppositely charged iron rods. The charged insulated conductor wires of the apparatus exerted a strong force to capture the leaf miner adults that entered the electric field. However, the force of this apparatus was insufficient to capture larger insects such as adult houseflies.

Another electrostatic approach was the development of an arc (spark) discharge-exposing apparatus. The arc-discharge exposer (ADE) was originally devised to eradicate warehouse pests, such as rice weevil, *Sitophilus oryzae* (Linnaeus) (Coleoptera: Curculionidae), nesting in dried postharvest products [17,18], and Kakutani et al. [19] applied it to a pigsty window to kill the mosquitoes, *Culex tritaeniorhynchus* Giles (Diptera: Culicidae), that transmit Japanese encephalitis between pigs and humans. Matsuda et al. [20] utilized the arc discharge-exposing technique to simultaneously control weeds and houseflies emerging from the soil in a greenhouse. The proposed device consisted of two-storied ADEs. In each layer, identical iron plates were placed in parallel at a defined interval and fixed in an iron frame. Two layers of fixed iron plates were used, one (lower floor of the two-storied apparatus) for weed control and the other (upper) for fly control. For weed control, all of the iron plates were negatively charged, and the negative charges that accumulated on the plates were released to weed shoots through an arc discharge when the shoots entered the first floor. Houseflies were introduced into the space between the negatively charged and grounded plates on the second floor, and then subjected to an arc discharge from the charged plates. Both plant shoots and adult houseflies are electrically conductive; thus, they were killed by discharge exposure in the electric field between the charged iron plate and the ground soil, and between the charged and grounded plates. However, the complex configuration of this method discourages ordinary greenhouse workers from personally setting it up. The objective of this study was to propose a simple ADE that could be easily established by greenhouse workers.

Arcing is an electrical phenomenon caused by a high-voltage negative charge moving in the air from the charged conductor to the ground via grounded conductors [21]. The conductor is negatively charged by linking it to a negative-voltage generator. A negative charge accumulates on the surface of the conductor and positively polarizes the grounded conductor facing the charged conductor at a specified distance as a result of electrostatic induction [22]. An electric field is generated in the space between two metal nets [23]. The intensity of the arcing is determined by the voltage applied to the conductor and the distance between the opposite poles (charged and grounded conductors); larger voltages and shorter distances generate stronger arcing [21]. The stronger arcing can kill insect pests [17–20] and weeds [20,24] more effectively and in a shorter time after they enter the electric field. The insects that enter this electric field are exposed to an instantaneous exposure of high-voltage arc discharge from the charged conductor linked to the voltage generator [23]. In the present study, we used two identical expanded metal nets for the

oppositely charged conductors. The apparatus was constructed simply by pairing these nets in parallel at a given spacing; one was linked to a negative-voltage generator, and the other was linked to a grounded line. For practical applications, we used a pulse-charging-type voltage generator, which is commonly used with electric fences to repel wild animals. Electric fences are ubiquitous and essential in modern agriculture. Accidents associated with agricultural electric fences are very rare [25]. Although unintentional human contact with electric fences occurs regularly, it results in little more than temporary discomfort [25].

In this study, we aimed to determine: the optimal pole distance for arcing to houseflies without effects due to changes in greenhouse relative humidity (RH), the intensity of the sound generated by the pulsed arc-discharge exposure, and the number of pulsed arc discharges required to kill the houseflies. In addition, we clarified the two-step arcing system in the present apparatus, which enables the apparatus to cope with successive invasions by multiple houseflies. Based on the results obtained, this study is aimed to evaluate the feasibility of the present ADE for housefly control and provide an experimental basis for developing a promising physical method for managing adult houseflies emerging from underground pupae in the soil beds of greenhouses.

2. Materials and Methods

2.1. Insect Species

Adult houseflies (*M. domestica*) were purchased from Sumika Technoservice (Hyogo, Japan) and reared on a certified diet (MF; Oriental Yeast Co., Ltd., Tokyo, Japan) [26] in a closed 30 mL transparent acrylic vessel. Insect rearing was conducted in a growth chamber (25 ± 0.5 °C, 12 h photoperiod, 4000 lux) from the egg to adult stages. Pupae found on the medium were individually transferred onto fresh medium in a 20 mL vial for isolation, and the vial mouth was covered with gauze. The sex of adult flies emerging from the pupal stage was determined based on the sexual dimorphism of the external morphology of *M. domestica* [27]. The body sizes of adult male and female houseflies (length from head to wing edge) were measured using 30 randomly collected adult test insects: 6.3 ± 0.3 mm (male) and 8.8 ± 0.4 mm (female). Both pupae and adult houseflies were used in this study.

2.2. Experimental Instrument

2.2.1. Formation of an Electric Field by Two Oppositely Charged Metal Nets

Two identical metal nets (expanded steel nets) (30×30 cm²; thickness, 0.8 mm) (Okutani Ltd., Kobe, Japan) (Figure S1A) were horizontally held with polypropylene clamps (insulator). The upper net was linked to a direct current (DC) voltage generator (pulse-charge type; pulse interval, 1 sec; usable voltage, -10 kV; Suematsu Denshi, Kumamoto, Japan) (Figure S1B) to supply a negative charge to the metal net, and the lower net was linked to a grounded line. A negative-voltage generator, driven by a solar cell (Figure S1B), was used as a booster to enhance the initial voltage (12 V) to a desired voltage (in this case, -10 kV).

The role of a negative-voltage generator is to pick up negative charge from the ground using the enhanced voltage and supply it to a conductor linked to the voltage generator. A negative charge accumulates on the surface of the charged conductor and forms an electric field in the space around the charged conductor. If the grounded conductor is placed inside the electric field, the negative charge on the charged conductor pushes negative electricity (free electrons) out of the grounded conductor by electrostatic induction [22]. Eventually, the grounded conductor becomes positively charged. This positively charged grounded conductor acts as a recipient pole of negative charge released from the negatively charged conductor. In the present configuration, a single-charged dipolar electric field was formed in the space between the negatively charged metal net (NC-MN) and the grounded metal net (G-MN) (Figure 1). The occurrence of an arc discharge between two opposite poles is determined by the applied voltage and the pole distance (distance between the NC-MN and G-MN). In this study, the applied voltage was fixed to -10 kV, and the pole distance was adjusted for proper arcing.

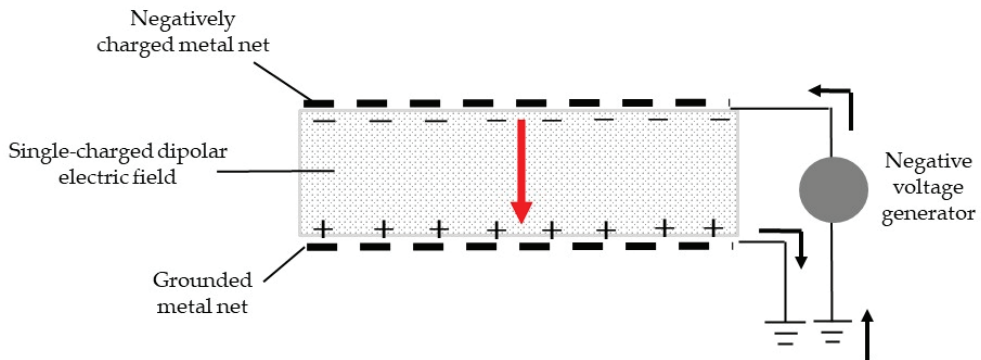


Figure 1. Schematic representation of a single-charged dipolar electric field formed between a negatively charged metal net and a grounded metal net. The black arrow represents the movement of the negative current, and the red arrow represents the movement of electricity through arcing.

2.2.2. Arcing between Two Oppositely Charged Metal Nets

In the preliminary experiment, the two metal nets (NC-MN and G-MN) were held horizontally using polypropylene (insulator) clamps in the cabinet; the RH was controlled at 25%, 50%, 75%, or 98%, and the distance between the nets was changed gradually until an arc discharge occurred between them to determine the distance that caused discharge at each RH. In this system, both metal nets generated the ground-to-ground circuit of electric current when a discharge occurred between them (Figure 1). Based on the results obtained, the following arcing experiments for houseflies were conducted at a pole distance of 6 mm, whereas no arc discharge occurs if the RH changes in a greenhouse.

2.3. Arcing to Adult Houseflies

2.3.1. Carbon Dioxide (CO₂) Anesthetization of Adult Houseflies

For immobilization, adult houseflies were anesthetized by CO₂ exposure according to a method described previously [28]. Briefly, vials containing an insect were placed in a non-vacuum glass desiccator (jar capacity, 5 L), and CO₂ gas (Air Water West Japan Inc., Osaka, Japan) was continuously introduced into the desiccator at 10 kg/cm² for 4–5 min. The air in the desiccator was simultaneously removed via the exhaust port of the desiccator lid. The introduction of CO₂ was stopped when all insects were anesthetized. In the present CO₂ treatment, all of the anesthetized houseflies awoke from anesthesia within 5 min.

2.3.2. Arc-Discharge Exposure Assay for Adult Houseflies

Arc-discharge exposure of houseflies was conducted using the experimental instrument shown in Figure 2A, in which three transparent acrylic cylinders of different lengths were placed vertically between the NC-MN and G-MN, beneath the G-MN and on a polypropylene plate, and beneath the polypropylene plate. The top cylinder (6 mm in length) was marked with lines every 2 mm to create three zones. An immobilized adult housefly was transferred into the bottom of the lowest cylinder (9 mm length) beneath the plate. After the housefly awoke from anesthesia, the plate was withdrawn to allow it to climb the cylinder wall (Figure 2B); it was then subjected to arc-discharge exposure from the NC-MN when it entered Zone 1 (Z1) (Figure 2C). The fly was thrown to the bottom of the lowest cylinder (Figure 2C) (cylinder-climbing assay). In this experiment, we confirmed the occurrence of arcing in both male and female houseflies when they reached the lowest zone (Z1). As the houseflies that were subjected to the arc-discharge exposure were thrown to the bottom of the lowest cylinder, we counted the number of repeated climbing trials by the discharged exposed houseflies until they died. Twenty adult houseflies of each sex were used, and separate experiments were repeated five times.

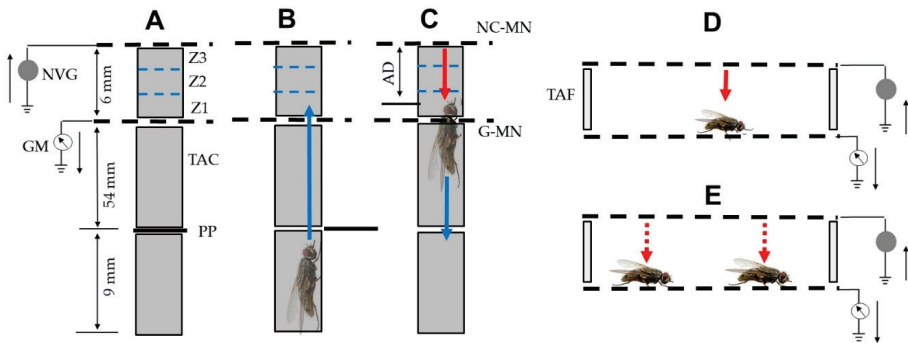


Figure 2. The experimental set-up for delivering an arc discharge to adult houseflies. (A) The apparatus consisted of two metal nets and three transparent acrylic cylinders (TACs) of different lengths. The upper net was linked to a pulse-type negative-voltage generator (NVG), and the lower net was linked to a grounded line. The top cylinder (6 mm in length) was placed vertically between the two metal nets, the middle cylinder (54 mm in length) was placed beneath the grounded metal net (G-MN) and on a polypropylene plate (PP), and the third cylinder (9 mm in length) was placed beneath the PP. The top cylinder was marked with lines every 2 mm to create three zones (Z1–3). (B,C) A climbing housefly (B) and its falling pathway following arc-discharge exposure (C). An adult housefly was placed in the lowest cylinder, and the PP was drawn out to allow the housefly to climb up the wall of the middle cylinder. The housefly was subjected to arc discharge from the negatively charged metal net (NC-MN) when it entered the upper cylinder on the G-MN and was within the arc distance (AD). (D,E) Another experimental set-up for exposing a housefly (or houseflies) transferred onto the G-MN. Two metal nets were separated by a transparent acrylic frame (TAF). Single (D) and double (E) CO₂-anesthetized houseflies were transferred onto the G-MN. The black arrow represents the movement of the negative current. The solid red arrow represents the movement of electricity through arcing, and the dotted red arrow represents selective arcing to one of the two houseflies. The blue arrow represents the pathway taken as the fly climbs and falls. A galvanometer (GM) was integrated into the grounded line to detect the electric current caused by the arc-discharge exposure.

In all experiments, we measured the magnitude of the electric current and the intensity of the sound, which reflected the arc-discharge exposure. The electric current was detected by a galvanometer (Sanwa Electric Instrument, Tokyo, Japan) integrated into the grounded lines. The sound produced by the arc discharge was measured in decibels using a sound-level meter (Sato Tech, Kanagawa, Japan). The sound profile was recorded with a spectrum analyzer integrated into the sound-level meter. Twenty adult houseflies of each sex were used, and each individual experiment was repeated five times.

2.4. Relationship between Autonomous Stoppage of Arc-Discharge Exposure and Loss of Body Water in Houseflies

2.4.1. Effect on Houseflies of Autonomous Stoppage of Arcing on the G-MN

In this experiment, we fabricated another instrument (Figure 2D) to ensure arc-discharge exposure to houseflies on the G-MN. The instrument consisted of the NC-MN and G-MN, which were separated by a square transparent acrylic frame (wall thickness, 1 mm; height, 6 mm). First, single CO₂-anesthetized male and female adult houseflies (body sizes 6, 7, 8, and 9 mm) were collected randomly, individually transferred onto the G-MN, and subjected to arcing by switching on the voltage generator after they awoke and began to crawl on the net (on-net-crawling assay). In this system, as pulsed arcing was continuously applied to the same fly at 1 s intervals, we switched off the generator immediately after the first arcing finished and examined the survival of the discharge-exposed fly. Similarly, we examined the survival of houseflies that were continuously exposed two to five times.

Second, we randomly collected single anesthetized houseflies of different sizes (without respect to sex), measured their body size and weight, transferred them individually

onto the G-MN, and switched on the voltage generator after they awoke. After the arcing stopped autonomously, we confirmed their death and re-measured their weight to determine the loss of body water. In each housefly, we determined the time taken for the arc to stop autonomously. Twenty houseflies were used to examine the relationship between the duration of the continuous arcing and body size. Additionally, we also determined the time taken for the arc to stop autonomously in cases when two houseflies were transferred onto the G-MN (Figure 2E).

2.4.2. Measurement of the Body Water Content of Houseflies

The body water content of a housefly was determined using the loss-on-drying (LOD) method [29]. Houseflies of different body sizes (6, 7, 8, and 9 mm) were weighed and placed in a thermostatic convection oven set to 30 °C to dehydrate. At intervals, insects were removed from the oven and weighed. This procedure was continued until the weight remained constant. Then, the difference between the initial and final weights was calculated to determine the moisture (body water) vaporized. Using a weight-loss calibration curve (Figure S1A), houseflies that lost different proportions of their body water were collected and transferred onto the G-MN to examine the occurrence or non-occurrence of arcing to their bodies (Figure S1B).

2.5. Construction of the Arc-Discharge Exposure

Figure 3A shows the structure of the arc-discharge exposure (ADE), which consisted of two identical expanded steel nets (100 × 90 cm², strand thickness, 0.5 mm). One was linked to a voltage generator and the other to a grounded line. These metal nets were adhered to both the upper and lower faces of a square polypropylene frame (wall width, 10 mm; wall height, 6 mm) by a silylated polyurethane adhesive (Figure 3B), creating a separation interval of 6 mm between the two nets. A fiberglass reinforced plastic (FRP) grating (100 × 90 cm²; 9 mm depth; 4095 cubic cells) (Figure S1C) (Chubu Corporation, Mie, Japan) was used to provide the flies with a climbing path. Six identical gratings (54 mm height) were stuck to each other and placed beneath the G-MN. Another single grating (54 mm height) was placed beneath the polypropylene plate (Figure 3A). The plate located between the two gratings was drawn out to provide a climbing path for flies in the cells of the lower grating at the start of the experiment.

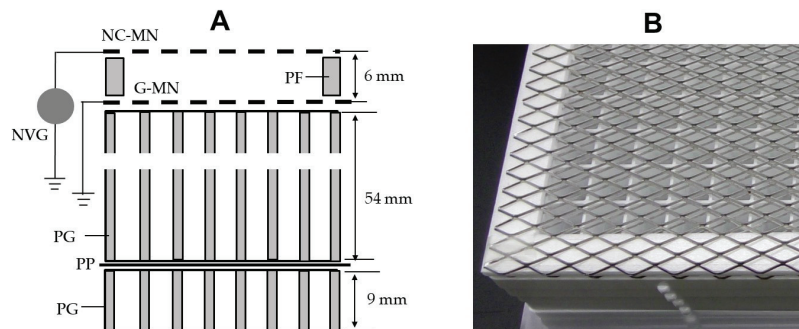


Figure 3. Schematic (A) and photograph (B) are representations of an arc-discharge exposure (ADE) consisting of two metal nets, two gratings, and a pulse-type negative-voltage generator (NVG) (cross-sectional view). A square polypropylene frame (PF) (6 mm in height) was placed between the negatively charged metal net (NC-MN) and the grounded metal net (G-MN). A plastic grating (PG) 54 mm in height was placed beneath the G-MN. Another grating (9 mm in height) was placed beneath the polypropylene plate (PP), which was positioned between the two gratings and withdrawn before the experiment. Pupae or CO₂-anesthetized adult houseflies were placed in separate cells of the lower grating.

2.6. Application of the ADE to Control Houseflies Emerging from Underground Pupae

In this experiment, we randomly collected pupae on the rearing medium (with no regard to their maturity) and embedded them into the soil in the cells of the lowest grating of an ADE that was placed in a greenhouse (July 2022; diurnal temperature range, 16–38 °C). We used 100, 200, 300, and 400 pupae in separate experiments. These pupae were individually transferred to separate cells (single pupa/cell). The experiments ran for 2 weeks. At the end of each experiment, we counted the number of dead adult houseflies on the bottom of the grating and on the G-MN. In addition, we dug pupae out of the soil to check the success or failure of adult emergence. In the first round of experiments, the number of pupae was increased stepwise from 100 to 300, and the experiment was conducted once for each number of pupae. In the second round, we used 400 pupae and repeated the same experiment five times.

2.7. Assessment of the Ability of the ADE to Control Adult Housefly Invasions

In this experiment, different numbers (25, 50, 100, and 150) of CO₂-anesthetized houseflies were individually transferred into the separate cells of the lowest grating of the ADE on the assumption that multiple adult houseflies would emerge from underground pupae, climb the cell wall and enter the arcing zone of the ADE. The experiments were continued for 3 days. We confirmed that all flies attempted to climb the grating wall and were exposed to the pulsed arc discharge. At the end of the experiment, we counted the number of dead houseflies on the bottom of the lowest grating and on the G-MN. In the first round of the experiments, we increased the number of adult houseflies stepwise from 50 to 100 in individual experiments, and the experiment was conducted once for each number of flies. In the second round, we used 150 adult houseflies and conducted the same experiment five times.

2.8. Statistical Analysis

All experiments were repeated five times; all data are presented as means with standard deviations. Analyses were performed using the EZR software version 1.54 (Jichi Medical University, Saitama, Japan) to identify significant differences among conditions and correlations among factors, as shown in the figures and tables.

3. Results and Discussion

3.1. Prevention of Target-Independent Arcing

The factors affecting arc discharge between the NC-MN and G-MN of the apparatus were the voltage applied to the NC-MN, the distance between the two nets (pole distance), and the change in vapor concentration in the air between the poles [21]. In the present apparatus, the applied voltage was fixed to −10 kV, and the pole distance and water-vapor concentration (RH) in the air were the parameters tested. The air conductivity between the two nets changed in response to changes in the RH of the air, with air conductivity increasing (i.e., higher amounts of electricity being transferred) under higher RH [30]. This implied that under higher RH, the arcing occurred at greater distances between the NC-MN and G-MN. We investigated the pole distances resulting in arc discharge between the nets under different RH conditions (Figure 4). As expected, the pole distance resulting in arc discharge increased as the RH increased. The change in the RH of the greenhouse over a year (recorded in 2021) was between 32% and 96%. Based on these data, the safe pole distance that did not result in arc discharge between the two nets was more than 6 mm, regardless of changes in the RH. In the following experiment, we examined possible arcing to houseflies at a pole distance of 6 mm. Incidentally, the temperature changes (between 5 and 50 °C) tested did not affect the generation of an arc discharge by the apparatus (data not shown).

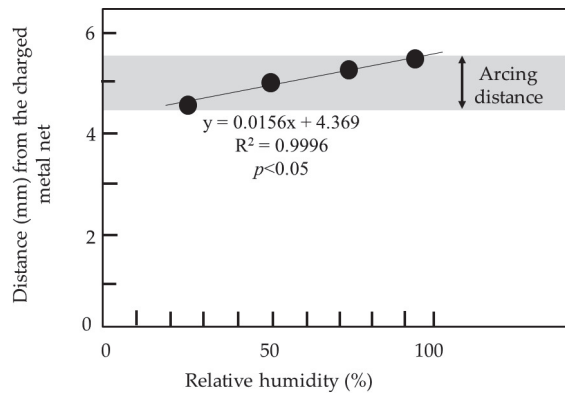


Figure 4. The distance from the pole required to cause arcing under different relative humidity (RH) conditions. Two identical expanded metal nets (negatively charged and grounded metal nets) were horizontally arranged, and the arcing distance (distance from the charged net) was determined by changing the distance between them at each RH.

3.2. Arcing to Kill Houseflies

Figure 4 indicates that the NC-MN was able to strike an arc discharge to a grounded conductor within positions at 4.5–5.5 mm from the NC-MN, depending on the RH. Houseflies received arc-discharge exposure [20,31] due to the conductive nature of their outer surface cuticle structure [32,33]. In the experiments, we examined whether the houseflies received discharge exposure from the NC-MN when they moved within this arcing distance. In the cylinder-climbing assay, we settled two cylinders on and beneath the G-MN, respectively, and marked the upper cylinder with lines to create zones. We then determined in which zone of the cylinder the housefly was subjected to an arc-discharge exposure from the NC-MN. In this experimental design, Z1 (4–6 mm from the NC-MN) was expected to be the first arcing site. We confirmed that all houseflies were subjected to arc-discharge exposure in this zone (Figure 2C).

The arcing is the movement of negative electricity in the air toward the grounded conductor by breaking down the resistivity of the air [21]. In the configuration of the instrument, negative electricity was picked up from the ground by a voltage generator and supplied to the metal net linked to the voltage generator. Using the applied voltage (−10 kV), the electricity on the metal net was released toward the conductor (housefly) in the electric field through the arc discharge. For successful arcing, it was essential for the electricity to flow back to the ground, and arcing did not occur if the grounded line of the G-MN was removed. Nevertheless, our attempt to detect the movement of electricity (i.e., the flow of electric current) from the G-MN to the ground was unsuccessful because of its low magnitude, i.e., below the detection limit (0.01 μ A) of the current detector used. The sound was detectable and was shown to reliably indicate the occurrence of arc-discharge exposure to the houseflies, which allowed us to determine the numbers of arc-discharge exposures to houseflies based on the numbers and intensities of the sounds recorded. The intensity of the arc-discharge sound was an important parameter in the determination of the force required to push the fly down (Figure 2A–C). The arc-discharge sound was a sonic boom caused by the shock wave from the high-speed electrons moving in the electric field, and its intensity was an indicator of the impact strength of the shock wave produced by the arc-discharge exposure. Video S1 shows male and female houseflies that were violently thrown down to the bottom of the cylinder by a single arc-discharge exposure. Matsuda et al. [20] reported that the strength of the impact produced by the arc-discharge exposure was in direct proportion to the intensity of the arc-discharge sound; in fact, both male and female houseflies underwent arcing with the same sound intensity (Figure 5A). The housefly has an inherent habit of climbing upward [34]. In fact, they did so even

after they experienced arc-discharge exposure, as a result of which they were repeatedly exposed to harmful arc discharges. Eventually, both houseflies were killed by three to four arc-discharge exposures (Figure 5B).

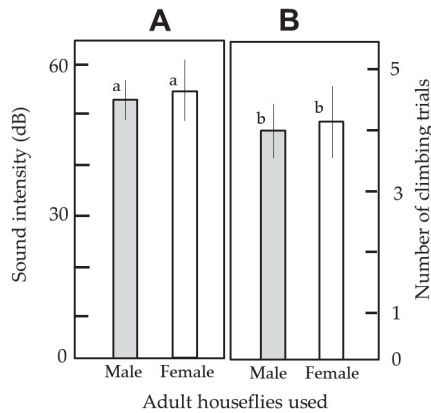


Figure 5. (A) The intensity of the sound produced by arc-discharge to a housefly climbing up the cylinder wall and reaching the arcing zone of the arc-discharge exposurer (ADE) in the cylinder-climbing assay. (B) Number of climbing trials by houseflies exposed repeatedly to arc-discharge exposure until they died. We used 20 insects of each sex. Means \pm standard deviation were calculated from five experimental replicates. The letters (a, b) on each column indicate no significant difference ($p < 0.05$) according to Tukey's test.

In the second experiment, we examined the lethal effects of arc-discharge exposure on the survival of the houseflies on the G-MN (on-net-crawling assay) (Figure 2D). Figure 6 shows the number of arc-discharge exposures required to kill the houseflies on the G-MN. The houseflies on the G-MN became motionless immediately after their first exposure to the arc discharge and were then subjected to subsequent arcing at the same position. The arc-discharge exposure was harmful, and the flies were killed by four pulsed arc-discharge exposures. There was no significant difference in survival rates between the male and female houseflies.

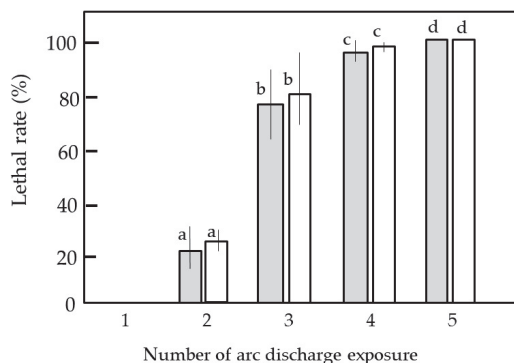


Figure 6. The mortality of the houseflies that were transferred onto the grounded metal net (G-MN) facing the negatively charged metal net (NC-MN) of the arc-discharge exposurer (ADE). Anesthetized male (gray) and female (open column) houseflies were individually transferred onto the G-MN and subjected to an arc discharge from the NC-MN. After 1–5 arc-discharge exposures, their survival was examined. We used 20 insects of each sex. Means \pm standard deviation were calculated from five experimental replicates. Different letters (a–d) on each column indicate significant differences ($p < 0.05$) according to Tukey's test.

For the same target, arc-discharge exposure continued regardless of whether it lived or died. In cases where single houseflies were introduced into the electric field, the arcing stopped autonomously after a lapse of 10–40 min. Figure 7 indicates that there was a linear relationship between the body size of the houseflies and the duration of the arcing, with larger houseflies requiring longer for arcing to finish.

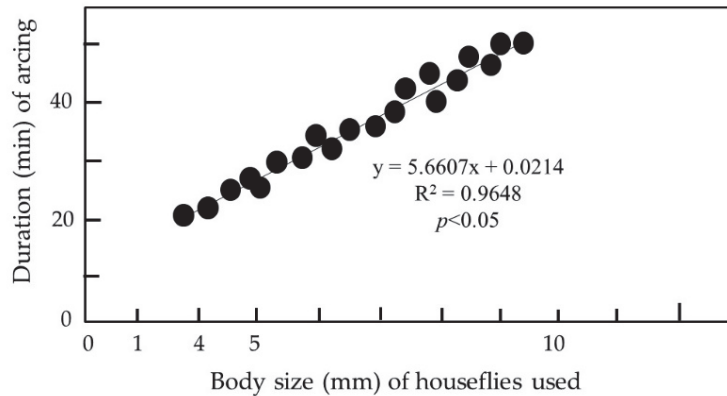


Figure 7. Relationship between the body size of houseflies and the length of time required for the arc-discharge exposure of houseflies to stop autonomously.

There was a need to determine why the arcing stopped autonomously. The most important outcome of this assay was that the weight of the houseflies decreased remarkably at the time arcing stopped (Table 1). The reduction in body weight implied a loss of water from the houseflies. Takikawa et al. [31] reported that the loss of body water resulted in a decline in the conductance of houseflies. Our supplementary experiment also indicated that the houseflies that approximately 50% of their body water by dehydration received no arcing due to reduced conductance, i.e., an increase in resistivity in the water-depleted houseflies due to the arc-discharge exposure (Figure S1B). Matsuda et al. [24] reported that continuous pulsed arc-discharge exposure to the growing stem tip of the kudzu plant (*Pueraria montana*) raised the temperature of the exposed region, implying that an increase in temperature caused the vaporization of body water.

Table 1. Change in the weight of houseflies before and after continuous pulsed arc-discharge exposure.

| Size (mm) of Houseflies Used | Weight (mg) | | Percentage of Body Water Lost | Duration (min) of Continuous Arcing |
|------------------------------|---------------|--------------|-------------------------------|-------------------------------------|
| | Before Arcing | After Arcing | | |
| 6 | 13.5 ± 0.8 a | 6.5 ± 0.5 a | 48.6 ± 2.5 a | 18.8 ± 1.8 a |
| 7 | 17.1 ± 0.7 b | 8.3 ± 0.6 b | 48.4 ± 3.5 a | 30.3 ± 2.0 b |
| 8 | 23.5 ± 0.5 c | 11.5 ± 0.7 c | 49.1 ± 3.4 a | 40.2 ± 2.7 c |
| 9 | 29.2 ± 0.6 d | 14.9 ± 0.7 d | 51.1 ± 2.3 a | 49.8 ± 1.3 d |

Twenty houseflies were used for each body size category. The means and standard deviations were calculated from five repetitions of the experiments. The letters (a–d) on the means in each vertical column indicate significant differences ($p < 0.05$) according to Tukey’s method.

Additionally, we simultaneously transferred two houseflies onto the G-MN and examined the duration of the continuous pulsed arc-discharge exposure of these two houseflies. In this case, arcing occurred to either of the two houseflies, whichever was closer to the NC-MN at the timing of arcing. Their antennae, wings, and legs were the sites that received the arcing from the NC-MN. Subtle changes in the positions of these organs affected the selective arcing from the NC-MN. Both houseflies died shortly after several arc-discharge exposures, whereas the arcing continued for some time. Eventually, the arcing stopped autonomously after a lapse of 20–80 min (data not shown).

3.3. Practical Application of the ADE to Control Houseflies Emerging from the Soil

3.3.1. Successful Grounding of the ADE

In this study, we fabricated an ADE operated by a pulse-type voltage generator. The prerequisite for normal functioning by the apparatus was to ensure successful grounding, to pick up the negative charge from the earth's ground by the voltage generator and send it back to the ground. In the laboratory experiments, we inserted the ground-line plug of the voltage generator into the ground-contact outlet of a wall socket, which was equipped with a conductive pipe or rod physically driven into the earth to a minimum depth of 8 feet (about 2.5 m) to protect buildings against fire resulting from leakage of electricity [35]. In the greenhouse experiments, it was necessary to create an effective ground for the voltage generator because the dry surface layer of the field could increase the ground resistance (earth resistance), thereby impeding the current flow to the ground [36]. For the pulse-type voltage generator used in this study, the manufacturer recommended a 50 cm steel rod driven into the ground completely. As a result of this grounding procedure, the apparatus was able to produce pulsed arc discharges at all 200 points tested inside and outside the greenhouse.

3.3.2. Construction of the ADE and Its Two-Step Arcing System to Control Houseflies

The two-net system was able to deliver an arc discharge to adult houseflies that were about to enter the space (electric field) between the two nets and that had already entered the electric field. Because the discharge-exposed houseflies are killed, this system can be used to manage houseflies. Based on this feature, we devised the ADE (Figure 3A) as a simple physical tool to effectively kill adult houseflies emerging from underground pupae in a greenhouse soil bed. The combination of a multicell grating with the two nets provided a climbing path for the houseflies on the soil to guide them to the killing site in the apparatus. The impact generated by the arc-discharge exposure was so strong that the houseflies that climbed up to the arcing zone were thrown down to the soil surface. Importantly, the ADE was able to control the houseflies that slipped through the first arcing. The second arcing was strong enough to make houseflies on the net motionless with a single hit. For practical use of the ADE, we attempted to clarify the population size limit of adult houseflies that the ADE could control in the first stage of defense.

The NC-MN generated a pulsed arc discharge to the nearest housefly in the electric field at 1 s intervals. In our preliminary measurement, the pace of climbing by the houseflies was 1.9 ± 0.3 mm/sec (average of 50 flies). The probability of passing through the first arcing was determined by the relationship between the interval of pulsed arcing and the climbing pace achieved by multiple houseflies climbing synchronously. Figure 8A1 shows the hypothetical case in which three houseflies simultaneously entered the electric field, where the housefly on the left side (nearest to the NC-MN) was first subjected to the arcing and thrown down. Other houseflies could move forward for 1 sec, and the second arcing occurred toward the second housefly that was nearest to the NC-MN (Figure 8A2). The investigation then turned to the third fly. In this case, before the third arcing, the houseflies that climbed over the G-MN were then subjected to an arc-discharge exposure (Figure 8A3). This implied that the third housefly could pass through the first defense mechanism of the apparatus. As mentioned earlier, the housefly that was subjected to the arc-discharge exposure was rendered motionless by the first single arcing of the second defense mechanism and was then continuously exposed to the pulsed arcing.

The houseflies on the G-MN underwent pulsed arc-discharge exposure continuously (Figure 8B1) (Video S1B). This arc-discharge exposure continued until the arc stopped autonomously. Figure 8B2 shows an uncommon case in which two houseflies entered the arcing zone simultaneously before the arcing for the preceding fly had stopped autonomously. Of these two flies, the earlier one was subjected to the arcing and thrown down before entering, whereas the second fly was able to climb over the net before being subjected to the arcing (Figure 8B3). Thus, a series of coincidences led to the existence of two houseflies on the G-MN (in the electric field). These two houseflies were motionless,

and whichever one was closer to the NC-MN was subjected to the arcing each time during the continuous arc-discharge exposure. This situation continued until the arcing stopped autonomously. Although the probability of these events was expected to be extremely low, understanding their possibility was essential for the successful management of houseflies by the apparatus.

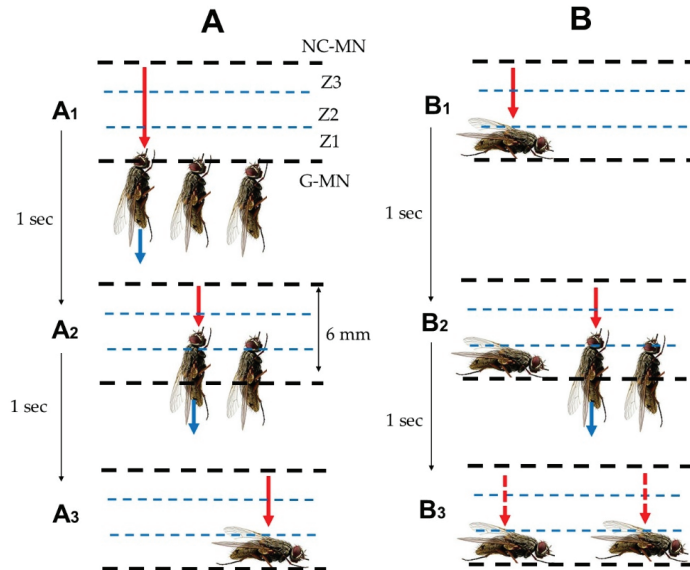


Figure 8. Schematic representation of the standby and follow-up arcing to multiple houseflies that entered the arcing zone of the arc-discharge exposur (ADE) simultaneously. **(A)** Simultaneous entry to the first arcing zone (Z1) by three houseflies. The housefly on the left, which was nearest to the first arcing zone (Z1) by three houseflies. The housefly on the left, which was nearest to the negatively charged metal net (NC-MN), was the first to be subjected to arc discharge from the NC-MN and thrown down (A1). The other flies moved into Zone 2 (Z2) for 1 sec, and a second fly was subjected to the arcing (A2). Before the third arcing, the last fly climbed over the grounded metal net (G-MN) and was subjected to arc discharge (A3). **(B)** Simultaneous entry by two houseflies to the arcing zone in which the first fly had been present. The housefly that remained in the electric field was subjected to a pulsed arc-discharge exposure (B1) continuously until the next fly entered and moved close to the NC-MN. Of the two flies that entered the arcing zone simultaneously, the one that was closest to the NC-MN was subjected to the arcing and thrown down (B2). The second fly was subjected to arcing only after it had climbed over the G-MN (B3). The solid red arrow represents arcing to the fly from the NC-MN. The dotted red arrow represents selective arcing to one of the two flies, i.e., whichever fly was closest to the NC-MN at the moment of arcing. The blue arrow represents the pathway taken as the fly falls.

3.3.3. Application of the ADE to Adult Houseflies Emerging from Underground Pupae

According to our records for the past three years, in which flypapers (sticky paper ribbons) were hung over the soil beds, and the numbers of trapped houseflies were counted, their occurrence (during the 3-month summer season) was between 8 and 62 per m². However, this approach provided no information about how many houseflies escaped from the trap and, more importantly, how many houseflies emerged simultaneously from the soil bed. In the experiment, we established the ADE in a greenhouse, embedded 100–400 pupae into the soil of separate cells of the lowest grating of the ADE (single pupa/cell), and surveyed the working of the ADE during the period of the experiment (2 weeks). The access of the houseflies that emerged from pupae to the electric field of the ADE was estimated based on the total number of arc-discharge sounds. If no adult housefly was detected on the G-MN, it was considered that all of the houseflies that reached the arcing zone were

thrown down to the soil surface by the arcing of the first dense mechanism (Table 2). In the experiment, more than 90% of the embedded pupae produced adult houseflies within 5–10 days. However, emergence was highly irregular, and therefore there was no chance that multiple houseflies (more than three houseflies) entered the arcing zone. This uneven emergence of adult houseflies probably depended on the different maturities of the pupae used. Eventually, we detected no adult houseflies on the G-MN, neither in the stepwise applications of 100–300 pupae nor in the repeated applications of the highest number of pupae (400 pupae). In conclusion, the study revealed that at <400 pupae/m², there was no opportunity for the ADE to undertake the second-step measures to control houseflies.

Table 2. Evaluation of the ability of the arc-discharge exposer (ADE) to control adult houseflies emerging from underground pupae by continuous pulsed arc-discharge exposures.

| No. of Pupae Used ^a | No. of Disable Pupae Bearing No Adults | No. of Dead Adult Houseflies on BLG ^b | No. of Dead Adult Houseflies on G-MN |
|--------------------------------|--|--|--------------------------------------|
| 100 | 6 | 94 | 0 |
| 200 | 12 | 188 | 0 |
| 300 | 4 | 296 | 0 |
| 400 | 11 | 389 | 0 |
| | 7 | 393 | 0 |
| | 25 | 375 | 0 |
| | 11 | 389 | 0 |
| | 10 | 390 | 0 |

^a Pupae at different stages of maturity were collected randomly and embedded into the soil of separate cells of the lowest grating (L-grating). Adult houseflies that emerged from pupae climbed the cell of the upper grating (U-grating), which was set on the L-grating, and were subjected to arcing from the negatively charged metal net (NC-MN) when they reached the arcing zone above the grounded metal net (G-MN), which covered the U-grating.

^b Bottom of the L-grating.

3.3.4. Capability of the ADE to Control Adult Houseflies Invading Successively

In the second experiment in a greenhouse, we directly applied adult houseflies to the ADE to set up an acute situation in which adult houseflies (in this case, 25–150 adults) simultaneously emerged from underground pupae and successively invaded the ADE. The experiment was designed to actualize the events hypothesized in Figure 7. However, in the preliminary application of the 25–150 houseflies, no fly was detected on the G-MN. Eventually, in one of five repeated applications of 150 adult houseflies, we detected one housefly on the G-MN (Table 3). Conversely, numerous dead houseflies were confirmed on the bottom of the lowest grating, which had been thrown down by the arcing during the first defense of the ADE. The study indicated that if the number of synchronously emerging adult houseflies did not exceed 200, the ADE was able to effectively cope with successive invasions by multiple houseflies using the first defense measures. The second arcing was a fallback measure to respond to the few houseflies that overcame the first defense.

Table 3. Evaluation of the ability of the arc-discharge exposer (ADE) to control successive invasions by adult houseflies.

| No. of Adult Houseflies Used ^a | No. of Dead Houseflies on BLG ^b | No. of Dead Houseflies on G-MN |
|---|--|--------------------------------|
| 25 | 25 | 0 |
| 50 | 50 | 0 |
| 100 | 100 | 0 |
| 150 | 150 | 0 |
| | 149 | 1 |
| | 150 | 0 |
| | 150 | 0 |
| | 150 | 0 |

^a Anesthetized adult houseflies were placed in separate cells of the lowest grating (L-grating). These flies climbed up the wall of the upper grating (U-grating), reached the L-grating, and entered the arcing zone above the grounded metal net (G-MN), where they were subjected to arcing from the negatively charged metal net (NC-MN) and then thrown down to the bottom of the L-grating. ^b Bottom of the lower grating.

The impact of the arc-discharge exposure was strong enough to kill adult houseflies. However, this arcing technique has not proven applicable to all fly species that emerge from underground pupae. The apparatus was found to be unsuitable for tomato leaf miner flies because of their small body size. If the metal net was not completely flat, the point that protruded most from the net surface became the site that received the arcing from the charged metal net. If the size of the fly was smaller than the vertical drop (i.e., the distance between the highest and lowest sites on the G-MN), it remained on the metal net without undergoing arcing from the NC-MN. Theoretically, only flies larger than the vertical drop were specifically targeted for arcing. Alternatively, another type of electrostatic tool, which consisted of a pair of insulated and non-insulated metal nets, was successfully applied to capture the smaller flies emerging from underground pupae [16].

The most useful feature of the ADE is its simple structure, which enables ordinary workers to fabricate and improve the apparatus cheaply using common materials based on their own requirements. The most important feature of the ADE is that it provides pulsed arc-discharge exposure to the nearest target from the NC-MN, and therefore it is possible to scale up the present system simply by linking additional ADEs together with an electric line. The arcing system of the ADE is operated safely using a pulse-type voltage generator, which is widely used with electric fences to deter wild animals without harming people [25]. Thus, the present study provided the experimental basis for the development of a new physical method for managing houseflies emerging from soil beds in greenhouses.

4. Conclusions

The electrostatic apparatus described here is a newly developed device that can be applied to net the surface of soil beds in a greenhouse to manage the emergence of adult houseflies from the ground by exposing them to an arc discharge. The convex array over the whole surface of an expanded metal net is the site from which a spark can be discharged to targets at any location. The target-responsible arc-discharge exposure treatment was extremely effective at pushing invading houseflies down into the soil surface through the destructive force generated by the arc-discharge exposure. The apparatus was developed by pairing commercially available expanded metal nets and connecting one to a negative-voltage generator and the other to a ground line. The study developed a simple physical method for an insecticide-independent pest-management approach that can be integrated into sustainable crop-production systems in greenhouses.

Supplementary Materials: The following supporting information can be downloaded at: <https://www.mdpi.com/article/10.3390/agronomy13020310/s1>, Figure S1: (A) An expanded steel net with diamond-shaped meshes. (B) A pulse-type voltage generator operated by a solar panel. (C) A fiberglass reinforced plastic (FRP) grating with square cells; Video S1: (A) Arc-discharge exposure from the negatively charged metal net (NC-MN) to adult male (left) and female (right) houseflies that reached the arcing zone above the grounded metal net (G-MN) of the arc-discharge exposer (ADE). (B) Arc-discharge exposure of an adult housefly (female) transferred onto the G-MN.

Author Contributions: Conceptualization, H.T. and Y.M.; methodology, Y.M. and K.K.; software, Y.M. and K.K.; validation, H.T., Y.M. and K.K.; formal analysis, Y.M.; investigation, Y.M. and K.K.; resources, Y.M.; data curation, K.K.; writing—original draft preparation, H.T.; writing—review and editing, Y.M. and K.K.; visualization, Y.M.; supervision, H.T.; project administration, Y.M. All authors have read and agreed to the published version of the manuscript.

Funding: This research received no external funding.

Data Availability Statement: Not applicable.

Conflicts of Interest: The authors declare no conflict of interest.

References

- Green, J.M. Current state of herbicides in herbicide-resistant crops. *Pest Manag. Sci.* **2014**, *70*, 1351–1357. [CrossRef] [PubMed]
- Heap, I. Global perspective of herbicide-resistant weeds. *Pest Manag. Sci.* **2014**, *70*, 1306–1315. [CrossRef] [PubMed]

3. Helps, J.C.; Paveley, N.D.; White, S.; van den Bosch, F. Determinants of optimal insecticide resistance management strategies. *J. Theor. Biol.* **2020**, *503*, 110383. [CrossRef] [PubMed]
4. Sparks, T.C.; Storer, N.; Porter, A.; Slater, R.; Nauen, R. Insecticide resistance management and industry: The origins and evolution of the Insecticide Resistance Action Committee (IRAC) and the mode of action classification scheme. *Pest Manag. Sci.* **2021**, *77*, 2609–2619. [CrossRef] [PubMed]
5. van den Bosch, F.; Gilligan, C.A. Models of fungicide resistance dynamics. *Annu. Rev. Phytopathol.* **2008**, *46*, 123–147. [CrossRef]
6. Hawkins, N.J.; Fraaije, B.A. Fitness penalties in the evolution of fungicide resistance. *Annu. Rev. Phytopathol.* **2018**, *56*, 339–360. [CrossRef]
7. Alam, M.J.; Zurek, L. Association of *Escherichia coli* O157:H7 with houseflies on a cattle farm. *Appl. Environ. Microbiol.* **2004**, *70*, 7578–7580. [CrossRef]
8. Ahmad, A.; Nagaraja, T.G.; Zurek, L. Transmission of *Escherichia coli* O157:H7 to cattle by house flies. *Prev. Vet. Med.* **2007**, *80*, 74–81. [CrossRef]
9. Russell, J.B.; Jarvis, G.N. Practical mechanisms for interrupting the oral-fecal lifecycle of *Escherichia coli*. *Mol. Microbiol. Biotechnol.* **2001**, *3*, 265–272.
10. Mukherjee, A.; Cho, S.; Scheftel, J.; Jawahir, S.; Smith, K.; Diez-Gonzalez, F. Soil survival of *Escherichia coli* O157:H7 acquired by a child from garden soil recently fertilized with cattle manure. *J. Appl. Microbiol.* **2006**, *101*, 429–436. [CrossRef]
11. Brandl, M.T. Plant lesions promote the rapid multiplication of *Escherichia coli* O157:H7 on postharvest lettuce. *Appl. Environ. Microbiol.* **2008**, *74*, 5285–5289. [CrossRef] [PubMed]
12. Ibekwe, A.M.; Grieve, C.M.; Papiernik, S.K.; Yang, C.-H. Persistence of *Escherichia coli* O157:H7 on the rhizosphere and phyllosphere of lettuce. *Let. Appl. Microbiol.* **2009**, *49*, 784–790. [CrossRef] [PubMed]
13. Luo, Y.; He, Q.; McEvoy, J.L. Effect of storage temperature and duration on the behavior of *Escherichia coli* O157:H7 on packaged fresh-cut salad containing romaine and Iceberg lettuce. *J. Food Sci.* **2010**, *75*, M390–M397. [CrossRef]
14. Petrikovszki, R.; Zalai, M.; Bogdányi, F.T.; Ferenc Tóth, F. The effect of organic mulching and irrigation on the weed species composition and the soil. *Plants* **2020**, *9*, 66. [CrossRef]
15. Wang, K.; Sun, X.; Long, B.; Li, F.; Yang, C.; Chen, J.; Ma, C.; Xie, D.; Wei, Y. Green production of biodegradable mulch films for effective weed control. *ACS Omega* **2021**, *6*, 32327–32333. [CrossRef] [PubMed]
16. Nonomura, T.; Toyoda, H. Soil surface-trapping of tomato leaf-miner flies emerging from underground pupae with a simple electrostatic cover of seedbeds in a greenhouse. *Insects* **2020**, *11*, 878. [CrossRef]
17. Matsuda, Y.; Takikawa, Y.; Nonomura, T.; Kakutani, K.; Okada, K.; Shibao, M.; Kusakari, S.; Miyama, K.; Toyoda, H. Selective electrostatic eradication of *Sitophilus oryzae* nesting in stored rice. *J. Food Technol. Press* **2018**, *2*, 15–20.
18. Kakutani, K.; Takikawa, Y.; Matsuda, Y. Selective arcing electrostatically eradicates rice weevils in rice grains. *Insects* **2021**, *12*, 522. [CrossRef]
19. Kakutani, K.; Matsuda, Y.; Takikawa, Y.; Nonomura, T.; Okada, K.; Shibao, M.; Kusakari, S.; Miyama, K.; Toyoda, H. Electrocutation of mosquitoes by a novel electrostatic window screen to minimize mosquito transmission of Japanese encephalitis viruses. *Int. J. Sci. Res.* **2018**, *7*, 47–50.
20. Matsuda, Y.; Shimizu, K.; Sonoda, T.; Takikawa, Y. Use of electric discharge for simultaneous control of weeds and houseflies emerging from soil. *Insects* **2020**, *11*, 861. [CrossRef]
21. Kaiser, K.L. Air breakdown. In *Electrostatic Discharge*; Kaiser, K.L., Ed.; Taylor & Francis: New York, NY, USA, 2006; pp. 1–93.
22. Griffith, W.T. Electrostatic phenomena. In *The Physics of Everyday Phenomena, a Conceptual Introduction to Physics*; Bruflo, D., Loehr, B.S., Eds.; McGraw-Hill: New York, NY, USA, 2004; pp. 232–252.
23. Toyoda, H.; Kusakari, S.; Matsuda, Y.; Kakutani, K.; Xu, L.; Nonomura, T.; Takikawa, Y. Structure and functions of discharge-generating screens. In *An Illustrated Manual of Electric Field Screens: Their Structures and Functions*; Toyoda, H., Ed.; RAEFSS Publishing Department: Nara, Japan, 2019; pp. 75–85.
24. Matsuda, Y.; Takikawa, Y.; Kakutani, K.; Nonomura, T.; Okada, K.; Kusakari, S.; Toyoda, H. Use of pulsed arc discharge exposure to impede expansion of the invasive vine *Pueraria montana*. *Agriculture* **2020**, *10*, 600. [CrossRef]
25. Burke, M.; Odell, M.; Bouwer, H.; Murdoch, A. Electric fences and accidental death. *Forensic Sci. Med. Pathol.* **2017**, *13*, 196–208. [CrossRef]
26. Izumi, N.; Sajiki, J. Effects of bisphenol A (BPA) on sex ratio of a housefly. *Bull. Public Health Lab. Chiba Prefect.* **2003**, *27*, 14–17.
27. Dubendorfer, A.; Hediger, M.; Burghardt, G.; Bopp, D. *Musca domestica*, a window on the evolution of sex-determining mechanisms in insects. *Int. J. Dev. Biol.* **2002**, *46*, 75–79. [PubMed]
28. Nilson, T.L.; Sinclair, B.J.; Roberts, S.P. The effects of carbon dioxide anesthesia and anoxia on rapid cold-hardening and chill coma recovery in *Drosophila melanogaster*. *J. Insect Physiol.* **2006**, *52*, 1027–1033. [CrossRef] [PubMed]
29. Bizzi, C.A.; Barin, J.S.; Hermes, A.L.; Mortari, S.R.; Flores, É.M.M. A fast microwave-assisted procedure for loss on drying determination in saccharides. *J. Braz. Chem. Soc.* **2011**, *22*, 376–381. [CrossRef]
30. Jonassen, N. Abatement of static electricity. In *Electrostatics*, 2nd ed.; Jonassen, N., Ed.; Kluwer Academic Publishers: Boston, MA, USA, 2002; pp. 101–120.
31. Takikawa, Y.; Takami, T.; Kakutani, K. Body water-mediated conductivity actualizes the insect-control functions of electric fields in houseflies. *Insects* **2020**, *11*, 561. [CrossRef]

32. McGonigle, D.G.; Jackson, C.W. Effect of surface material on electrostatic charging of houseflies (*Musca domestica* L.). *Pest Manag. Sci.* **2002**, *58*, 374–380. [CrossRef]
33. McGonigle, D.G.; Jackson, C.W.; Davidson, J.L. Triboelectrification of houseflies (*Musca domestica* L.) walking on synthetic dielectric surfaces. *J. Electrostat.* **2002**, *54*, 167–177. [CrossRef]
34. National Fire Protection Association. About the NEC®/Grounding & Bonding. Available online: <https://www.nfpa.org/NEC/About-the-NEC/Grounding-and-bonding> (accessed on 21 November 2022).
35. Nor, N.M.; Rajab, R.R.; Ramar, K. Validation of the calculation and measurement techniques of earth resistance values. *Am. J. Appl. Sci.* **2008**, *5*, 1313–1317. [CrossRef]
36. Matsuda, Y.; Nonomura, T.; Kakutani, K.; Kimbara, J.; Osamura, K.; Kusakari, S.; Toyoda, H. Avoidance of an electric field by insects: Fundamental biological phenomenon for an electrostatic pest-exclusion strategy. *J. Phys. Conf. Ser.* **2015**, *646*, 0120031–0120034. [CrossRef]

Disclaimer/Publisher’s Note: The statements, opinions and data contained in all publications are solely those of the individual author(s) and contributor(s) and not of MDPI and/or the editor(s). MDPI and/or the editor(s) disclaim responsibility for any injury to people or property resulting from any ideas, methods, instructions or products referred to in the content.



Article

Target-Size-Dependent Application of Electrostatic Techniques for Pest Management in Greenhouses

Yoshinori Matsuda ^{1,*} and Hideyoshi Toyoda ²

¹ Laboratory of Phytoprotection Science and Technology, Faculty of Agriculture, Kindai University, Nara 631-8505, Japan

² Research Association of Electric Field Screen Supporters, Nara 631-8505, Japan

* Correspondence: ymatsuda@nara.kindai.ac.jp

Abstract: Two new electrostatic devices were developed to manage greenhouse insect pests. One was an electrostatic insect catcher (EIC) to trap small flying pests, and the other was an arc-discharge zapper (ADZ) to kill larger insects emerging from soil beds. The EIC consisted of negatively charged insulated conductor plates (NIPs) and grounded conductor plates (GCPs), which were alternately arrayed in parallel at defined intervals. The ADZ had the same framework as the EIC, except that the NIPs were replaced with negatively charged non-insulated iron plates (NNPs). The EIC formed a non-discharging electric field between the NIP and GCP to create an attractive force to capture insects. By contrast, the ADZ formed a discharge-generating electric field between the NNP and GCP that killed insects. The EIC was effectively applied to small pests, such as whiteflies, thrips, leaf miners, winged aphids, and shore flies, that can pass through the conventional insect-proof nets installed on greenhouse windows. The ADZ was effective for adult houseflies emerging from pupae in soil beds. Our electrostatic devices are useful for controlling insect pests of different sizes.

Keywords: arc discharge zapper; electrostatic insect catcher; green peach aphid; housefly; physical control; shore fly; tomato leaf miner; western flower thrips; whitefly

Citation: Matsuda, Y.; Toyoda, H. Target-Size-Dependent Application of Electrostatic Techniques for Pest Management in Greenhouses. *Agronomy* **2023**, *13*, 125. <https://doi.org/10.3390/agronomy13010125>

Academic Editor: Christos Athanassiou

Received: 8 December 2022
Revised: 23 December 2022
Accepted: 27 December 2022
Published: 30 December 2022



Copyright: © 2022 by the authors. Licensee MDPI, Basel, Switzerland. This article is an open access article distributed under the terms and conditions of the Creative Commons Attribution (CC BY) license (<https://creativecommons.org/licenses/by/4.0/>).

1. Introduction

Electrostatic techniques have been developed to precipitate airborne biotic and abiotic nuisances (such as airborne fungal spores, flying insect pests, pollen grains causing pollinosis, and tobacco smoke particles) in various environments [1]. The major electrostatic principle used in these approaches is the formation of an electric field. An electric field is the space surrounding an electric charge that exerts a perceptible force on another electric charge [2]. A negative charge is supplied to a conductor by connecting it to a direct current (DC) negative voltage generator (NVG). An NVG is a booster that enhances an initial voltage (12 V) to a desired voltage using a transformer and Cockcroft circuit integrated into a voltage generator [3]. Using this enhanced voltage, an NVG draws negative charge (free electrons) from a ground and supplies it to a conductor linked to the voltage generator. Negative charge accumulates on the conductor and generates an electric field in the surrounding space. If a grounded conductor is placed inside the electric field, the negative charge on the charged conductor polarizes the grounded conductor positively by electrostatic induction [4]. Eventually, the opposite charges on the conductor and grounded conductor form a dipolar electric field in the space between them. In this study, based on this electrostatic theory, we constructed two different physical tools to control insect pests.

First, we produced a device to capture flying insect pests in a dipolar electric field. Kakutani et al. [5] proposed such a device using an insulated metal wire and a non-insulated, grounded metal net. They tested it on the vinegar fly, *Drosophila melanogaster* Meigen (Diptera, Drosophilidae). A negative charge on the insulated wire pushed negative electricity (free electrons) out of the fly body and onto the grounded metal net. Eventually,

the fly became positively electrified and was drawn to the negatively charged, insulated wire. They referred to this phenomenon as “discharge-mediated positive electrification of an insect.” This method worked because of the highly conductive nature of the cuticle layer of the insect body [6–10]. The same group found that the mechanism is effective for many insect species (across 8 orders and 15 genera) [11]. Building on this idea, our electric-field-based insect-capturing device employed a pair of identical metal plates: one was insulated with a soft polyvinyl chloride resin and linked to a continuous-charge voltage generator, while the other was noninsulated and linked to a grounded line. The use of the two parallel metal plates enabled an even pole distance (the distance between the two plates) to be created over the entire surface of the plates, which was expected to have the same attractive force for target insects at any location along the plate. More importantly, an insulative coating on the charged metal plate would effectively prevent accidental electrocution of workers.

Next, a device was produced to kill insects via an arc discharge. This concept was originally used to manage the rice weevil, *Sitophilus oryzae* Linnaeus (Coleoptera: Curculionidae), a warehouse pest that nests in stored rice [12,13]. In previous studies, two identical conductors (metal nets or plates) were placed in parallel at a defined interval to form a dipolar electric field between them. One conductor was linked to an NVG, and the other was linked to a grounded line. Because the negatively charged conductor was not insulated, the negative charge on the conductor was discharged toward the insect when it entered the electric field (the space between the two conductors). Insects were killed by the strong impact of the discharge [12,13]. However, because of the high risk of electrocution with this system, it was essential to furnish the device with an insulation guard. Thus, in our arc-discharge-based device reported herein, we used a pulse-charge-type voltage generator, which is commonly used in electric fences to repel wild animals. Electric fences are ubiquitous and essential in modern agriculture. Accidents in association with agricultural electric fences are very rare [14]. Although unintentional human contact with electric fences occurs regularly, it causes little more than temporary discomfort [14].

A total of six pest species were targeted and tested with two devices that had different body sizes; these are listed in Table S1. All pests in the small- and middle-size groups were able to pass through a conventionally woven “insect-proof” net (1–1.5 mm mesh size) installed on the windows of greenhouses. Most greenhouse plants are vulnerable to direct attacks by these pests as well as serious infections caused by viral, bacterial, and fungal pathogens that are carried by these vectors. In particular, whiteflies, thrips, and aphids transmit viral pathogens: tomato yellow leaf curl virus [15,16], tomato spotted wilt tospovirus [17,18], and cucumber mosaic virus [19], respectively. Shore flies in the middle-sized group were also able to pass through the net and transfer rhizosphere fungal pathogens (*Verticillium dahliae* and *Fusarium oxysporum* f. sp. *radicis-lycopersici*) [20,21]. Vinegar flies have been targeted as a potential vector of various bacterial and fungal pathogens [22]. The most problematic pest in our greenhouses was the viruliferous whitefly. Tomato plants suffer from viral diseases every year in our greenhouses [23], whereas other pests seldom cause problems. Thus, the establishment of a reliable control method for whiteflies was extremely important in the present study.

Although houseflies in the large size group were not able to pass through the net, they were frequently transferred to greenhouse soil beds from cattle manure used for fertilization [24]. Cattle manure is the major organic fertilizer in our greenhouse cultivation system and is typically applied once or twice each year. Unfortunately, it frequently contains the larvae of houseflies, and therefore adult flies frequently emerge during plant cultivation. Houseflies can transmit pathogenic *Escherichia coli* O157 [25,26], causing food poisoning in people who ingest foods contaminated with this pathogen. *E. coli* O157 is originally present in the intestines of cattle and sheep, where it does not cause disease [25–27]. However, housefly larvae develop in animal feces [25], and the microbes they ingest remain viable in their excreta; consequently, they carry and disseminate *E. coli* for several days [25] and thus

pose a threat to public health [28–30]. Therefore, the management of adult houseflies that emerge from underground is of critical importance.

In an effort to give greenhouse managers/researchers flexibility in what tool would be best for their current situation, we designed the two devices mentioned above. The main distinction between the two devices is that one features an iron plate that is covered with a soft polyvinyl chloride resin and linked to a continuous-charge type voltage generator; the other is not insulated and is linked to a pulse-charge type voltage generator. We call the former the electrostatic insect catcher (EIC) and the latter the arc-discharge zapper (ADZ). These works are unique challenges to develop new physical methods for pest control, and the newly devised apparatuses possess simple structures, allowing ordinary greenhouse workers to fabricate or improve them for their own requirements and exert prominent control functions to target insect pests.

2. Materials and Methods

2.1. Insects

Adult whiteflies (*B. tabaci*), vinegar flies (*D. melanogaster*), western flower thrips (*F. occidentalis*), wingless female green peach aphids (*M. persicae*), and pupae of houseflies (*M. domestica*) and tomato leaf miners (*L. sativae*) were purchased from Sumika Technoservice (Hyogo, Japan). Pupae of greenbottle flies (*L. sericata*) were purchased from the Japan Maggot Company (Okayama, Japan). Although vinegar fly *D. melanogaster* and greenbottle fly *L. sericata* were not pests of greenhouse plants, they were added as supplements to the medium- and large-size groups, respectively.

Houseflies and greenbottle flies were reared on a certified diet (MF; Oriental Yeast Co., Ltd., Tokyo, Japan) [31] in a closed 30 mL transparent acrylic vessel. The rearing was conducted in a growth chamber (25 ± 0.5 °C, 12 h photoperiod, 4000 lux) from the egg to adult stages. Pupae found in the medium were individually transferred into fresh medium in a 20 mL vial for isolation, and the vial mouth was covered with gauze. The sexes of adult flies that emerged from the pupal stage were determined based on the sexual dimorphism of their external morphology [32,33]. For immobilization, adult houseflies and greenbottle flies were anesthetized by CO₂ exposure according to a method described previously [34]. The vials containing insects were placed in a non-vacuum glass desiccator (jar capacity: 5 L) into which CO₂ gas (Air Water West Japan Inc., Osaka, Japan) was continuously introduced at 10 kg/cm² for 4–5 min. The air in the desiccator was simultaneously exhausted from an exhaust port on the desiccator lid. The introduction of CO₂ was stopped when all insects were anesthetized. In the CO₂ treatment, all of the anesthetized flies awoke within 5 min. These immobilized flies were used in the experiments.

Adult vinegar flies were reared on blue medium (Wako Pure Chemical, Osaka, Japan) under the above conditions, and newly emerged adults (15–24 h after eclosion) were used as active flies for experiments. The whiteflies were reared on 10-day-old kidney bean (*Phaseolus vulgaris* L. ‘Nagauzura-saitou’) seedlings [35] in a phytotron (22–34 °C). Adult western flower thrips and wingless adult female green peach aphids were reared on water-swollen seeds and 1-week-old broad-bean (*Vicia faba* L. “GB-Blend”) seedlings in a growth chamber according to the methods of Murai [36] and Murai and Loomans [37]. Pupae of tomato leaf miners were maintained in a growth chamber until the adults emerged. Adult shore flies were collected from a hydroponic tomato greenhouse and maintained on a lawn of green algae (*Chlamydomonas reinhardtii* Dangeard). The lawn was cultured on a sponge cube soaked in hydroponic culture solution in a transparent 2 L culture bottle; the bottle opening was covered with a woven net of 0.6 mm mesh [38]. The test insects were held in a temperature-controlled growth chamber (26 ± 2 °C, 35–45% relative humidity, and a 16 h photoperiod with 4000 lux from fluorescent lamps). The hatched winged adult female green peach aphids and newly emerged adults of other test insects (whiteflies, western flower thrips, tomato leaf miners, vinegar flies, and shore flies) were collected with an insect aspirator (Wildco, Yulee, FL, USA).

Table S1 shows the mean body sizes of the insects (i.e., length from head to wing tip), where 20 adults of each species were measured.

2.2. Experimental Instrument for an Insect-Capturing Assay

2.2.1. Fabrication of the Instrument

Figure 1 shows the structure of the instrument used to capture insects. The instrument consisted of two identical iron plates ($30 \times 20 \text{ mm}^2$; thickness, 1 mm) horizontally arranged at defined separation intervals (5 or 10 mm). One plate was coated with a soft polyvinyl chloride resin for insulation (coating thickness, 2 mm; resistivity, $2 \times 10^8 \Omega\text{cm}$) (Sonoda Seisakusho, Osaka, Japan) and linked to a direct current (DC) negative voltage generator (NVG) (continuous-charge type; applicable voltage, -0.1 to -10 kV) (Max Electronics, Tokyo, Japan). The voltage generator was operated by a lithium storage battery (12 V). The other plate was non-insulated and linked to a grounded line. In this instrument, the negative charge that accumulated on the surface of the charged conductor plate dielectrically polarized an insulating cover, positively on the inner surface and negatively on the outer surface [39]. The negative charge on the insulated conductor plate (ICP) generated a monopolar electric field in the surrounding space (Figure 1A). When the grounded conductor plate (GCP) entered the monopolar electric field, the negative charge on the ICP polarized it positively to form a dipolar electric field between them (Figure 1B). Any insect that entered the dipolar electric field was deprived of free electrons from its body, causing it to be positively polarized. This drew the polarized insect to the negatively charged ICP (NIP) [5].

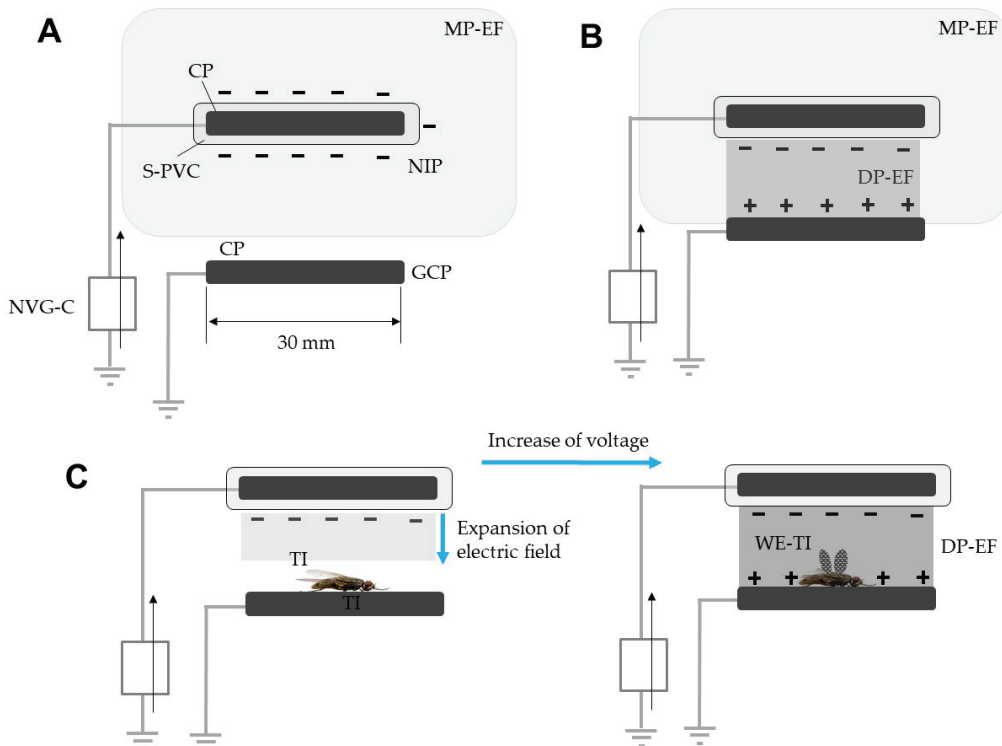


Figure 1. Structure of an experimental instrument for capturing insects and the formation of monopolar and dipolar electric fields. (A) Two identical conductor (iron) plates (CPs) were horizontally arranged;

the upper plate was insulated with a soft polyvinyl chloride (S-PVC) resin and linked to a negative voltage generator (continuous-charge type) (NVC-C), and the lower plate was non-insulated and linked to a grounded line (cross-sectional view). A negatively charged insulated conductor plate (NIP) formed a monopolar electric field (MP-EF) in the surrounding space. A grounded conductor plate (GCP) was located outside the MP-EF. (B) When the GCP entered the MP-EF, it was positively polarized by the negative surface of the NIP as a result of electrostatic induction; eventually, a dipolar electric field (DP-EF) was formed between the two plates. (C) Determination of the expansion of the electric field based on a wing erectness phenomenon observed with a test insect (TI) that entered the dipolar electric field. The electric field was expanded in direct proportion to the increase in the voltage applied to the insulated conductor plate. The insect lifted its wings (WE-TI) when it entered the electric field. The black arrows represent the direction of the movement of negative electricity.

2.2.2. Electric Field Expansion with an Increase in Voltage

First, we evaluated the area of the electric field generated by the NIP (its reach). Kakutani et al. [5] reported that an insect in an electric field first lifts its wings in response to the attractive force of the conductor and is then drawn to it by an increase in the applied voltage. In the present study, we adopted this wing erectness phenomenon as a sign that an insect had encountered a field. We placed two rectangular polypropylene (insulator) spacers (length: 20 mm; width: 3 mm; height: 5 mm) at both ends of the GCP to create a separation interval of 5 mm between the NIP and GCP. As the monopolar electric field produced by the NIP was expanded by an increase in the voltage applied (Matsuda et al. 2006), we placed a test insect (an adult whitefly) onto the GCP and raised the voltage gradually until the insect lifted its wings. At that point, we considered that a dipolar electric field was formed between the NIP and GCP (Figure 1C). In addition, we fabricated the instruments at 6 to 10 mm intervals and determined the voltage that formed the dipolar electric field between the two plates at these interval settings, using the wing erectness method mentioned above.

2.2.3. Insect-Capturing Assay

Next, we ran an experiment using the instrument with two plates spaced by a 5 mm interval. The ICP was negatively charged at different voltages (0.1 to 10 kV). Test insects (without respect to their sex) belonging to the small- and middle-size groups (Table S1) were transferred individually onto the GCP using an insect aspirator. Because adult houseflies and greenbottle flies were too large to transfer that way, they were immobilized by CO₂ anesthetization and then gently transferred onto the GCP with bamboo forceps. The edges of the forceps were covered with rubber caps. After the flies awoke from anesthesia, the voltage was applied. Twenty insects were used for each species and each voltage to determine the rate of capture at a given voltage.

2.3. Experimental Instrument for Exposing Insects to an Arc Discharge

2.3.1. Fabrication of the Instrument

Figure 2 shows the second experimental instrument used to expose an insect to an arc discharge. The instrument consisted of two identical iron plates (30 × 20 mm²; thickness, 2 mm) horizontally arranged at a defined interval. One plate was non-insulated and linked to a pulse-charge-type NVG (pulse interval, 1 s; usable voltage, −10 kV) (Suematsu Denshi, Kumamoto, Japan), and the other plate was linked to a grounded line. The voltage generator was operated by a lithium storage battery (12 V) powered by a solar panel. In this instrument, the pole distance determined the occurrence of arcing. In the first experiment, the GCP was lifted gradually and settled at the position where the arcing by the NNP occurred (Figure 2). At this position, a dipolar electric field was formed between the NNP and GCP, and arcing occurred [40]. In this instrument, pulsed arcing occurred continuously in the electric field at an interval of 1 s.

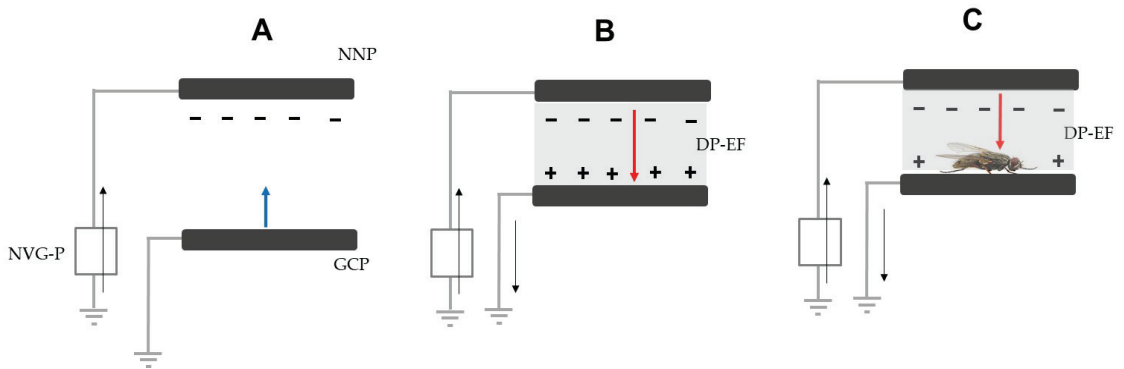


Figure 2. (A, B) Schematic representation of arc-discharge generation by an experimental instrument. The instrument consisted of a negatively charged non-insulated conductor plate (NNP) linked to a negative voltage generator (pulse-charge type) (NVG-P), and a grounded conductor plate (GCP). The GCP was lifted gradually (blue arrow) (A) and settled in a position that caused an arcing (red arrow) by the NNP (B), where a dipolar electric field (DP-EF) was formed between the two plates to positively polarize the GCP. In this position, the pulsed arcing continuously occurs at an interval of 1 s. The arcing was preferentially directed to an insect that was located on the GCP (C).

2.3.2. Exposure of Insects to an Arc Discharge

Next, we introduced insects into an electric field in which pulsed arcing occurred continuously to examine whether the arcing was preferentially directed toward them (Figure 2). Small- and intermediate-sized insects were individually transferred onto the GCP of the charged instrument with an insect aspirator; large ones were first immobilized as described above. We examined whether preferential arcing was dependent on the body size of the insect. We used 20 insects from each species. We measured the weight of insects before and after they were subjected to arcing to estimate the loss of body water due to the arcing treatment.

2.4. Construction and Practical Application of the EIC and ADZ

2.4.1. Construction of the EIC and ADZ

Next, the practical application of each device was tested (Figure 3). The two devices were constructed on an identical framework, namely, the NIPs and GCPs or NNPs and GCPs were alternately arrayed in parallel at an interval of 5 mm in the EIC and ADZ, respectively. The NIPs and NNPs were linked to a continuous- and pulse-charge-type voltage generator, respectively. In both devices, the plates were fixed with two polypropylene props that were pierced into the holes on both ends of the plates, and the separation interval between the plates was created using polypropylene cylindrical spaces with a height of 5 mm.

2.4.2. Insect-Capturing Assay

An insect-capturing assay was conducted in a closed cabinet (2 m^3) placed in a greenhouse (Figure 4A). In this experiment, the EIC ($30 \times 30\text{ cm}^2$) was furnished with a yellow board to attract phototactic insects to the vicinity of the device (Figure 4B). A yellow board was prepared by coloring a thick piece of paper with a watercolor paste (Turner Color Works Ltd., Osaka, Japan). Its Munsell hue/value/chroma index [41] was 7Y8.5/11 (yellow), which corresponded to the coloration of a commercially available yellow sticky trap (Horiver yellow trap; Arysta LifeScience Corp., Tokyo, Japan). The coloration of the yellow board was measured using an RGB-1002 color analyzer (Sato Shoji Inc., Kanagawa, Japan). Whiteflies were used as a model insect for phototactic insects. Two yellow-boarded EICs, two commercial yellow sticky traps of the same size as the EIC, and two potted tomato

(*Solanum lycopersicum* cv. Momotaro Fight) plants (1-month-old seedlings; 40 cm high from the pot bottom to the plant top) were placed on the concyclic points at regular intervals, and a vessel containing 20 whiteflies was placed at the central point of a circle. In this experiment, 24 and 48 h after the insects were released, we counted the number of test insects that had been captured by the EICs and sticky trap plates, the number of test insects that had reached the plant, and the number of test insects that remained in the vial or on the walls and ceiling of the cabinet. The experiments were conducted separately and repeated five times.

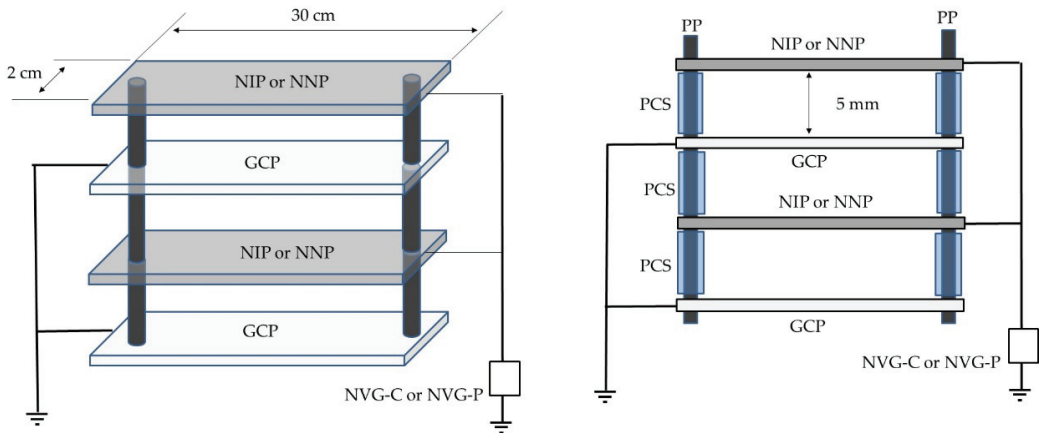


Figure 3. Schematic representation of an identical framework for an electrostatic insect catcher (EIC) and arc-discharge zapper (ADZ). The devices consisted of identical conductor (iron) plates, polypropylene props (PPs), polypropylene cylindrical spacers (PCSs), and a negative voltage generator. Negatively charged insulated conductor plates (NIPs) and grounded conductor plates (GCPs) or negatively charged non-insulated conductor plates (NNPs) and GCPs were arranged in parallel at an interval of 5 mm to fabricate the EIC and ADZ, respectively. The plates were fixed with the PCSs, which were poked into the holes on both sides of the plates, and the separation intervals between the plates were made by the PCSs that passed through the PPs. The EIC and ADZ were linked to the continuous-charge and pulse-charge types of negative voltage generators (NVG-C and NVG-P, respectively).

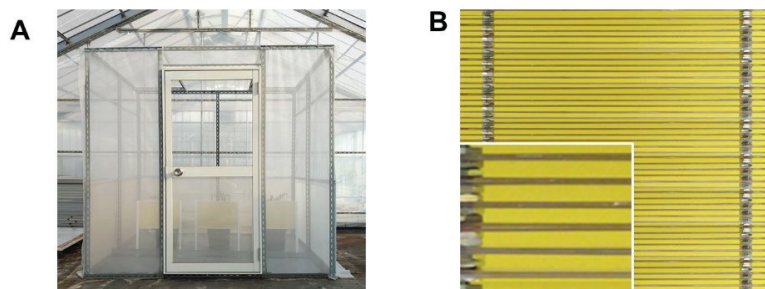


Figure 4. (A) A closed, small, cubic cabinet placed inside a greenhouse for conducting an insect-capturing assay. (B) An electrostatic insect catcher (EIC) furnished with a yellow board to attract phototactic insect pests. The insert in B shows an enlarged part of the EIC.

2.4.3. Arc-Discharge Exposure Assay

The ADZ was applied to kill adult houseflies that emerged from pupae in the soil bed of a greenhouse. In this test, we utilized the strong impact of the arc discharge to strike houseflies that climbed on to the apparatus. For this purpose, we set the plates of the ADZ vertically and placed them on a plastic grid ($30 \times 30 \text{ cm}^2$; 20 mm height) that consisted of multiple cells (Figure 5A). The cells provided a climbing path for the houseflies on the soil surface to the arcing site of the ADZ. In the first experiment, CO_2 -anesthetized male and female houseflies were individually transferred to the bottom of the grating cells. The houseflies climbed along the wall of the cell and were subjected to the arc discharge when they reached the arcing zone, which forced them down to the bottom of the cell (Figure 5B). Due to their inherent habit of climbing upward [42], the flies continued to climb even after they were subjected to the arc discharge and knocked down to the bottom of the grating. We therefore counted the number of climbing trials until they died. In the second experiment, we transferred different numbers (25, 50, 75, and 100 adults) of anesthetized houseflies (without respect to their sex) to separate cells to create a situation in which multiple adult houseflies invaded successively. In the first round of experiments, we increased the numbers of adult houseflies stepwise from 25 to 75 in individual experiments, and the experiment was conducted once for each number of flies. In the second round, we used 100 and 110 adult houseflies and conducted the same experiment five times for each. At the end of the experiment (after 2 days), we counted the number of dead houseflies on the bottom of the cells.

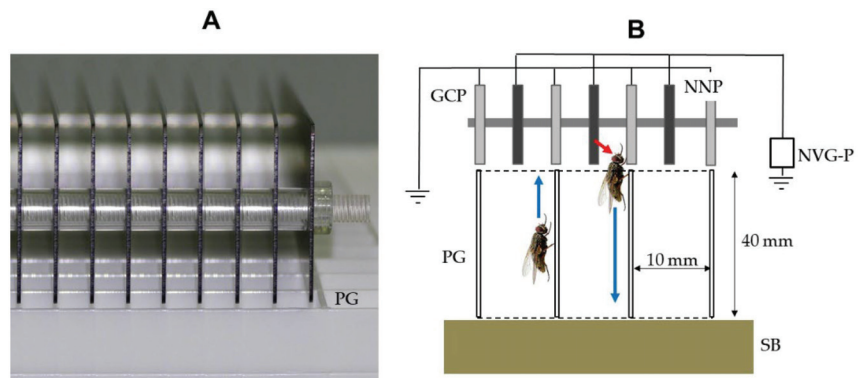


Figure 5. Photograph (A) and schematic representation (B) of an arc-discharge zapper (ADZ) placed on a plastic grating (PG). The ADZ, which consisted of negatively charged non-insulated conductor (iron) plates (NNPs) linked to a pulse-charge type voltage generator (NVG-P) and grounded conductor plates (GCPs), was placed on a plastic grating (40 mm height, 10 mm square cells). Houseflies anesthetized with CO_2 were transferred to the bottom of the separate cells of the PG placed on a soil bed (SB). After awaking from anesthesia, they climbed along the wall of the cell (blue arrow) and were subjected to an arc discharge (red arrow) from the NNP when they reached the arcing zone, then were knocked downward (blue arrow) by the strong impact of the arc discharge.

2.5. Statistical Analysis

All experiments were repeated five times, and all data are presented as means with standard deviations. The analyses were performed using the EZR software version 1.54 (Jichi Medical University, Saitama, Japan) to identify any significant differences among the results obtained under different test conditions, which are shown in the figure and table legends.

3. Results and Discussion

3.1. Construction of the EIC

3.1.1. Expansion of the Electric Field of the NIP by Increasing the Applied Voltage

The electric field of the NIP expanded as the voltage was increased; as described above, we measured the field area based on the wing erectness method (using whiteflies). Figure 6 shows the voltages required to connect the NIP and GCP with an electric field in the instruments where the intervals of the two plates were 5 to 10 mm. At a separation interval of 5 mm, the electrostatic force on the whitefly was initially detectable at around 0.5 kV, with the flies erecting their wings and seemingly bracing against the NIP attraction force. Video S1 shows this behavior. The longer separation intervals (6 and 7 mm) required higher voltages (−5 and −9.5 kV, respectively). At <8 mm, no whitefly displayed wing erectness with the application of the highest voltage (−10 kV), indicating that the electric field did not reach the GCP. Based on these results, we first settled the GCP at a position 5 mm from the NIP, at which point we were able to use a wider range of voltages (−0.5 to −10 kV). The use of a higher voltage reinforced the electric field intensity, and led to the exertion of a stronger force on the insects in the electric field.

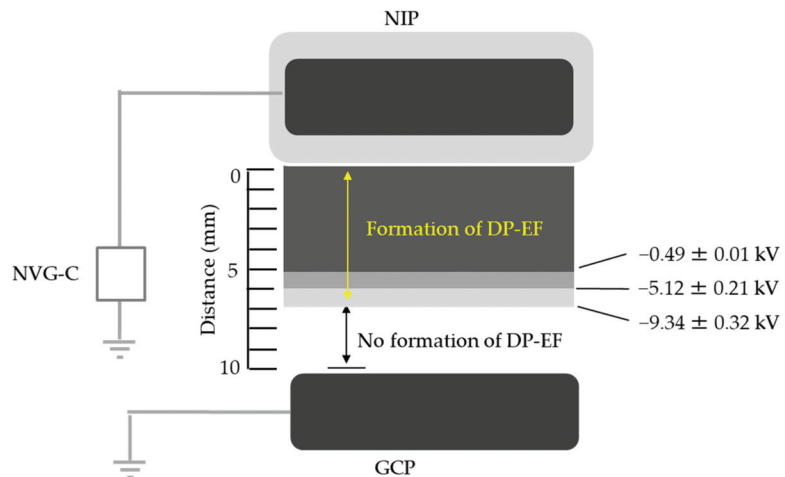


Figure 6. The voltages required to form a dipolar electric field (DP-EF) between a negatively charged insulated conductor (iron) plate (NIP) and a grounded conductor plate (GCP), which were spaced by different distances (5–10 mm). The NIP was linked to a negative voltage generator (continuous-charge type) (NVG-C) and charged with different voltages (−0.1 to −10 kV).

3.1.2. Insect-Capturing Ability

All test insects were transferred individually onto the GCP of the insect-capturing instrument that was negatively charged with different voltages (−0.1 to −10 kV). Table 1 shows the percentage of captured insects at each voltage. Higher voltages were required to capture larger insects. For example, for whiteflies (small insects) and vinegar flies (intermediate), charging at −1 and −4 kV, respectively, was sufficient to capture all insects. Videos S2A and S2B demonstrate the strong capture of an adult whitefly at −1 kV and a vinegar fly at −4 kV, respectively. At lower voltages, however, the attractive force was insufficient, and the insects ultimately escaped from the trap. All small and intermediate insects were captured at <−3.1 kV (Table 1).

Table 1. Percentage of insects captured by an experimental instrument consisting of a negatively charged insulated conductor (iron) plate (NIP) and a grounded non-insulated conductor plate (GCP) at a separation interval of 5 mm.

| Test Insects * | Negative Voltage (–kV) Applied | | | | | | | | | | | |
|----------------|--------------------------------|--------------|-------|-------|--------------|--------------|--------------|--------------|-------|-------|-------|-------|
| | 0.4 | 0.6 | 0.8 | 1 | 1.2 | 1.6 | 2 | 3 | 4 | 6 | 8 | 10 |
| WH | 0 | 42.1 ± 5.3 a | 100 a | 100 a | 100 a | 100 a | 100 a | 100 a | 100 a | 100 a | 100 a | 100 a |
| WFT | 0 | 0 b | 0 b | 0 b | 36.8 ± 2.7 b | 91.3 ± 2.2 b | 100 a | 100 a | 100 a | 100 a | 100 a | 100 a |
| TLM | 0 | 0 b | 0 b | 0 b | 48.6 ± 4.2 b | 95.6 ± 3.2 b | 100 a | 100 a | 100 a | 100 a | 100 a | 100 a |
| SF | 0 | 0 b | 0 b | 0 b | 0 c | 18.8 ± 2.2 c | 48.3 ± 2.7 b | 79.3 ± 4.9 b | 100 a | 100 a | 100 a | 100 a |
| VF | 0 | 0 b | 0 b | 0 b | 0 c | 20.5 ± 5.1 c | 54.6 ± 3.9 b | 84.9 ± 2.8 b | 100 a | 100 a | 100 a | 100 a |
| GPA-w | 0 | 0 b | 0 b | 0 b | 0 c | 0 d | 68.7 ± 3.5 c | 97.3 ± 4.2 c | 100 a | 100 a | 100 a | 100 a |
| HF-m | 0 | 0 b | 0 b | 0 b | 0 c | 0 d | 0 d | 0 d | 0 b | 0 b | BF ** | BF |
| GBF-m | 0 | 0 b | 0 b | 0 b | 0 c | 0 d | 0 d | 0 d | 0 b | 0 b | BF | BF |
| HF-f | 0 | 0 b | 0 b | 0 b | 0 c | 0 d | 0 d | 0 d | 0 b | 0 b | BF | BF |
| GBF-f | 0 | 0 b | 0 b | 0 b | 0 c | 0 d | 0 d | 0 d | 0 b | 0 b | BF | BF |

* Refer to Table 1 for the abbreviations of insect names. Insect species are ordered from top (smallest) to bottom (largest) according to their body sizes. ** bridge is formed by an inset body between the NIP and GCP. Twenty insects were used for each voltage and each species. The means ± standard deviations were calculated from five experimental replicates. The different letters (a–d) within a column indicate significant differences ($p < 0.05$) according to Tukey’s test.

The attractive force of the instrument (5 mm interval) was sufficient to draw large insects (houseflies and greenbottle flies) to the NIP at >–8 kV. However, their capture was considered abnormal because a bridge was established between the opposite poles by the insect body, which was large enough to touch both poles (Figure 7A) (Video S3A). In this case, the flies formed a direct route for the electric current to flow between the opposite poles. The current flow erased the surface accumulation of negative charge (i.e., loss of attractive force) and eventually caused the insulating coating to break down.

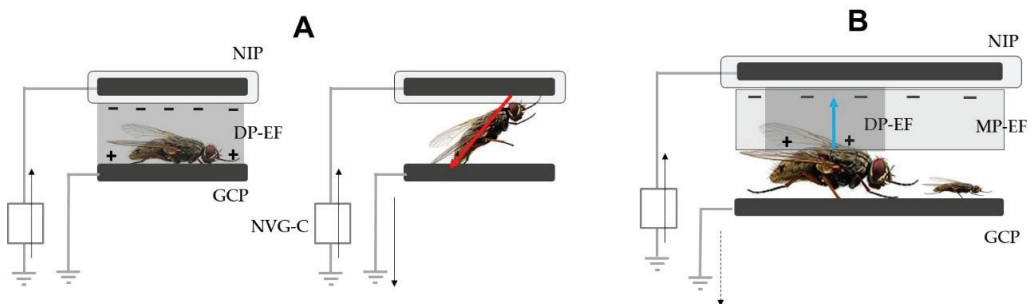


Figure 7. (A) Formation of an insect body bridge between the negatively charged insulated conductor plate (NIP), which was linked to a negative voltage generator (continuous-charge type) (NVG-C), and the grounded conductor plate (GCP). The electric current (red arrow) moved over a direct route (i.e., the insect body) between the two plates. (B) Formation of an insect-mediated opposite pole to the NIP. A large fly (housefly and greenbottle fly) on the GCP reached a monopolar electric field (MP-EF) to create a dipolar electric field (DP-EF) between the NIP and the fly. Eventually, the fly was positively electrified and drawn to the NIP (blue arrow). At this distance between the NIP and GCP, small insects did not reach the MP-EF and were therefore not drawn to the NIP. The solid black arrow represents the direction of movement of the negative charge (free electrons), and the dotted black arrow represents an insect-derived transient electric current caused by its positive electrification.

To solve this problem, it was essential to make the separation distance wider. A separation interval of 10 mm was wide enough to avoid this problem. At this distance, the NIP was not able to expand its monopolar electric field to the GCP even when the highest voltage (–10 kV) was applied; the expansion at –10 kV was approximately 7 mm (Figure 6). However, large flies (houseflies and greenbottle flies) reached the monopolar

electric field (MP-EF) and formed a dipolar electric field between the NIP and themselves when they were located on the GCP (Figure 7B). In this situation, the flies were deprived of free electrons and became positively polarized, eventually being drawn to the NIP (Table 2). In both fly species, male flies were smaller than females, and therefore lower voltages (−8 kV) were sufficient to capture them, while a charge of −9 kV was necessary to capture female adults. Video S3B shows the successful capture of a female adult housefly at −9 kV.

Table 2. Capture of insects with different body sizes by an experimental instrument consisting of a negatively charged insulated conductor (iron) plate (NIP) and a grounded non-insulated conductor plate (GCP) at a separation interval of 10 mm.

| Insects Used * | Negative Voltage (−kV) Applied | | | | | | |
|----------------|--------------------------------|--------------|--------------|--------------|-------|-------|-------|
| | 5 | 5.5 | 6 | 7 | 8 | 9 | 10 |
| WH | 0 | 0 a | 0 a | 0 a | 0 a | 0 a | 0 a |
| WFT | 0 | 0 a | 0 a | 0 a | 0 a | 0 a | 0 a |
| TLM | 0 | 0 a | 0 a | 0 a | 0 a | 0 a | 0 a |
| SF | 0 | 0 a | 0 a | 0 a | 0 a | 0 a | 0 a |
| VF | 0 | 0 a | 0 a | 0 a | 0 a | 0 a | 0 a |
| GPA-w | 0 | 0 a | 0 a | 0 a | 0 a | 0 a | 0 a |
| HF-m | 0 | 12.1 ± 0.5 b | 78.6 ± 0.1 b | 100 b | 100 b | 100 b | 100 b |
| GBF-m | 0 | 13.6 ± 0.2 b | 82.3 ± 0.3 b | 100 b | 100 b | 100 b | 100 b |
| HF-f | 0 | 0 a | 22.2 ± 0.4 c | 84.5 ± 0.6 c | 100 b | 100 b | 100 b |
| GBF-f | 0 | 0 a | 24.6 ± 0.8 c | 86.7 ± 0.8 c | 100 b | 100 b | 100 b |

* Refer to Table 1 for the abbreviations of insect names. Insect species are ordered from the top (smallest) to the bottom (largest) according to their body sizes. Twenty insects for each voltage and each species were used. The means ± standard deviations were calculated from five experimental replicates. The different letters (a–c) within a column indicate significant differences ($p < 0.05$) according to Tukey's test.

In addition, as shown in Table 2, not all insects in the small and medium-sized groups were captured at this separation distance because they did not reach the monopolar electric field of the NIP (Figure 7B). From these results, we concluded that it is impossible to capture all insects in the three groups using an instrument with a separation interval of either 5 or 10 mm.

3.2. Construction of the ADZ and Preferential Arcing for Insects

The NNP was able to generate pulsed arcings at an interval of 1 s toward the GCP when the separation interval between them was settled at 5 mm. In this experiment (described above), all male and female housefly and greenbottle fly adults were preferentially subjected to pulsed arcing after they were introduced to the electric field (Figure 8A). The impact produced by the arc discharge was so strong that the flies were rendered motionless by the first pulsed arcing (Video S4A). The arcing continued for a while and then stopped automatically. This automatic stoppage was due to a decline in body conductance caused by the loss of body water [43,44]. We confirmed that the insects that received continuous pulsed arcing had lost more than 50% of their body water. Small/intermediate insects did not receive preferential arcing, with arcing continuing between the two plates regardless of the presence of an insect on the G-MN (Figure 8B). Preferential arcing did not occur even when the distance between the two plates was shortened (4 and 3 mm). These results suggest that insect body size is of critical importance or receives a certain amount of electric charge. The capacitance is defined as the ability of the conductor to store or receive an electrical charge and depends on the shape and size of the conductor (i.e., larger conductors receive a larger electric charge) [45]. In our interpretation, it was essential for the conductor (the insect) to have a sufficient capacitance to receive the total electric charge released by the charged conductor (the NNP) through an arc discharge. Consequently, the capacitances of small/intermediate insects were too small to receive arcing. Accordingly, we conclude that the arc discharge method is suitable only to control houseflies.

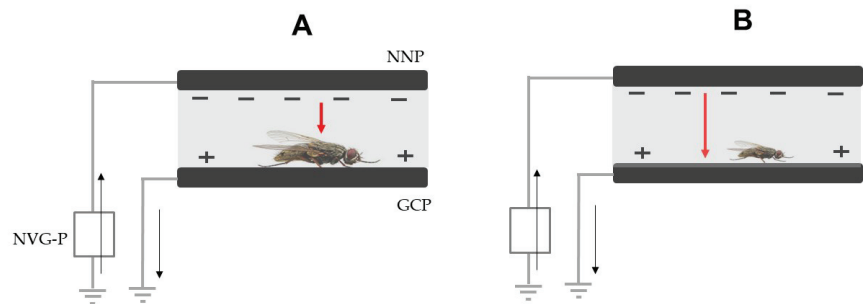


Figure 8. Schematic representation of preferential (A) and non-preferential (B) arcing to an insect in the electric field. The instrument consisted of a negatively charged non-insulated conductor plate (NNP), which was linked to a negative voltage generator (pulsed-charging type) (NVG-P), and a grounded conductor plate (GCP). (A) Larger insects were introduced into the electric field where a pulsed arc was generated and preferentially subjected to an arc discharge (red arrow) from the NNP. (B) No preferential arcing occurred to small insects, and the arcing occurred between the two plates as before. The black arrow indicates the movement of negative electricity.

3.3. Practical Application of the EIC and ADZ

Of the insects used in the present study, whiteflies and houseflies are the most intractable pests in our greenhouse for tomato cultivation [23,24], and therefore it was important to evaluate the feasibility of the new devices for these two insect pests. The EIC had the ability to capture insects that entered its electric field; however, it could not attract insects beyond a certain distance from the apparatus. This weakness was compensated for by adding a yellow-colored plate to the apparatus because many harmful flying insect pests, including whiteflies, winged aphids, leaf miners, thrips, and shore flies, are effectively attracted to yellow objects [46]. This was effective for luring distant whiteflies into the electric field of the device. The attraction-and-capture provided by the device was equivalent to a commercial yellow sticky trap (Figure 9), indicating the effectiveness of the EIC in greenhouse operations. Interestingly, whiteflies exhibited a stronger photoselectivity to the yellow-colored traps than the host tomato plant. These results strongly suggest that the EIC combined with a yellow board is useful as an on-site method to control flying phototactic insect pests in a greenhouse.

For practical use of the ADZ, we used the impact of the arc discharge to knock down adult houseflies that climbed onto the device. For this purpose, we set all of the plates vertically and placed them on a plastic grating (Figure 5A). The separate cells of the grating enabled adult houseflies on the soil surface to climb up to the arcing zone of the ADZ, as described above. As previously described, the flies repeatedly climbed up, were impacted by the arc, and eventually died. Both male and female houseflies were killed after three or four discharges (Figure 10) (Video S4B). These results indicate that the method was effective for killing adult houseflies of either sex that climbed onto the device from the soil surface.

According to our records over the past 3 years, in which flypapers (sticky paper ribbons) were suspended over the soil beds and the number of trapped houseflies were counted, their occurrence (during the 3-month summer season) was between 8 and 62 per m². However, this approach provided no information about how many houseflies escaped from the trap or, more importantly, how many houseflies emerged simultaneously from the soil bed. In the second experiment in a greenhouse, we directly applied adult houseflies to the ADZ to set up an acute situation in which adult houseflies (in this case, 25–110 adults) simultaneously emerged from underground pupae and successively invaded the ADZ. In the preliminary application of the 25–75 houseflies, all flies were detected as dead bodies on the bottom of the grating (Table 3). Moreover, in five repeated applications of 100 and

110 adult houseflies, we confirmed that the newly developed device was able to kill all houseflies even when 100 flies invaded successively (Table 3), whereas one or two flies escaped from the device in the case of 110 houseflies. These results indicate that if the number of synchronously emerging adult houseflies does not exceed 100, the ADZ would be able to effectively cope with successive invasions by multiple houseflies.

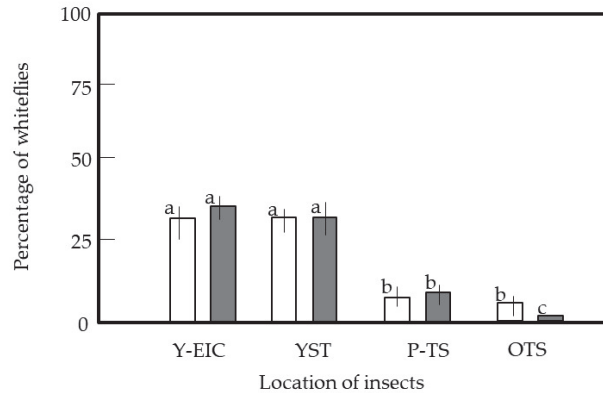


Figure 9. Assay of the preferential attraction of whiteflies to a yellow-colored electrostatic insect catcher (Y-EIC), a yellow sticky trap (YST), and a potted tomato seedling (P-TS), which were placed in concyclic positions at equal distances. A vessel containing test insects was placed at the central position of a circle. Adult whiteflies were used as test insects. In all experiments, the destinations of test insects were recorded 1 day (open) and 2 days (gray column) after their release. OTS represents other places, such as in the vial or on the floor, wall, and ceiling of the cabinet. Twenty insects were used in each experiment, and the means and standard deviations were calculated from five replicates of the experiments. The letters a–c in each vertical column indicate significant differences ($p < 0.05$) according to Tukey’s test.

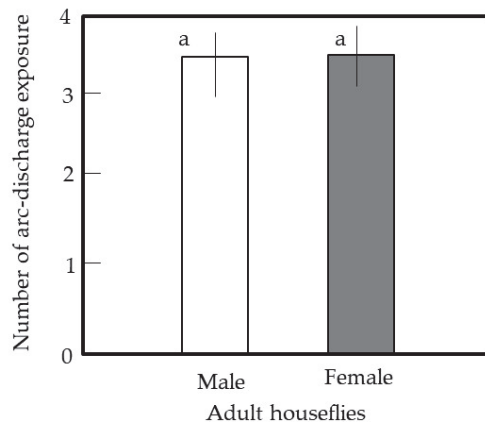


Figure 10. Number of arc-discharge exposures required to kill adult houseflies that climbed up to the arc discharge zapper (ADZ). The flies climbed along the wall of the cell of the grating placed beneath the ADZ and were subjected to the arc discharge when they reached the arcing zone of the device. They were knocked down to the bottom of the cell. The flies attempted several climbing trials and were exposed to repeated arc discharges until they died. Twenty insects were used in each experiment, and the means and standard deviations were calculated from five replicates of the experiments. The letter “a” in each vertical column indicates no significant difference ($p < 0.05$) according to Tukey’s test.

Table 3. Evaluation of the capability of the arc discharge zapper (ADZ) used to control successive invasions of adult houseflies.

| Number of Adult Houseflies Used ^a | Number of Dead Houseflies on the Bottom of the Grating | Number of Houseflies that Escaped from the ADZ |
|--|--|--|
| 25 | 25 | 0 |
| 50 | 50 | 0 |
| 75 | 75 | 0 |
| 100 | 100 | 0 |
| | 100 | 0 |
| | 100 | 0 |
| | 100 | 0 |
| | 100 | 0 |
| 110 | 98 | 2 |
| | 100 | 0 |
| | 99 | 1 |
| | 99 | 1 |
| | 98 | 2 |

^a Adult houseflies anesthetized by CO₂ were placed in separate cells of the grating. These flies climbed along the wall of the grating and reached the arcing zone of the ADZ, where they were subjected to arcing from the negatively charged non-insulated conductor plate (NNP), and then were knocked down to the bottom of the grating.

The two unique devices devised in this study (the ADZ and EIC) to manage greenhouse insect pests are both simple and easy to fabricate. The ADZ is slightly easier to fabricate and was operated safely using a pulse-charge-type voltage generator. However, its application is restricted to larger insect pests, such as houseflies. These pests are too large to pass through a conventional insect-proof net, but they are typically introduced to greenhouses as larvae in manure. Housefly management may therefore be a specific problem limited to greenhouses that utilize cattle manure. By contrast, the invasion of small flying insect pests that can pass through insect nets is common in ordinary open greenhouses. The EIC had a higher utility value for managing harmful insect pests, such as whiteflies, thrips, aphids, leaf miners, and shore flies, which are common pests. More importantly, its insect-trapping function was strengthened by adding a yellow-colored plate, which attracted insects that were some distance from the device. The EIC requires insulation of its charged metal plates; for this, we used a soft polyvinylchloride resin. Unfortunately, the coating had to be applied by a professional producer, and it will therefore be essential to prepare a substitutable coating method if the device is to be produced by greenhouse workers. Several commercially available electrostatic dissipative (ESD) materials covering the range of desired resistivities are potential candidates for insulating charged metal plates. The identification of a suitable ESD tape would make it possible to reconstruct the ADZ into an EIC merely by applying it to the metal plate for charging, because the devices share the same framework.

4. Conclusions

We constructed two electrostatic devices with a common framework to manage greenhouse insect pests. The key difference between the two devices was the presence or absence of an insulation coating on the metal plates used for charging. The charged insulated metal plates generated an electrostatic force to trap small flying insects, while the charged non-insulated metal plates generated an arc discharge to kill adult houseflies that emerged from underground pupae. Both devices are simple to fabricate and could be used as a new physical tool for physical pest management in greenhouse crop production.

Supplementary Materials: The following supporting information can be downloaded at: <https://www.mdpi.com/article/10.3390/agronomy13010125/s1>. Table S1: Average body sizes (from head to wing edge) of the adult insects tested, Video S1: Lifting of the wings of an adult whitefly placed on a grounded conductor (iron) plate (GCP) facing the negatively charged insulated conductor plate (NIP) of an insect-capturing instrument, Video S2: Capture of an adult whitefly (A) and vinegar fly (B) with a negatively charged insulated conductor plate (NIP) at -1 and -3 kV, respectively, Video S3: (A) Bridge formation between a negatively charged insulated conductor plate (NIP) and a grounded conductor plate (GCP) (5 mm interval) by an adult female housefly at a -8 kV-charge. (B) Capture of an adult female housefly with the NIP (-9 kV-charge), which was positioned 10 mm from the GCP, Video S4: (A) Arc-discharge to an adult female housefly located on a grounded conductor plate (GCP) facing a negatively charged non-insulated conductor plate (NNP). (B) The removal of a housefly from the bottom of the cylinder by the strong impact of an arc discharge

Author Contributions: Conceptualization, H.T. and Y.M.; methodology, H.T. and Y.M.; software, Y.M.; validation, H.T. and Y.M.; formal analysis, Y.M.; investigation, Y.M.; resources, Y.M.; data curation, H.T. and Y.M.; writing—original draft preparation, H.T.; writing—review and editing, Y.M.; visualization, Y.M.; supervision, H.T.; project administration, Y.M. All authors have read and agreed to the published version of the manuscript.

Funding: This research received no external funding.

Institutional Review Board Statement: Not applicable.

Informed Consent Statement: Not applicable.

Data Availability Statement: Not applicable.

Conflicts of Interest: The authors declare no conflict of interest.

References

1. Matsuda, Y.; Toyoda, H. Novel electrostatic devices for managing biotic and abiotic nuisances in environments. *Open Access J. Sci.* **2018**, *2*, 337–353.
2. Jones, E.; Childers, R. Electric charge and electric field. In *Physics*, 3rd ed.; McGraw-Hill: Boston, MA, USA, 2002; pp. 495–525.
3. Wegner, H.E. Electrical charging generators. In *McGraw-Hill Encyclopedia of Science and Technology*, 9th ed.; Geller, E., Moore, K., Well, J., Blumet, D., Felsenfeld, S., Martin, T., Rappaport, A., Wagner, C., Lai, B., Taylor, R., Eds.; The Lakeside Press: New York, NY, USA, 2002; pp. 42–43.
4. Griffith, W.T. Electrostatic phenomena. In *The Physics of Everyday Phenomena, a Conceptual Introduction to Physics*; Brufloodt, D., Loehr, B.S., Eds.; McGraw-Hill: New York, NY, USA, 2004; pp. 232–252.
5. Kakutani, K.; Matsuda, Y.; Haneda, K.; Sekoguchi, D.; Nonomura, T.; Kimbara, J.; Osamura, K.; Kusakari, S.; Toyoda, H. An electric field screen prevents captured insects from escaping by depriving bioelectricity generated through insect movements. *J. Electrostat.* **2012**, *70*, 207–211. [CrossRef]
6. Ishay, J.S.; Shimony, T.B.; Shalom, A.B.; Kristianpoller, N. Photovoltaic effects in the oriental hornet, *Vespa orientalis*. *J. Insect. Physiol.* **1992**, *38*, 37–48. [CrossRef]
7. McGonigle, D.G.; Jackson, C.W. Effect of surface material on electrostatic charging of houseflies (*Musca domestica* L.). *Pest Manag. Sci.* **2002**, *58*, 374–380. [CrossRef] [PubMed]
8. McGonigle, D.G.; Jackson, C.W.; Davidson, J.L. Triboelectrification of houseflies (*Musca domestica* L.) walking on synthetic dielectric surfaces. *J. Electrostat.* **2002**, *54*, 167–177. [CrossRef]
9. Honna, T.; Akiyama, Y.; Morishima, K. Demonstration of insect-based power generation using a piezoelectric fiber. *Comp. Biochem. Physiol. Part B Biochem. Mol. Biol.* **2008**, *151*, 460. [CrossRef]
10. Moussian, B. Recent advances in understanding mechanisms of insect cuticle differentiation. *Insect Biochem. Mol. Biol.* **2010**, *40*, 363–375. [CrossRef]
11. Kakutani, K.; Matsuda, Y.; Haneda, K.; Nonomura, T.; Kimbara, J.; Kusakari, S.; Osamura, K.; Toyoda, H. Insects are electrified in an electric field by deprivation of their negative charge. *Ann. Appl. Biol.* **2012**, *160*, 250–259. [CrossRef]
12. Matsuda, Y.; Takikawa, Y.; Nonomura, T.; Kakutani, K.; Okada, K.; Shibao, M.; Kusakari, S.; Miyama, K.; Toyoda, H. Selective electrostatic eradication of *Sitophilus oryzae* nesting in stored rice. *J. Food Technol. Pres.* **2018**, *2*, 15–20.
13. Kakutani, K.; Takikawa, Y.; Matsuda, Y. Selective arcing electrostatically eradicates rice weevils in rice grains. *Insects* **2021**, *12*, 522. [CrossRef]
14. Burke, M.; Odell, M.; Bouwer, H.; Murdoch, A. Electric fences and accidental death. *Forensic Sci. Med. Pathol.* **2017**, *13*, 196–208. [CrossRef] [PubMed]
15. Fukuta, S.; Kato, S.; Yoshida, K.; Mizukami, Y.; Ishida, A.; Ueda, J.; Kanbe, M.; Ishimoto, Y. Detection of tomato yellow leaf curl virus by loop-mediated isothermal amplification reaction. *J. Virol. Methods* **2003**, *112*, 35–40. [CrossRef] [PubMed]

16. Riley, D.G.; Srinivasan, R. Integrated management of tomato yellow leaf curl virus and its whitefly vector in tomato. *J. Econ. Entomol.* **2019**, *112*, 1526–1540. [CrossRef] [PubMed]
17. Houle, J.L.; Kennedy, G.G. Tomato spotted wilt virus can infect resistant tomato when western flower thrips inoculate blossoms. *Plant Dis.* **2017**, *101*, 1666–1670. [CrossRef] [PubMed]
18. He, Z.; Guo, J.-F.; Reitz, S.R.; Lei, Z.-R.; Wu, S.-Y. A global invasion by the thrip, *Frankliniella occidentalis*: Current virus vector status and its management. *Insect Sci.* **2020**, *27*, 626–645. [CrossRef]
19. Rendina, N.; Nuzzaci, M.; Scopa, A.; Cuypers, A.; Sofo, A. Chitosan-elicited defense responses in cucumber mosaic virus (CMV)-infected tomato plants. *J. Plant Physiol.* **2019**, *234–235*, 9–17. [CrossRef]
20. Gillespie, D.R.; Menzies, J.G. Fungus gnats vector *Fusarium oxysporum* f. sp. *radicislycopersici*. *Ann. Appl. Biol.* **1993**, *23*, 539–544. [CrossRef]
21. El-Hamalawi, Z.A. Attraction, acquisition, retention and spatiotemporal distribution of soilborne plant pathogenic fungi by shore flies. *Ann. Appl. Biol.* **2008**, *152*, 169–177. [CrossRef]
22. Hubhachen, Z.; Pointon, H.; Perkins, J.A.; Van Timmeren, S.; Pittendrigh, B.; Isaacs, R. Resistance to multiple insecticide classes in the vinegar fly *Drosophila melanogaster* (Diptera: Drosophilidae) in Michigan vineyards. *J. Econ. Entomol.* **2022**, *18*, 155. [CrossRef]
23. Nonomura, T.; Matsuda, Y.; Kakutani, K.; Takikawa, Y.; Kimbara, J.; Osamura, K.; Kusakari, S.; Toyoda, H. Prevention of whitefly entry from a greenhouse entrance by furnishing an airflow-oriented pre-entrance room guarded with electric field screens. *J. Agric. Sci.* **2014**, *6*, 172–184. [CrossRef]
24. Matsuda, Y.; Shimizu, K.; Sonoda, T.; Takikawa, Y. Use of electric discharge for simultaneous control of weeds and houseflies emerging from soil. *Insects* **2020**, *11*, 861. [CrossRef] [PubMed]
25. Alam, M.J.; Zurek, L. Association of *Escherichia coli* O157:H7 with houseflies on a cattle farm. *Appl. Environ. Microbiol.* **2004**, *70*, 7578–7580. [CrossRef] [PubMed]
26. Ahmad, A.; Nagaraja, T.G.; Zurek, L. Transmission of *Escherichia coli* O157:H7 to cattle by house flies. *Prev. Vet. Med.* **2007**, *80*, 74–81. [CrossRef] [PubMed]
27. Russell, J.B.; Jarvis, G.N. Practical mechanisms for interrupting the oral-fecal lifecycle of *Escherichia coli*. *Mol. Microbiol. Biotechnol.* **2001**, *3*, 265–272.
28. Brandl, M.T. Plant lesions promote the rapid multiplication of *Escherichia coli* O157:H7 on postharvest lettuce. *Appl. Environ. Microbiol.* **2008**, *74*, 5285–5289. [CrossRef]
29. Ibekwe, A.M.; Grieve, C.M.; Papiernik, S.K.; Yang, C.-H. Persistence of *Escherichia coli* O157:H7 on the rhizosphere and phyllosphere of lettuce. *Lett. Appl. Microbiol.* **2009**, *49*, 784–790. [CrossRef]
30. Luo, Y.; He, Q.; McEvoy, J.L. Effect of storage temperature and duration on the behavior of *Escherichia coli* O157:H7 on packaged fresh-cut salad containing romaine and Iceberg lettuce. *J. Food Sci.* **2010**, *75*, M390–M397. [CrossRef]
31. Izumi, N.; Sajiki, J. Effects of bisphenol A (BPA) on sex ratio of a housefly. *Bull. Public Health Lab. Chiba Prefecture.* **2003**, *27*, 14–17.
32. Dubendorfer, A.; Hediger, M.; Burghardt, G.; Bopp, D. *Musca domestica*, a window on the evolution of sex-determining mechanisms in insects. *Int. J. Dev. Biol.* **2002**, *46*, 75–79.
33. Rognes, K. First record of the sheep greenbottle fly *Lucilia cuprina* (Wiedemann, 1830) from Europe (Diptera: Calliphoridae) with additional Spanish records of Calliphorida, Muscidae and Sarcophagidae. *Eos* **1993**, *69*, 41–44.
34. Nilson, T.L.; Sinclair, B.J.; Roberts, S.P. The effects of carbon dioxide anesthesia and anoxia on rapid cold-hardening and chill coma recovery in *Drosophila melanogaster*. *J. Insect. Physiol.* **2006**, *52*, 1027–1033. [CrossRef] [PubMed]
35. Tanaka, N.; Matsuda, Y.; Kato, E.; Kokabe, K.; Furukawa, T.; Nonomura, T.; Honda, K.; Kusakari, S.; Imura, T.; Kimbara, J.; et al. An electric dipolar screen with oppositely polarized insulators for excluding whiteflies from greenhouses. *Crop Prot.* **2008**, *27*, 215–221. [CrossRef]
36. Murai, T. Rearing method for clones of some aphids on tick bean, *Vicia faba*. *Bull. Shimane Agric. Exp. Stat.* **1991**, *25*, 78–82.
37. Murai, T.; Loomans, A.J.M. Evaluation of an improved method for mass-rearing of thrips and a thrips parasitoid. *Entomol. Exp. Appl.* **2001**, *101*, 281–289. [CrossRef]
38. Nonomura, T.; Matsuda, Y.; Bingo, M.; Onishi, M.; Matsuda, K.; Harada, S.; Toyoda, H. Algicidal effect of 3-(3-indolyl)butanoic acid, a control agent of the bacterial wilt pathogen, *Ralstonia solanacearum*. *Crop Prot.* **2001**, *20*, 935–939. [CrossRef]
39. Halliday, D.; Resnick, R.; Walker, J. Electric discharge and electric fields. In *Fundamentals of Physics*; Johnson, S., Ford, E., Eds.; John Wiley & Sons: New York, NY, USA, 2005; pp. 561–604.
40. Kaiser, K.L. Air breakdown. In *Electrostatic Discharge*; Kaiser, K.L., Ed.; Taylor & Francis: New York, NY, USA, 2006; pp. 1–93.
41. Munsell Color Company. Munsell Hue Circle Poster. Available online: <https://munsell.com/color-blog/munsell-hue-circle-poster/> (accessed on 20 November 2022).
42. Matsuda, Y.; Nonomura, T.; Kakutani, K.; Kimbara, J.; Osamura, K.; Kusakari, S.; Toyoda, H. Avoidance of an electric field by insects: Fundamental biological phenomenon for an electrostatic pest-exclusion strategy. *J. Phys. Conf. Ser.* **2015**, *646*, 0120031–0120034. [CrossRef]
43. Kakutani, K.; Matsuda, Y.; Toyoda, H. A simple and safe electrostatic method for managing houseflies emerging from underground pupae. *Agronomy* **2022**. (submitted).
44. Takikawa, Y.; Takami, T.; Kakutani, K. Body water-mediated conductivity actualizes the insect-control functions of electric fields in houseflies. *Insects* **2020**, *11*, 561. [CrossRef]

45. Halliday, D.; Resnick, R.; Walker, J. Capacitance. In *Fundamentals of Physics*; Johnson, S., Ford, E., Eds.; John Wiley & Sons: New York, NY, USA, 2005; pp. 656–681.
46. NC State Extension Publications. Insects Found on Yellow Sticky Traps in the Greenhouse. Available online: <https://content.ces.ncsu.edu/insects-found-on-yellow-sticky-traps-in-the-greenhouse/> (accessed on 20 November 2022).

Disclaimer/Publisher’s Note: The statements, opinions and data contained in all publications are solely those of the individual author(s) and contributor(s) and not of MDPI and/or the editor(s). MDPI and/or the editor(s) disclaim responsibility for any injury to people or property resulting from any ideas, methods, instructions or products referred to in the content.

Review

Directions from Nature: How to Halt the Tomato Brown Rugose Fruit Virus

Mireille van Damme ¹, Romanos Zois ¹, Martin Verbeek ², Yuling Bai ¹ and Anne-Marie A. Wolters ^{1,*}

¹ Plant Breeding, Wageningen University & Research, Droevendaalsesteeg 1, 6708 PB Wageningen, The Netherlands; mireille.vandamme@wur.nl (M.v.D.); romanos.zois@wur.nl (R.Z.); bai.yuling@wur.nl (Y.B.)

² Biointeractions and Plant Health, Wageningen University & Research, Droevendaalsesteeg 1, 6708 PB Wageningen, The Netherlands; martin.verbeek@wur.nl

* Correspondence: anne-marie.wolters@wur.nl

Abstract: Tomato brown rugose fruit virus (ToBRFV) is a recently emerged serious viral threat to tomato production. The virus is named after its symptoms consisting of characteristic brown wrinkled (rugose) patches on the fruits of infected tomato plants. ToBRFV is a member of the genus *Tobamovirus* and a very stable mechanically transmitted virus. So far, most tomato cultivars are susceptible, enabling a swift spread of ToBRFV. In this review, we present strategies to halt devastating disease outbreaks of ToBRFV based on the collective research data of various tobamovirus–plant interactions. Viruses, like ToBRFV, are biotrophic pathogens with small genomes. Hence viral proliferation depends on various host factors, also termed susceptibility (S) genes. However, S genes often have an intrinsic function for the host plant. Thus, mutations in S genes may lead to pleiotropic phenotypes. Therefore, identifying mutant variants of S genes with no pleiotropic effects is essential for exploring impaired S genes in breeding tomatoes resistant to ToBRFV.

Keywords: ToBRFV; tobamovirus; tomato; *Solanum lycopersicum*; disease; S gene; durable resistance

Citation: van Damme, M.; Zois, R.; Verbeek, M.; Bai, Y.; Wolters, A.-M.A. Directions from Nature: How to Halt the Tomato Brown Rugose Fruit Virus. *Agronomy* **2023**, *13*, 1300. <https://doi.org/10.3390/agronomy13051300>

Academic Editor: Rohit Mago

Received: 4 April 2023

Revised: 24 April 2023

Accepted: 26 April 2023

Published: 5 May 2023



Copyright: © 2023 by the authors. Licensee MDPI, Basel, Switzerland. This article is an open access article distributed under the terms and conditions of the Creative Commons Attribution (CC BY) license (<https://creativecommons.org/licenses/by/4.0/>).

1. Introduction: Tomato Crop Model for Viral Immunity

Tomato (*Solanum lycopersicum* L.) has become one of the most important and extensively grown fruit/vegetable crops, with global production increasing by over 49 million tonnes between 2000 and 2019 [1]. Tomato belongs to the dicot Solanaceae family. Solanaceous plants share a high degree of sequence similarity, and this enables comparative genetic studies [2]. Other major crop plants within this family include potato, pepper, eggplant, tobacco, and petunia [3].

Tomato is a model crop for genetic research because the genome sequence is available, it can easily be transformed, and interspecific crosses can be generated between tomato cultivars and many wild relative *Solanum* species. Tomato is also a model plant for studying immunity because it is susceptible to a wide range of pathogens, including viruses. At least 312 viruses, satellite viruses, or viroid species in 22 families and 39 genera are associated with tomatoes [4]. This is likely the highest number of recorded viral and related species in a single crop. However, we should consider that this number could still increase because viral interactions are intensively studied and monitored in tomatoes. Moreover, before discussing in more detail different tomato factors that play a role during tomato–viral interactions, we will introduce tomato brown rugose fruit virus (ToBRFV) because, as stated by Johanna Westerdijk in 1917: ‘knowledge of a disease and the way to fight it, must be based on an understanding of the physiology of both the host plant and the parasite’. In this review, we discuss aspects of the tobamovirus–plant interaction that could potentially lead to ToBRFV-resistant tomato genotypes.

2. ToBRFV Is a Tobamovirus

A virus consists of one or a few small nucleic acid molecules, generally protected by a protein coat, that can only multiply within the living cells of a host. Moreover, since viruses are so small, it took decades before scientific consensus agreed they existed.

2.1. Tobamoviruses Are the First Described Viruses

Around 1900, viruses were identified by three pioneers in plant pathology [5,6]. Adolf Mayer described the tobacco mosaic disease and found that the disease could be transferred between plants. Dmitri Ivanovsky and Martinus Beijerinck independently showed that the infectious agent of tobacco mosaic disease is within the filtrate of infected plant sap. Beijerinck named the agent that could replicate and multiply in living plants as “contagium vivum fluidum” (contagious living fluid) and the new pathogen virus (liquid poison) to specify its non-bacterial nature [7]. In 1939 the first electron micrographs of a virus, tobacco mosaic virus (TMV), were produced by Gustav Kausche, Edgar Pfankuch, and Helmut Ruska (reviewed by [5]). In 1958 Rosalind Franklin speculated that TMV was not solid but hollow and carried a single-stranded RNA molecule [8]. Consequently, the discovery of viruses, pathogens with a hitherto unknown lifestyle, was made by three plant pathologists who wanted to halt the tobacco mosaic disease. They were assisted by fellow scientists who could visualize the viral particles and their content.

2.2. Pathogenic Tomato Viruses

The tomato crop is susceptible to many different plant viruses. Viruses can be classified into seven “Baltimore classes” (I–VII) depending on their genome and how messenger RNA is generated during viral genome replication. A viral genome can be double-stranded (ds)DNA (I), single-stranded (ss)DNA (II), dsRNA (III), positive ssRNA (IV), negative ssRNA (V), RNA reverse-transcribing viruses with positive RNA (VI), and DNA reverse-transcribing viruses with dsDNA or RNA-DNA (VII) [9]. Pathogenic tomato viruses belong to several classes. They are transmitted and spread in different ways. The economically most important viruses for tomato crops are transmitted by whiteflies (e.g., members of the genera *Begomovirus*, *Crinivirus*, *Torradovirus*), aphids (members of the genera *Potyvirus*, *Cucumovirus*, *Alfamovirus*), and thrips (*Orthotospovirus*) [10]. However, members of the genus *Tobamovirus* (Baltimore class IV), such as ToBRFV, tomato mosaic virus (ToMV), and tomato mottle mosaic virus (ToMMV), are not transmitted by insect vectors but by contact and in low percentages via seed [11,12].

2.3. The Genome Organisation of ToBRFV

The ssRNA(+) genome of ToBRFV is about 6400 nucleotides in length containing four open reading frames (ORF) (Figure 1). ORF1 and ORF2 encode two replication (REP)-associated proteins of ~126 kDa and ~183 kDa. The latter protein is synthesized by readthrough of the ~126 kDa protein ORF. ORF3 encodes a movement protein (MP) of ~30 kDa and ORF4 a coat protein (CP) of ~17.5 kDa. ORF3 and ORF4 are translated from subgenomic RNAs. Since ToBRFV only encodes a limited number of proteins, it is expected that these viral proteins have multiple functions to establish viral proliferation.

Comparison of the tomato-infecting tobamoviruses TMV, ToMV, ToMMV, and ToBRFV genome sequences showed that their sequences are very similar, with approximately 90% nucleotide (nt) identity and the concatenated ORF amino acid sequence with approximately 80% amino acid (aa) identity (Figure 2). The relationships among the different tobamoviral species were determined by comparison of complete concatenated ORF amino acid sequences and shown in a phylogenetic tree (on the left in Figure 2) [13]. Our phylogenetic analysis of nucleotide and amino acid levels indicates that ToBRFV-IL is most similar to TMV (91.58% identity on nucleotide and 81.57% identity on amino acid levels).

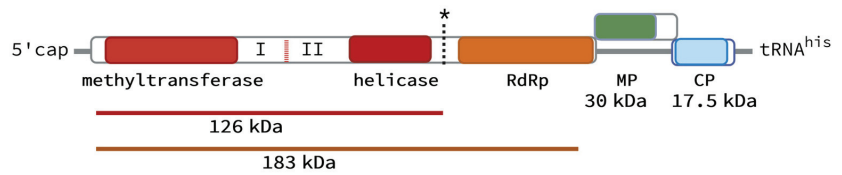


Figure 1. Schematic representation of the tomato brown rugose fruit virus (ToBRFV) genome organization adapted from Pfam (<https://pfam.xfam.org/search/sequence> (accessed on 1 December 2022)). The 6392-bp genomic sequence of ToBRFV-IL (Israeli) strain (NCBI: KX619418.1) was used. Four open reading frames (ORFs) corresponding to proteins are indicated by three open boxes. They encode a 126-kDa (top, shorter red line) and a 183-kDa (bottom, longer orange line) replication (REP) protein by readthrough of an amber stop codon, UAG (black asterisk), a 30-kDa movement protein (MP; green box, shifted up to indicate different reading frame than other ORFs), and a 17.5-kDa coat protein (CP; blue box). The first REP protein (126 kDa) contains two domains depicted by solid red boxes, a helicase, and a methyltransferase; in between the predicted domains, two non-conserved regions are located (indicated by I and II). The second REP protein of 183 kDa contains an additional RNA-dependent RNA polymerase (RdRp, solid orange box) domain at the C-terminus. The molecular weight of the proteins was predicted by Compute pI/Mw (https://web.expasy.org/cgi-bin/compute_pi/pi_tool (accessed on 1 December 2022)).

| | Identity to ToBRFV-IL in % | |
|-----------|----------------------------|-------|
| | nt | AA |
| YMV | 59.64 | 59.21 |
| ToMMV | 89.22 | 80.62 |
| ToMV | 90.87 | 80.88 |
| ToBRFV-IL | 100 | 100 |
| TMV | 91.58 | 81.57 |

Figure 2. Phylogenetic tree of 4 tomato-infecting tobamoviruses, with the Youcai mosaic virus (YMV) that infects plants from the rosid clade, was used as an outgroup [13]. The phylogenetic tree, a neighbor-joining tree without distance corrections with real branch length, was generated by Clustal Omega (<https://www.ebi.ac.uk/Tools/services/> (accessed on 1 December 2022)). Percentage of nucleotide (nt) and amino acid (aa) sequence identity of viral sequence compared to ToBRFV-IL is indicated to the right of each of the five tobamoviruses. Used genome sequences are from NCBI; YMV (NC_004422.1), TMV (NC_001367.1), ToMV (NC_002692.1), ToMMV (NC_022230.1), and ToBRFV (KX619418.1).

3. ToBRFV Spread, Symptoms, and Host Range

Tobamoviruses spread mechanically, and viral particles enter the plant cells after wounding the epidermal cells. Therefore, the virus will spread rapidly with all plant handling, and a gentle touch is already sufficient as virus concentrations are very high even in trichomes [14]. Bumblebees can transmit the virus, but they are not considered vectors as the mode of transmission is mechanical [15]. The presence of ToBRFV in tomatoes was first reported in the fall of 2014 in southern Israel and during the spring of 2015 in Jordan. Both virus isolates were similar and termed corresponding to the disease symptoms “tomato brown rugose fruit virus” (ToBRFV) [16,17]. Subsequently, ToBRFV was detected and reported (between 2018 and 2023) on tomatoes and other plants in more than 25 countries all over the world [18].

3.1. ToBRFV Disease Symptoms in Tomato

The ToBRFV-caused symptoms on tomatoes are similar to those caused by TMV, ToMV, and ToMMV. They are not easily distinguished from other viral tomato symptoms, e.g., cucumber mosaic virus (CMV), or even herbicide effects [19,20]. ToBRFV disease symptoms in tomatoes can be severe. The most obvious ones are curling, malformation of the leaves (shoestring or fern leaf), and stunting of the whole plant (Figure 3). Additional symptoms on the leaves are mosaic discoloration, mottling, and necrosis. Deformation and necrosis can also occur on the stem. In Figure 3, the bottom left panel shows deformation and anthocyanin accumulation on the stem. Additionally, ToBRFV infection reduces fruit number due to early flower abortion and reduced fruit size. Figure 3, bottom right panel, shows the reduced fruit number of Micro-Tom plants. Mock-treated Micro-Tom plants yielded an average of 55 fruits per plant, while ToBRFV-infected plants yielded 22.4.

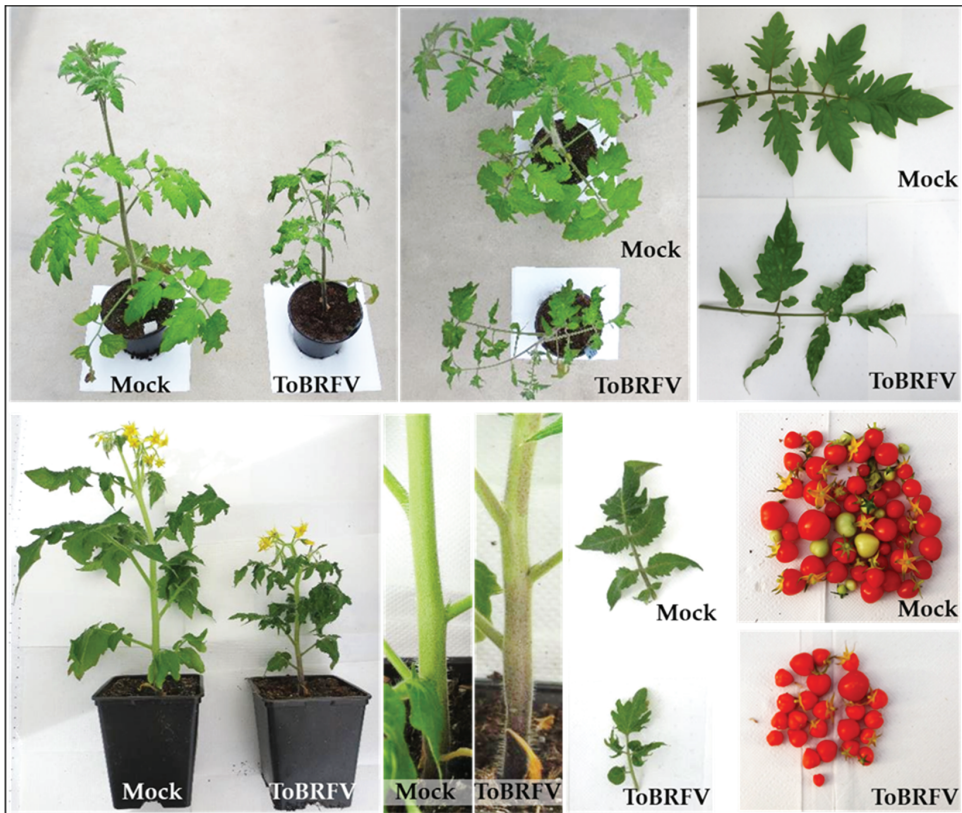


Figure 3. ToBRFV symptoms on tomato Moneymaker plants (top panels) and Micro-Tom plants (bottom panels). Pictures of 5-week-old plants, 4 weeks post-Mock or ToBRFV inoculation. Tomato fruits harvested from ~3-month-old Mock-treated and ToBRFV-infected Micro-Tom plants are shown in the bottom right panels.

Although the disease is termed tomato brown rugose fruit virus, neither discoloration (marbling) nor brown wrinkled (rugose) patches could be detected on Micro-Tom or Moneymaker fruits, whether ToBRFV inoculation was performed on 10-day-old seedlings or mature plants just before fruit set under greenhouse conditions. However, others detected fruits with marbling, yellow patches, brown rugosity, and deformation symptoms on tomato cultivars Piccolo, Kivu, and Moneymaker [21]. Symptom development can

vary due to environmental growth conditions (temperature), age during viral infection initiation, and the genetic background of the tomato plant [22]. In addition, as expected, when ToBRFV is present in a greenhouse compartment, the virus swiftly spreads. Two ToBRFV-contaminated tomato plants, corresponding to <0.5% of the total crop arsenal, could contaminate the entire tomato crop (98.96%) under normal cultivation procedures within 9 months [23].

3.2. Additional Host Plants of ToBRFV

In addition to tomatoes, ToBRFV has been reported in sweet pepper plants in Jordan and Sicily (Italy) [16,24]. The host range of ToBRFV was evaluated for 31 plant species from seven families, and 20 plant species (encompassing four families) showed local symptoms or the presence of ToBRFV in systemic leaves [25]. The various host plants include petunia, pepper, tobacco, and tomato (from the Solanaceae), globe amaranth, quinoa and lamb's quarters (from Amaranthaceae), rosy periwinkle (from Apocynaceae), lilac tassel flower and crown daisy (from Asteraceae) [25]. Probably these 20 plant species and many of the thus far unidentified host plants will never be tested for the presence of ToBRFV either because ToBRFV infection causes only mild symptoms or because the host plant has no economic impact. However, the various ornamental species and weeds can still facilitate ToBRFV viral spread.

3.3. Preventing ToBRFV Distribution

To better understand the worldwide distribution of ToBRFV, all countries should investigate and report the absence or presence of ToBRFV in all known host plants, not only tomatoes. Obviously, this is not a realistic task, and eliminating ToBRFV by eradicating all the infected host plants is impossible. The current geographical overview of ToBRFV expansion solely based on reported occurrences does not reflect the true global spreading of the virus. Possibly, measuring ToBRFV in waste water (all over the world), similar to the detection of the COVID-19 virus, and indicating positive locations on the world map would give a more realistic overview.

To halt the spreading of ToBRFV and the possibility of new ToBRFV variants evolving, tomato cultivars with durable ToBRFV resistance are required. Although ToBRFV is a recently emerged virus species, its high genomic similarity to the three tobamoviruses TMV, ToMV, and ToMMV (Figure 2) is helpful in deducing the biological function of the viral proteins and how they can establish disease. Furthermore, the extensive knowledge and comparable life style among the different tomato tobamoviruses can help us to combat the tomato brown rugose fruit disease in tomato. Four strategies that can be utilized by the plant as a defense against viral disease are given in the next paragraph.

4. Viral Disease Resistance Strategies in Plants

Four well-known strategies that plants use to become resistant against plant viruses are (1) RNA silencing mediated by the plant, (2) the presence of dominant plant resistance proteins (R-proteins), (3) plant hormone-mediated resistance, and (4) absence of a functional plant susceptibility factors (S-factors). Resistance strategies can differ in expected durability, and a strategy with high durability (+++) is preferred. Simultaneously, a specific strategy can have a negative impact on plant physiology and lead to pleiotropy, and a strategy with a low pleiotropic likelihood (−) is preferred. The durability of the pleiotropic effect on the plant as a result of the chosen resistance strategy is based on current knowledge and discussed for each strategy.

4.1. ToBRFV Resistance Conferred by Host-Based Viral RNA Silencing

RNA silencing encompasses the plant's first layer of viral defense (Figure 4, box 1). Viral RNA is converted into viral double-stranded RNA (dsRNA) by RNA-dependent RNA polymerase encoded by the plant. Similar to Pathogen Associated Molecular Patterns (PAMPS), viral dsRNA can be considered a Virus-Associated Molecular Pattern (VAMP).

The viral dsRNA is recognized by Dicer-like (DCL) plant enzymes, and DCLs process viral dsRNA into virus-derived small interfering RNAs (vsiRNAs). These vsiRNAs are incorporated in the RNA silencing complex (RISC), where single vsiRNA strands act as RNA guides for viral RNA silencing (reviewed by [26]). Mutations in genes that play a role in the plant RNA silencing mechanism often have a significant impact on plant physiology because the plant RNA silencing mechanism plays a key role in plant development [27], indicated by a single + for the likelihood of pleiotropy in Figure 4 beside box 1. In addition, successful plant viruses express viral suppressors of RNA silencing (VSRs) that attenuate or block this defense. VSRs are produced from the first ORF of tobamoviruses and are part of the 126-kDa replicase (REP) protein (top horizontal red line in Figure 1) [28]. The 126-kDa protein (P126) consists of four parts, methyltransferase, helicase, and two non-conserved regions, I and II (Figure 1). The methyltransferase, helicase, and non-conserved region II each possess RNA silencing-suppression activity [29].

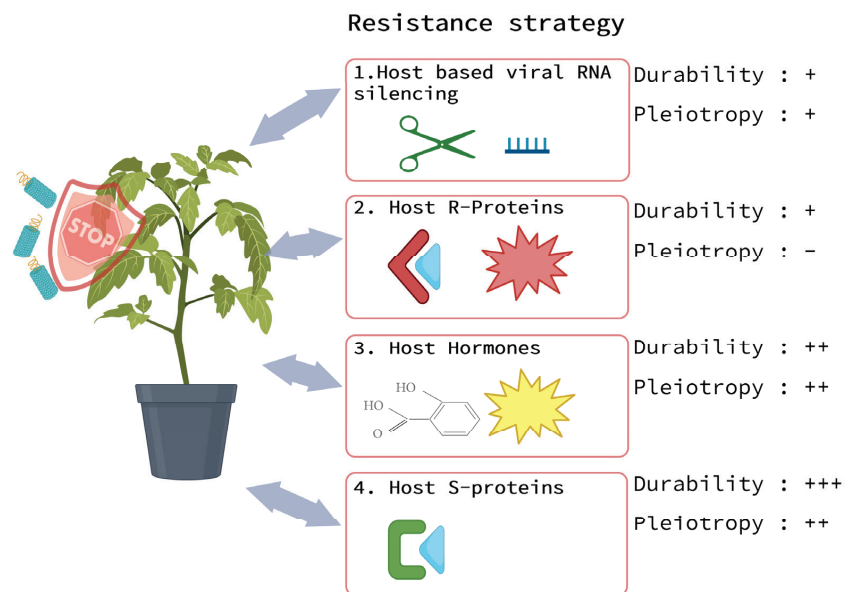


Figure 4. Four strategies for plant resistance against tobamoviruses. For each strategy, the expected durability and likelihood of pleiotropic plant phenotypes are indicated by plus (+) or minus (–).

VSRs target various factors of the silencing pathway. P126 of TMV interferes with HEN1-mediated methylation and accumulation of novel miRNAs, while P130 of ToMV blocks the siRNA accumulation. Crucifer-infecting-TMV P122 binds to siRNAs and miRNAs, thereby preventing their incorporation into RISC, and also enhances AGO1 downregulation via miR168 upregulation [28,30]. The production of P126 as the first viral protein with a combined function of replication and VSR is a perfect viral survival strategy since the viral genome is most exposed to silencing-mediated RNA degradation during its replication. Therefore, due to the production of VSRs, the strategy of RNA silencing mediated by the plant is expected not to be highly durable (indicated by a single + beside box 1 in Figure 4).

4.2. ToBRFV Resistance Conferred by Host Resistance (R) Proteins

Viral proliferation can also be inhibited by a host R protein-mediated defense response, the second strategy (Figure 4). R genes are usually dominant genes that provide full or partial resistance to pathogens [31]. Most plant R proteins are encoded by nucleotide-binding leucine-rich repeat receptor (NLR) genes. More than 200 NLR genes identified from dif-

ferent plant species can prevent viral proliferation [32]. Dominant R proteins directly or, in most cases, indirectly sense and interact with a viral protein, also termed effector [32] (Figure 4, box 2). The sensing or recognition between NLRs and their cognate viral protein usually triggers rapid localized cell death, also termed the hypersensitive response (HR), indicated by the red star in Figure 4, box 2. Two NLR encoding R proteins for resistance against tobamoviruses were identified, the N protein from tobacco yielding resistance to TMV and Tm-2/Tm-2² from tomato yielding resistance to ToMV and TMV [33,34]. However, not all viral dominant R proteins code for NLRs. The tomato Tm-1 R protein against TMV has a triosephosphate isomerase (TIM)-barrel-like domain and unknown function [35]; for several R proteins against viruses, the sensed or interacting viral protein that leads to resistance is known. The Tm-2/Tm-2² protein detects the MP of TMV and ToMV. Detection or sensing of the helicase domain from the TMV REP protein by the host N and/or Tm-1 protein results in resistance (reviewed by [32]). Although R proteins are successfully used to halt viral proliferation and prevent disease, the achieved resistance is mostly only effective against one viral species. In addition, viral genomes have a high mutation frequency due to their rapid replication rate and generation of large populations [36]. Viruses with RNA genomes, such as ToBRFV, are expected to have the highest mutation frequency since RNA polymerases lack proofreading activity [36]. Another source of genetic variation is caused by recombination between two viral species, which is known to occur when multiple viral species are present in a single host plant [36]. The high genetic variability of tobamoviruses potentially leads to changes in viral proteins that overcome the R-protein-based resistance due to the inability to sense the altered viral protein. For example, initially, the two allelic R proteins Tm-2 and Tm-2² were successfully exploited to halt ToMV viral disease in tomatoes. But in 1993, two ToMV isolates (from Japan and Europe) broke the Tm-2² resistance [37]. These ToMV isolates had three amino acid changes in their MP [37,38]. Furthermore, currently, none of the three dominant resistance genes Tm-1, Tm-2/Tm-2² used in tomato cultivars provide complete resistance to ToBRFV disease [39].

4.3. Search for Additional ToBRFV Host Resistance (R) Proteins

Currently, wild tomato accessions are explored to identify additional/novel R proteins against ToBRFV. Multiple ToBRFV resistance traits are described in patents by various breeding companies. A dominant ToBRFV resistance trait conferred by a CC-NBS-LRR gene was found on chromosome 8 of the *S. habrochaites* LYC4943 accession [40]. A recessive ToBRFV resistance trait was found on chromosome 11 from *S. pimpinellifolium* accession PI79532 (LA2348) [41]. Patent WO2019110130 describes a *polygenic* ToBRFV resistance trait based on three loci (located on chromosomes 6, 11, and 12) from three different *S. pimpinellifolium* accessions [42]. Interestingly, some identified novel ToBRFV resistance traits involve alleles and loci of the previously ‘broken’ *Tm* genes. Zinger et al. (2021) reported a tomato genotype resistant to ToBRFV. The ToBRFV resistance of this accession depends on a locus on chromosome 2 that includes the Tm-1 gene, in combination with a locus on chromosome 11 (associated with tolerance to ToBRFV) [43]. In addition, the presence of the Tm-1 locus with at least one of the two recessive loci on chromosome 9 (fruit tolerance) and chromosome 11 (foliar tolerance) can lead to resistant plants [44]. Finally, a recent patent describes a gain-of-function in resistance to ToBRFV and ToMV by amino acid changes in the protein sequence of Tm-2² [45]. The recent claims and findings on novel ToBRFV-resistant sources indicate the great desire to halt this pathogen in tomatoes.

Although the novel identified R genes lead to ToBRFV-resistant tomato cultivars, the occurrence of resistance-breaking viral isolates and newly evolving species, as seen in the past, is likely to occur (also illustrated by a single plus (+) for durability in Figure 4). One benefit of this strategy is that the R proteins-based resistance is widely used and rarely leads to pleiotropy (indicated by a minus (−) for pleiotropy in Figure 4 beside box 2). Therefore, a good approach would be to stack multiple R genes within a single tomato cultivar. The application of multiple R proteins will increase the durability of the disease resistance

significantly. The disadvantage of this strategy is that the introgression of multiple R genes in each cultivar requires a lot of time and effort.

4.4. Hormone-Based ToBRFV Resistance

Another complex viral resistance strategy is mediated by hormone-based resistance (box 3 in Figure 4). The complexity is caused by the crosstalk between different hormone signaling pathways [46]. Crosstalk refers to the phenomenon that different hormones regulate each other; e.g., the accumulation of salicylic acid (SA) can cause a reduction in jasmonic acid (JA). Additionally, various hormones are affected by the viral presence, as viruses hijack host components to deregulate the plant hormone production in order to proliferate. Zhao and Li [39] composed a graphical summary of six different viral outcomes/effects (replication, accumulation, symptom development, virus movement, host resistance, and insect vector relationship) by eight different hormones, including SA, JA, ethylene (ET), abscisic acid (ABA), gibberellic acid (GA), auxin, cytokinin and brassinosteroids (BRs) for 19 plant viruses. Their main conclusion is that changes in hormone levels are tightly coordinated with viral movement, replication, symptom development, and defense responses and directly affect viral disease outcomes. ABA accumulation has a negative effect on TMV accumulation, movement, and symptom development. The induction of ABA signaling causes a down-regulation of callose-degrading enzymes, resulting in callose accumulation at the plasmodesmata (PD), which leads to restricted viral cell-to-cell movement [47]. ET accumulation has a negative effect on TMV accumulation and symptom development but a positive effect on the accumulation of viral crucifer-infecting tobacco mosaic virus (TMV-cg) [46]. SA accumulation has a negative effect on TMV and ToMV accumulation [46]. In addition, exogenous application of SA, JA, or a combination resulted in reduced levels of TMV in *N. benthamiana* plants. Therefore enhanced SA and JA levels possibly activate systemically induced defense in tobacco leaves against TMV [48]. Exogenous application of BR in tobacco also enhanced resistance to TMV, independent of SA accumulation [49]. BRs modulate plant–pathogen interactions, but depending on the involved plant species and the pathogen’s lifestyle, BRs induce resistance or susceptibility. The presence of BR induces resistance to most biotrophic pathogens and susceptibility to necrotrophic and hemibiotrophic pathogens. Importantly, BRs do not always enhance plant viral defense, as there is evidence that BRs induce viral susceptibility [50].

Overall, resistance based on altered hormone levels can lead to durable virus resistance, and this strategy is marked by ++ behind box 3 in Figure 4. Simultaneously, hormones, especially the balance between hormones, influence all stages of the tomato composite leaf development [51]. Therefore, the predicted effect on pleiotropy is indicated with ++ beside box 3 in Figure 4. Remarkably, the shoestring/fern leaf symptoms on the ToBRFV-infected tomato leaves (Figure 3) resemble a phenotype caused by hormonal imbalance in non-infected tomato plants.

4.5. ToBRFV Resistance Based on Dysfunctional Host Susceptibility (S) Proteins

Viral proliferation depends on the presence of a considerable number of host susceptibility (S-) factors. Therefore, the fourth resistance strategy (box 4 in Figure 4) depends on the absence of crucial S-factor(s). The absence of some host S-factors can prevent or inhibit viral proliferation. Therefore, this type of resistance is expected to be highly durable, illustrated by +++ in Figure 4 beside box 4. However, this may be accompanied by slight to severe pleiotropic effects on plant morphology and fitness, marked by ++ in Figure 4. In the next section of this review, we will discuss why we consider the S-factor-based viral resistance strategy as the preferred strategy to achieve durable ToBRFV resistance.

Until now, at least 115 plant host factors that could affect viral proliferation for at least 52 different viral species have been identified (based on current literature studies). Thirty-eight S-factors that could or are proven to affect tobamoviral proliferation, including references, are presented in Supplemental Table S1. In the next section, we discuss the molecular role of 11 plant host factors (indicated in bold in Supplemental Table S1) in more

detail and in what manner they are instrumental for tobamovirus viral proliferation (also illustrated in Figure 5). Obviously, plant host factors that are nonessential for the fitness of the host are preferred; these would be scored as—for pleiotropy.

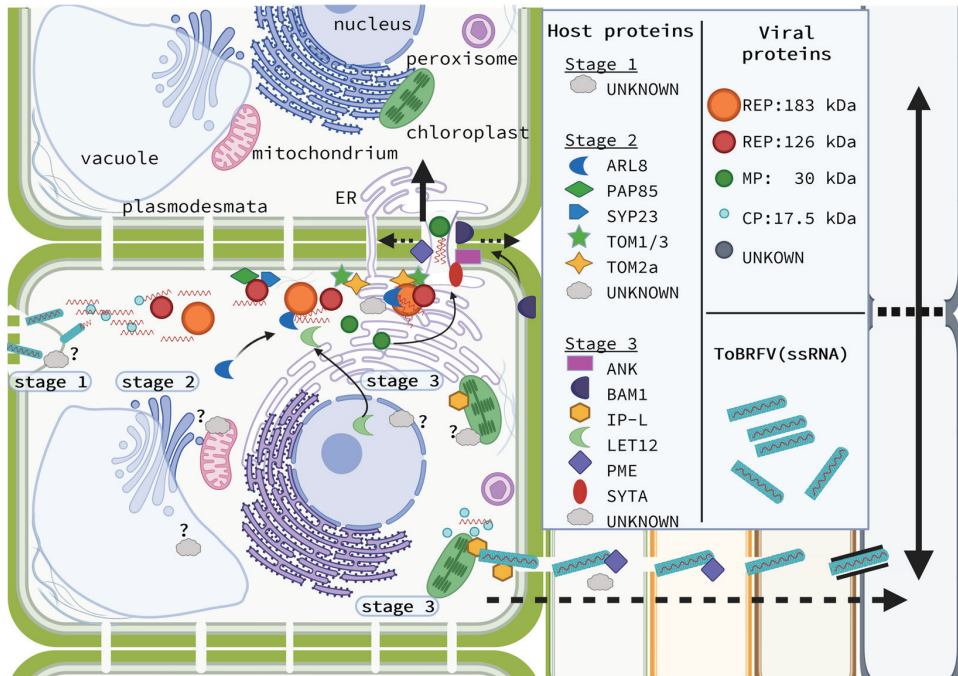


Figure 5. Schematic tobamovirus–plant interaction and the involved viral and plant host factors. Viral proteins are shown as circles in different colors: REP (red and orange), MP (green), and CP (blue). Plant proteins are depicted by the different symbols and colors. Thus far, grey is unknown proteins, cloud-shaped with question mark for plant proteins, and circle for viral proteins. The three stages vital for virus proliferation within the host are 1—host cell entrance, 2—replication and translation within the host cytosol, and 3—viral movement and spreading, short- or long-distance. Viral spreading to adjacent cells occurs through plasmodesmata (short distance), while viral particles are transported to the vascular bundle for long distance. The interactions are shown for twelve selected plant proteins discussed in the text. These include proteins important for tobamovirus replication and translation (stage 2; ARL8, PAP85, SYP23, TOM1/3, and TOM2a) and viral movement and spread (stage 3; ANK, BAM1, IP-L, LeT12, PME, and SYTA).

5. Molecular Factors of Plant Host and Tobamoviruses That Are Instrumental for Viral Proliferation

To make maximal use of their limited genomes, viruses exploit the machinery and metabolism of a living host cell for their life cycle. The viral proliferation of tobamoviruses can be divided into three stages: (1) entrance, (2) replication and translation, and (3) movement and spread through the plant vascular tissue (Figure 5) [52].

For each stage, viral and plant proteins are expected to collectively contribute to viral proliferation. As the life cycle of ToBRFV conceivably resembles that of TMV, based on the genome structure and sequence similarity (Figures 1 and 2), it is likely that ToBRFV exploits similar host cell components as TMV (or ToMV and ToMMV) to cause disease. Therefore, in this review, we propose the host factors required for TMV and/or ToMV proliferation as the host factors for ToBRFV proliferation [52]. Figure 5 illustrates the three stages of the ToBRFV life cycle in the plant and how virus and plant proteins together

could contribute to enhancing tobamovirus viral proliferation. Due to the mechanical transmission of tobamoviruses, most host factors are utilized by the virus during the second and third stages. Plant proteins that associate with the viral REP play a key role during the second stage, and those that associate with viral MP or CP are more relevant during the third stage. Obviously, as research continues, the depicted interactions and locations are not set in stone, and additional viral and plant proteins that take part in the ToBRFV proliferation remain to be discovered.

5.1. Stage 1: Viral Entrance

Plant cells have cell walls that act as the first barrier against the invasion of pathogens. To overcome this, many plant viruses have to take advantage of different biological vectors or physical damage (wounding) of the plant tissue caused by environmental stresses to enter plant cells. For example, ToBRFV enters the host cell through mechanical wounding of the plant tissue, which either transiently opens the plasma membrane (PM) or allows pinocytosis (endocytosis of fluids) [52]. Therefore, no host proteins are likely required for tobamoviral entrance or are not identified yet (only hypothetical proteins are illustrated in Figure 5). A putative role for the viral CP that interacts with a plant protein could be envisioned, but thus far entrance of tobamoviruses is known to rely only on a damaged cell.

5.2. Stage 2: Viral Replication and Translation

For the second stage, replication and translation, the REP proteins, REP-126-130 kDa and REP-180-183 kDa, play a central role. The viral REP proteins (indicated by red and orange circles in Figure 5) can interact directly or indirectly with host proteins to build the tobamovirus replication complex. Figure 5 depicts a set of plant proteins that directly interact and/or are part of the replication complex.

Details for each plant protein and how it might function in the replication complex and enhance viral replication and translation are provided below.

ARL8 (ADP-ribosylation factor-like 8, blue crescent shape in Figure 5) is a GTPase highly conserved in eukaryotic cells from animals to plants. The 180-kDa REP protein of ToMV interacts with ARL8 from *Nicotiana tabacum*, and the absence of the ARL8 protein in Arabidopsis inhibits intracellular TMV and ToMV virus multiplication [53]. Arabidopsis has two ARL8 homologs, and only a double knock-out of both *AtARL8* genes led to the inhibition of TMV and ToMV viral proliferation [53]. Tomato has four ARL8 homologs, and solely knocking out *SlARL8a* was insufficient to reduce ToBRFV viral proliferation [54]. How the absence of ARL8 could lead to viral resistance is still unknown. Research in human cells showed that ARL8b regulates lysosomal motility and the fusion of lysosomes with late endosomes [55–57]. Lysosomes are organelles needed for the clearing and recycling of cellular components, also known as autophagy. Depending on the plant-virus pathogenesis system, autophagy can function as an antiviral mechanism or promote viral infection [58,59]. A putative role of autophagy in viral proliferation and whether viral S genes take part in the molecular mechanism of autophagy will be further discussed in Section 5.4.

PAP85 (Pokeweed antiviral protein, green rhombus shape in Figure 5) was originally identified in field beans (*Vicia faba* L.) as vicilin, a 7S seed globulin representing approximately 30% of the storage protein in mature seeds [60]. Remarkably, vicilins are mostly reported as defensive proteins against fungi and insects, probably due to their capacity to bind chitin [61,62]. In Arabidopsis, PAP85 is involved in membrane modification for transportation, and its transcript accumulates during the last stage of silique development [63]. Arabidopsis PAP85 interacts with the 126-kDa REP protein of TMV at the endoplasmic reticulum (ER) [64]. The interaction between PAP85 and P126 results in ER transition, formation, and transfer of small vesicles from ER to Golgi early in the infection process [64]. In general, newly synthesized proteins and lipids are transported from the ER to the PM via the Golgi apparatus. Viruses are known to hijack the secretory pathway that leads to membrane rearrangements for their life cycle (reviewed by [65]). Presumably, tobamoviruses exploit PAP85 for this function.

SYP22 and SYP23 (Figure 5, blue pentagon arrow shape) are also important for vesicle trafficking and interact with the methyltransferase domain of the 126-kDa REP TMV protein. SYP proteins are soluble N-ethylmaleimide-sensitive fusion protein attachment protein receptors (SNAREs) [66]. The presence of SYP22 and/or SYP23 is necessary for TMV accumulation [67]. SNAREs associate with membranes and mediate the fusion of vesicle membranes with target membranes. SNARE proteins form highly stable protein–protein interactions, a SNARE complex. SNAREs can be classified according to their subcellular localization, t (target)- and v (vesicle)-SNAREs, or to their structure, with the presence of a conserved glutamine (Q) or arginine (R) residue in the center of the SNARE domain [68]. t-SNAREs have a Q residue and are termed Q-SNARE, and v-SNAREs have an R and are termed R-SNARE. A functional SNARE complex consists of one set of Qa-, Qb-, Qc-, and R-SNARE proteins with a four-helical bundle assembled by four SNARE motifs. The three types of Q-SNAREs, Qa, Qb, and Qc, are determined by their position in the SNARE complex [68]. The SYP2 SNARE subfamily (SYP21, SYP22, and SYP23) belongs to the Qa-SNAREs. In general, a Qa-SNARE is the core SNARE protein that regulates the formation of a SNARE complex at the target membrane. In Arabidopsis, the functions of SYP21, SYP22, and SYP23 are expected to be redundant and interchangeable [69,70]. Vesicle transport mediated by SYP22 is important for shoot gravitropism and morphogenesis. The predicted localization sites of SYP22 and SYP23 are cytosol, vacuole, or pre-vacuole compartment. SYP22 forms a SNARE complex with a v-SNARE, e.g., VAMP711, and the complex is localized to tonoplasts and the pre-vacuolar compartment [70]. SYP22 also interacts with R-SNARE VAMP727, and both bind to the PM-bound receptor BRASSI-NOSTEROID INSENSITIVE1 (BRI1), resulting in BR accumulation. BRs are plant-specific steroidal compounds essential for normal growth and development [50]. Accumulation of BR enhanced plant defense, e.g., against root-knot nematodes [71,72]. Possibly, the absence of a functional SYP2 protein may lead to an imbalance of hormones leading to viral resistance.

Arabidopsis TOM1 (Tobamovirus multiplication 1, green star shape in Figure 5) and TOM3 (a paralog of TOM1) have been shown to interact with the tobamovirus helicase domain from the 130-kDa/180-kDa REP proteins [73,74]. The Arabidopsis TOM1/TOM3 double mutant completely suppressed TMV replication [73]. TOM1 and TOM3 are predicted to be seven-pass transmembrane proteins. Therefore TOM1/3 could form a link between the host membrane and the tobamovirus replication proteins [52,74,75]. The effectivity of TOM1 and TOM3 as S proteins for TMV has been shown for various plant species besides Arabidopsis, including *C. annuum*, *N. benthamiana*, and tomato [76,77]. In tomato, both paralogs TOM1 and TOM3 have two homologs. Recent data showed that a quadruple knock-out mutant of all four homologs in tomatoes displayed resistance to four tobamoviruses: TMV, ToMV, YMV, and ToBRFV [78]. Presumably, based on the phylogenetic tree (Figure 4), ToMMV accumulation will also be inhibited in the quadruple tomato mutant. However, when only three of the four homologs were mutated, the virus could still multiply. Moreover, in the triple knock-out tomato plants, mutant viruses emerged that were multiplying more efficiently than the wild-type ToBRFV [78].

Arabidopsis TOM2a (orange cross shape in Figure 5) interacts with itself and the TOM1 integral membrane protein [79]. Both the Arabidopsis *tom2-1* mutant that lacks TOM2a, and the tobacco genotype TI203 containing a natural TOM2a variant, showed reduced tobamovirus viral accumulation [79,80]. In addition, tomato CRISPR-Cas9 knock-out mutants of TOM2a displayed enhanced resistance against TMV [80]. TOM2a encodes a 280-amino acid putative four-pass transmembrane protein with a C-terminal farnesylation signal, i.e., CaaX motif, that undergoes farnesylation [79]. Farnesylation is a post-translational protein modification by which an isoprenyl group is added to a cysteine residue. Farnesylation mediates protein–protein interactions and protein–membrane interactions [81]. RNA viruses such as ToBRFV lack post-translational protein modification enzymes. Instead, they probably use the host to modify their proteins and/or post-transcriptionally modified

host proteins (e.g., the TOM1–TOM2a complex) to allocate to the membrane to promote viral proliferation.

5.3. Stage 3: Viral Movement and Spread

For the third stage, viral movement and spread, plant viruses move from cell to cell via plasmodesmata (PD), indicated as short distance, and via the phloem (sieve elements), indicated as long distance (Figure 5). PD are unique membrane-lined cytoplasmic nanobridges that connect plant cells for cell-to-cell movement [82]. Due to studies on the role of viral MP in cell-to-cell movement, it was discovered that plant proteins could also move between cells via PD [83]. Microinjection of fluorescently-labeled viral MP revealed that MP proteins could increase the size exclusion limit of PD to facilitate the movement of viral RNA, MP, and other proteins to surrounding cells [83]. Six host factors that facilitate viral movement were selected and are depicted in Figure 5. Although most of the host proteins that facilitate the viral movement and spreading interact with the tobamoviral MP or CP protein, the REP from TMV was also shown to have a role in viral movement [84,85]. Most of the discussed proteins in this review interact directly with the viral MP (ANK, BAM1, PME, and SYTA), while LeT12 co-localizes with MP, and IP-L interacts with CP. The depicted proteins in Figure 5 are ANK (pink rectangle shape), BAM1 (blue semicircle shape), IP-L (orange pentagon shape), LeT12 (green crescent shape), PME (purple rhombus shape), and SYTA (oval red shape).

The plant ankyrin repeat-containing protein ANK probably promotes short-distance viral spread. The binding of the viral MP protein to the plant ANK protein results in the reduction of callose levels at the plasmodesmata, also termed callose sphincters. This causes the relaxation of the PD, which promotes viral cell-to-cell movement through the PD [86]. The ANK repeat domain-containing proteins comprise one of the largest known protein superfamilies in plants [87]. ANK proteins can mediate protein–protein interactions, and most plant ANK proteins play crucial roles in defense responses [87]. Still, ANKs' role in viral proliferation is not well understood.

BAM1 (Barley any meristem 1) is a receptor-like kinase (RLK) from Arabidopsis that interacts with MP from TMV. Viral movement through PD by BAM1 is independent of its kinase activity [88]. Arabidopsis mutants *bam1-3* and *bam2-3* both showed reduced levels of TMV RNA accumulation when compared to wild-type plants at 6 days post-inoculation [88]. Interestingly, BAM1 and BAM2 were previously identified to interact with a small protein (C4) of tomato yellow leaf curl virus (TYLCV) at the PM and PD. TYLCV contains a DNA genome and is unrelated to tobamoviruses. BAM1 is required for the cell-to-cell spread of RNA silencing. In addition, in this case, the kinase activity of BAM1 does not seem to be required [89]—the targeting of BAM1 by C4 of TYLCV results in the suppression of intercellular spreading of RNA silencing. In C4-overexpressing transgenic tomato plants, four RLK genes (including BAM1 and BAM2) transcript levels were reduced. Therefore, the TYLCV C4 could compromise the RLK-mediated plant defense system. For tobamoviruses, it is not yet known whether the absence of BAM1 also causes reduced viral spread due to the reduction of cell-to-cell spread of RNA silencing or RLK-mediated plant defense.

The tobacco-interacting protein-L (IP-L) is a host protein interacting with the ToMV CP. IP-L was previously identified as an 'elicitor-responsive protein' gene [90]. For the protein–protein interaction, the N-terminal helical region of IP-L (155 aa) and two α -helical domains of ToMV CP are essential [91]. Both proteins, IP-L and ToMV CP, co-localize in the chloroplast thylakoid membranes [91]. This localization could explain the occurrence of chlorosis during viral infection because the interaction of ToMV CP with IP-L may affect chloroplast function and stability. Multiple studies of chloroplast protein–viral protein interactions have shown that the chloroplast is a common target of plant viruses for viral pathogenesis or propagation [92]. TMV infection induces the transcript levels of IP-L, and the reduction of IP-L transcripts in *N. benthamiana* resulted in delayed systemic ToMV symptoms at 7 days post-inoculation [90,93]. How IP-L supports viral proliferation is still unknown. For several viruses, the role of chloroplasts and associated proteins

during viral proliferation has been described [94]. For example, the MP of ToMV and TMV interact with the small subunit of Rubisco (RbCS). This interaction takes place in the cytoplasm prior to the re-localization of RbCS to the chloroplasts of *N. benthamiana*. Silencing of *NbRbCS* in susceptible *N. benthamiana* plants enhanced local virus infectivity but delayed the development of systemic viral symptoms [95]. Additionally, *NbRbCS* silencing compromises Tm-2²-dependent resistance in transgenic Tm-2² *N. benthamiana* (ToMV-resistant) plants [95]. Thus, hijacking light-dependent or light-induced chloroplast factors by tobamovirus in plants can enhance local viral proliferation and/or prevent R protein-based viral defense.

LeT12 (*Lycopersicon esculentum* clone 12) is a class II knotted-like homeodomain protein (KNOX2) isolated from a tomato cDNA library [96]. The tomato LeT12 protein is a host factor in stages 2 and 3. The closest homolog of tomato LeT12 in tobacco is NTH201. NTH201 regulates the formation of VRC and the accumulation of TMV MP [97]. Silencing of the *NTH201* gene transcript caused a delay in viral RNA accumulation and viral spread in TMV-infected tobacco plants [97]. Although NTH201 was observed to migrate from the nucleus to cytoplasm and PD, where NTH201 colocalized with MP, no direct interaction between NTH201 and TMV MP was detected [97]. The closest Arabidopsis homolog of LeT12 is Knotted1-like homeobox gene 4 (*KNAT4*). *KNAT4* is one of the four Arabidopsis *KNOX2* genes, together with *KNAT3*, *KNAT5*, and *KNAT7*, expressed in the inflorescence stems [98]. *KNAT3* and *KNAT7* may play a significant role in secondary cell wall formation as detected by mutation analysis [98]. Single gene mutations of *KNAT4* and *KNAT5* did not result in obvious morphological cell wall phenotypes in Arabidopsis, indicating possible redundancy in gene function, or *KNAT4* and *KNAT5* have another role, and absence does not lead to direct cell wall malformation. Still, modification of the plant cell wall by tobamoviruses is a likely strategy to improve viral spreading.

The tomato and citrus pectin methylesterase (PME) interacts with the MP from TMV, Turnip vein-clearing virus (TVCV, crucifer-infecting RNA tobamovirus), or Cauliflower mosaic virus (CaMV, DNA pararetrovirus) [99]. PMEs catalyze the de-methylesterification of pectin resulting in the release of protons and methanol. Methanol emission triggers the expression of methanol-induced genes, including β -1,3-glucanases. β -1,3-glucanases degrade callose locally deposited at the cell wall-embedded neck region of PD to restrict cell-to-cell communication and viral spreading. PME-dependent methanol emission triggers PD dilation, and the accumulated protons in the apoplast lead to acidification of the cell wall. This results in cell wall loosening due to the activation of several cell wall-degrading enzymes [100]. Dorokhov and coworkers identified an additional or contradicting role of PME, in which PME suppresses TMV RNA accumulation. They showed that PME levels increase due to the presence of TMV (or other pathogens), and this resulted in rapid siRNA accumulation indicative of induced RNA silencing [101,102]. In Figure 5, we have only depicted the PD dilation by PME, enhancing the viral spread, with the PD outward dashed arrow. Directed mutagenesis of PME will elucidate whether tobamovirus movement is inhibited by a non-functional or reduced functional PME.

The final host factor is synaptotagmin A (SYTA). SYTA is a protein that localizes to endosomes in plant cells and is essential to form ER-PM contact sites (EPCSs). The MP from TMV (and viruses from other genera) interact with SYTA to allocate the MPs to PD and to alter the PDs. The combination of MP allocation to and altering of the PD can facilitate tobamovirus cell-to-cell movement [103–105]. In Arabidopsis, the absence of SYTA/SYT1 affects the formation of the ER immobile tubules [106]. Two SYT1 interacting proteins, SYT5 and SYT7, were identified and shown to contribute together with SYT1 to enhance PD permeability for tobamoviral MP [107]. Because SYTA is suggested to assist viral movement through the PD, this protein is indicated near the PD (Figure 5).

5.4. Identification of Additional Host Factors Based on Host Processes That Are Manipulated by Tobamoviruses

Most identified host proteins reside in the cytosol/lysosomes or at the cell membrane. Host factors that function in the mitochondria or vacuole are, to our knowledge, not (yet) identified (depicted with the grey cloud shapes and a question mark in Figure 5). The number of *host* (*susceptibility*) factors currently identified is limited due to the identification method, co-purification with viral proteins. As a result, susceptibility-related host factors that do not directly interact or associate with a viral protein will be overlooked. Some S factors were identified via a forward genetics approach, e.g., TOM1, TOM2a, and TOM3 [73–75,79,108]. If existing, forward genetic screens of mutant plant populations will allow the identification of additional and non-viral protein-interacting host proteins. The drawback of forward genetic screens is that these will only disclose single proteins that result in a clear reduction of viral titer. This method will not reveal proteins that facilitate the virus proliferation if multiple or redundant proteins are required in concert. In addition, mutations that cause strong pleiotropic or lethal effects will be eliminated from the screen, and the corresponding host factors will not be identified.

In this review, we have focused on the utilization of host protein factors that interact with viral proteins. The absence of these specific host factors can lead to resistance. However, the identification of tobamoviral resistance can also be based on exploring which mechanisms are manipulated by the virus since these factors could also lead to novel and durable resistance. For example, viral resistance can be based on altered hormonal balance, membrane composition, apoptosis pathway, vesicle trafficking, or RNAi silencing mechanism of the host plant. For each mechanism, examples of S factors have been found.

S factors that alter the hormonal balance are discussed in Section 4.4. Altered membrane composition by plant cell fortification (discussed in Section 5.3), caused by PME-based callose deposition or overexpression of PME inhibitors (PMEIs) in tobacco and Arabidopsis plants, limits viral movement and reduces susceptibility to TMV and TVCV [100]. Autophagy can inhibit viral proliferation. Some S factors are negative regulators of autophagy, and their absence will trigger autophagy [58,59]. Five of the six host proteins in stage 2 (discussed in Section 5.2) prevent autophagy. However, autophagy can also have a pro-viral role, and several viruses have evolved strategies to use autophagy to their benefit. Therefore, only the autophagy-related genes (ATGs) with a pro-viral function should be further explored as S factors to combat viral infections of plants [58,59,109]. Importantly, the induction of autophagy and resistance depends on which plant proteins interact/bind with the viral helicase domain. The binding of the viral helicase to the N and/or Tm-1 R proteins can enhance autophagy resulting in resistance. In contrast, binding the viral helicase to the S proteins could prevent autophagy, enhancing susceptibility. For example, ARL8 binding to the REP protein could promote viral proliferation. ARL8 also interacts with TOM1 [53]. TOM1/3, TOM2a and ARL8 are essential to the tobamovirus replication complex. In human cells, the knockdown of ARL8b resulted in an increased fusion of autophagosomes with lysosomes [110]. The presence of ARL8 could promote viral infection by preventing the fusion of autophagosomes with lysosomes, as such inhibiting autophagy. In addition, SNARE motif-containing proteins, such as SYP23, are also required for autophagosome-lysosome fusion. Thus, we could postulate that host targets are incorporated into the VRC complex to prevent autophagy.

Another mechanism that is linked to the above S factors is membrane trafficking. SYP23 contains a SNARE motif, and TOM1/3 and TOM2a are putative transmembrane proteins. The TOM1/3 and TOM2a proteins could function in cell or vesicle membranes. A major role was found for endomembrane deformation during virus replication of ssRNA(+) viruses such as ToBRFV (reviewed by [111]). Additional host proteins that associate with VRC and are part of the intracellular membrane are interesting S factor candidates to explore.

Finally, studying the RNAi silencing mechanism and factors involved in this pathway can also lead to the identification of potential S factors. Plants produce small noncoding

RNAs (sRNAs) that can alter viral proliferation (reviewed by [112]), including miRNAs. miRNAs are derived and excised from primary nonprotein-coding MIR transcripts that form stem-loop structures [113]. Three main modes of miRNA antiviral defense response could be anticipated. A plant miRNA could (1) directly target and silence viral RNA, (2) trigger the biogenesis of siRNA resulting in RNA silencing, or (3) target the mRNA of an S gene resulting in the absence of the viral S factor from the host. An example of the first mode by miRNAs is from two miRNAs from cotton (*Gossypium arboreum*), Ga-miR398 and Ga-miR2950. Both miRNAs can target multiple ORFs of the Cotton leaf curl Multan virus (CLCuMuV), leading to enhanced viral immunity [114]. Interestingly, for TMV, an opposite role of miRNAs in viral proliferation has been found. The presence of TMV in tobacco (*N. benthamiana*) causes the accumulation of two miRNAs, Nb-miR6019 and Nb-miR6020, which results in the cleavage and silencing of the mRNA of the resistance gene N, leading to enhanced susceptibility [115]. It would be interesting to identify and utilize the promotor of the two miRNAs to produce viral dsRNA fragments that halt viral proliferation.

Another method that is currently successfully applied to halt viruses is the application of topical dsRNA delivery. Topical dsRNA application is sometimes referred to as a ‘plant vaccine’. However, technically it is not a vaccine because the dsRNA only works temporarily (10–20 days) when the pathogen is present [116]. The use of dsRNA production in-planta driven by a promotor induced in the presence of a virus could lead to a more durable solution. However, as the application of genetically modified plants is restricted in the European Union, other approaches need to be considered.

5.5. Antisense Oligonucleotide Therapeutics: Targeting the Secondary RNA Structures from ToBRFV for Durable Resistance

Although the discovery of the first viruses occurred in plants by plant pathologists, new insights from the fast-evolving human virology field may lead to solutions for plant breeding. For example, research on the human severe acute respiratory syndrome coronavirus 2 (SARS-CoV-2), the causal agent of Coronavirus Disease 2019 (COVID-19), could lead to new insights or solutions for durable plant virus resistance. SARS-CoV-2 virus, like ToBRFV, contains a single-stranded positive-sense RNA genome. The SARS-CoV-2 genome is ~30 kb RNA, and the secondary RNA structure of the entire SARS-CoV-2 virus genome was recently described [117].

The secondary RNA structure of ToBRFV is probably vital to evade plant-based RNA silencing, the first layer of viral defense by the host plant. For TMV, secondary RNA structures for the 5′ and 3′ parts of the genome have been described, but a genome-wide predicted RNA structure is still missing [118]. Secondary RNA structures from multiple animal viruses can be targeted by small molecules that affect interactions, structural stability, or conformational changes and thereby block processes that are essential for viral replication [119]. Can the secondary RNA structure of ToBRFV also be targeted by small molecular inhibitors? Comparison of human (SARS-CoV2), Pengolin, Porcine, and Bat coronaviruses resulted in the identification of conserved sites with persistent single-stranded sequences in the SARS-CoV2 and other coronavirus genomes in vivo [117]. These regions might represent ideal targets for the design of antisense oligonucleotide therapeutics, already proven to represent a promising approach for the treatment of infections by other RNA viruses [117].

The ToBRFV RNA molecule is only ~6.4 kb. It may be interesting to investigate whether a full genome comparison of secondary RNA structures from several tobamoviruses would also result in the identification of conserved sites with persistent single-stranded sequences. Antisense oligonucleotide therapeutics in tomatoes could also cause conformational changes or instability of secondary ToBRFV RNA structures and, as such, inhibit viral replication leading to durable ToBRFV resistance.

6. Conclusion and Future Directions towards Durable ToBRFV Tomato Resistance

Mutant S gene alleles can provide viral-resistant plants, and the abovementioned host factors for tobamoviruses are excellent candidates for which mutant alleles should be identified. Mutant alleles can be obtained by non-targeted chemical mutagenesis (e.g., EMS) or targeted mutagenesis using, e.g., CRISPR/Cas9 technology. Genome editing by CRISPR/Cas9 is well established in tomatoes and is the ideal method to explore and generate S gene-based resistance against ToBRFV. However, caution is required, as was shown by a CRISPR/Cas9 knock-out study on the well-known *eIF4E* and *eIF4G* S genes for potyviruses [120]. Knocking out *eIF4E1* in Arabidopsis resulted in clover yellow vein virus (CIYVV) resistance but simultaneously increased turnip mosaic virus (TuMV) susceptibility. This is probably because potyviruses, such as both CIYVV and TuMV, hijack different *eIF4E* factors, and the strategy of developing resistance by *eIF4E* loss-of-function could be jeopardized by existing or emerging viruses that are able to recruit the remaining *eIF4* paralogs in the plant [120].

As in the European Union, the application of CRISPR/Cas9 technology to generate mutations is restricted, and alternative methods to generate durable ToBRFV resistance have to be explored. A search for natural variants of a gene impacting the function of the encoded protein may be considered, especially if the complete absence of a functional S protein causes undesired pleiotropic effects.

6.1. The Use of Allelic Polymorphisms of Susceptibility Genes for Durable Resistance

Previously, some well-known S genes were identified from naturally occurring polymorphic alleles. These include *eIF4E* and *eIF4G* for resistance to potyviruses in Arabidopsis and pepper [121,122] and *pelota* for resistance against geminiviruses in tomato and pepper [123,124]. Thus, allelic variants of susceptibility genes (S genes) can be utilized to achieve recessively inherited disease resistance. The identification of natural variation in R proteins from wild tomato relatives is already a valuable source in tomato breeding. Wild relatives genetically related to cultivated species (*Solanum lycopersicum*), allowing compatible crosses, present a great opportunity to increase the genetic diversity in tomato breeding programs for disease resistance. Furthermore, such allelic S gene variants can be introgressed into cultivated tomatoes to obtain durable ToBRFV resistance. Currently, with the large list of identified host S genes, allelic S gene variants that could potentially contribute to ToBRFV resistance can be readily identified in the available genome sequences of various crop and wild tomato species. For example, ToBRFV-resistant tomato could be obtained using allelic variants of some of our discussed S genes since the absence of TOM1/3 led to ToMV or TMV resistance in tomato, pepper (*Capsicum annuum*) and tobacco (*N. benthamiana*) [76,125,126]. In addition, recently, allelic variants of TOM2a were claimed to be the main cause of ToBRFV resistance in wild tomato accessions [127].

The combination of available literature on tobamoviruses S gene candidates, wild tomato resources, genome sequences of the various wild species, single nucleotide polymorphism (SNP) detection methods, molecular techniques, and breeding methods make this reverse genetics approach to obtain durable resistant ToBRFV tomatoes accessible.

6.2. The Best Strategy for Durable Resistance Is the Absence of Susceptibility Genes

In this review, we highlighted four strategies to achieve durable ToBRFV-resistance in tomatoes (Figure 4). Although the second strategy (host R proteins) does not show a high risk of pleiotropy, viral genomes can adjust fast and break the resistance. The best strategy for durable resistance is an absence of functional susceptibility genes because viruses fully depend on host proteins for their proliferation due to the small number of viral proteins. As illustrated in the previous sections, most viral proteins interact with S proteins. Therefore, we need to investigate which amino acids from the S protein are relevant for viral protein binding and responsible for the S factor function. Simultaneously, we should identify which amino acid variants of the S protein can prevent viral protein binding and proliferation while maintaining the intrinsic protein function for the host plant.

Deployment of S protein variants that lost their viral “helper” ability but kept their intrinsic in planta function is expected to result in durable virus resistance.

Supplementary Materials: The following supporting information can be downloaded at: <https://www.mdpi.com/article/10.3390/agronomy13051300/s1>. Table S1: Tomato homologs of selected tobamoviral S genes from the literature including additional references [128–160]. Genes in bold are discussed in the text.

Funding: M.v.D., A.-M.A.W., M.V. and Y.B. are funded by a grant from the Top Sector for Horticulture and Starting Materials in the Netherlands (project LWV19106), and R.Z. is funded by a grant from the European Union’s Horizon 2020 research and innovation program (under grant agreement No 101000570).

Acknowledgments: The authors would like to thank all anonymous reviewers for commenting on earlier versions of this paper.

Conflicts of Interest: The authors declare no conflict of interest.

References

1. FAO. *World Food and Agriculture—Statistical Yearbook 2021*; Food and Agriculture Organization of the United Nations: Rome, Italy, 2021. [CrossRef]
2. Rosli, H.G.; Martin, G.B. Functional genomics of tomato for the study of plant immunity. *Brief. Funct. Genom.* **2015**, *14*, 291–301. [CrossRef] [PubMed]
3. D’Arcy, W.G.; Berry, P.E. Solanales. Available online: <https://www.britannica.com/plant/Solanales> (accessed on 30 March 2023).
4. Rivarez, M.P.S.; Vucurovic, A.; Mehle, N.; Ravnikar, M.; Kutnjak, D. Global Advances in Tomato Virome Research: Current Status and the Impact of High-Throughput Sequencing. *Front. Microbiol.* **2021**, *12*, 671925. [CrossRef] [PubMed]
5. Lustig, A.; Levine, A.J. One hundred years of virology. *J. Virol.* **1992**, *66*, 4629–4631. [CrossRef] [PubMed]
6. Bos, L. Beijerinck’s work on tobacco mosaic virus: Historical context and legacy. *Philos. Trans. R. Soc. Lond. Ser. B Biol. Sci.* **1999**, *354*, 675–685. [CrossRef] [PubMed]
7. Centre, D.S. Corona Crisis from a Historical Perspective. Available online: <https://heritage.tudelft.nl/en/exhibitions/corona-chronicles> (accessed on 30 March 2023).
8. Creager, A.N.; Morgan, G.J. After the double helix: Rosalind Franklin’s research on Tobacco mosaic virus. *Isis* **2008**, *99*, 239–272. [CrossRef]
9. Koonin, E.V.; Dolja, V.V.; Krupovic, M.; Varsani, A.; Wolf, Y.I.; Yutin, N.; Zerbini, F.M.; Kuhn, J.H. Global Organization and Proposed Megataxonomy of the Virus World. *Microbiol. Mol. Biol. Rev.* **2020**, *84*, e00061-19. [CrossRef]
10. Hanssen, I.M.; Lapidot, M.; Thomma, B.P. Emerging viral diseases of tomato crops. *Mol. Plant Microbe Interact.* **2010**, *23*, 539–548. [CrossRef]
11. Dombrovsky, A.; Smith, E. *Seed Transmission of Tobamoviruses: Aspects of Global Disease Distribution*; Jimenez-Lopez, J., Ed.; InTech: Rijeka, Croatia, 2017. [CrossRef]
12. Salem, N.M.; Sulaiman, A.; Samarah, N.; Turina, M.; Vallino, M. Localization and Mechanical Transmission of Tomato Brown Rugose Fruit Virus in Tomato Seeds. *Plant Dis.* **2022**, *106*, 275–281. [CrossRef]
13. Gibbs, A.J.; Wood, J.; Garcia-Arenal, F.; Ohshima, K.; Armstrong, J.S. Tobamoviruses have probably co-diverged with their eudicotyledonous hosts for at least 110 million years. *Virus Evol.* **2015**, *1*, vev019. [CrossRef]
14. Avni, B.; Gelbart, D.; Sufirin-Ringwald, T.; Zemach, H.; Belausov, E.; Kamenetsky-Goldstein, R.; Lapidot, M. ToBRFV Infects the Reproductive Tissues of Tomato Plants but Is Not Transmitted to the Progenies by Pollination. *Cells* **2022**, *11*, 2864. [CrossRef]
15. Levitzky, N.; Smith, E.; Lachman, O.; Luria, N.; Mizrahi, Y.; Bakelman, H.; Sela, N.; Laskar, O.; Milrot, E.; Dombrovsky, A. The bumblebee *Bombus terrestris* carries a primary inoculum of Tomato brown rugose fruit virus contributing to disease spread in tomatoes. *PLoS ONE* **2019**, *14*, e0210871. [CrossRef] [PubMed]
16. Salem, N.; Mansour, A.; Ciuffo, M.; Falk, B.W.; Turina, M. A new tobamovirus infecting tomato crops in Jordan. *Arch. Virol.* **2016**, *161*, 503–506. [CrossRef]
17. Luria, N.; Smith, E.; Reingold, V.; Bekelman, I.; Lapidot, M.; Levin, I.; Elad, N.; Tam, Y.; Sela, N.; Abu-Ras, A.; et al. A New Israeli Tobamovirus Isolate Infects Tomato Plants Harboring *Tm-2²* Resistance Genes. *PLoS ONE* **2017**, *12*, e0170429. [CrossRef]
18. Tomato Brown Rugose Fruit Virus (ToBRFV). Available online: <https://gd.eppo.int/taxon/tobrfv/reporting> (accessed on 30 March 2023).
19. Plant Virus Snapshots: Cucumber Mosaic Virus. Available online: <https://www.virtigation.eu/plant-virus-snapshots-cucumber-mosaic-virus/> (accessed on 30 March 2023).
20. Lewis Ivey, M.L.; Sidhu, J. Diagnosing Off-Target 2,4-D and Glyphosate Herbicide Damage to Tomato. Available online: https://www.lsu.edu/agriculture/plant/extension/hcpl-publications/herbicide_injury_tomato_ppcp-veg-004.pdf (accessed on 30 March 2023).

21. Zhang, S.K.; Griffiths, J.S.; Marchand, G.; Bernards, M.A.; Wang, A.M. Tomato brown rugose fruit virus: An emerging and rapidly spreading plant RNA virus that threatens tomato production worldwide. *Mol. Plant Pathol.* **2022**, *23*, 1262–1277. [CrossRef]
22. Scholthof, K.B. Tobacco mosaic virus: A model system for plant biology. *Annu. Rev. Phytopathol.* **2004**, *42*, 13–34. [CrossRef]
23. Panno, S.; Caruso, A.G.; Barone, S.; Lo Bosco, G.; Rangel, E.A.; Davino, S. Spread of Tomato Brown Rugose Fruit Virus in Sicily and Evaluation of the Spatiotemporal Dispersion in Experimental Conditions. *Agronomy* **2020**, *10*, 834. [CrossRef]
24. Panno, S.; Caruso, A.G.; Davino, S. First Report of Tomato Brown Rugose Fruit Virus on Tomato Crops in Italy. *Plant Dis.* **2019**, *103*, 1443. [CrossRef]
25. Chanda, B.; Gilliard, A.; Jaiswal, N.; Ling, K.S. Comparative analysis of host range, ability to infect tomato cultivars with *Tm-2²* gene, and real-time reverse transcription PCR detection of tomato brown rugose fruit virus. *Plant Dis.* **2021**, *105*, 3643–3652. [CrossRef]
26. Gaffar, F.Y.; Koch, A. Catch me if you can! RNA silencing-based improvement of antiviral plant immunity. *Viruses* **2019**, *11*, 673. [CrossRef]
27. Meins, F., Jr.; Si-Ammour, A.; Blevins, T. RNA silencing systems and their relevance to plant development. *Annu. Rev. Cell Dev. Biol.* **2005**, *21*, 297–318. [CrossRef]
28. Csorba, T.; Kontra, L.; Burgyan, J. viral silencing suppressors: Tools forged to fine-tune host-pathogen coexistence. *Virology* **2015**, *479–480*, 85–103. [CrossRef] [PubMed]
29. Wang, M.B.; Masuta, C.; Smith, N.A.; Shimura, H. RNA silencing and plant viral diseases. *Mol. Plant Microbe Interact.* **2012**, *25*, 1275–1285. [CrossRef] [PubMed]
30. Kubota, K.; Tsuda, S.; Tamai, A.; Meshi, T. Tomato mosaic virus replication protein suppresses virus-targeted posttranscriptional gene silencing. *J. Virol.* **2003**, *77*, 11016–11026. [CrossRef] [PubMed]
31. Kourelis, J.; van der Hoorn, R.A.L. Defended to the Nines: 25 Years of Resistance Gene Cloning Identifies Nine Mechanisms for R Protein Function. *Plant Cell* **2018**, *30*, 285–299. [CrossRef] [PubMed]
32. de Ronde, D.; Butterbach, P.; Kormelink, R. Dominant resistance against plant viruses. *Front. Plant Sci.* **2014**, *5*, 307. [CrossRef] [PubMed]
33. Lanfermeijer, F.C.; Dijkhuis, J.; Sturre, M.J.; de Haan, P.; Hille, J. Cloning and characterization of the durable tomato mosaic virus resistance gene *Tm-2²* from *Lycopersicon esculentum*. *Plant Mol. Biol.* **2003**, *52*, 1037–1049. [CrossRef]
34. Lanfermeijer, F.C.; Warmink, J.; Hille, J. The products of the broken *Tm-2* and the durable *Tm-2²* resistance genes from tomato differ in four amino acids. *J. Exp. Bot.* **2005**, *56*, 2925–2933. [CrossRef]
35. Watanabe, Y.; Kishibayashi, N.; Motoyoshi, F.; Okada, Y. Characterization of *Tm-1* gene action on replication of common isolates and a resistance-breaking isolate of TMV. *Virology* **1987**, *161*, 527–532. [CrossRef]
36. Rubio, L.; Galipienso, L.; Ferriol, I. Detection of Plant Viruses and Disease Management: Relevance of Genetic Diversity and Evolution. *Front. Plant Sci.* **2020**, *11*, 1092. [CrossRef]
37. Weber, H.; Schultze, S.; Pflitzner, A.J. Two amino acid substitutions in the tomato mosaic virus 30-kilodalton movement protein confer the ability to overcome the *Tm-2²* resistance gene in the tomato. *J. Virol.* **1993**, *67*, 6432–6438. [CrossRef]
38. Yan, Z.Y.; Ma, H.Y.; Wang, L.; Tettey, C.; Zhao, M.S.; Geng, C.; Tian, Y.P.; Li, X.D. Identification of genetic determinants of tomato brown rugose fruit virus that enable infection of plants harbouring the *Tm-2²* resistance gene. *Mol. Plant Pathol.* **2021**, *22*, 1347–1357. [CrossRef]
39. Hak, H.; Spiegelman, Z. The tomato brown rugose fruit virus movement protein overcomes *Tm-2²* resistance in tomato while attenuating viral transport. *Mol. Plant Microbe Interact.* **2021**, *34*, 1024–1032. [CrossRef] [PubMed]
40. Ykema, M.; Verweij, C.W.; De la Fuente van Bentem, S.; Perefarras, F.M.P. Tomato Plant Resistant to Tomato Brown Rugose Fruit Virus. US 2021/0238627 A1, 5 August 2021.
41. Fontanet, L.; Skoneczka, J.; Lionneton, E.; Lederer, J. Resistance in Plants of *Solanum lycopersicum* to the ToBRFV. WO 2021/245282 A1, 9 December 2021.
42. Hamelink, R.; Kalisvaart, J.; Rashidi, H. TBRFV Resistant Tomato Plant. WO 2019/110130 A1, 13 June 2019.
43. Zinger, A.; Lapidot, M.; Harel, A.; Doron-Faigenboim, A.; Gelbart, D.; Levin, I. Identification and Mapping of Tomato Genome Loci Controlling Tolerance and Resistance to Tomato Brown Rugose Fruit Virus. *Plants* **2021**, *10*, 179. [CrossRef] [PubMed]
44. Ashkenazi, V.; Rotem, Y.; Ecker, R.; Nashilevitz, S.; Barom, N. Resistance in Plants of *Solanum lycopersicum* to the Tobamovirus Tomato Brown Rugose Fruit Virus. WO 2020/249798 A1, 17 December 2020.
45. Lindbo, J. Tomato Plants Resistant to ToBRFV, TMV, TOMV and TOMMV and Corresponding Resistance Genes. WO 2022/117884 A1, 9 June 2022.
46. Zhao, S.; Li, Y. Current understanding of the interplays between host hormones and plant viral infections. *PLoS Pathog.* **2021**, *17*, e1009242. [CrossRef] [PubMed]
47. Alazem, M.; Lin, N.S. Antiviral Roles of Abscisic Acid in Plants. *Front. Plant Sci.* **2017**, *8*, 1760. [CrossRef]
48. Zhu, F.; Xi, D.H.; Yuan, S.; Xu, F.; Zhang, D.W.; Lin, H.H. Salicylic acid and jasmonic acid are essential for systemic resistance against tobacco mosaic virus in *Nicotiana benthamiana*. *Mol. Plant Microbe Interact.* **2014**, *27*, 567–577. [CrossRef] [PubMed]
49. Nakashita, H.; Yasuda, M.; Nitta, T.; Asami, T.; Fujioka, S.; Arai, Y.; Sekimata, K.; Takatsuto, S.; Yamaguchi, I.; Yoshida, S. Brassinosteroid functions in a broad range of disease resistance in tobacco and rice. *Plant J.* **2003**, *33*, 887–898. [CrossRef]
50. Yu, M.H.; Zhao, Z.Z.; He, J.X. Brassinosteroid signaling in plant-microbe interactions. *Int. J. Mol. Sci.* **2018**, *19*, 4091. [CrossRef]
51. Schwartz, I.; Levy, M.; Ori, N.; Bar, M. Hormones in tomato leaf development. *Dev. Biol.* **2016**, *419*, 132–142. [CrossRef]

52. Liu, C.; Nelson, R.S. The cell biology of Tobacco mosaic virus replication and movement. *Front. Plant Sci.* **2013**, *4*, 12. [CrossRef]
53. Nishikiori, M.; Mori, M.; Dohi, K.; Okamura, H.; Katoh, E.; Naito, S.; Meshi, T.; Ishikawa, M. A host small GTP-binding protein ARL8 plays crucial roles in tobamovirus RNA replication. *PLoS Pathog.* **2011**, *7*, e1002409. [CrossRef] [PubMed]
54. Kravchik, M.; Shnaider, Y.; Abebie, B.; Shtarkman, M.; Kumari, R.; Kumar, S.; Leibman, D.; Spiegelman, Z.; Gal-On, A. Knockout of SITOM1 and SITOM3 results in differential resistance to tobamovirus in tomato. *Mol Plant Pathol* **2022**, *23*, 1278–1289. [CrossRef] [PubMed]
55. Rosa-Ferreira, C.; Munro, S. Arl8 and SKIP act together to link lysosomes to kinesin-1. *Dev. Cell* **2011**, *21*, 1171–1178. [CrossRef] [PubMed]
56. Khatter, D.; Sindhwani, A.; Sharma, M. Arf-like GTPase Arl8: Moving from the periphery to the center of lysosomal biology. *Cell. Logist.* **2015**, *5*, e1086501. [CrossRef]
57. Garg, S.; Sharma, M.; Ung, C.; Tuli, A.; Barral, D.C.; Hava, D.L.; Veerapen, N.; Besra, G.S.; Hacohen, N.; Brenner, M.B. Lysosomal trafficking, antigen presentation, and microbial killing are controlled by the Arf-like GTPase Arl8b. *Immunity* **2011**, *35*, 182–193. [CrossRef]
58. Yang, M.; Ismayil, A.; Liu, Y. Autophagy in Plant-Virus Interactions. *Annu. Rev. Virol.* **2020**, *7*, 403–419. [CrossRef]
59. Huang, X.; Chen, S.; Yang, X.; Yang, X.; Zhang, T.; Zhou, G. Friend or Enemy: A Dual Role of Autophagy in Plant Virus Infection. *Front. Microbiol.* **2020**, *11*, 736. [CrossRef]
60. Bassüner, R.; Nong, V.; Jung, R.; Saalbach, G.; Müntz, K. The primary structure of the predominating vicilin storage protein subunit from field bean seeds (*Vicia faba* L. var. minor cv. Fribo). *Nucleic Acids Res.* **1987**, *15*, 9609. [CrossRef]
61. Ferreira, R.B.; Monteiro, S.; Freitas, R.; Santos, C.N.; Chen, Z.; Batista, L.M.; Duarte, J.; Borges, A.; Teixeira, A.R. The role of plant defence proteins in fungal pathogenesis. *Mol. Plant Pathol.* **2007**, *8*, 677–700. [CrossRef]
62. Cândido Ede, S.; Pinto, M.F.; Pelegrini, P.B.; Lima, T.B.; Silva, O.N.; Pogue, R.; Grossi-de-Sá, M.F.; Franco, O.L. Plant storage proteins with antimicrobial activity: Novel insights into plant defense mechanisms. *FASEB J.* **2011**, *25*, 3290–3305. [CrossRef]
63. Parcy, F.; Valon, C.; Raynal, M.; Gaubier-Comella, P.; Delseny, M.; Giraudat, J. Regulation of gene expression programs during Arabidopsis seed development: Roles of the ABI3 locus and of endogenous abscisic acid. *Plant Cell* **1994**, *6*, 1567–1582. [CrossRef] [PubMed]
64. Chen, C.E.; Yeh, K.C.; Wu, S.H.; Wang, H.L.; Yeh, H.H. A vicilin-like seed storage protein, PAP85, is involved in tobacco mosaic virus replication. *J. Virol.* **2013**, *87*, 6888–6900. [CrossRef] [PubMed]
65. Hassan, Z.; Kumar, N.D.; Reggiori, F.; Khan, G. How Viruses Hijack and Modify the Secretory Transport Pathway. *Cells* **2021**, *10*, 2535. [CrossRef]
66. Sanderfoot, A.A.; Assaad, F.F.; Raikhel, N.V. The Arabidopsis Genome. An Abundance of Soluble N-Ethylmaleimide-Sensitive Factor Adaptor Protein Receptors1. *Plant Physiol.* **2000**, *124*, 1558–1569. [CrossRef]
67. Ibrahim, A.; Yang, X.; Liu, C.; Cooper, K.D.; Bishop, B.A.; Zhu, M.; Kwon, S.; Schoelz, J.E.; Nelson, R.S. Plant SNAREs SYP22 and SYP23 interact with Tobacco mosaic virus 126 kDa protein and SYP2s are required for normal local virus accumulation and spread. *Virology* **2020**, *547*, 57–71. [CrossRef]
68. Lipka, V.; Kwon, C.; Panstruga, R. SNARE-ware: The role of SNARE-domain proteins in plant biology. *Annu. Rev. Cell Dev. Biol.* **2007**, *23*, 147–174. [CrossRef] [PubMed]
69. Ohtomo, I.; Ueda, H.; Shimada, T.; Nishiyama, C.; Komoto, Y.; Hara-Nishimura, I.; Takahashi, T. Identification of an allele of VAM3/SYP22 that confers a semi-dwarf phenotype in Arabidopsis thaliana. *Plant Cell Physiol.* **2005**, *46*, 1358–1365. [CrossRef] [PubMed]
70. Fujiwara, M.; Uemura, T.; Ebine, K.; Nishimori, Y.; Ueda, T.; Nakano, A.; Sato, M.H.; Fukao, Y. Interactomics of Qa-SNARE in Arabidopsis thaliana. *Plant Cell Physiol* **2014**, *55*, 781–789. [CrossRef]
71. Zhang, H.; He, Y.; Tan, X.; Xie, K.; Li, L.; Hong, G.; Li, J.; Cheng, Y.; Yan, F.; Chen, J.; et al. The Dual Effect of the Brassinosteroid Pathway on Rice Black-Streaked Dwarf Virus Infection by Modulating the Peroxidase-Mediated Oxidative Burst and Plant Defense. *Mol. Plant Microbe Interact.* **2019**, *32*, 685–696. [CrossRef]
72. Zhu, X.F.; Liu, Y.; Gai, X.T.; Zhou, Y.; Xia, Z.Y.; Chen, L.J.; Duan, Y.X.; Xuan, Y.H. SNARE proteins SYP22 and VAMP727 negatively regulate plant defense. *Plant Signal. Behav.* **2019**, *14*, 1610300. [CrossRef]
73. Yamanaka, T.; Imai, T.; Satoh, R.; Kawashima, A.; Takahashi, M.; Tomita, K.; Kubota, K.; Meshi, T.; Naito, S.; Ishikawa, M. Complete inhibition of tobamovirus multiplication by simultaneous mutations in two homologous host genes. *J. Virol.* **2002**, *76*, 2491–2497. [CrossRef] [PubMed]
74. Yamanaka, T.; Ohta, T.; Takahashi, M.; Meshi, T.; Schmidt, R.; Dean, C.; Naito, S.; Ishikawa, M. TOM1, an Arabidopsis gene required for efficient multiplication of a tobamovirus, encodes a putative transmembrane protein. *Proc. Natl. Acad. Sci. USA* **2000**, *97*, 10107–10112. [CrossRef] [PubMed]
75. Ishikawa, M.; Naito, S.; Ohno, T. Effects of the tom1 mutation of Arabidopsis thaliana on the multiplication of tobacco mosaic virus RNA in protoplasts. *J. Virol.* **1993**, *67*, 5328–5338. [CrossRef] [PubMed]
76. Kumar, S.; Dubey, A.K.; Karmakar, R.; Kini, K.R.; Mathew, M.K.; Prakash, H.S. Inhibition of TMV multiplication by siRNA constructs against TOM1 and TOM3 genes of Capsicum annum. *J. Virol. Methods* **2012**, *186*, 78–85. [CrossRef] [PubMed]
77. Wen, Y.; Lim, G.X.; Wong, S.M. Profiling of genes related to cross protection and competition for NbTOM1 by HLSV and TMV. *PLoS ONE* **2013**, *8*, e73725. [CrossRef]

78. Ishikawa, M.; Yoshida, T.; Matsuyama, M.; Kouzai, Y.; Kano, A.; Ishibashi, K. Tomato brown rugose fruit virus resistance generated by quadruple knockout of homologs of TOBAMOVIRUS MULTIPLICATION1 in tomato. *Plant Physiol.* **2022**, *189*, 679–686. [CrossRef]
79. Tsujimoto, Y.; Numaga, T.; Ohshima, K.; Yano, M.A.; Ohsawa, R.; Goto, D.B.; Naito, S.; Ishikawa, M. Arabidopsis TOBAMOVIRUS MULTIPLICATION (TOM) 2 locus encodes a transmembrane protein that interacts with TOM1. *EMBO J.* **2003**, *22*, 335–343. [CrossRef]
80. Hu, Q.; Zhang, H.; Zhang, L.; Liu, Y.; Huang, C.; Yuan, C.; Chen, Z.; Li, K.; Larkin, R.M.; Chen, J.; et al. Two TOBAMOVIRUS MULTIPLICATION 2A homologs in tobacco control asymptomatic response to tobacco mosaic virus. *Plant Physiol.* **2021**, *187*, 2674–2690. [CrossRef]
81. Galichet, A.; Gruissem, W. Protein farnesylation in plants—conserved mechanisms but different targets. *Curr. Opin. Plant Biol.* **2003**, *6*, 530–535. [CrossRef]
82. Benitez-Alfonso, Y.; Faulkner, C.; Ritzenthaler, C.; Maule, A.J. Plasmodesmata: Gateways to local and systemic virus infection. *Mol. Plant Microbe Interact.* **2010**, *23*, 1403–1412. [CrossRef]
83. Lucas, W.J.; Wolf, S. Connections between virus movement, macromolecular signaling and assimilate allocation. *Curr. Opin. Plant Biol.* **1999**, *2*, 192–197. [CrossRef] [PubMed]
84. Hirashima, K.; Watanabe, Y. Tobamovirus replicase coding region is involved in cell-to-cell movement. *J. Virol.* **2001**, *75*, 8831–8836. [CrossRef] [PubMed]
85. Hirashima, K.; Watanabe, Y. RNA helicase domain of tobamovirus replicase executes cell-to-cell movement possibly through collaboration with its nonconserved region. *J. Virol.* **2003**, *77*, 12357–12362. [CrossRef] [PubMed]
86. Ueki, S.; Spektor, R.; Natale, D.M.; Citovsky, V. ANK, a host cytoplasmic receptor for the Tobacco mosaic virus cell-to-cell movement protein, facilitates intercellular transport through plasmodesmata. *PLoS Pathog.* **2010**, *6*, e1001201. [CrossRef]
87. Vo, K.T.X.; Kim, C.-Y.; Chandran, A.K.N.; Jung, K.-H.; An, G.; Jeon, J.-S. Molecular insights into the function of ankyrin proteins in plants. *J. Plant Biol.* **2015**, *58*, 271–284. [CrossRef]
88. Tran, P.T.; Citovsky, V. Receptor-like kinase BAM1 facilitates early movement of the Tobacco mosaic virus. *Commun. Biol.* **2021**, *4*, 511. [CrossRef]
89. Rosas-Diaz, T.; Zhang, D.; Fan, P.; Wang, L.; Ding, X.; Jiang, Y.; Jimenez-Gongora, T.; Medina-Puche, L.; Zhao, X.; Feng, Z.; et al. A virus-targeted plant receptor-like kinase promotes cell-to-cell spread of RNAi. *Proc. Natl. Acad. Sci. USA* **2018**, *115*, 1388–1393. [CrossRef]
90. Li, Y.; Wu, M.Y.; Song, H.H.; Hu, X.; Qiu, B.S. Identification of a tobacco protein interacting with tomato mosaic virus coat protein and facilitating long-distance movement of virus. *Arch. Virol.* **2005**, *150*, 1993–2008. [CrossRef]
91. Zhang, C.; Liu, Y.; Sun, X.; Qian, W.; Zhang, D.; Qiu, B. Characterization of a specific interaction between IP-L, a tobacco protein localized in the thylakoid membranes, and Tomato mosaic virus coat protein. *Biochem. Biophys. Res. Commun.* **2008**, *374*, 253–257. [CrossRef]
92. Zhao, J.; Zhang, X.; Hong, Y.; Liu, Y. Chloroplast in Plant-Virus Interaction. *Front. Microbiol.* **2016**, *7*, 1565. [CrossRef]
93. Liu, C.; Pu, Y.; Peng, H.; Lv, X.; Tian, S.; Wei, X.; Zhang, J.; Zou, A.; Fan, G.; Sun, X. Transcriptome sequencing reveals that photoinduced gene IP-L affects the expression of PsbO to response to virus infection in *Nicotiana benthamiana*. *Physiol. Mol. Plant Pathol.* **2021**, *114*, 101613. [CrossRef]
94. Bhattacharyya, D.; Chakraborty, S. Chloroplast: The Trojan horse in plant-virus interaction. *Mol. Plant Pathol.* **2018**, *19*, 504–518. [CrossRef] [PubMed]
95. Zhao, J.; Liu, Q.; Zhang, H.; Jia, Q.; Hong, Y.; Liu, Y. The rubisco small subunit is involved in tobamovirus movement and *Tm-2²*-mediated extreme resistance. *Plant Physiol.* **2013**, *161*, 374–383. [CrossRef]
96. Janssen, B.J.; Williams, A.; Chen, J.J.; Mathern, J.; Hake, S.; Sinha, N. Isolation and characterization of two knotted-like homeobox genes from tomato. *Plant Mol. Biol.* **1998**, *36*, 417–425. [CrossRef] [PubMed]
97. Yoshii, A.; Shimizu, T.; Yoshida, A.; Hamada, K.; Sakurai, K.; Yamaji, Y.; Suzuki, M.; Namba, S.; Hibi, T. NTH201, a novel class II KNOTTED1-like protein, facilitates the cell-to-cell movement of Tobacco mosaic virus in tobacco. *Mol. Plant Microbe Interact.* **2008**, *21*, 586–596. [CrossRef] [PubMed]
98. Wang, S.; Yamaguchi, M.; Grienenberger, E.; Martone, P.T.; Samuels, A.L.; Mansfield, S.D. The Class II KNOX genes KNAT3 and KNAT7 work cooperatively to influence deposition of secondary cell walls that provide mechanical support to Arabidopsis stems. *Plant J.* **2020**, *101*, 293–309. [CrossRef] [PubMed]
99. Chen, M.H.; Sheng, J.; Hind, G.; Handa, A.K.; Citovsky, V. Interaction between the tobacco mosaic virus movement protein and host cell pectin methylesterases is required for viral cell-to-cell movement. *EMBO J.* **2000**, *19*, 913–920. [CrossRef]
100. Lionetti, V.; Raiola, A.; Cervone, F.; Bellincampi, D. How do pectin methylesterases and their inhibitors affect the spreading of tobamovirus? *Plant Signal. Behav.* **2014**, *9*, e972863. [CrossRef]
101. Dorokhov, Y.L.; Frolova, O.Y.; Skurat, E.V.; Ivanov, P.A.; Gasanova, T.V.; Sheveleva, A.A.; Ravin, N.V.; Makinen, K.M.; Klimyuk, V.I.; Skryabin, K.G.; et al. A novel function for a ubiquitous plant enzyme pectin methylesterase: The enhancer of RNA silencing. *FEBS Lett.* **2006**, *580*, 3872–3878. [CrossRef]
102. Gasanova, T.V.; Skurat, E.V.; Frolova, O.; Semashko, M.A.; Dorokhov Iu, L. Pectin methylesterase as a factor of plant transcriptome stability. *Mol. Biol.* **2008**, *42*, 478–486. [CrossRef]

103. Lewis, J.D.; Lazarowitz, S.G. Arabidopsis synaptotagmin SYTA regulates endocytosis and virus movement protein cell-to-cell transport. *Proc. Natl. Acad. Sci. USA* **2010**, *107*, 2491–2496. [CrossRef] [PubMed]
104. Uchiyama, A.; Shimada-Beltran, H.; Levy, A.; Zheng, J.Y.; Javia, P.A.; Lazarowitz, S.G. The Arabidopsis synaptotagmin SYTA regulates the cell-to-cell movement of diverse plant viruses. *Front. Plant Sci.* **2014**, *5*, 584. [CrossRef] [PubMed]
105. Levy, A.; Zheng, J.Y.; Lazarowitz, S.G. Synaptotagmin SYTA forms ER-plasma membrane junctions that are recruited to plasmodesmata for plant virus movement. *Curr. Biol.* **2015**, *25*, 2018–2025. [CrossRef]
106. Ishikawa, K.; Tamura, K.; Ueda, H.; Ito, Y.; Nakano, A.; Hara-Nishimura, I.; Shimada, T. Synaptotagmin-associated endoplasmic reticulum-plasma membrane contact sites are localized to immobile er tubules. *Plant Physiol.* **2018**, *178*, 641–653. [CrossRef] [PubMed]
107. Ishikawa, K.; Tamura, K.; Fukao, Y.; Shimada, T. Structural and functional relationships between plasmodesmata and plant endoplasmic reticulum-plasma membrane contact sites consisting of three synaptotagmins. *New Phytol.* **2020**, *226*, 798–808. [CrossRef] [PubMed]
108. Ishikawa, M.; Obata, F.; Kumagai, T.; Ohno, T. Isolation of mutants of Arabidopsis thaliana in which accumulation of tobacco mosaic virus coat protein is reduced to low levels. *Mol. Gen. Genet.* **1991**, *230*, 33–38. [CrossRef]
109. Kushwaha, N.K.; Hafren, A.; Hofius, D. Autophagy–virus interplay in plants: From antiviral recognition to proviral manipulation. *Mol. Plant Pathol.* **2019**, *20*, 1211–1216. [CrossRef]
110. Trivedi, P.C.; Bartlett, J.J.; Pulinilkunnil, T. Lysosomal Biology and Function: Modern View of Cellular Debris Bin. *Cells* **2020**, *9*, 1131. [CrossRef]
111. Agaoua, A.; Bendahmane, A.; Moquet, F.; Dogimont, C. Membrane Trafficking Proteins: A New Target to Identify Resistance to Viruses in Plants. *Plants* **2021**, *10*, 2139. [CrossRef]
112. Mengistu, A.A.; Tenkegna, T.A. The role of miRNA in plant–virus interaction: A review. *Mol. Biol. Rep.* **2021**, *48*, 2853–2861. [CrossRef]
113. Meyers, B.C.; Axtell, M.J.; Bartel, B.; Bartel, D.P.; Baulcombe, D.; Bowman, J.L.; Cao, X.; Carrington, J.C.; Chen, X.; Green, P.J.; et al. Criteria for annotation of plant MicroRNAs. *Plant Cell* **2008**, *20*, 3186–3190. [CrossRef] [PubMed]
114. Akmal, M.; Baig, M.S.; Khan, J.A. Suppression of cotton leaf curl disease symptoms in Gossypium hirsutum through over expression of host-encoded miRNAs. *J. Biotechnol.* **2017**, *263*, 21–29. [CrossRef] [PubMed]
115. Li, F.; Pignatta, D.; Bendix, C.; Brunkard, J.O.; Cohn, M.M.; Tung, J.; Sun, H.; Kumar, P.; Baker, B. MicroRNA regulation of plant innate immune receptors. *Proc. Natl. Acad. Sci. USA* **2012**, *109*, 1790–1795. [CrossRef]
116. Niehl, A.; Soinenen, M.; Poranen, M.M.; Heinlein, M. Synthetic biology approach for plant protection using dsRNA. *Plant Biotechnol. J.* **2018**, *16*, 1679–1687. [CrossRef]
117. Manfredonia, I.; Nithin, C.; Ponce-Salvatierra, A.; Ghosh, P.; Wirecki, T.K.; Marinus, T.; Ogando, N.S.; Snijder, E.J.; van Hemert, M.J.; Bujnicki, J.M.; et al. Genome-wide mapping of SARS-CoV-2 RNA structures identifies therapeutically-relevant elements. *Nucleic Acids Res.* **2020**, *48*, 12436–12452. [CrossRef] [PubMed]
118. Zimmern, D. An extended secondary structure model for the TMV assembly origin, and its correlation with protection studies and an assembly defective mutant. *EMBO J.* **1983**, *2*, 1901–1907. [CrossRef]
119. Hermann, T. Small molecules targeting viral RNA. *Wiley Interdiscip. Rev. RNA* **2016**, *7*, 726–743. [CrossRef]
120. Zafirov, D.; Giovanazzo, N.; Bastet, A.; Gallois, J.-L. When a knockout is an Achilles’ heel: Resistance to one potyvirus species triggers hypersusceptibility to another one in Arabidopsis thaliana. *Mol. Plant Pathol.* **2021**, *22*, 334–347. [CrossRef]
121. Duprat, A.; Caranta, C.; Revers, F.; Menand, B.; Browning, K.S.; Robaglia, C. The Arabidopsis eukaryotic initiation factor (iso)4E is dispensable for plant growth but required for susceptibility to potyviruses. *Plant J.* **2002**, *32*, 927–934. [CrossRef]
122. Ruffel, S.; Dussault, M.H.; Palloix, A.; Moury, B.; Bendahmane, A.; Robaglia, C.; Caranta, C. A natural recessive resistance gene against potato virus Y in pepper corresponds to the eukaryotic initiation factor 4E (eIF4E). *Plant J.* **2002**, *32*, 1067–1075. [CrossRef]
123. Lapidot, M.; Karniel, U.; Gelbart, D.; Fogel, D.; Evenor, D.; Kutsher, Y.; Makhbash, Z.; Nahon, S.; Shlomo, H.; Chen, L.; et al. A Novel Route Controlling Begomovirus Resistance by the Messenger RNA Surveillance Factor Pelota. *PLoS Genet.* **2015**, *11*, e1005538. [CrossRef] [PubMed]
124. Koeda, S.; Onouchi, M.; Mori, N.; Pohan, N.S.; Nagano, A.J.; Kesumawati, E. A recessive gene pepy-1 encoding Pelota confers resistance to begomovirus isolates of PepYLCIV and PepYLCAV in Capsicum annum. *Theor. Appl. Genet.* **2021**, *134*, 2947–2964. [CrossRef] [PubMed]
125. Ali, M.E.; Ishii, Y.; Taniguchi, J.-i.; Waliullah, S.; Kobayashi, K.; Yaeno, T.; Yamaoka, N.; Nishiguchi, M. Conferring virus resistance in tomato by independent RNA silencing of three tomato homologs of Arabidopsis TOM1. *Arch. Virol.* **2018**, *163*, 1357–1362. [CrossRef]
126. Chen, B.; Jiang, J.H.; Zhou, X.P. A TOM1 homologue is required for multiplication of Tobacco mosaic virus in Nicotiana benthamiana. *J. Zhejiang Univ. Sci. B* **2007**, *8*, 256–259. [CrossRef] [PubMed]
127. Kalisvaart, J.; Ludeking, D.J.W.; Roovers, A.J.M. Gene leading to ToBRFV resistance in *S. lycopersicum*. WO 2022/013452 A1, 20 January 2022.
128. Chen, L.; Zhang, L.; Li, D.; Wang, F.; Yu, D. WRKY8 transcription factor functions in the TMV-cg defense response by mediating both abscisic acid and ethylene signaling in Arabidopsis. *Proc. Natl. Acad. Sci. USA* **2013**, *110*, E1963–E1971. [CrossRef]
129. Fichtenbauer, D.; Xu, X.M.; Jackson, D.; Kragler, F. The chaperonin CCT8 facilitates spread of tobamovirus infection. *Plant Signal. Behav.* **2012**, *7*, 318–321. [CrossRef]

130. Ouibrahim, L.; Mazier, M.; Estevan, J.; Pagny, G.; Decroocq, V.; Desbiez, C.; Moretti, A.; Gallois, J.-L.; Caranta, C. Cloning of the Arabidopsis rwm1 gene for resistance to Watermelon mosaic virus points to a new function for natural virus resistance genes. *Plant J.* **2014**, *79*, 705–716. [CrossRef]
131. Lin, J.W.; Ding, M.P.; Hsu, Y.H.; Tsai, C.H. Chloroplast phosphoglycerate kinase, a gluconeogenetic enzyme, is required for efficient accumulation of Bamboo mosaic virus. *Nucleic Acids Res.* **2007**, *35*, 424–432. [CrossRef]
132. Poque, S.; Pagny, G.; Ouibrahim, L.; Chague, A.; Eyquard, J.P.; Caballero, M.; Candresse, T.; Caranta, C.; Mariette, S.; Decroocq, V. Allelic variation at the rpv1 locus controls partial resistance to Plum pox virus infection in Arabidopsis thaliana. *BMC Plant Biol.* **2015**, *15*, 159. [CrossRef]
133. Orjuela, J.; Deless, E.F.; Kolade, O.; Chéron, S.; Ghesquière, A.; Albar, L. A recessive resistance to rice yellow mottle virus is associated with a rice homolog of the CPR5 gene, a regulator of active defense mechanisms. *Mol. Plant Microbe Interact.* **2013**, *26*, 1455–1463. [CrossRef]
134. Carrasco, J.L.; Ancillo, G.; Castelló, M.J.; Vera, P. A novel DNA-binding motif, hallmark of a new family of plant transcription factors. *Plant Physiol.* **2005**, *137*, 602–606. [CrossRef] [PubMed]
135. Hwang, J.; Oh, C.-S.; Kang, B.-C. Translation elongation factor 1B (eEF1B) is an essential host factor for Tobacco mosaic virus infection in plants. *Virology* **2013**, *439*, 105–114. [CrossRef] [PubMed]
136. Hashimoto, M.; Neriya, Y.; Keima, T.; Iwabuchi, N.; Koinuma, H.; Hagiwara-Komoda, Y.; Ishikawa, K.; Himeno, M.; Maejima, K.; Yamaji, Y.; et al. EXA1, a GYF domain protein, is responsible for loss-of-susceptibility to plantago asiatica mosaic virus in Arabidopsis thaliana. *Plant J.* **2016**, *88*, 120–131. [CrossRef]
137. Yusa, A.; Neriya, Y.; Hashimoto, M.; Yoshida, T.; Fujimoto, Y.; Hosoe, N.; Keima, T.; Tokumaru, K.; Maejima, K.; Netsu, O.; et al. Functional conservation of EXA1 among diverse plant species for the infection by a family of plant viruses. *Sci. Rep.* **2019**, *9*, 5958. [CrossRef] [PubMed]
138. Taylor, D.N.; Carr, J.P. The GCD10 subunit of yeast eIF-3 binds the methyltransferase-like domain of the 126 and 183 kDa replicase proteins of tobacco mosaic virus in the yeast two-hybrid system. *J. Gen. Virol.* **2000**, *81*, 1587–1591. [CrossRef]
139. Kramer, S.R.; Goregaoker, S.P.; Culver, J.N. Association of the Tobacco mosaic virus 126 kDa replication protein with a GDI protein affects host susceptibility. *Virology* **2011**, *414*, 110–118. [CrossRef]
140. Conti, G.; Rodriguez, M.C.; Manacorda, C.A.; Asurmendi, S. Transgenic Expression of Tobacco mosaic virus Capsid and Movement Proteins Modulate Plant Basal Defense and Biotic Stress Responses in Nicotiana tabacum. *Mol. Plant-Microbe Interact.* **2012**, *25*, 1370–1384. [CrossRef]
141. Zou, L.J.; Deng, X.G.; Han, X.Y.; Tan, W.R.; Zhu, L.J.; Xi, D.H.; Zhang, D.W.; Lin, H.H. Role of Transcription Factor HAT1 in Modulating Arabidopsis thaliana Response to Cucumber mosaic virus. *Plant Cell Physiol.* **2016**, *57*, 1879–1889. [CrossRef]
142. Whitham, S.A.; Quan, S.; Chang, H.S.; Cooper, B.; Estes, B.; Zhu, T.; Wang, X.; Hou, Y.M. Diverse RNA viruses elicit the expression of common sets of genes in susceptible Arabidopsis thaliana plants. *Plant J.* **2003**, *33*, 271–283. [CrossRef]
143. Carr, T.; Wang, Y.; Huang, Z.; Yeakley, J.M.; Fan, J.-B.; Whitham, S.A. Tobamovirus infection is independent of HSP101 mRNA induction and protein expression. *Virus Res.* **2006**, *121*, 33–41. [CrossRef]
144. Gorovits, R.; Moshe, A.; Ghanim, M.; Czosnek, H. Recruitment of the host plant heat shock protein 70 by Tomato yellow leaf curl virus coat protein is required for virus infection. *PLoS ONE* **2013**, *8*, e70280. [CrossRef] [PubMed]
145. Zhang, L.; Chen, H.; Brandizzi, F.; Verchot, J.; Wang, A. The UPR branch IRE1-bZIP60 in plants plays an essential role in viral infection and is complementary to the only UPR pathway in yeast. *PLoS Genet.* **2015**, *11*, e1005164. [CrossRef] [PubMed]
146. Sasaki, N.; Ogata, T.; Deguchi, M.; Nagai, S.; Tamai, A.; Meshi, T.; Kawakami, S.; Watanabe, Y.; Matsushita, Y.; Nyunoya, H. Over-expression of putative transcriptional coactivator KELP interferes with Tomato mosaic virus cell-to-cell movement. *Mol. Plant Pathol.* **2009**, *10*, 161–173. [CrossRef] [PubMed]
147. Sheshukova, E.V.; Komarova, T.V.; Pozdyshev, D.V.; Ershova, N.M.; Shindyapina, A.V.; Tashlitsky, V.N.; Sheval, E.V.; Dorokhov, Y.L. The intergenic interplay between aldose 1-epimerase-like protein and pectin methylesterase in abiotic and biotic stress control. *Front. Plant Sci.* **2017**, *8*, 1646. [CrossRef] [PubMed]
148. Bilgin, D.D.; Liu, Y.; Schiff, M.; Dinesh-Kumar, S. P58IPK, a plant ortholog of double-stranded RNA-dependent protein kinase PKR inhibitor, functions in viral pathogenesis. *Dev. Cell* **2003**, *4*, 651–661. [CrossRef]
149. Vijayapalani, P.; Maeshima, M.; Nagasaki-Takekuchi, N.; Miller, W.A. Interaction of the trans-frame potyvirus protein P3N-PIPO with host protein PCaP1 facilitates potyvirus movement. *PLoS Pathog.* **2012**, *8*, e1002639. [CrossRef] [PubMed]
150. Yang, P.; Lüpken, T.; Habekuss, A.; Hensel, G.; Steuernagel, B.; Kilian, B.; Ariyadasa, R.; Himmelbach, A.; Kumlehn, J.; Scholz, U. PROTEIN DISULFIDE ISOMERASE LIKE 5-1 is a susceptibility factor to plant viruses. *Proc. Natl. Acad. Sci. USA* **2014**, *111*, 2104–2109. [CrossRef]
151. Amari, K.; Boutant, E.; Hofmann, C.; Schmitt-Keichinger, C.; Fernandez-Calvino, L.; Didier, P.; Lerich, A.; Mutterer, J.; Thomas, C.L.; Heinlein, M. A family of plasmodesmal proteins with receptor-like properties for plant viral movement proteins. *PLoS Pathog.* **2010**, *6*, e1001119. [CrossRef]
152. Dunoyer, P.; Thomas, C.; Harrison, S.; Revers, F.; Maule, A. A cysteine-rich plant protein potentiates Potyvirus movement through an interaction with the virus genome-linked protein VPg. *J. Virol.* **2004**, *78*, 2301–2309. [CrossRef]
153. Naderpour, M.; Lund, O.S.; Santana, G.; Blair, M.; Johansen, E. Potyviral VPG-interacting proteins and bean common mosaic virus resistance in *Phaseolus vulgaris* L. *BIC* **2010**, *53*, 44–45.

154. Feng, Z.; Xue, F.; Xu, M.; Chen, X.; Zhao, W.; Garcia-Murria, M.J.; Mingarro, I.; Liu, Y.; Huang, Y.; Jiang, L. The ER-membrane transport system is critical for intercellular trafficking of the NSm movement protein and tomato spotted wilt tospovirus. *PLoS Pathog.* **2016**, *12*, e1005443. [CrossRef] [PubMed]
155. Yoshii, M.; Yamazaki, M.; Rakwal, R.; Kishi-Kaboshi, M.; Miyao, A.; Hirochika, H. The NAC transcription factor RIM1 of rice is a new regulator of jasmonate signaling. *Plant J.* **2010**, *61*, 804–815. [CrossRef] [PubMed]
156. Maio, F.; Arroyo-Mateos, M.; Bobay, B.G.; Bejarano, E.R.; Prins, M.; van den Burg, H.A. A lysine residue essential for geminivirus replication also controls nuclear localization of the tomato yellow leaf curl virus rep protein. *J. Virol.* **2019**, *93*, e01910–e01918. [CrossRef] [PubMed]
157. Ohshima, K.; Taniyama, T.; Yamanaka, T.; Ishikawa, M.; Naito, S. Isolation of a Mutant of *Arabidopsis thaliana* Carrying Two Simultaneous Mutations Affecting Tobacco Mosaic Virus Multiplication within a Single Cell. *Virology* **1998**, *243*, 472–481. [CrossRef]
158. Pena, E.J.; Ferriol, I.; Sambade, A.; Buschmann, H.; Niehl, A.; Elena, S.F.; Rubio, L.; Heinlein, M. Experimental virus evolution reveals a role of plant microtubule dynamics and TORTIFOLIA1/SPIRAL2 in RNA trafficking. *PLoS ONE* **2014**, *9*, e105364. [CrossRef]
159. Ye, C.; Verchot, J. Role of unfolded protein response in plant virus infection. *Plant Signal. Behav.* **2011**, *6*, 1212–1215. [CrossRef]
160. Ye, C.; Dickman, M.B.; Whitham, S.A.; Payton, M.; Verchot, J. The Unfolded Protein Response Is Triggered by a Plant Viral Movement Protein. *Plant Physiol.* **2011**, *156*, 741–755. [CrossRef]

Disclaimer/Publisher’s Note: The statements, opinions and data contained in all publications are solely those of the individual author(s) and contributor(s) and not of MDPI and/or the editor(s). MDPI and/or the editor(s) disclaim responsibility for any injury to people or property resulting from any ideas, methods, instructions or products referred to in the content.



Resistance to Anthracnose Rot Disease in *Capsicum*

Lei Cui ^{1,2}, Michiel C. van den Munckhof ², Yuling Bai ² and Roeland E. Voorrips ^{2,*}¹ College of Agriculture, Shanxi Agricultural University, Taiyuan 030031, China² Plant Breeding, Wageningen University & Research, P.O. Box 386, 6700 AJ Wageningen, The Netherlands

* Correspondence: roeland.voorrips@wur.nl

Abstract: Pepper (*Capsicum* spp.) is an important vegetable crop worldwide with high economic and nutritional value. The *Capsicum* genus comprises more than 30 species, of which *C. annuum*, *C. baccatum*, *C. frutescens*, and *C. pubescens* are the five domesticated ones. Anthracnose fruit rot, caused by *Colletotrichum* spp., is one of the most destructive fungal diseases of pepper. In this review, we compiled up-to-date information from 40 publications on anthracnose resistance in *Capsicum* species. In total, 375 accessions were described as showing different levels of resistance against *Colletotrichum* spp. These accessions belonged to different species, including *C. annuum* (160), *C. baccatum* (86), *C. chacoense* (4), *C. chinense* (90), and *C. frutescens* (16), as well as 19 accessions of which the species were not reported. High levels of resistance were mainly present in *C. baccatum* and *C. chinense*. For some of the resistant accessions, resistance genes or quantitative trait loci (QTL) were reported. Using associated molecular markers, we located 31 QTLs and 17 resistance-related genes in the recently published *Capsicum* genomes, including *C. annuum* CM334 version 1.6, *C. chinense* version 1.2, and *C. baccatum* version 1.2. Our results could be helpful for making use of some reported accessions in the breeding of pepper cultivars with resistance to anthracnose rot disease.

Keywords: *Capsicum* spp.; anthracnose; *Colletotrichum* spp.; resistance; screening; QTL; in silico mapping; breeding

1. Introduction

The *Capsicum* species, or pepper, is commonly used as a vegetable and a spice. The economic importance of pepper is highlighted by its global annual production in 2017 of approximately 31.5 million tons for fresh pepper and 3.6 million tons for dried pepper [1]. Although pepper originates from South America, most of the world's production currently takes place in Asia, which contributes to more than 65% of the total.

Capsicum belongs to the Solanaceae family. Currently, 38 *Capsicum* species are recognized, including the five important domesticated species: *C. annuum*, *C. baccatum*, *C. chinense*, *C. frutescens*, and *C. pubescens* [2,3]. The *Capsicum* species is diploid ($n = 12$). Its genome is, in general, quite complex, and contains a large amount of repetitive DNA sequences, which has resulted in genome sizes above 3 Gb [4,5]. Because of the large genome size, the development of reference sequences has been delayed compared with other Solanaceous crops, for instance, tomato (900 Mb, Tomato Genome Consortium) [6] and potato (844 Mb, Potato Genome Sequencing Consortium) [7]. Until now, five *Capsicum* genomes have been completely sequenced, of which three are *C. annuum* and the others are *C. baccatum* and *C. chinense* [4,5,8]. The five pepper genomes are *C. annuum* cv. CM334 (3.06 Gb with 34,903 annotated genes); cv. Zunla-1 (3.35 Gb), a wild accession Chiltepin of *C. annuum* var. *glabriusculum* (3.48 Gb); *C. baccatum* PBC81 (3.9 Gb); and *C. chinense* PI 159236 (3.2 Gb).

Anthracnose is a major disease of pepper caused by a complex of *Colletotrichum* species, mainly occurring in the (sub-)tropics during the wet season. The prevalence of anthracnose is usually associated with a high amount of inoculum in the soil, which is the primary source of infection. Secondary spread occurs rapidly through conidial dispersion in air or

Citation: Cui, L.; van den Munckhof, M.C.; Bai, Y.; Voorrips, R.E. Resistance to Anthracnose Rot Disease in *Capsicum*. *Agronomy* **2023**, *13*, 1434. <https://doi.org/10.3390/agronomy13051434>

Academic Editor: Imre J. Holb

Received: 14 April 2023

Revised: 9 May 2023

Accepted: 14 May 2023

Published: 22 May 2023



Copyright: © 2023 by the authors. Licensee MDPI, Basel, Switzerland. This article is an open access article distributed under the terms and conditions of the Creative Commons Attribution (CC BY) license (<https://creativecommons.org/licenses/by/4.0/>).

surface water, or even by insects such as fruit flies (*Dacus* spp.) [9,10]. *Colletotrichum* is able to infect pepper plants at all developmental stages. The major species causing anthracnose in seedlings, leaves, and stems is *C. coccodes* [11,12]. The most prevalent and virulent species causing fruit rot are *C. scovillei* (previously known as *C. acutatum*), *C. siamense* (previously known as *C. gloeosporioides*), and *C. truncatum* (previously known as *C. capsici*) [13–17]. The taxonomy of *Colletotrichum* species has recently been revised based on pathogenicity and multi-gene phylogenetic analyses [18]. Typical anthracnose fruit rot symptoms, found on both green and ripe fruit, are black sunken necrotic tissues with water-soaked rings of wet acervuli [19] (Figure 1), leading to a loss of market value. The annual yield loss of pepper due to anthracnose has been reported to vary from 10% [20] to 50% [21], and can sometimes even be as high as 80% [22].



Figure 1. Typical anthracnose symptoms after pinprick inoculation with *C. siamense* (previously known as *C. gloeosporioides*) on a red ripe fruit of chili.

Control measures against anthracnose include the application of chemical fungicides, seed sterilization or cleaning, crop rotation, and biological control [23,24]. The frequent application of fungicides leads to environmental pollution and promotes the development of fungicide-resistant *Colletotrichum* strains [25,26]. As an alternative, growing resistant cultivars is considered to be the most effective and economic method to combat this disease. However, unlike for several other major pepper diseases, no commercial anthracnose-resistant cultivars have been released. The main factor that hinders anthracnose resistance breeding is the polygenic nature of the resistance and large variation in pathotypes [27]. Nevertheless, a vast number of *Capsicum* accessions have been evaluated worldwide, and anthracnose resistance has been identified in domesticated species including *C. annuum*, *C. baccatum*, *C. chinense*, and *C. frutescens* [28–31]. In addition, a few accessions from the wild species *C. chacoense* were reported to be resistant [30]. Genetic studies on some of these resistant accessions have identified monogenic (both dominantly and recessively inherited) and polygenic factors contributing to resistance, with the latter representing the most common type of resistance [15,21,25,26,28,32–34].

As many of these genetic studies were performed prior to the release of the genome sequences, the locations of the genes/quantitative trait loci (QTLs) were not reported in relation to a common genome or map, and are hence hard to compare. Therefore, we aimed to provide a comprehensive overview of current knowledge on anthracnose resistance in pepper in terms of the source and genetics of the identified resistance, as well as the chromosomal locations of the reported anthracnose resistance genes and QTLs. This effort could provide a new starting point for making use of the identified resistant sources in breeding programs.

2. Bioassays for Evaluating Anthracnose Resistance

A key factor for success in breeding for anthracnose resistance is the methods used for inoculation and evaluation. Inoculation can be performed on fruits, either detached or still on the plant, or on whole plants (Table 1). To determine foliar resistance, pepper plants at various growth stages have been inoculated with conidial suspension via foliar spray [35,36]. For fruit bioassays, two approaches are widely used: the fruit is either not wounded or wounded prior to inoculation [19,37]. The wound inoculation ensures direct entry of the spores without considering the cuticle and epidermis as the primary defense

barrier [25,38]. This can be achieved either via a so-called pinprick method [39,40] or via a microinjection procedure [16,41]. Non-wound inoculation delivers the conidia spores onto the fruit either via droplets (detached fruits) or via spraying (in planta or detached) [42,43].

Most screening studies have been based on bioassays of detached fruits at different maturity stages, mainly the mature green and ripe stages (Table 1). In *Capsicum* species, fruit maturity is a well-documented factor that influences the expression of anthracnose resistance. Genetic analyses in populations derived from *C. chinense* PBC932 and *C. baccatum* PBC80 have revealed that resistance in mature green and ripe fruit is controlled by different genes [22,28,43,44]. Mongkolporn et al. [44] reported that detached fruits of accession PBC932 at the mature green stage were more resistant than at the ripening stage. Two linked genes are responsible for resistance at the mature green and ripe fruit stages [22]. In contrast, the ripe fruit of accession PBC80 was more resistant than the mature green fruit [28,43]. In PBC80, resistance at the ripe fruit stage is controlled by a dominant gene, while an independent recessive gene mediates resistance in mature green fruit [28,43].

For evaluating anthracnose resistance, various assessment methods have been used by different research groups (Table 1). For example, a high resistance score has been based on four aspects: low incidence (the proportion of diseased plants/fruits of the total number of plants/fruits assessed) [39,45], low severity (lesion size as a proportion of fruit size) [31,36,46], low infection rate (the fraction of inoculations resulting in a lesion) [26,47], and low AUDPC value (the area under the disease progress curve) [16,48]. In some studies, different aspects are combined. For example, disease severity and incidence were converted to the disease severity index [44,49–51], while in other studies, lesion diameter was measured as well as the infection rate [25], disease incidence [26], and AUDPC [48].

Table 1. Inoculation and evaluation methods used in previous studies to evaluate anthracnose resistance and susceptibility.

| Pathogen ^a | Bioassay ^b | Inoculation Method ^c | Disease Evaluation Method ^d | Phenotypic Responses ^e | Reference |
|--|-----------------------|---------------------------------|---|---|------------------|
| <i>C. scovillei</i> | 1 | 1 | DSI | R (1<-3); IR (3<-6); S (6-9) | [52] |
| | 2 | 1/2 | DSI | HR (0); R (0.1-1.9); MR (2.0-2.9); S (3.0-4.9); HS (5) | [30] |
| | 4 | 4 | Infection rate | R (infection rate < 10%) | [53] |
| | 3 | 3 | DI | HR (0<-10%); R (10<-20%); MR (20<-40%); S (40<-70%); HS (>70%) | [45] |
| | 3 | 3 | DSI, AUDPC, IP, LP | R (low value for AUDPC, and high values for IP and LP) | [16] |
| <i>C. brevisporum</i> | 3 | 3 | DSI | HR (1); R (3); MR (4); MS (6); S (8); HS (10) | [41] |
| | 5 | 3 | DSI based on LS | R (<10%); MR (11-20%); S (21-40%); HS (>41%) | [36] |
| | 6 | 1 | DSI based on LS (foliar) | 1 (SL); 2 (>1 mm); 3 (1%); 4 (5%); 5 (10%); 6 (25%) | [36] |
| | 7 | 2 | DSI based on LS | R (0-1.0); MR (1.1-2.0); MS (2.1-3.0); S (3.1-4.0); HS (4.1-5.0) | [40] |
| <i>C. capsici</i> | - | 4 | DSI based on DI | I (0%); R (1-5%); MR (6-25%); S (26-50%); HS (51-100%) | [51] |
| | 7 | 1 | DSI based on LS | R (<20%); MR (21-40%); MS (41-60%); S (>60%) | [46] |
| <i>C. coccodes</i> | 6 | 1/2 | DSI based on LS | SL (0); R (0.1-10%); MR (10.1-25%); MS (25.1-50%); S (50.1-75%); HS (75.1-100%) | [31] |
| | 6 | 1/5 | DSI and AUDPC | Index (0-5) | [54] |
| <i>C. siamense</i> | 3 | 3 | DSI | HR (1); R (3); MR (4); MS (6); S (8); HS (10) | [55] |
| | 8 | 6/3 | DSI and AUDPC | HR (1); R (3); MR (4); MS (6); S (8); HS (10) | [48] |
| <i>C. scovillei</i> | 7 | 2 | DSI based on DI | I (0); R (1); MR (2); S (3); HS (4) | [39] |
| | 2 | 3 | Lesion diameter and infection frequency | | [26,47] |
| <i>C. capsici, C. siamense</i> | 3 | 2 | | | [25] |
| | 2 | 3 | LI | | [56] |
| <i>C. scovillei, C. capsici, C. siamense, C. truncatum</i> | 8 | 1/3 | DSI based on LS | HR (0); R (1); MR (3); MS (5); S (7); HS (9) | [28,44,49,50,57] |
| | 3 | 1 | DI, lesion diameter, LGR, AUDPC, IP | R (low values for AUDPC, DI, lesion diameter, and LGR; high values for IP) | [58] |

^a *C. scovillei* (previously known as *C. actitatum*), *C. siamense* (previously known as *C. gloeosporioides*), and *C. truncatum* (previously known as *C. capsici*). ^b 1: detached immature green fruit; 2: detached mature green fruit; 3: detached mature green and ripe fruits; 4: immature green and ripe red fruits on plants; 5: detached (im)mature fruits; 6: chili plants; 7: detached ripe fruits; 8: unripe and ripe fruit detached/on plants. ^c 1: spray; 2: pinpricking wounding; 3: microinjection; 4: natural field inoculation; 5: soil-drench method; 6: dropping spores on the pericarp. ^d Disease incidence (DI): percentage of fruit infected with inoculation sites at which lesion diameter > 4 mm; lesion growth rate (LGR): the measurement of lesion growth over time and calculated in mm/day; incubation period (IP) and latent period (LP), the number of days from inoculation to the appearance of symptoms; lesion incidence (LI): percentage of inoculation sites at which lesions ≤ 4 mm in diameter; percent lesion size (LS): lesion size as a proportion of fruit size; DSI: disease severity index; AUDPC: area under the disease progress curve. ^e Codes are interpreted from the original studies. Immune: I; symptomless: SL; highly resistant: HR; resistant: R; intermediate resistance: IR; moderately resistant: MR; susceptible: S; highly susceptible: HS. Between brackets, the original phenotypic classes or measurements are shown.

3. Sources of Anthracnose Resistance in *Capsicum* Germplasm

Breeding for resistance to anthracnose in pepper was started in the early 1990s by Korean and Indian chili breeders [59]. Their breeding programs mainly relied on moderate resistance obtained from *C. annuum* sources (cv. Perennial and Chungryong), which is the most widely cultivated *Capsicum* species [59,60]. Aiming to identify resistance at a high level, disease tests have been performed worldwide in a large number of *Capsicum* accessions. In total, 375 resistant accessions have been identified in the cultivated *Capsicum* species corresponding to *C. annuum* (160), *C. baccatum* (86), *C. chinense* (90), and *C. frutescens* (16) as well as in the wild species *C. chacoense* (4) and 19 accessions of unreported species [28–31] (Tables 2 and S1).

Table 2. Summary of identified sources of *Capsicum* accessions resistant to *Colletotrichum* species.

| <i>Colletotrichum</i> Species ^a | <i>Capsicum</i> Species ^b | | | | | |
|--|--------------------------------------|--------------------|---------------------|--------------------|----------------------|----------------------|
| | <i>C. annuum</i> | <i>C. baccatum</i> | <i>C. chacoense</i> | <i>C. chinense</i> | <i>C. frutescens</i> | <i>Capsicum</i> spp. |
| <i>C. scovillei</i> | 18 | 46 | 4 | 21 | 7 | - |
| <i>C. capsici</i> | 76 | 22 | - | 13 | 8 | 4 |
| <i>C. siamense</i> | 31 | 18 | - | 41 | - | 15 |
| <i>C. coccodes</i> | 1 | - | - | - | 1 | - |
| <i>C. brevisporum</i> | - | - | - | 15 | - | - |
| <i>C. dematium</i> | 7 | - | - | - | - | - |
| <i>C. truncatum</i> | 9 | - | - | - | - | - |
| <i>Colletotrichum</i> spp. | 18 | - | - | - | - | - |
| Total | 160 | 86 | 4 | 90 | 16 | 19 |

^a *C. scovillei* (previously known as *C. acutatum*); *C. siamense* (previously known as *C. gloeosporioides*), and *C. truncatum* (previously known as *C. capsici*); resistance to multiple species (*Colletotrichum* spp.), including *C. capsica* (syn. *C. truncatum*), *C. siamense*, and *C. scovillei* was identified in 18 *C. annuum* accessions. ^b *Capsicum* spp. denotes that the *Capsicum* species was not mentioned in the corresponding reports; “-” no such report. *Capsicum* accessions resistant to *Colletotrichum* spp. were summarized from the following references: [13,16,25,26,28,30,31,35,36,39,41, 44–49,51–56,59,61–70].

In these screening, six *Colletotrichum* species were used, of which three (*C. scovillei*, *C. truncatum*, and *C. siamense*) are prevalent worldwide and three (*C. coccodes*, *C. brevisporum*, and *C. dematium*) are common in Asia [19]. In most of the screens, a single *Colletotrichum* species was used. In a few cases, *C. annuum* accessions were evaluated against multiple *Colletotrichum* spp., leading to the identification of 18 accessions with broad resistance (Table 2).

In order to avoid redundant screenings in future studies, we summarize and present accessions identified as susceptible (Table S2). This panel included 255 accessions of the following species: *C. annuum* (167 accessions), *C. baccatum* (31), *C. chinense* (38), and *C. frutescens* (19).

4. Breeding for Anthracnose Resistance in *Capsicum*

Some of the resistant accessions of *C. annuum*, *C. baccatum*, and *C. chinense* listed in Table 2 have been used as donors for anthracnose resistance (Table 3). However, the resistance identified in *C. baccatum* is difficult to transfer into elite *C. annuum* lines, as an interspecific crossing barrier exists between both species [52]. As a result, one or multiple bridge crosses or embryo rescues are necessary in order to introgress the resistance into *C. annuum* [67]. For example, hybrids of *C. baccatum* PBC80 with elite *C. annuum* cultivars have been obtained with the aid of embryo rescue [71]. On the other hand, resistance in the accessions of *C. annuum* and *C. chinense* is generally easier to introduce into existing *C. annuum* lines.

The development of resistant cultivars can be facilitated with prior knowledge of the genetic basis of resistance and associated molecular markers for marker-assisted selection (MAS). The very first genetic map of anthracnose resistance in pepper was derived from an interspecific population between *C. annuum* and a resistant *C. chinense* accession,

PRI95030 [25] (Table 3). More recent genetic maps have been constructed and genetic analysis has been conducted in several populations derived from the main resistance sources, including *C. chinense* PBC932 [15]; *C. baccatum* PBC80 [34], PBC81 [29,72], PI594137 [47], and 881045 (Cbp) [33]. In addition, genetic studies have also been based on resistance obtained from *C. annuum* sources including cv. Perennial, cv. Chungryong, cv. Punjab Lal, and accessions 83–168, which are not highly resistant (Table 3). Results from these genetic studies indicate that the estimated inheritance of resistance depends not only on the *Colletotrichum* species and methods used for inoculation, but also on the fruit stages and the other parental lines used in the study (Table 3). For example, a single recessive gene model was suggested for the resistance of *C. chinense* PBC932 against *C. truncatum* (previously known as *C. capsici*) infection at different maturity stages in a cross with *C. annuum* cv. Bangchang (Table 3) [22], while polygenic resistance against *C. scovillei* was found at the mature green and ripe fruit stages in crosses between PBC 932 and *C. annuum* 9955-15 [72] or 77013 [15]. The inheritance of *Colletotrichum* spp. resistance derived from *C. baccatum* accessions PBC80, PBC81, and PI594137, from either intraspecific populations or an interspecific cross with *C. annuum*, was shown to be controlled by single or multiple genes at different maturity stages [28,29,43,47]. In contrast, monogenic resistance was found to be responsible for resistance to *C. truncatum* (previously known as *C. capsici*) in *C. annuum* accessions 83–168 [73], and to *C. scovillei* in *C. baccatum* accessions PI594137 [47] and PBC80 [34].

To introgress anthracnose resistance into a *C. annuum* line, backcrossing is one of the most important techniques used in breeding [74]. Successful resistant lines have been obtained from the backcrossing of resistant sources of *C. baccatum* and *C. chinense* with a recurrent elite *C. annuum* cultivar. At the AVRDC (the World Vegetable Center), five *C. annuum* lines, namely AVPP1102-B, AVPP0513, AVPP0719, AVPP0207, and AVPP1004-B, were found to be promising in terms of fruit yield and tolerance to anthracnose [45]. Two *C. annuum* varieties from IVEGRI (the Indonesian Vegetables Research Institute), Lembang-1 and Tanjung-2, have been reported to possess moderate resistance [75]. There have been multiple anthracnose-resistant *C. annuum* lines reported in India, including PBC-380, BS-20, BS28, Taiwan-2, Pant C-1 [31], LLS, VI047018 (derived from *C. chinense* PBC932), Breck-2, VI046804 (derived from *C. baccatum* PBC80), Breck-1, Jaun, and VI046805 (derived from *C. baccatum* PBC81) [76].

Table 3. *Capsicum* accessions used in anthracnose resistance breeding.

| Genetic Source <i>Capsicum</i> spp. | Accession | Resistance Level ^a | Population | | Colletotrichum spp. ^b | Inoculation Method | Genetic Mechanism ^c | | | Reference |
|---|-----------------|----------------------------------|---|---------------------------------------|--|-------------------------|--------------------------------|-----------------------|------------|-----------|
| | | | Type | Susceptible Parent | | | Mature Green | Ripe | Ripe | |
| <i>C. annuum</i> | Chungryong | MR | F ₂ , BC ₁ | <i>C. annuum</i> PI244670 | <i>C. denatumum</i> , <i>C. siamense</i> | Detached pinpricking | Partial dominant * | Partial dominant * | [59,68] | |
| | Perennial | MR | F ₂ , BC ₁ , BC ₂ | <i>C. annuum</i> 'Kolascat E-14' | <i>C. truncatum</i> | - | Polygenic | na | [60,68] | |
| | 83-168 | MR | F ₂ , BC ₁ | <i>C. annuum</i> 'KKU-Cluster' | <i>C. capsici</i> | Detached dropping | Single dominant | na | [73] | |
| | Punjab Lal | R | F ₂ | <i>C. annuum</i> 'PT 12-3' | <i>C. scovillei</i> , <i>C. capsici</i> | Detached pinpricking | Polygenic | Polygenic | [77] | |
| <i>C. chinense</i> | GBUEL104 | HR | F ₂ , BC ₁ , BC ₂ | <i>C. annuum</i> GBUEL103 | <i>C. scovillei</i> | Detached microinfection | Two dominant QTLs * | Two dominant QTLs * | [41] | |
| | PR95030 | HR | F ₂ | <i>C. annuum</i> 'Jatilaba' | <i>C. siamense</i> , <i>C. capsici</i> | Detached pinpricking | na | Polygenic | [25] | |
| | PBC932 | R | F ₂ , BC ₁ , BC ₃ | <i>C. annuum</i> '9955-15' | <i>C. scovillei</i> | Detached microinfection | Two dominant genes * | Polygenic recessive * | [72] | |
| | PBC932 | HR | F ₂ , BC ₁ | <i>C. annuum</i> 'Yeaju', 'Bangchang' | <i>C. capsici</i> | Detached microinfection | Single recessive * | Single recessive * | [22,26] | |
| | PBC932 | R | BC ₁ | <i>C. annuum</i> '77013' | <i>C. scovillei</i> | Detached microinfection | Polygenic dominant * | Polygenic dominant * | [15] | |
| | PI594137 | R | F ₂ , BC ₁ | <i>C. baccatum</i> Golden-aji | <i>C. scovillei</i> | Detached microinfection | Single dominant | na | [47] | |
| | PBC80 | HR | F ₂ , BC ₁ | <i>C. baccatum</i> CA1316 | <i>C. scovillei</i> | Detached microinfection | Single recessive * | Single dominant * | [28,34,43] | |
| | PBC81 | HR | F ₂ , BC ₁ | <i>C. annuum</i> SP26, Matikas | <i>C. scovillei</i> , <i>C. capsici</i> | Detached microinfection | Polygenic * | Polygenic * | [29,78] | |
| | 881045 (CbP) | R | F ₂ | <i>C. baccatum</i> Golden-aji | <i>C. scovillei</i> | Detached microinfection | na | Polygenic | [33] | |

^a Highly resistant: HR; resistant: R; moderate resistance: MR; ^b *C. scovillei* (previously known as *C. acutatum*), *C. siamense* (previously known as *C. glaberrimoides*), and *C. truncatum* (previously known as *C. capsici*); ^c * resistance in mature green and ripe fruit controlled by distinct genes; na: genetic information not available as mapping has not been performed.

5. Location of Anthracnose Resistance on the Pepper Genome

Knowledge on the localization of resistance genes and QTLs is of utmost importance when it comes to the development of markers linked to the resistance, subsequent gene introgression, and identification of allelic variants present in novel (wild) material. Many studies have been devoted to this aim, and their output, including resistant sources, *Colletotrichum* strains, linkage maps, and linked/flanking markers, is summarized in Table S3. However, for many of the genes and QTLs reported to date, their localization on the corresponding genome is not available due to the lack of reference sequences at the time of their first report. With the availability of the three pepper genomes [4,5,8], we attempted to map previously reported genes and QTLs on the chromosomes (Tables 4 and S3, Figure 2). After retrieving the reported sequences of associated markers, primer pairs, fragments, and genes, in silico mapping was performed on the corresponding genomes (*C. annuum* CM334 version 1.6, *C. chinense* version 1.2, or *C. baccatum* version 1.2) using BLASTN (nucleotide-to-nucleotide BLAST) in TBtools software [79]. For BLASTN, sequences of two categories were used. The first category is for AFLP markers and other PCR markers for which sequences of the amplified fragments are known. Amplicon sequences (>100 bp) were used, and the chromosome with the most likely hit (E-value below 1×10^{-5}) was chosen. The second category is for when the amplicon sequences are unknown. Primer sequences of about 20 bp were used and the setting was then set for short query sequences with an E-value threshold of 1000. When multiple markers could be used for one QTL, the chromosome anchored by the majority of markers was chosen. Some QTLs could not be anchored since their flanking markers had hits on different chromosomes.

In total, 56 QTLs were reported from 11 studies (Table 4), and 31 of them were anchored using the in silico mapping approach. The BLAST hits (markers flanking and/or within the QTL regions) were found across all 12 *Capsicum* spp. chromosomes (Tables 4 and S3, Figure 2).

In the *C. chinense* accession PBC932, a major QTL for resistance to *C. scovillei* on the bottom of chromosome 5 was consistently detected in different studies [80–83]. The interval is flanked by the markers P5in-2266-404 and P5in-2268-978 within a physical distance of 164 kb in the physical map [82]. Additionally, many other QTLs were identified in the study of Sun et al. [15], of which four were likely located on chromosomes 3 (AnRGo12), 5 (AnRGo5_AnRGT5), 7 (AnRgo7), and 10 (AnRGo10/AnR_{GD}10). For resistance to *C. capsici*, three QTLs were found, with two of them mapped to chromosomes 9 (QTLUL) and 11 (QTL-L4) [84].

In *C. baccatum* PBC80, monogenic resistance to *C. truncatum* (previously known as *C. capsici*) was found that could be inherited either dominantly or recessively [22,26]. In the study of Suwor et al. [81], a major contributing QTL (LG12) against *C. scovillei* was identified that could be anchored to chromosome 12.

In *C. baccatum* PBC81, many QTLs were identified in three independent studies [72,85,86]. In the study of Lee et al. [86], one QTL (CcR9) for resistance to *C. truncatum* (previously known as *C. capsici*) could be mapped to chromosome 3, while the other one (CaR12.2) for resistance against *C. scovillei* could be mapped to chromosome 12. Three QTLs (RA80f6_r1, RA80f6_g1, and RA80f6_g2) conferring *C. scovillei* resistance were mapped to chromosomes 4, 8, and 3, respectively [72].

In *C. baccatum* var. *pendulum* 881045, Kim et al. [33] found more than 15 QTLs contributing the resistance to *C. scovillei*. A major QTL, An9.1, could be mapped to the top of chromosome 1. A few minor QTLs could be assigned to chromosomes 3 (An8.1/An8.2), 4 (An4.1), 6 (An7.2–7.4), and 10 (An 13.1).

In *C. chinense* PRI195030, four QTLs were detected [25], of which only two could be mapped, including the QTLs H1 on chromosome 2 for *C. scovillei* resistance and B1 on chromosome 7 for resistance to *C. truncatum* (previously known as *C. capsici*) and *C. scovillei*. Other QTLs could not be assigned to any chromosomes since their associated markers are mapped to different chromosomes.

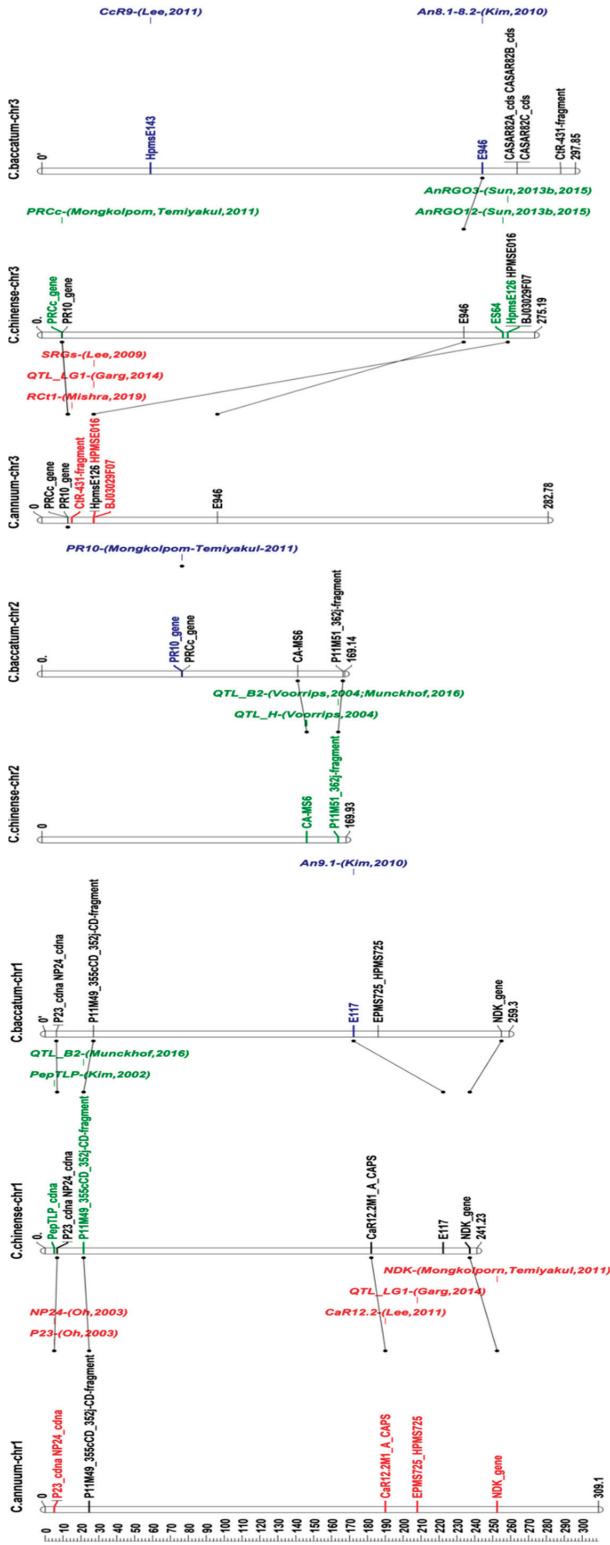
Table 4. Published QTL studies on anthracnose resistance.

| Study | QTL | Flanking Marker(s) | LOD ^a | R ² ^b | In Silico Mapping Chromosome | Colletotrichum Species | Resistant Source | | Fruit Stage ^c | Trait ^d | |
|-----------|---------|--|----------------------|-----------------------------|------------------------------|---|---|--------------------|--------------------------|--------------------|---------|
| | | | | | | | Capsicum Species | Accession | | | |
| [25] | B1 | E7M51_184cCD | 3.9–9.3 | 16.3–77.1 | 7 | <i>C. capsici</i> , <i>C. scovillei</i> | | | | | |
| | | P11M49_355cCD_352cCD P11M51_362j | | | 1 | | | | | | |
| | B2 | E37M51_184cCD | 2.7–4.7 | 30.2–51.8 | 7 | <i>C. scovillei</i> | <i>C. chinense</i> | PRI95030 | F | L.A, IF | |
| | | E37M51_251j P11M51_280 P11M51_362j | | | 10 12 2 | | | | | | |
| | H1 | P11M50_137j; P14M58_199cCD | 2.9–3.7 | 13.4–20.5 | 2 | <i>C. capsici</i> | | | | LD | |
| | G1 | hpms1-166, hpms1-274 | 2.8 | 7.6 | 7 | | | | | | |
| | | hpms1-155 hpms2-24 | | | 8 | | | | | | |
| | [85] | QTL_LG1 | hpms1-216, hpms1-274 | | | - | <i>C. scovillei</i> | <i>C. baccatum</i> | PBC81 | GF, RF | DI, TLD |
| | | QTL_LG7 | AF039662 | | | - | | | | | |
| | | QTL_LG9 | C31 | | | 9 | | | | | |
| | | QTL_LG10 | G28 | | | 11 | <i>C. capsici</i> | <i>C. chinense</i> | PBC92 | GF | LA |
| | [84] | QTL_L4 | C41 | 4.6 | 14.4 | 1 | | | | | |
| QTL_L3 | | E117 | 4–4.1 | 2–8.4 | 3 | | | | | DA | |
| An8-1-8.2 | | E946 | 4–4.1 | 2–8.4 | 3 | | | | | DR | |
| An8-1-8.2 | | E946 | 3.1 | 0.6 | 4 | | | | | - | |
| An4.1 | | E1540 | 2.5–3.8 | 4.9–37.5 | 6 | <i>C. scovillei</i> | <i>C. baccatum</i> var. <i>pendulatum</i> | 881045 | F | DR | |
| An7-2-7.4 | | E672, E384 | 2.9 | 15.4 | 10 | | | | | DA | |
| An13.1 | | E246 | 2.7–3.6 | 12.8–30.1 | - | | | | | DA | |
| An3-1-3.3 | | E63M82_270, E65M81_450 | 2.9 | 3.9 | - | | | | | DR | |
| An5.1 | | E74M79_370, E77M81_320 | | | - | | | | | DR | |
| An6.1 | | me02em03_04, me02em02_05 | 2.8 | 0.9 | - | | | | | DR | |
| [33] | An7.1 | E76M83_250, E65M80_420 | 3.4 | 11.3 | - | | | | | DA | |
| | An7.5 | E77M83_320, E75M83_450 | 3.9 | 6.9 | - | | | | | DR | |
| | An8.3 | E70M84_380, E71M79_295 | 3.3 | 15.2 | - | <i>C. scovillei</i> | <i>C. baccatum</i> var. <i>pendulatum</i> | | F | DR | |
| | An8.4 | E71M79_330, E67M79_250 | 3.8 | 20.5 | - | | | | | DR | |
| | An9.2 | E76M83_350, E75M81_480 | 3 | 10.8 | - | | | | | DA | |
| | CaR12.2 | CaR12.2ML_A_CAPS CaR12.2ML_B_CAPS | 7.8–9.6 | 11.9–20.5 | 1 12 | <i>C. scovillei</i> | | | GF, RF | TLD | |
| [29] | CaR9 | HpmsE143 | 13.4–15.9 | 57.5–78.9 | 3 | <i>C. capsici</i> | <i>C. baccatum</i> | PBC81 | | DI, TLD, OLD | |
| | CaR12.1 | EtagMcag11, EtecMcga05 | 4.7 | 17.9 | - | <i>C. scovillei</i> | | | RF | TLD | |
| | CcRC | EaacMcgc02, EaatMcgc07 | 6.7 | 10.6 | - | <i>C. capsici</i> | | | | DI | |

Table 4. Cont.

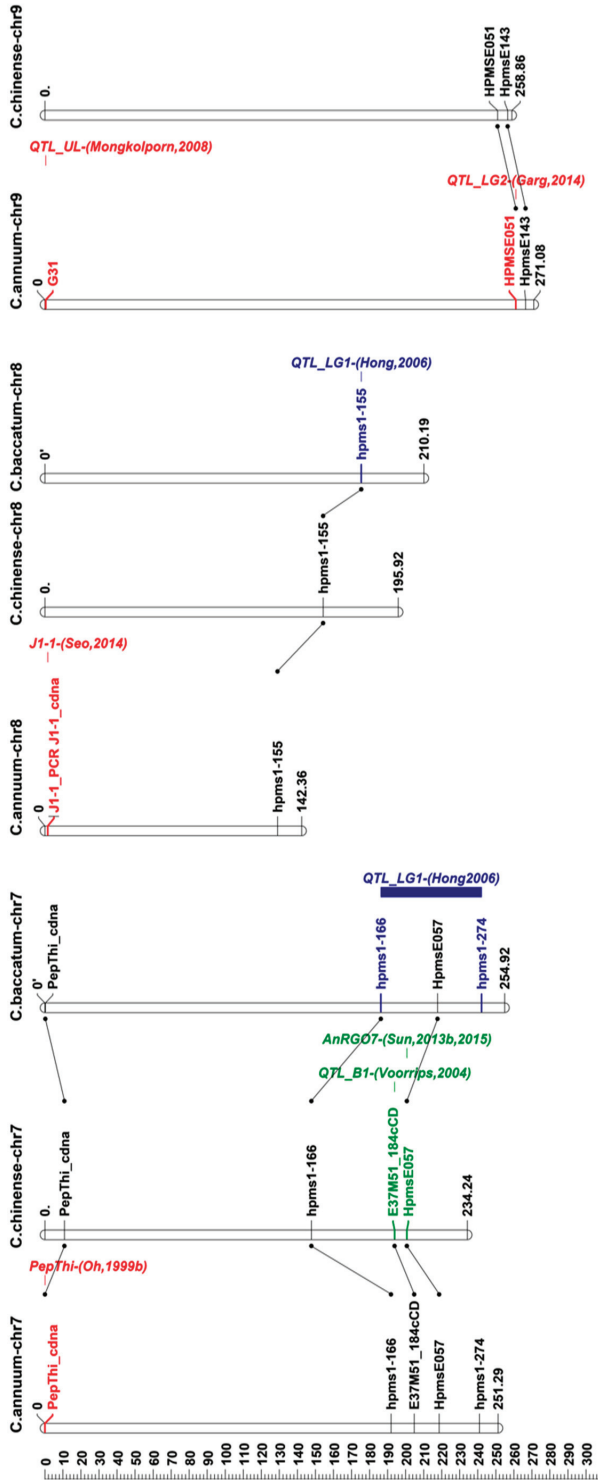
| Study | QTL | Flanking Marker(s) | LOD ^a | R ² ^b | In Silico Mapping Chromosome | Colletotrichum Species | Resistant Source | | Fruit Stage ^c | Trait ^d |
|-------|---|---|---------------------|-----------------------------|------------------------------|------------------------|--------------------|-----------------|--------------------------|--------------------|
| | | | | | | | CapSicum Species | Accession | | |
| [77] | QTL_LG1 | EFMS725, HPMS725 | 3.4–5.8 | 16.7–71 | 1 | | | | | |
| | QTL_LG2 | HPMSE016 | 2.1–4.9 | 7.2–18 | 3 | <i>C. scovillei</i> | <i>C. annuum</i> | Punjab Lal | GF, RF | IP |
| | QCcR4fp-ivr1.1 QCcG-hiivr1.1 | CAMS020, HPMSE016 HPMS725, CAMS644 | 3.5 | 14.2 | 9 | <i>C. capsici</i> | | | | IP, LA |
| [80] | QTL_AR | A518_InDel_98b, A518_seq_281b, A518_primer_89c | 2.3 | 2.9 | 5 | <i>C. scovillei</i> | <i>C. chinense</i> | PBC932 | GF | OLD |
| | AnRCo3 | HpmsE126 ES382 | 2.3 | 2.9 | 3 | | | | | OLD |
| [15] | AnRCo12 | ES64, EpmS745 | 2.7 | 3.1 | 4 | | | | | OLD |
| | AnRCo5_AnRGr5 | InDel-HpmsE116, InDel | 31.9–32.3 | 60.5–62.4 | 3 | | | | | OLD, TLD |
| | AnRCo7 | HpmsE057 | 2.2 | 2.5 | 7 | <i>C. scovillei</i> | <i>C. chinense</i> | PBC932 | GF | OLD |
| | AnRCo10, AnRCo10 AnRCo5, AnRCo5, AnRGr5, AnRGr5 | C2_A14g03400, Gp20068 HpmsE116 | 2.2–2.3 2.7–12.3 | 2.9–4.7 9.3–33.2 | 10 - | | | | | GF, RF |
| [81] | P5 | ES118, ES181 | 2.8 | 5.4 | - | | | | GF | DI |
| | LG12 | SCAR-InDel | | | 5 | | <i>C. chinense</i> | PBC932 | GF | LD |
| [82] | AnRCo5 | SSK-HpmsE032 P5in-2266-404, P5in-2268-978 | 24.4 | 69.3 | 12 5 | <i>C. scovillei</i> | <i>C. baccatum</i> | PBC80 PBC932 | GF | TLD |
| | RA8016_r1 | SNP_305/331 | 4 | 17.7 | 4 | <i>C. scovillei</i> | <i>C. chinense</i> | | GF | |
| [72] | RA8016_g1 | SNP_541/571 | 5.2 | 20.2 | 8 | | | | GF, RF | IP |
| | RA8016_g2 | SNP_228/218 | 3.5 | 12.8 | 3 | <i>C. scovillei</i> | <i>C. baccatum</i> | PBC81 | GF, RF | |

^a LOD: likelihood of odds ratio; ^b R²: percentage of phenotypic variance explained by each QTL; ^c GF: green fruit; RF: red fruit; F: fruit (undefined); ^d DI: disease incidence, TLD: true lesion diameter, OLD: overall lesion diameter, IP: Infection percentage, LA: lesion area, DR: disease rate, DA: disease area, IF: infection frequency.



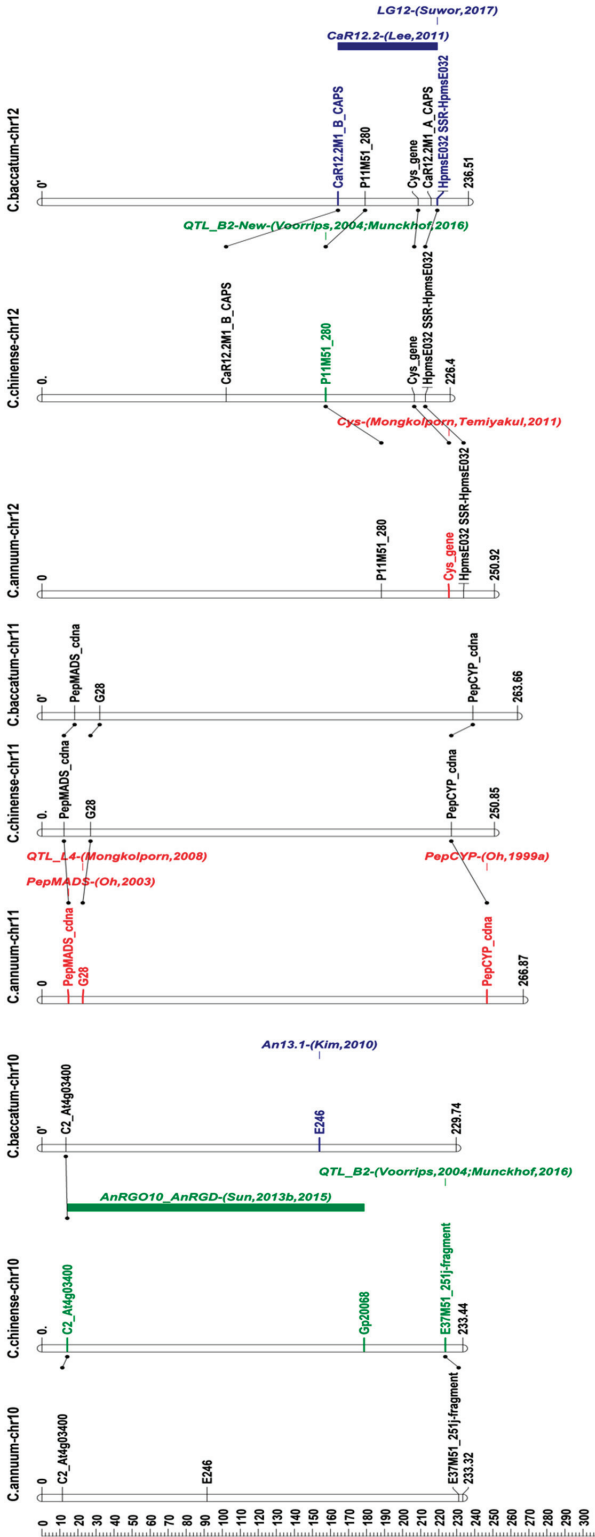
(A)

Figure 2. Cont.



(C)

Figure 2. Cont.



(D)

Figure 2. Anthracnose resistance-associated QTLs, genes, and fragments projected on the physical chromosomes of *C. annuum* CM334 version 1.6, *C. chinense* version 1.2, and *C. baccatum* version 1.2. Positions are in million base pairs. QTLs and genes are displayed as bars or indicators shown to the right of the chromosomes. Their names as given by the authors are maintained, and the study from which they originate is indicated between brackets. Molecular markers flanking the QTLs are indicated on the corresponding chromosomes. Synteny links are represented by black lines. Depending on the origin of resistance sources, molecular markers, QTLs, and genes are displayed in different colors (i.e., red for *C. annuum*, green for *C. chinense*, and blue for *C. baccatum*). Information was visualized using MapChart 2.3 [87]. (A) Physical maps of chromosomes 1–3 of *C. annuum* CM334 version 1.6, *C. chinense* version 1.2, and *C. baccatum* version 1.2; (B) physical maps of chromosomes 4–6; (C) physical maps of chromosomes 7–9; (D) physical maps of chromosomes 10–12.

In *C. annuum* PT-12-3, among the four reported QTLs, only QTL_LG2 could be assigned to chromosome 9 [68].

6. Defense Mechanisms of Anthracnose Resistance Caused by *Colletotrichum* spp.

The complete resistance of *C. chinense* accession PBC932 and *C. baccatum* accessions PBC80 and PBC81 is due to a hypersensitive reaction (HR) [12,22,28]. The immune response consists of slight tissue necrosis and localized cell death surrounding the inoculation site on the detached fruits [22,28,88]. The infected cells themselves have thickened cell walls or a thickened cuticle layer and have high levels of reactive oxygen species [12,88].

To understand the molecular mechanisms of defense against anthracnose, differential *Capsicum* spp.–*Colletotrichum* spp. pathosystems have been used to evaluate the expression of defense-related genes or the production of antimicrobial compounds. Based on an expression study with the *C. truncatum*-resistant accession Bhut Jolokia (obtained from a cross between *C. frutescens* and *C. chinense*), Mishra et al. [89] identified a number of defense-related genes, including *PDF1.2*, lipoxygenase *Lox3*, *PR2*, *PR5*, and transcription factors (*WRKY33* and *CaMYB*), as possibly being involved in the resistance response.

In *C. baccatum* accession PBC80, pathogen-responsive gene 10 (*PR10*) was differentially expressed upon *C. scovillei* infection [90]. This gene is located on *C. baccatum* chromosome 2 at 78.2 Mb. In *C. baccatum* accession P27 challenged with *Colletotrichum* spp., the resistant response was dependent on the ripening stage and correlated with the accumulation of the metabolites butane-2,3-diol, fructose, and phenolics, and superoxide dismutase and peroxidase activities [58].

In the incompatible interaction of *C. annuum* cv. Nokkwang with *C. siamense*, six defense-responsive genes, including cytochrome P450, a *PepCYP* gene, a thionin-like gene (*PepThi*), a defensin gene (*J1-1*) [91], a pepper thaumatin-like gene (*PepTLP*), a MADS-box gene (*PepMADS*) [92], and a pepper esterase gene (*PepEST*) [93], were reported, of which *PepCYP* was mapped towards the bottom of chromosome 11, *PepThi* on the distal top of chromosome 7, *J1-1* on the top of chromosome 8, *PepTLP* on chromosome 1 at 5.08 Mb, *PepMADS* on chromosome 11 at 14.7 Mb, and *PepEST* on chromosome 4 at 208.98 Mb. Moreover, the salicylic acid-induced protection of ripe pepper fruits of cv. Nokkwang against *C. siamense* was associated with highly expressed SA-responsive genes (SRGs) [94]. A SRG, namely BJ03029B07, was located at the top of *C. annuum* chromosome 6, and BJ03028G01 was located towards the bottom of this chromosome. Additionally, BJ03028G01 co-localized with QTL An7.2–7.4. The possible involvement of these genes in anthracnose resistance controlled by the QTL An7.2–7.4 needs to be studied. In *C. annuum* cv. Hanbyul, a systemic acquired resistance gene (*CASAR8.2*) with three cDNA clones (*CASAR82A*, -B, and -C) was strongly associated with resistance to *C. coccodes* [95]. This gene was mapped to the top of chromosome 5. *C. annuum* UENF 1381, in response to *C. siamense*, produced abundant amounts of antimicrobial peptides such as defensin, lipid transfer protein, and protease inhibitor [70]. The quantification of secondary metabolites produced during the interaction between the resistant *C. annuum* accessions GBUEL104 and *C. siamense* revealed that high concentrations of caffeic and chlorogenic acid were produced, and their differential expression depended on the fruit development stage and the time that had elapsed post-inoculation [55].

7. Conclusions

Anthracnose fruit rot disease is caused by a complex of *Colletotrichum* species. It causes significant yield losses and has become a constraint for *Capsicum* production. The ultimate means of achieving the sustainable control of anthracnose is to breed for anthracnose resistance. Worldwide screenings have mostly identified resistant accessions in *C. baccatum* and *C. chinense*. In this study, we summarized information on *Capsicum* accessions that have been tested and shown to be either resistant or susceptible to *Colletotrichum* spp. Generally, *C. annuum* lacks anthracnose resistance, but the introgression of resistance from resistant *C. chinense* and *C. baccatum* accessions has resulted in multiple breeding lines. A

large number of genes and QTLs conferring anthracnose resistance that were anchored to the *C. chinense* and *C. baccatum* genomes were identified in various sources in the present study using an in silico mapping approach. Our results may be useful and informative for clarifying the locations of genes/QTLs from different sources for resistance to anthracnose rot disease in pepper, as well as for the introgression of resistance from donor accessions into elite cultivars.

Supplementary Materials: The following supporting information can be downloaded at: <https://www.mdpi.com/article/10.3390/agronomy13051434/s1>, Table S1: Published data on *Capsicum* accessions resistant to *Colletotrichum* species; Table S2: Published data on *Capsicum* accessions susceptible to *Colletotrichum* species; Table S3: Sequences from primer pairs, genes, proteins, or cDNA clones used in the in silico mapping of anthracnose resistance genes/QTLs [96–103].

Author Contributions: Conceptualization, Y.B. and R.E.V.; data curation, L.C. and M.C.v.d.M.; visualization and writing—original draft preparation, L.C.; writing—review and editing, L.C., M.C.v.d.M., Y.B. and R.E.V. All authors have read and agreed to the published version of the manuscript.

Funding: L.C. acknowledges financial support from the China Scholarship Council (201908140029).

Data Availability Statement: Not applicable.

Conflicts of Interest: The authors declare no conflict of interest.

References

1. FAO. FAOSTAT. 2017. Available online: <http://faostat.fao.org> (accessed on 13 November 2021).
2. Bosland, P.W.; Votava, E.J.; Votava, E.M. Peppers: Vegetable and spice capsicums. In *Crop Production Science in Horticulture*; CABI: Cambridge, UK, 2012; Volume 22.
3. Ramchiary, N.; Kehie, M.; Brahma, V.; Kumaria, S.; Tandon, P. Application of genetics and genomics towards *Capsicum* translational research. *Plant Biotechnol. Rep.* **2013**, *8*, 101–123. [CrossRef]
4. Kim, S.; Park, M.; Yeom, S.-I.; Kim, Y.-M.; Lee, J.M.; Lee, H.-A.; Seo, E.; Choi, J.; Cheong, K.; Kim, K.-T.; et al. Genome sequence of the hot pepper provides insights into the evolution of pungency in *Capsicum* species. *Nat. Genet.* **2014**, *46*, 270–278. [CrossRef] [PubMed]
5. Kim, S.; Park, J.; Yeom, S.-I.; Kim, Y.-M.; Seo, E.; Kim, K.-T.; Kim, M.-S.; Lee, J.M.; Cheong, K.; Shin, H.-S.; et al. New reference genome sequences of hot pepper reveal the massive evolution of plant disease-resistance genes by retroduplication. *Genome Biol.* **2017**, *18*, 210. [CrossRef] [PubMed]
6. Sato, S.; Tabata, S.; Hirakawa, H.; Asamizu, E.; Shirasawa, K.; Isobe, S.; Kaneko, T.; Nakamura, Y.; Shibata, D.; Aoki, K.; et al. The tomato genome sequence provides insights into fleshy fruit evolution. *Nature* **2012**, *485*, 635–641. [CrossRef]
7. Potato Genome Sequencing Consortium. Genome sequence and analysis of the tuber crop potato. *Nature* **2011**, *475*, 189. [CrossRef]
8. Qin, C.; Yu, C.; Shen, Y.; Fang, X.; Chen, L.; Min, J.; Cheng, J.; Zhao, S.; Xu, M.; Luo, Y.; et al. Whole-genome sequencing of cultivated and wild peppers provides insights into *Capsicum* domestication and specialization. *Proc. Natl. Acad. Sci. USA* **2014**, *111*, 5135–5140. [CrossRef]
9. Amusa, N.; Kehinde, I.; Adegbite, A. Pepper (*Capsicum frutescens*) fruit anthracnose in the humid forest region of south-western Nigeria. *Nutr. Food Sci.* **2004**, *34*, 130–134. [CrossRef]
10. Sang, M.K.; Shrestha, A.; Kim, D.-Y.; Park, K.; Pak, C.H.; Kim, K.D. Biocontrol of *Phytophthora* blight and anthracnose in pepper by sequentially selected antagonistic rhizobacteria against *Phytophthora capsici*. *Plant Pathol. J.* **2013**, *29*, 154–167. [CrossRef]
11. Oh, I.S.; In, M.S.; Woo, I.S.; Lee, S.K.; Yu, S.H. Anthracnose of pepper seedling caused by *Colletotrichum coccodes* (Wallr.) Hughes. *Korean J. Mycol.* **1988**, *16*, 151–156.
12. Kim, K.-H.; Yoon, J.-B.; Park, H.-G.; Park, E.W.; Kim, Y.H.; Kim, J.-B.Y.K.-H.; Mongkolporn, O.; Taylor, P.W.J.; Yan, G.; Baidoo, R.; et al. Structural modifications and programmed cell death of chili pepper fruit related to resistance responses to *Colletotrichum gloeosporioides* infection. *Phytopathology* **2004**, *94*, 1295–1304. [CrossRef]
13. Kim, S.H.; Yoon, J.B.; Do, J.W.; Park, H.G. Resistance to anthracnose caused by *Colletotrichum acutatum* in chili pepper (*Capsicum annuum* L.). *J. Crop Sci. Biotechnol.* **2007**, *10*, 277–280.
14. Madhavan, S.; Paranidharan, V.; Velazhahan, R. RAPD and virulence analyses of *Colletotrichum capsici* isolates from chilli (*Capsicum annuum*). *J. Plant Dis. Prot.* **2010**, *117*, 253–257. [CrossRef]
15. Sun, C.; Mao, S.L.; Zhang, Z.H.; Palloix, A.; Wang, L.H.; Zhang, B.X. Resistances to anthracnose (*Colletotrichum acutatum*) of *Capsicum* mature green and ripe fruit are controlled by a major dominant cluster of QTLs on chromosome P5. *Sci. Hortic.* **2015**, *181*, 81–88. [CrossRef]
16. de Almeida, C.L.P.; Bento, C.D.S.; Sudré, C.P.; Pimenta, S.; Gonçalves, L.S.A.; Rodrigues, R. Genotype-Ideotype distance index and multivariate analysis to select sources of anthracnose resistance in *Capsicum* spp. *Eur. J. Plant Pathol.* **2019**, *156*, 223–236. [CrossRef]

17. Oo, M.M.; Oh, S.-K. First report of anthracnose of chili pepper fruit caused by *Colletotrichum truncatum* in Korea. *Plant Dis.* **2020**, *104*, 564. [CrossRef]
18. Mongkolporn, O.; Taylor, P.W.J. Chili anthracnose: *Colletotrichum* taxonomy and pathogenicity. *Plant Pathol.* **2018**, *67*, 1255–1263. [CrossRef]
19. Mongkolporn, O. Anthracnose disease in *Capsicum*. In *Capsicum: Breeding Strategies for Anthracnose Resistance*; CRC Press: Boca Raton, FL, USA, 2018; pp. 47–71.
20. Saxena, A.; Raghuvanshi, R.; Gupta, V.K.; Singh, H.B. Chilli anthracnose: The epidemiology and management. *Front. Microbiol.* **2016**, *7*, 1527. [CrossRef]
21. Pakdeevaporn, P.; Wasee, S.; Taylor, P.W.J.; Mongkolporn, O. Inheritance of resistance to anthracnose caused by *Colletotrichum capsici* in *Capsicum*. *Plant Breed.* **2005**, *124*, 206–208. [CrossRef]
22. Mahasuk, P.; Khumpeng, N.; Wasee, S.; Taylor, P.W.J.; Mongkolporn, O. Inheritance of resistance to anthracnose (*Colletotrichum capsici*) at seedling and fruiting stages in chili pepper (*Capsicum* spp.). *Plant Breed.* **2009**, *128*, 701–706. [CrossRef]
23. Marvel, J.K. Biology and control of pepper anthracnose. Ph.D. Thesis, Virginia Tech, Blacksburg, VA, USA, 2003.
24. Than, P.P.; Prihastuti, H.; Phoulivong, S.; Taylor, P.W.J.; Hyde, K.D. Chilli anthracnose disease caused by *Colletotrichum* species. *J. Zhejiang Univ. Sci. B* **2008**, *9*, 764–778. [CrossRef]
25. Voorrips, R.E.; Finkers, R.; Sanjaya, L.; Groenwold, R. QTL mapping of anthracnose (*Colletotrichum* spp.) resistance in a cross between *Capsicum annuum* and *C. chinense*. *Theor. Appl. Genet.* **2004**, *109*, 1275–1282. [CrossRef]
26. Kim, S.H.; Yoon, J.B.; Do, J.W.; Park, H.G. A major recessive gene associated with anthracnose resistance to *Colletotrichum capsici* in chili pepper (*Capsicum annuum* L.). *Breed. Sci.* **2008**, *58*, 137–141. [CrossRef]
27. Mongkolporn, O.; Taylor, P.W.J. *Capsicum*. In *Wild Crop Relatives: Genomic and Breeding Resources*; Kole, C., Ed.; Springer: Berlin/Heidelberg, Germany, 2011; pp. 43–57.
28. Mahasuk, P.; Taylor, P.W.J.; Mongkolporn, O. Identification of two new genes conferring resistance to *Colletotrichum acutatum* in *Capsicum baccatum* L. *Phytopathology* **2009**, *99*, 1100–1104. [CrossRef]
29. Lee, J.; Hong, J.-H.; Do, J.W.; Yoon, J.B. Identification of QTLs for resistance to anthracnose to two *Colletotrichum* species in pepper. *J. Crop. Sci. Biotechnol.* **2010**, *13*, 227–233. [CrossRef]
30. Kim, S.-G.; Ro, N.-Y.; Hur, O.-S.; Ko, H.-C.; Gwag, J.-G.; Huh, Y.-C. Evaluation of resistance to *Colletotrichum acutatum* in pepper genetic resources. *Res. Plant Dis.* **2012**, *18*, 93–100. [CrossRef]
31. Garg, R.; Kumar, S.; Kumar, R.; Loganathan, M.; Saha, S.; Kumar, S.; Rai, A.B.; Roy, B.K. Novel source of resistance and differential reactions on chilli fruit infected by *Colletotrichum capsici*. *Australas. Plant Pathol.* **2012**, *42*, 227–233. [CrossRef]
32. Yoon, J.; Park, H. Trispecies bridge crosses, (*Capsicum annuum* × *C. chinense*) × *C. baccatum*, as an alternative for introgression of anthracnose resistance from *C. baccatum* into *C. annuum*. *Hortic. Environ. Biotechnol.* **2005**, *46*, 5–9.
33. Kim, S.; Kim, K.T.; Yang, E.Y.; Cho, M.C.; Jamal, A.; Chae, Y.; Pae, D.H.; Hwang, J.K. Identification of quantitative trait loci associated with anthracnose resistance in chili pepper (*Capsicum* spp.). *Korean J. Hortic. Sci. Technol.* **2010**, *28*, 1014–1024.
34. Mahasuk, P.; Struss, D.; Mongkolporn, O. QTLs for resistance to anthracnose identified in two *Capsicum* sources. *Mol. Breed.* **2016**, *36*, 1–10. [CrossRef]
35. Chang, S.H.; Chung, B.K. Studies on the varietal resistance and effects of nutrients for fungal growth of pepper anthracnose disease caused by *Colletotrichum dematium* fsp. *capsicum*. *Korean J. Mycol.* **1985**, *13*, 227–233.
36. Souza, L.C.S.; Assis, L.A.G.; Catarino, A.D.M.; Hanada, R. Screening of chilli pepper genotypes against anthracnose (*Colletotrichum brevisporum*). *Emir. J. Food Agric.* **2020**, *31*, 919–929. [CrossRef]
37. De Silva, D.D.; Ades, P.K.; Crous, P.W.; Taylor, P.W.J. *Colletotrichum* species associated with chili anthracnose in Australia. *Plant Pathol.* **2017**, *66*, 254–267. [CrossRef]
38. Auyong, A.S.M.; Ford, R.; Taylor, P.W.J. The role of cutinase and its impact on pathogenicity of *Colletotrichum truncatum*. *J. Plant Pathol. Microbiol.* **2015**, *6*, 259. [CrossRef]
39. Angadi, H.D.; Naik, M.K.; Patil, M.G. Evaluation of chilli genotypes against anthracnose disease. *Veg. Sci.* **2003**, *30*, 164–165.
40. Vanan, T.; Khirbat, S.K.; Mehra, R. Reaction of detached fruits of chilli (*Capsicum annuum* L.) varieties to isolates of *Colletotrichum capsici* (Syd.) Butler and Bisby. *J. Spices Aromat. Crops.* **2005**, *14*, 145–147.
41. Giacomini, R.M.; Ruas, C.D.F.; Moreira, A.F.P.; Guidone, G.H.M.; Baba, V.Y.; Rodrigues, R.; Gonçalves, L.S.A. Inheritance of anthracnose resistance (*Colletotrichum scovillei*) in ripe and unripe *Capsicum annuum* fruits. *J. Phytopathol.* **2020**, *168*, 184–192. [CrossRef]
42. Kanchana-udomkan, C.; Taylor, P.W.J.; Mongkolporn, O. Development of a bioassay to study anthracnose infection of chili fruit caused by *Colletotrichum capsici*. *Thai J. Agric. Sci.* **2004**, *37*, 293–297.
43. Mahasuk, P.; Chinthaisong, J.; Mongkolporn, O. Differential resistances to anthracnose in *Capsicum baccatum* as responding to two *Colletotrichum* pathotypes and inoculation methods. *Breed. Sci.* **2013**, *63*, 333–338. [CrossRef]
44. Mongkolporn, O.; Montri, P.; Supakaew, T.; Taylor, P.W.J. Differential reactions on mature green and ripe chili fruit infected by three *Colletotrichum* spp. *Plant Dis.* **2010**, *94*, 306–310. [CrossRef]
45. Hasyim, A.; Setiawati, W.; Sutarya, R. Screening for resistance to anthracnose caused by *Colletotrichum acutatum* in chili pepper (*Capsicum annuum* L.) in Kediri, East Java. *Adv. Agric. Bot.* **2014**, *6*, 104–118.

46. Wasee, S.; Pongpisuttha, R.; Patarapuwadol, S.; Saridnirun, P.; Tangchitsomkid, N. Pepper (*Capsicum* spp.) germplasm management under Thailand conditions. In Proceedings of the SEAVEG 2012 High Value Vegetables in Southeast Asia: Production, Supply and Demand, Chiang Mai, Thailand, 24–26 January 2012; Volume 44.
47. Kim, S.H.; Yoon, J.B.; Park, H.G. Inheritance of anthracnose resistance in a new genetic resource, *Capsicum baccatum* PI594137. *J. Crop. Sci. Biotechnol.* **2008**, *11*, 13–16.
48. Silva, S.A.M.; Rodrigues, R.; Gonçalves, L.S.; Sudré, C.P.; Bento, C.S.; Carmo, M.G.; Medeiros, A.M. Resistance in *Capsicum* spp. to anthracnose affected by different stages of fruit development during pre- and post-harvest. *Trop. Plant Pathol.* **2014**, *39*, 335–341. [CrossRef]
49. Mishra, R.; Rout, E.; Joshi, R.K. Identification of resistant sources against anthracnose disease caused by *Colletotrichum truncatum* and *Colletotrichum gloeosporioides* in *Capsicum annuum* L. *Proc. Natl. Acad. Sci. India Sect. B Boil. Sci.* **2019**, *89*, 517–524. [CrossRef]
50. Mishra, R.; Mohanty, J.N.; Mahanty, B.; Joshi, R.K. A single transcript CRISPR/Cas9 mediated mutagenesis of *CaERF28* confers anthracnose resistance in chilli pepper (*Capsicum annuum* L.). *Planta* **2021**, *254*, 1–17. [CrossRef] [PubMed]
51. Prasath, D.; Ponnuswami, V.; Muralidharan, V. Source of resistance to anthracnose (*Colletotrichum capsici*) disease in *Capsicum* species. *Indian J. Agric. Sci.* **2007**, *77*, 473–474.
52. AVRDC. Genetic enhancement: Pepper unit. In *AVRDC Report 2004*; Kalb, T., Ed.; Asian Vegetable Research and Development Center: Shanhuah, Taiwan, 2004; pp. 41–66.
53. Cho, M.C.; Lin, S.W.; Shieh, S.C.; Suwor, P.; Kim, S.Y.; Techawongstien, S.; Kumar, S. Revisiting anthracnose-resistant *Capsicum* germplasm: Preliminary field evaluation. In *Breakthroughs in the Genetics and Breeding of Capsicum and Eggplant, Proceedings of the XV EUCARPIA Meeting on Genetics and Breeding of Capsicum and Eggplant, Torino, Italy, 2–4 September 2013*; Lanteri, S., Rotino, G.L., Eds.; Comitato per L'organizzazione degli Eventi (COE) DISAFA; Università degli Studi di Torino: Torino, Italy, 2013; pp. 363–366.
54. Hong, J.K.; Hwang, B.K. Influence of inoculum density, wetness duration, plant age, inoculation method, and cultivar resistance on infection of pepper plants by *Colletotrichum coccodes*. *Plant Dis.* **1998**, *82*, 1079–1083. [CrossRef]
55. Baba, V.Y.; Constantino, L.V.; Ivamoto-Suzuki, S.T.; Moreira, A.F.P.; Madeira, T.B.; Nixdorf, S.L.; Rodrigues, R.; Gonçalves, L.S.A. *Capsicum-Colletotrichum* interaction: Identification of resistance sources and quantification of secondary metabolites in unripe and ripe fruits in response to anthracnose infection. *Sci. Hortic.* **2019**, *246*, 469–477. [CrossRef]
56. AVRDC. Vegetables in cereal-based systems: Off-season tomato, pepper and eggplant. In *AVRDC Report 1998*; Stares, J., Ed.; Asian Vegetable Research and Development Center: Shanhuah, Taiwan, 1999; pp. 2–36.
57. Montri, P.; Taylor, P.W.J.; Mongkolporn, O. Pathotypes of *Colletotrichum capsici*, the causal agent of chili anthracnose, in Thailand. *Plant Dis.* **2009**, *93*, 17–20. [CrossRef]
58. Padilha, H.K.M.; Madruga, N.D.A.; Aranha, B.C.; Hoffmann, J.F.; Crizel, R.L.; Barbieri, R.L.; Chaves, F.C. Defense responses of *Capsicum* spp. genotypes to post-harvest *Colletotrichum* sp. inoculation. *Phytoparasitica* **2019**, *47*, 557–573. [CrossRef]
59. Park, H.K.; Kim, B.S.; Lee, W.S. Inheritance of resistance to anthracnose (*Colletotrichum* spp.) in pepper (*Capsicum annuum* L.). I. Genetic analysis of anthracnose resistance by diallel crosses. *J. Korean Soc. Hortic. Sci.* **1990**, *31*, 91–105.
60. Ahmed, N.; Dey, S.K.; Hundal, J.S. Inheritance of resistance to anthracnose in chilli. *Indian Phytopathol.* **1991**, *44*, 402–403.
61. Hirdaypal, S.; Jarnail, S.; Kaur, S. Resistant sources to fruit rot (*Colletotrichum capsici*) in pepper (*Capsicum annuum* L.). *J. Res. Punjab Agric. Univ.* **1990**, *27*, 419–420.
62. Henz, G.P.; Boiteux, L.S.; Lima, M.F. Reaction of *Capsicum* spp. fruits to *Colletotrichum gloeosporioides*. *Capsicum Eggplant Nwsl.* **1993**, *12*, 79–80.
63. AVRDC. Vegetables in cereal-based systems: Off-season tomato, pepper and eggplant. In *AVRDC Report 1999*; Koizumi, M., Abbass, D., Stares, J., Eds.; Asian Vegetable Research and Development Center: Shanhuah, Taiwan, 2000; pp. 2–36.
64. AVRDC. *Annual Report 2013*; AVRDC-The World Vegetable Center: Shanhuah, Taiwan, 2014; pp. 14–27.
65. Kaur, N.; Dhiman, J.S.; Khurana, D.S. Physiological and biochemical traits analysis of *Capsicum annuum* L. germplasm for resistance to *Colletotrichum capsici*. *J. Cell Plant Sci.* **2011**, *2*, 12–21.
66. Pereira, M.J.Z.; Junior, N.S.M.; Sussel, A.A.B.; Sala, F.C.; de Costa, C.P.; Boiteux, L.S. Reação de acessos de *Capsicum* e de progênies de cruzamentos interespecíficos a isolados de *Colletotrichum acutatum*. *Hortic. Bras.* **2011**, *29*, 569–576. [CrossRef]
67. Babu, B.S.; Pandravada, S.; Rao, R.P.; Anitha, K.; Chakrabarty, S.; Varaprasad, K. Global sources of pepper genetic resources against arthropods, nematodes and pathogens. *Crop. Prot.* **2011**, *30*, 389–400. [CrossRef]
68. Garg, R.; Loganathan, M.; Saha, S.; Roy, B.K. Chilli anthracnose: A review of causal organism, resistance source and mapping of gene. In *Microbial Diversity and Biotechnology in Food Security*; Kharwar, R., Upadhyay, R., Dubey, N., Raghuvanshi, R., Eds.; Springer: New Delhi, India, 2014; pp. 589–610.
69. Machenahalli, S.R.; Nargund, V.; Sridevi, O. Reaction of chilli genotypes against fruit rot complex. *Int. J. Life Sci.* **2016**, *11*, 715–719.
70. Maracahipes, C.; Taveira, G.B.; Mello, E.O.; Carvalho, A.O.; Rodrigues, R.; Perales, J.; Teixeira-Ferreira, A.; Silva, M.S.; Rocha, G.L.; Fernandes, K.V.S.; et al. Biochemical analysis of antimicrobial peptides in two different *Capsicum* genotypes after fruit infection by *Colletotrichum gloeosporioides*. *Biosci. Rep.* **2019**, *39*. [CrossRef]
71. Manzur, J.P.; Fita, A.; Prohens, J.; Rodríguez-Burruezo, A. Successful wide hybridization and introgression breeding in a diverse set of common peppers (*Capsicum annuum*) using different cultivated Ají (*C. baccatum*) accessions as donor parents. *PLoS ONE* **2015**, *10*, e0144142. [CrossRef]

72. Kethom, W.; Mongkolporn, O. New QTLs for anthracnose resistance identified in *Capsicum baccatum* 'PBC80'-derived recombinant inbred lines. *Euphytica* **2021**, *217*, 1–12. [CrossRef]
73. Lin, Q.; Kanchana-udomkan, C.; Jaunet, T.; Mongkolporn, O. Genetic analysis of resistance to pepper anthracnose caused by *Colletotrichum capsici*. *Thai J. Agric. Sci.* **2002**, *35*, 259–264.
74. Ridzuan, R.; Rafii, M.Y.; Ismail, S.I.; Yusoff, M.M.; Miah, G.; Usman, M. Breeding for anthracnose disease resistance in chili: Progress and prospects. *Int. J. Mol. Sci.* **2018**, *19*, 3122. [CrossRef]
75. Setiawati, W.; Udiarto, B.K.; Soetiarso, T.A. The effect of variety and planting system of chili pepper on incidence of whiteflies. *J. Hortic.* **2008**, *18*, 55–61.
76. Reddy, M.K.; Srivastava, A.; Kumar, S.; Kumar, R.; Chawda, N.; Ebert, A.W.; Vishwakarma, M. Chilli (*Capsicum annum* L.) breeding in India: An overview. *SABRAO J. Breed Genet.* **2014**, *46*, 160–173.
77. Garg, R. Genetics of Host Pathogen Interaction Resistance to Anthracnose in Chilli. Ph.D. Thesis, Banaras Hindu University, Uttar Pradesh, India, 2011.
78. Yoon, J.B.; Do, J.W.; Kim, S.H.; Park, H.G. Inheritance of anthracnose (*Colletotrichum acutatum*) resistance in *Capsicum* using interspecific hybridization. *Korean J. Agric. Sci.* **2009**, *27*, 140–144.
79. Chen, C.; Chen, H.; He, Y.; Xia, R. TBtools, a toolkit for biologists integrating various biological data handling tools with a user-friendly interface. *BioRxiv* **2018**, *1*, 289660.
80. Wang, Y.W. Development of Sequence Characterized Amplified Region (SCAR) Markers Associated with Pepper Anthracnose (*Colletotrichum acutatum*) Resistance. Master's Thesis, National Chiayi University, Chiayi, Taiwan, 2011.
81. Suwor, P.; Sanitchon, J.; Thummabenjapone, P.; Kumar, S.; Techawongstien, S. Inheritance analysis of anthracnose resistance and marker-assisted selection in introgression populations of chili (*Capsicum annum* L.). *Sci. Hortic.* **2017**, *220*, 20–26. [CrossRef]
82. Zhao, Y.; Liu, Y.; Zhang, Z.; Cao, Y.; Yu, H.; Ma, W.; Zhang, B.; Wang, R.; Gao, J.; Wang, L. Fine mapping of the major anthracnose resistance QTL AnRGO5 in *Capsicum chinense* 'PBC932'. *BMC Plant Biol.* **2020**, *20*, 189. [CrossRef]
83. Sun, C.Y.; Mao, S.L.; Zhang, Z.H. QTLs analysis of anthracnose (*Colletotrichum acutatum*) resistance in pepper (*Capsicum* spp.). In *Breakthroughs in the Genetics and Breeding of Capsicum and Eggplant, Proceedings of the XV EUCARPIA Meeting on Genetics and Breeding of Capsicum and Eggplant, Torino, Italy, 2–4 September 2013*; Lanteri, S., Rotino, G.L., Eds.; Comitato per L'organizzazione degli Eventi (COE) DISAFA; Università degli Studi di Torino: Torino, Italy, 2013; pp. 169–176.
84. Mongkolporn, O. Mapping genes conferring resistance to anthracnose (*Colletotrichum capsici*) and development of molecular markers for the selection of anthracnose resistance trait in chili. 2008; unpublished.
85. Hong, J.H.; Do, J.W.; Park, H.G. Species-Specific QTLs Associated with Anthracnose Resistance to Different *Colletotrichum* spp. in an Introgressed BC₁F₂ Population from *Capsicum annum* × *C. baccatum*. Master's Thesis, Seoul National University, Seoul, Republic of Korea, 2006.
86. Lee, J.; Do, J.W.; Yoon, J.B. Development of STS markers linked to the major QTLs for resistance to the pepper anthracnose caused by *Colletotrichum acutatum* and *C. capsici*. *Hortic. Environ. Biotechnol.* **2011**, *52*, 596–601. [CrossRef]
87. Voorrips, R.E. MapChart: Software for the graphical presentation of linkage maps and QTLs. *J. Hered.* **2002**, *93*, 77–78. [CrossRef] [PubMed]
88. Ranathunge, N.P.; Mongkolporn, O.; Ford, R.; Taylor, P.W.J. *Colletotrichum truncatum* pathosystem on *Capsicum* spp.: Infection, colonization and defence mechanisms. *Australas. Plant Pathol.* **2012**, *41*, 463–473. [CrossRef]
89. Mishra, R.; Nanda, S.; Rout, E.; Chand, S.K.; Mohanty, J.N.; Joshi, R.K. Differential expression of defense-related genes in chilli pepper infected with anthracnose pathogen *Colletotrichum truncatum*. *Physiol. Mol. Plant Pathol.* **2017**, *97*, 1–10. [CrossRef]
90. Soh, H.C.; Park, A.R.; Park, S.; Back, K.; Yoon, J.B.; Park, H.G.; Kim, Y.S. Comparative analysis of pathogenesis-related protein 10 (PR10) genes between fungal resistant and susceptible peppers. *Eur. J. Plant Pathol.* **2011**, *132*, 37–48. [CrossRef]
91. Oh, B.-J.; Ko, M.K.; Kostenyuk, I.; Shin, B.; Kim, K.S. Coexpression of a defensin gene and a thionin-like gene via different signal transduction pathways in pepper and *Colletotrichum gloeosporioides* interactions. *Plant Mol. Biol.* **1999**, *41*, 313–319. [CrossRef]
92. Oh, B.-J.; Ko, M.-K.; Kim, K.S.; Kim, Y.S.; Lee, H.H.; Jeon, W.B.; Im, K.H. Isolation of defense-related genes differentially expressed in the resistance interaction between pepper fruits and the anthracnose fungus *Colletotrichum gloeosporioides*. *Mol. Cells* **2003**, *15*, 349–355.
93. Ko, M.K.; Jeon, W.B.; Kim, K.S.; Lee, H.H.; Seo, H.H.; Kim, Y.S.; Oh, B.-J. A *Colletotrichum gloeosporioides*-induced esterase gene of nonclimacteric pepper (*Capsicum annum*) fruit during ripening plays a role in resistance against fungal infection. *Plant Mol. Biol.* **2005**, *58*, 529–541. [CrossRef]
94. Lee, S.; Hong, J.-C.; Jeon, W.B.; Chung, Y.-S.; Sung, S.; Choi, D.; Joung, Y.H.; Oh, B.-J. The salicylic acid-induced protection of non-climacteric unripe pepper fruit against *Colletotrichum gloeosporioides* is similar to the resistance of ripe fruit. *Plant Cell Rep.* **2009**, *28*, 1573–1580. [CrossRef]
95. Lee, S.; Hwang, B. Identification of the pepper SAR8.2 gene as a molecular marker for pathogen infection, abiotic elicitors and environmental stresses in *Capsicum annum*. *Planta* **2003**, *216*, 387–396. [CrossRef]
96. Yi, G.; Lee, J.M.; Lee, S.; Choi, D.; Kim, B.-D. Exploitation of pepper EST-SSRs and an SSR-based linkage map. *Theor. Appl. Genet.* **2006**, *114*, 113–130. [CrossRef]
97. Portis, E.; Nagy, I.; Sasvári, Z.; Stágel, A.; Barchi, L.; Lanteri, S. The design of *Capsicum* spp. SSR assays via analysis of in silico DNA sequence, and their potential utility for genetic mapping. *Plant Sci.* **2007**, *172*, 640–648. [CrossRef]
98. Minamiyama, Y.; Tsuru, M.; Hirai, M. An SSR-based linkage map of *Capsicum annum*. *Mol. Breed.* **2006**, *18*, 157–169. [CrossRef]

99. Lee, J.M.; Nahm, S.H.; Kim, Y.M.; Kim, B.D. Characterization and molecular genetic mapping of microsatellite loci in pepper. *Theor. Appl. Genet.* **2003**, *108*, 619–627. [CrossRef]
100. Li, G.; Quiros, C.F. Sequence-related amplified polymorphism (SRAP), a new marker system based on a simple PCR reaction: Its application to mapping and gene tagging in *Brassica*. *Theor. Appl. Genet.* **2001**, *103*, 455–461. [CrossRef]
101. Kim, Y.S.; Park, J.Y.; Kim, K.S.; Ko, M.K.; Cheong, S.J.; Oh, B.-J. A thaumatin-like gene in nonclimacteric pepper fruits used as molecular marker in probing disease resistance, ripening, and sugar accumulation. *Plant Mol. Biol.* **2002**, *49*, 125–135. [CrossRef] [PubMed]
102. Seo, H.H.; Park, S.; Park, S.; Oh, B.J.; Back, K.; Han, O.; Kim, J.; Kim, Y.S. Overexpression of a defensin enhances resistance to a fruit-specific anthracnose fungus in pepper. *PLoS ONE* **2014**, *21*, e97936. [CrossRef] [PubMed]
103. Park, S.; Kim, S.H.; Park, H.G.; Yoon, J.B. *Capsicum* germplasm resistant to pepper anthracnose differentially interact with *Colletotrichum* isolates. *Hortic. Environ. Biotechnol.* **2009**, *50*, 17–23.

Disclaimer/Publisher’s Note: The statements, opinions and data contained in all publications are solely those of the individual author(s) and contributor(s) and not of MDPI and/or the editor(s). MDPI and/or the editor(s) disclaim responsibility for any injury to people or property resulting from any ideas, methods, instructions or products referred to in the content.



Article

Identification of Two Novel Loci Underlying Tolerance to *Clavibacter michiganensis* Originating from *Solanum arcanum* LA2157

Eleni Koseoglou^{1,2}, Matthijs Brouwer¹, Derek Mudadirwa¹, Jan M. Van der Wolf³, Richard G. F. Visser^{1,*} and Yuling Bai¹

- ¹ Plant Breeding, Wageningen University & Research, 6708 WG Wageningen, The Netherlands; eleni.koseoglou@wur.nl (E.K.); matthijs.brouwer@wur.nl (M.B.); derekmudadirwa@gmail.com (D.M.); bai.yuling@wur.nl (Y.B.)
- ² Graduate School Experimental Plant Sciences, Wageningen University & Research, 6708 WG Wageningen, The Netherlands
- ³ Biointeractions & Plant Health, Wageningen University & Research, 6708 WG Wageningen, The Netherlands; jan.vanderwolf@wur.nl
- * Correspondence: richard.visser@wur.nl

Abstract: *Clavibacter michiganensis* (*Cm*) is a tomato phytopathogenic bacterium. Outbreaks of *Cm* can result in severe yield and economic losses. To date, no resistance to *Cm* has been identified. Screening of wild tomato accessions has resulted in the identification of several sources of tolerance to *Cm*. The genetic background of tolerance provided by these sources is polygenic and complex. Previous results from advanced lines of a cross between *Solanum arcanum* LA2157 and *S. lycopersicum* showed that introgression lines carrying a locus of *S. arcanum* LA2157 on chromosome 7 had high levels of tolerance to *Cm*. We set out to functionally characterize this locus, in an effort to identify the gene(s) underlying the observed tolerance. Testing of near isogenic lines (NILs) containing a fixed LA2157 introgression on chromosome 7 did not lead to the expected results, as high susceptibility was observed in some NILs homozygous for the *S. arcanum* LA2157 allele. Therefore, we employed whole genome sequencing in combination with a bulk segregant analysis to identify loci involved in the observed tolerant phenotype. Our results suggest that two additional loci on chromosomes 2 and 4 together with the locus on chromosome 7 are required for tolerance to *Cm*.

Keywords: tomato bacterial canker; tolerance; quantitative trait loci (QTL); bulk segregant analysis; k-mer analysis

Citation: Koseoglou, E.; Brouwer, M.; Mudadirwa, D.; Van der Wolf, J.M.; Visser, R.G.F.; Bai, Y. Identification of Two Novel Loci Underlying Tolerance to *Clavibacter michiganensis* Originating from *Solanum arcanum* LA2157. *Agronomy* **2023**, *13*, 953. <https://doi.org/10.3390/agronomy13040953>

Academic Editor: José David Flores-Félix

Received: 7 February 2023
Revised: 20 March 2023
Accepted: 21 March 2023
Published: 23 March 2023



Copyright: © 2023 by the authors. Licensee MDPI, Basel, Switzerland. This article is an open access article distributed under the terms and conditions of the Creative Commons Attribution (CC BY) license (<https://creativecommons.org/licenses/by/4.0/>).

1. Introduction

Resistance and tolerance represent the two major mechanisms of plant defences to pathogens [1]. Even though both resistance and tolerance result in the survival and reproduction of the host, the two mechanisms act in distinct ways [2]. Resistance acts by limiting the multiplication of the pathogen, while tolerance aims at the reduction of the effects of infection regardless of the pathogen population size [1,2].

The gram-positive phytopathogenic bacterium *Clavibacter michiganensis* (*Cm*) is responsible for bacterial canker of tomato (*Solanum lycopersicum*), one of the most destructive diseases of cultivated tomato [3,4]. The spread of the pathogen over long distances is primarily facilitated by contaminated seeds, while cultural practices can lead to a rapid spread of the pathogen in infected crops, resulting in severe disease outbreaks [5–8].

Cm colonizes the vasculature of tomato plants, leading to systemic infections. Severity of the disease depends on several factors, including the route of infection, environmental conditions, the tomato genotype, the developmental stage of the plant at the time of infection, and the virulence of the infecting strain [8–11]. The most commonly observed symptoms of the disease are wilting of leaves and leaflets, cankers on the stems and petioles

of infected plants, as well as discoloration and necrosis of the xylem [3,4]. Localized infections of tomato fruits can lead to the development of necrotic spots, known as bird's eye spots, while local infections of aerial parts can result in marginal leaf necrosis and white blister-like spots on the stems and leaves of plants [12,13]. Control of the pathogen is currently limited to the "good seed and plant practice" (GSPP) protocol, which aims at decreasing the risks of introduction and spread of the pathogen [14]. Chemical and biological agents for the control of *Cm* do not provide satisfactory levels of protection, while resistance to the pathogen has yet to be identified.

Early studies claimed several sources of resistance to the pathogen. Nevertheless, bacterial titres of the infected plants in these early studies were not assessed. Recent research that included the quantification of bacterial populations in wild accessions has only reported sources of tolerance. Based on these recent results, we cannot definitely conclude that the reported resistance was indeed resistance and not merely tolerance. For the purposes of this manuscript, we will refer to resistance and tolerance based on the terminology used in the original papers.

In most cases, the reported resistance conferred by wild accessions was found to be polygenic and complex (Table 1). An (unreported) accession of *Solanum pimpinellifolium*, which was used for the development of line "Bulgaria 12" (or PI 330727), was the first wild species reported to be resistant to *Cm* [15]. In other *S. pimpinellifolium* accessions, A129 and A134, several loci (ranged from four to 11) with additive effects were reported for the resistance observed in *S. pimpinellifolium*. However, no map positions of these loci were reported [15]. *S. habrochaites* LA407 is one of the most well-described sources conferring resistance to *Cm*. Initial genetic studies in crosses of *S. habrochaites* LA407 with *S. lycopersicum* resulted in one to three genetic loci linked to tolerance to *Cm* derived from *S. habrochaites* LA407 [16]. Further studies of the crosses resulted in the mapping of two QTLs on chromosomes 2 and 5 with an epistatic effect [17,18].

The polygenic nature of resistance to *Cm* was further demonstrated between inter- and intraspecific crosses of *S. arcanum* and *S. lycopersicum* [11,19,20]. The interspecific cross between *S. arcanum* LA2157 and *S. lycopersicum* cv. Solentos yielded three resistance quantitative trait loci (QTLs) located on tomato chromosomes 5, 7 and 9. The three QTLs were found to be additive, with the QTL on chromosome 7 having the biggest contribution to resistance [19]. Further fine-mapping of backcrosses between *S. arcanum* LA2157 and *S. lycopersicum* cv. MoneyMaker (MM) reduced the size of the previously identified QTLs on chromosomes 5 and 7. In addition, two novel QTLs on tomato chromosomes 6 and 11 were identified [21]. Subsequent fine-mapping of the QTL on chromosome 7 concluded that a single ~211 kb introgression on chromosome 7 is enough to confer high tolerance to *Cm*. Based on the tomato reference genome, 15 genes were reported to be present on the ~211 kb introgression [22]. Finally, an intraspecific backcross population between the resistant *S. arcanum* LA2157 and susceptible *S. arcanum* LA2172 resulted in the identification of five QTLs on chromosomes 1, 6, 7, 8 and 10 of tomato [20]. In parallel to the fine-mapping of the backcrosses between *S. arcanum* LA2157 and *S. lycopersicum* cv. MM, bacterial enumeration in these crosses concluded that the bacterial titres were not different from the susceptible parent [21]. Therefore, the observed lack of symptoms was due to tolerance, rather than the previously reported resistance.

In contrast to most studies reporting multiple loci involved in resistance/tolerance to *Cm*, a dominant locus derived from *S. arcanum* var. *humifusum* linked to resistance has been reported on chromosome 4 of tomato [23]. Even though it was suggested that a single dominant gene was responsible for the observed resistance, the authors concluded that the resistance level was dependent on the presence of other modifier genes. Therefore, in our view, this source should also be considered as polygenic.

In an effort to identify novel sources of tomato resistance to *Cm*, 24 wild species were screened in our laboratory (Plant Breeding, WUR). The screen led to the report of three previously undescribed highly tolerant accessions, namely *S. pimpinellifolium* G1.1554, *S. neorickii* LA735 and *S. neorickii* LA2072 [11]. Further mapping studies of recombinant

inbred lines (RILs) derived from crosses between *S. pimpinellifolium* Gl.1554 and cv. MM, resulted in the identification of five QTLs on tomato chromosomes 1, 2, 7, 8, and 12. The QTL on chromosome 7 was found to have a major contribution to the observed tolerance [24].

Table 1. Overview of loci associated with tolerance to *Cm* derived from wild accessions.

| Tolerance Source | Susceptible Parent | Population | Tolerance/Resistance Type | Reference |
|---|---|--|---|-----------|
| <i>S. habrochaites</i> LA407 | <i>S. lycopersicum</i> cv. Ohio 86120 | F ₂ | QTLs Rcm 2.0 on chromosome 2 (Chr2) and Rcm 5.1 on Chr5 | [13] |
| <i>S. arcanum</i> LA2157 | <i>S. lycopersicum</i> cv. Solentos | F ₂ | QTLs on Chr5, Chr7 and Chr9 | [19] |
| <i>S. arcanum</i> LA2157 | <i>S. lycopersicum</i> cv. MM | Recombinant inbred lines (RILs) | QTLs on Chr5, Chr7, Chr6 and, Chr11 | [21] |
| <i>S. arcanum</i> LA2157 | <i>S. lycopersicum</i> cv. MM | Recombinant inbred lines (RILs) | ~211 kb introgression on Chr7 | [22] |
| <i>S. pimpinellifolium</i> Gl. 1554 | <i>S. lycopersicum</i> cv. MM | Recombinant inbred lines (RILs) | QTLs on Chr1, Chr2, Chr7, Chr8, and Chr12 | [24] |
| <i>S. arcanum</i> LA2157 | <i>S. arcanum</i> LA2172 | Backcross (BC) of intraspecific cross | QTLs on Chr1, Chr6, Chr7, Chr8, and Chr10 | [20] |
| <i>S. arcanum</i> var. <i>humifusum</i> | <i>S. lycopersicum</i> × <i>S. chilense</i> LA460 | F ₂ BC population of three genome hybrid <i>S. lycopersicum</i> line Cm 180 | Dominant gene on Chr4 (with modifier genes) | [23] |

In this study, we aimed to functionally characterize the 15 genes previously reported to be present on the ~211 kb LA2157 introgression, with the intention of identifying the gene(s) underlying the observed tolerance [22]. We used a BC₃S₆ line and its selfing with a fixed introgression on chromosome 7. Surprisingly, during our disease assays, we could not confirm the results previously reported. Therefore, we employed marker analysis as well as whole genome sequencing in combination with bulk segregant analysis (BSA) to identify loci involved in the observed tolerant phenotypes.

2. Materials and Methods

2.1. Plant Materials

In this study, we used an BC₃S₆ near isogenic line (NIL) PV175136 and its selfing PV185517. The material was developed from the original F₂ population between the tolerant accession *Solanum arcanum* LA2157 and the susceptible *Solanum lycopersicum* cv. Solentos [19]. Shortly, progeny containing the identified QTLs described by van Heusden et al. [19] were backcrossed to *Solanum lycopersicum* cv. Moneymaker (cv. MM) to obtain BC₃S₆ NILs. Selfing of BC₃S₆ NIL PV175136 gave rise to PV185571, which was used in this study. The susceptible cv. MM was used as a control.

2.2. Bacterial Strains and Growth Conditions

Cm strain NCPBB382 was used in the bioassays. Prior to plant inoculation, the strain was grown at 25 °C on TBY plates (10 g L⁻¹ tryptone, 5 g L⁻¹ yeast extract, 5 g L⁻¹ sodium chloride, 15 g L⁻¹ bacteriological agar) for two days. For the preparation of the inoculum, bacterial cells were resuspended in Ringer's buffer to a final concentration of ~10⁸ cfu/mL (OD₆₀₀ = 0.1).

2.3. Disease Assays

Tomato plants at the fourth true leaf stage were inoculated using a petiole clipping off method. The petioles of the first two fully expanded leaves were clipped off with razor blades immersed in the bacterial inoculum, and 5 µL of the bacterial inoculum was directly pipetted on the lowest wound created on the stem. For the first experiment, 27 plants (*n* = 27) from line PV175136 were inoculated. In the next two subsequent experiments, 54 (*n* = 54) and 73 (*n* = 73) plants from line PV185517 were used in the experiments, respectively.

Symptom development was monitored for up to 20 days post inoculation (dpi). A disease index (DI) scale based on the development of wilting symptoms on the leaves was used

(0; no symptoms, 1; one leaf wilting, 2; <2/3 of leaves wilting, 3; 2/3 of leaves wilting, 4; 3/4 of leaves wilting, 5; all leaves wilting). A threshold of 2.5 was used to categorize plants as tolerant < 2.5 or susceptible \geq 2.5, as at this value, more than half of the leaves were scored as wilting.

2.4. Development of Cleaved Amplified Polymorphic Sequences (CAPS) Markers

In previous research, it was described that NIL PV175136 contained a fixed 697 kb introgression on chromosome 7 [22]. To confirm the introgression size on chromosome 7, six in-gene CAPS markers flanking the reported introgression region (physical position SOL07-1060331 to SOL07-1784948) were designed. Genes in the region were mined from the available annotated ITAG3.2 genes on Jbrowser. Single nucleotide polymorphisms (SNPs) between *S. arcanum* LA2157 and *S. lycopersicum* cv. MM were identified, based on the *de novo* genome sequence of *S. arcanum* LA2157 [25] and the tomato genome ITAG 2.4 (SolGenomics). Polymorphic CAPS markers were developed based on the identified SNPs.

2.5. Genomic DNA Isolation and Genotypic

Genomic DNA (gDNA) was isolated from cotyledons of young tomato plants using a modified cetyl trimethylammonium bromide (CTAB) extraction method [26]. Gene specific primers were designed for the amplification of the allelic variants. Following amplification, the amplification products were incubated with the appropriate restriction enzyme at 37 °C overnight. The digested products were visualized on 2% agarose gel for the detection of the alleles present in each sample.

2.6. DNA Isolation and Pooling

Whole-genome sequencing (WGS) of a susceptible and a resistant pool of 14 plants, each was performed to identify loci involved in the observed phenotypes. Genomic DNA of plants was extracted from leaves that were flash frozen in liquid nitrogen and stored at -80 °C, using a modified (CTAB) extraction method [26]. DNA concentration of each sample was assessed using a Qubit Fluorometer (Invitrogen). Samples were cleaned with the Genomic DNA & Concentrator™-10 (Zymo Research). For each bulk, 28.57 ng of gDNA of each individual was pooled. For the WGS experiment, 400 ng of (pooled) gDNA were used for the library preparation and sequencing. Sequencing was performed on an Illumina Novaseq 6000 platform producing 151 bp paired end reads at a $35 \times$ depth (Novogene Europe, Cambridge, UK).

2.7. Comparative Subsequence Sets Analysis (CoSSA)

A modified version of the CoSSA workflow was used for the identification of bulk-specific k-mers [27].

Using the KMC software package, k-mer databases with $k = 31$ and a minimum frequency of 2 were constructed from the susceptible and the resistant set of reads. Using the total number of k-mers in these databases, assuming the k-mer frequency to be Poisson distributed and estimating the total genome size to be 950 Mb, the rate parameter was estimated for both the susceptible and resistant set. From the two k-mer sets, two other databases were derived: all k-mers from the resistant set that were not in the susceptible set, and all k-mers from the susceptible set were not included in the resistant set. Then, these two new databases with uniquely resistant and uniquely susceptible k-mers were filtered to only k-mers with frequencies within the confidence interval of 99.9% for ploidy 1 or 2. These intervals were computed with the previously derived Poisson distributions. For each bulk, using the filtered k-mer database, all reads containing at least 15 (half the k-mer size) k-mers were selected. The two sets of selected reads were mapped against tomato reference genome SL4.0, just as both full sets of reads. For both the filtered and full sets of reads, coverage was computed using a bin equal to the k-mer size. As for the k-mer databases, rate parameters for the assumed Poisson distributions from the read depths were estimated. Using these distributions, for each bulk, the coverage bins were

filtered to have both a total and selected read coverage within the confidence interval of 99.9% for ploidy 1 or 2. Because either 50% or 100% of the reads in each bin is expected to be selected, with the assumed underlying binominal distribution, a confidence boundary of 99.9% for the coverage fraction not to correspond with 25% of the total coverage was computed and applied. Finally, the selected bins were required to be covered by at least 10 uniquely mapped selected k-mers. This resulted in the filtered coverage of the 12 tomato chromosomes for both the R- and S-bulks.

2.8. Protein-Protein Interaction Network Prediction

For the prediction of potential protein-protein interactions between the two newly mapped loci on chromosomes 2 and 4 of tomato and the 15 mapped genes on the QTL on chromosome 7, we used the reference sequences of genes *Solyc02g084740.4* and *Solyc04g081190.3* as queries on the STRING database for functional protein association networks (<https://string-db.org/>, accessed 12 July 2022) using the default settings.

2.9. Protein Prediction of *S. arcanum* LA2157 Alleles

To predict the protein sequences produced by the *S. arcanum* LA2157 allelic variants, the coding sequence (CDS) of the genes was predicted based on the CDS of the *S. lycopersicum* allele. The CDS was then used on the expasy translate tool (<https://web.expasy.org/translate/>, accessed 12 July 2022) to predict the open reading frames and the protein sequences. The default settings were used in the prediction of the proteins.

3. Results

3.1. Phenotypic and Genotypic Evaluation of Lines PV175136 and PV185517

In an effort to confirm previous results, we used the line PV175136 and its selfing PV185517 derived from an initial cross between *S. arcanum* LA2157 and *S. lycopersicum* cv. Solentos, which carry the QTL on chromosome 7 homozygously and were tolerant to *Cm* [22].

To monitor the presence of the LA2157 introgression on chromosome 7, we developed cleaved amplified polymorphic sequence (CAPS) markers (Q7M1 to Q7M9, Supplementary Table S1) flanking the previously reported QTL region [22]. Marker analysis confirmed that these two lines are homozygous for the expected 697 kb introgression (physical position; SOL07-1060331 to SOL07-1784948) from *S. arcanum* LA2157 (Table 2).

Table 2. CAPS markers analysis of the QTL on chromosome 7 in line PV175136. In the table, a number of plants with segregating phenotypes is given. A = homozygous for *S. arcanum* LA2157 allele, M = homozygous for *S. lycopersicum* cv. MM, S = susceptible, T = tolerant.

| PV175136 Line | Q7M1 | Q7M7 | Q7M2 | Q7M3 | Q7M4 | Q7M5 | Q7M9 | Disease Index | Phenotype |
|---------------|------|------|------|------|------|------|------|---------------|-----------|
| PV175136_5 | M | A | A | A | A | M | M | 4 | S |
| PV175136_13 | M | A | A | A | A | M | M | 5 | S |
| PV175136_20 | M | A | A | A | A | M | M | 2.5 | S |
| PV175136_29 | M | A | A | A | A | M | M | 0 | T |
| PV175136_4 | M | A | A | A | A | M | M | 0.25 | T |
| PV175136_27 | M | A | A | A | A | M | M | 0.25 | T |

In our first experiment, the PV175136 line was inoculated with *Cm*. On average, a significant reduction of wilting symptoms was observed in family PV175136 compared to the susceptible control cv. MM at 20 dpi. However, we also recorded two plants that were highly susceptible ($DI \geq 2.5$) in the PV175136 line (Figure 1).

To confirm these results, we decided to repeat the bioassays on a line derived from the selfing of PV175136-8. Prior to the infection of the plants, we confirmed that the PV185517 line carried the introgression on chromosome 7 homozygously (Table 3). Two independent experiments were performed with line PV185517. Our results were in accordance with what we previously observed for line PV175136. On average, the symptom development of line PV185517 was significantly lower than the susceptible cv. MM at 20 dpi (Figure 2a,b).

Nevertheless, we observed both highly tolerant ($0 \leq DI < 2.5$) and highly susceptible ($2.5 \leq DI \leq 5$) plants in the PV185517 family (Figure 2c,d).

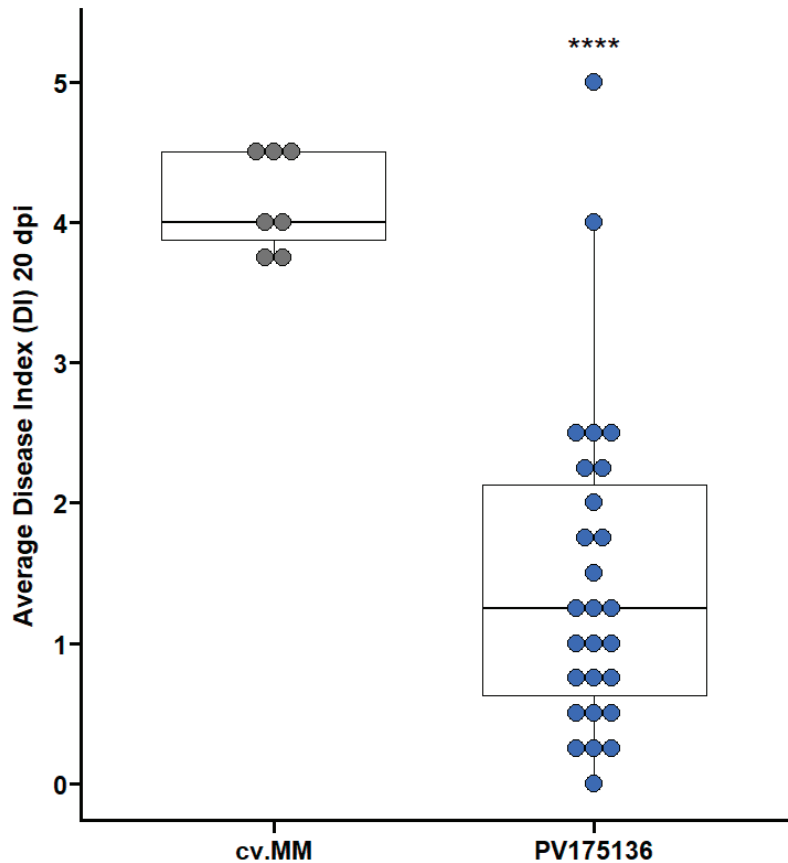


Figure 1. Phenotypic evaluation of line PV175136. Average disease index (DI) of the introgression line PV175136 and the susceptible background cv. MM at 20 days after inoculation with *Clavibacter michiganensis* NCPBB382. Centre lines indicate medians; the box limits indicate the 25th and 75th percentiles. (Student's *t*-test, **** $p \leq 0.00$).

Table 3. CAPS markers analysis of the QTL on chromosome 7 in line PV185517. In the table, a number of plants with segregating phenotypes is given. A = homozygous for *S. arcanum* LA2157 allele, M = homozygous for *S. lycopersicum* cv. MM, S = susceptible, T = tolerant.

| PV185517 Line | Q7M1 | Q7M7 | Q7M2 | Q7M3 | Q7M4 | Q7M5 | Q7M9 | Disease Index | Phenotype |
|---------------|------|------|------|------|------|------|------|---------------|-----------|
| PV185517_14 | M | A | A | A | A | M | M | 5 | S |
| PV185517_18 | M | A | A | A | A | M | M | 3.75 | S |
| PV185517_31 | M | A | A | A | A | M | M | 5 | S |
| PV185517_37 | M | A | A | A | A | M | M | 0 | T |
| PV185517_39 | M | A | A | A | A | M | M | 0 | T |
| PV185517_40 | M | A | A | A | A | M | M | 0 | T |

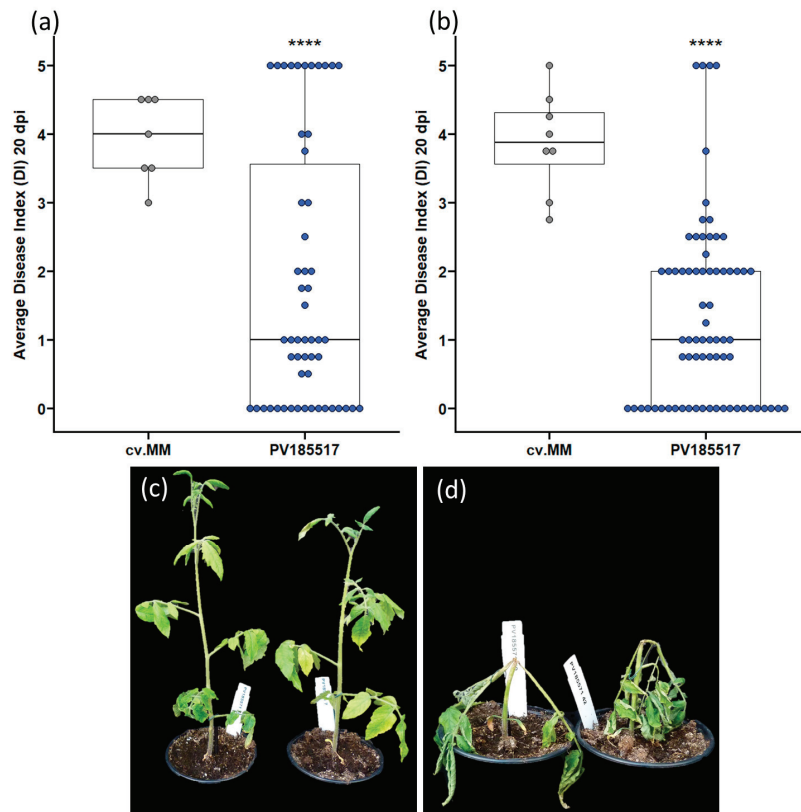


Figure 2. Phenotypic evaluation of line PV185517. (a,b) Average disease index (DI) of introgression line PV185517 and the susceptible background cv. MM at 20 days after inoculation with *Clavibacter michiganensis* NCPBB382. (a,b) represent two independent experiments. Phenotype of (c) tolerant plants and (d) susceptible plants in the PV185517 family. Centre lines indicate medians; the box limits indicate the 25th and 75th percentiles. (Student's *t*-test, **** $p \leq 0.00$).

3.2. Additional QTLs on Chromosomes 5 and 9 Do Not Contribute to the Observed Tolerance

Since susceptible plants were observed in these two homozygous introgression lines, we speculated that another previously reported QTL from the initial cross, on either chromosome 5 or chromosome 9, was still segregating in the tested line [21]. To investigate this possibility, markers were run along the previously described genomic regions on chromosomes 5 (physical position; 39,792,518 ... 61,792,631) and 9 (physical position; 52,411 ... 4,698,709). Eight markers were run along each region on chromosomes 5 and 9. Only one single nucleotide polymorphism (SNP) (52533C > G) was identified between cv. MM and line PV185517. However, no segregation of the SNP was found between the plants of line PV185517, suggesting that this SNP was not responsible for the observed phenotypic segregation in the line.

3.3. Tolerance to *Cm* Requires QTL7 in Combination with Two Additional Loci on Chromosomes 2 and 4

To identify sequence variants linked to *Cm* tolerance in the PV185517 family, we combined whole genome sequencing (WGS) with bulk segregant analysis (BSA). We selected 14 fully resistant and 14 susceptible plants of PV185517 from the two independent experiments to compose the resistant bulk (R-bulk) and the susceptible bulk (S-bulk), respectively. Two higher peaks with different k-mer frequencies were observed for the R-bulk, one

between positions 43,262,484 . . . 48,143,527 (6.98 Mb) on tomato chromosome 2, and the other between positions 63,165,755 . . . 63,767,930 (602 kb) on chromosome 4 (Figure 3). Several lower k-mer peaks were observed on other genomic regions (Figure 3). These lower k-mer peaks could be mapped due to lack of coverage in the S bulk, a hypothesis that still requires validation. On the mapped loci on chromosomes 2 and 4, only two genes contained k-mers that were specific to the R-bulk (Supplementary Table S2). These were genes *Solyc02g084740.4* coding for cytochrome P450/CYP90C1 and *Solyc04g081190.3* encoding vsf-1 on tomato chromosomes 2 and 4, respectively. Allele frequencies in the R-bulk for genes *Solyc02g084740.4* and *Solyc04g081190.3* were estimated to be 0.57 and 0.6, respectively. Further inspection of the sequencing data revealed that both sequences of the genes mapped on the R-bulk were identical to the *S. arcanum* LA2157 allele. Several S-bulk specific k-mers were also linked to genes specifically present in the S-bulk (Supplementary Table S3). Further analysis of the sequencing data revealed that the S-bulk specific k-mers were identical to the susceptible cv. MM sequences.

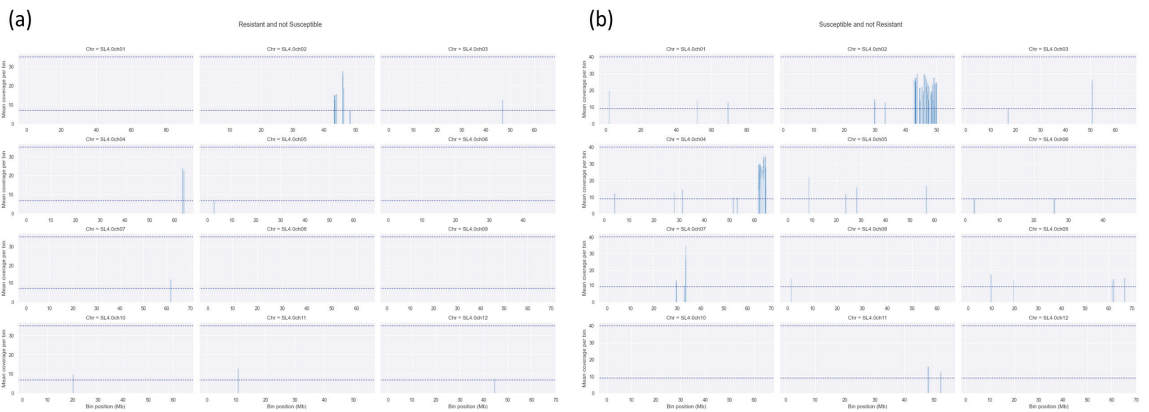


Figure 3. Loci linked to tolerance and susceptibility to *Cm* mapped on chromosomes 2 and 4 of tomato. Density graphs of unique k-mers mapped to bins equal to k-mer size on the tomato (*S. lycopersicum*) reference genome ITAG 4.0. (a) Blue vertical lines indicate loci associated with tolerance, (b) blue vertical lined indicate loci associated with susceptibility.

3.4. Changes in the Amino Acid Sequence of Produced by the *S. arcanum* LA2157 Allelic Variant Lead to Changed Proteins

To detect for potential protein interactions between our new mapped genes on chromosomes 2 and 4 and the 15 genes mapped on QTL on chromosome 7 (Supplementary Table S4), we searched the STRING database for functional protein association networks. No interactions were detected on the database. The database, however, only allowed for the use of the sequences of the *S. lycopersicum* reference genome. We therefore decided to predict the protein sequences encoded by the *S. arcanum* LA2157 alleles and detect amino acid substitutions that could potentially result in changed protein-protein interactions. Alignment of the predicted *S. arcanum* LA2157 and the *S. lycopersicum* CYP90C1 (*Solyc02g084740.4*) proteins revealed a premature stop codon, leading to protein truncation and potential loss-of-function of the *S. arcanum* LA2157 protein. In addition, five amino acid changes were detected between the protein sequences. Of the five amino acid changes we predicted two which lead to changes in the amino acids charge. The pL167Q change results in a non-polar to polar amino acid substitution, whereas the pK255I substitution results in from a positively charged amino acid to a non-polar one (Figure 4).



Figure 4. Alignment of the *S. lycopersicum* CYP90C1 protein against the predicted protein of the *S. arcanum* LA2157 allelic variant. Amino acids in red indicate changes between the two proteins.

After alignment of the predicted *S. arcanum* LA2157 and the *S. lycopersicum* vsf-1 (*Solyc04g081190.3*) proteins, we detected 8 amino acid changes between the protein sequences (Figure 5).

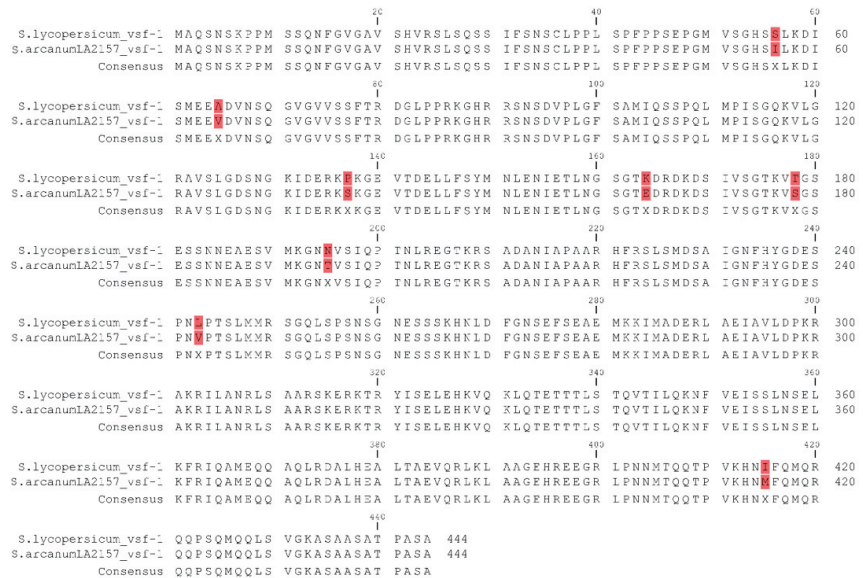


Figure 5. Alignment of the *S. lycopersicum* vsf-1 protein against the predicted protein of the *S. arcanum* LA2157 allelic variant. Amino acids in red indicate changes between the two proteins.

Of the eight amino acid changes we predicted in the *S. arcanum* LA2157 protein, three were predicted to result in changes in the amino acid charge. The p.S56I change results in a polar to non-polar amino acid substitution. The p.P137S substitution results in a non-polar to polar amino acid change, while the p.K164E substitution results in a change from a basic to an acidic amino acid.

4. Discussion

Wild *Solanum* species harbour genetic diversity that can be used as a valuable source of disease resistance. Screenings of wild tomato accessions have resulted in the identification of several sources of tolerance to *Cm* [11,17,19,24]. Loci or markers closely linked to tolerance to *Cm* have been mapped on most of the tomato chromosomes (Figure 6). Colocalization of QTLs between studies have been reported for the QTLs mapped from crosses between *S. arcanum* LA2157 and *S. lycopersicum* [19,21,22]. Of the mapped QTLs, introgressions derived from *S. arcanum* LA2157 and *S. pimpinellifolium* GI. 1554 on chromosome 7 of tomato have been reported to have a major effect in tolerance [19,21].

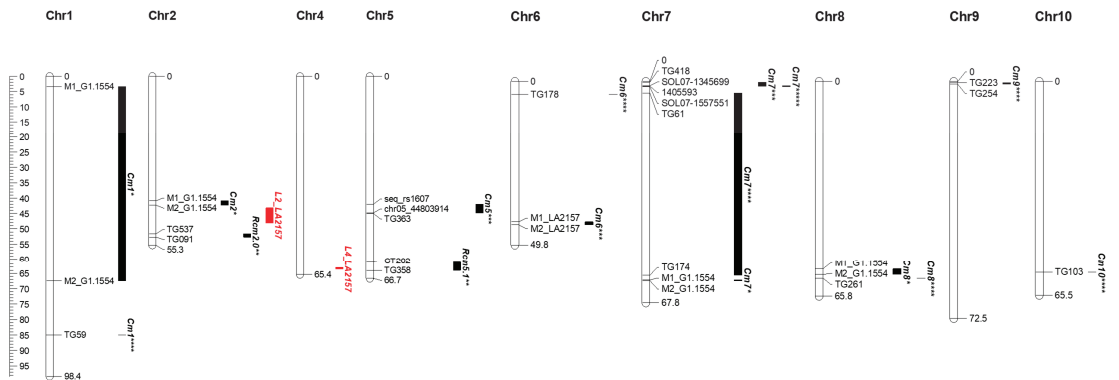


Figure 6. Overview of mapped QTLs reported to be linked to tolerance to *Cm*. Physical positions (Mb) of previously described QTLs linked to tolerance to *Cm* mapped on the *Solanum lycopersicum* genome. Bars indicate the QTL intervals determined by two flanking markers or one closely linked marker. Red bars indicate the newly mapped loci linked to tolerance on chromosomes 2 and 4 of tomato. References: ** [18], **** [23], * [25], *** [26], ** [28]. It has long been speculated that morphological differences in the vascular system of wild tomato accessions might be responsible for the described tolerance to *Cm* [11,17,29]. Interestingly, both genes we mapped on chromosomes 2 and 4 could be related to vascular morphology. Gene *Solyc02g084740.4* (*cytochrome P450/CYP90C1*) belongs to the cytochrome P450 family. *Solyc02g084740.4* is an ortholog of the *Arabidopsis* *ROTUNDIFOLIA3* (*ROT3*) gene, which is involved in brassinosteroid (BR) biosynthesis and polar cell elongation [30,31]. The *CYP90C1* protein encodes a C-23 hydroxylase, which acts redundantly with *CYP90D1* in BR biosynthesis in *Arabidopsis* [31]. BRs have been found to be important in several developmental processes of plants, including cell elongation, cell diving, and vascular differentiation [32]. Mutations in the *Arabidopsis* *CYP90C1* gene have been shown to result in dwarf phenotypes, as well as to affect the expansion of cells in the stems of mutants and the arrangement of pith cells [29].

In our laboratory (Plant Breeding, WUR), efforts to identify the genes underlying the tolerance observed in crosses between *S. arcanum* LA2157 and *S. lycopersicum* resulted in a list of 15 genes in a ~211 kb introgression on the major QTL on chromosome 7. Data also suggested that the introgression on chromosome 7 alone were enough to confer high tolerance to *Cm* [22].

In this study, we set out to functionally characterize these 15 genes in the described region on chromosome 7. As a first step, we decided to confirm that the QTL on chromosome 7 alone is enough to confer high tolerance to *Cm*, as previously reported. A BC₃S₆ line and its selfing lines were used in our disease assays. During our disease assays, we

indeed recorded a significant reduction in wilting symptoms on a line level. Nonetheless, we repeatedly observed phenotypic segregation between the plants in the line, with plants being highly tolerant or highly susceptible to the pathogen (Figures 1 and 2).

Previously, it was reported that the combination of the QTL on chromosome 7 with either of the QTLs on chromosomes 5 or 9 leads to high levels of tolerance [19]. After marker analysis on the previously reported regions on chromosomes 5 and 9 of the line, we could not detect co-segregation of other QTLs with the observed segregating phenotypes (Tables 1 and 2, Figures 1 and 2).

By combining whole genome sequencing with a bulk segregant analysis, we identified two loci on tomato chromosomes 2 (6.98 Mb) and 4 (602 kb) contributing to the observed tolerance (Figure 3). Two genes with distinguishing k-mers on the loci on chromosomes 2 and 4 were mapped. Those were genes *Solyc02g084740.4* and *Solyc04g081190.3*, coding for cytochrome P450/CYP90C1 and transcription factor VASCULAR SPECIFIC FACTOR-1 (*vsf-1*), respectively. Interestingly, a single dominant gene originating from *S. arcanum* var. *humifusum* was also reported on tomato chromosome 4 [23]. The position of the gene, however, was not mapped, and therefore, we cannot conclude if it co-localizes with the locus we mapped on chromosome 4.

VSF-1 is a development-related member of the bZIP family of transcription factors, and is expressed in vascular tissues [33]. Analysis of interactors of *VSF-1* has revealed a strong interaction with the promoter of structural glycine-rich cell wall protein GRP1.8, which is specifically deposited on protoxylem and metaxylem cells [34,35]. Functional analysis of the rice homolog of *VSF-1* (*RF2a*) reported that mutation of *RF2a* results in non-uniform lignification of the xylem, as well as alteration in phloem development [36].

Upon inspection of the sequencing data of the two genes mapped on the R-specific bulk, we could confirm that the SNPs present on the k-mers mapped to the genes were identical to the *S. arcanum* LA2157 allelic variant. We were able to show that differences in the coding sequences of the *S. arcanum* LA2157 alleles both genes result in the production of altered proteins (Figures 4 and 5). In the case of *Solyc02g084740.4* (*cytochrome P450/CYP90C1*), SNPs in the *S. arcanum* LA2157 allelic variant result in the production of a truncated protein. Amino acid substitutions in the proteins produced by allelic variants may influence protein-protein interactions [36]. Therefore, it is likely that changed interactions between the newly mapped loci on chromosomes 2 and 4 with the QTL on chromosome 7 result in tolerance. Based on the loci that we have mapped, molecular markers can be developed. Marker analysis of susceptible and resistant plants of the PV185517 line can confirm the involvement of the loci in tolerance. The use of molecular markers can also verify if the lower peaks mapped are minor loci or due to lack of sequencing coverage. As a next step, functional analysis of genes in the regions important for tolerance can further aid in the identification of the genes underlying the tolerant phenotype. In addition, morphological studies of the vascular systems of tolerant and susceptible plants might uncover differences that support the hypothesis that vascular changes are responsible for the observed tolerance.

Supplementary Materials: The following supporting information can be downloaded at: <https://www.mdpi.com/article/10.3390/agronomy13040953/s1>, Table S1. Details of CAPS markers used in this study; Table S2. Locations on the *S. lycopersicum* ITAG4.0 reference genome with resistant specific coverage; Table S3. Locations on the *S. lycopersicum* ITAG4.0 reference genome with susceptible specific coverage; Table S4. Genes mapped on QTL on chromosome 7; Computer code S1. Computer code developed for the Bulk Segregant Analysis (BSA).

Author Contributions: Conceptualization, E.K. and Y.B.; Methodology, E.K. and M.B.; Software, M.B.; Validation, E.K. and D.M.; Formal Analysis, E.K.; Investigation, E.K.; Resources, Y.B., J.M.V.d.W. and R.G.F.V.; Data Curation, E.K. and M.B.; Writing—Original Draft Preparation, E.K.; Writing—Review & Editing, Y.B., J.M.V.d.W. and R.G.F.V.; Visualization, Y.B.; Supervision, Y.B., J.M.V.d.W. and R.G.F.V.; Project Administration, Y.B.; Funding Acquisition, Y.B. and E.K. All authors have read and agreed to the published version of the manuscript.

Funding: This research was (partially) funded by NWO Science domain (NWO-ENW) project 8440590003, which is financed by the Dutch Research Council (NWO).

Data Availability Statement: The data presented in this study are openly available in European Nucleotide Archive (ENA), with reference number PRJEB59321.

Conflicts of Interest: The authors declare no conflict of interest. R.G.F.V is a member of the editorial board of *Agronomy*. The funders had no role in the design, in the collection, analyses or interpretation of data, in the writing of the manuscript, or in the decision to publish the results. The results described in this paper were part of the PhD study of Eleni Koseoglou and as such have appeared in a modified version in her PhD thesis entitled “Identification of susceptibility determinants in the tomato-*Clavibacter michiganensis* pathosystem”, Chapter 6, pages 143–173, Wageningen University and Research, DOI: 10.18174/574581, and ISBN: 978-94-6447-339-1.

References

- Pagán, I.; García-Arenal, F. Tolerance to Plant Pathogens: Theory and Experimental Evidence. *Int. J. Mol. Sci.* **2018**, *19*, 810. [CrossRef] [PubMed]
- Roy, B.A.; Kirchner, J.W. Evolutionary Dynamics of Pathogen Resistance and Tolerance. *Evolution* **2000**, *54*, 51–63. [CrossRef] [PubMed]
- Eichenlaub, R.; Gartemann, K.-H. The *Clavibacter michiganensis* Subspecies: Molecular Investigation of Gram-Positive Bacterial Plant Pathogens. *Annu. Rev. Phytopathol.* **2011**, *49*, 445–464. [CrossRef]
- Gartemann, K.-H.; Kirchner, O.; Engemann, J.; Gräfen, I.; Eichenlaub, R.; Burger, A. *Clavibacter michiganensis* subsp. *michiganensis*: First steps in the understanding of virulence of a Gram-positive phytopathogenic bacterium. *J. Biotechnol.* **2003**, *106*, 179–191. [CrossRef]
- Tancos, M.A.; Chalupowicz, L.; Barash, I.; Manulis-Sasson, S.; Smart, C.D. Tomato Fruit and Seed Colonization by *Clavibacter michiganensis* subsp. *michiganensis* through External and Internal Routes. *Appl. Environ. Microbiol.* **2013**, *79*, 6948–6957. [CrossRef]
- Sen, Y.; van der Wolf, J.; Visser, R.G.F.; van Heusden, S. Bacterial Canker of Tomato: Current Knowledge of Detection, Management, Resistance, and Interactions. *Plant Dis.* **2015**, *99*, 4–13. [CrossRef]
- Frenkel, O.; Bornstein, M.; Shulhani, R.; Sharabani, G.; Sofer, M.; Abo-Moch, F.; Lofthouse, M.; Manulis-Sasson, S.; Shtienberg, D. Secondary spread of *Clavibacter michiganensis* subsp. *michiganensis* in nurseries and the conditions leading to infection of tomato seedlings. *Eur. J. Plant Pathol.* **2016**, *144*, 569–579. [CrossRef]
- Sharabani, G.; Manulis-Sasson, S.; Borenstein, M.; Shulhani, R.; Lofthouse, M.; Chalupowicz, L.; Shtienberg, D. The significance of guttation in the secondary spread of *Clavibacter michiganensis* subsp. *michiganensis* in tomato greenhouses. *Plant Pathol.* **2013**, *62*, 578–586. [CrossRef]
- Sharabani, G.; Shtienberg, D.; Borenstein, M.; Shulhani, R.; Lofthouse, M.; Sofer, M.; Chalupowicz, L.; Barel, V.; Manulis-Sasson, S. Effects of plant age on disease development and virulence of *Clavibacter michiganensis* subsp. *michiganensis* on tomato. *Plant Pathol.* **2013**, *62*, 1114–1122. [CrossRef]
- Sharabani, G.; Manulis-Sasson, S.; Chalupowicz, L.; Borenstein, M.; Shulhani, R.; Lofthouse, M.; Sofer, M.; Frenkel, O.; Dror, O.; Shtienberg, D. Temperature at the early stages of *Clavibacter michiganensis* subsp. *michiganensis* infection affects bacterial canker development and virulence gene expression. *Plant Pathol.* **2014**, *63*, 1119–1129. [CrossRef]
- Sen, Y.; Feng, Z.; Vandenbroucke, H.; Van Der Wolf, J.; Visser, R.G.F.; Van Heusden, A.W. Screening for new sources of resistance to *Clavibacter michiganensis* subsp. *michiganensis* (Cmm) in tomato. *Euphytica* **2013**, *190*, 309–317. [CrossRef]
- Medina-Mora, C.M.; Hausbeck, M.K.; Fulbright, D.W. Bird’s Eye Lesions of Tomato Fruit Produced by Aerosol and Direct Application of *Clavibacter michiganensis* subsp. *michiganensis*. *Plant Dis.* **2001**, *85*, 88–91. [CrossRef] [PubMed]
- Chalupowicz, L.; Barash, I.; Reuven, M.; Dror, O.; Sharabani, G.; Gartemann, K.-H.; Eichenlaub, R.; Sessa, G.; Manulis-Sasson, S. Differential contribution of *Clavibacter michiganensis* ssp. *michiganensis* virulence factors to systemic and local infection in tomato. *Mol. Plant Pathol.* **2017**, *18*, 336–346. [CrossRef] [PubMed]
- EFSA. Scientific Opinion on the pest categorisation of *Clavibacter michiganensis* subsp. *michiganensis* (Smith) Davis et al.. *EFSA J.* **2014**, *12*, 3721. [CrossRef]
- Thyr, B.D. Inheritance of Resistance to *Corynebacterium michiganense* in Tomato. *Phytopathology* **1976**, *66*, 1116–1119. [CrossRef]
- Francis, D.M.; Kabelka, E.; Bell, J.; Franchino, B.; St Clair, D. Resistance to Bacterial Canker in Tomato (*Lycopersicon hirsutum* LA407) and its Progeny Derived from Crosses to *L. esculentum*. *Plant Dis.* **2001**, *85*, 1171–1176. [CrossRef]
- Coaker, G.L.; Francis, D.M. Mapping, genetic effects, and epistatic interaction of two bacterial canker resistance QTLs from *Lycopersicon hirsutum*. *Theor. Appl. Genet.* **2004**, *108*, 1047–1055. [CrossRef]
- Kabelka, E.; Franchino, B.; Francis, D.M. Two Loci from *Lycopersicon hirsutum* LA407 Confer Resistance to Strains of *Clavibacter michiganensis* subsp. *michiganensis*. *Phytopathology* **2002**, *92*, 504–510. [CrossRef]
- Van Heusden, A.W.; Koornneef, M.; Voorrips, R.E.; Brüggemann, W.; Pet, G.; Vrieling-van Ginkel, R.; Chen, X.; Lindhout, P. Three QTLs from *Lycopersicon peruvianum* confer a high level of resistance to *Clavibacter michiganensis* ssp. *michiganensis*. *Theor. Appl. Genet.* **1999**, *99*, 1068–1074. [CrossRef]

20. Sandbrink, J.M.; Van Ooijen, J.W.; Purimahua, C.C.; Vrieling, M.; Verkerk, R.; Zabel, P.; Lindhout, P. Localization of genes for bacterial canker resistance in *Lycopersicon peruvianum* using RFLPs. *Theor. Appl. Genet.* **1995**, *90*, 444–450. [CrossRef]
21. Sen, Y. Bacterial Canker Resistance in Tomato. Ph.D. Thesis, Wageningen University & Research, Wageningen, The Netherlands, 2014; p. 140.
22. Muniroh binti Mohd Nadzir, M. Different Approaches of Combating Bacterial Canker in Tomato: In Pursuit of Resistance. Ph.D. Thesis, Wageningen University & Research, Wageningen, The Netherlands, 2018; p. 149.
23. Vulkova, Z.V.; Sotirova, V.G. Study of the three-genome hybrid *Lycopersicon esculentum* Mill.—*L. chilense* Dun.—*L. peruvianum* var ‘*humifusum*’ Mill. and its use as a source for resistance. *Theor. Appl. Genet.* **1993**, *87*, 337–342. [CrossRef] [PubMed]
24. Sen, Y.; Manrique, M.J.; Kabaş, A.; Visser, R.G.F.; Heusden, A.W. Qtl Mapping of *Clavibacter Michiganensis* Subsp. *Michiganensis* (cmm) Resistance Originating from *Solanum Pimpinellifolium* g1.1554. *Res. Sq.* **2021**. [CrossRef]
25. Aflitos, S.; Schijlen, E.; De Jong, H.; De Ridder, D.; Smit, S.; Finkers, R.; Wang, J.; Zhang, G.; Li, N.; Mao, L.; et al. Exploring genetic variation in the tomato (*Solanum* section *Lycopersicon*) clade by whole-genome sequencing. *Plant J.* **2014**, *80*, 136–148. [CrossRef]
26. Doyle, J. *DNA Protocols for Plants*; Springer: Berlin/Heidelberg, Germany, 1991; pp. 283–293.
27. Prodhomme, C.; Esselink, D.; Borm, T.; Visser, R.G.F.; Van Eck, H.J.; Vossen, J.H. Comparative Subsequence Sets Analysis (CoSSA) is a robust approach to identify haplotype specific SNPs; mapping and pedigree analysis of a potato wart disease resistance gene Sen3. *Plant Methods* **2019**, *15*, 60. [CrossRef]
28. Ohnishi, T.; Szatmari, A.M.; Watanabe, B.; Fujita, S.; Bancos, S.; Koncz, C.; Lafos, M.; Shibata, K.; Yokota, T.; Sakata, K.; et al. C-23 hydroxylation by Arabidopsis CYP90C1 and CYP90D1 reveals a novel shortcut in brassinosteroid biosynthesis. *Plant Cell* **2006**, *18*, 3275–3288. [CrossRef] [PubMed]
29. Peritore-Galve, F.C.; Miller, C.; Smart, C.D. Characterizing Colonization Patterns of *Clavibacter michiganensis* during Infection of Tolerant Wild *Solanum* Species. *Phytopathology* **2020**, *110*, 574–581. [CrossRef]
30. Kim, G.-T.; Tsukaya, H.; Uchimiya, H. The *ROTUNDIFOLIA3* gene of *Arabidopsis thaliana* encodes a new member of the cytochrome P-450 family that is required for the regulated polar elongation of leaf cells. *Genes Dev.* **1998**, *12*, 2381–2391. [CrossRef]
31. Oh, M.-H.; Honey, S.H.; Tax, F.E. The Control of Cell Expansion, Cell Division, and Vascular Development by Brassinosteroids: A Historical Perspective. *Int. J. Mol. Sci.* **2020**, *21*, 1743. [CrossRef] [PubMed]
32. Li, D.; Fu, F.; Zhang, H.; Song, F. Genome-wide systematic characterization of the bZIP transcriptional factor family in tomato (*Solanum lycopersicum* L.). *BMC Genom.* **2015**, *16*, 771. [CrossRef]
33. Ringli, C.; Keller, B. Specific interaction of the tomato bZIP transcription factor *VSF-1* with a non-palindromic DNA sequence that controls vascular gene expression. *Plant Mol. Biol.* **1998**, *37*, 977–988. [CrossRef]
34. Torres-Schumann, S.; Ringli, C.; Heierli, D.; Amrhein, N.; Keller, B. In vitro binding of the tomato bZIP transcriptional activator *VSF-1* to a regulatory element that controls xylem-specific gene expression. *Plant J.* **1996**, *9*, 283–296. [CrossRef] [PubMed]
35. Dai, S.; Petruccelli, S.; Ordiz, M.I.; Zhang, Z.; Chen, S.; Beachy, R.N. Functional Analysis of *RF2a*, a Rice Transcription Factor. *J. Biol. Chem.* **2003**, *278*, 36396–36402. [CrossRef] [PubMed]
36. Teng, S.; Srivastava, A.K.; Schwartz, C.E.; Alexov, E.; Wang, L. Structural assessment of the effects of Amino Acid Substitutions on protein stability and protein protein interaction. *Int. J. Comput. Biol. Drug Des.* **2010**, *3*, 334. [CrossRef] [PubMed]

Disclaimer/Publisher’s Note: The statements, opinions and data contained in all publications are solely those of the individual author(s) and contributor(s) and not of MDPI and/or the editor(s). MDPI and/or the editor(s) disclaim responsibility for any injury to people or property resulting from any ideas, methods, instructions or products referred to in the content.

Review

Fungi Parasitizing Powdery Mildew Fungi: *Ampelomyces* Strains as Biocontrol Agents against Powdery Mildews

Márk Z. Németh¹, Diána Seress¹ and Teruo Nonomura^{2,3,*}

¹ Centre for Agricultural Research, Plant Protection Institute, P.O. Box 102, H-1525 Budapest, Hungary; nemeth.mark@atk.hu (M.Z.N.); seress.diana@atk.hu (D.S.)

² Laboratory of Phytoprotection, Science and Technology, Faculty of Agriculture, Kindai University, Nara 631-8505, Japan

³ Agricultural Technology and Innovation Research Institute, Kindai University, Nara 631-8505, Japan

* Correspondence: nonomura@nara.kindai.ac.jp; Tel.: +81-742-43-5194

Abstract: Among the mycoparasites, *Ampelomyces* strains are studied in detail, particularly regarding their use as biocontrol agents (BCAs) of powdery mildew (PM) fungi, including their potential to replace conventional agrochemicals. *Ampelomyces* strains are characterized morphologically; their ribosomal DNA internal transcribed spacer (rDNA-ITS) regions and actin gene (*ACT*) fragments were sequenced and their mycoparasitic activity was analyzed. In the interaction between *Ampelomyces* strains and PM fungi, the spores of the mycoparasites germinate on plant leaves, and their hyphae then penetrate the hyphae of PM fungi. *Ampelomyces* hyphae continue their growth internally, initiating the atrophy of PM conidiophores and eventually their complete collapse. Following the successful destruction of PM hyphae by *Ampelomyces*, the mycoparasite produces new intracellular pycnidia in PM conidiophores. The progeny spores released by mature pycnidia become the sources of subsequent infections of intact PM hyphae. As a result, the number of *Ampelomyces*-inoculated PM colonies gradually declines, and the conidial release of PM colonies is inhibited after the first treatment. Almost all conidiophores of 5- and 10-day-old *Ampelomyces*-inoculated PM colonies undergo complete atrophy or collapse. Methodological advances and in-depth analyses of the *Ampelomyces*–PM interaction were recently published. In this review, we summarize the genetic and phylogenetic diversity, the timing of mycoparasitism and pycnidogenesis, the results of quantitative and visual analyses using electrostatic and digital microscopy technologies, the PM biocontrol potential of *Ampelomyces*, and the potential commercialization of the mycoparasites. The information provided herein can support further biocontrol and ecological studies of *Ampelomyces* mycoparasites.

Citation: Németh, M.Z.; Seress, D.; Nonomura, T. Fungi Parasitizing Powdery Mildew Fungi: *Ampelomyces* Strains as Biocontrol Agents against Powdery Mildews. *Agronomy* **2023**, *13*, 1991. <https://doi.org/10.3390/agronomy13081991>

Academic Editor: Ivo Toševski

Received: 29 June 2023

Revised: 24 July 2023

Accepted: 26 July 2023

Published: 27 July 2023



Copyright: © 2023 by the authors. Licensee MDPI, Basel, Switzerland. This article is an open access article distributed under the terms and conditions of the Creative Commons Attribution (CC BY) license (<https://creativecommons.org/licenses/by/4.0/>).

Keywords: biological control; digital microscopic technique; hyperparasite; hyperparasitism; integrated control; mycoparasite; plant protection

1. Introduction

Powdery mildew (PM) is a serious disease affecting many crops [1,2]. The leaf damage caused by the fungus significantly reduces crop productivity [3,4]. While fungicides can be sprayed before or after PM colonies appear on host leaves to control the disease, frequent application of commercial fungicides can lead to resistance [5–7]. To avoid fungicide resistance and the environmental problems caused by fungicide residues, new control strategies that are independent of chemical methods are needed to control PM. Biological control offers an alternative method to prevent or suppress PM in crops by exploiting the antagonism between micro-organisms. Mycoparasitic fungi parasitize other fungi and they include a diverse group of parasites. These fungi absorb nutrients from their mycohosts through haustoria or other special interfaces between their cell walls and membranes. Alternatively, they invade the hyphae of their mycohosts, growing from cell to cell in the latter's hyphae, conidia, and conidiophores while absorbing nutrients from the infection structures [8,9].

Kiss [10,11] examined all known fungal antagonists of PM, whether found in the field or tested as potential biocontrol agents (BCAs) of PM infections, including species without any record of a natural antagonistic relationship. More than 40 fungal taxa were shown to suppress the growth and sporulation of PM fungi. Of these, *Aphanocladium album* [12], *Pseudozyma flocculosa*, *Moesziomyces rugulosus* [13,14], *Gjaerumia minor* [15,16], *Lecanicillium lecanii* [14], and *Ampelomyces quisqualis* [17,18] are well known as BCAs against PM.

The mycoparasitic fungus *Ampelomyces quisqualis* Cesati ex Schlechtend (syn. *Cicimobolus cesatii* de Bary; [17,18]) is a slow-growing pycnidial fungus widely distributed in PM colonies and naturally occurring worldwide [19–21], where it acts as a hyperparasite of strains infecting cultivated and wild plants [10,21–23]. The *Ampelomyces* strains produce progeny spores in mature pycnidia, which develop intracellularly in the hyphae of PM fungi in nature and then suppress mycelial growth, sporulation, and conidial germination of their mycohosts [9–11]. Therefore, this mycoparasitic fungus gained much attention as BCAs for controlling the PMs. The life cycle, mode of action, and biocontrol potential of hyperparasitic fungi were reviewed [9,11,24] with the aim of guiding future research in fungal and plant ecology, as well as in the development of products for the control of plant diseases [25]. However, quantitative data on the impact of hyperparasitism on host fungi are lacking. Thus, in this work, we review (1) the interactions between *Ampelomyces* strains and PM fungi (mycohosts) with respect to the morphological and physiological characteristics and phylogenetic placement of *Ampelomyces* strains; (2) the visualization and impact of fungal hyperparasitism (infection process and pycnidogenesis) on mycohost survival by using a digital microscopic technique; (3) the quantitative impact of fungal hyperparasitism on the suppression of conidial release from PM colonies infected with *Ampelomyces* strains by incorporating a recent methodological advance; and (4) the practical aspects of using *Ampelomyces* strains as BCAs. Finally, (5) summarizing experimental results, we provide an ideal spray inoculation system for the effective use of *Ampelomyces* as a BCA, as well as in research.

2. Powdery Mildew Fungi

PM fungi (Erysiphaceae) are obligate biotrophic pathogens of more than 10,000 host plant species, including important crops, and are responsible for serious losses in agriculture, horticulture, and forestry [1,26–28]. The sporulation of many PM anamorphs is intense (Figure 1A), and the produced conidia (Figure 1B) spread rapidly [29,30]. While regularly applied fungicides are used to control PM, its frequent and inadequate use can lead to the emergence of fungicide resistance [7,31,32], as demonstrated in cucurbit PM fungi [5,6,33–36]. In addition, plant leaves retain fungicides that are not completely decomposed by microorganisms, and the fungicides may also have negative side effects on plant physiology [37] as well as biodiversity [38]. Thus, to avoid drug resistance and environmental problems, new strategies for the control of PM that are independent of chemical methods are needed.

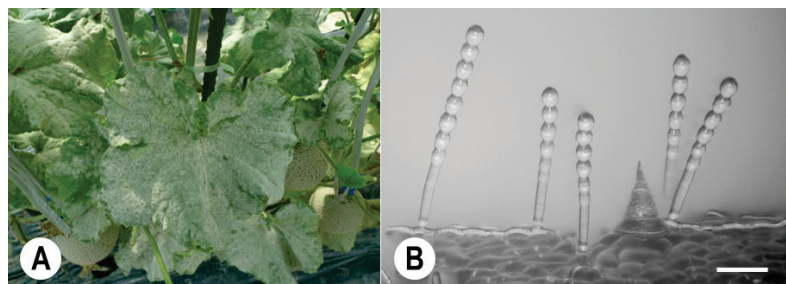


Figure 1. Photograph of powdery mildew (PM) disease caused by *Podosphaera xanthii* on melon leaves, and a micrograph of conidiophores formed in the fungal colonies. (A) Melon PM disease involving the whole leaf. (B) Melon PM conidiophores observed using a digital microscope (KH-2700 DM). The conidiophores have normal catenate conidia, forming chains. Bar: 60 μ m.

3. *Ampelomyces*, a Genus in Need of Taxonomic Revision

Ampelomyces quisqualis was first described from the PM fungus *Erysiphe necator* [17]. However, de Bary [39] used the name *Cicinnobolus cesatii* for the same fungus instead, and the latter became the most commonly used name until the 1970s. However, based on priority, the former name is taxonomically correct [40]. Based on the presumed, but experimentally unproven specialization to host fungi, or based on the host plant of PM infected with *Ampelomyces*, a number of different species were described in the genus. There are more than 40 formally valid descriptions of *Ampelomyces* species in the literature (see [41]). However, as it seems there is no narrow host specificity (see below) in the genus, in recent decades, the name *A. quisqualis* was used for the fungus, hinting that the *Ampelomyces* genus would be monotypic. However, considerable genetic variation characterizes the genus *Ampelomyces*. Between each genetic group, the sequence difference in the ribosomal DNA internal transcribed spacer (rDNA-ITS) region may be as high as 19% [41,42], with even greater variability in actin (*ACT*) sequences [43]. Although lineages that can be separated in the genus are presumably separate species [42,44,45], formally described species do not correspond to the phylogenetic groupings obtained on the basis of DNA sequences. In addition, for some proposed *Ampelomyces* species there are several published names, and a taxonomic revision of the genus is accordingly necessary [42,46]. However, a polyphasic, comprehensive analysis based on colony morphology, micromorphology, and phylogeny is yet to be conducted. In this work, therefore, we do not use the formally existing species names, but rather the terms *Ampelomyces* species or *Ampelomyces* strains, as recommended [47].

4. *Ampelomyces* as an Ecofriendly Biocontrol Agent against PM

Ampelomyces strains were reported in association with more than 65 species (eight genera) of Erysiphaceae from across the world [12,21,22,48–61]. The interactions between mycoparasitic fungi and their mycohosts take place exclusively on the surfaces of aerial plant organs [21,24,62].

In the 19th century, mycologists clearly recognized that some fungi were parasites of PM (e.g., *A. quisqualis* Cesati ex Schlechtend. [17]; *Byssocystis textilis* Riess [63]; and *Cicinnobolus cesatii* [39]). The first study of *A. quisqualis* was carried out by De Bary [39], who identified the fungus as an intracellular parasite of Erysiphaceae. De Bary [39] also showed that *Ampelomyces* hyphae grow within the mycelia of PM, spreading from cell to cell through septal pores, with pycnidia produced in one or two cells of the hyphae, conidiophores, and conidia of their mycohosts. Emmons [49] later conducted an extensive cytological study, describing in detail the penetration, growth, and sporulation of *Ampelomyces* in the ascomata of PM. Shortly thereafter, Yarwood [64] described the treatment of PM-infected plants using a conidial suspension of *Ampelomyces*, the first experiment demonstrating the biocontrol of a plant pathogenic fungus. Since then, hyperparasitic fungi of the genus *Ampelomyces* began to be applied as BCAs against PM fungi in various crops worldwide [9,10,23,44,46,65,66], thus demonstrating their utility as an ecofriendly method of PM disease management.

There is little on the physiological, biochemical, and molecular interactions between *Ampelomyces* strains and their host fungi; therefore, overall, little is known about the molecular mechanism of the mycoparasitism exerted by *Ampelomyces* [65,67]. A few studies reported that enzymatic, and also mechanical processes play a role during penetration into PM structures. Appressorium-like structures were observed at the penetration sites [68]. Five to ten days later, the mycoparasite degrades the cytoplasm of the host [49,69]. This suggests that the interaction becomes necrotrophic at a later stage. The activity of several hydrolytic enzymes (such as chitinases, proteases [70], β -glucosidase, β -N-acetylglucosaminidase, acid phosphatase, ribonuclease, β -1,3-glucanase, and α -1,4-glucanase [71,72]) was demonstrated in *Ampelomyces* strains. It was suggested [72] that *Ampelomyces* probably interferes with the energy metabolism and protein and cell wall synthesis of the host. Based on transcription studies, several other genes are differentially expressed during mycoparasitism, including lipases, oxygenases, and peptidases [65]. In addition to enzymatic

processes, another underexplored mechanism, toxin biosynthesis, may also take place during mycoparasitism [65].

5. Morphological and Molecular Analyses, and the Identification of *Ampelomyces* Strains

Based on morphological and molecular phylogenetic analyses, Németh et al. [61] recently identified hyperparasites isolated from different PM species in Japan as *Ampelomyces* Cesati ex Schlechtend. Spores of Japanese hyperparasitic strains were produced in pycnidia, which develop intracellularly in the mycelia of PM fungi. The spores are unicellular, hyaline, ellipsoid–ovoid to doliiform (size range: $5.7\text{--}9.2 \times 2.6\text{--}5.0 \mu\text{m}$), mostly guttulate, and embedded in a mucilaginous matrix within swollen ampulliform or pyriform pycnidia [61]. The spores germinate *ca.* 15–20 h after their inoculation, forming elongated hyphae that branch under conditions of high relative humidity (RH). Hyphae formed from the spores reach a length of $6.2\text{--}78.2 \mu\text{m}$ 48 h after inoculation. Fungal colonies slowly and concentrically spread after the inoculation of a single mature pycnidium in the centre of Czapek–Dox agar medium supplemented with 2% malt extract. The colony area reaches $148.4\text{--}391.3 \text{ mm}^2$ at 20 days post-inoculation (dpi). Isolates significantly differ in their germination rate and hyphal length, but not in their colony area. The strains grow slowly, with an *in vitro* radial growth rate of $0.5\text{--}1.0 \text{ mm day}^{-1}$. Thus, the morphological and physiological characteristics of the Japanese strains clearly resemble those of *A. quisqualis* isolates [41,59,60,69,73].

As noted above, molecular analyses based on the rDNA-ITS region and *ACT* fragment revealed considerable genetic diversity among *Ampelomyces* strains [42–45,62,74,75]. Using sequences from these two loci, Németh et al. [61] confirmed the existence of at least five different phylogenetic lineages within the genus *Ampelomyces*, and showed that the newly isolated Japanese strains belong to three major clades. The authors analyzed the phenotypic characteristics of *Ampelomyces* strains isolated from four different PM samples, and four different strains isolated from the same PM sample. There were no morphological characteristics that could clearly be associated with a given genotype or clade. The four strains isolated from the same PM sample, however, differed significantly in their measured hyphal lengths, germination rates, and the number of spores that developed in single pycnidia, as well as strong evidence of strain-level differences, as reported in other studies [46,70]. Whether the differences in the phenotypic characteristics of different strains of *Ampelomyces* are related to an as-yet unrevealed genetic diversity or are simply caused by phenotypic plasticity is currently unknown. The possibility of strain-level differences, however, needs to be considered in studies aimed at the development of *Ampelomyces* as BCAs.

6. *Ampelomyces* Strains May Be Associated with, but Are Not Specific to, Their Host PM Species

The specificity of *Ampelomyces* was investigated using two fundamentally different approaches: by isolating *Ampelomyces* from a diverse range of PM fungi and then investigating possible associations between the interacting partners and via cross-inoculation experiments.

“Some degree of mycohost specialization” and “evidence for narrow host specialization” were reported for *Ampelomyces* based on the genetic clustering of strains according to the mycohost [44,75,76]. However, other studies that employed a similar methodology obtained different results. Several *Ampelomyces* strains, all isolated from grapevine PM naturally infected by *Ampelomyces*, belong to four different genetic clades [43]. After a similar sampling, *Ampelomyces* strains isolated solely from *Arthrocladiella mougeotii* were assigned to three different clades [77]. These studies suggest that *Ampelomyces* strains isolated from a given PM fungal species can belong to genetically different groups, and isolates from different host fungi can belong to the same genetic group [41–44,47,77,78]. Taken together, these results support the lack of host specificity of *Ampelomyces*.

Host specificity was also experimentally investigated in other studies. In cross-inoculation experiments carried out by De Bary [39], *Ampelomyces* mycoparasites col-

lected from a given PM species were shown to also produce intracellular pycnidia in the mycelia of other PM species. In other cross-inoculation experiments, including *in vitro* studies [42,70,74,79] and field experiments [46,77,80] involving different *Ampelomyces* strains and several PM species, these mycoparasitic strains did not show strict host specificity; instead, they were capable of infecting many host species irrespective of the original host, producing intracellular pycnidia in the mycelia of other species of Erysiphaceae [39,42,46,47,70,74,77,79–81]. Following inoculation tests with Japanese isolates and five PM species, Németh et al. [61] observed the degeneration and constriction of parasitized hyphae of all five PM species tested, as well as pycnidial formation in the hyphae and conidiophores of four PM fungi. These results show that Japanese *Ampelomyces* strains can infect PM hyphae irrespective of the original host, as they produced intracellular pycnidia in the mycelia of four out of the five tested mycohosts. Additional experiments showed that *Ampelomyces* strains from apple PM naturally infect *Golovinomyces orontii* (s. l.), the tobacco PM fungus, and *P. xanthii* causing cucumber PM [77]. These results and those of several other studies [39,70,74,77,82] support the lack of host specificity with the tested *Ampelomyces* strains.

Seemingly contradictory results were obtained with *B. graminis*. A previous study reported the lack of pycnidial production of a strain isolated from *E. artemisiae* in *B. graminis* on barley [60], which is similar to the findings of Németh et al. [61]. Other studies reported typical mycoparasitism, including the formation of intracellular pycnidia, in *B. graminis* conidiophores on cereals (wheat and barley) by *Ampelomyces* strains isolated from PM infecting dicots [59,62,79,83,84]. The contradictory results might be due to unfavourable experimental conditions, as described by Kiss [10], and not to the inability of *Ampelomyces* strains to infect *B. graminis*. It should be noted, however, that *Ampelomyces* strains seem to parasitize PM fungi less commonly, such as *B. graminis* infecting monocot plants, than PM species on dicotyledonous plants [59].

However, even in the absence of a strict host association between *Ampelomyces* and PM fungi, i.e., no species specificity, qualitative differences between *Ampelomyces* strains in their ability to infect different PM fungi cannot be ruled out. In a previous study, *Ampelomyces* mycoparasites formed more pycnidia in colonies of the original host than in those of other PM fungi [82]. In other studies, the opposite was observed, namely that *Ampelomyces* strains isolated from different PM species were similarly capable of parasitizing colonies of other PM species, regardless of the original host, both *in vitro* and in field experiments [46,74,77]. In their mycoparasitic tests with Japanese *Ampelomyces* strains, Németh et al. [61] used five PM species maintained in the greenhouse: *B. graminis* f. sp. *hordei* race 1 KBP-01 (on barley *Hordeum vulgare* L. cv. 'Kobinkatagi'), *E. neolyopersici* (= *Pseudoidium neolyopersici*) KTP-03 (on tomato *Solanum lycopersicum* Mill. cv. 'Moneymaker'), *E. trifoliorum* KRCP-4N (on red clover *Trifolium pratense* L., cv. 'Megium'), *P. aphanis* KSP-7N (on strawberry *Fragaria* × *ananassa* Duchesne cv. 'Sagahonoka'), and *P. xanthii* KMP-6N (on melon *Cucumis melo* L., cv. 'Earl's Favourite'). Then, PM-infected plants were spray-inoculated with spore suspensions and then the mycoparasitic activity was scored. Japanese *Ampelomyces* strains successfully infected all five PM isolates and formed mature pycnidia in four out of five mycohost colonies (*E. trifoliorum*, *E. neolyopersici*, *P. aphanis*, and *P. xanthii*). The tested strains infected melon PM more heavily than the other hosts, as reflected by the formation of a larger number of pycnidia at 14 dpi. However, there were no significant differences in the mycoparasitic activity of the eight Japanese *Ampelomyces* strains based on three-level scoring.

Understanding host specificity is complicated by the existence of strain-level differences between *Ampelomyces* strains, as in laboratory experiments, strong differences in the mycoparasitic ability of different *Ampelomyces* strains were observed [46,70], including with respect to the PM species [70]. However, in general, the most effective *Ampelomyces* strains are very effective not only against the original host, but also against other PM species [46,70]. Those observations imply that the degree of mycoparasitism does not depend on the original host fungus [46], nor is it a general characteristic of individual genetic clades; rather, it reflects differences at the strain level. Indeed, the contradictory

results obtained in experimental work might be partially explained by differences at the strain level.

A summary of the available data leads to the conclusion that they do not contradict the possibility of a “certain degree of host specialization” [44] among these mycoparasites. However, as this conclusion conflicts with the experimental evidence, strict (exclusive) host specialization can in fact be ruled out, and it instead suggests structural specificity [85], defined as the ability of a given parasite to parasitize different host fungi but in different proportions or with different abundances depending on the host [85]. This holds true for *Ampelomyces*. Structural specificity can also result in an apparent association with host fungi without implying a narrow host specialization. This is well demonstrated by *Ampelomyces* strains associated with the causal agent of apple PM (*P. leucotricha*): while these strains are mostly found in *P. leucotricha*, they easily colonize other mycohosts as well [74,77].

From a practical point of view, the lack of strict host specificity [24] allows a single *Ampelomyces* strain to be applied as a BCA against a wide range of PM species. Several studies demonstrated the biocontrol potential of *Ampelomyces* species against PM on various crops, such as *E. trifoliorum* on red clover [64], *P. leucotricha* on apple [84,86], *P. xanthii* on cucumber [19,20,66,76,79,86–92] and melon [93–95], *E. necator* on grapevine [22,76,82,92,96,97], *B. hordei* on barley [59,83], and *B. graminis* on wheat [83], and several other species as well [64,76,79,86,89,98–102].

7. Latest Results on *Ampelomyces*—PM Interaction

7.1. Methodological Considerations of Spray Inoculation of *Ampelomyces* Spores onto PM Colonies

The effective control of PM using mycoparasitic strains requires a method for inoculating hyperparasite spores onto PM fungal colonies. *Ampelomyces* is usually spray-inoculated onto PM-infected plants as a spore suspension, with the applications repeated several times during the season to ensure a high level of control [79,103]. Gu and Ko [104] reported that the concentration of hyperparasite spores is an important factor affecting their germination and infection in pathogens, as spore germination decreases rapidly at spore concentrations $>10^6$ spores mL^{-1} , due to the production of self-inhibitory compounds. In our spray inoculation system, spore suspensions of *Ampelomyces* are diluted to 5×10^5 spores mL^{-1} , and polyoxyethylene sorbitan monolaurate (Tween 20) is added to a final concentration of 0.05%. With this method, spores of *Ampelomyces* germinate successfully 15–20 h after spray inoculation onto PM-inoculated plant leaves at high RH [61,95].

7.2. Infection Processes of *Ampelomyces* Strains in PM Fungi

In Németh et al. [62], *A. quisqualis* transformants expressing an integrated green fluorescent protein (GFP) gene could be visualized in PM fungi and PM-infected leaves, which allowed for the localization of mycoparasitic fungi in PM hyphae. The method described by Suzuki et al. [105] was used to visualize tri-trophic interactions among mycoparasites, mycohosts, and plant cells. Further insights into mycoparasitism, including direct observations of the infection process of *Ampelomyces* strains, were obtained in real-time using high-fidelity digital microscopy (KH-2700 DM; Hirox, Tokyo, Japan) to monitor mycoparasite–mycohost interactions and thus determine how and when mycoparasites invade PM structures. The infection process of *Ampelomyces* strains in tomato PM *E. neolyopersici* on leaf type I trichomes of common tomato (*S. lycopersicum* Mill. cv. ‘Mon-eymaker’) and in melon PM colonies was also observed using digital microscopy (KH-2700 DM). Németh et al. [61] visually followed the infection of tomato PM colonies and subsequent conidiogenesis of an *Ampelomyces* strain. Foot cells and generative cells (GCs) of PM conidiophores began to atrophy at 5–6 dpi, with the formation of intracellular pycnidia of the hyperparasite strain initiated in basal cells of the conidiophores at 6–8 dpi, followed by the complete collapse of the conidiophores at 10–14 dpi. Kimura et al. [95] observed the degeneration and constriction of hyphae in melon PM *P. xanthii* prior to intracellular pycnidial formation in the hyphae (ex. conidiophores). Infection and conidiogenesis by the tested hyperparasitic *Ampelomyces* strain were very similar in melon PM fungus and in

tomato PM fungus, as reported by Németh et al. [61]. Interestingly, almost all intracellular pycnidia were produced in conidiophores of the mycohost.

Based on earlier work and our detailed microscopic analysis, the approximate time course of infection, the events that take place in the mycoparasites once they entered the mycohosts (PM fungi), and the morphological changes in a mycoparasite-infected mycohost can be summarized as follows: *Ampelomyces* hyphae within parasitized PM conidia are spread by wind [20,106,107] and spores are dispersed, e.g., by rain splash [68,108]. The processes that, after spore germination, allow *Ampelomyces* to penetrate and parasitize hyphae of PM fungi may be mechanical [68] or enzymatic [70,71]. Penetration of mycohost structures by the hyperparasite *Ampelomyces* can occur within 24 h [68,93]. The mycoparasite hyphae continue their growth in PM structures, extending from cell to cell through the septal pores, and further ramifying throughout the mycohost hyphae [68,69]. The mycohost invasion by *Ampelomyces* leads to atrophy in 5–6 dpi and then to complete disruption of the mycohost conidiophores at 7 dpi. Disruption of the cytoplasm of the fungal hosts causes the reduced growth and eventually the death of the host fungus [22,69,82]. During the course of infection, *Ampelomyces* produces intracellular pycnidia in the hyphae or conidiophores of their mycohosts at 5–10 dpi [19,68,81]. In contrast to other pycnidial mycoparasites, such as *Coniothyrium minitans* Campbell [109–111], toxin production by *Ampelomyces* was not detected [112].

7.3. Pycnidial Development of *Ampelomyces* Strains in PM Fungi

Spores of *Ampelomyces* strains are produced in pycnidia that develop intracellularly in the mycelia of PM fungi [92]. The pycnidia of *Ampelomyces* are formed ubiquitously in PM colonies (Figure 2A), with a change in colour from pale yellow (immature) to black (mature) over time [95]. The number of pycnidia of *Ampelomyces* per melon PM colony was shown to increase with the age of the PM colony [95]. Mature pycnidia have a size range of $40.2\text{--}84.2 \times 22.6\text{--}48.1 \mu\text{m}$, and a single mature pycnidium produces 199.4–1492.7 spores by 14 dpi [61]. Both the number of spores developed in a single pycnidium and the sizes of pycnidia among strains can significantly differ [61].

Detailed observations on pycnidial development were obtained using tomato and melon PM colonies infected with *Ampelomyces* strains following spray inoculation [61,95]. Almost all pycnidia were produced in conidiophores of the mycohost (Figure 2B). Following infection of tomato PM fungi, the first signs of atrophy were seen in foot cells and GCs of the conidiophores (normal noncatenate conidia) at 5–6 dpi. Intracellular pycnidia of *Ampelomyces* were initially produced mostly in the basal cells of the conidiophores at 6–8 dpi, during which time *Ampelomyces* hyphae and pycnidia continued to elongate in the host hyphae. The conidiophores completely collapsed at 10–14 dpi. In melon PM fungus, intracellular pycnidia of *Ampelomyces* initiated within GCs of the conidiophores (normal catenate conidia, forming chains) at 6–8 dpi. Single conidia formed at the top of the conidiophores and began to atrophy at 7–9 dpi, with complete atrophy at 10–11 dpi and complete collapse of the conidiophores at 11–12 dpi. PM hyphae containing conidiophores on melon leaves also underwent complete collapse. Melon PM colonies were therefore unable to scatter their asexual progeny conidia from the conidiophores. Pycnidia of *Ampelomyces* matured within 12–14 days. In the presence of water, *Ampelomyces* spores were released from intracellular pycnidia by the rupture of both the pycnidial and the PM cell walls (Figure 2C). The released mature spores served as sources of subsequent infections for PM hyphae.

7.4. Quantitative Analysis of PM Conidia Released from *Ampelomyces*-Parasitized PM Colonies under Greenhouse Conditions

In the natural environment, the asexual conidia produced by PM fungi on conidiophores (Figure 1B) are dispersed by wind over large areas and are the source of host plant infection [113–116]. *Ampelomyces* mycoparasites suppress both asexual and sexual sporulation of the attacked PM mycelia by colonizing and destroying conidiophores [24].

Philipp et al. [88] observed that parasitized PM colonies can continue their radial growth, but their sporulation is stopped soon after *Ampelomyces* penetrates their mycelia. Similarly, Shishkoff, and McGrath [91] showed that *Ampelomyces* could not prevent the spread of PM colonies *in vitro*, but the parasite caused a reduction in the inoculum produced by each colony. In addition, if *Ampelomyces* is to be used as a BCA, its growth and spread must outpace that of PM fungi (mycohosts). The conidiation rate of PM colonies depends on several factors, including the inoculum density, physiological patterns of the host plant, and abiotic factors [29,117,118]. Intense conidiation and spread of PM fungi will prevent their successful control by *Ampelomyces* mycoparasites applied as BCAs. In these cases, the effect of *Ampelomyces* will be limited to a reduction in disease severity and a milder impact of the PM fungus on the infected plants.

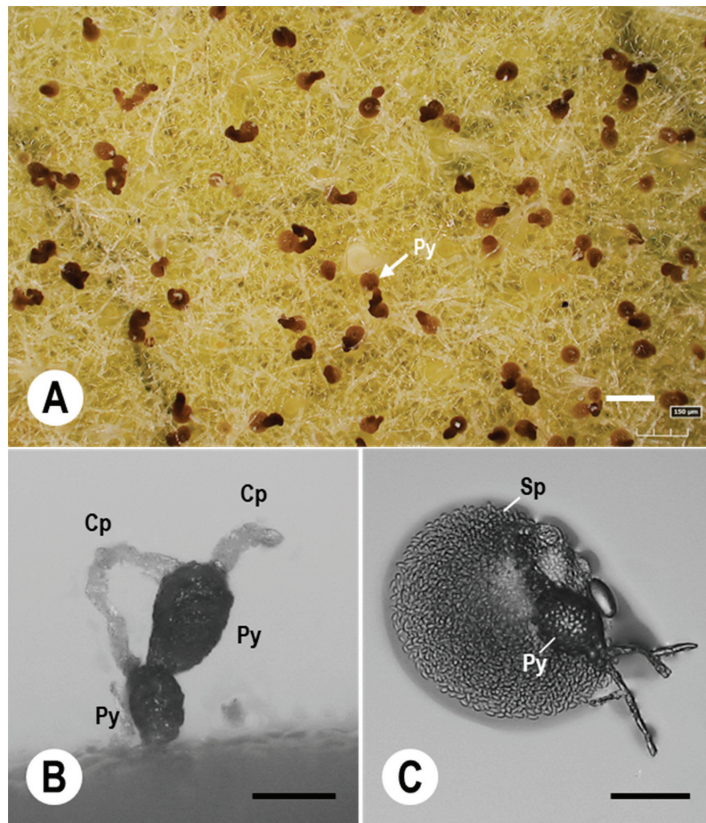


Figure 2. Digital micrographs of *P. xanthii* colonies and conidiophores on melon leaves spray-inoculated with spores of a Japanese *Ampelomyces* strain. (A) Digital microscopy images of pycnidia (Py) of an *Ampelomyces* strain cultivated in plastic boxes at 70–80% relative humidity (RH) and under growth chamber conditions; the images were taken at 10 days post-inoculation (dpi) of 15-day-old melon PM colonies. (B) Pycnidia (Py) of the *Ampelomyces* strain that developed in melon PM conidiophores (Cp). The pycnidia were successfully produced in generative cells of the conidiophores at high RH (70–80%). (C) *Ampelomyces* spores released from a pycnidium after treatment with a 10 µL drop of distilled water. Mature pycnidia (Py) released abundant progeny spores (Sp). Bars: 150 µm (A,B), and 60 µm (C).

Recent methodological advances and the use of an electrostatic spore collector system facilitated the quantification of conidial release from PM colonies. In a study in which an electrostatic rotational spore collector consisting of a dielectrically polarized insulator

drum was used for this purpose, a single melon and strawberry PM colony maintained under greenhouse conditions was found to release an average of 12.6×10^4 conidia and 6.7×10^4 conidia throughout its lifespan, respectively [119,120]. The collection device had no detrimental effect on the survival of the fungus; the electrostatically collected conidia produced normally elongated hyphae and formed conidiophores that produce living progeny conidia [119,120].

The same methodology was employed to study *Ampelomyces*–PM interactions. Using electrostatic and digital microscopy techniques, Kimura et al. [95] estimated the control effects and infection efficiency of an *Ampelomyces* strain against a melon PM fungus. The aim of their study was to determine whether asexual PM progeny conidia, which are a source of host plant infection, are released from *Ampelomyces*-inoculated melon PM colonies at different developmental stages (5-, 10-, and 15-day-old colonies). The authors found that the number of conidia released from 5- to 10-day-old melon PM colonies after spray inoculation with mycoparasite spores decreased gradually, with no release by 3–5 dpi and 4–11 dpi, respectively. Thus, conidial release from melon PM colonies was suppressed completely by the application of an *Ampelomyces* strain under greenhouse conditions. However, the complete prevention of progeny conidial release from 15-day-old melon PM colonies required two spray inoculations with the mycoparasite; a single treatment was insufficient. In response to a single inoculation, 5-, 10-, and 15-day-old melon PM colonies ceased their expansion at 4, 5, and 2 dpi, respectively. After electrostatic spore collection, conidiophores in uninoculated melon PM colonies had a normal morphology, forming conidial chains under greenhouse conditions, whereas conidiophores and hyphae in inoculated melon PM colonies either atrophied or collapsed, with a clear decrease in the number of normal conidiophores. There were no normal melon PM conidiophores per single 5- and 10-day-old melon PM colonies following a single spray inoculation of hyperparasite spores, unlike in 15-day-old colonies. Based on these results, for successful disease control, PM colonies should be spray-inoculated with hyperparasitic fungal spores during early developmental stages (e.g., when the colonies are 5–10 days old, or as soon as PM is detected on host leaves). If older colonies (e.g., >15 days old) are spray-inoculated with mycoparasite spores, a few normal conidiophores will persist due to suboptimal control by *Ampelomyces* strains, allowing PM fungi to scatter progeny conidia from the colonies. During that period, some of the conidiophores of the invaded mycelium will continue to produce fresh conidia, although they might already be infected, and will thus contain intracellular hyphae of *Ampelomyces* [107].

8. Practical Application of *Ampelomyces* Strains as Biocontrol Agents of PM

Yarwood [64] first showed the potential of *Ampelomyces* as a BCA by demonstrating the control of clover PM (*E. polygoni*) in a basic experiment that reproduced the events of a natural epidemic recorded in the previous year. On the other hand, there was also a problem with the emergence of fungicide resistance to chemical control agents. Therefore, from the 1970s, interest in the biological controls of PMs increased. Kiss [121] determined that potential BCAs need to be active in the phyllosphere because PM fungi are biotrophic pathogens infecting the aerial parts of their host plants. The first significant trial of *Ampelomyces* was reported by Jarvis and Slingsby [19], who used conidial suspensions of the mycoparasite to successfully control cucumber PM in greenhouse trials. Control was enhanced when application was interspersed with water sprays. The many other positive examples in which *Ampelomyces* was subsequently used to control PM on several crops paved the way for commercialization [24,66,96,97,122]. In addition, Sundheim and Tronsmo [123] recommended *Ampelomyces*-based fungal biocontrol products in plant protection practice as they can be used without any risk to human health. The absence of nontarget effects of *Ampelomyces* biocontrol procedures was reported as well [62,124].

Ampelomyces-based BCAs can also be applied prophylactically [125–127], as the mycoparasite can survive on leaves without immediate contact with the targeted PM fungus, as demonstrated experimentally [62].

The most successful biocontrol experiments using *Ampelomyces* were carried out in greenhouses, under high RH [19,20,103], and in the field, where free water was frequently available on the treated leaves [79,82]. However, the efficacy of *Ampelomyces* was shown to decrease rapidly at a RH < 85–90% [125,126] or <90–95% [88,128,129]. This high RH requirement of *Ampelomyces* is a major obstacle to its use as a reliable BCA. Our tested *Ampelomyces* strain also did not produce intracellular pycnidia in PM hyphae under greenhouse conditions that included a low RH, but it did produce them in PM hyphae in growth chambers with a high RH [95]. These results, as well as those of previous studies [19,20,22,24,61,81,82], demonstrate the importance of high-RH conditions for hyperparasitic *Ampelomyces* strains to produce intracellular pycnidia in mycohost hyphae. The inability to form pycnidia may explain the suboptimal biocontrol of *Ampelomyces* at low RH.

The high RH requirement of *Ampelomyces* must be addressed before the mycoparasite can be used in biocontrol [125,129]. In attempts to enhance the efficacy of *Ampelomyces* at lower RHs, Epton and Hamed El Nil [130] selected isolates that were able to germinate at a higher vapor deficit than wild types. In an alternative approach, a number of additives, such as an emulsion of 1% paraffin oil [128], a 0.3% mineral oil surfactant [97], 0.5% Tween 20 [46], or 0.01% Tween 80 [92], were shown to increase the biocontrol performance of *Ampelomyces* at lower RHs, although some of these additives can control PM directly [14,98,131,132]. To observe the effects of the BCA alone requires the use of surfactants at concentrations that do not affect the development of PM hyphae [61,95].

9. Formulation and Commercialization of *Ampelomyces* as BCAs

The scale-up of *Ampelomyces* inoculum for biocontrol purposes was one of the crucial steps towards its commercialization and practical application in plant protection. Szejnberg et al. [133] developed and patented (European Patent Office, publ. no. 0353662/1988) a simple, inexpensive method for the production of large amounts of *Ampelomyces* spores in fermenters. The different formulations were tested in various crops, particularly grapevine. An improved product (AQ10™ Biofungicide) registered in 1995 for use in the control of grapevine PM was subsequently also registered for use in other fruits and vegetables in conjunction with the wetting agent (formulated as water-dispersible granules) Add-Q, a spray adjuvant recommended for use together with AQ10 biofungicides [125,126]. However, Shishkoff and McGrath [91] found that in the control of cucumber PM, Add-Q was as effective alone as when combined with AQ10. Therefore, the effect of the additives should be clearly distinguished from that of *Ampelomyces* when assessing the efficacy of a BCA [125].

Other studies likewise showed that the efficacy of biocontrol achieved with commercial anti-PM biofungicide products, including AQ10® (Ecogen Incorporated, Langhorne, PA, USA) [97], Q-fect® (Green Biotech, Paju, South Korea), Powderycare® (AgriLife, Medak, India) [10,44,65], and Bio-Dewcon 2.00 WP (India) [66], varies significantly. Some trials reported that *Ampelomyces* treatment was ineffective, others suggested only very limited control of PM [90,91,129,132], others reported suboptimal control [90,134], and still others reported satisfactory results [95,102,135,136], including a level of control comparable to that using conventional fungicides [122]. These contradictions might result from experimental differences, such as humidity [10], differences in the mycoparasitic activities of individual *Ampelomyces* strains [10,70], and/or from physiological differences between genetically similar or uniform strains of *Ampelomyces* [46,70,76].

Recently, the large-scale production of a new strain, CPA-9 was reported [136]. Formulation was also developed, and the efficiency of the formulated product was demonstrated [102].

10. An Ideal Spray Inoculation System for the Effective Use of *Ampelomyces* as a BCA

An efficient inoculation method of *Ampelomyces* spores to PM colonies is needed for *in vitro* experimental studies of the fungus, as well as for its successful use as a BCA. Based on the experimental results and the studies conducted to date, a list of criteria for the

delivery of *Ampelomyces* as a BCA in an optimal spray inoculation system can be compiled as follows: (1) The selected strains should have exceptional mycoparasitic abilities [46,70]. (2) Adding a surfactant as a wetting agent [46,95,97,122,128] increases efficacy. (3) Spraying should be conducted at high RH, such as in the early morning or late afternoon [122]. (4) Alternatively, although technically less feasible, PM colonies can be inoculated with mycoparasite spores at night, when conidiophores do not release progeny conidia, in contrast with during the day, when progeny conidia are actively released [95,119,120]. (5) For effective control, young colonies should be targeted, i.e., as soon as PM fungi are observable on host leaves (e.g., in 5- to 10-day-old colonies), when the leaf incidence of PM is still low (<10%) [95,122]. (6) Efficiency can be further improved by adding interspersed water sprays [19] and by repeated applications [79,95,103]. In demonstration trials, spraying with *Ampelomyces* was as effective as conventional fungicides [122] when conditions were optimized. In addition, because *A. quisqualis* tolerates a number of pesticides applied in plant protection [20,81,87,93,102], it can be included in integrated plant protection programs [102].

11. Conclusions

Ampelomyces strains were demonstrated to be able to suppress PM development. The lack of their strict host species specificity enables the use of *Ampelomyces* strains as a BCA against a wide range of PM fungi. There are, however, problems associated with the taxonomy of the genus, and occasional difficulties with their practical use. Considerable knowledge gaps concerning *Ampelomyces* include the molecular and biochemical processes during mycoparasitism, which are largely understudied. For the study these, genomic [23] and transcriptomic [65] resources are available, and an efficient transformation system [62], as well as a toolbox for gene knockout [67] were developed. These provide a basis for future studies aimed at deciphering the molecular background of mycoparasitism.

On the other hand, there were some recent advances in the study of these mycoparasites, facilitating the use of *Ampelomyces* strains for the effective control of PM fungi. These findings and the experimental results reported in this review lead to the development of an ideal spray inoculation system for the delivery of hyperparasitic fungi to control PM pathogens. The spray inoculation system should aid experimental research on *Ampelomyces*, and also its practical use as a BCA. Due to the recent methodological advancements and newest results on the biology of the fungus, *Ampelomyces* strains have the potential to be used as effective BCAs against PM fungi as an eco-friendly alternative to conventional fungicides.

Author Contributions: Conceptualization, T.N.; methodology, M.Z.N., D.S. and T.N.; resources, M.Z.N. and T.N.; data curation, M.Z.N., D.S. and T.N.; writing—original draft preparation, M.Z.N. and T.N.; writing—review and editing, M.Z.N. and T.N.; visualization, M.Z.N. and T.N.; supervision, M.Z.N. and T.N.; project administration, T.N. All authors have read and agreed to the published version of the manuscript.

Funding: This research was supported by the János Bolyai Research Scholarship of the Hungarian Academy of Sciences, awarded to Márk Z. Németh (BO/00221/21/4).

Data Availability Statement: Referred data sets are available in earlier publications, or from the current author on reasonable request.

Acknowledgments: The authors thank professional editors, native speakers of English, for checking the English of this document.

Conflicts of Interest: The authors declare no conflict of interest.

References

- Kiss, L.; Vaghefi, N.; Bransgrove, K.; Dearnaley, J.D.W.; Takamatsu, S.; Tan, Y.P.; Marston, C.; Liu, S.-Y.; Jin, D.-N.; Adorada, D.L.; et al. Australia: A continent without native powdery mildews? The first comprehensive catalog indicates recent introductions and multiple host range expansion events, and leads to the re-discovery of *Salmonomyces* as a new lineage of the Erysiphales. *Front. Microbiol.* **2020**, *11*, 1571. [CrossRef]
- Vaghefi, N.; Kusch, S.; Németh, M.Z.; Seress, D.; Braun, U.; Takamatsu, S.; Panstruga, R.; Kiss, L. Beyond nuclear ribosomal DNA sequences: Evolution, taxonomy, and closest known saprobic relatives of powdery mildew fungi (Erysiphaceae) inferred from their first comprehensive genome-scale phylogenetic analyses. *Front. Microbiol.* **2022**, *13*, 903024. [CrossRef] [PubMed]
- Spencer, D.M. Powdery mildew of strawberries. In *The Powdery Mildews*; Spencer, D.M., Ed.; Academic Press: New York, NY, USA, 1978; pp. 355–358.
- Keinath, T.P.; Wintermantel, W.M.; Zitter, T.A. *Compendium of Cucurbit Diseases*; APS Press: St. Paul, MN, USA, 2017.
- Miyamoto, T.; Hayashi, K.; Ogawara, T. First report of the occurrence of multiple resistance to Flutianil and Pyriofenone in field isolates of *Podosphaera xanthii*, the causal fungus of cucumber powdery mildew. *Eur. J. Plant Pathol.* **2020**, *156*, 953–963. [CrossRef]
- Miyamoto, T.; Hayashi, K.; Okada, R.; Wari, D.; Ogawara, T. Resistance to succinate dehydrogenase inhibitors in field isolates of *Podosphaera xanthii* on cucumber: Monitoring, cross-resistance patterns and molecular characterization. *Pestic. Biochem. Physiol.* **2020**, *169*, 104646. [CrossRef] [PubMed]
- Vielba-Fernández, A.; Polonio, A.; Ruiz-Jiménez, L.; de Vicente, A.; Pérez-García, A.; Fernández-Ortuño, D. Fungicide resistance in powdery mildew fungi. *Microorganisms* **2020**, *8*, 1431. [CrossRef]
- Jeffries, P.; Young, T.W.K. *Interfungal Parasitic Relationships*; CABI Publishing: Wallingford, UK, 1994.
- Prahl, R.E.; Khan, S.; Deo, R.C. *Ampelomyces* mycoparasites of powdery mildews—A review. *Can. J. Plant Pathol.* **2023**. [CrossRef]
- Kiss, L. A review of fungal antagonists of powdery mildews and their potential as biocontrol agents. *Pest Manag. Sci.* **2003**, *59*, 475–483. [CrossRef] [PubMed]
- Kiss, L. Intracellular mycoparasites in action: Interactions between powdery mildew fungi and *Ampelomyces*. In *Stress in Yeasts and Filamentous Fungi*; Avery, S.V., Stratford, M., van West, P., Eds.; Academic Press: Cambridge, MA, USA, 2008; Volume 27, pp. 37–52.
- Hijwegen, T.; Buchenauer, H. Isolation and identification of hyperparasitic fungi associated with Erysiphaceae. *Neth. J. Plant Pathol.* **1984**, *90*, 79–84. [CrossRef]
- Jarvis, W.R.; Shaw, L.A.; Traquair, J.A. Factors affecting antagonism of cucumber powdery mildew by *Stephanoascus flocculosus* and *S. rugulosus*. *Mycol. Res.* **1989**, *92*, 162–165. [CrossRef]
- Verhaar, M.A.; Hijwegen, T.; Zadoks, J.C. Glasshouse experiments on biocontrol of cucumber powdery mildew (*Sphaerotheca fuliginea*) by the mycoparasites *Verticillium lecanii* and *Sporothrix rugulosa*. *Biol. Cont.* **1996**, *6*, 353–360. [CrossRef]
- Hoch, H.C.; Provvidenti, R. Mycoparasitic relationships: Cytology of the *Sphaerotheca fuliginea*-*Tilletiopsis* sp. interaction. *Phytopathology* **1979**, *69*, 359–362. [CrossRef]
- Hijwegen, T. Biological control of cucumber powdery mildew by *Tilletiopsis minor*. *Neth. J. Plant Pathol.* **1986**, *92*, 93–95. [CrossRef]
- Cesati, V. *Ampelomyces quisqualis* Ces. *Bot. Ztg.* **1852**, *10*, 301–302.
- Yarwood, C.E. An overwintering pycnidial stage of *Cicinnobolus*. *Mycologia* **1939**, *31*, 420–422. [CrossRef]
- Jarvis, W.R.; Slingsby, K. The control of powdery mildew of greenhouse cucumber by water sprays and *Ampelomyces quisqualis*. *Plant Dis. Repr.* **1977**, *61*, 728–730.
- Sundheim, L. Control of cucumber powdery mildew by the hyperparasite *Ampelomyces quisqualis* and fungicides. *Plant Pathol.* **1982**, *31*, 209–214. [CrossRef]
- Kiss, L. Natural occurrence of *Ampelomyces* intracellular mycoparasites in mycelia of powdery mildew fungi. *New Phytol.* **1998**, *140*, 709–714. [CrossRef]
- Falk, S.P.; Gadoury, D.M.; Cortesi, P.; Pearson, R.C.; Seem, R.C. Parasitism of *Uncinula necator* cleistothecia by the mycoparasite *Ampelomyces quisqualis*. *Phytopathology* **1995**, *85*, 794–800. [CrossRef]
- Huth, L.; Ash, G.J.; Idnurm, A.; Kiss, L.; Vaghefi, N. The “bipartite” structure of the first genome of *Ampelomyces quisqualis*, a common hyperparasite and biocontrol agent of powdery mildews, may point to its evolutionary origin from plant pathogenic fungi. *Genome Biol. Evol.* **2021**, *13*, evab182. [CrossRef]
- Kiss, L.; Russell, J.C.; Szentiványi, O.; Xu, X.; Jeffries, P. Biology and biocontrol potential of *Ampelomyces* mycoparasites, natural antagonists of powdery mildew fungi. *Biocont. Sci. Technol.* **2004**, *14*, 635–651. [CrossRef]
- Manjunatha, L.; Singh, S.; Ravikumara, B.M.; Narasa Reddy, G.; Senthikumar, M. *Ampelomyces*. In *Beneficial Microbes in Agro-ecology*; Amaresan, N., Senthil Kumar, M., Annapurna, K., Kumar, K., Sankaranarayanan, A., Eds.; Academic Press: Amsterdam, The Netherlands, 2020; Chapter 44; pp. 833–860. [CrossRef]
- Matsuda, Y.; Kashimoto, K.; Takikawa, Y.; Aikami, R.; Nonomura, T.; Toyoda, H. Occurrence of new powdery mildew on greenhouse tomato cultivars. *J. Gen. Plant Pathol.* **2001**, *67*, 294–298. [CrossRef]
- White, J.F., Jr.; Johnston, S.A.; Wang, C.L.; Chin, C.K. First report of powdery mildew in greenhouse-grown tomatoes in New Jersey. *Plant Dis.* **1997**, *81*, 227. [CrossRef] [PubMed]
- Braun, U.; Cook, R.T.A. *Taxonomic Manual of the Erysiphales (Powdery Mildews)*; CBS-KNAW Fungal Biodiversity Centre: Utrecht, The Netherlands, 2012.
- Yarwood, C.E. Powdery mildews. *Bot. Rev.* **1957**, *23*, 235–301. [CrossRef]

30. Braun, U. A monograph of the Erysiphales (powdery mildews). *Beih. Nova Hedwig*. **1987**, *89*, 1–700.
31. Rallos, L.E.E.; Baudoin, A.B. Co-occurrence of two allelic variants of CYP51 in *Erysiphe necator* and their correlation with over-expression for DMI resistance. *PLoS ONE* **2016**, *11*, e0148025. [CrossRef]
32. Pintye, A.; Németh, M.Z.; Molnár, O.; Horváth, Á.; Spitzmüller, Z.; Szalóki, N.; Pal, K.; Váczy, K.; Kovács, G. Improved DNA extraction and quantitative real-time PCR for genotyping *Erysiphe necator* and detecting the DMI fungicide resistance marker A495T, using single ascocarps. *Phytopathol. Medit.* **2020**, *59*, 97–106. [CrossRef]
33. Huggenberger, F.; Collins, M.A.; Skylakakis, G. Decreased sensitivity of *Sphaerotheca fuliginea* to fenarimol and other ergosterol-biosynthesis inhibitors. *Crop Prot.* **1984**, *3*, 137–149. [CrossRef]
34. McGrath, M.T.; Shishkoff, N. Resistance to triadimefon and benomyl: Dynamics and impact on managing cucurbit powdery mildew. *Plant Dis.* **2001**, *85*, 147–154. [CrossRef]
35. McGrath, M.T.; Shishkoff, N. First report of the cucurbit powdery mildew fungus (*Podosphaera xanthii*) resistant to strobilurin fungicides in the United States. *Plant Dis.* **2003**, *87*, 1007. [CrossRef]
36. Lebeda, A.; Sedláková, B. Fungicide resistance in population of cucurbit powdery mildew. *J. Plant Pathol.* **2008**, *90*, S2.142.
37. Petit, A.N.; Fontaine, F.; Vatsa, P.; Clément, C.; Vaillant-Gaveau, N. Fungicide impacts on photosynthesis in crop plants. *Photosyn. Res.* **2012**, *111*, 315–326. [CrossRef] [PubMed]
38. Geiger, F.; Bengtsson, J.; Berendse, F.; Weisser, W.W.; Emmerson, M.; Morales, M.B.; Ceryngier, P.; Liira, J.; Tschirntke, T.; Winqvist, C.; et al. Persistent negative effects of pesticides on biodiversity and biological control potential on European farmland. *Basic Appl. Ecol.* **2010**, *11*, 97–105. [CrossRef]
39. De Bary, A. *Eurotium, Erysiphe, Cicinnobolus*: Nebst Bemerkungen über die Geschlechtsorgane der Ascomyceten. In *Beiträge zur Morphologie und Physiologie der Pilze*; De Bary, A., Woronin, M., Eds.; Verlag von C. Winter: Frankfurt, Germany, 1870; pp. 1–95.
40. Rogers, D. On *Cicinnobolus*. *Mycologia* **1959**, *51*, 96–98. [CrossRef]
41. Kiss, L.; Nakasone, K.K. Ribosomal DNA internal transcribed spacer sequences do not support the species status of *Ampelomyces quisqualis*, a hyperparasite of powdery mildew fungi. *Curr. Genet.* **1998**, *33*, 362–367. [CrossRef] [PubMed]
42. Liang, C.; Yang, J.; Kovács, G.M.; Szentiványi, O.; Li, B.; Xu, X.; Kiss, L. Genetic diversity of *Ampelomyces* mycoparasites isolated from different powdery mildew species in China inferred from analyses of rDNA ITS sequences. *Fungal Div.* **2007**, *24*, 225–240.
43. Pintye, A.; Bereczky, Z.; Kovács, G.M.; Nagy, L.G.; Xu, X.; Legler, S.E.; Váczy, Z.; Váczy, K.Z.; Caffi, T.; Rossi, V.; et al. No indication of strict host associations in a widespread mycoparasite: Grapevine powdery mildew (*Erysiphe necator*) is attacked by phylogenetically distant *Ampelomyces* strains in the field. *Phytopathology* **2012**, *102*, 707–716. [CrossRef]
44. Park, M.-J.; Choi, Y.-J.; Hong, S.-B.; Shin, H.-D. Genetic variability and mycohost association of *Ampelomyces quisqualis* isolates inferred from phylogenetic analyses of ITS rDNA and actin gene sequences. *Fungal Biol.* **2010**, *114*, 235–247. [CrossRef]
45. Prah, R.E.; Khan, S.; Deo, R.C. The role of internal transcribed spacer 2 secondary structures in classifying mycoparasitic *Ampelomyces*. *PLoS ONE* **2021**, *16*, e0253772. [CrossRef]
46. Legler, S.E.; Pintye, A.; Caffi, T.; Gulyás, S.; Bohár, G.; Rossi, V.; Kiss, L. Sporulation rate in culture and mycoparasitic activity, but not mycohost specificity, are the key factors for selecting *Ampelomyces* strains for biocontrol of grapevine powdery mildew (*Erysiphe necator*). *Eur. J. Plant Pathol.* **2016**, *144*, 723–736. [CrossRef]
47. Kiss, L. Genetic diversity in *Ampelomyces* isolates, hyperparasites of powdery mildew fungi, inferred from RFLP analysis of the rDNA ITS region. *Mycol. Res.* **1997**, *101*, 1073–1080. [CrossRef]
48. Hino, I.; Kato, H. *Cicinnoboli* parasitic on mildew fungi. *Bull. Miyazaki Coll. Agric. For.* **1929**, *1*, 91–98.
49. Emmons, C.W. *Cicinnobolus cesatii*, a study in host-parasite relationships. *Bull. Torrey Bot. Club* **1930**, *57*, 421–439. [CrossRef]
50. Blumer, S. Die Erysiphaceen Mitteleuropas mit besonderer Berücksichtigung der Schweiz. *Beitr. Zur Kryptogamenflora Schweiz* **1933**, *7*, 1–483.
51. Clare, B.G. *Ampelomyces quisqualis* (*Cicinnobolus cesatii*) on Queensland Erysiphaceae. *Univ. Qld. Pap.* **1964**, *4*, 147–149.
52. Belsare, S.W.; Moniz, L.; Deo, V.B. The hyperparasite *Ampelomyces quisqualis* Ces. from Maharashtra State, India. *Biovigyanam* **1980**, *6*, 173–176.
53. Hanlin, R.T.; Tortolero, O. *Brasiliomyces*, a new host for *Ampelomyces*. *Mycotaxon* **1984**, *21*, 459–462.
54. Nagy, S.G.; Vajna, L. *Ampelomyces* fajok előfordulása lisztharagombákban Magyarországon. *Mikológiai Közlemények* **1990**, *29*, 103–112. (In Hungarian)
55. Puzanova, L.A. Distribution of hyperparasites from the genus *Ampelomyces* Ces. ex Schlecht. on the powdery mildew fungi in northern Caucasus and their importance in disease control. *Mikol. I Fitopatol.* **1991**, *25*, 438–442. (In Russian)
56. Tsay, J.G.; Tung, B. *Ampelomyces quisqualis* Ces. ex Schlecht., a hyperparasite of the asparagus bean powdery mildew pathogen *Erysiphe polygoni* in Taiwan. *Trans. Mycol. Soc. R.O.C.* **1991**, *6*, 55–58.
57. Paulech, C.; Herrera, S.; Fernet, E. Phytopathogenic micromycetes of the family Erysiphaceae distributed in Cuba. *Ceska Mykol.* **1993**, *46*, 303–314. (In Slovakian)
58. Shin, H.-D. Isolation and identification of hyperparasites against powdery mildew fungi in Korea. *Kor. J. Mycol.* **1994**, *22*, 355–365. (In Korean)
59. Kiss, L. Graminicolous powdery mildew fungi as new natural hosts of *Ampelomyces* mycoparasites. *Can. J. Bot.* **1997**, *75*, 680–683. [CrossRef]
60. Ranković, B. Hyperparasites of the genus *Ampelomyces* on powdery mildew fungi in Serbia. *Mycopathologia* **1997**, *139*, 157–164. [CrossRef]

61. Németh, M.Z.; Mizuno, Y.; Kobayashi, H.; Seress, D.; Shishido, N.; Kimura, Y.; Takamatsu, S.; Suzuki, T.; Takikawa, Y.; Kakutani, K.; et al. *Ampelomyces* strains isolated from diverse powdery mildew hosts in Japan: Their phylogeny and mycoparasitic activity, including timing and quantifying mycoparasitism of *Pseudoidium neolycopersici* on tomato. *PLoS ONE* **2021**, *16*, e0251444. [CrossRef] [PubMed]
62. Németh, M.Z.; Pintye, A.; Horváth, Á.N.; Vági, P.; Kovács, G.M.; Gorfer, M.; Kiss, L. Green fluorescent protein transformation sheds more light on a widespread mycoparasitic interaction. *Phytopathology* **2019**, *109*, 1404–1416. [CrossRef] [PubMed]
63. Riess, H. Uber *Byssocystis textilis*. *Hedwigia* **1852**, *1*, 23.
64. Yarwood, C.E. *Ampelomyces quisqualis* on clover mildew. *Phytopathology* **1932**, *22*, 31.
65. Siozios, S.; Tosi, L.; Ferrarini, A.; Ferrari, A.; Tonomi, P.; Bellin, D.; Maurhofer, M.; Gessler, C.; Delledonne, M.; Pertot, I. Transcriptional reprogramming of the mycoparasitic fungus *Ampelomyces quisqualis* during the powdery mildew host-induced germination. *Phytopathology* **2015**, *105*, 199–209. [CrossRef]
66. Sivakumar, T.; Balabaskar, P.; Renganathan, P.; Sanjeevkumar, K. To evaluate the bio-efficacy and phytotoxicity of powder formulation of Biodewcon (*Ampelomyces quisqualis* 2.00% Wp) against powdery mildew (*Sphaerotheca fuliginea*) in cucumber crop. *Plant Arch.* **2020**, *20*, 3811–3815.
67. Németh, M.Z.; Li, G.; Seress, D.; Pintye, A.; Molnár, O.; Kovács, G.M.; Kiss, L.; Gorfer, M. What is the role of the nitrate reductase (*euknr*) gene in fungi that live in nitrate-free environments? A targeted gene knock-out study in *Ampelomyces* mycoparasites. *Fungal Biol.* **2021**, *125*, 905–913. [CrossRef] [PubMed]
68. Sundheim, L.; Krekling, T. Host-parasite relationships of the hyperparasite *Ampelomyces quisqualis* and its powdery mildew host *Sphaerotheca fuliginea*. *Phytopath. Z.* **1982**, *104*, 202–210. [CrossRef]
69. Hashioka, Y.; Nakai, Y. Ultrastructure of pycnidial development and mycoparasitism of *Ampelomyces quisqualis* parasitic on Erysiphales. *Trans. Mycol. Soc. Jpn.* **1980**, *21*, 329–338.
70. Angeli, D.; Puopolo, G.; Maurhofer, M.; Gessler, C.; Pertot, I. Is the mycoparasitic activity of *Ampelomyces quisqualis* biocontrol strains related to phylogeny and hydrolytic enzyme production? *Biol. Cont.* **2012**, *63*, 348–358. [CrossRef]
71. Rotem, Y.; Yarden, O.; Szejnberg, A. The mycoparasite *Ampelomyces quisqualis* expresses *exgA* encoding and *exo-β-1,3*-glucanase in culture and during mycoparasitism. *Phytopathology* **1999**, *89*, 631–638. [CrossRef]
72. Philipp, W.D. Extracellular enzymes and nutritional physiology of *Ampelomyces quisqualis* Ces., hyperparasite of powdery mildew, *in vitro*. *J. Phytopathol.* **1985**, *114*, 274–283. [CrossRef]
73. Vaidya, S.; Thakur, V.S. *Ampelomyces quisqualis* Ces.—A mycoparasite of apple powdery mildew in western Himalayas. *Indian Phytopathol.* **2005**, *58*, 250–251.
74. Szentiványi, O.; Kiss, L.; Russell, J.C.; Kovács, G.M.; Varga, K.; Jankovics, T.; Lesemann, S.; Xu, X.-M.; Jeffries, P. *Ampelomyces* mycoparasites from apple powdery mildew identified as a distinct group based on single-stranded conformation polymorphism analysis of the rDNA ITS region. *Mycol. Res.* **2005**, *109*, 429–438. [CrossRef] [PubMed]
75. Liyanage, K.K.; Khan, S.; Brooks, S.; Mortimer, P.E.; Karunarathna, S.C.; Xu, J.; Hyde, K.D. Morpho-molecular characterization of two *Ampelomyces* spp. (Pleosporales) strains mycoparasites of powdery mildew of *Hevea brasiliensis*. *Front. Microbiol.* **2018**, *9*, 1–10. [CrossRef]
76. Angeli, D.; Maurhofer, M.; Gessler, C.; Pertot, I. Existence of different physiological forms within genetically diverse strains of *Ampelomyces quisqualis*. *Phytoparasitica* **2012**, *40*, 37–51. [CrossRef]
77. Kiss, L.; Pintye, A.; Kovács, G.M.; Jankovics, T.; Fontaine, M.C.; Harvey, N.; Xu, X.; Nicot, P.C.; Bardin, M.; Shykoff, J.A.; et al. Temporal isolation explains host-related genetic differentiation in a group of widespread mycoparasitic fungi. *Mol. Ecol.* **2011**, *20*, 1492–1507. [CrossRef]
78. Pintye, A.; Ropars, J.; Harvey, N.; Shin, H.-D.; Leyronas, C.; Nicot, P.C.; Giraud, T.; Kiss, L. Host phenology and geography as drivers of differentiation in generalist fungal mycoparasites. *PLoS ONE* **2015**, *10*, e0120703. [CrossRef]
79. Szejnberg, A.; Galper, S.; Mazar, S.; Lisker, N. *Ampelomyces quisqualis* for biological and integrated control of powdery mildews in Israel. *J. Phytopathol.* **1989**, *124*, 285–295. [CrossRef]
80. Paratt, S.R.; Laine, A.-L. Pathogen dynamics under both bottom-up host resistance and top-down hyperparasite attack. *J. Appl. Ecol.* **2018**, *55*, 2976–2985. [CrossRef] [PubMed]
81. Philipp, W.-D.; Crüger, G. Parasitismus von *Ampelomyces quisqualis* auf echten Mehлтаupilzenal von Gurken und anderen Gemüsearten. *Z. Pflanzenkrankh. Pflanzenschutz* **1979**, *86*, 129–142.
82. Falk, S.P.; Gadoury, D.M.; Pearson, R.C.; Seem, R.C. Partial control of grape powdery mildew by the mycoparasite *Ampelomyces quisqualis*. *Plant Dis.* **1995**, *79*, 483–490. [CrossRef]
83. Mairovich, G.; Marder, J.B.; Shtienberg, D.; Szejnberg, A. Studies of biological control of powdery mildew in cereals by the hyperparasite *Ampelomyces quisqualis*. *Phytoparasitica* **1996**, *24*, 157–158.
84. Szentiványi, O.; Kiss, L. Overwintering of *Ampelomyces* mycoparasites on apple trees and other plants infected with powdery mildews. *Plant Pathol.* **2003**, *52*, 737–746. [CrossRef]
85. Poulin, R.; Krasnov, B.R.; Mouillot, D. Host specificity in phylogenetic and geographic space. *Trends Parasitol.* **2011**, *27*, 355–361. [CrossRef]
86. Szejnberg, A. Biological control of powdery mildews by *Ampelomyces quisqualis*. *Phytopathology* **1979**, *69*, 1047.
87. Sundheim, L. *Ampelomyces quisqualis*, a hyperparasitic fungus in biological control of powdery mildews on greenhouse cucumber. *Acta Hort.* **1984**, *156*, 229–236. [CrossRef]

88. Philipp, W.-D.; Grauer, U.; Grossmann, F. Ergänzende Untersuchungen zur biologischen und integrierten Bekämpfung von Gurkenmehltau unter Glass durch *Ampelomyces quisqualis*. Z. Pflanzenkrankh. Pflanzenschutz **1984**, *91*, 438–443.
89. Szejnberg, A.; Mazar, S. Biocontrol of cucumber and carrot powdery mildew by *Ampelomyces quisqualis*. Phytopathology **1985**, *75*, 1301–1302.
90. Dik, A.J.; Verhaar, M.A.; Bélanger, R.R. Comparison of three biological control agents against cucumber powdery mildew (*Sphaerotheca fuliginea*) in semi-commercial-scale glasshouse trials. Eur. J. Plant Pathol. **1998**, *104*, 413–423. [CrossRef]
91. Shishkoff, N.; McGrath, M.T. AQ10 biofungicide combined with chemical fungicides or AddQ spray adjuvant for control of cucurbit powdery mildew in detached leaf culture. Plant Dis. **2002**, *86*, 915–918. [CrossRef] [PubMed]
92. Angeli, D.; Saharan, K.; Segarra, G.; Sicher, C.; Pertot, I. Production of *Ampelomyces quisqualis* conidia in submerged fermentation and improvements in the formulation for increased shelf-life. Crop Prot. **2017**, *97*, 135–144. [CrossRef]
93. Szejnberg, A.; Mazar, S. Studies on the hyperparasite *Ampelomyces quisqualis* and preliminary trials on biological control of powdery mildew. Phytoparasitica **1983**, *11*, 219–220.
94. Romero, D.; Rivera, M.E.; Cazorla, F.M.; De Vicente, A.; Pérez-García, A. Effect of mycoparasitic fungi on the development of *Sphaerotheca fusca* in melon leaves. Mycol. Res. **2003**, *107*, 64–71. [CrossRef]
95. Kimura, Y.; Németh, M.Z.; Numano, K.; Mitao, A.; Shirakawa, T.; Seress, D.; Takikawa, Y.; Kakutani, K.; Matsuda, Y.; Kiss, L.; et al. Hyperparasitic fungi against melon powdery mildew pathogens: Quantitative analysis of conidia released from single colonies of *Podosphaera xanthii* parasitized by *Ampelomyces*. Agronomy **2023**, *13*, 1204. [CrossRef]
96. Hofstein, R.; Fridlender, B. Development of production, formulation and delivery systems. In Brighton Crop Protection Conference, Pest and Diseases; British Crop Protection Council: Farnham, UK, 1994; Volume 3, pp. 1273–1280.
97. Hofstein, R.; Daoust, R.A.; Aeschlimann, J.P. Constrains to the development of biofungicides: The example of “AQ10”, a new product for controlling powdery mildews. Entomophaga **1996**, *41*, 455–460. [CrossRef]
98. Pasini, C.; D’Aquila, F.; Curir, P.; Gullino, M.L. Effectiveness of antifungal compounds against rose powdery mildew (*Sphaerotheca pannosa* var. *rosae*) in glasshouses. Crop Prot. **1997**, *16*, 251–256. [CrossRef]
99. Pertot, I.; Zasso, R.; Amsalem, L.; Baldessari, M.; Angeli, G.; Elad, Y. Integrating biocontrol agents in strawberry powdery mildew control strategies in high tunnel growing systems. Crop Prot. **2008**, *27*, 622–631. [CrossRef]
100. Gautam, A.K.; Avasthi, S. *Ampelomyces quisqualis* Ces.—A mycoparasite of *Euphorbia hirta* powdery mildew in Himachal Pradesh, India. J. Phytopathol. Pest Manag. **2016**, *3*, 64–70.
101. Parratt, S.R.; Barrès, B.; Penczykowski, R.M.; Laine, A.L. Local adaptation at higher trophic levels: Contrasting hyperparasite-pathogen infection dynamics in the field and laboratory. Mol. Ecol. **2017**, *26*, 1964–1979. [CrossRef] [PubMed]
102. Carbó, A.; Teixidó, N.; Usall, J.; Solsona, C.; Torres, R. Formulated *Ampelomyces quisqualis* CPA-9 applied on zucchini leaves: Influence of abiotic factors and powdery mildew mycoparasitization. Eur. J. Plant Pathol. **2021**, *161*, 37–48. [CrossRef]
103. Philipp, W.-D.; Beuther, E.; Hermann, D.; Klinkert, F.; Oberwalder, C.; Schmidtke, M.; Straub, B. Zur Formulierung des Mehltauhyperparasiten *Ampelomyces quisqualis* Ces. Z. Pflanzenkrankh. Pflanzenschutz **1990**, *97*, 120–132.
104. Gu, Y.H.; Ko, W.H. Water agarose medium for studying factors affecting germination of conidia of *Ampelomyces quisqualis*. Mycol. Res. **1997**, *101*, 422–424. [CrossRef]
105. Suzuki, T.; Murakami, T.; Takizumi, Y.; Ishimaru, H.; Kudo, D.; Takikawa, Y.; Matsuda, Y.; Kakutani, K.; Bai, Y.; Nonomura, T. Trichomes: Interaction sites of tomato leaves with biotrophic powdery mildew pathogens. Eur. J. Plant Pathol. **2018**, *150*, 115–125. [CrossRef]
106. Speer, E.O. *Ampelomyces cesati* (Fungi, Sphaeropsidales). Taxon **1978**, *27*, 549–562. [CrossRef]
107. Kiss, L.; Pintye, A.; Zséli, G.; Jankovics, T.; Szentiványi, O.; Hafez, Y.M.; Cook, R.T.A. Microcyclic conidiogenesis in powdery mildews and its association with intracellular parasitism by *Ampelomyces*. Eur. J. Plant Pathol. **2010**, *126*, 445–451. [CrossRef]
108. Zeng, L.F.; Jiang, Y.C. An investigation of parasitic fungi on *Erysiphe* spp. RoPP **1986**, *65*, 419.
109. Machida, K.; Trifonov, L.S.; Ayer, W.A.; Lu, Z.-X.; Laroche, A.; Huang, H.C.; Cheng, K.J.; Zantige, J.L. 3(2H)-Benzofuranones and chromanes from liquid cultures of the mycoparasitic fungus *Coniothyrium minitans*. Phytochemistry **2001**, *58*, 173–177. [CrossRef] [PubMed]
110. McQuilken, M.P.; Gemmell, J.; Whipps, J.M. Some nutritional factors affecting production of biomass and antifungal metabolites of *Coniothyrium minitans*. Biocont. Sci. Technol. **2002**, *12*, 443–454. [CrossRef]
111. McQuilken, M.P.; Gemmell, J.; Hill, R.A.; Whipps, J.M. Production of macrospheptide A by the mycoparasite *Coniothyrium minitans*. FEMS Microbiol. Lett. **2003**, *219*, 27–31. [CrossRef] [PubMed]
112. Beuther, E.; Philipp, W.D.; Grossmann, F. Untersuchungen zum hyperparasitismus von *Ampelomyces quisqualis* auf gurkenmehltau (*Sphaerotheca fuliginea*). Phytopath. Z. **1981**, *101*, 265–270. [CrossRef]
113. Aylor, D.E. The role of intermittent wind in the dispersal of fungal pathogens. Annu. Rev. Phytopathol. **1990**, *28*, 73–92. [CrossRef]
114. Brown, J.K.M.; Hovmöller, M.S. Aerial dispersal of pathogens on the global and continental scales and its impact on plant disease. Science **2002**, *297*, 537–541. [CrossRef]
115. Nonomura, T.; Matsuda, Y.; Yamashita, S.; Akahoshi, H.; Takikawa, Y.; Kakutani, K.; Toyoda, H. Natural woody plant, *Mallotus japonicus*, as an ecological partner to transfer different pathotypic conidia of *Oidium neolycopersici* to greenhouse tomatoes. Plant Protect. Sci. **2013**, *49*, S33–S40. [CrossRef]

116. Suzuki, T.; Iwasaki, S.; Hisazumi, H.; Miyamoto, A.; Ogami, H.; Takikawa, Y.; Kakutani, K.; Matsuda, Y.; Nonomura, T. Inhibitory effects of blue light-emitting diode irradiation on *Podosphaera xanthii* conidial release and infection of melon seedlings. *Agriculture* **2022**, *12*, 198. [CrossRef]
117. Rouse, D.I.; MacKenzie, D.R.; Nelson, R.R. Density dependent sporulation of *Erysiphe graminis* f. sp. *tritici*. *Phytopathology* **1984**, *74*, 1176–1180. [CrossRef]
118. Bushnell, W.R. The role of powdery mildew research in understanding host-parasite interaction: Past, present, and future. In *The Powdery Mildews: A Comprehensive Treatise*; Bélanger, R.R., Bushnell, W.R., Dik, A.J., Carver, T.L.W., Eds.; APS Press: St. Paul, MN, USA, 2002; pp. 1–12.
119. Suzuki, T.; Nakamura, R.; Takagi, N.; Takikawa, Y.; Kakutani, K.; Matsuda, Y.; Matsui, K.; Nonomura, T. Quantitative analysis of the lifelong production of conidia released from single colonies of *Podosphaera xanthii* on melon leaves using electrostatic techniques. *Austral. Plant Pathol.* **2019**, *48*, 297–307. [CrossRef]
120. Ayabe, S.; Kimura, Y.; Umei, N.; Takikawa, Y.; Kakutani, K.; Matsuda, Y.; Nonomura, T. Real-time collection of conidia released from living single colonies of *Podosphaera aphanis* on strawberry leaves under natural conditions with electrostatic techniques. *Plants* **2022**, *11*, 3453. [CrossRef]
121. Kiss, L. The role of hyperparasites in host plant–parasitic fungi relationships. In *Biotic Interactions in Plant–Pathogen Associations*; Jeger, M.J., Spence, N.J., Eds.; CABI Publishing: Wallingford, UK, 2001; pp. 227–236.
122. Daoust, R.A.; Hofstein, R. *Ampelomyces quisqualis*, a new biofungicide to control powdery mildew in grapes. In *Brighton Crop Protection Conference, Pest and Diseases*; British Crop Protection Council: Farnham, UK, 1996; Volume 1, pp. 33–40.
123. Sundheim, L.; Tronsmo, A. Hyperparasites in biological control. In *Biocontrol of Plant Diseases*; Mukerji, K.G., Garg, K.L., Eds.; CRC Press: Boca Raton, FL, USA, 1988; Volume 1, pp. 53–69.
124. Kiss, L. How dangerous is the use of fungal biocontrol agents to nontarget organisms? *New Phytol.* **2004**, *163*, 453–455. [CrossRef] [PubMed]
125. Paulitz, T.C.; Bélanger, R.R. Biological control in greenhouse systems. *Annu. Rev. Phytopathol.* **2001**, *39*, 103–133. [CrossRef] [PubMed]
126. Bélanger, R.R.; Labbé, C. Control of powdery mildews without chemicals: Prophylactic and biological alternatives for horticultural crops. In *The Powdery Mildews: A Comprehensive Treatise*; Bélanger, R.R., Bushnell, W.R., Dik, A.J., Carver, T.L.W., Eds.; APS Press: St. Paul, MN, USA, 2002; pp. 256–267.
127. Kaur, L.; Gupta, B.; Sharma, I.M.; Joshi, A.K. Eco-friendly management of powdery mildew of mango through biocontrol agents. *Int. J. Curr. Microbiol. Appl. Sci.* **2018**, *7*, 392–396. [CrossRef]
128. Philipp, W.-D.; Hellstern, A. Biologische Mehlaubekämpfung mit *Ampelomyces quisqualis* bei reduzierter Luftfeuchtigkeit. *Z. Pflanzenkrankh. Pflanzenschutz* **1986**, *93*, 384–391.
129. Verhaar, M.A.; Keressies, A.; Hijwegen, T. Effect of RH on mycoparasitism of rose powdery mildew with and without treatments with mycoparasites. *Z. Pflanzenkrankh. Pflanzenschutz* **1999**, *106*, 158–165.
130. Epton, H.A.S.; Hamed El Nil, Y.F. Improvement in the hyperparasitic activity of *Ampelomyces quisqualis* in the biocontrol of powdery mildew of cucumber. *IOBC/WPRS Bull.* **1993**, *16*, 86–89.
131. Hijwegen, T. Biological control of cucumber powdery mildew with *Tilletiopsis minor* under greenhouse conditions. *Neth. J. Plant Pathol.* **1992**, *98*, 221–225. [CrossRef]
132. McGrath, M.T.; Shishkoff, N. Evaluation of biocompatible products for managing cucurbit powdery mildew. *Crop Prot.* **1999**, *18*, 471–478. [CrossRef]
133. Szejnberg, A.; Galper, S.; Lisker, N. Conditions for pycnidial production and spore formation by *Ampelomyces quisqualis*. *Can. J. Microbiol.* **1990**, *36*, 193–198. [CrossRef]
134. Gilardi, G.; Manker, D.C.; Garibaldi, A.; Gullino, M.L. Efficacy of the biocontrol agents *Bacillus subtilis* and *Ampelomyces quisqualis* applied in combination with fungicides against powdery mildew of zucchini. *J. Plant Dis. Prot.* **2008**, *115*, 208–213. [CrossRef]
135. Hijwegen, T. Effect of seventeen fungicolous fungi on sporulation of cucumber powdery mildew. *Neth. J. Plant Pathol.* **1988**, *94*, 185–190. [CrossRef]
136. Carbó, A.; Torres, R.; Usall, J.; Ballesta, J.; Teixidó, N. Biocontrol potential of *Ampelomyces quisqualis* strain CPA-9 against powdery mildew: Conidia production in liquid medium and efficacy on zucchini leaves. *Sci. Hortic.* **2020**, *267*, 109337. [CrossRef]

Disclaimer/Publisher’s Note: The statements, opinions and data contained in all publications are solely those of the individual author(s) and contributor(s) and not of MDPI and/or the editor(s). MDPI and/or the editor(s) disclaim responsibility for any injury to people or property resulting from any ideas, methods, instructions or products referred to in the content.



Article

Hyperparasitic Fungi against Melon Powdery Mildew Pathogens: Quantitative Analysis of Conidia Released from Single Colonies of *Podosphaera xanthii* Parasitised by *Ampelomyces*

Yutaka Kimura ^{1,†}, Márk Z. Németh ^{2,†}, Kana Numano ¹, Asami Mitao ¹, Tomomi Shirakawa ³, Diána Seress ², Yoshihiro Takikawa ⁴, Koji Kakutani ⁵, Yoshinori Matsuda ¹, Levente Kiss ^{2,6} and Teruo Nonomura ^{1,7,*}

- ¹ Laboratory of Phytoprotection, Science and Technology, Faculty of Agriculture, Kindai University, Nara 631-8505, Japan; walk011kimu_ax000@icloud.com (Y.K.); mano0823kaa@gmail.com (K.N.); 2011410196f@nara.kindai.ac.jp (A.M.); ymatsuda@nara.kindai.ac.jp (Y.M.)
- ² Plant Protection Institute, Centre for Agricultural Research, H-1525 Budapest, Hungary; nemeth.mark@atk.hu (M.Z.N.); seress.diana@atk.hu (D.S.); kiss.levente@atk.hu or levente.kiss@usq.edu.au (L.K.)
- ³ Biological Evaluation Group, Agrochemicals Research Center, Research & Development Division, Mitsui Chemicals Agro, Inc., Yasu-shi 520-2362, Japan; tomomi.shirakawa@mitsuichemicals.com
- ⁴ Plant Center, Institute of Advanced Technology, Kindai University, Wakayama 642-0017, Japan; takikawa@waka.kindai.ac.jp
- ⁵ Pharmaceutical Research and Technology Institute, Kindai University, Osaka 577-8502, Japan; 934097@kindai.ac.jp
- ⁶ Centre for Crop Health, University of Queensland, Toowoomba, QLD 4350, Australia
- ⁷ Agricultural Technology and Innovation Research Institute, Kindai University, Nara 631-8505, Japan
- * Correspondence: nonomura@nara.kindai.ac.jp; Tel.: +81-742-43-5194
- † These authors contributed equally to this work.

Citation: Kimura, Y.; Németh, M.Z.; Numano, K.; Mitao, A.; Shirakawa, T.; Seress, D.; Takikawa, Y.; Kakutani, K.; Matsuda, Y.; Kiss, L.; et al. Hyperparasitic Fungi against Melon Powdery Mildew Pathogens: Quantitative Analysis of Conidia Released from Single Colonies of *Podosphaera xanthii* Parasitised by *Ampelomyces*. *Agronomy* **2023**, *13*, 1204. <https://doi.org/10.3390/agronomy13051204>

Academic Editor: Francesco Calzarano

Received: 8 March 2023
 Revised: 19 April 2023
 Accepted: 22 April 2023
 Published: 24 April 2023



Copyright: © 2023 by the authors. Licensee MDPI, Basel, Switzerland. This article is an open access article distributed under the terms and conditions of the Creative Commons Attribution (CC BY) license (<https://creativecommons.org/licenses/by/4.0/>).

Abstract: In this study, we evaluated the effectiveness of hyperparasitic fungi in controlling powdery mildew (PM). In a greenhouse, we spray-inoculated single colonies of the melon PM-causing fungus *Podosphaera xanthii* strain KMP-6N at three different fungal developmental stages (i.e., 5, 10, and 15 days old) with spores of the hyperparasitic fungus *Ampelomyces* sp. strain Xs-q. After spray inoculation, we collected and counted KMP-6N conidia produced as asexual progeny from PM colonies using an electrostatic rotational spore collector. Collector insulator films were replaced at 24 h intervals until KMP-6N ceased to release additional progeny conidia. Conidial releases from each of the single Xs-q-inoculated KMP-6N colonies gradually reduced, then stopped within ca. 4 and 8 days of the first treatment in 5- and 10-day-old KMP-6N colonies, and within ca. 20 days of the second spray treatment in 15-day-old KMP-6N colonies, respectively. The total numbers of asexual progeny conidia collected from single 5-, 10-, and 15-day-old colonies were ca. 156, 1167, and 44,866, respectively. After electrostatic spore collection, conidiophores in Xs-q-uninoculated KMP-6N colonies appeared normal, whereas almost all conidiophores in 5- and 10-day-old Xs-q-inoculated KMP-6N colonies were completely deformed or collapsed due to the infection of the hyperparasitic fungus. This is the first study to apply electrostatic and digital microscopic techniques to clarify the impact of fungal hyperparasitism on mycohost survival, and, in particular, to assess quantitatively and visually the suppression of conidial release from any PM colonies infected with *Ampelomyces*.

Keywords: biological control; catenated conidia; conidiophores; *Cucumis melo*; electrostatic field; electrostatic spore collector; mycoparasites; pycnidium formation

1. Introduction

Powdery mildew (PM) is a serious disease affecting many crops, including cucurbits in many countries [1–13]. PM causes leaf damage and significantly reduces cucurbit

productivity [4,9,14]. In Japan, a severe PM outbreak occurred in melon (*Cucumis melo* cv. 'Earl's Favourite') cultivated hydroponically in a greenhouse [15]. The fungus isolated from PM-infected melon leaves was identified as *Podosphaera xanthii* (syn. *Podosphaera fuliginea*, *Sphaerotheca fuliginea*, *Sphaerotheca fusca*; anamorph: *Fibroidium*) based on morphological and genetic characteristics including ribosomal DNA internal transcribed spacer sequences (rDNA-ITS) [15].

Growers spray fungicides before or after PM colonies appear on host leaves, to control disease. However, frequent application can cause resistance to commercial fungicides in the fungi causing PM, as shown in diseased cucurbit plants [16–22]. To avoid fungicide resistance and environmental problems caused by fungicide residues, new control strategies that are independent of chemical methods are needed to control PM. The hyperparasitic fungus *Ampelomyces quisqualis* is a slow-growing pycnidial fungus that is widely distributed among PMs (family Erysiphaceae) [23–26] and acts as a hyperparasite of PM fungi that infect cultivated and wild plants [26–30] including *P. xanthii* Pollacci on cucumber [24,25,31–37] and melon [38,39]. *Ampelomyces* isolates have been developed as commercial biofungicide products and applied as biocontrol agents (BCAs) against PMs in various crops [29,30,40–42]; these agents include AQ10 (Ecogen Inc., Langhorne, PA, USA), Q-fect (Green Biotech, Paju, South Korea), and Powderycare (AgriLife, Medak, India). These hyperparasitic fungi kill PM-causing fungi by invading and destroying their cytoplasm [28,43,44]. The life cycles, modes of action, and biocontrol potential of hyperparasitic fungi have been reviewed previously [45,46]. Recently, Németh et al. [47] visualised *A. quisqualis* transformants expressing an integrated green fluorescent protein (GFP) gene in PM-causing fungi and PM-infected leaves, and they clarified the localisation of hyperparasitic fungi in PM hyphae. In addition, Németh et al. [48] analysed the infection processes of *Ampelomyces* strains used as BCAs against *Erysiphe neolycopersici* that developed on tomato cv. 'Moneymaker' trichome cells using high-fidelity digital microscopy to clarify aspects of the biology and infection sites of these hyperparasitic fungi in their mycohosts.

PM-causing fungi produce asexual conidia on conidiophores, which are the source of host plant infection; conidia are dispersed by wind over large areas [49–52]. In a previous study, we collected and quantitatively analysed all progeny conidia released from single living colonies of a fungus causing melon PM throughout their lifetime under greenhouse conditions, using an electrostatic rotational spore collector consisting of a dielectrically polarised insulator drum [53]. The insulators of the collection device are electrified through dielectric polarisation caused by a charged conductor, so that the polarised dipole insulators produce a non-uniform electric field around them, creating an electrostatic force [54,55]. Because violently projected wind-dispersed fungal spores become electrically charged at the moment of release [56], conidia are attracted to both negatively and positively polarised insulator cylinders by this electrostatic force, as demonstrated previously in tomato PM [57,58]. The collection device has no detrimental effect on the survival of the fungus, even when exposed to electrostatic force throughout its lifetime; conidia collected via electrostatic force produce normally elongated hyphae and form conidiophores that produce living progeny conidia [53,59].

In this study, we applied our previously developed electrostatic spore collection system, incorporating a recent methodological advance [48], to collect all progeny conidia released from single *P. xanthii* KMP-6N colonies spray-inoculated with a Japanese strain of *Ampelomyces*, and estimated the impact of this hyperparasitic fungus on melon PM colonies through quantitative analysis of the total number of *P. xanthii* KMP-6N conidia attracted to the insulators. The results of this study will contribute to developing strategies for the practical application of *Ampelomyces* strains as BCAs against melon PMs. To our knowledge, this is the first study to apply electrostatic and digital microscopic techniques to study the impact of fungal hyperparasitism on mycohost survival and, in particular, to assess quantitatively and visually the suppression of conidial release from any PM colonies infected with *Ampelomyces*.

2. Materials and Methods

2.1. Plant Materials and Cultivation

Melon seeds (*Cucumis melo* cv. 'Earl's Favourite'; F1 hybrid plants derived from a 'Natsukei-1' × 'Natsukei-4' cross) were supplied by the Yuasa Experimental Farm, Kindai University (Wakayama, Japan). The seeds were placed on wet filter paper in Petri dishes and germinated for 3–4 days in a growth chamber (LH-240N; Nippon Medical and Chemical Instruments, Osaka, Japan) under continuous illumination ($22.2 \mu\text{mol m}^{-2} \text{s}^{-1}$; 380–750 nm) with white (full-spectrum) fluorescent lamps (FL40SS W/37; Mitsubishi, Tokyo, Japan) at $25 \pm 2 \text{ }^\circ\text{C}$. The germinated seedlings were placed on polyurethane cubic sponge supports (3 cm × 3 cm × 3 cm) that were inserted into 30 mL cylindrical plastic containers (diameter, 3 cm; length, 5 cm) containing 20 mL of hydroponic nutrient solution (4.0 mM KNO_3 , 1.5 mM $\text{Ca}(\text{NO}_3)_2$, 1.0 mM MgSO_4 , 0.66 mM $\text{NH}_4\text{H}_2\text{PO}_4$, 0.057 mM FeEDTA , 0.048 mM H_3BO_3 , and 0.009 mM MnSO_4) [15] and incubated for 14 days under controlled conditions ($25 \pm 1 \text{ }^\circ\text{C}$; 40–50% relative humidity (RH); continuous illumination at $59.5 \mu\text{mol m}^{-2} \text{s}^{-1}$). Light intensity was measured using an LI-250A light meter (LI-COR, Tokyo, Japan) fitted with a quantum sensor that measures photosynthetically active radiation (400–700 nm).

The 14-day-old seedlings were transferred to a polystyrene plate (61.5 cm × 60.5 cm × 3.0 cm) floating in hydroponic nutrient solution in a hydroponic culture trough (67.0 cm × 65.5 cm × 21.0 cm) (Home Hyponica 303; Kyowa, Osaka, Japan) on a growing table (height, 100 cm) in a pathogen-free nursery greenhouse (10.0 m × 6.0 m; $26 \pm 3 \text{ }^\circ\text{C}$) [57]. The seedlings were further cultivated until used for experiments. Three plants were used to maintain the PM fungus, and 25 plants were used in experiments to collect asexual progeny conidia released from single colonies of PM-causing fungal isolates with or without hyperparasite inoculation using the electrostatic collector, as described previously [53].

2.2. Fungal Materials, Culture, Inoculation, and Incubation

2.2.1. *Podosphaera xanthii* KMP-6N

A single conidium from melon leaves displaying PM symptoms was isolated in 2013 in Japan. Subsequently, the isolate was identified on the morphological characteristics and sequence of the rDNA-ITS region amplified by polymerase chain reaction (PCR). The Japanese isolate of *P. xanthii* KMP-6N [15,52,53] was used in this study. Asexual mature conidia were collected from conidiophores on KMP-6N-infected melon leaves using a pencil-type electrostatic insulator probe. The electrified probe formed an electrostatic field around it and attracted mature conidia from conidiophores. The insulator probe consisted of an ebonite rod with a pointed tip (diameter, 4 mm; length, 7 cm; tip diameter, 5 μm); it was mounted on the micromanipulator of a KH-2700 high-fidelity digital microscope (KH-2700 DM; Hirox, Tokyo, Japan). Conidia were inoculated onto the true leaves of 14-day-old healthy melon seedlings (cv. 'Earl's Favourite'), as described previously [15]. The KMP-6N isolate was maintained for 14 days by incubation in an electrostatic screen (ES) chamber, which excludes airborne pathogens, installed in a greenhouse (10.0 m × 6.0 m) at $26 \pm 3 \text{ }^\circ\text{C}$ and 30–55% RH under illumination at $190.6\text{--}400.4 \mu\text{mol m}^{-2} \text{s}^{-1}$ [57], or in an LH-240N growth chamber at $25 \pm 1 \text{ }^\circ\text{C}$ at 40–50% RH under continuous illumination at $22.2 \mu\text{mol m}^{-2} \text{s}^{-1}$ [15]. A pressed KMP-6N specimen is preserved in the Herbarium Preservation Section of Kindai University (Nara, Japan).

2.2.2. *Ampelomyces* Strain Xs-q

Hyperparasitic fungi were isolated from the PM fungal sample (*P. xanthii*) collected from a naturally infected host plant (*Xanthium stramonium*) in November 2017 in Mie Prefecture in Japan. The strains were characterised based on morphological characteristics and sequences of rDNA-ITS regions and actin gene (*ACT*) fragments, and identified as *Ampelomyces* spp. One of the Japanese *Ampelomyces* sp. strains designated as Xs-q was used in this study [48]. Xs-q colonies were cultured on Czapek-Dox agar medium supplemented with 2% malt extract (MCzA; 3 g NaNO_3 , 1 g K_2HPO_4 , 0.5 g KCl , 0.5 g MgSO_4 , 15 g agar and 20 g malt extract) and maintained at $25 \pm 2 \text{ }^\circ\text{C}$ and continuous illumination at

22.2 $\mu\text{mol m}^{-2} \text{s}^{-1}$. The Xs-q strain was subcultured on MCzA medium every 2 months. Sporulating colonies (30 days old) were flushed with 1.0–1.5 mL of sterile distilled water and the colony was scraped with a sterile scalpel to produce spore suspensions. The concentration of the suspension was measured using a haemocytometer (Nippon Rinsho Kikai Kogyo Co. Ltd., Tokyo, Japan) and then it was diluted to 5×10^5 spores mL^{-1} . Polyoxyethylene sorbitan monolaurate (Tween 20; Nacalai Tesque, Tokyo, Japan) was added to a final concentration of 0.05%. This suspension was used for inoculations.

2.2.3. Inoculation Experiments for Observing Mycoparasitism in Melon PM

Single KMP-6N conidia were inoculated onto the leaves of 14-day-old melon seedlings using the insulator probe and incubated under pathogen-free greenhouse conditions for 5, 10, or 15 days post-inoculation (dpi). The 5-, 10-, and 15-day-old KMP-6N colonies on melon leaves (Figure 1A–C) were drenched by spraying with the density-adjusted spore suspension (5×10^5 spores mL^{-1}) of *Ampelomyces* strain Xs-q, and all seedlings were placed in plastic boxes (70–80% RH). Seedlings not inoculated with Xs-q were used as controls. Gauze pads soaked with sterile tap water were placed in the boxes. The boxes were closed and incubated for 10–20 days in LH-240N growth chambers at 25 ± 1 °C and 40–50% RH under continuous illumination at 22.2 $\mu\text{mol m}^{-2} \text{s}^{-1}$. Ten 14-day-old melon seedlings were used in each experiment.

2.3. Morphological Observation and Infection Processes of *Ampelomyces* Strain Xs-q Inoculated onto Hyphae of *P. xanthii* KMP-6N

Following incubation for 14 days of the KMP-6N-infected melon seedlings spray-inoculated with *Ampelomyces* strain Xs-q (14 dpi), the length and width of mature Xs-q pycnidia and spores were measured on glass slides under the KH-2700 DM. To facilitate release of spores from pycnidia, a drop of distilled water (10 μL) was added to the samples. Data are presented as means \pm standard deviation (SD) of five replicates (20 pycnidia and 100 spores per replication). The number of spores per pycnidium was also evaluated using the KH-2700 DM. Data are presented as means \pm SD of five replicates (5 pycnidia per replication).

The infection processes of *Ampelomyces* strain Xs-q in KMP-6N colonies were observed using the KH-2700 DM. Xs-q hyphal development was photographed for 14 days following the spray inoculation of Xs-q spores onto 10-day-old KMP-6N colonies using the 0.5" interline transfer charge-coupled device (CCD) camera of the KH-2700 DM. Ten KMP-6N conidiophores, one per melon leaf, were selected for consecutive observation of the pycnidial development of the Xs-q strain. Digital micrographs were analysed using the Adobe Photoshop v5.0 software (Adobe Systems, San Jose, CA, USA) to optimise the contrast of the images without altering the original data.

2.4. Conidial Collector and Electrostatic Spore Collection

The rotational electrostatic spore collector consisted of a copper conductor film (250 mm \times 10 mm \times 0.5 mm) wound around an insulated round plastic container (diameter, 8 cm; height, 5 cm), a direct current HVA 10K202NA electrostatic voltage generator (Logy Electric, Tokyo, Japan), a transparent insulator film (260 mm \times 60 mm \times 0.5 mm) made with polypropylene (Hapila, Tokyo, Japan), and a WH3311 timer mechanism (Matsushita Electric Works, Osaka, Japan) [53]. The conductor was connected to the negative terminal of the electrostatic voltage generator, and a current was supplied from the voltage generator to the conductor. The outer insulator film, which was negatively polarised and charged with static electricity (5.2×10^{-1} nC), was placed at ca. 2 cm (Figure 2, distance A) from the apex of a fungal colony formed on a melon leaf to collect all released asexual progeny conidia, as described previously [53]. The negative charge on the outer surface of the electrified insulator film generated an electrostatic field and created an attractive force [53,57,60,61], thereby trapping KMP-6N conidia that entered the field (Figure 2). The insulator film achieved a complete rotation in 24 h at the collection site and was therefore removed from

the apparatus at 24 h intervals to be replaced with a new insulator film. Then, the conidia attracted to these insulator films from each KMP-6N colony were counted.

2.5. Electrostatic Activation of the Insulator Film

The transparent insulator film was dielectrically polarised by providing impressed potential supplied from the voltage generator to the conductor film (positively on the conductor film side; negatively on the opposite conidium collection side; Figure 2). The potential of the conductor film was controlled by the voltage generator, and the potential difference (kV) between the insulator surface and ground level (i.e., the voltage) was measured using an electrostatic field meter (FMX-002; Simco, Kobe, Japan). The surface electrostatic charge of the insulator film was measured by touching the film surface with the probe (tip diameter, 50 μm) of a coulometer (NK-1001; Kasuga Denki, Kanagawa, Japan).

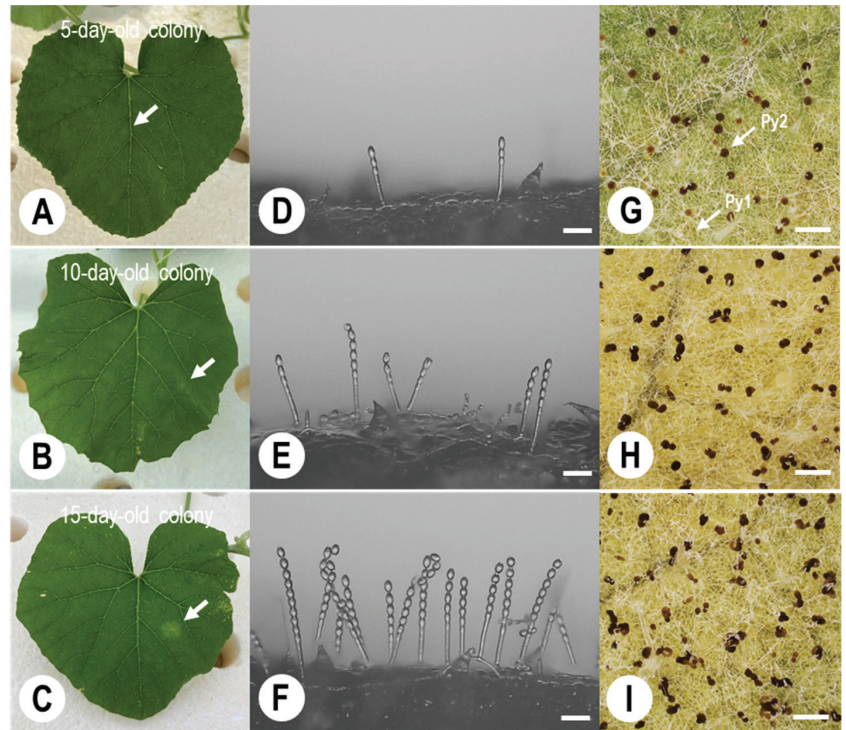


Figure 1. Photographs and micrographs of *Podosphaera xanthii* Pollacci KMP-6N colonies and conidiophores on melon leaves spray-inoculated with spores of the Japanese *Ampelomyces* strain Xs-q. (A–C) Single 5-day-old (A), 10-day-old (B), and 15-day-old (C) KMP-6N colonies were prepared by inoculating KMP-6N conidia onto leaves of melon seedlings. Arrows show the growth of single KMP-6N colonies on melon leaves at different fungal developmental stages. (D–F) KMP-6N conidiophores in single 5-day-old (D), 10-day-old (E), and 15-day-old (F) KMP-6N colonies observed using a digital microscope (KH-2700 DM). KMP-6N conidiophores had normal catenate conidia, forming chains. (G–I) KH-2700 DM images of pycnidia of the Xs-q strain produced in plastic boxes at 70–80% relative humidity (RH) under growth chamber conditions at 10 days post-inoculation (dpi) onto 5-day-old (G), 10-day-old (H), and 15-day-old (I) KMP-6N colonies. The Xs-q pycnidia changed in colour from pale yellow to black as they matured; Py1 and Py2 indicate immature and mature pycnidia, respectively. Bars represent 60 μm (D–F) and 300 μm (G–I).

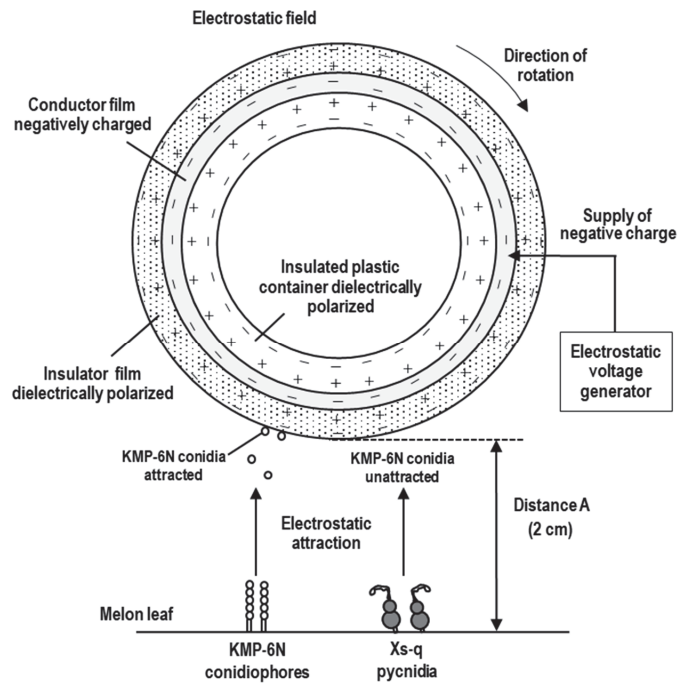


Figure 2. An electrostatic spore collector system for collecting progeny conidia released from KMP-6N colonies with and without spray inoculation with hyperparasite spores (cross-sectional view). The electrostatic voltage generator produced a negative charge, which was transferred to the conductor film, inducing a positive image charge on the surface of the insulator film. Dielectric polarisation produced a negative surface charge on the opposite side of the insulator film, and an electrostatic field formed around the dielectrically polarised insulator film. The dielectrically polarised insulated plastic container was timed to revolve once every 24 h. KMP-6N progeny conidia from normal conidiophores were collected on the insulator film by electrostatic attraction. The insulator film (5.2×10^{-1} nC) was placed at <2 cm from a KMP-6N colony on a melon leaf (distance A).

2.6. Consecutive Collection of KMP-6N Conidia Released from Single *Ampelomyces*-Treated Colonies

Experiments were conducted to estimate the number of asexual progeny conidia released from single KMP-6N colonies over periods of 3–28 days after spray inoculation with Xs-q spores. In the greenhouse, mature conidia were collected from conidiophores using the electrostatic insulator probe and transferred onto well-developed young leaves of 14-day-old melon seedlings. A melon seedling grown in an ES-chamber installed in a greenhouse (25 ± 2 °C; 30–55% RH) [57] bearing a single KMP-6N colony on a leaf (Figure 1A–C) was drenched by spraying with Xs-q spores (5×10^5 spores mL⁻¹) and placed under the electrostatic conidial collection apparatus (Figure 2). Uninoculated melon seedlings each bearing a single 5-day-old KMP-6N colony were used as controls. The collection apparatus was operated continuously throughout definite experimental periods that ranged from 5 to 32 days. The insulator film was continuously charged (5.2×10^{-1} nC) until it was replaced with a new insulator film (film change duration, 30 s). A total of 5–32 films were used during each experiment. The total conidia deposited on each film were counted every 5 h after collection using the KH-2700 DM. The numbers of conidia collected per h were estimated by pooling the counts for each 60 min interval. Conidium collection experiments were conducted after a single spray inoculation of Xs-q spores onto 5-, 10-, and 15-day-old KMP-6N colonies, and during a double spray inoculation of Xs-q spores onto 15-day-old KMP-6N colonies. One PM colony per melon leaf was sampled

at each colony developmental stage, with five replicates. The second spray inoculation of Xs-q spores (5×10^5 spores mL⁻¹) onto 15-day-old KMP-6N colonies was conducted at ca. 4–5 days after the first spray inoculation, by which conidial release had restarted.

Conidiophores of KMP-6N colonies on melon leaves and on the insulator films were viewed using the objective zoom lens (MX-5030RZII; $\times 250$) of the KH-2700 DM, focused on the side of the leaf or the insulator film. Digitalised images of conidia and conidiophores were obtained using a CCD camera and adjusted using Adobe Photoshop.

2.7. Microscopic Observation of Melon PM Colonies Inoculated with Xs-q Spores

KMP-6N conidia were collected from five colonies per colony developmental stage. After the final collection, leaf segments (ca. 3 cm \times 3 cm) were cut from leaves of plants inoculated with Xs-q spores. The samples were fixed and chlorophyll was removed by boiling for 1–2 min in an alcoholic lactophenol solution containing 10 mL glycerol, 10 mL phenol, 10 mL lactic acid, 10 mL distilled water, and 40 mL 99.8% ethanol, and then the fixed samples were stained with 0.1% Aniline Blue (Nacalai Tesque) dissolved in distilled water, as described previously [62]. The stained colonies were observed using a light microscope (BX-60 LM; Olympus, Tokyo, Japan) and photographed using a digital camera (EOS KISSX6i; Canon, Tokyo, Japan) mounted on the microscope. The total numbers of normal conidiophores formed in five individual colonies per colony developmental stage were calculated, and the mycelial areas of the colonies were calculated using the ImageJ software (National Institutes of Health, Bethesda, MD, USA). Data are presented as means \pm SD of five replicates.

2.8. Statistical Analyses

The areas and morphological characteristics of KMP-6N colonies, and total numbers of progeny conidia collected from single KMP-6N colonies at each colony developmental stage, were analysed using the EZR v1.54 software (Jichi Medical University, Saitama, Japan). Significant differences were evaluated at a level of $p < 0.05$ using Tukey's test.

3. Results

3.1. Morphological Observations of *Ampelomyces* Strain Xs-q in KMP-6N Colonies

We observed 5-, 10-, and 15-day-old KMP-6N colonies (Figure 1A–C) formed on melon leaves under greenhouse conditions and examined the morphology of their conidiophores (Figure 1D–F). The KMP-6N conidiophores had catenate conidia with fibrosin bodies and were produced in chains. The numbers of KMP-6N conidiophores increased as the colonies grew. After inoculation with *Ampelomyces* strain Xs-q, the strain grew vigorously, and elongated parasitic hyphae entered into KMP-6N hyphae (Figure 3A), followed by the complete collapse of the KMP-6N conidiophores at ca. 10–14 dpi. Xs-q pycnidia were produced in 5-, 10-, and 15-day-old KMP-6N colonies (Figure 1G–I) and changed in colour from pale yellow (immature) to black (mature) over time. The number of Xs-q pycnidia per KMP-6N colony increased with the growth stage (age) of the colony (Figure 1G–I, Table 1). At 14 dpi, Xs-q pycnidia in infected KMP-6N colonies were ovoid structures, $54.1 \pm 6.4 \times 37.1 \pm 5.6$ μ m in size. Numerous Xs-q spores were released from intracellular pycnidia by the rupture of the pycnidial wall (Figure 3B). Xs-q spores with unicellular, hyaline, and ellipsoid–ovoid to doliiform morphology were $6.7 \pm 0.5 \times 2.8 \pm 0.4$ μ m in size. There was an average of 1111.6 Xs-q spores per mature pycnidium, i.e., at 14 dpi, with a significant difference between 10- and 15-day-old KMP-6N colonies, but not between 5- and 10-day-old colonies (Table 1).

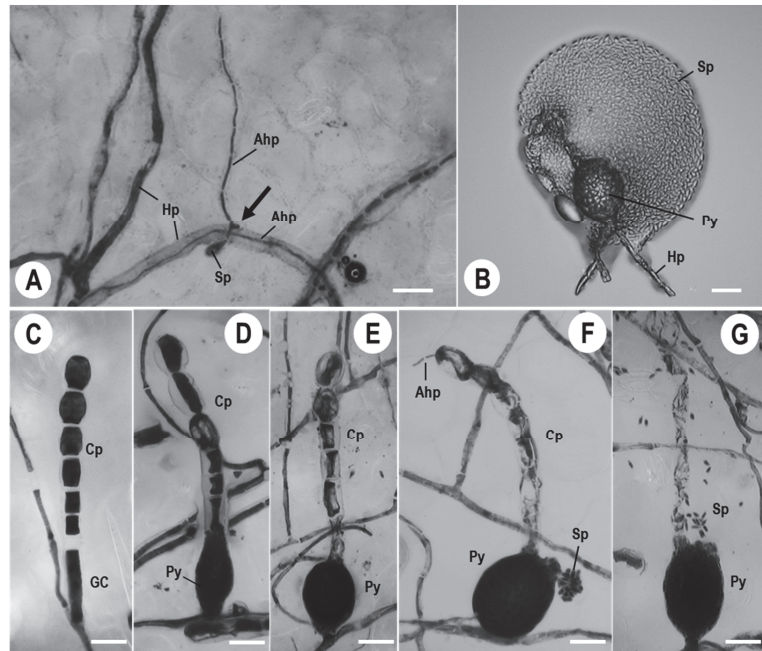


Figure 3. Infection of the Japanese *Ampelomyces* strain Xs-q in *P. xanthii* KMP-6N colonies. (A) Light micrograph of Xs-q hyphae that invaded and grew vigorously into KMP-6N hyphae. (B) Digital micrograph of Xs-q spores released from a pycnidium after treatment with a 10 μ L drop of distilled water. (C–G) Morphological changes in KMP-6N conidiophores parasitised by Xs-q. (C) Normal KMP-6N conidiophore. (D) Xs-q pycnidium initiated in generative cell (GC) of a KMP-6N conidiophore. (E) Mature intracellular pycnidium produced in a GC of a KMP-6N conidiophore. (F) The hyperparasitic Xs-q strain produced intracellular pycnidia in GCs, and Xs-q hyphae grew out from conidial cells at the apex of the KMP-6N conidiophore. (G) Abundant Xs-q spores released from mature pycnidia. KMP-6N conidiophores atrophied and collapsed without releasing progeny conidia. Light micrographs were taken at 0 (C), 6 (D), 8 (E), 10 (F), and 12 days (G) after spray inoculation with Xs-q spores onto 10-day-old KMP-6N mycelia. Bars represent 10 μ m (A) and 20 μ m (B–G). Ahp, Xs-q hypha; Cp, KMP-6N conidiophore; Hp, KMP-6N hypha; Sp, Xs-q spore; Py, Xs-q pycnidium.

Table 1. Numbers of *Ampelomyces* strain Xs-q pycnidia formed per *Podosphaera xanthii* KMP-6N colony and of Xs-q spores produced per mature pycnidium at different KMP-6N colony developmental stages.

| Colony | Times of Spray Inoculation | Numbers of Pycnidia in a Single Colony ^x | Numbers of Spores Produced in a Mature Pycnidium ^y |
|-------------|----------------------------|---|---|
| 5 days old | Once | 313.7 \pm 125.6 a | 745.3 \pm 287.3 a |
| 10 days old | Once | 1602.1 \pm 220.5 b | 851.0 \pm 372.3 a |
| 15 days old | Once | 2321.0 \pm 399.5 c | 1738.5 \pm 494.2 b |

^x Xs-q pycnidia were counted in each powdery mildew KMP-6N colony at 14 days after spray inoculation with Xs-q spores. ^y Xs-q spores in newly formed mature pycnidia were counted 14 days post-inoculation (dpi). Different letters in each column indicate significant differences ($p < 0.05$, Tukey's test).

3.2. KMP-6N Conidiophore Morphology following Invasion by *Ampelomyces* Strain Xs-q

Normal KMP-6N conidiophores exhibited different morphology following invasion by Xs-q parasitic hyphae (Figure 3C). Intracellular Xs-q pycnidia were initiated (Figure 3D)

and then completely formed in generative cells (GCs) of KMP-6N conidiophores (Figure 3E). Thereafter, Xs-q parasitic hyphae grew outward from conidia formed at the top of KMP-6N conidiophores in whose GCs the mature intracellular pycnidia were produced (Figure 3F), and some Xs-q spores were released from mature intracellular pycnidia in GCs (Figure 3G). Consequently, KMP-6N conidiophores collapsed completely. Histochemical staining in cells forming KMP-6N conidiophores changed greatly following invasion by parasitic Xs-q hyphae (Figure 3).

3.3. Pycnidial Development of *Ampelomyces* Strain Xs-q in KMP-6N Conidiophores

Normal KMP-6N conidiophores developed on melon leaves prior to inoculation with Xs-q spores (Figure 4A). After inoculation, intracellular Xs-q pycnidia initiated within GCs of the conidiophores at ca. 6–8 dpi. Single PM conidia formed at the top of the conidiophores started to degenerate at ca. 7–9 dpi (Figure 4B); then, they were completely degenerated at ca. 10–11 dpi (Figure 4C). The conidiophores collapsed completely by ca. 11–12 dpi (Figure 4D). KMP-6N hyphae containing conidiophores on melon leaves also collapsed completely. Thus, KMP-6N was unable to produce asexual progeny conidia successfully from its conidiophores after this time period. Xs-q pycnidia matured within ca. 12–14 days. Xs-q spores were released from mature intracellular pycnidia after treatment with a 10 μ L drop of distilled water (Figure 4E).

3.4. Quantitative Analysis of KMP-6N Conidia Released from Parasitised PM Colonies under Greenhouse Conditions

Figure 5 shows electrostatic conidial collection from and morphological characteristics of conidiophores in KMP-6N colonies with and without Xs-q inoculation after the insulator film was negatively electrified. Progeny conidia were successfully attracted from the PM colonies after spraying with water (Figure 5A). By contrast, no progeny conidia were attracted from the colonies of 8 days after spray inoculation with Xs-q spores (8 dpi) (Figure 5B). Conidiophores in uninoculated KMP-6N colonies showed an usual morphology, forming conidial chains (Figure 5C,E), whereas those of inoculated colonies were abnormal and destroyed at 8 days after inoculation with Xs-q (8 dpi) (Figure 5D,F). We plotted the total conidia collected per 1 h from each of five KMP-6N colonies at each colony developmental stage to estimate the numbers of progeny conidia released (Figure 6). Progeny conidia were also collected from a single uninoculated 5-day-old KMP-6N colony over a period of ca. 30 days (the colony lifespan) after spraying with water as an experimental control (Figure 6A). Progeny conidia could be electrostatically collected during the daytime, but not at night (Figure 6A). No conidia could be collected from 5- and 10-day-old KMP-6N colonies after inoculation with Xs-q spores (Figure 6B,C), regardless of the colony developmental stage. Thus, conidial release from 5- and 10-day-old KMP-6N colonies decreased gradually, stopping completely by ca. 3–5 dpi and ca. 7–9 dpi, respectively (Figure 6B,C). However, in 15-day-old KMP-6N colonies, conidial releases did not stop completely after the first Xs-q spore inoculation (Figure 6D), and they began to increase again at ca. 5–6 dpi until the end of the colony lifespan was reached at ca. 22–28 days (Figure 6D). A second spray inoculation of Xs-q spores caused the number of KMP-6N conidia to decrease again, eventually stopping by ca. 16–18 days after the second inoculation (Figure 6E). The duration and total number of conidial releases by individual KMP-6N colonies throughout their lifespans are shown in Table 2. The KMP-6N colony areas and numbers of normal conidiophores per KMP-6N colony before and after one or two spray inoculations with Xs-q are also listed in Table 2. KMP-6N colony expansion ceased at ca. 4, 5, and 2 dpi in 5-, 10-, and 15-day-old colonies, respectively, after a single inoculation. KMP-6N colonies were measured after conidial releases had stopped completely; therefore, KMP-6N colonies were slightly larger in area after inoculation than before inoculation (Table 2). After electrostatic spore collection, conidiophores in uninoculated KMP-6N colonies were normal under greenhouse conditions, whereas conidiophores and hyphae in inoculated KMP-6N colonies were either deformed or collapsed, and the numbers of normal conidiophores clearly decreased

(Table 2). Thus, there were no normal KMP-6N conidiophores per single 5- and 10-day-old KMP-6N colonies following a single spray inoculation of Xs-q spores, except in 15-day-old colonies. No Xs-q pycnidia formed in KMP-6N colonies at any colony developmental stage under our greenhouse conditions (low RH) throughout these experiments.

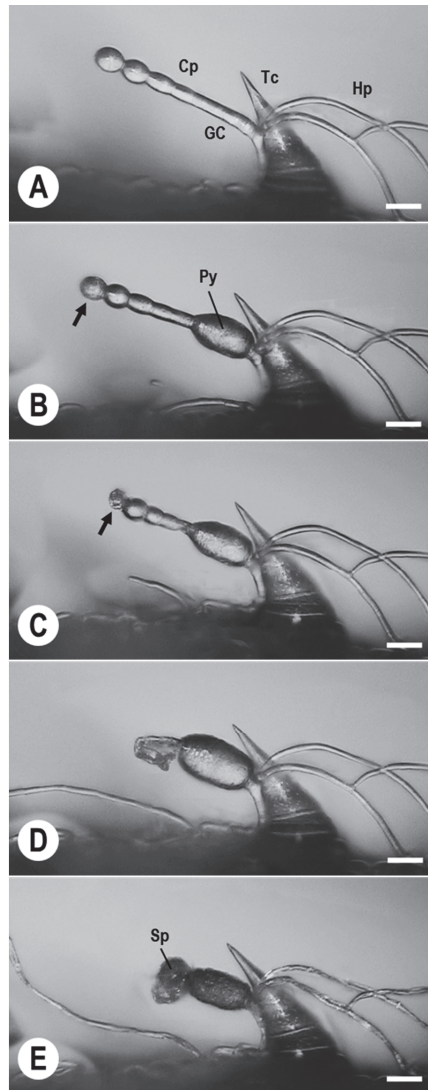


Figure 4. Pycnidial development of the Xs-q strain in KMP-6N conidiophores. A KMP-6N mycelium formed on a melon leaf at 10 dpi with a KMP-6N conidium using a micromanipulation technique. Digital micrographs were taken from the same view at 0 (A), 10 (B), 11 (C), 12 (D), and 14 days (E) after spray inoculation of Xs-q spores onto 10-day-old KMP-6N mycelium. KMP-6N conidiophores (Cp) that formed near a trichome cell (Tc) on a melon leaf atrophied completely after invasion by Xs-q hyphae into KMP-6N hyphae (Hp). Xs-q pycnidia (Py) were successfully produced in generative cells (GC) of KMP-6N conidiophores at high RH (80–90%). Mature pycnidia released abundant progeny spores (Sp). Arrow indicates atrophied conidial cells at the top of KMP-6N conidiophores. Bars represent 20 μm .

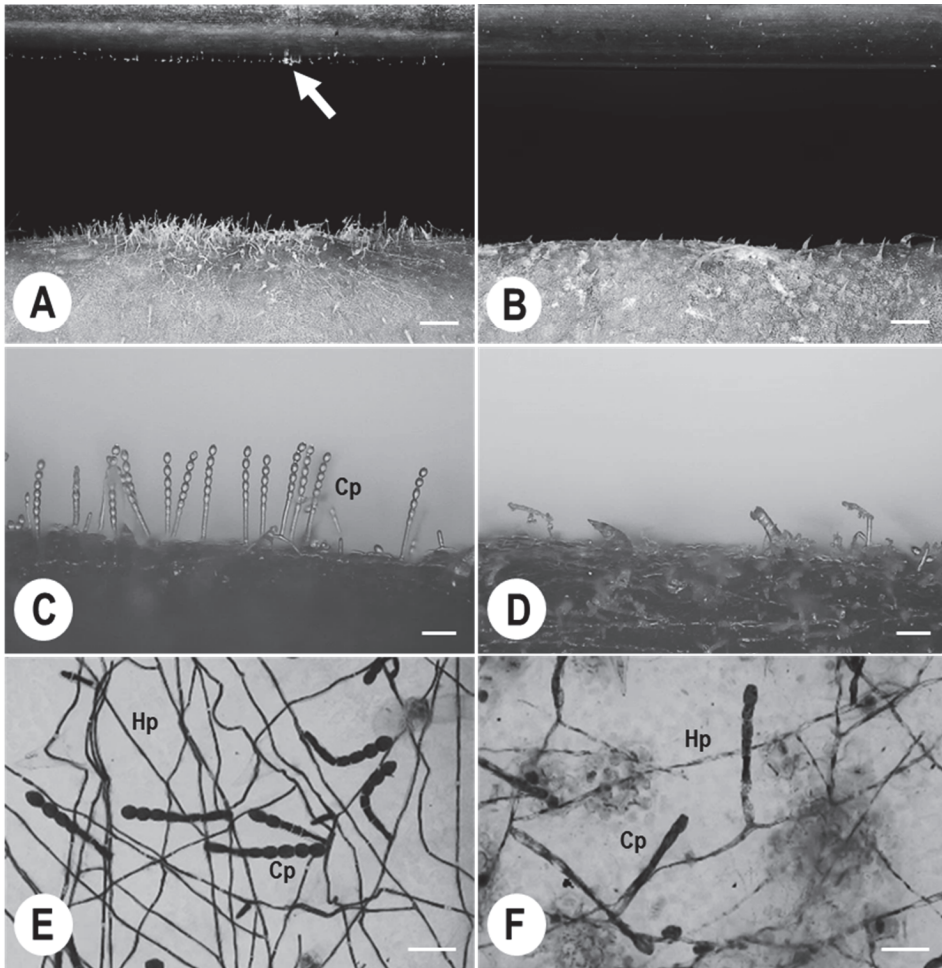


Figure 5. Micrographs of conidiophores and colonies in Xs-q-uninoculated (A,C,E) or Xs-q-inoculated (B,D,F) 10-day-old KMP-6N colonies after electrostatic attraction of conidia to the insulator film under greenhouse conditions. (A,B) Digital micrographs showing the attraction of progeny conidia released from Xs-q-uninoculated (A) and Xs-q-inoculated (B) KMP-6N colonies to an electrostatic insulator film. An insulator film carrying a charge of 1.0 nC was placed at 2000 μm from the apex of the conidiophore. Micrographs were taken at 8 days after the start of electrostatic spore collection. Conidia (arrow) were attracted to the insulator film in (A), whereas no conidia were captured in (B). (C,D) Digital micrographs showing Xs-q-uninoculated (C) and Xs-q-inoculated (D) KMP-6N colonies at 8 days after the electrostatic collector was applied. Conidiophores (Cp) were normal and developed conidia in chains in (C) but developed abnormally and atrophied completely without forming Xs-q pycnidia in (D). (E,F) Light micrographs showing KMP-6N hyphae (Hp) and conidiophores (Cp) in histochemically stained Xs-q-uninoculated (E) and Xs-q-inoculated (F) KMP-6N colonies at 8 days after the electrostatic insulator was applied. Conidiophores (Cp) were normal with the development of conidial cell chains in (E), but were atrophied completely without forming Xs-q pycnidia in (F). Bars represent 500 μm (A,B) and 60 μm (C–F).

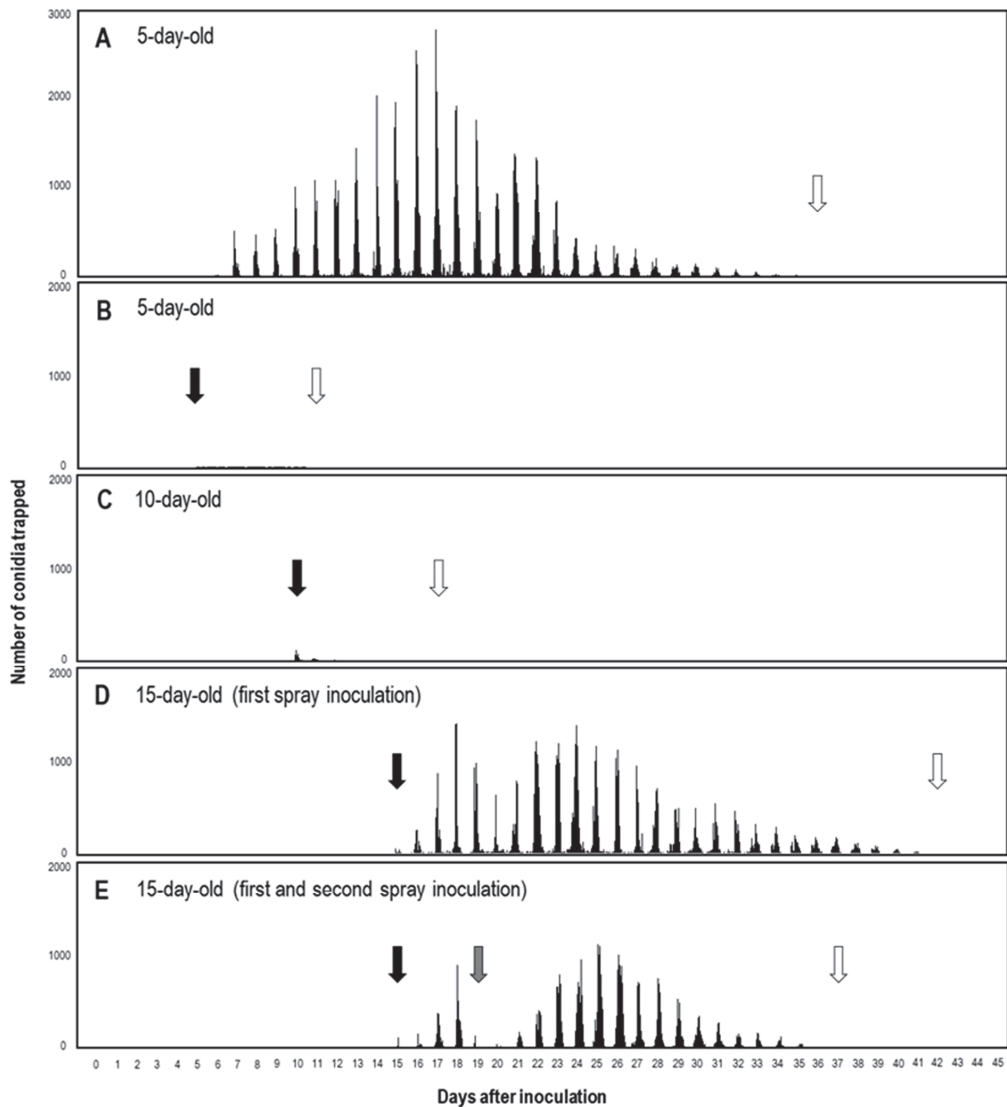


Figure 6. Numbers of progeny conidia collected from *P. xanthii* Pollacci KMP-6N colonies without (A) or with (B–E) spray inoculation with Xs-q spores on melon leaves. Electrostatic conidial collection was conducted during definite periods until conidial release stopped from uninoculated 5-day-old (A) or spray-inoculated 5-day-old (B), 10-day-old (C), and 15-day-old KMP-6N colonies with single Xs-q spore application (D) or double Xs-q spore application (E). Data are plotted for 1 h periods. Open arrows indicate no conidia were released from KMP-6N colonies; the day on which KMP-6N conidial releases stopped completely is indicated. Black and grey arrows indicate first and second spray inoculation, respectively.

Table 2. Development of Xs-q-uninoculated and Xs-q spray-inoculated KMP-6N colonies on melon leaves throughout the conidiation period, assessed by directly counting KMP-6N progeny conidia continuously collected on electrostatically activated insulator films under greenhouse conditions.

| Colony | Times of Spray Inoculation | Colony Area (cm ²) | | Number of Normal Conidiophores in a Single Colony | | Duration of Conidial Seccession (Day) | Total Conidia Collected from Xs-q-Inoculated Colonies ^y |
|---------------------------|----------------------------|--------------------------------|--------------------------------|---|--------------------------------|---------------------------------------|--|
| | | Before Inoculation | After Inoculation ^w | Before Inoculation | After Inoculation ^x | | |
| 5 days old | One | 0.02 ± 0.02 a | 0.04 ± 0.02 a | 12.0 ± 10.6 a | 0 a | 4.6 ± 0.9 a | 156.2 ± 108.3 a |
| 10 days old | One | 0.32 ± 0.13 b | 0.46 ± 0.14 b | 752.1 ± 170.4 b | 0 a | 8.2 ± 0.8 b | 1167.0 ± 745.9 b |
| 15 days old | One | 0.98 ± 0.14 c | 1.21 ± 0.15 c | 1130.7 ± 145.9 c | 864.8 ± 91.2 b | 24.6 ± 3.0 c | 61,530.4 ± 8785.3 c |
| 15 days old | Twice | 0.94 ± 0.18 c | 1.10 ± 0.15 c | 1255.3 ± 179.4 c | 654.4 ± 45.6 c | 20.4 ± 1.1 d | 44,866.4 ± 7654.7 d |
| Uninoculated ^z | One (water) | 0.05 ± 0.02 a | 2.00 ± 0.16 d | 15.4 ± 4.0 a | 1409.0 ± 100.1 d | 28.2 ± 2.2 c | 124,761.0 ± 12,157.4 e |

^w KMP-6N colonies were measured when conidial releases stopped completely after spray inoculation with Xs-q spores. ^x Normal conidiophores per KMP-6N colony were counted when conidial releases stopped completely after spray inoculation with Xs-q spores. ^y Total KMP-6N conidia collected using the electrostatic spore collector were summed for each colony throughout its lifespan. ^z Single colonies were spray-inoculated with water, as a control. Electrostatic spore collection was conducted throughout the lifespan of each KMP-6N colony. Data were analysed after conidial releases from the colony had stopped completely. Different letters in each column indicate significant differences ($p < 0.05$, Tukey's test).

4. Discussion

Hyperparasitic fungi in the genus *Ampelomyces* have been used as BCAs against PM fungi in various crops worldwide [29,40,41,46], as an eco-friendly method for PM disease management. Based on morphological and molecular phylogenetic analyses, Németh et al. [48] recently identified hyperparasites isolated from different PM species in Japan as *Ampelomyces* spp. Spores of Japanese hyperparasitic strains produced in pycnidia, which develop intracellularly in the mycelia of PM fungi, are unicellular, hyaline, mostly guttulate, and embedded in a mucilaginous matrix within swollen ampulliform or pyriform pycnidia [48]. These strains always grew slowly, with an *in vitro* radial growth rate of 0.5–1.0 mm day⁻¹ on MCzA. Thus, the morphological and physiological characteristics of the Japanese strains were clearly similar to those of previously reported *A. quisqualis* isolates [30,44,63–66].

To control PMs effectively with these hyperparasitic Japanese strains, we established a method for inoculating hyperparasite spores onto PM fungal colonies. The concentration of hyperparasite spores is an important factor affecting their germination and infection in pathogens, as spore germination decreases rapidly at spore concentrations of >10⁶ spores mL⁻¹, due to the production of self-inhibitory substances [67]. In the present study, we adjusted the spore concentration to 5 × 10⁵ spores mL⁻¹ for spray inoculations. Our results agreed with those of Németh et al. [48], because the spores of the tested Japanese *Ampelomyces* strain germinated successfully at 15–20 h after spray inoculation onto PM-inoculated melon leaves at high RH.

Previous studies have reported that penetration by the hyperparasite *A. quisqualis* into mycohost structures can occur within 24 h [38,68], and that its hyphae of hyperparasites continue to grow internally and produce intracellular pycnidia in the mycelia or conidiophores of mycohosts at 5–8 days [24,69] or 7–10 days [42,68] after penetration. After infection, the hyperparasites further ramify throughout the mycohost hyphae, resulting in its reduced growth and eventual death [44]. Németh et al. [48] visually clarified the infection processes and conidiogenesis of a Japanese *Ampelomyces* strain in tomato PM colonies; the foot and GCs of PM conidiophores began to degenerate by ca. 5–6 dpi, and intracellular pycnidia of the hyperparasite strain initiated in basal cells of the conidiophores at ca. 6–8 dpi, followed by the complete collapse of the conidiophores at ca. 10–14 dpi. In the present study, we consecutively observed the degeneration and constriction of hyphae in *P. xanthii*, followed by intracellular pycnidial formation in the hyphae (ex. Conidiophores). The infection

processes and conidiogenesis of the tested hyperparasitic *Ampelomyces* strain in the melon PM fungus were very similar to those of a tomato PM fungus reported by Németh et al. [48]. Interestingly, almost all intracellular pycnidia were produced in conidiophores, but not in the hyphae, of the mycohost, as observed by DM, and *Ampelomyces* hyphae that invaded the PM conidiophores grew out of conidia that formed at the top of the conidiophores.

In this study, we applied electrostatic and DM techniques to estimate quantitatively the control effects and infection efficiency of a Japanese hyperparasitic *Ampelomyces* strain against a melon PM fungus, to determine whether asexual PM progeny conidia, which are a source of host plant infection, are released from *Ampelomyces*-inoculated melon PM colonies at different developmental stages. Previous studies have determined the numbers of progeny conidia released by PM colonies throughout their lifespans, to clarify the conidial dispersal process using negatively polarised Insulator plates [60], probes [70], and drums [53,59]. Using a negatively polarised insulator drum, one study demonstrated that a single melon PM colony releases an average of 12.6×10^4 conidia throughout its lifespan under greenhouse conditions [53]; the dielectrically polarised insulator drum only detached mature conidia from conidiophores. Interestingly, Suzuki et al. [53] observed the vigorous release of conidia from melon PM colonies in the daytime, whereas very few conidia were released at night. The conidial release from colonies also largely reflected seasonal day length and light intensity [53]. These studies demonstrate that the use of an electrostatic spore collector system is crucial for the elucidation of ecological characteristics such as conidial release from PM colonies, which otherwise might be impossible to analyse.

In the present study, we also found that PM isolate KMP-6N actively released asexual progeny conidia during the day, and few at night, from colonies with and without spray inoculation of Xs-q spores (see Figure 6). Moreover, the numbers of conidia released from 5- and 10-day-old KMP-6N colonies after spray inoculation with Xs-q spores decreased gradually and stopped completely after ca. 4 dpi and ca. 8 dpi, respectively. Thus, we were able to suppress conidial releases completely from KMP-6N colonies by the application of a Japanese *Ampelomyces* strain under greenhouse conditions. However, we were only able to stop progeny conidial releases completely from 15-day-old KMP-6N colonies after two spray inoculations of Xs-q spores; a single spray treatment was insufficient to achieve this. Thus, our results strongly suggest that PM colonies should be inoculated with hyperparasitic fungal spores in the early developmental stages (e.g., when colonies are 5–10 days old, or as soon as PM is detected on host leaves) to successfully control the disease.

Ampelomyces hyperparasites are transported for long distances by wind [25,71,72] and spores in pycnidia can be dispersed by rain splash [68,73] to parasitise mycohosts over broad areas. In older colonies (e.g., >15 days old) spray-inoculated with Xs-q spores, a few normal conidiophores survived due to suboptimal control with *Ampelomyces*, allowing melon PM fungi to scatter progeny conidia widely from the colonies. To suppress the spread of PM, it may be more effective to inoculate PM colonies with Xs-q spores at night, when conidiophores do not release progeny conidia, than during the day, when progeny conidia are actively released. Interestingly, our tested *Ampelomyces* strain did not produce intracellular pycnidia in PM hyphae under our greenhouse conditions (low RH) but did produce them in PM hyphae under our growth chamber conditions (high RH). It appears that the hyperparasitic *Ampelomyces* strain requires high-RH conditions to produce intracellular pycnidia in mycohost hyphae. Similar results were observed in previous studies [24,45,48,69].

To elucidate the process of conidial release from hyperparasitic fungus-inoculated pathogenic PM colonies, we counted the PM conidia captured by our electrostatic spore collection apparatus to estimate quantitatively the ability of a hyperparasitic fungus to control cucurbit PM disease. To our knowledge, this is the first report describing pycnidial formation by hyperparasitic fungi within cucurbit PM hyphae using a DM, to determine directly the duration of conidial release from hyperparasite-inoculated PM colonies at different colony developmental stages and apply electrostatic techniques to determine the

total number of progeny conidia released from live PM colonies after inoculation with a hyperparasitic fungus. The findings of the present study will provide important insights into the ecological interactions between hyperparasitic *Ampelomyces* strains and PM mycohosts. Because *A. quisqualis* has been reported to tolerate a number of fungicides [25,32,38,69], it shows potential for application in combination with other pathogen control agents. Therefore, in a future study, we will examine the tolerance of Japanese *Ampelomyces* strains to commercial fungicides and focus on their use as practical BCAs against PMs.

5. Conclusions

In this study, we quantitatively and visually evaluated the suppressive effects of *Ampelomyces* Japanese Xs-q strain on the development of conidiophores and colonies of the melon PM isolate KMP-6N, to support the practical application of this hyperparasitic fungus as a biocontrol agent (BCA). In the first experiment, we monitored pycnidial formation of the Xs-q strain in conidiophores of the KMP-6N isolate using DM technology. Intracellular pycnidia of Xs-q were produced in KMP-6N conidiophores incubated in a growth chamber until ca. 10–14 dpi with Xs-q spores. KMP-6N conidiophores atrophied completely and did not release asexual progeny conidia. This is the first report to describe the pycnidial formation processes of a hyperparasitic fungus in melon PM conidiophores. In a second experiment, KMP-6N conidia were collected from Xs-q-inoculated KMP-6N colonies at different developmental stages under greenhouse conditions using an electrostatic spore collector. Conidial releases from 5- and 10-day-old KMP-6N colonies stopped after a single spray inoculation of Xs-q spores, whereas those from 15-day-old KMP-6N colonies did not stop. Therefore, we suggest that younger colonies should be targeted, as soon as melon PM fungi are observable on host leaves (e.g., in 5–10-day-old colonies) for the effective control of PM fungi using *Ampelomyces* strains. In addition, these results will lead to the establishment of ideal spray inoculation systems of hyperparasitic fungi to PM pathogens. These findings offer valuable insights into the development of hyperparasitic fungi as BCAs against PMs.

Author Contributions: Conceptualisation, Y.K., M.Z.N. and T.N.; methodology, Y.K., M.Z.N., D.S., L.K. and T.N.; software, Y.K. and Y.T.; validation, T.S., K.K., Y.M. and T.N.; formal analysis, Y.K. and T.S.; investigation, Y.K., K.N. and A.M.; resources, Y.K. and T.N.; data curation, Y.K. and T.N.; writing—original draft preparation, Y.K. and T.N.; writing—review and editing, M.Z.N., L.K. and T.N.; visualization, Y.M., M.Z.N., L.K. and T.N.; supervision, M.Z.N., L.K. and T.N.; project administration, L.K. and T.N. All authors have read and agreed to the published version of the manuscript.

Funding: This work was supported by a Grant for Agricultural Technology and Innovation Research Institute, Kindai University, by the János Bolyai Research Scholarship of the Hungarian Academy of Sciences (awarded to Márk Z. Németh; BO/00221/21/4), and by the Hungarian Scientific Research Fund (NKFIH OTKA FK142735).

Institutional Review Board Statement: Not applicable.

Informed Consent Statement: Not applicable.

Data Availability Statement: Data sets analysed during the current study are available from the current author on reasonable request.

Acknowledgments: The English in this document has been checked by at least two professional editors, both native speakers of English.

Conflicts of Interest: The authors declare no conflict of interest.

References

1. Sowell, G., Jr. Population shift of *Sphaerotheca fuliginea* on musk melon. *J. Am. Soc. Hortic. Sci.* **1982**, *112*, 156–160.
2. Reifschneider, F.J.B.; Boiteux, L.S.; Occhiena, E.M. Powdery mildew on melon (*Cucumis melo*) caused by *Sphaerotheca fuliginea* in Brazil. *Plant Dis.* **1985**, *69*, 1069–1070.
3. Mohamed, Y.F.; Bardin, M.; Nicot, P.C.; Pitrat, M. Causal agents of powdery mildew of cucurbits in Sudan. *Plant Dis.* **1995**, *79*, 634–636. [CrossRef]

4. Hosoya, K.; Narisawa, K.; Pitrat, M.; Ezura, H. Race identification in powdery mildew (*Sphaerotheca fuliginea*) on melon (*Cucumis melo*) in Japan. *Plant Breed.* **1999**, *118*, 259–262. [CrossRef]
5. Del Pino, D.; Olalla, L.; Pérez-García, A.; Rivera, M.E.; García, S.; Moreno, R.; Torés, J.A. Occurrence of races and pathotypes of cucurbit powdery mildew in southeastern Spain. *Phytoparasitica* **2002**, *30*, 459–466. [CrossRef]
6. Krístková, E.; Lebeda, A.; Sedláková, B. Virulence of Czech cucurbit powdery mildew isolates on *Cucumis melo* genotypes MR-1 and PI 124112. *Sci. Hortic.* **2004**, *99*, 257–265. [CrossRef]
7. Krístková, E.; Lebeda, A.; Sedláková, B. Species spectra, distribution and host range of cucurbit powdery mildews in the Czech Republic, and in some other European and Middle Eastern countries. *Phytoparasitica* **2009**, *37*, 337–350. [CrossRef]
8. Tomason, Y.; Gibson, P.T. Fungal characteristics and varietal reactions of powdery mildew species on cucurbits in steppes of Ukraine. *Agron. Res.* **2006**, *4*, 549–562.
9. Pérez-García, A.; Romero, D.; Fernández-Ortuño, D.; López-Ruiz, F.; De Vicente, A.; Torés, J.A. The powdery mildew fungus *Podosphaera fusca* (synonym *Podosphaera xanthii*), a constant threat to cucurbits. *Mol. Plant Pathol.* **2009**, *10*, 153–160. [CrossRef]
10. Hong, Y.-J.; Hossain, M.R.; Kim, H.-T.; Park, J.-I.; Nou, I.-S. Identification of two new races of *Podosphaera xanthii* causing powdery mildew in melon in South Korea. *Plant Pathol. J.* **2018**, *34*, 182–190. [CrossRef]
11. Kiss, L.; Vaghefi, N.; Bransgrove, K.; Dearnaley, J.D.W.; Takamatsu, S.; Tan, Y.P.; Marston, C.; Liu, S.Y.; Jin, D.N.; Adorada, D.L.; et al. Australia: A continent without native powdery mildews? The first comprehensive catalogue indicates recent introductions and multiple host range expansion events, and leads to the re-discovery of *Salmonomyces* as a new lineage of the Erysiphales. *Front. Microbiol.* **2020**, *11*, 1571. [CrossRef] [PubMed]
12. Kelly, L.A.; Vaghefi, N.; Bransgrove, K.; Fechner, N.A.; Stuart, K.; Pandey, A.K.; Sharma, M.; Németh, M.Z.; Liu, S.Y.; Tang, S.R.; et al. One crop disease, how many pathogens? *Podosphaera xanthii* and *Erysiphe vignae* sp. nov. identified as the two species that cause powdery mildew of mungbean (*Vigna radiata*) and black gram (*V. mungo*) in Australia. *Phytopathology* **2021**, *111*, 1193–1206. [CrossRef] [PubMed]
13. Vaghefi, N.; Kusch, S.; Németh, M.Z.; Seress, D.; Braun, U.; Takamatsu, S.; Panstruga, R.; Kiss, L. Beyond nuclear ribosomal DNA sequences: Evolution, taxonomy, and closest known saprobic relatives of powdery mildew fungi (Erysiphaceae) inferred from their first comprehensive genome-scale phylogenetic analyses. *Front. Microbiol.* **2022**, *13*, 903024. [CrossRef] [PubMed]
14. Keinath, A.P.; Wintermantel, W.M.; Zitter, T.A. *Compendium of Cucurbit Diseases and Pests*, 2nd ed.; The American Phytopathological Society Press: St. Paul, MN, USA, 2017.
15. Takikawa, Y.; Nonomura, T.; Miyamoto, S.; Okamoto, N.; Murakami, T.; Matsuda, Y.; Kakutani, K.; Kusakari, S.; Toyoda, H. Digital microscopic analysis of developmental process of conidiogenesis by powdery mildew pathogens isolated from melon leaves. *Phytoparasitica* **2015**, *43*, 517–530. [CrossRef]
16. Huggenberger, F.; Collins, M.A.; Skylakakis, G. Decreased sensitivity of *Sphaerotheca fuliginea* to fenarimol and other ergosterol-biosynthesis inhibitors. *Crop Prot.* **1984**, *3*, 137–149. [CrossRef]
17. Lebeda, A.; Sedláková, B. Fungicide resistance in population of cucurbit powdery mildew. *J. Plant Pathol.* **2008**, *90*, S2.142.
18. McGrath, M.T.; Shishkoff, N. Resistance to triadimefon and benomyl: Dynamics and impact on managing cucurbit powdery mildew. *Plant Dis.* **2001**, *85*, 147–154. [CrossRef]
19. McGrath, M.T.; Shishkoff, N. First report of the cucurbit powdery mildew fungus (*Podosphaera xanthii*) resistant to strobilurin fungicides in the United States. *Plant Dis.* **2003**, *87*, 1007. [CrossRef]
20. Miyamoto, T.; Hayashi, K.; Ogawara, T. First report of the occurrence of multiple resistance to Flutianil and Pyriofenone in field isolates of *Podosphaera xanthii*, the causal fungus of cucumber powdery mildew. *Eur. J. Plant Pathol.* **2020**, *156*, 953–963. [CrossRef]
21. Miyamoto, T.; Hayashi, K.; Okada, R.; Wari, D.; Ogawara, T. Resistance to succinate dehydrogenase inhibitors in field isolates of *Podosphaera xanthii* on cucumber: Monitoring, cross-resistance patterns and molecular characterization. *Pestic. Biochem. Physiol.* **2020**, *169*, 104646. [CrossRef]
22. Vielba-Fernández, A.; Polonio, A.; Ruiz-Jiménez, L.; de Vicente, A.; Pérez-García, A.; Fernández-Ortuño, D. Fungicide resistance in powdery mildew fungi. *Microorganisms* **2020**, *8*, 1431. [CrossRef] [PubMed]
23. Cesati, V. *Ampelomyces quisqualis* Ces. Bot. Ztg. **1852**, *10*, 301–302.
24. Jarvis, W.R.; Slingsby, K. The control of powdery mildew of greenhouse cucumber by water sprays and *Ampelomyces quisqualis*. *Plant Dis. Reprtr.* **1977**, *61*, 728–730.
25. Sundheim, L. Control of cucumber powdery mildew by the hyperparasite *Ampelomyces quisqualis* and fungicides. *Plant Pathol.* **1982**, *31*, 209–214. [CrossRef]
26. Kiss, L. Natural occurrence of *Ampelomyces* intracellular mycoparasites in mycelia of powdery mildew fungi. *New Phytol.* **1998**, *140*, 709–714. [CrossRef]
27. Yarwood, C.E. An overwintering pycnidial stage of *Cicinnobolus*. *Mycologia* **1939**, *31*, 420–422. [CrossRef]
28. Falk, S.P.; Gadoury, D.M.; Cortesi, P.; Pearson, R.C.; Seem, R.C. Parasitism of *Uncinula necator* cleistothecia by the mycoparasite *Ampelomyces quisqualis*. *Phytopathology* **1995**, *85*, 794–800. [CrossRef]
29. Kiss, L. A review of fungal antagonists of powdery mildews and their potential as biocontrol agents. *Pest Manag. Sci.* **2003**, *59*, 475–483. [CrossRef]
30. Huth, L.; Ash, G.J.; Idnurm, A.; Kiss, L.; Vaghefi, N. The “bipartite” structure of the first genome of *Ampelomyces quisqualis*, a common hyperparasite and biocontrol agent of powdery mildews, may point to its evolutionary origin from plant pathogenic fungi. *Genome Biol. Evol.* **2021**, *13*, evab182. [CrossRef]

31. Szejnberg, A. Biological control of powdery mildews by *Ampelomyces quisqualis*. *Phytopathology* **1979**, *69*, 1047.
32. Sundheim, L. *Ampelomyces quisqualis*, a hyperparasitic fungus in biological control of powdery mildews on greenhouse cucumber. *Acta Hort.* **1984**, *156*, 229–236. [CrossRef]
33. Szejnberg, A.; Mazar, S. Biocontrol of cucumber and carrot powdery mildew by *Ampelomyces quisqualis*. *Phytopathology* **1985**, *75*, 1301–1302.
34. Szejnberg, A.; Galper, S.; Mazar, S.; Lisker, N. *Ampelomyces quisqualis* for biological and integrated control of powdery mildews in Israel. *J. Phytopathol.* **1989**, *124*, 285–295. [CrossRef]
35. Dik, A.J.; Verhaar, M.A.; Bélanger, R.R. Comparison of three biological control agents against cucumber powdery mildew (*Sphaerotheca fuliginea*) in semi-commercial-scale glasshouse trials. *Eur. J. Plant Pathol.* **1998**, *104*, 413–423. [CrossRef]
36. Shishkoff, N.; McGrath, M.T. AQ10 biofungicide combined with chemical fungicides or AddQ spray adjuvant for control of cucurbit powdery mildew in detached leaf culture. *Plant Dis.* **2002**, *86*, 915–918. [CrossRef] [PubMed]
37. Angeli, D.; Maurhofer, M.; Gessler, C.; Pertot, I. Existence of different physiological forms within genetically diverse strains of *Ampelomyces quisqualis*. *Phytoparasitica* **2012**, *40*, 37–51. [CrossRef]
38. Szejnberg, A.; Mazar, S. Studies on the hyperparasite *Ampelomyces quisqualis* and preliminary trials on biological control of powdery mildew. *Phytoparasitica* **1983**, *11*, 219–220.
39. Romero, D.; Rivera, M.E.; Cazorla, F.M.; De Vicente, A.; Pérez-García, A. Effect of mycoparasitic fungi on the development of *Sphaerotheca fusca* in melon leaves. *Mycol. Res.* **2003**, *107*, 64–71. [CrossRef]
40. Park, M.-J.; Choi, Y.-J.; Hong, S.-B.; Shin, H.-D. Genetic variability and mycohost association of *Ampelomyces quisqualis* isolates inferred from phylogenetic analyses of ITS rDNA and actin gene sequences. *Fungal Biol.* **2010**, *114*, 235–247. [CrossRef]
41. Siozios, S.; Tosi, L.; Ferrarini, A.; Ferrari, A.; Tononi, P.; Bellin, D.; Maurhofer, M.; Gessler, C.; Delledonne, M.; Pertot, I. Transcriptional reprogramming of the mycoparasitic fungus *Ampelomyces quisqualis* during the powdery mildew host-induced germination. *Phytopathology* **2015**, *105*, 199–209. [CrossRef]
42. Legler, S.E.; Pintye, A.; Caffi, T.; Gulyás, S.; Bohár, G.; Rossi, V.; Kiss, L. Sporulation rate in culture and mycoparasitic activity, but not mycohost specificity, are the key factors for selecting *Ampelomyces* strains for biocontrol of grapevine powdery mildew (*Erysiphe necator*). *Eur. J. Plant Pathol.* **2016**, *144*, 723–736. [CrossRef]
43. Falk, S.P.; Gadoury, D.M.; Pearson, R.C.; Seem, R.C. Partial control of grape powdery mildew by the mycoparasite *Ampelomyces quisqualis*. *Plant Dis.* **1995**, *79*, 483–490. [CrossRef]
44. Hashioka, Y.; Nakai, Y. Ultrastructure of pycnidial development and mycoparasitism of *Ampelomyces quisqualis* parasitic on Erysiphales. *Trans. Mycol. Soc. Japan* **1980**, *21*, 329–338.
45. Kiss, L.; Russell, J.C.; Szentiványi, O.; Xu, X.; Jeffries, P. Biology and biocontrol potential of *Ampelomyces* mycoparasites, natural antagonists of powdery mildew fungi. *Biocont. Sci. Technol.* **2004**, *14*, 635–651. [CrossRef]
46. Kiss, L. Intracellular mycoparasites in action: Interactions between powdery mildew fungi and *Ampelomyces*. In *Stress in Yeasts and Filamentous Fungi*; Avery, S.V., Stratford, M., van West, P., Eds.; Academic Press: Cambridge, MA, USA, 2008; Volume 27, pp. 37–52.
47. Németh, M.Z.; Pintye, A.; Horváth, Á.N.; Vági, P.; Kovács, G.M.; Gorfer, M.; Kiss, L. Green fluorescent protein transformation sheds more light on a widespread mycoparasitic interaction. *Phytopathology* **2019**, *109*, 1404–1416. [CrossRef] [PubMed]
48. Németh, M.Z.; Mizuno, Y.; Kobayashi, H.; Seress, D.; Shishido, N.; Kimura, Y.; Takamatsu, S.; Suzuki, T.; Takikawa, Y.; Kakutani, K.; et al. *Ampelomyces* strains isolated from diverse powdery mildew hosts in Japan: Their phylogeny and mycoparasitic activity, including timing and quantifying mycoparasitism of *Pseudoidium neolyopersici* on tomato. *PLoS ONE* **2021**, *16*, e0251444. [CrossRef]
49. Aylor, D.E. The role of intermittent wind in the dispersal of fungal pathogens. *Annu. Rev. Phytopathol.* **1990**, *28*, 73–92. [CrossRef]
50. Brown, J.K.M.; Hovmöller, M.S. Aerial dispersal of pathogens on the global and continental scales and its impact on plant disease. *Science* **2002**, *297*, 537–541. [CrossRef]
51. Nonomura, T.; Matsuda, Y.; Yamashita, S.; Akahoshi, H.; Takikawa, Y.; Kakutani, K.; Toyoda, H. Natural woody plant, *Mallotus japonicus*, as an ecological partner to transfer different pathotypic conidia of *Oidium neolyopersici* to greenhouse tomatoes. *Plant Protect. Sci.* **2013**, *49*, S33–S40. [CrossRef]
52. Suzuki, T.; Iwasaki, S.; Hisazumi, H.; Miyamoto, A.; Ogami, H.; Takikawa, Y.; Kakutani, K.; Matsuda, Y.; Nonomura, T. Inhibitory effects of blue light-emitting diode irradiation on *Podosphaera xanthii* conidial release and infection of melon seedlings. *Agriculture* **2022**, *12*, 198. [CrossRef]
53. Suzuki, T.; Nakamura, R.; Takagi, N.; Takikawa, Y.; Kakutani, K.; Matsuda, Y.; Matsui, K.; Nonomura, T. Quantitative analysis of the lifelong production of conidia released from single colonies of *Podosphaera xanthii* on melon leaves using electrostatic techniques. *Austral. Plant Pathol.* **2019**, *48*, 297–307. [CrossRef]
54. Griffith, W.T. Electrostatic phenomena. In *The Physics of Everyday Phenomena: A Conceptual Introduction to Physics*; Brufloodt, D., Loehr, B.S., Eds.; McGraw-Hill: New York, NY, USA, 2004; pp. 232–252.
55. Halliday, D.; Resnick, R.; Walker, J. Electric charge. In *Fundamentals of Physics*; Johnson, S., Ford, E., Eds.; John Wiley & Sons: New York, NY, USA, 2005; pp. 561–579.
56. Leach, C.M. An electrostatic theory to explain violent spore liberation by *Drechslera turcica* and other fungi. *Mycologia* **1976**, *68*, 63–86. [CrossRef]

57. Matsuda, Y.; Ikeda, H.; Moriura, N.; Tanaka, N.; Shimizu, K.; Oichi, W.; Nonomura, T.; Kakutani, K.; Kusakari, S.; Higashi, K.; et al. A new spore precipitator with polarized dielectric insulators for physical control of tomato powdery mildew. *Phytopathology* **2006**, *96*, 967–974. [CrossRef] [PubMed]
58. Shimizu, T.; Matsuda, Y.; Nonomura, T.; Ikeda, H.; Tamura, N.; Kusakari, S.; Kimbara, J.; Toyoda, H. Dual protection of hydroponic tomatoes from rhizosphere pathogens *Ralstonia solanacearum* and *Fusarium oxysporum* f. sp. *radicis-lycopersici* and airborne conidia of *Oidium neolycopersici* with an ozone-generative electrostatic spore precipitator. *Plant Pathol.* **2007**, *56*, 987–997. [CrossRef]
59. Ayabe, S.; Kimura, Y.; Umei, N.; Takikawa, Y.; Kakutani, K.; Matsuda, Y.; Nonomura, T. Real-time collection of conidia released from living single colonies of *Podosphaera aphanis* on strawberry leaves under natural conditions with electrostatic techniques. *Plants* **2022**, *11*, 3453. [CrossRef]
60. Moriura, N.; Matsuda, Y.; Oichi, W.; Nakashima, S.; Hirai, T.; Nonomura, T.; Kakutani, K.; Kusakari, S.; Higashi, K.; Toyoda, H. An apparatus for collecting total conidia of *Blumeria graminis* f. sp. *hordei* from leaf colonies using electrostatic attraction. *Plant Pathol.* **2006**, *55*, 367–374. [CrossRef]
61. Suzuki, T.; Nishimura, S.; Yagi, K.; Nakamura, R.; Takikawa, Y.; Matsuda, Y.; Kakutani, K.; Nonomura, T. Effects of light quality on conidiophore formation of the melon powdery mildew pathogen *Podosphaera xanthii*. *Phytoparasitica* **2018**, *94*, 1105–1110. [CrossRef]
62. Sameshima, T.; Kashimoto, K.; Kida, K.; Matsuda, Y.; Nonomura, T.; Kakutani, K.; Nakata, K.; Kusakari, S.; Toyoda, H. Cytological events in tomato leaves inoculated with conidia of *Blumeria graminis* f. sp. *hordei* and *Oidium neolycopersici* KTP-01. *J. Gen. Plant Pathol.* **2004**, *70*, 7–10. [CrossRef]
63. Kiss, L. Graminicolous powdery mildew fungi as new natural hosts of *Ampelomyces* mycoparasites. *Can. J. Bot.* **1997**, *75*, 680–683. [CrossRef]
64. Kiss, L.; Nakasone, K.K. Ribosomal DNA internal transcribed spacer sequences do not support the species status of *Ampelomyces quisqualis*, a hyperparasite of powdery mildew fungi. *Curr. Genet.* **1998**, *33*, 362–367. [CrossRef]
65. Ranković, B. Hyperparasites of the genus *Ampelomyces* on powdery mildew fungi in Serbia. *Mycopathologia* **1997**, *139*, 157–164. [CrossRef] [PubMed]
66. Pintye, A.; Ropars, J.; Harvey, N.; Shin, H.D.; Leyronas, C.; Nicot, P.C.; Giraud, T.; Kiss, L. Host phenology and geography as drivers of differentiation in generalist fungal mycoparasites. *PLoS ONE* **2015**, *10*, e0120703. [CrossRef]
67. Gu, Y.H.; Ko, W.H. Water agarose medium for studying factors affecting germination of conidia of *Ampelomyces quisqualis*. *Mycol. Res.* **1997**, *101*, 422–424. [CrossRef]
68. Sundheim, L.; Krekling, T. Host-parasite relationships of the hyperparasite *Ampelomyces quisqualis* and its powdery mildew host *Sphaerotheca fuliginea*. *Phytopath. Z.* **1982**, *104*, 202–210. [CrossRef]
69. Philipp, W.-D.; Crüger, G. Parasitismus von *Ampelomyces quisqualis* auf echten mehlaupilzen an gurken und anderen gemüsearten. *Z. Pflanzenkrankh. Pflanzenschutz* **1979**, *86*, 129–142.
70. Nonomura, T.; Matsuda, Y.; Xu, L.; Kakutani, K.; Takikawa, Y.; Toyoda, H. Collection of highly germinative pseudochain conidia of *Oidium neolycopersici* from conidiophores by electrostatic attraction. *Mycol. Res.* **2009**, *113*, 364–372. [CrossRef] [PubMed]
71. Speer, E.O. *Ampelomyces cesati* (Fungi, Sphaeropsidales). *Taxon* **1978**, *27*, 549–562. [CrossRef]
72. Kiss, L.; Pintye, A.; Zséli, G.; Jankovics, T.; Szentiványi, O.; Hafez, Y.M.; Cook, R.T.A. Microcyclic conidiogenesis in powdery mildews and its association with intracellular parasitism by *Ampelomyces*. *Eur. J. Plant Pathol.* **2010**, *126*, 445–451. [CrossRef]
73. Zeng, L.F.; Jiang, Y.C. An investigation of parasitic fungi on *Erysiphe* spp. *RoPP* **1986**, *65*, 419.

Disclaimer/Publisher’s Note: The statements, opinions and data contained in all publications are solely those of the individual author(s) and contributor(s) and not of MDPI and/or the editor(s). MDPI and/or the editor(s) disclaim responsibility for any injury to people or property resulting from any ideas, methods, instructions or products referred to in the content.

MDPI
St. Alban-Anlage 66
4052 Basel
Switzerland
www.mdpi.com

Agronomy Editorial Office
E-mail: agronomy@mdpi.com
www.mdpi.com/journal/agronomy



Disclaimer/Publisher's Note: The statements, opinions and data contained in all publications are solely those of the individual author(s) and contributor(s) and not of MDPI and/or the editor(s). MDPI and/or the editor(s) disclaim responsibility for any injury to people or property resulting from any ideas, methods, instructions or products referred to in the content.



Academic Open
Access Publishing

[mdpi.com](https://www.mdpi.com)

ISBN 978-3-7258-0896-0